Harmicini amidnoga tipa kao potencijalni antimalarici

Marinović, Marina

Sveučilište u Zagrebu

FARMACEUTSKO-BIOKEMIJSKI FAKULTET

Marina Marinović

HARMICINI AMIDNOGA TIPA KAO POTENCIJALNI ANTIMALARICI

DOKTORSKI RAD

Zagreb, 2023.

Sveučilište u Zagrebu

FARMACEUTSKO-BIOKEMIJSKI FAKULTET

Marina Marinović

HARMICINI AMIDNOGA TIPA KAO POTENCIJALNI ANTIMALARICI

DOKTORSKI RAD

Mentor: prof. dr. sc. Zrinka Rajić

Zagreb, 2023.

University of Zagreb

FACULTY OF PHARMACY AND BIOCHEMISTRY

Marina Marinović

AMIDE-TYPE HARMICINES AS POTENTIAL ANTIMALARIAL AGENTS

DOCTORAL DISSERTATION

Supervisor: Professor Zrinka Rajić, PhD

Zagreb, 2023

Doktorski rad je predan na ocjenu Fakultetskom vijeću Farmaceutsko-biokemijskog fakulteta Sveučilišta u Zagrebu radi stjecanja akademskog stupnja doktora znanosti u znanstvenom području biomedicine i zdravstva, polje farmacija, grana farmacija.

Doktorski rad je izrađen u Zavodu za farmaceutsku kemiju Farmaceutsko-biokemijskog fakulteta Sveučilišta u Zagrebu u suradnji s Institutom za tropsku medicinu Sveučilišta u Tübingenu (Njemačka) i Institutom za molekularnu medicinu, Medicinskog fakulteta Sveučilišta u Lisabonu (Portugal), u sklopu doktorskog studija „Farmaceutsko-biokemijske znanosti" Farmaceutsko-biokemijskog fakulteta Sveučilišta u Zagrebu. Rad je financiran sredstvima projekta „Derivati harmina kao potencijalni antimalarici" (UIP-2017-05-5160) Hrvatske zaklade za znanost. Rad doktorandice Marine Marinović financiran je iz projekta „Projekt razvoja karijera mladih istraživača – izobrazba novih doktora znanosti" Hrvatske zaklade za znanost koji je financirala Europska unija iz Europskog socijalnog fonda i projekta Jačanje znanstveno-istraživačkih i inovacijskih kapaciteta Farmaceutsko-biokemijskog fakulteta Sveučilišta u Zagrebu (FarmInova) koji je financiran iz Europskoga fonda za regionalni razvoj, Operativni program konkurentnosti i kohezije za razdoblje 2014. – 2020, poziv „Ulaganje u organizacijsku reformu i infrastrukturu u sektoru istraživanja, razvoja i inovacija".

Zahvale

Zahvaljujem mentorici, prof. dr. sc. Zrinki Rajić na stručnom vodstvu, svim savjetima, idejama, strpljivosti i pomoći tijekom izrade doktorskog rada.

Izv. prof. dr. sc. Ivani Perković na prenesenom znanju, svim savjetima i velikodušnosti.

Doc. dr. sc. Hrvoju Rimcu za pomoć pri izradi QSAR modela.

Doc. dr. sc. Kristini Pavić na ugodnom društvu, pomoći, savjetima i dijeljenju slano-slatkih delicija.

Veliko hvala kolegi i prijatelju Goranu (dr. sc. Gogiću) na: 1) nesebičnosti, 2) savjetima, 3) podršci, 4) razgovorima i raspravama, 5) zajedničkom pranju suđa, 6) smijehu i 7) stalnoj spremnosti na riječi: „E Gogić ajde dođi vidjet pločicu!"

Svim članovima Zavoda za farmaceutsku kemiju, na svoj podršci i lijepim trenutcima, posebno hvala tehničarki Ljiljani Jurkin što je uvijek bila spremna pomoći.

Asistentskoj ekipi na druženju, hodničkim razgovorima i međusobnoj podršci.

Barbari Rubinić, Luci Udovičić i Karmeli Klarić, koje su pri izradi svojih diplomskih radova i/ili radova za Rektorovu nagradu doprinijele izradi dijela doktorata.

Beskrajno hvala mojoj obitelji: braći, šogoricama, nećacima i sestričnama, na svoj ljubavi i podršci koju su imali za mene, a najveće hvala mojim roditeljima, vaša bezuvjetna ljubav učinila je da sve ovo bude moguće. Volim vas!

Hvala svim mojim prijateljima, posebno Ireni, mojoj cimki na svim razgovorima, podršci i razumijevanju.

Veliko hvala mojim credićima, jer: „Vi prekrasni ljudi, sa vama mogu, cijelu noć biti budna i sanjati na nogama, sanjati na nogama." Hvala vam na svim lijepim trenutcima, prijateljstvu, smijehu i ispjevanim pjesmama.

SAŽETAK

U prvom dijelu istraživanja ovog doktorskog rada sintetizirano je četrdeset harmicina amidnoga tipa (**7a-h**, **13a-h**, **19a-h**, **22a-h**, **25a-f**, **i-p**), hibridnih spojeva harmina/srodnih β-karbolinskih alkaloida i cimetne kiseline/odabranih derivata cimetne kiseline (DCK-a) međusobno povezanih amidnom vezom. U tu svrhu pripravljeni su amini **6**, **12**, **18**, **21** i **24**, čime je primarna amino skupina uvedena u pet položaja β-karbolina: 1, 3, 6, 7 i 9. U idućem koraku sintetizirani su harmicini amidnoga tipa reakcijama povezivanja dobivenih amina s cimetnom kiselinom/DCK-ima korištenjem standardnih reakcijskih uvjeta (HATU/DIEA). Harmicini su karakterizirani spektroskopskim (^{1}H, ^{13}C NMR, IR) i spektrometrijskim (MS) tehnikama te im je određeno talište. Svim spojevima ispitano je antiplazmodijsko djelovanje *in vitro* na eritrocitnu fazu životnog ciklusa dva soja *Plasmodium falciparum* (*Pf*3D7 i *Pf*Dd2), hepatocitnu fazu životnog ciklusa *P. berghei* i citotoksičnost na humanu staničnu liniju hepatocelularnog karcinoma (HepG2).

U drugom dijelu istraživanja provedena je analiza kvantitativnog odnosa strukture i djelovanja (engl. *quantitative structure-activity relationship*, QSAR). Antiplazmodijsko djelovanje harmicina na eritrocitnu fazu *Pf*3D7 povezano je s pripadajućim izračunatim molekulskim deskriptorima te je primjenom metode višestruke linearne regresije dobiven prediktivni model ovisnosti log IC_{50} o dvije varijable: izoelektričnoj točki (p*I*) i Abrahamovom deskriptoru E (Abr E). Model je validiran unutarnjom 10-strukom unakrsnom validacijom.

U trećem dijelu istraživanja, za provedbu vanjske validacije modela predložene su strukture 356 novih harmicina te su im, prema dobivenom modelu, izračunate predviđene IC_{50} vrijednosti. Potom je odabrano, sintetizirano i karakterizirano ukupno 19 harmicina: šest harmicina amidnoga tipa (**25k-p**), 11 harmicina karbamatnog tipa (**28a-k**) i dva harmicina ureidnog tipa (**32b**,**c**) u položaju N-9 β-karbolina, te je ispitano njihovo antiplazmodijsko djelovanje *in vitro* na eritrocitnu fazu životnog ciklusa plazmodija (*Pf*3D7 i *Pf*Dd2). Na temelju dobivenih rezultata izračunate su razlike između eksperimentalnih i predviđenih vrijednosti i srednja apsolutna pogreška predviđanja. Najjače djelovanje, gotovo dva reda veličine jače od harmina, pokazali su harmicini amidnoga tipa u položaju N-9 β-karbolina (**25b-e**,**i**,**j**).

Rezultati ovog doktorskog rada predstavljaju temelj za daljnji razvoj novih harmicina amidnoga tipa s pojačanim antiplazmodijskim djelovanjem.

Ključne riječi: β-karbolin, harmicini, DCK, sinteza, antiplazmodijsko djelovanje, QSAR

SUMMARY

Introduction

Malaria, caused by parasites of the genus *Plasmodium*, is one of the most important life-threatening infectious diseases in humans. According to World Health Organization, 241 million malaria cases and 627 000 deaths were reported in 2020, mainly in tropical and subtropical regions. Over the past two decades, malaria cases and deaths have declined worldwide, but progress is now stagnating due to the widespread emergence of multidrug-resistant strains. Several strategies are currently being used in parallel to combat this disease, including vector control methods, vaccine development, and novel drugs. RTS,S/AS01 is the leading malaria vaccine, but has shown only moderate efficacy in preventing clinical *P. falciparum* malaria. In addition, first-line treatments, including artemisinin-based combination therapies (ACTs), are also at risk due to the emergence of resistant *P. falciparum* strains in Southeast Asia and Africa, so there is an urgent need to discover and develop new drugs with different mechanisms of action. One attractive approach commonly used in drug discovery is molecular hybridization. A hybrid combining two or more bioactive molecules offers the potential to increase the efficacy of each bioactive molecule and overcome drug resistance. In this work, harmine/β-carboline and cinnamic acid derivatives (CADs), were covalently linked, resulting in harmicines. Harmine is a naturally occurring β-carboline alkaloid and a potent and selective inhibitor of *P. falciparum* Hsp90. Cinnamic acid and its derivatives are also natural products whose numerous biological activities, including antimalarial activity, have been extensively reported. In this work, the synthesis, characterization and biological evaluation of harmicines were reported. In addition, detailed QSAR study was performed, leading to a predictive model that enabled the design and synthesis of new harmicines**.**

Materials and methods

The preparation of the amide-type harmicines (AT) was straightforward and involved: 1) synthesis of the primary β-carboline amines **6**, **12**, **18**, **21**, and **24** and 2) coupling reactions with cinnamic acid and various CADs. The β-carboline amines **6**, **12**, and **18** in positions C-1, C-3, and O-6, respectively, were prepared *via* a multistep reaction pathway. Pictet-Spengler condensation of 1) tryptamine with 2,2-dimethoxyacetaldehyde, 2) tryptophan methyl ester with acetaldehyde dimethyl acetal, 3) 5-methoxytryptamine with acetaldehyde dimethyl acetal and subsequent oxidation of the tetrahydro-β-carboline intermediates resulted in the preparation of the corresponding β-carbolines **2**, **9** and **15**, respectively. The acetal group of β-carboline **2** was hydrolyzed in a CH_3COOH/H_2O mixture, and the obtained aldehyde **3** was reduced with $LiAlH_4$ to give alcohol **4**. The ester groups of β-carbolines **9a** and **9b** were reduced under similar

reaction conditions, yielding alcohol **10**. Alcohols **4** and **10** reacted with 2-azido-1,3-dimethylimidazolinium hexafluorophosphate (ADMP) and 1,8-diazabicyclo[5.4.0]undec-7-ene (DBU) to give azides **5** and **11**, respectively. Reduction of azides with H_2/Pd/C gave rise to amines **6** and **12**. The ether group of β-carboline **15** was hydrolyzed in a CH_3COOH/HBr mixture. Subsequently, the obtained phenol **16** was alkylated with $BocNH(CH_2)_2Br$ in the presence of Cs_2CO_3 and tetrabutylammonium hydrogen sulfate (TBAHS) to give the Boc-protected amine **17**. The latter was converted to amine **18** after the removal of the Boc protecting group in HCl. The synthesis of amines in the positions O-7 and N-9 was carried out by the alkylation of harmole (obtained by hydrolysis of harmine in a CH_3COOH/HBr mixture) or harmine with $BocNH(CH_2)_2Br$ in the presence of Cs_2CO_3. The resulting Boc-protected amines **20** and **23** were converted to amines **21** and **24** as described previously.

For the preparation of carbamate- and ureido-type harmicines, CADs were converted into corresponding alcohols and amines. First, CADs were converted to acyl chlorides **26b-k** using $SOCl_2$ and DMF in toluene, which were immediately reduced with $NaBH_4$, either in a mixture of THF and MeOH, giving alcohols **27b-d**, or in a mixture of diethyl ether and MeOH, yielding alcohols **27e-k**. Cinnamyl alcohols **27b**,**c** were then converted to azides **29b**,**c** with ADMP in the presence of DBU and reduced to amines **30b**,**c** with $LiAlH_4$. Reaction of BtcCl and β-carboline amine **24** in the presence of TEA in DCM gave harmine benzotriazolide (**31**).

All chemicals were obtained from commercial sources. The progress of the chemical reactions was monitored by thin-layer chromatography (TLC). The synthesized products were purified by extraction, column chromatography, trituration with diethyl ether/petroleum ether and fully characterized by ^{1}H and ^{13}C NMR, IR and MS.

Harmicines' antimalarial activities against the erythrocytic and hepatic stages of the *Plasmodium* life cycle and cytotoxicity against the hepatocellular carcinoma cell line (HepG2) were investigated. Antimalarial activity against the erythrocytic stage was evaluated *in vitro* against two *P. falciparum* laboratory strains: 3D7 (CQ-sensitive) and Dd2 (CQ-resistant), using the histidine-rich protein-2 assay (HRP-2), with CQ and harmine as positive controls. Antimalarial activity against hepatic stages of the *Plasmodium* life cycle was evaluated *in vitro* against hepatocellular carcinoma cells (Huh7) infected with *P. berghei* using a bioluminescence assay, with primaquine (PQ) and harmine as positive controls. AT harmicines were initially tested at two concentrations, 1 and 10 µM. Cytotoxicity against HepG2 was evaluated using the neutral red assay. For safety evaluation, a selectivity index (SI) was calculated for each compound tested as a fraction of the ratio between the IC_{50} values for HepG2 and the *Pf*3D7 strain.

In addition, a QSAR study was performed to correlate the biological activity with structural and physicochemical properties of AT harmicines, *i.e.* the molecular descriptors using multiple linear regression (MLR) technique. The molecular descriptors for 40 synthesized AT harmicines were generated using the online platform Chemicalize.com, the web tool Swissadme.ch and the software programs MarvinSketch, ACD/ChemSketch, Mnova and ChemDraw Professional. A total set of molecular descriptors were statistically processed in R 4.0.3 using RStudio 1.3.1093 and the libraries "tidyverse," "ggplot2," "readxl," and "caret." First, the initial set of molecular descriptors was reduced by removing descriptors with "0" and constant values for each compound. Then, the correlation matrix was calculated and descriptors with correlation coefficient > 0.95 and < -0.95 were removed. A reduced set of 67 molecular descriptors was subjected to a stepwise forward regression procedure to determine which combination of descriptors was most strongly correlated with the logarithm of the IC_{50} value against the *Pf*3D7 strain. The predictive model was constructed by selecting two descriptors, isoelectric point (pI) and Abraham descriptor E (Abr E) based on the calculated statistical parameters (R^2, coefficient of determination; R_a^2, adjusted coefficient of determination; p value; F value; MAE, mean absolute error; and RMSE, root mean square error). Internal validation of the constructed model was performed with 10-fold cross-validation. Subsequently, the constructed model was used to calculate the predictive log IC_{50} values of 356 newly designed harmicines.

Results and discussion

AT harmicines **7**, **13**, **19**, **22**, and **25** were prepared by coupling reactions of cinnamic acid/CADs and β-carboline-based amines **6**, **12**, **18**, **21**, and **24**, respectively, using HATU and DIEA in DCM. The target hybrids were obtained in good to excellent yields. CT harmicines were prepared in the position N-9 by reacting β-carboline-based amine **24**, CDI, and cinnamyl alcohols **27a-k** using two different approaches. Preparation of CT harmicines **28a-d** started with a reaction of amine **24** and CDI in DMF, followed by the *in situ* reaction of the obtained precursor with cinnamyl alcohols **27a-d**. On the other hand, in the synthetic pathway leading to CT harmicines **28e-k**, in the first step cinnamyl alcohols **27e-k** reacted with CDI. After isolation of the obtained precursor, reaction with amine **24** gave rise to CT harmicines in low to moderate yields. Reaction of cinnamyl amines **30b**,**c** and harmine benzotriazolide **31** gave UT harmicines **32b**,**c** in moderate yield.

The results of the *in vitro* screening of harmicines' antiplasmodial activity against the erythrocytic stage of two *P. falciparum* strains (*Pf*3D7 and *Pf*Dd2) showed that all compounds

exert higher activity than the parent compound harmine (IC_{50} values in low micromolar and submicromolar concentrations), with the exception of AT harmicines (**7a-h**) in the position C-1, which were inactive at the highest concentration tested. In general, harmicines were more active against *Pf*3D7 strain. The most active compounds among all harmicines were AT harmicines in the position N-9 (**25b-e**,**i**,**j**), which showed at least two orders of magnitude stronger activities (IC_{50} = 0.04 – 0.09 µM) against the *Pf*3D7 strain, than the parent compound harmine. AT harmicines in the position C-3 were the least active against both strains, while O-6 and O-7 AT harmicines showed good to moderate activities, except α-CH_3-substituted AT harmicine in the position O-7 (**22h**), which showed the weakest activity among all harmicines. In the series of CT harmicines, *p*-NO_2-substituted harmicine **28k** showed the strongest activities against both strains (IC_{50} (*Pf*3D7) = 0.36 ± 0.001 µM and IC_{50} (*Pf*Dd2) = 0.33 ± 0.04 µM). Among UT harmicines, *m*-CF_3-substituted harmicine **32c** exhibited two-fold stronger activity against *Pf*3D7 (IC_{50} = 0.22 ± 0.04 µM) than the *p*-propoxy-substituted harmicine **32b** (IC_{50} = 0.42 ± 0.0004 µM).

On the other hand, the results of harmicines' antiplasmodial activity screening against hepatic stages of *P. berghei* were modest. As expected, all AT harmicines, except **7a** and **7b**, were more active at 10 µM. The marked cytotoxicity to Huh7 cells observed with most of the harmicines precluded the determination of the corresponding IC_{50} values. Only *m*-CF_3-substituted AT harmicine in the position N-9 (**25i**) was selected for IC_{50} determination. The IC_{50} value obtained was 4.3-fold lower than the IC_{50} value of the reference drug primaquine (1.94 ± 0.68 µM versus 8.4 ± 3.4 µM).

The results of the cytotoxicity assay showed that AT harmicines in the position O-6 **19e-g** and CT harmicines **28a**,**c** were not cytotoxic at all in the highest concentration tested. The least cytotoxic compound with IC_{50} = 350.31 ± 13.02 µM was unsubstituted AT harmicine in the position N-9 (**25a**). The most selective compound was AT harmicine **25i** (SI = 1105), followed by **25b** (*m*-F-substituted AT harmicine, SI = 773). Notably, the latter harmicines were among the most active compounds.

The QSAR model for prediction of antiplasmodial activity (log IC_{50} against the *Pf*3D7 strain) was constructed as follows: the initial set of molecular descriptors was reduced and after applying forward stepwise regression method followed by selecting two descriptors (pI and Abr E), the linear model was obtained. The quality of the constructed QSAR model was evaluated based on various statistical parameters (R^2 = 0.89, R_a^2 = 0.88, MAE_{MLR} = 0.248, $RMSE_{MLR}$ = 0.310, F-test = 148.4). The coefficient of determination and the adjusted coefficient of determination indicate the goodness of fit, and both values were greater than the required

criteria ($R^2 > 0.6$). The constructed QSAR model was also validated by 10-fold cross-validation and by calculating statistical parameters: $Q^2 = 0.85$, $MAE_{CV} = 0.282$, $RMSE_{CV} = 0.355$. The value of Q^2 was greater than the required value of 0.5, indicating high predictive power of the model obtained. For confirmation, a series of 356 novel harmicines was designed, and their log IC_{50} values were calculated. Further, we created and synthesized a focused library of novel AT (**25k-p**), CT (**28a-k**), and UT (**32b**,**c**) harmicines, and evaluated their antiplasmodial activities against the erythrocytic stage of *P. falciparum*.

Conclusion

In this thesis we represent design, synthesis, *in vitro* evaluation of antiplasmodial activity as well as cytotoxicity and QSAR study of novel harmicines. By applying molecular hybridization approach, *i.e.* conjugation of harmine with various CADs, we have successfully prepared hybrid compounds harmicines. The most of harmicines exhibited pronounced antiplasmodial activities against the erythrocytic stage of *P. falciparum*, which was higher than that of the parent compound harmine. In addition, structures and biological activities of 40 novel AT harmicines served as a basis for the creation of QSAR model, followed by the prediction, selection, and synthesis of novel AT, CT, and UT harmicines. The most active and selective harmicines were AT harmicines prepared in the position N-9 of the β-carboline ring. Thus, those harmicines could be considered as lead compounds for further development of novel antimalarial agents.

Keywords: β-carboline, harmicines, CAD, synthesis, antiplasmodial activity, QSAR

SADRŽAJ

PRILOG A

PRILOG B

TEMELJNA DOKUMENTACIJSKA KARTICA/BASIC DOCUMENTATION CARD

KRATICE

ACT	kombinirana terapija koja se temelji na artemizininu (engl. *artemisinin-based combination therapy*)
ADMA	acetaldehid-dimetil acetal
ADMP	2-azido-1,3-dimetilimidazolinijev heksafluorofosfat
ANN	umjetne neuronske mreže (engl. *Artificial Neural Network*)
ATP	adenozin-trifosfat
ATR	prigušena totalna refleksija (engl. *attenuated total reflection*)
B16F-10	stanična linija mišjeg melanoma
BDNF	moždano-neurotrofni faktor
Bel-7402	humana stanična linija hepatocelularnog karcinoma
BGC-823	humana stanična linija adenokarcinoma želuca
Boc	*tert*-butiloksikarbonil
BtcCl	klorid 1-benzotriazol karboksilne kiseline
BtH	benzotriazol (1*H*-benzo[*d*][1,2,3]triazol)
BxPC-3	humana stanična linija adenokarcinoma gušterače
CAT	katalaza
CADD	računalno potpomognuto dizajniranje lijekova (engl. *Computer Aided Drug Design*)
CDI	1,1'-karbonildiimidazol
CDK	kinaze ovisne o ciklinima (engl. *cyclin dependent kinases*)
COX-2	ciklooksigenaza-2
CFPAC-1	humana stanična linija adenokarcinoma gušterače
CV	unakrsna validacija (engl. *cross-validation*)
C6	humana stanična linija glioblastoma
DABCO	1,4-diazabiciklo(2.2.2)oktan
DBU	1,8-diazabiciklo(5.4.0)undek-7-en
DCK	derivat cimetne kiseline
DDQ	2,3-dikloro-5,6-dicijano-1,4-benzokinon
DHA	dihidroartemizinin
DIEA	*N*,*N*-diizopropiletilamin
DMF	*N*,*N*-dimetilformamid

DMSO	dimetilsulfoksid
DNA	deoksiribonukleinska kiselina (engl. *deoxyribonucleic acid*)
DPP	difenilfosforilazid
DYRK	tirozin-fosforilirana i regulirana kinaza dvostruke specifičnosti
EGFR	receptor epidermalnog faktora rasta
ESI	ionizacija elektroraspršenjem
EtOH	etanol
FDA	Američka agencija za hranu i lijekove (engl. *Food and Drug Administration*)
HATU	1-[*bis*(dimetilamino)metilen]-1*H*-1,2,3-triazolo(4,5-*b*)piridinijev 3-oksid heksafluorofosfat
HepG2	humana stanična linija hepatocelularnog karcinoma
HL60	humana stanična linija leukemije
Huh-7	humana stanična linija hepatocelularnog karcinoma
IC_{50}	koncentracija spoja koja inhibira rast stanica za 50 %
IR	infracrveno elektromagnetsko zračenje (engl. *infrared radiation*)
LBDD	dizajniranje lijekova temeljeno na ligandu (engl. *ligand-based drug design*)
LDL	lipoproteini male gustoće (engl. *low-density lipoprotein*)
LPS	lipopolisaharid
MAE	srednja apsolutna pogreška (engl. *mean absolute error*)
MAO-A	monoaminooksidaza-A
MD	simulacije molekulske dinamike (engl. *molecular dynamics*)
MCF-7	humana stanična linija adenokarcinoma dojke
MC3T3-E1	mišja preosteoblastna stanična linija
MGC-803	humana stanična linija adenokarcinoma želuca
MKN-45	humana stanična linija adenokarcinoma želuca
MLR	višestruka linearna regresija (engl. *multiple linear regression*)
MS	masena spektrometrija
MW	mikrovalno zračenje (engl. *microwave radiation*)
NB4	humana stanična linija leukemije
NSCLC	karcinom pluća ne-malih stanica
NMR	nuklearna magnetska rezonancija
N206	humana stanična linija neuroblastoma

OECD	Organizacija za ekonomsku suradnju i razvoj (engl. *Organisation for Economic Cooperation and Development*)
PABA	*p*-aminobenzojeva kiselina
PANC-1	humana stanična linija adenokarcinoma gušterače
PLS	parcijalna regresija najmanjih kvadrata (engl. *Partial Least Square*)
Pd/C	paladij na ugljenu
*Pf*Dd2	soj otporan na klorokin vrste *Plasmodium falciparum*
*Pf*Hsp90	protein toplinskog šoka 90 vrste *Plasmodium falciparum*
*Pf*K1	soj otporan na klorokin, pirimetamin i sulfadoksin vrste *Plasmodium falciparum*
*Pf*NF54	soj osjetljiv na klorokin vrste *Plasmodium falciparum*
*Pf*W2	soj otporan na klorokin, kinin, pirimetamin, ciklogvanil i sulfadoksin vrste *Plasmodium falciparum*
*Pf*3D7	soj osjetljiv na klorokin vrste *Plasmodium falciparum*
PiRBC	eritrociti inficirani plazmodijem (engl. *Plasmodium-infected red blood cells*
PPARγ	γ receptor aktiviran proliferatorom peroksizoma
PQ	primakin
QSAR	kvantitativni odnos strukture i djelovanja (engl. *quantitative stucture-activity relationship*)
QSPR	kvantitativni odnos strukture i svojstva (engl. *Quantitative Structure-Property Activity*)
RMSE	korijen srednje kvadratne pogreške (engl. *root mean square error*)
RT112	humana stanična linija karcinoma mokraćnog mjehura
RT4	humana stanična linija karcinoma mokraćnog mjehura
SAR	odnos strukture i djelovanja (engl. *stucture-activity relationship*)
SBDD	dizajniranje lijekova temeljen na strukturi (engl. *structure-based drug design*, SBDD)
SGC-7901	humana stanična linija adenokarcinoma želuca
SKOV-3	humana stanične linija karcinoma jajnika
SMMC-7721	humana stanična linija hepatocelularog karcinoma
SOD	superoksid dismutaza
SW1990	humana stanična linija adenokarcinoma gušterače
SW620	humana stanična linija adenokarcinoma debelog crijeva

SW480	humana stanična linija adenokarcinoma debelog crijeva
SW780	humana stanična linija karcinoma mokraćnog mjehura
SZO	Svjetska zdravstvena organizacija
TBTU	2-(1*H*-benzotriazol-1-il)-1,1,3,3-tetrametilaminijev tetrafluoroborat
TEA	trietilamin
TFA	trifluoroctena kiselina (engl. *trifluoroacetic acid*)
THβC	tetrahidro-β-karbolin (engl. *tetrahydro-β-carboline*)
THF	tetrahidrofuran
TLC	tankoslojna kromatografija (engl. *thin layer chromatography*)
TMS	tetrametilsilan
TNF-α	faktora nekroze tumora-α
TPC-1	humana stanična linija karcinoma štitnjače
t_t	temperatura taljenja
TWC	komatogram ukupne valne duljine (engl. *total wavelength chromatogram*)
UV	ultraljubičasto zračenje (engl. *ultraviolet*)
U87	humana stanična linija glioblastoma
U373	humana stanična linija glioblastoma
VEGF	vaskularni endotelni faktor rasta

1. UVOD

1.1. MALARIJA

Malarija je zarazna bolest koju uzrokuju tkivno-krvne protozoe roda *Plasmodium,* a prijenosnici malarije ženke su komarca roda *Anopheles*. Najrasprostranjenija je u suptropskim i tropskim područjima koja pružaju pogodne uvjete za život i razmnožavanje komarca (1, 2). Malarijom se godišnje zarazi više od 200 milijuna ljudi, a najugroženija skupina su djeca, trudnice, osobe s oslabljenim imunosnim sustavom i putnici. Pema izvještaju Svjetske zdravstvene organizacije (SZO) broj povezanih smrtnih slučajeva u 2020. godini iznosio je 627 000, od čega su 77 % bila djeca mlađa od pet godina. Također je zabilježen blagi porast smrtnosti u odnosu na 2019. godinu (558 000), a procjenjuje se da je od ukupno 69 000 dodatnih smrtnih slučajeva, 47 000 uvjetovano novonastalom pandemijom uzrokovanom SARS-CoV-2 virusom (2, 3).

Malariju kod ljudi uzrokuje pet patogenih vrsta: *P. falciparum, P. malariae, P. ovale, P. vivax* i *P. knowlesi*. Među navedenima najopasniji su *P. falciparum* i *P. vivax*, a odgovorni su za više od 95 % slučajeva malarije u svijetu. *P. falciparum* prevladava u većim dijelovima Afrike i jugoistočne Azije, području zapadnog Pacifika i području istočnog Mediterana, dok je *P. vivax* najrasprostranjeniji u Srednjoj i Južnoj Americi te Jugoistočnoj Aziji (najviše u Indiji) (2–5).

Životni ciklus plazmodija podijeljen je u dvije faze: spolna faza, koja se odvija u ženki komaraca *Anopheles* (vektor), i nespolna faza u čovjeku (domaćin). Spolna faza započinje u komarcu spajanjem gameta, pri čemu nastaje sporozoit, oblik koji se ubodom zaraženog komarca prenosi u čovjeka, čime započinje nespolna faza. Sporozoiti krvotokom čovjeka vrlo brzo dospijevaju do jetre. Diobom sporozoita dolazi do nastanka velikog broja merozoita, koji uzrokuju pucanje hepatocita. Sporozoiti vrsta *P. vivax* i *P. ovale* mogu prijeći u hipnozoite, latentne oblike koji se zadržavaju u jetri i odgovorni su za relaps bolesti mjesecima ili čak godinama nakon primarne infekcije. Odlaskom u krvotok merozoiti inficiraju eritrocite. U eritrocitnoj fazi također dolazi do nespolnog razmnožavanja, tzv. eritrocitne shizogonije, pri čemu merozoiti sazrijevaju preko prstenastog oblika u trofozoite, a zatim u zrele shizonte, koji uzrokuju pucanje eritrocita i inficiranje novih. Nakon nekoliko ciklusa diobe i sazrijevanja, neki od merozoita se diferenciraju u gametocite. Ponovnim ubodom ženke komarca gametociti dospijevaju u želudac komarca, gdje započinje spolna faza i ciklus se ponavlja (6–9). Životni ciklus plazmodija prikazan je na Slici 1.

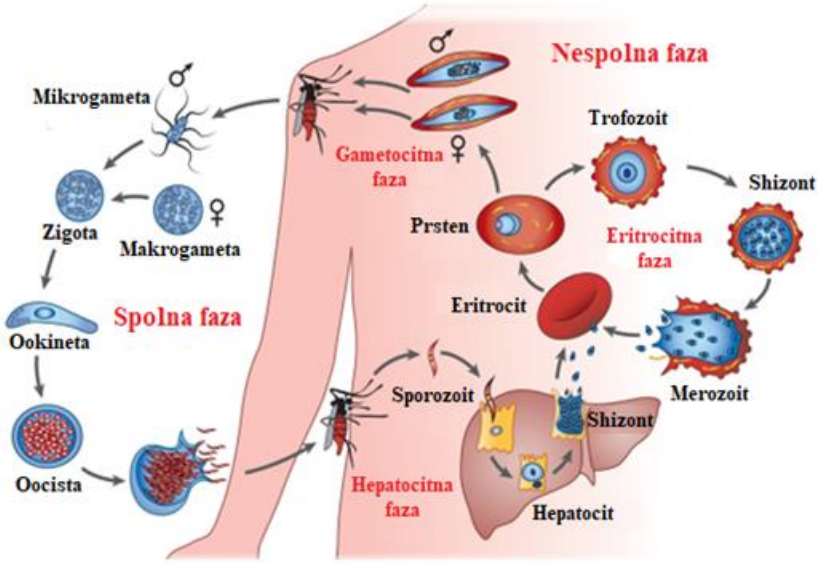

Slika 1. Životni ciklus plazmodija (prilagođeno prema(10))

Klinički simptomi malarije povezani su s eritrocitnom fazom životnog ciklusa plazmodija, dok je hepatocitna faza asimptomatska. Pojava prvih simptoma ovisi o vrsti parazita koji je uzrokovao infekciju, a u prosjeku se javljaju 10 do 15 dana od uboda. Vrijeme inkubacije *P. vivax* najčešće traje 12 do 17 dana, *P. falciparum* 9 do 14 dana, *P. ovale* 16 do 18 dana, a *P. malariae* 18 do 40 dana. Kod nekomplicirane malarije simptomi su često blagi i nespecifični, a uključuju vrućicu, glavobolju, tresavicu, zimicu, bol u mišićima, povraćanje, opću slabost. Međutim, ako se pravovremeno i pravovaljano ne liječi, malarija uzrokovana vrstom *P. falciparum* može prijeći u teški oblik bolesti (komplicirana malarija), koji karakteriziraju teška anemija i hemoglobinurija, sindrom akutnog respiratornog distresa, hipoglikemija, plućni edem, a nerijetko dolazi do akutnog zatajenja bubrega, metaboličke acidoze te cerebralne malarije za koju je karakterističan poremećaj svijesti i koma. U slučaju komplicirane malarije čest je smrtni ishod bolesti (6, 11, 12).

Razni su pristupi koje SZO preporučuje u smjernicama za kontrolu malarije. Neki od njih usmjereni su na kontrolu vektora bolesti, a podrazumijevaju uporabu zaštitnih mreža tretiranih insekticidima i raspršivanje insekticida u zatvorenom prostoru (jedanput do dvaput godišnje). Ostali pristupi u kontroli bolesti uključuju razvoj brzih dijagnostičkih testova, cjepiva i lijekova za liječenje i profilaksu malarije (3, 6).

Veliki napredak u kontroli malarije uočen je razvojem RTS,S/AS01 (Mosquirix) cjepiva. Iako ne pruža potpunu zaštitu, smanjio je broj teških slučajeva u djece, a od listopada 2021. godine SZO preporučuje upotrebu navedenog cjepiva za prevenciju malarije u djece u područjima visokog prijenosa *P. falciparum* malarije (3, 8, 13).

Glavni pristup u prevenciji i kontroli malarije i dalje uključuje upotrebu lijekova za profilaksu i liječenje. Osim kompleksnosti bolesti i razvoja rezistencije plazmodija na postojeću terapiju, dodatan utjecaj na kontrolu malarije ima i činjenica da veći dio farmaceutske industrije napušta istraživanje i razvoj lijekova zbog nedostatka profita, a sve ovo rezultira činjenicom da napredak u suzbijanju malarije stagnira unazad nekoliko godina (2, 6).

1.1.1. Lijekovi u terapiji malarije

Većina trenutno dostupnih lijekova koji se koriste u terapiji malarije djeluje na eritrocitnu fazu životnog ciklusa plazmodija. Mogu se podijeliti u pet glavnih skupina: derivati kinolina, antifolati, naftokinoni, artemizinini i antibiotici. Obzirom na razvoj rezistencije plazmodija, za učinkovito liječenje najčešće se koristi kombinirana terapija, a odabir i doziranje ovisi o vrsti parazita, dostupnosti lijekova, prisutnosti rezistencije i težini kliničkog slučaja (1, 14, 15).

Derivati kinolina. Povijesno gledano derivati kinolina su najupotrebljavaniji antimalarici. Prvi lijek iz ove skupine je kinin, a od prvotne izolacije 1820. pa sve do 1940. godine bio je jedini lijek koji se koristio u terapiji malarije. Pojava rezistentnih sojeva plazmodija zabilježena je 1910. godine. Od 2006. godine se više ne koristi kao prva linija liječenja malarije, ali je i dalje na listi esencijalnih lijekova SZO-e za liječenje malarije kada kombinirana terapija koja se temelji na artemizininu (engl. *artemisnin-based combination therapy,* ACT) nije dostupna (14–17).

Zbog pojave rezistencije i nuspojava (cinkonizam) razvijeni su 4-aminokinolini (klorokin, amodiakin, piperakin), koji u svojoj strukturi sadrže amino skupinu vezanu za kinolinski prsten. Bazični karakter ovih spojeva omogućava im zadržavanje u prehrambenoj vakuoli parazita gdje ispoljavaju svoje antimalarijsko djelovanje. Stvaranjem kompleksa sa slobodnim hemom sprječavaju polimerizaciju hemozoina, pri čemu dolazi do nakupljanja toksičnog hema, što u konačnici dovodi do smrti parazita. Zbog svoje učinkovitosti, niske toksičnosti i niske cijene proizvodnje klorokin je postao široko primjenjivani lijek u liječenju malarije uzrokovane svim vrstama plazmodija. Razvoj rezistencije plazmodija na klorokin započeo je 1950-ih godina, a do danas je poznato nekoliko sojeva rezistentnih na klorokin. Također se nalazi na listi esencijalnih lijekova SZO-e za liječenje *P. vivax* malarije u područjima gdje rezistencija nije razvijena. Amodiakin je prvi put sintetiziran 1948. godine, a zbog svoje toksičnosti više se ne koristiti kao monoterapija. Danas se upotrebljava za liječenje nekomplicirane *P. falciparum* malarije u kombinaciji s artezunatom. Piperakin je razvijen 1960-ih godina i pokazao je učinkovitost protiv sojeva rezistentnih na klorokin. Prema kemijskoj

strukturi je *bis*-kinolin te njegov točan mehanizam djelovanja nije poznat, ali se pretpostavlja da djeluje analogno 4-aminokinolinima. Pojava rezistencije zabilježena je 1980-ih godina u područjima gdje se koristio kao monoterapija, stoga se danas koristi kao dio ACT kao lijek partner dihidroartemizininu (8, 14–17).

8-Aminokinolini (primakin, tafenokin) su derivati kinolina, čiji mehanizam djelovanja nije u potpunosti razjašnjen. Primakin je u kliničku upotrebu uveden 1950-ih godina, a djeluje na hepatocitnu fazu svih vrsta plazmodija, na gametocitnu fazu *P. falciparum*, a također sprječava relaps malarije djelujući na hipnozoite *P. vivax* i *P. ovale*. U odnosu na primakin, tafenokin posjeduje sposobnost inhibicije polimerizacije hemozoina, što mu omogućuje da djeluje i na krvne shizonte, a upotrebljava se za liječenje *P. vivax* malarije. Također djeluje na latentne hipnozoite *P. vivax* i *P. ovale* stoga se, kao i primakin, koristi u profilaktičkom liječenju malarije. Međutim, ovi lijekovi uzrokuju hemolitičku anemiju u pacijenata s manjkom glukoza-6-fosfat dehidrogenaze, što ograničava njihovu upotrebu (8, 14–16, 18, 19).

Meflokin, lumefantrin i halofantrin su derivati kinolina, a spadaju u skupinu arilaminoalkohola. Meflokin je lijek koji je razvijen 1970-ih godina za liječenje klorokin-rezistentne malarije. Posjeduje snažno shizontocidno djelovanje, a točan mehanizam djelovanja nije još razjašnjen. Istraživanja pokazuju da, poput 4-aminokinolina, inhibira polimerizaciju hemozoina, a novija istraživanja pokazuju da se veže na 80S podjedinicu ribosoma vrste *P. falciparum*, čime sprječava sintezu proteina. Izaziva ozbiljne nuspojave u središnjem živčanom sustavu, pa se stoga ne koristi kao monoterapija već u kombinaciji s artezunatom za liječenje nekomplicirane malarije u djece. Pojava rezistencije na ovaj lijek zabilježena je 1980-ih godina. Lumefantrin je prvi put sintetiziran 1976. godine, a upotrebljava se kao dio ACT kao lijek partner artemeteru. Iako mu mehanizam nije u potpunosti razjašnjen pretpostavlja se da inhibira polimerizaciju hemozoina. Halofantrin je razvijen između 1965. i 1975. godine, a koristio se za liječenje malarije uzorkovane svim vrstama plazmodija. Pojava kardiotoksičnosti ograničava njegovu primjenu pa se danas koristi samo za liječenje komplicirane malarije (8, 14–16, 20).

Pironaridin je naftiridin, derivat kinolina razvijen 1970-ih godina. Pokazao se učinkovitim protiv svih sojeva rezistentnih na klorokin i već se više od 40 godina koristi kao dio ACT u kombinaciji s artezunatom za liječenje *P. falciparum* i *P. vivax* malarije (8, 14, 16, 20).

Antifolati. Antifolati su skupina antimalarijskih lijekova koji djeluju kao krvni shizontocidi (eritrocitna faza plazmodija), a posjeduju i protutumorsko djelovanje. Obzirom na mehanizam antimalarijskog djelovanja mogu se podijeliti u dvije grupe. U prvu grupu antifolata ubrajaju se sulfonamidi, odn. sulfadoksin. Sulfadoksin je strukturno sličan *p*-aminobenzojevoj

kiselini (PABA), a antimalarijsko djelovanje ostvaruje inhibicijom dihidropteroat sintetaze vrste *P. falciparum*, enzima ključnog u sintezi nukleinskih kiselina. Zbog toksičnosti i niske učinkovitosti ne upotrebljava se kao monoterapija već u kombinaciji s pirimetaminom (8, 14–16, 20).

U drugu grupu antifolata spadaju pirimetamin i progvanil koji antimalarijsko djelovanje ostvaruju inhibicijom dihidrofolat reduktaze plazmodija, sprječavajući na taj način redukciju dihidrofolata u tetrahidrofolat koji je neophodan za sintezu deoksinukleotida potrebnih u sintezi DNA. Pirimetamin je razvijen 1950-ih godina i najčešće se koristi u kombinaciji sa sulfadoksinom za profilaksu i liječenje malarije. Nažalost, 1976. godine zabilježena je rezistencija na ovu kombinaciju lijekova stoga se danas često koriste u kombinaciji s kininom ili kao dio ACT u kombinaciji s artezunatom. Progvanil je bigvanidin, prolijek koji se u organizmu pomoću enzima CYP 2C19 metabolizira u aktivni metabolit ciklogvanil. Prvi je antimalarijski lijek u skupini antifolata, a zbog niske toksičnosti se upotrebljava u profilaksi i liječenju *P. falciparum* malarije. Od 2000-te godine se koristi u kombinaciji s atovakvonom, čime se postiže sinergistički učinak (8, 14–16, 20).

Naftokinoni. Atovakvon je naftokinon sintetiziran 1991. godine. Trenutno je jedini lijek koji selektivno inhibira citokrom bc1 plazmodija u lancu prijenosa elektrona, a u terapiji malarije koristi se u kombinaciji s progvanilom (8, 15, 20).

Artemizinini. Artemizinin je seskviterpenski lakton otkriven 1972. godine. Pokazao se učinkovitim protiv svih rezistentnih sojeva vrste *P. falciparum*, a vrlo brzo su sintetizirani njegovi strukturni analozi, artemeter i artezunat, prolijekovi koji se u organizmu metaboliziraju u aktivni metabolit dihidroartemizinin. Artemizinin i njegovi derivati djeluju na rani stadij razvoja parazita u eritrocitnoj fazi što omogućava brzu eliminaciju plazmodija i sprječavanje razvoja težeg oblika bolesti. Također imaju i gametocitno djelovanje čime sprječavaju transmisiju malarije. Budući da djeluju kratko, koriste se u raznim kombinacijama s dugodjelujućim lijekovima (artemeter-lumefantrin, dihidroartemeter-piperakin, artezunat-amodiakin, artezunat-meflokin, artezunat-sulfadoksin-pirimetamin, artezunat-pironaridin, dihidroartemizinin-piperakin) kao ACT. Od 2006. godine SZO preporučuje ACT kao prvu linije liječenja *P. falciparum* malarije. Mehanizam djelovanja artemizinina i njegovih derivata temelji se na redukciji endoperoksidnog mosta od strane slobodnih Fe^{2+} iona, koji potječu iz hemoglobina, pri čemu nastaju radikali koji uzrokuju alkiliranje i uništavanje proteina (primjerice proteasom, *Pf*ATP6) ključnih za preživljavanje plazmodija. Rezistencija na artemizinin uočena je 2008. godine u Kambodži, dok se 2018. godine križna rezistencija na kombinaciju dihidroartemizinin-piperakin pojavila u Jugoistočnoj Aziji (8, 14–16, 20–22).

Antibiotici. Tetraciklini (doksiciklin, tetraciklin), makrolidi (azitromicin) i klindamicin su antibiotici, koji se u terapiji malarije najčešće koriste kao dodatak kininu za liječenje *P. falciparum* malarije. Osim toga, doksiciklin se još koristi u profilaksi malarije (8, 15, 20). Djeluju na ribosome plazmodija i inhibiraju sintezu polipeptida u apikoplastu čime postižu selektivno djelovanje. Najjače antimalarijsko djelovanje među navedenim antibioticima pokazuje azitromicin (8, 15, 20, 23).

Popis lijekova koji se koriste u terapiji malarije dan je u Tablici 1.

Tablica 1. Lijekovi u terapiji malarije (14–16, 20, 24)

Skupina	**Podskupina**	**Lijek (godina razvoja)**	**Rezistencija**	**Terapijska primjena**	**Mehanizam djelovanja**
Derivati kinolina	alkaloidi kininovca	kinin (1820.)	od 1910.	liječenje kompliciranе i nekompliciranе *P. falciparum* malarije	inhibicija polimerizacije hemozoina
	4-aminokinolini	klorokin (1945.)	od 1957.	liječenje *P. vivax, P. malariae, P. ovale* malarije	
		amodiakin (1948.)	razvijena rezistencija	ACT (artezunat + amodiakin), liječenje nekompliciranе *P. falciparum* malarije	
		piperakin (1960.)	od 1980-ih	ACT (DHA[a] + piperakin)	
	8-aminokinolini	primakin (1950.)	nije zabilježena rezistencija	liječenje i profilaksa *P. vivax, P. ovale* malarije, liječenje gemetocitnog stadija *P. falciparum* malarije	nije u potpunosti razjašnjen
		tafenokin (1978.)	nije zabilježena rezistencija	liječenje i profilaksa *P. vivax, P. ovale* malarije	
	arilaminoalkoholi	meflokin (1977.)	od 1982.	profilaksa, ACT (artezunat + meflokin)	
		lumefantrin (1976.)	nije zabilježena rezistencija	ACT (artemeter + lumefantrin) liječenje nekompliciranе malarije	
		halofantrin (1975.)	razvijena rezistencija	liječenje kompliciranе *P. falciparum* malarije	
	benzonaftiridini	pironaridin (1970.)	nije zabilježena rezistencija	ACT (artezunat + pironaridin)	

Antifolati	diaminopirimidini	pirimetamin (1952.)	od 1967.	liječenje *P. falciparum* malarije u kombinaciji sa sulfadoksinom	inhibicija dihidrofolat reduktaze
	bigvanidini	progvanil (1948.)	od 2000.	liječenje *P. falciparum* malarije u kombinaciji s atovakvonom	
	sulfonamidi	sulfadoksin (1967.)	od 1967.	liječenje nekomplicirane *P. falciparum* malarije, ACT (artezunat + sulfadoksin + pirimetamin)	inhibicija dihidropteroat sintetaze
Naftokinoni	hidroksinaftokinon	atovakvon (1991.)	od 2000.	liječenje *P. falciparum* malarije u kombinaciji s progvanilom	inhibicija citokrom bc1 kompleksa
Artemizinini	seskviterpenski laktoni	artemeter	od 2001.	ACT (artemeter + lumefantrin)	stvaranje slobodnih radikala reakcijom endoperoksida s Fe^{2+} ionima hema
		artezunat	od 2008.	liječenje komplicirane malarije, ACT (meflokin, amodiakin, pironaridin, sulfadoksin pirimetamin)	
		DHA[a]	od 2018.	liječenje komplicirane *P. falciparum* malarije ACT (DHA + piperakin)	
Antibiotici	tetraciklini	doksiciklin, tetraciklin	nije zabilježena rezistencija	liječenje *P. falciparum* malarije u kombinaciji s kininom	inhibicija sinteze proteina vezanjem na ribosome plazmodija
	makrolidi	azitromicin	nije zabilježena rezistencija	*in vitro* i *in vivo* studije sinergističkog učinka u kombinaciji s kininom, artezunatom, klorokinom u liječenju nekomplicirane *P. falciparum* malarije	inhibicija sinteze proteina vezanjem na ribosome plazmodija
	linkozamidi	klindamicin	nije zabilježena rezistencija	u kombinaciji s kininom za liječenje nekomplicirane *P. falciparum* malarije	inhibicija sinteze proteina vezanjem na ribosome plazmodija

[a] DHA - dihidroartemizinin

Zbog brzog razvoja rezistentnih sojeva plazmodija, istraživanja u terapiji malarije kontinuirano su usmjerena na pronalazak učinkovitih antimalarijskih lijekova. Idealan antimalarik trebao bi brzo djelovati (na ranije faze plazmodija), biti siguran, nadvladavati rezistenciju te imati niske troškove proizvodnje kako bi bio dostupan endemskim zemljama (koje su većinom siromašne zemlje). Brzo djelovanje i liječenje (npr. trodnevni antimalarijski režim) osigurava suradljivost pacijenata, omogućava brzo uklanjanje parazita (prije razvoja teškog oblika malarije) i smanjuje mogućnost razvoja rezistencije. Također, otkrićem spoja s novim mehanizmom djelovanja mogao bi se izbjeći razvoj unakrsne rezistencije i postići sinergistički učinak s postojećim antimalarijskim lijekovima (6, 15).

Najčešće korišteni pristupi u otkriću i razvoju učinkovitog antimalarijskog lijeka uključuju kemijske modifikacije postojećih antimalarijskih lijekova koji gube svoju učinkovitost, zatim prenamjenu postojećih lijekova koji se koriste u drugom polju medicine, razvoj nove kombinirane terapije dostupnih antimalarijskih lijekova, pronalazak učinkovitih prirodnih produkata i spojeva koji će djelovati na više faza životnog ciklusa plazmodija, molekulska hibridizacija i razvoj cjepiva (Slika 2) (1, 25).

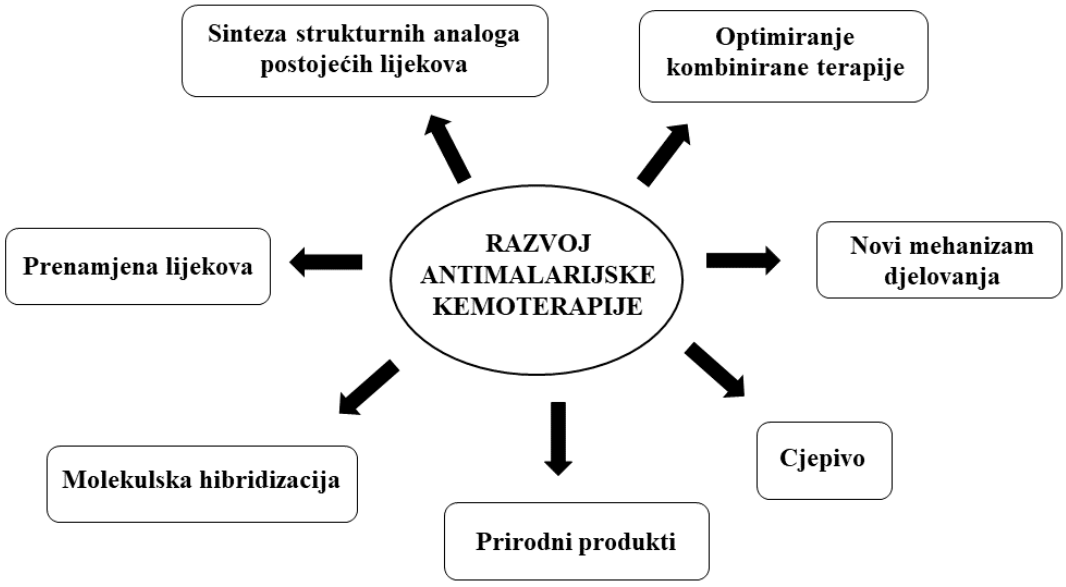

Slika 2. Pristupi u razvoju antimalarijske kemoterapije

1.2. MOLEKULSKA HIBRIDIZACIJA

Molekulska hibridizacija je racionalni pristup dizajniranja lijekova koji uključuje kovalentno povezivanje dviju biološki aktivnih molekula ili njihovih farmakofora s ciljem dobivanja jedinstvene hibridne molekule s poboljšanim djelovanjem. Popularan je pristup koji su koristile brojne istraživačke skupine za razvoj potencijalnih lijekova u terapiji karcinoma, AIDS-a i tuberkuloze, a danas je posebno značajan u procesu razvoja novih antimalarijskih lijekova (26–28).

Hibridne molekule mogu se podijeliti prema:

1. načinu interakcije pojedinačnih molekula/farmakofora s biološkom metom:
    - djelovanje na istu metu,
    - djelovanje na različite mete,
    - istovremeno djelovanje na povezane/slične mete;
2. obliku pojedinih sastavnica (lijek/prolijek):
    - obje molekule u aktivnom obliku,
    - jedna molekula prolijek, druga u aktivnom obliku,
    - obje molekule prolijekovi;
3. načinu povezivanja molekula:
    - konjugati – molekule povezane poveznicom koja nije prisutna u njihovim strukturama,
    - fuzionirani hibridi – molekule su direktno povezane, bez poveznice,
    - integrirani hibridi – integriranje struktura pojedinačnih molekula u jedinstvenu manju molekulu,
    - konjugati s poveznicom koja se cijepa – molekule povezane poveznicom koja se u organizmu metabolizira te dolazi do otpuštanja pojedinih lijekova (26).

Shematski prikaz podjele hibridnih molekula prikazan je na Slici 3.

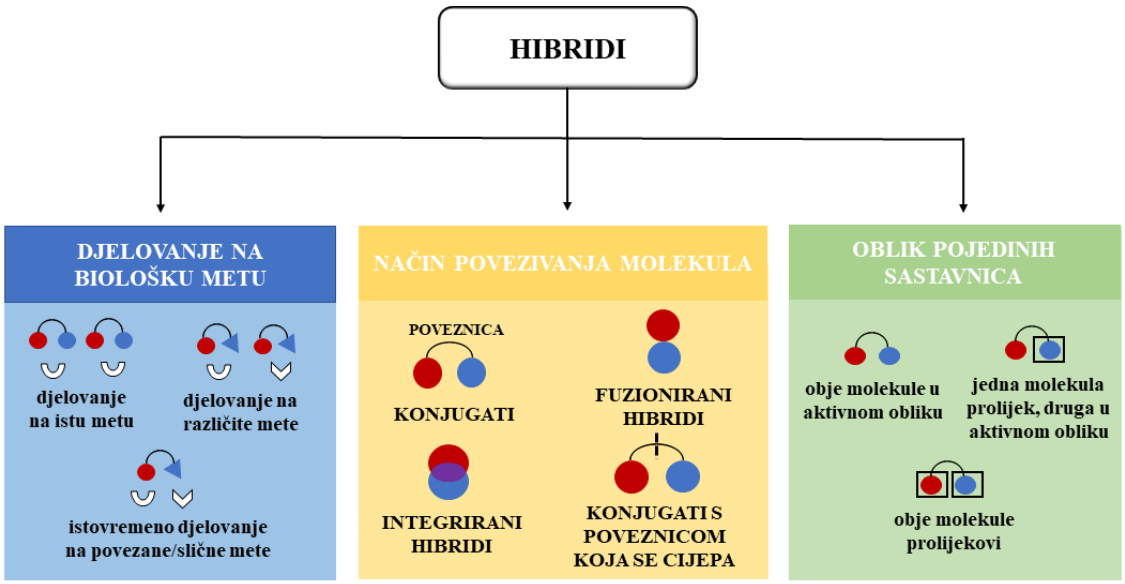

Slika 3. Podjela hibridnih spojeva

Brojne su prednosti primjene hibridnih molekula nad kombiniranom terapijom. Jedna od mogućih prednosti je djelovanje na više bioloških meta, pri čemu se djelovanje može ostvariti različitim mehanizmima ili putem trećeg jedinstvenog mehanizma djelovanja. Nadalje, primjenom hibridnih molekula mogao bi se postići sinergistički učinak, smanjiti toksičnost pojedinačnih spojeva i izbjeći neželjene međusobne interakcije lijekova. Ovim pristupom bi se također mogla smanjiti vjerojatnost razvoja rezistencije i troškovi proizvodnje lijeka, što je od izuzetne važnosti u terapiji malarije (26–29).

1.3. PRIRODNI PRODUKTI

Pojam prirodnih produkata obuhvaća sve kemijske tvari koje potječu iz živih organizama kao što su biljke, gljive, mikroorganizmi, morski organizmi, kralješnjaci i beskralješnjaci (30). Priroda je neiscrpan izvor biološki aktivnih prirodnih produkata, a vrlo su važni u procesu otkrića i razvoja lijekova. Mogu se koristiti izravno kao lijekovi, poslužiti kao sirovine u sintezi složenijih, polusintetskih lijekova ili biti korisni spojevi uzori u otkriću novoga lijeka (31). Iako je upotreba biološki aktivnih prirodnih produkata u obliku biljnih pripravaka poznata još od davnina, njihova izolacija i karakterizacija u svrhu otkrića i razvoja novih lijekova započela je tek u 19-om stoljeću. Prvi prirodni produkt koji je korišten izravno u terapiji bio je morfin. Izoliran je iz maka (*Papaver somniferum*, Papaveraceae), a na tržište ga je stavio Merck 1826. godine. Nešto kasnije razvijena je acetilsalicilna kiselina, prvi polusintetski derivat prirodnog

produkta, salicilne kiseline, izoliranog iz kore vrbe (*Salix alba*, Salicaceae), kojeg je na tržište stavio Bayer 1899. godine (32).

Važnost prirodnih produkata u otkriću i razvoju novih lijekova procijenili su Newman i Cragg 2019 godine. Procjenu su proveli za lijekove koje je odobrila Američka agencija za hranu i lijekove (engl. *Food and Drug Administration*, FDA) u razdoblju od 1981. do listopada 2019. godine. FDA je u navedenom razdoblju odobrila ukupno 1881 lijek, od čega je nemodificiranih prirodnih produkata bilo 71 (3,8 %), biljnih lijekova bilo je 14 (0,8 %), derivata prirodnih produkata 356 (18,9 %) te sintetskih lijekova s prirodnim produktom kao farmakoforom 65 (3,2 %). Prirodni produkti i njihovi strukturni analozi dali su veliki doprinos u protutumorskoj terapiji i terapiji zaraznih bolesti. U navedenom razdoblju najviše je odobreno protutumorskih lijekova (247) od čega je 18 nemodificiranih prirodnih produkata, 43 derivata prirodnih produkata i 13 sintetski dobivenih lijekova s prirodnim produktom kao farmakoforom, zatim antivirusnih lijekova (186) koji uključuju 6 derivata prirodnih produkata i 26 sintetskih lijekova s prirodnim produktom kao farmakoforom, te antibakterijskih lijekova (162) od kojih je 11 nemodificiranih prirodnih produkata i 78 derivata prirodnih produkata (33). Također, veliki broj spojeva dobivenih iz prirodnih izvora u raznim je fazama kliničkih ispitivanja, što ukazuje na održivost i važnost upotrebe prirodnih produkata u razvoju novih lijekova (32).

Biljke su zbog svoje biološke raznolikosti najbogatiji izvor prirodnih produkata koji nude strukturnu raznolikost i širok izbor kemijskih spojeva u razvoju novih lijekova (30). To potvrđuju i brojni lijekovi koji se danas koriste u terapijama raznih bolesti, a koji su izravno ili neizravno dobiveni iz biljaka. Neki od njih navedeni su u Tablici 2.

Tablica 2. Izabrani prirodni produkti i derivati prirodnih produkata izolirani iz biljaka i njihova terapijska primjena (32–65)

Ljekovita tvar	**Prirodni izvor**	**Terapijska primjena**
tiotropij (derivat atropina)	velebilje (*Atropa belladonna*, Solanaceae)	bronhodilatator u terapiji kronične opstrukcijske plućne bolesti
apomorfin (derivat morfina)	mak (*Papaver somniferum*, Papaveraceae)	liječenje Parkinsonove bolesti
nitizinon (derivat leptospermona)	četkovac (*Callistemon citrinus*, Myrtaceae)	liječenje odraslih i djece s potvrđenom dijagnozom nasljedne tirozinemije tipa 1
galantamin	visibaba (*Galanthus nivalis*, Amaryllidaceae)	liječenje Alzheimerove bolesti
paklitaksel	pacifička tisa (*Taxus brevifolia*, Taxaceae)	liječenje karcinoma pluća ne-malih stanica, jajnika, dojke i Kaposijevog sarkoma
topotekan (derivat kamptotecina)	*Camptotheca acuminata*, Nyssaceae	liječenje metastatskog karcinoma jajnika i karcinoma pluća malih stanica
irinotekan (derivat kamptotecina)	*Camptotheca acuminata*, Nyssaceae	liječenje karcinoma debelog crijeva i kolorektalnog karcinoma
etopozid (derivat podofilotoksina)	*Podophyllum peltatum*, Berberidaceae	liječenje karcinom testisa, jajnika, karcinoma pluća malih stanica, akutne mijeloične leukemije, non-Hodgkinovog i Hodgkinovog limfoma i gestacijske trofoblastične neoplazije
silimarin (mješavina flavonolignana)	sikavica (*Silybum marianum*, Gaertneri)	liječenje raznih bolesti jetre
dronabinol	konoplja (*Cannabis sativa*, Cannabaceae)	liječenje anoreksije osoba oboljelih od AIDS-a, ublažavanje kemoterapijom indiciranih mučnina i povraćanja
kanabidiol	konoplja (*Cannabis sativa*, Cannabaceae)	dodatna terapija za napadaje povezane s Lennox-Gastautovim i Dravetovim sindromom
kapsaicin	paprika (*Capsicum annuum*, Solanaceae)	liječenje periferne neuropatske boli
kodein	mak (*Papaver somniferum*, Papaveraceae)	liječenje akutne umjerene boli
kokain	koka (*Erythroxylum coca*, Erythroxylaceae)	lokalna anestezija
digoksin	vunasti naprstak (*Digitalis lanata*, Scrophulariaceae)	liječenje kroničnog srčanog zatajivanja
pilokarpin	*Pilocarpus microphyllus*, Rutaceae	snižavanje visokog očnog tlaka
kolhicin	jesenski mrazovac (*Colchicum autumnale*, Colchicaceae)	liječenje akutnog gihta, liječenje upalnih simptoma obiteljske mediteranske groznice
natrijev kromoglikat	kela (*Ammi visnaga*, Apiaceae)	ublažavanje i liječenje alergijskog konjunktivitisa

Strukture odabranih prirodnih produkata (paklitaksel, kamptotecin, kolhicin, kapsaicin, dronabinol, kanabidiol, galantamin) i derivata prirodnih produkata (nitizinon, apomorfin, tiotropij) izoliranih iz biljaka koji se koriste kao lijekovi prikazane su na Slici 4.

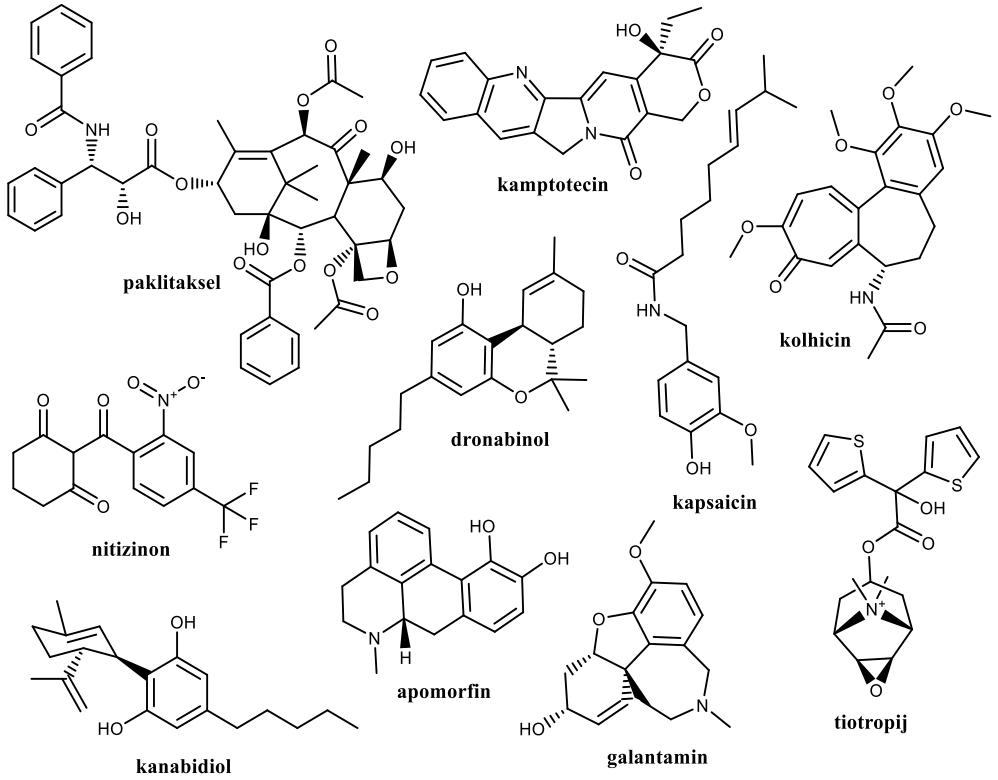

Slika 4. Strukture prirodnih produkata i njihovih derivata koji se koriste kao lijekovi (66–68)

Prirodni produkti su imali veliku ulogu u terapiji malarije. Kinin je antimalarik koji je zajedno s drugim alkaloidima 1820. godine izoliran iz kore kininovca (*Cinchona officinalis*, Rubiaceae), čiji se prah još u 17. stoljeću koristio kao antipiretik. Od svoga otkrića pa sve do sredine 20. stoljeća bio je jedini dostupni antimalarik, a njegova je struktura poslužila je kao spoj uzor za sintezu učinkovitijih antimalarika, derivata kinolina, kao što su klorokin, primakin i drugi (Slika 5) (69).

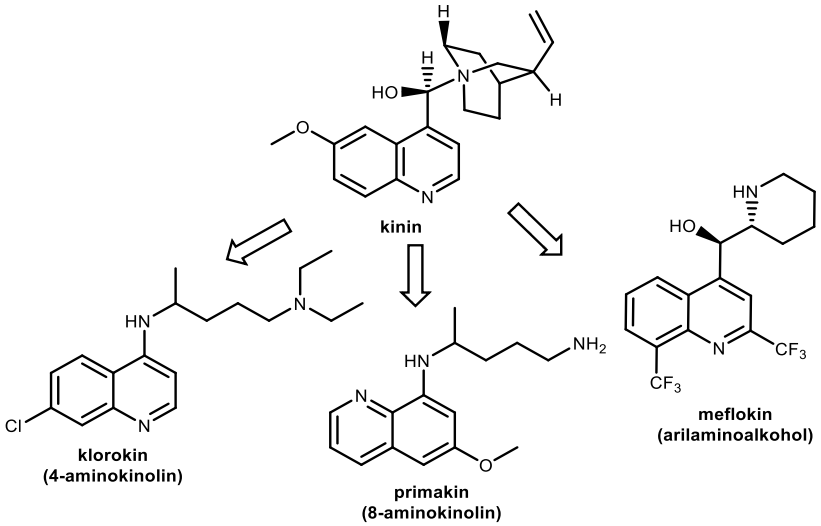

Slika 5. Strukture kinina, klorokina, primakina i meflokina (7)

Veliko otkriće u terapiji malarije dogodilo se 1972. godine kada je tim kineskih znanstvenika predvođen Tu Youyou izolirao artemizinin iz slatkog pelina (*Artemisia annua,* Asteraceae). Ubrzo nakon identifikacije i karakterizacije sintetizirani su i njegovi strukturni analozi artemeter, artezunat i dihidroartemizinin. Koliko je ovo otkriće važno svjedoči i činjenica da je profesorica Tu za njegovo otkriće dobila 2015. godine Nobelovu nagradu za fiziologiju i medicinu (70). Strukture artemizinina i njegovih strukturnih analoga dihidroartemizinina, artezunata i artemetera prikazane su na Slici 6.

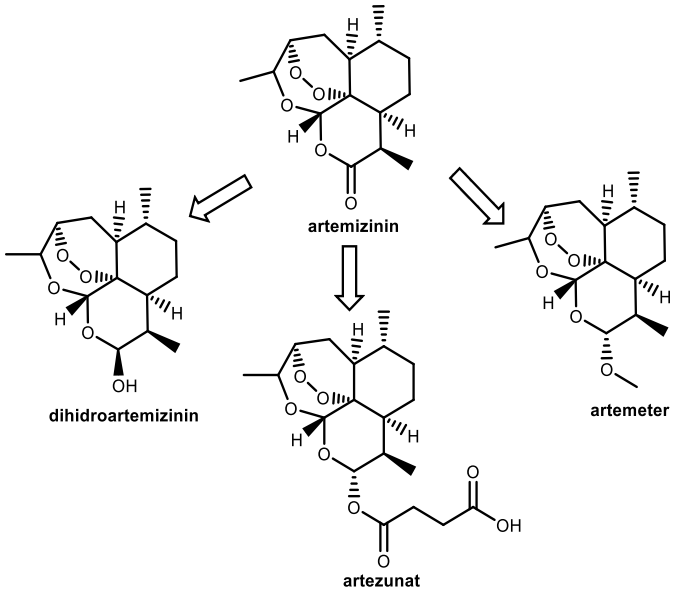

Slika 6. Strukture artemizinina i njegovih strukturnih analoga dihidroartemizinina, artezunata i artemetera (70)

Atovakvon ubrajamo u skupinu naftokinona, a razvijen je iz prirodnog produkta lapahola izoliranog iz *Tabebuia avellanedae*, Bignoniaceae 1882. godine (Slika 7). Lapahol je također naftokinon, a posjeduje slabo antimalarijsko djelovanje (71).

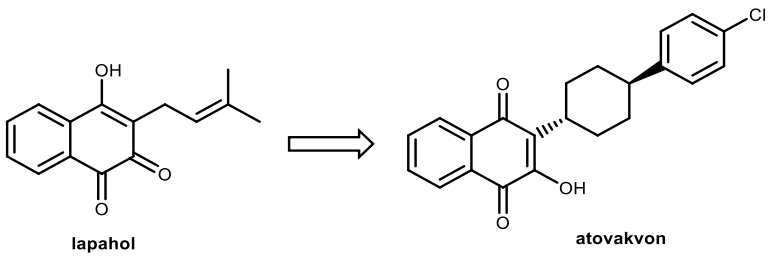

Slika 7. Strukture lapahola i naftokinona

U terapiji malarije danas se koriste i razni antibiotici, koji su također dobiveni iz prirodnih produkata. Tetraciklin i doksiciklin su polusintetski derivati klortetraciklina, izoliranog 1945. godine iz bakterije *Streptomyces aureofaciens*, azitromicin ubrajamo u skupinu makrolida, a dobiven je iz eritromicina A, koji je izoliran 1952. godine iz *Streptomyces erythreus* (72, 73). Konačno, klindamicin je polusintetski antibiotik, pripravljen iz linkomicina, izoliranog iz *Streptomyces lincolnensis* (74).

Unatoč brojnim prednostima i uspješnim primjerima upotrebe prirodnih produkata, sintetski lijekovi i dalje čine glavninu novoodobrenih lijekova, iz nekoliko razloga. Primjerice, identifikacija biološki aktivnih prirodnih produkata od interesa može biti vrlo izazovna i zahtjevna, a pristup dovoljnim količinama biološkog materijala za izolaciju i karakterizaciju biološki aktivnog prirodnog produkta također može biti jedan od ograničavajućih faktora. Osim toga, brojni se prirodni produkti ne mogu sintetizirati zbog njihove strukturne složenosti, a sinteza strukturnih analoga za istraživanje odnosa strukture i djelovanja u optimizaciji vodećeg prirodnog produkta može biti zahtjevna, dugotrajna ili financijski neisplativa. Međutim, prirodni produkti i dalje ostaju predmet istraživanja farmaceutske industrije, posebice u razvoju lijekova za rak ili infektivne bolesti, gdje njihova strukturna raznolikost daje nadu za razvoj novih inovativnih lijekova (34, 35).

1.3.1. β-Karbolini

β-Karbolini pripadaju velikoj skupini indolskih alkaloida. Široko su rasprostranjeni u biljnom svijetu, a nalaze se još i u tkivu sisavaca, morskim organizmima, kukcima, mikroorganizmima, prehrambenim proizvodima i duhanskom dimu (75–77). U svojoj strukturi sadrže triciklički *9H*-pirido[3,4-*b*]indolni prsten, a slovo β označava položaj dušikovog atoma u piridinskom prstenu, stoga su osim β-karbolina poznati još i α-, γ- i δ-karbolini (78). Prema stupnju zasićenosti piridinskog prstena mogu se podijeliti na: 1) potpuno nezasićene β-karboline, 2) djelomično zasićene 3,4-dihidro-β-karboline i 3) potpuno zasićene odnosno 1,2,3,4-tetrahidro-β-karboline (THβC) (Slika 8) (79). Piridinski dušik bazičnijeg je karaktera u odnosu na indolni dušikov atom, a ovisno o pH i otapalu, β-karbolini mogu postojati u četiri oblika: kation, neutralni oblik, zwitterion i anion (76, 80).

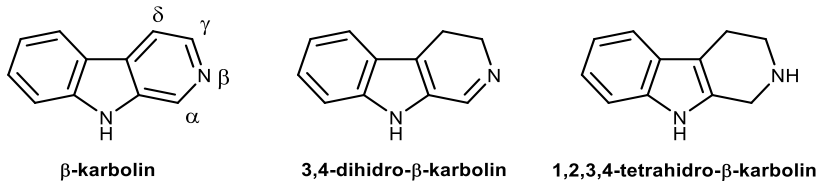

Slika 8. Strukture β-karbolina, 3,4-dihidro-β-karbolina i 1,2,3,4-tetrahidro-β-karbolina (79)

Harmalin je prvi β-karbolin, izoliran 1841. godine iz sjemenki sirijske rutvice (*Peganum harmala*, Nitrariaceae) (81). Od tada pa sve do danas, iz prirodnih izvora izolirano je više od 500 β-karbolina i to najviše iz biljaka, iz porodica: Rubiaceae, Nitrariaceae Malpighiaceae, Passifloraceae, Rutaceae, Simaroubaceae, Amaranthaceae i Caryophyllaceae (76, 77). Također su izolirani iz različitih morskih beskralješnjaka poput hidrozoida (*Aglaophenia*), mahovnjaka (*Cribricellina, Catenicella*), mekih koralja (*Lignopsis*), plaštenjaka (*Eudistoma*, *Didemnum*, *Lissoclinum, Ritterella, Pseudodistoma*) i raznih spužvi. Među plaštenjacima se posebno ističe rod *Eudistoma* kao bogat izvor biološki aktivnih β-karbolina. Identificirano je više od 100 alkaloida koji su poznati po zajedničkom nazivu eudistomini, a većina ih je pokazala izvrsno antimikrobno, protutumorsko i/ili antivirusno djelovanje (76, 80). Druga velika skupina strukturno kompleksnih, prirodnih β-karbolina su manzamini. Prvi predstavnik iz ove skupine je manzamin A, a izvorno je izoliran iz spužve roda *Haliclona* pronađene uz obalu Okinawe (76). Manzamin, uz iznimku skupine manzamina C, karakterizira spojeni i premošteni kondenzirani tetra- ili pentaciklički prstenasti sustav vezan na položaj C-1 β-karbolinskog prstena (82, 83). Do danas je izolirano više od 80 manzaminskih alkaloida iz različitih vrsta morskih spužvi (*Acanthostrongylophora ingens, Amphimedon* sp., *Acanthostrongylophora* sp.),

a brojni se odlikuju snažnim antiparazitskim, protutumorskim ili antimikrobnim djelovanjem. Nadalje, u prirodi su pronađene i N-metilne kvaterne soli β-karbolina. Jedan od takvih spojeva je nostokarbolin izoliran iz cijanobakterije *Nostoc* 78-12A, a pokazuje značajno antimalarijsko djelovanje (76). β-Karbolini su pronađeni i u određenim vrstama škorpiona. Stachel i suradnici izolirali su i detektirali β-karboline norharman i 3-karboksilnu kiselinu norharmana iz kutikule škorpiona vrste *Centruroides vittatus* i *Pandinus imperator,* a upravo su ovi spojevi odgovorni za njihova fluorescentna svojstva (84).

Prisutnost određenih β-karbolina dokazana je i u prehrambenim proizvodima pa se tako harman i norharman, u određenim količinama, mogu naći u kukuruzu, ječmu, soji, kavi i nadomjescima za kavu (kava od cikorije), u alkoholnim pićima kao što su pivo, vino, viski, sake i votka, kao i u mesu, ribi, povrću i voću (85, 86). Prisutnost β-karbolina u prehrambenim namirnicama ukazuje na činjenicu da je upravo prehrana važan egzogeni izvor ovih spojeva u sisavaca i ljudi. Međutim, istraživanja su pokazala kako se neki od strukturno jednostavnijih β-karbolina, poput harmina, harmana, harmalina, norharmana i određenih THβC endogeno sintetiziraju kondenzacijom indoloamina kao što su triptofan i triptamin i aldehida ili piruvata, a pronađeni su u plazmi, trombocitima i urinu te jetri i mozgu ljudi i drugih sisavaca (80).

Brojni su literaturni podaci koji izvještavaju kako se β-karbolini, osim izolacijom iz izuzetno bogatih prirodnih izvora, mogu dobiti sintetskim putem. Najpopularniji način sinteze β-karbolina uključuje Pictet-Spenglerovu reakciju u kojoj kondenzacijom β-ariletilamina i aldehida u prisutnosti kiselog katalizatora dolazi do zatvaranja prstena (87). Mehanizam Pictet-Spenglerove reakcije prikazan je na Slici 9.

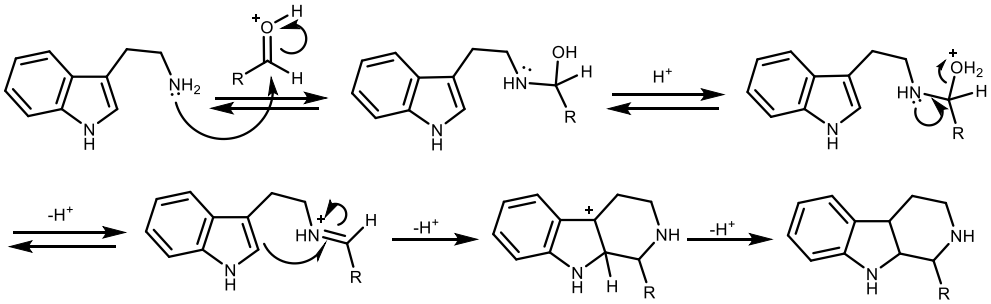

Slika 9. Mehanizam Pictet-Spenglerove kondenzacije (87)

Pictet-Spenglerova kondenzacija je otkrivena 1911. godine kada su Amé Pictet i Theodor Spengler kondenzacijom 2-feniletanamina i dimetoksimetana, koristeći HCl kao kiseli katalizator, sintetizirali tetrahidroizokinolin (Slika 10a). Opseg Pictet-Spenglerove kondenzcije proširio se 1928. godine kada je Tatsui reakcijom triptamina i aldehida u prisutnosti sumporne

kiseline sintetizirao 1-metil-1,2,3,4-tetrahidro-β-karbolin (Slika 10b), čime se otvorila mogućnost sinteze raznih supstituiranih i kondenziranih THβC (88–90).

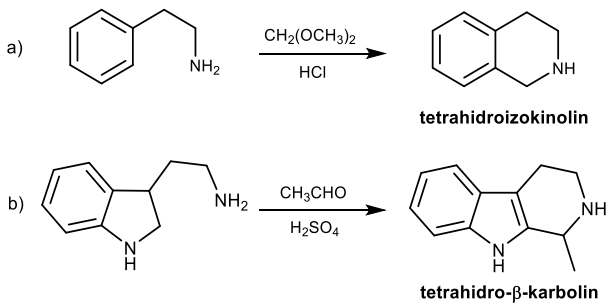

Slika 10. Sinteza: a) tetrahidroizokinolina i b) tetrahidro-β-karbolina Pictet-Spenglerovom kondenzacijom (90)

Daljnja istraživanja su pokazala kako se Pictet-Spenglerova kondenzacija može provesti i u aprotonskim otapalima, a često i bez prisutnosti kiselog katalizatora, dajući vrlo visoke prinose (88, 80). U reakcijama se umjesto aldehida mogu koristiti i zaštićeni aldehidi, ketoni, α-aminonitrili, α-halo-α-feniltio derivati i brojni drugi (91). Nadalje, ispitivana je i stereoselektivna sinteza THβC te su brojne studije pokazale kako se kontroliranim reakcijskim uvjetima i odabirom odgovarajućih reagenasa može postići stereoselektivnost (90, 92). Budući da se Pictet-Spenglerovom kondenzacijom dobivaju THβC, za pripravu aromatskih β-karbolina potrebno je provesti korak oksidacije. Najčešće upotrebljavani reagens za oksidaciju je paladij na ugljenu, a još se upotrebljava elementarni sumpor, kalijev permanganat, 2,3-dikloro-5,6-dicijano-1,4-benzokinon (DDQ), a nešto rjeđe selenov dioksid (88). Iako je razvijen čitav niz sintetskih metoda za dobivanje β-karbolina, Pictet-Spenglerova kondenzacija je od svoga otkrića pa sve do danas ostala vodeća metoda u sintezi izokinolinskih i indolnih alkaloida.

Zbog raznolikosti bioloških aktivnosti β-karbolini su privukli veliku pažnju znanstvenika. Danas su poznati brojni prirodni i sintetski spojevi koji u svojoj strukturi sadrže β-karbolin, a ispoljavaju široki raspon bioloških djelovanja kao što su protutumorsko, antitrombotsko, antimikrobno, antiparazitsko, antituberkulotsko, antivirusno, sedativno. Također je dokazano kako se interkaliraju u DNA, te su inhibitori brojnih enzima, poput kinaza ovisnih o ciklinima (CDK), topoizomeraze I i II, monoaminooksidaze, te fosfodiesteraze tipa 5. Neki od njih stupaju u interakciju s benzodiazepinskim receptorima, imidazolinskim I_2 i serotoninskim 5-HT_1 i 5-HT_2 receptorima (76, 77, 79, 80). Osim toga, svojstva fotoluminiscencije β-karbolina proširila su potencijalnu primjenu ovih spojeva kao fotosenzibilizatora u fotodinamičkoj terapiji (93).

Mnogi su biološki aktivni β-karbolini poslužili kao spojevi uzori za razvoj novih lijekova pa se tako na tržištu nalazi: tadalafil, rezerpin, dezerpidin, rescinamin, (antihipertenzivi), zatim ajmalin (antiaritmik) lurbinektedin (citostatik indiciran za liječenje odraslih osoba s metastatskim karcinomom pluća malih stanica) (79, 89, 94–98). Strukture navedenih lijekova prikazane su na Slici 11.

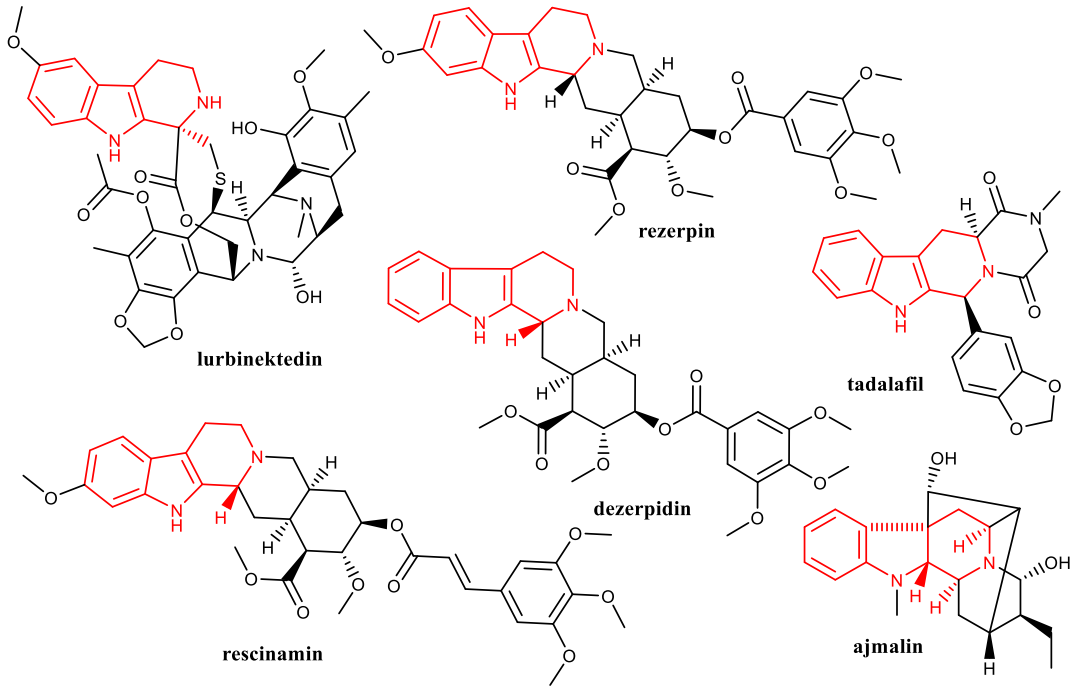

Slika 11. Strukture lijekova u kojima se nalazi strukturni motiv THβC-a (94–98)

Također, brojni se prirodni i sintetski β-karbolini odlikuju visokom antimalarijskom aktivnošću, a među njima se posebno ističe cipargamin koji se trenutno nalazi u fazi II kliničkih ispitivanja za liječenje *P. falciparum* malarije (14, 99). Strukture odabranih prirodnih (manzamin A, dihidrouzambarenzin, bisnikalaterin C, homofascaplizin A, nostokarbolin, tubulozin, harmin) i sintetskih β-karbolina s pripadajućim *in vitro* antimalarijskim djelovanjima na *P. falciparum* (sojevi W2, K1, NF54 i 3D7) prikazani su na Slici 12.

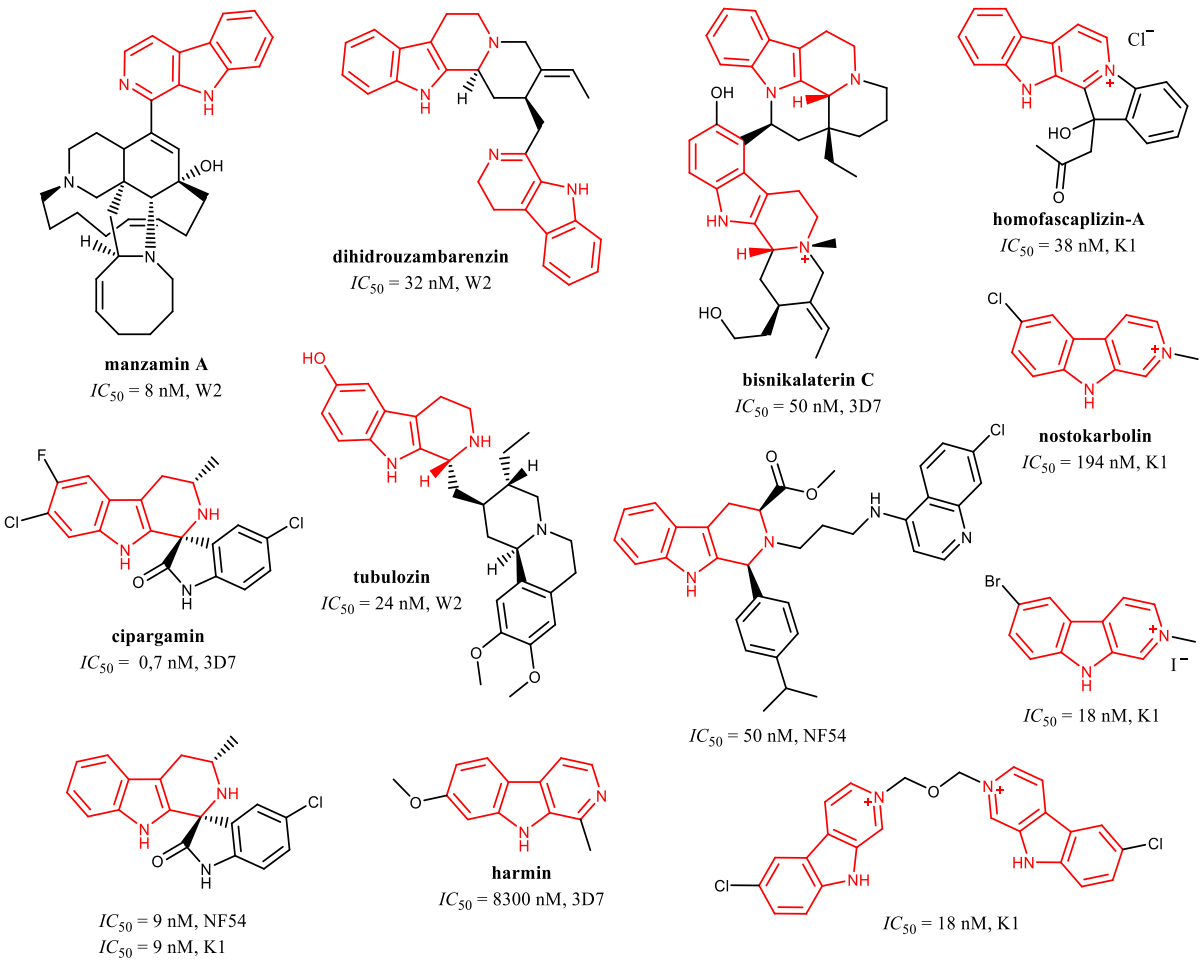

Slika 12. Strukture prirodnih i sintetskih β-karbolina s pripadajućim *in vitro* antimalarijskim djelovanjima (75, 77, 79)

1.3.1.1. Harmin

Harmin, odn. 7-metoksi-1-metil-9*H*-pirido[3,4-*b*]indol (Slika 13) je prirodni spoj molekulske formule $C_{13}H_{12}N_2O$ i relativne molekulske mase 212,25. Poznat je još pod nazivima telepatin, banisterin, leukoharmin. Na sobnoj temperaturi je krutina blijedo-žute boje s temperaturom tališta 264 – 265 °C, a topljivost u vodi mu je izuzetno niska. Na tržištu je dostupan u slobodnom obliku i kao hidrokloridna sol (100).

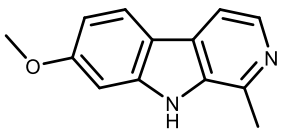

Slika 13. Struktura harmina (100)

Zbog prisutnosti indolnog i piridinskog prstena u svojoj strukturi harmin se odlikuje bazičnim svojstvima, a procijenjene pK_a vrijednosti iznose: pK_a = 6,15 (piridinski amin) i pK_a = 13,54 (indolni amin) (Slika 14) (101).

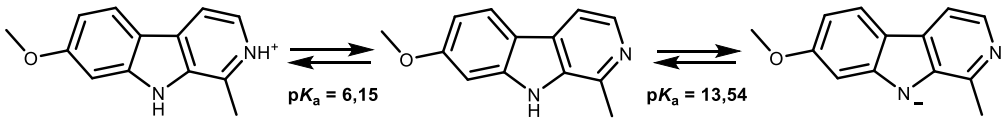

Slika 14. Konstante disocijacije harmina prema *chemicalize.com* (101)

Harmin pripada skupini harmala alkaloida, odn. β-karbolina, a izvorno je izoliran iz sjemenki sirijske rutvice (*Peganum harmala*, Nitrariaceae) 1847. godine (102). Sirijska rutvica (Slika 15) je biljka koja raste u sušnim područjima, a najrasprostranjenija je na Bliskom Istoku, u sjevernoj Africi i srednjoj Aziji (103).

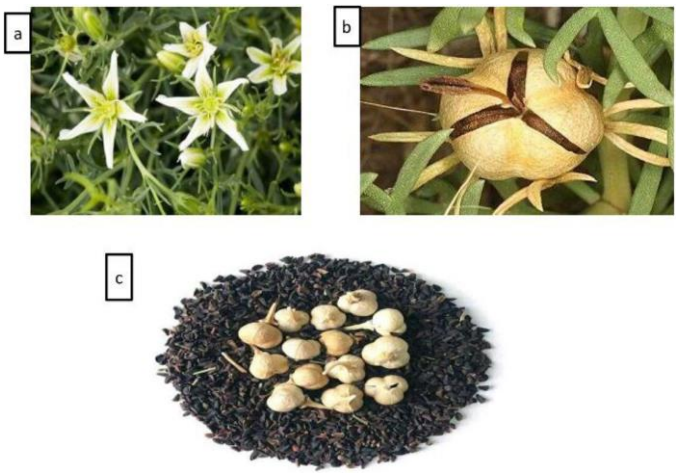

Slika 15. *Peganum harmala*: a) listovi i cvijet, b) plod, c) sjemenke (102)

Ekstrakti korijena i sjemena biljke *Peganum harmala* koristili su se dugi niz godina u tradicionalnoj medicini u Kini i na Bliskom Istoku za liječenje raka, malarije, upalnih procesa i raznih infekcija. Naknadom izolacijom i identifikacijom spojeva otkriveno je da su upravo harmala alkaloidi najodgovorniji za biološke učinke ovih ekstrakata, a najzastupljeniji harmala alkloidi u korijenu i sjemenu sirijske rutvice su harmin, harmalin, harmalol, tetrahidroharmin i hraman (Slika 16) (102–105).

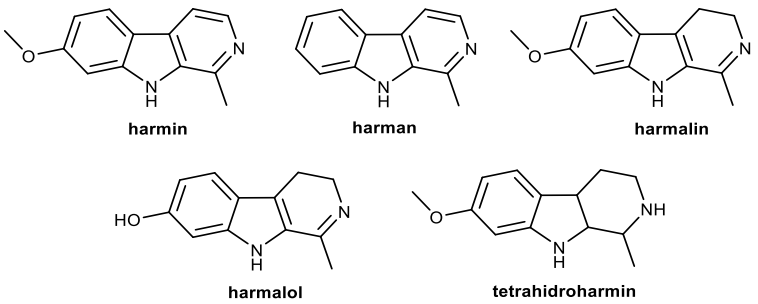

Slika 16. Strukture harmala alkaloida (harmina, harmana, harmalina, harmalola i tetrahidroharmina) (102, 103)

Osim sirijske rutvice, u kojoj je i najzastupljeniji među harmala alkaloidima, harmin se može naći u drugim biljnim vrstama, poput dušne loze (*Banisteriopsis caapi*, Malpighiaceae), u korijenu i lišću kineskog androfagisa (*Andrographis paniculata,* Acanthaceae), sjemenkama ljetnog čempresa (*Kochia scoparia,* Amaranthaceae), korijenu cecelja (*Oxalis tuberosa,* Oxalidaceae) i u ljubičastoj pasiflori (*Passiflora incarnata,* Passifloraceae) (106). Harmin se također može dobiti i sintetskim putem. Do danas je razvijeno nekoliko metoda, a najčešće su Bischler–Napieralski i Pictet-Spenglerova kondenzacija iz 6-metoksitriptamina (78).

1.3.1.1.1. Mehanizam antimalarijskog djelovanja harmina

Shahinas i suradnici ispitivali su afinitet vezanja harmina za protein toplinskog šoka 90 plazmodija (*Pf*Hsp90) kao potencijalan mehanizam antimalarijskog djelovanja harmina. Proteini toplinskog šoka (engl. *Heat shock proteins*, Hsp) su velika skupina evolucijski očuvanih molekularnih šaperona koji imaju ključnu ulogu u preživljavanju i razvoju stanica. Iako su otkriveni pri izlaganju stanica toplinskom stresu, povećana ekspresija ovih proteina javlja se i pri drugim vrstama stresa (hipoksija, ishemija, nedostatak hranjivih tvari, prisutnost teških metala, oksidativni stres, oštećenja izazvana UV-zračenjem, ozljede tkiva, upale i dr.). Imaju zaštitnu ulogu unutarstaničnih proteina od pogrešnog smatanja ili agregacije, zatim u popravku denaturiranih proteina, inhibiranju signalnih kaskada koje dovode do stanične smrti, te očuvanju unutarstaničnih signalnih puteva koji su bitni za preživljavanje stanica. Hsp proteini su podijeljeni obzirom na molekulsku masu koja je u rasponu od 8-150 kDa, a jedna od važnijih i proučavanijih obitelji šaperona je Hsp90 (90kDa). Domena na N-kraju Hsp90 sadrži visoko afinitetno vezno mjesto za adenozin-trifosfat (ATP), koje je bitno za ATP-azno djelovanje Hsp-a (107–109).

*Pf*Hsp90 je šaperon neophodan za razvoj parazita tijekom eritrocitne faze životnog ciklusa. Njegovom inhibicijom sprječava se razvoj parazita iz prstenastog stadija u stadij toforzoita (110). Ispitivanja koja su proveli Shahinas i suradnici dokazala su da harmin, vežući se na vezno mjesto za ATP, selektivno inhibira *Pf*Hsp90 u odnosu na humani Hsp90. Vezanjem harmina za N-kraj ATP-azne domene, inhibira se učinak *Pf*Hsp90, što može imati višestruke koristi. Primjerice, kombinacija harmina i postojećih antimalarika ili spojeva s antimalarijskim djelovanjem mogla bi dovesti do sinergističkog učinka. Štoviše, time bi se mogao spriječiti razvoj rezistencije te povratiti učinkovitost postojećih antimalarika (111).

1.3.1.1.2. Biološka djelovanja harmina

Brojni su literaturni pregledi koji, osim antimalarijskog, izvještavaju o širokom rasponu bioloških djelovanja harmina, a opisano je njegovo antimikrobno, antioksidativno, antiparazitsko, antitumorsko, osteoprotektivno, halucinogeno, antidepresivno, anksiolitičko, antivirusno, protuupalno, antidijabetičko i neuroprotektivno djelovanje (106).

Harmin je najviše istraživan zbog protutumorskog učinka kojeg ostvaruje različitim mehanizmima: interakcijom s DNA (interkalacijom i vezanjem u velike i male utore DNA), oštećenjem DNA, ometanjem replikacije i sinteze DNA te inhibicijom topoizomeraze, inhibicijom CDK-a, inhibicijom tirozin-fosforilirane i regulirane kinaze dvostruke specifičnosti (DYRK) i haspin kinaza, djelovanjem na vaskularni endotelni faktor rasta (VEGF), koji potencira procese tumorske angiogeneze (104, 106).

Istraživanja su pokazala da harmin izaziva apoptozu i inhibira proliferaciju i migraciju stanica humanog adenokarcinoma želuca (BGC-823, SGC-7901, MGC-803). Budući da enzim ciklooksigenaza-2 (COX-2) ima važnu ulogu u karcinogenezi i progresiji raka želuca provedena su istraživanja te je dokazano da harmin značajno smanjuje ekspresiju COX-2 u BGC-823 i SGC-7901 staničnim linijama. Harmin je izazvao zastoj staničnog ciklusa MGC-803 i SMMC-7721 stanica u G2 fazi aktivacijom p21 i Myt1 i deaktivacijom Cdc2. Osim toga, kombinacija harmina i paklitaksela pokazala je sinergistički učinak na inhibiciju proliferacije i na izazivanje apoptoze u SGC-7901 i MKN-45 staničnim linijama (104, 106).

Zatim je dokazano da harmin inhibicijom DYRK1A smanjuje ekspresiju Mcl-1 i čini stanice karcinoma pluća ne-malih stanica (NSCLC) osjetljivima na BCL-2 inhibitore. Štoviše, inhibicija DYRK1A smanjila je razine receptora epidermalnog faktora rasta (EGFR) u NSCLC stanicama. Harmin zaustavlja proliferaciju stanica adenokarcinoma dojke (MCF-7) inhibiranjem aktivnosti telomeraze preko p53/p21 ovisnog mehanizma (104).

Brojna istraživanja dokazala su da harmin inhibira proliferaciju stanica humanog hepatocelularnog karcinoma (Huh-7, SMMC-7721, HepG2, Bel-7402) i adenokarcinoma debelog crijeva (SW480, SW620). Nadalje, dokazano je da harmin inhibira proliferaciju, invaziju i migraciju tumorskih stanica melanoma (B16F-10) karcinoma mokraćnog mjehura (RT112, RT4, SW780, BIU87, 5637), karcinoma jajnika (SKOV-3), adenokarcinoma štitnjače (TPC-1), adenokarcinoma gušterače (PANC-1, CFPAC-1, SW-1990, BxPC-3), akutne leukemije (NB4, HL60), glioblastoma (C6, U87 i U373) i neuroblastoma (N206, CRL-213) (103, 104, 106).

Antidepresivni učinak harmina očituje se u njegovoj sposobnosti inhibicije monoaminooksidaze-A (MAO-A) čime smanjuje razgradnju neurotransmitera. Dokazano je da stupa u interakciju sa serotoninskim 5-HT2A receptorima te potiče adultnu neurogenezu i stimulira rast, migraciju i diferencijaciju neuralnih matičnih stanica *in vitro*. Istraživanja su pokazala da harmin povećava razinu moždano-neurotrofnog faktora (BDNF) u hipokampusu štakora, a sve ovo dodatno doprinosi njegovom antidepresivnom učinku (103, 104, 106).

Neuroprotektivni učinci harmina očituju se u smanjenju oksidativnog stresa i upalnih procesa. Istraživanja su pokazala da primjena harmina u visokim dozama (5, 10, 15 mg/kg) dovodi do povećanja razine antioksidativnih enzima superoksid dismutaze (SOD) i katalaze (CAT) u hipokampusu i prefrontalnom korteksu štakora. Harmin značajno smanjuje razinu interleukina-1 beta i faktora nekroze tumora-α (TNF-α), čime slabi apoptotična smrt neurona u hipokampusu. *In vivo* istraživanja su pokazala da harmin smanjuje smrt neurona zbog aktivacije glutamatnih transportera (GLT-1) koji smanjuju prekomjerne i neurotoksične razine glutamata. Također je otkriveno da je harmin snažni inhibitor tau fosforilacije i selektivni inhibitor protein kinaze DYRK1A, enzima koji je prekomjerno eksprimiran u brojnim bolestima i za koji se pretpostavlja da doprinosi ranom razvoju Alzheimerove bolesti u osoba s Downovim sindromom. Također je dokazano da harmin inhibira $CuSO_4$-potaknutu oksidaciju LDL-a (lipoprotein male gustoće, engl. *low-density lipoprotein*) i stvaranje slobodnih radikala. Brojna su istraživanja pokazala da u ovisnosti o koncentraciji sprječava lipidnu peroksidaciju prilikom enzimatskih i neenzimatskih stvaranja kisikovih radikala (103, 104, 106).

Također je dokazano da harmin inhibira enzim acetilkolinesterazu te potiče aktivnost kolin-acetiltransferaze. Na ovaj način bi harmin mogao ublažiti simptome oštećenja pamćenja u pacijenata s Alzheimerovom bolesti. Budući da mu lipofilni karakter omogućava prolazak krvno-moždane barijere pretpostavka je da se vodikovim vezama i π–π interakcijama veže za aktivne ostatke aminokiselina kolin-acetiltransferaze i tako potiče aktivnost enzima (104, 106).

Nedostatak zrelih β-stanica koje izlučuju inzulin jedan je od glavnih uzroka dijabetesa. Budući da inhibitori DYRK1A potiču proliferaciju β-stanica i poboljšavaju metabolizam glukoze, harmin kao učinkovit inhibitor DYRK1A enzima pokazuje veliki antidijabetički potencijal. Nadalje, istraživanja su pokazala da harmin regulira ekspresiju PPARγ (γ receptor aktiviran proliferatorom peroksizoma) preko Wnt signalnog puta čime se dodatno očituje njegov antidijabetički učinak (104).

Nadalje, istraživanja su dokazala da harmin, ovisno o koncentraciji, smanjuje razine interleukina-6, interleukina-1 beta i TNF-α u lipopolisaharidom (LPS)-induciranim RAW 264,7 mišjim makrofagima i THP-1 stanicama čime ostvaruje protuupalno djelovanje (103, 104, 106).

Harmin se također odlikuje i antimikrobnim svojstvima te je dokazan njegov učinak protiv raznih vrsta gljivica, kao što su *Fusarium oxysporum, Colletotrichum gloeosporioides* i *Physalospora piricola*. Nadalje, harmin pokazuje antivirusno djelovanje protiv virusa mozaika duhana, kao i antifungicidno djelovanje protiv *Puccinia sorghi*. Utvrđeno je da, ovisno o koncentraciji, sprječava infekcije virusom Herpes simplex. Daljnja istraživanja antivirusnog djelovanja harmina dokazala su da učinkovito smanjuje replikaciju enterovirusa (EV71) *in vitro* NF-κB signalnim putem, a nešto kasnije dokazani su i njegovi pozitivni učinci *in vivo* u miševima (104, 106).

Osteoprotektivno djelovanje harmina ostvaruje se u blokiranju resorpcije kostiju i RANKL-posredovane diferencijacije osteoklasta *in vitro* i *in vivo*. U mišjoj preosteoblastnoj staničnoj liniji (MC3T3-E1) potiče aktivnost alkalne fosfataze bez utjecaja na rast stanica (104, 106).

Harmin također djeluje kao fotosenzibilizator, a pokazao je i antiparazitsko djelovanje: *in vivo* i *in vitro* djelovanje protiv *Plasmodium falciparum, in vivo* antileišmanijsko djelovanje protiv *Leishmania infantum*, zatim djelovanje protiv parazita *Toxoplasma gondii* i *Trichomonas gallinae* (106).

Unatoč brojnim biološkim djelovanjima koje harmin posjeduje, niska bioraspoloživost i brojne nuspojave ograničavaju njegovu kliničku upotrebu. Stoga se danas brojnim kemijskim modifikacijama nastoji pojačati njegov učinak, poboljšati farmakokinetička svojstva te smanjiti neželjene nuspojave (104, 106).

1.3.1.1.3. Hibridni spojevi harmina s antimalarijskim djelovanjem

Istraživanja novih spojeva s potencijalnim antimalarijskim djelovanjem u Zavodu za farmaceutsku kemiju Farmaceutsko-biokemijskog fakulteta u posljednje četiri godine usmjerena su na derivatizaciju molekule harmina. Povezivanjem harmina s poznatim antimalaricima klorokinom, meflokinom i primakinom, te spojevima koji posjeduju antimalarijsko djelovanje kao što su cimetna kiselina i derivati cimetne kiseline (DCK-i), pripravljeno je niz hibridnih spojeva. Variranjem tipa i duljine poveznice kao i položaja derivatizacije u β-karbolinskom prstenu harmina nastoji se poboljšati djelovanje i postići selektivnost novih spojeva te dobiti uvid u odnos strukture i djelovanja.

Perković i suradnici su 2019. godine objavili rad u kojem su opisali sintezu hibridnih spojeva harmina i DCK-a (harmicini). Poveznica između dvije strukturne jedinice bio je 1*H*-1,2,3-triazol (Slika 17), a navedeni hibridi pripravljeni su bakrom (I) kataliziranom cikloadicijom azida i alkina, odnosno klik-kemijom u položajima N-9 i O-7 β-karbolina. Antiplazmodijsko djelovanje novosintetiziranih hibrida ispitano je *in vitro* te su gotovo svi pokazali jače djelovanje na eritrocitnu fazu *P. falciparum* u odnosu na početni spoj harmin. Ispitano je i antiplazmodijsko djelovanje odabranih hibrida na hepatocitnu fazu *P. berghei* te su svi pokazali jače djelovanje u odnosu na referentni lijek primakin. Među hibridima se posebno istaknuo *N*,*O*-bis-harmicin koji u *para* položaju benzenskog prstena cimetne kiseline sadrži metoksi skupinu. Ovaj spoj se, osim na eritrocitu fazu, pokazao najaktivnijim i na hepatocitnu fazu *P. berghei* s IC_{50} = 0,4 μM (75).

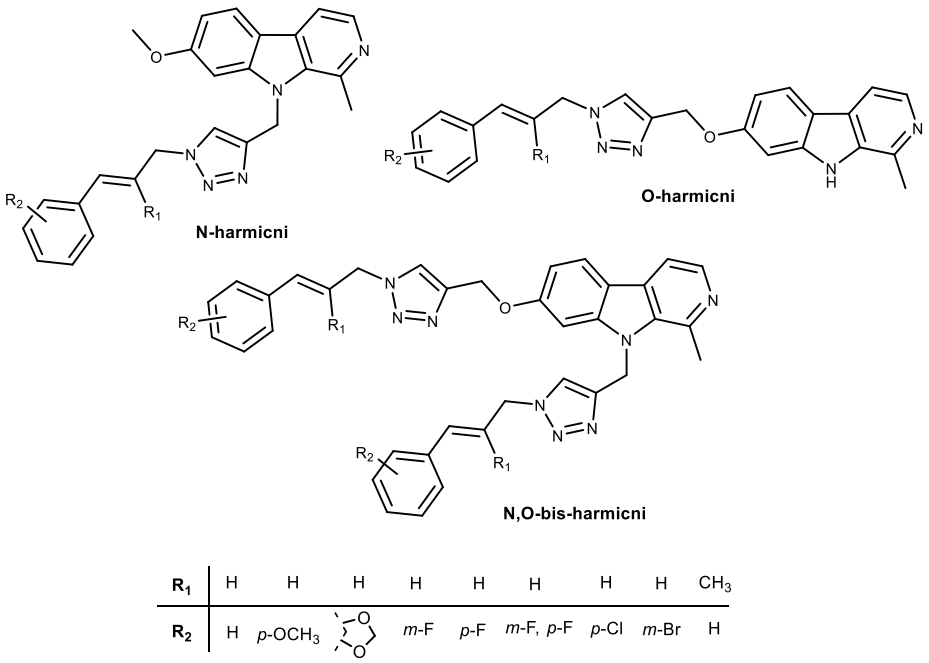

Slika 17. Strukture *N*-harmicina, *O*-harmicina, *N*,*O*-bis-harmicina

Poje i suradnici nastavili su istraživanje te su pripravili dodatne serije harmicina triazolskog tipa (TT), u položajima C-1, C-3, O-6 i N-9 (Slika 18). U odnosu na harmicine u položajima O-6 i N-9 harmicini TT u položajima C-1 i C-3 sadržavali su uz 1*H*-1,2,3-triazol dodatnu estersku skupinu u svojoj strukturi. Nadalje, harmicini TT u položaju N-9 sadržavali su hidroksilnu skupinu u položaju C-3 β-karbolina. Svim je harmicinima TT ispitano antimalarijsko djelovanje na eritrocitnu fazu *P. falciparum*, na dva soja (*Pf*3D7 i *Pf*Dd2) i hepatocitnu fazu *P. berghei*. Rezultati ispitivanja pokazali su da su najdjelotvorniji na eritrocitnu fazu bili O-6-supstituirani harmicini, a pokazali su aktivnost u mikromolarnim i submikromolarnim koncentracijama (IC_{50} (*Pf*3D7) = 0,26 – 0,61 μM; IC_{50} (*Pf*Dd2) = 0,73 – 2,28 μM). Najaktivniji među svim spojevima bio je *m*-Br-supstituirani harmicin koji je pokazao gotovo 32 puta jače djelovanje na *Pf*3D7 soj u odnosu na harmin. Harmicini u položaju N-9, izuzev harmicina u kojemu je R = *m*-Br, bili su manje djelotvorni u odnosu na harmin (112). Također, uspoređujući djelovanja prethodno sintetiziranih strukturnih analoga od strane Perković i suradnika (75) vidljivo je da uvođenje hidroksilne skupine u položaj 3 β-karbolina dovodi do smanjenja aktivnosti. Nadalje, harmicini u položajima C-1 i C-3, izuzev *m*-Br-supstituiranog harmicina u položaju 3, bili su inaktivni pri najvišim ispitivanim koncentracijama. Harmicini TT nisu pokazali značajnu aktivnost na hepatocitnu fazu, a djelovanja su pratila slijed N-9 ~ O-6 > C-3 > C-1 (112).

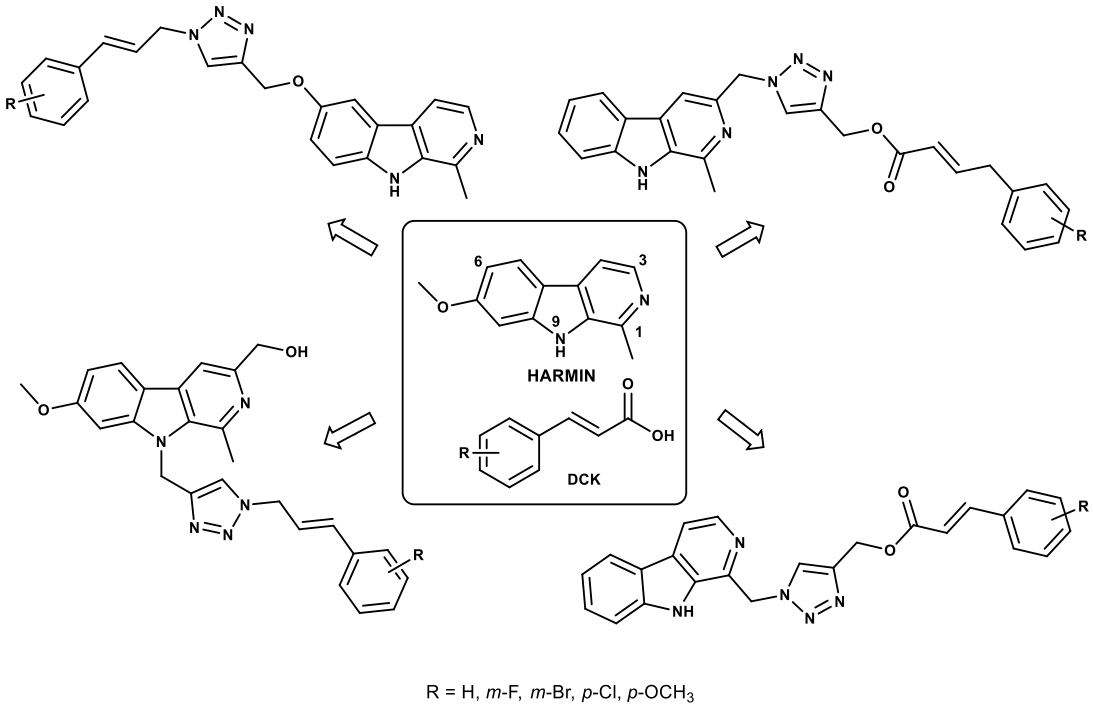

Slika 18. Strukture harmicina TT

Nova serija hibridnih spojeva harmina sintetizirana je od strane iste istraživačke skupine. Ukupno 18 harmicena - hibridih spojeva harmina i ferocena pripravljeno je povezivanjem strukturnih jedinica amidnom ili triazolnom poveznicom (AT i TT harmicini), a pripravljeni su u pet položaja β-karbolina (1, 3, 6, 7, i 9). Također je, osim vrste poveznice i položaja supstitucije, varirana i duljina poveznice te se tako, među navedenim hibridima, razlikuju oni u kojima je ferocen izravno vezan za amid/triazol i oni u kojima je ferocen preko metilenskog mosta vezan za amid/triazol. Harmicenima je ispitano antimalarijsko djelovanje *in vitro* na eritrocitnu fazu *P. falciparum*, na soj osjetljiv na klorokin (*Pf*3D7) i soj otporan na klorokin (*Pf*Dd2) te su gotovo svi pokazali jače antimalarijsko djelovanje na *Pf*3D7 soj, u mikromolarnim i submikromolarnim koncentracijama. Ukupno 7/18 harmicena ostvarilo je za jedan red veličine jače djelovanje u odnosu na harmin, dok su se dva harmicena pokazala inaktivnima. Među TT harmicenima jače djelovanje ostvarili su O-6- i O-7-supstituirani harmiceni dok su među AT harmicenima najjača djelovanja ostvarili O-7- i N-9-supstituirani harmiceni. Također je uočeno da duljina poveznice utječe na aktivnost, te je tako TT harmicen u položaju O-7 β-karbolina u kojemu je ferocen izravno vezan za triazol ostvario najjače djelovanje (IC_{50} (*Pf*3D7) = 0,15 ± 0,05 μM; IC_{50} (*Pf*Dd2) = 1,02 ± 0,52 μM), dok je njegov strukturni analog u kojemu je ferocen preko metilenskog mosta vezan za triazol bio inaktivan pri najvišim ispitivanim koncentracijama. Analogno TT harmicenima, među AT harmicenima aktivniji su bili oni u kojima je ferocen izravno vezan za amid (113). Strukture harmicena prikazane su na Slici 19.

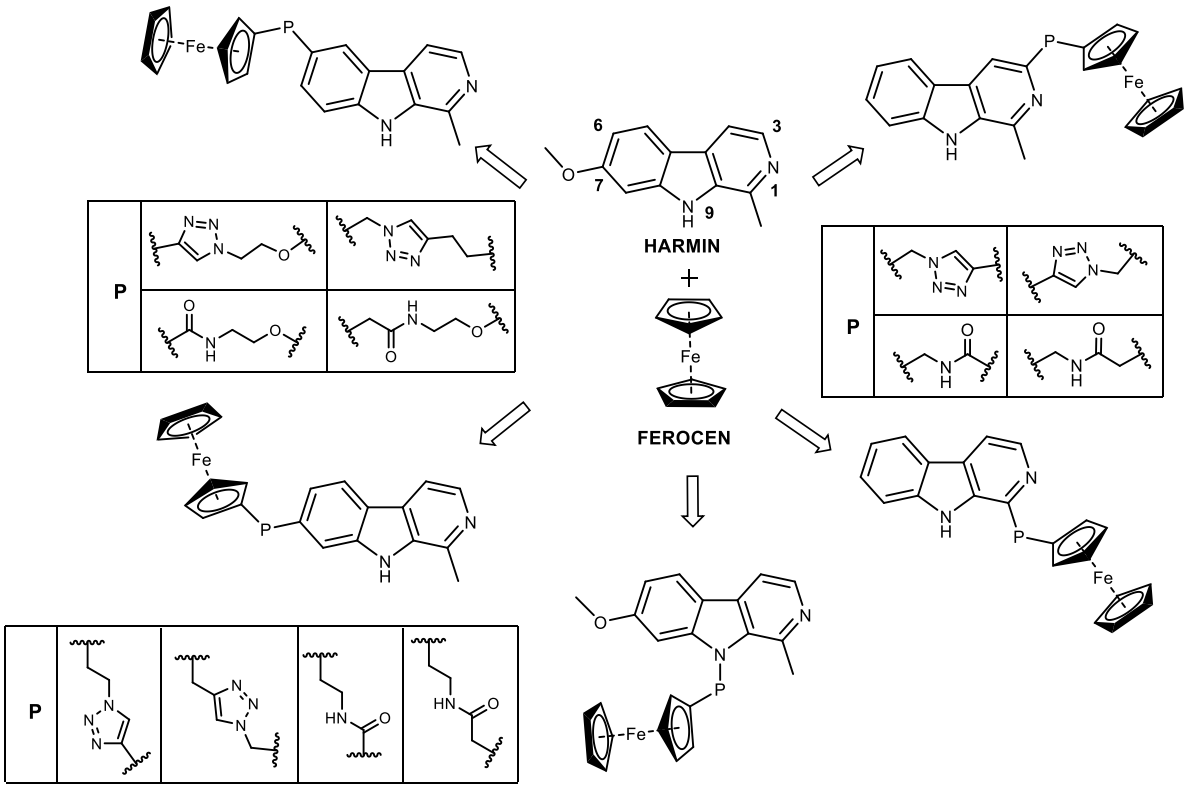

Slika 19. Strukture harmicena (113)

Ista je istraživačka skupina pripravila nove serije hibridnih spojeva, harmikine (Slika 20). Sintetizirane su dvije serije harmikina, amidi i triazoli (AT i TT harmikini), a navedeni hibridni spojevi pripravljeni su u pet položaja β-karbolina: 1, 3, 6, 7 i 9. Svim harmikinima ispitano je antimalarijsko djelovanje *in vitro* na eritrocitnu fazu *P. faciparum*, na soj osjetljiv na klorokin (*Pf*3D7) i sojeve otporne na klorokin (*Pf*Dd2, *Pf*K1 i *Pf*7G8). Svi harmikini pokazali su jače djelovanje (IC_{50} = 2 – 7110,3 nM) na eritrocitnu fazu (*Pf*3D7 i *Pf*Dd2) u odnosu na početni spoj harmin (IC_{50} = 8250 nM), pri čemu su amidi bili djelotvorniji. Amidni derivati u položaju N-9, ostvarili najbolja djelovanja na sve ispitivane sojeve. Također je uočeno da je amino skupina izravno vezana za kinolinski prsten u strukturi klorokina nužna za antimalarijsko djelovanje, a šest od ukupno sedam amida te četiri od osam triazola ostvarili su jače djelovanje na rezistentne sojeve *P. falciparum* (*Pf*Dd2, *Pf*K1 i *Pf*7G8) u odnosu na klorokin. Novosintetiziranim harmikinima također je ispitana sposobnost inhibicije polimerizacije hemozoina kao mogućeg mehanizma djelovanja te je uočeno da triazoli jače inhibiraju polimerizaciju hemozoina u odnosu na amide. Dobiveni rezultati nisu pratili slijed jačine antimalarijskog djelovanja na eritrocitnu fazu što ukazuje na to da novosintetizirani harmikini, osim inhibicije polimerizacije hemozoina, djeluju i na druge načine. U tu svrhu je, simulacijama molekulske dinamike,

ispitano vezanje amidnih derivata za *Pf*Hsp90, a rezultati su pokazali da se svi amidni derivati vežu za N-kraj ATP-azne domene navedenog proteina. Također je uočeno da je najpoželjniji položaj derivatizacije harmina N-9, što je u skladu s rezultatima *in vitro* antimalarijskog djelovanja na eritrocitnu fazu *P. falciparum* (114).

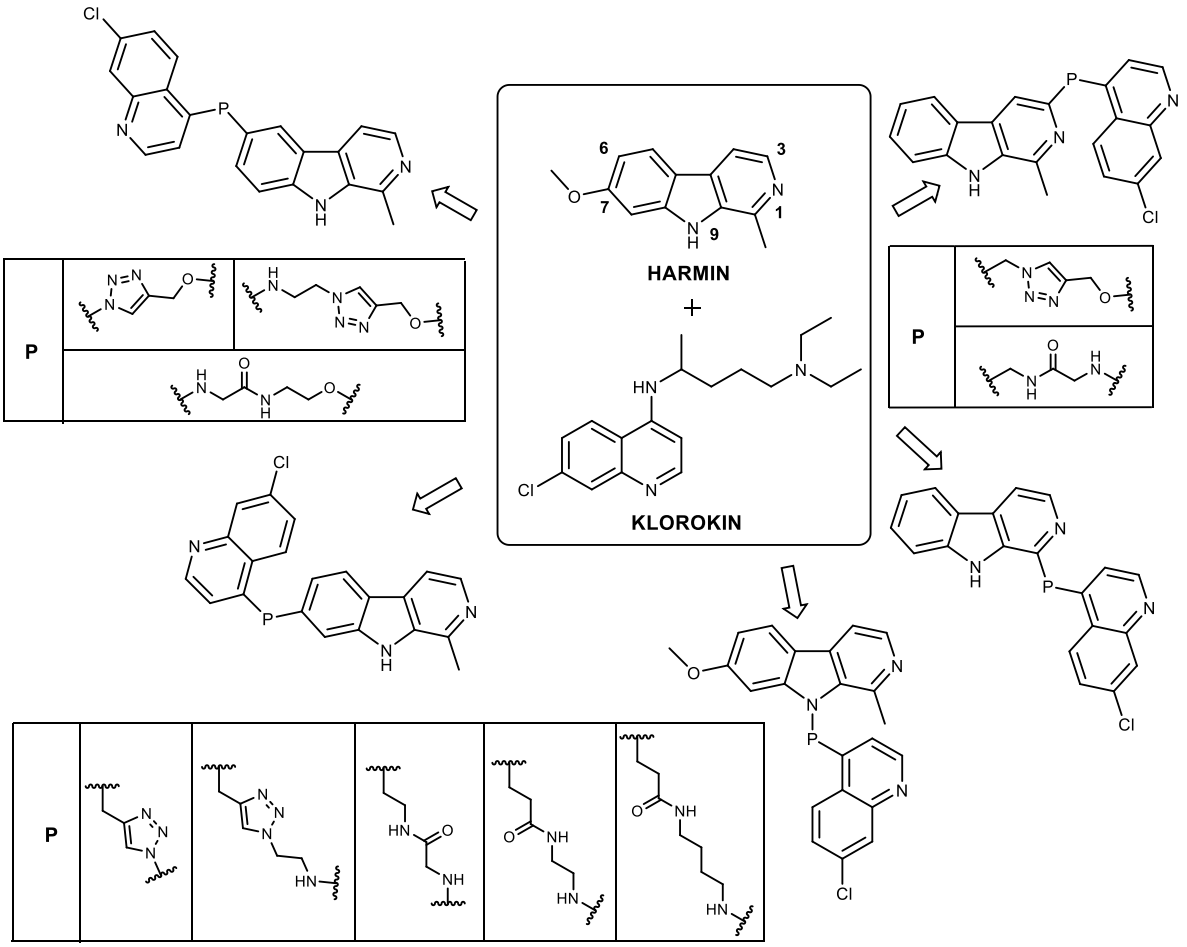

Slika 20. Strukture harmikina (114)

1.3.2. Cimetna kiselina

Cimetna kiselina ((2*E*)-3-fenilprop-2-enska kiselina) je prirodni spoj široko rasprostranjen u biljnom svijetu. Prisutna je u biljkama poput kineskog cimeta (*Cinnamomum cassia*, Lauraceae) i azijskog ginsenga (*Panax ginseng*, Araliaceae), voću, povrću i medu (115, 116). Biosinteza cimetne kiseline odvija se šikimatnim putem koji uključuje enzimatsku deaminaciju L-fenilalanina uz fenilalanin-amonij-liazu kojom se dobiva cimetna kiselina, a daljnjom hidroksilacijom i metilacijom nastaju njeni fenolni derivati. Neki od najzastupljenijih DCK-a su *p*-kumarinska, kavena, ferulična i sinapinska kiselina (Slika 21) (115, 117–119). Ove

kiseline se često nalaze u konjugiranom obliku i čine građevne blokove složenih polifenola, kao što su acilirani derivati flavonoidnih glikozida, a imaju niz uloga u biljkama kao što su zaštita od mikroorganizama ili drugih vanjskih štetnih učinaka te privlačenje oprašivača (115).

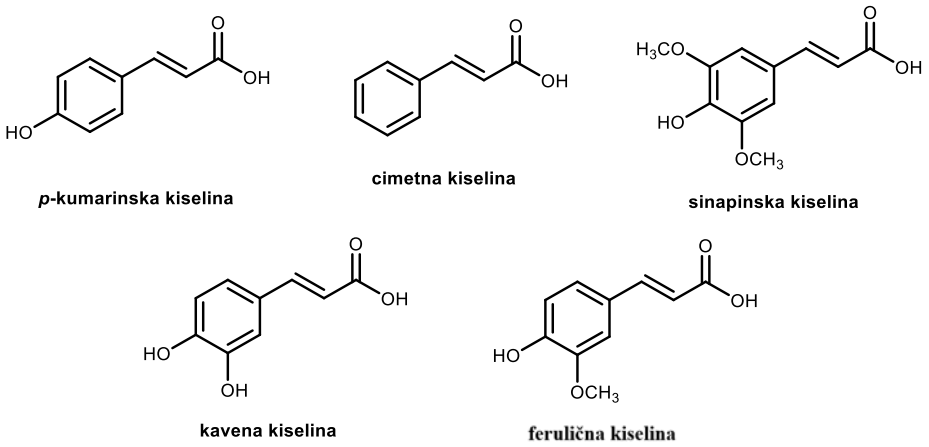

Slika 21. Strukture cimetne kiseline i fenolnih DCK-a (118)

Cimetna kiselina i DCK-i mogu se pripraviti sintetskim putem, a opisano je nekoliko metoda koje uključuju Knoevenagelovu kondenzaciju, Pechmanovu kondenzaciju, Claisenovu kondenzaciju, Perkinovu, Reformatskyjevu i Wittigovu reakciju. Danas se najčešće koristi Perkinova reakcija koja podrazumijeva aldolnu kondenzaciju aromatskog aldehida i alifatskih anhidrida karboksilnih kiselina u prisutnosti slabe baze npr. kalijevog ili natrijevog acetata (Slika 22) (120, 121).

Slika 22. Sinteza cimetne kiseline i DCK-a Perkinovom reakcijom (122)

Cimetna kiselina i DCK-i našli su široku primjenu u kozmetičkoj industriji, pa se tako cinamaldehid, cinamilni alkohol, dihidrocinamilni alkohol i cimetna kiselina koriste kao mirisni sastojci parfema, dok se esteri cimetne kiseline koji apsorbiraju UV zračenje koriste kao UV filteri u kremama za sunčanje. Cimetna kiselina se koristi u proizvodnji bojila, polimernoj industriji i poljoprivredi (115, 116, 120).

Osim toga, cimetna kiselina i DCK-i posjeduju niz bioloških djelovanja: antioksidativno, antimikrobno, antiparzitsko, protutumorsko, protuvirusno, protuupalno, neuroprotektivno, antidijabetičko, antituberkulotsko (116, 123, 124). Niska toksičnost, prisutnost benzenskog

prstena, α,β-nezasićene veze, koja je najčešće u *trans*-konfiguraciji i karboksilne skupine čini cimetnu kiselinu pogodnim spojem za sintezu novih biološki aktivnih spojeva (116, 118). Brojni su literaturni podaci koji izvještavaju o povezivanju DCK-a s poznatim lijekovima u cilju postizanja sinergističkog učinka i djelovanja na više meta (115).

Strukturni motiv cimetne kiseline nalazi se u brojnim odobrenim lijekovima: antitumorskim lijekovima panobinostatu, belinostatu, antitrombotskom lijeku ozagrelu, antialergijskim lijekovima cinarizinu, cinanserinu i tranilastu (Slika 23), te antihipertenzivu rescinaminu (Slika 11) (125).

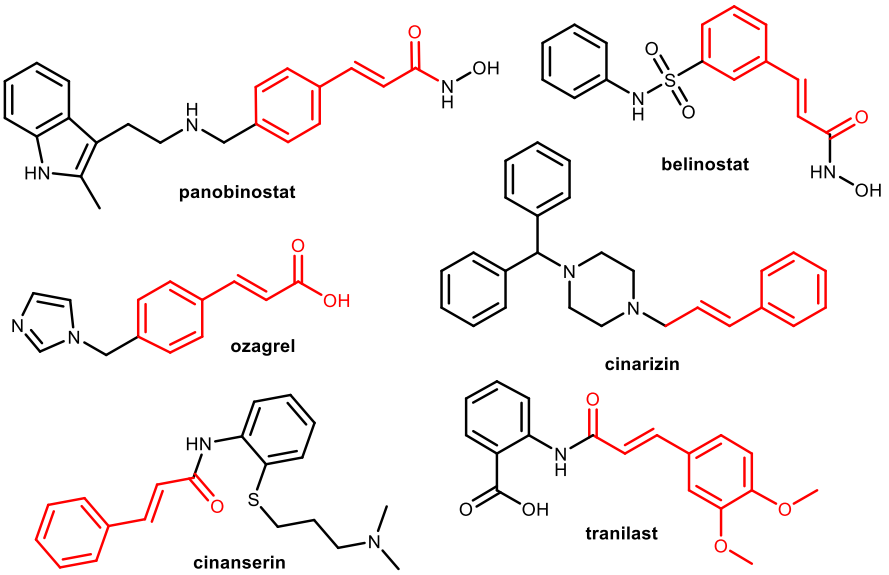

Slika 23. Strukture lijekova koji sadrže motiv cimetne kiseline (126)

1.3.2.1. Mehanizam antimalarijskog djelovanja DCK-a

Dva su moguća mehanizma antimalarijskog djelovanja DCK-a koja se očituju u inhibiraju rasta i razvoja plazmodija u eritrocitnoj fazi životnog ciklusa.

Prvi mehanizam antimalarijskog djelovanja DCK-a potvrdili su Kannani i Ginsburg u svojim istraživanjima koja su objavili 1992. godine. Naime, u eritrocitima inficiranim plazmodijem (engl. *Plasmodium-infected red blood cells*, PiRBC) razvojem plazmodija dolazi do znatnog povećanja potrošnje glukoze i stvaranja mliječne kiseline. Stoga plazmodij stvara nove puteve propusnosti u membranama eritrocita domaćina koji imaju važnu ulogu u unosu hranjivih tvari (ugljikohidrata, aminokiselina), uklanjanju nusprodukata (mliječne kiseline) i održavanju ionske ravnoteže. Ovim istraživanjem dokazano je da ispitani DCK-i sprječavaju izlučivanje laktata, glavnog produkta metabolizma plazmodija, iz PiRBC. Isto tako, DCK-i sprječavaju transmembranski prijenos ugljikohidrata i aminokiselina inhibicijom novih puteva

propusnosti te da utječu na smanjenje proizvodnje ATP-a u PiRBC, koji parazitu služi kao glavni izvor energije. Sve ovo u konačnici dovodi do sprječavanja razvoja parazita čime se očituje antimalarijsko djelovanje DCK-a (127, 128).

Drugi mehanizam antimalarijskog djelovanja DCK-a može se očitovati inhibicijom cistein proteaza plazmodija. Prisutnost α,β-nezasićene veze u strukturi DCK-a omogućava im da se Michaelovom adicijom kovalentno vežu za tiolne ostatke cisteina te ireverzibilno inhibiraju falcipain-2 i falcipain-3 proteaze, enzime koje su uključeni u degradaciju hemoglobina. Na ovaj način DCK-i mogu spriječiti rast i razvoj parazita u eritrocitnoj fazi životnog ciklusa (129).

1.3.2.2. Hibridi spojevi DCK-a s antimalarijskim djelovanjem

U pokušaju pronalaska učinkovitijih antimalarika Pérez i suradnici su, pristupom molekulske hibridizacije, sintetizirali niz hibrida u kojima su poznate antimalarike, klorokin i primakin povezivali sa strukturnim motivom cimetne kiseline. U sintezi ovih hibrida su, osim duljine i vrste poveznice, varirali položaj i vrstu supstituenta na benzenskom prstenu cimetne kiseline. Direktnim vezanjem 4-amino-7-klorkinolina i DCK-a amidnom poveznicom pripravili su hecine (engl. *heterocyclic-cinnamic acid conjugate*), a povezivanjem s dipeptidnom poveznicom hedicine (engl. *heterocyclic-dipeptide-cinnamic acid conjugate*) (Slika 24). Uočeno je kako se direktnim vezanjem 4-amino-7-klorkinolina i DCK-a gubi njihova aktivnost (IC_{50} > 10 μM), dok se uvođenjem dužih, dipeptidnih poveznica pojačava djelovanje (IC_{50} = 0,8 – 5,4 μM), uz iznimku spoja koji u *para* položaju cimetne kiseline sadrži -OCH_3 skupinu (IC_{50} = 10,8 μM). Budući da ovi spojevi u svojoj strukturi sadrže 4-amino-7-klorkinolin, ispitana je sposobnost inhibicije polimerizacije hemozoina kao mogućeg mehanizma djelovanja. Četiri od ukupno dvanaest dipeptidnih derivata pokazalo je svojstvo inhibicije polimerizacije hemozoina, dok izravno vezani derivati nisu inhibirali polimerizaciju hemozoina. Daljnja istraživanja pokazala su da se povećanjem lipofilnosti povećava antimalarijska aktivnost ovih spojeva, a kao optimalna poveznica pokazala se *n*-butilna. Svi hibridi s *n*-butilnom poveznicom ostvarili su značajno *in vitro* antimalarijsko djelovanje na eritrocitu fazu *P. falciparum* (IC_{50} = 11 – 59 nM), a najaktivniji su bili oni derivati koji u strukturi sadrže *para* supstituiranu cimetnu kiselinu (*p*-^{i}Pr, IC_{50} = 11,0 nM; *p*-Cl, IC_{50} = 11,6 nM; *p*-Me, IC_{50} = 16,9 nM; *p*-Br, IC_{50} = 18,2 nM) (115, 129, 130).

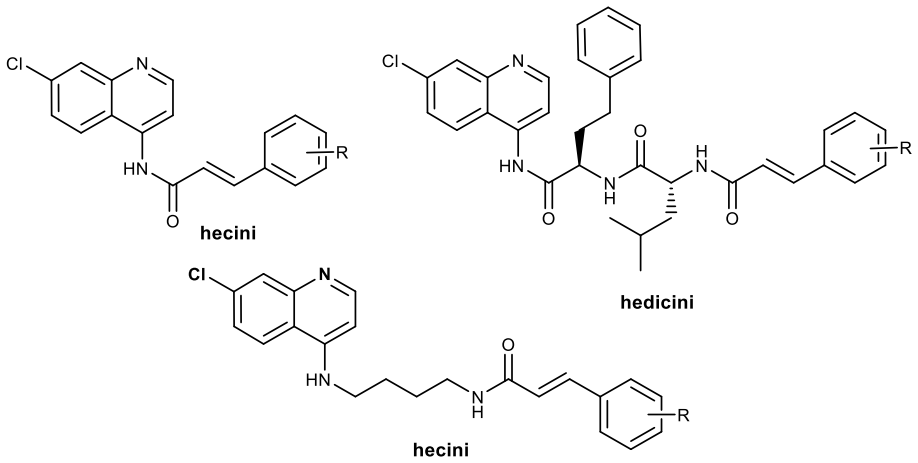

Slika 24. Hibridi 4-amino-7-klorkinolina i DCK-a (129, 130)

Kao nastavak istraživanja Pérez i suradnici sintetizirali su heflecine (engl. *heterocyclic-cinnamic conjugates*), niz spojeva u kojima su kao uvid u odnos strukture i djelovanja varirali: 1) heterocikličke prstenove 2) duljinu alifatske poveznice između cimetne kiseline i heterocikličkog prstena, 3) vrstu poveznice i 4) položaj i vrstu supstituenta na benzenskom prstenu cimetne kiseline (Slika 25). Ispitano je njihovo djelovanje na eritrocitnu fazu *P. falciparum in vitro*, na dva soja (3D7 i W2), pri čemu su svi pokazali jače antimalarijsko djelovanje na W2 soj. Prema dobivenim rezultatima zaključili su da duljina alifatskog lanca, vrsta poveznice i prisutnost 7-klorkinolina utječu na antimalarijsko djelovanje heflecina, dok vrsta supstituenta na benzenskom prstenu cimetne kiseline nije imala značajnu ulogu, ali je *para* položaj supstitucije bio poželjan. Najjače djelovanje (IC_{50} = 11 – 80 nM) pokazale su tri serije spojeva u kojima je heterociklički prsten bio 4-amino-7-klorkinolin, vrsta poveznice amid, dok su varirani duljina alifatskog lanca u poveznici kao i položaj i vrsta supstituenta na benzenskom prstenu cimetne kiseline. Uspoređujući međusobno ove tri serije spojeva učinkovitiji spojevi bili su oni koji u svojoj strukturi imaju butilnu poveznicu u odnosu na spojeve s propilnom ili pentilnom. Nadalje, uklanjanje klora u 4-amino-7-klorkinolinu dovelo je do smanjenja aktivnosti (do deset puta), a zamjenom amidne poveznice s esterskom dobiven je spoj koji je pokazao šest puta slabije djelovanje. Zamjena 7-klorkinolina s aromatskim (meflokin, piridin) ili heterocikličkim prstenom (morfolin) dovela je do potpunog gubitka aktivnosti. Ispitivanje djelovanja heflecina na hepatocitnu fazu *P. berghei* pokazalo je da neki spojevi ispoljavaju jače djelovanje (IC_{50} = 1,1 – 6,5 μM) u odnosu na primakin (IC_{50} = 7,5 μM). Ova istraživanja dokazala su da je N-cinamilna skupina važan farmakofor koji povećava *in vitro* antimalarijsko

djelovanje 7-klorkinolina, a ujedno su i prvi dokaz dvojnog antimalarijskog djelovanja derivata klorokina (131).

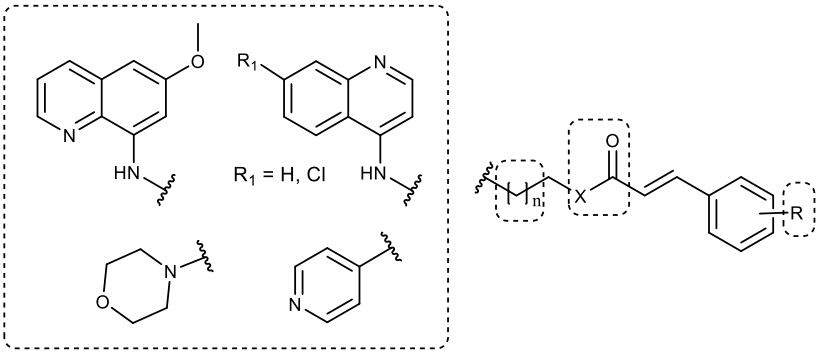

Slika 25. Strukturni parametri varirani u heflecina (131)

Gayam i Ravi su 2017. godine publicirali rad u kojem su opisali sintezu i biološko djelovanje N-cinamoiliranih derivata klorokina. U prvoj seriji spojeva 4-amino-7-klorkinolin i DCK-i bili su povezani amidnom poveznicom, a duljina alifatskog lanca u poveznici bila je etilna, dok je u drugoj seriji u poveznicu uvedena dodatna metoksifenilna skupina (Slika 26). DCK-i korišteni u sintezi ovih hibrida prethodno su pripravljeni reakcijom supstituiranih aldehida i malonske kiseline u DMF-u uz katalizator DABCO.

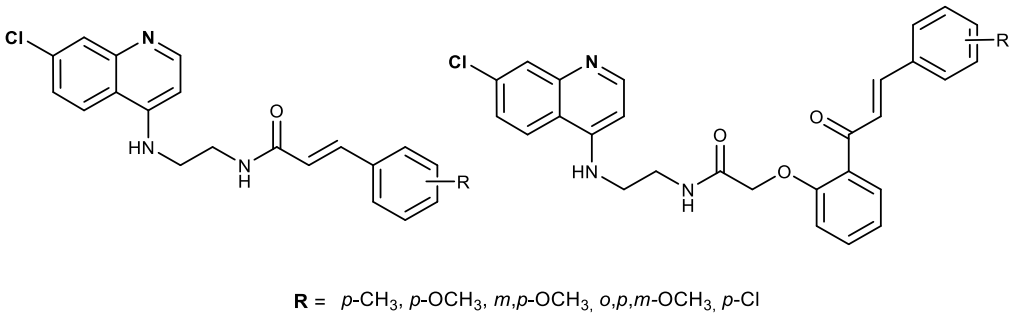

Slika 26. Strukture *N*-cinamoiliranih derivata 4-amino-7-klorkinolina (132)

Antiplazmodijsko djelovanje svih spojeva ispitano je *in vitro* na dva soja: soj osjetljiv na klorokin (*Pf*3D7) i soj otporan na klorokin (*Pf*K1) te su se pokazali značajno aktivnijima na soj *Pf*K1 (IC_{50} = 44 – 252 nM) u odnosu na klorokin (IC_{50} = 463 nM). Među navedenim serijama spojeva snažnije djelovanje ispoljavaju oni koji ne sadrže dodatnu metoksifenilnu skupinu u poveznici, pri čemu su najaktivniji bili oni spojevi koji u svojoj strukturi sadrže supstituent u *para* položaju benzenskog prstena cimetne kiseline (*p*-Cl, IC_{50} = 44 nM; *p*-Me, IC_{50} = 48 nM; *p*-OMe, IC_{50} = 59 nM), te su pokazali približno deset puta jače djelovanje na *Pf*K1 u odnosu na

klorokin. Također, zamjena benzenskog prstena cimetne kiseline s furanom te zamjena dvostruke veze cimetne kiseline eterom doprinijela je smanjenju aktivnosti (132).

Nadalje, Pérez i suradnici nastavili su istraživanje te su, analogno hecinima, sintetizirali primacine, hibride primakina i DCK-a koji su međusobno povezani amidnom poveznicom (Slika 27). Primacinima je ispitano antimalarijsko djelovanje na eritrocitnu fazu *P. falciparum* i hepatocitnu fazu *P. berghei*. Budući da primakin djeluje na tkivne shizonte svih vrsta plazmodija, a ujedno je i jedini antimalarik koji djeluje na hipnozoite - latentne oblike *P. vivax* i *P. ovale* u jetri, pretpostavka je bila da će navedeni hibridi pokazati dvojno djelovanje, odn. na eritrocitnu i hepatocitnu fazu plazmodija. Međutim, primacini su se, izuzev spoja u kojemu je R = *p*-^{i}Pr (IC_{50} = 4,84 μM), pokazali inaktivnima na eritrocitnu fazu, dok su na hepatocitnu fazu pokazali dva do tri puta jače djelovanje (IC_{50} = 1,38 – 2,39 μM) u odnosu na početni spoj primakin (IC_{50} = 7,50 μM) (133).

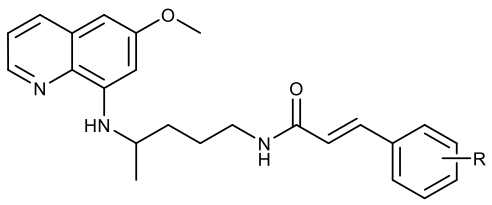

R = H, *p*-Me, *p*-^{i}Pr, *p*-OMe, *m*-F, *p*-F, *p*-Cl, *p*-Br, *o*-NO_2, *m*-NO_2, *p*-NO_2

Slika 27. Strukture primacina (133)

Primakin je dugi niz godina bio predmet istraživanja u Zavodu za farmaceutsku kemiju Farmaceutsko-biokemijskog fakulteta. U više znanstvenih radova koje su objavili Zorc i suradnici opisana je i sinteza hibrida primakina i DCK-a te im je ispitano antimalarijsko i protutumorsko djelovanje. Poveznica između ova dva farmakofora bila je amid ili acilsemikarbazid (Slika 28), a većina sintetiziranih hibrida pokazala je umjereno antimalarijsko djelovanje na eritrocitnu fazu *P. falciparum*. Serija spojeva u kojima je primakin preko amidne poveznice vezan za DCK-e ispoljila je jače djelovanje, uz iznimku spoja koji u svojoj strukturi sadrži acilsemikarbazidnu poveznicu i tri metoksi skupine na benzenskom prstenu cimetne kiseline, a koji je među navedenim hibridima bio najdjelotvorniji (IC_{50} = 4,5 μM) (134).

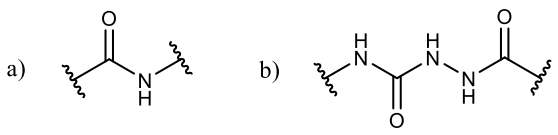

Slika 28. Poveznice u primakin-DCK-i hibridima: a) amidna b) acilsemikarbazidna (134)

Ohrabreni dobrim rezultatima dobivenim ispitivanjem antimalarijskog djelovanja derivata klorokina i primakina s derivatima cimetne kiseline, Pérez i suradnici proširili su istraživanje te su tako pripravili N-butilcinamoilirane derivate aminoakridina, a poveznica između aminoakridina i DCK-a također je bila amidna (Slika 29). Sinteza ovih derivata uključivala je samo dva reakcijska koraka: 1) uvođenje aminobutilnog lanca u strukturu aminoakridina reakcijom 9-klorakridina i 1,4-diaminobutana i 2) reakciju povezivanja DCK-a i aminoakridina uz *coupling* reagens TBTU i bazu DIEA u DMF-u. Navedenim spojevima je ispitano antimalarijsko djelovanje na eritrocitnu fazu *P. falciparum* (*Pf*W2) *in vitro* te su svi, osim derivata koji sadrži nesupstituiranu cimetnu kiselinu u svojoj strukturi, pokazali značajno antimalarijsko djelovanje s rasponom IC_{50} = 126 – 345 nM. Analogno prethodno sintetiziranim hibridima DCK-a i klorokina/primakina (hecini, hedicini, primacini) najaktivniji među novosintetiziranim hibridima bio je spoj koji sadrži *p*-^{i}Pr-supstituiranu cimetnu kiselinu (IC_{50} = 126 nM) potvrđujući da lipofilni razgranati supstituenti u *para* položaju benzenskog prstena cimetne kiseline doprinose povećanju antimalarijskog djelovanja.

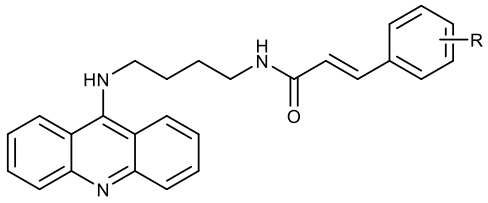

R = H, *p*-Me, *p*-^{i}Pr, *p*-OMe, *p*-F, *m*-F, *m*-NO_2

Slika 29. Strukture hibrida aminoakridina i DCK-a (135)

Tri derivata (R = *p*-^{i}Pr; *p*-OMe; *p*-F) su odabrana te im je ispitno antimalarijsko djelovanje *in vitro* na hepatocitnu fazu *P. berghei* i ostvarili su jače djelovanje u odnosu na primakin. Ispitivanja su također pokazala da su odabrani spojevi netoksični na Huh7 staničnu liniju pri maksimalnoj koncentraciji od 5 µM. Najaktivniji spoj (R = *p*-OMe) s IC_{50} = 3,2 µM ispoljio je gotovo 2,5 puta jače djelovanje od primakina (IC_{50} = 8 µM) što svrstava novosintetizirane hibride akridina među spojeve za razvoj novih potencijalnih antimalarijskih lijekova s dvojnim djelovanjem. Nadalje, ova istraživanja su pokazala da su upravo navedeni hibridi aminoakridina i DCK-a prvi spojevi djelotvorniji na hepatocitnu fazu u odnosu na primakin, a koji u svojoj strukturi ne sadrže kinolinski prsten (135).

Ista je istraživačka skupina, predvođena Paulom Gomes, nastavila i proširila istraživanje novih hibrida aminoakridina i DCK-a te su tako sintetizirali seriju spojeva koji, u odnosu na prvu generaciju, u strukturi aminoakridina sadrže metoksi skupinu u položaju 2 te klor u

položaju 6. Vodeći se dosadašnjim saznanjima o SAR-u, odabrali su amidnu poveznicu, butilnu alifatsku poveznicu i DCK-e sa supstituentom u *para* položaju benzenskog prstena (Slika 30).

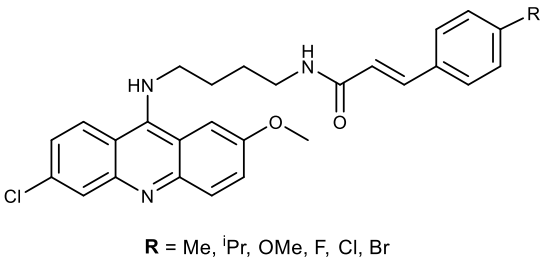

R = Me, ^{i}Pr, OMe, F, Cl, Br

Slika 30. Strukture druge generacije hibrida aminoakridina i DCK-a (136)

Svi su spojevi ispoljili izuzetno snažno djelovanje na eritrocitnu fazu *P. falciparum* s IC_{50} = 17 – 39 nM (*Pf*3D7), IC_{50} = 27 – 131 nM (*Pf*W2) i IC_{50} = 3 – 41 nM (*Pf*Dd2). U usporedbi s klorokinom svi su spojevi, izuzev spoja koji je kao supstituent na benzenskom prstenu imao metoksi skupinu, pokazali slabije djelovanje na soj *Pf*3D7, dok su na klorokin-rezistentne sojeve *Pf*W2 i *Pf*Dd2 ispoljili 2-4 puta odnosno 5-70 puta jače djelovanje. Novosintetizirani hibridi aminoakridina i DCK-a ostvarili su jače djelovanje u odnosu na analoge prve generacije, što ukazuje da uvođenje metoksi skupine u položaj 2 i klora u položaj 6 aminoakridinskog prstena doprinosi pojačanju antimalarijskog djelovanja. Nadalje, ispitano je antimalarijsko djelovanje svih hibrida na hepatocitnu fazu *P. berghei*, te su određene IC_{50} vrijednosti za spojeve s najsnažnijim djelovanjem, pri čemu su spojevi s R = F (IC_{50} = 1,6 µM) i R = Cl (IC_{50} = 1,8 µM) pokazali 4-5 puta jače djelovanje u odnosu na primakin (IC_{50} = 7,5 µM). Zatim su provedena ispitivanja inhibicije polimerizacije hemozoina *in vitro* kao njihovog mogućeg mehanizma djelovanja. Izuzev jednog hibrida druge generacije (R = Me), niti jedan drugi spoj (prve i druge generacije) nije inhibirao polimerizaciju hemozoina te tako mehanizam djelovanja ovih spojeva ostaje i dalje predmet istraživanja (136).

Novija istraživanja Paule Gomes i suradnika dovela su do sinteze ionskih tekućina, odn. organskih soli kao potencijalnih, učinkovitih antimalarika. Vođeni dosadašnjim saznanjima, metodom neutralizacije primakina i odabranih DCK-a, pripravili su ukupno šest ionskih tekućina (Slika 31) te su im ispitali antimalarijsko djelovanje *in vitro* na *P. falciparum* (3D7 i Dd2).

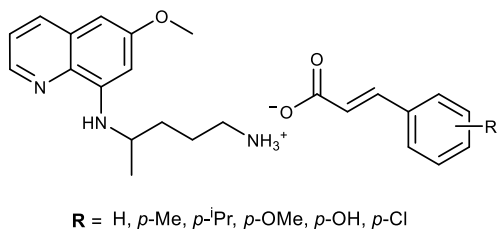

Slika 31. Strukture ionskih tekućina primakina i DCK-a (137)

Sve su ionske tekućine pokazale jače antimalarijsko djelovanje na eritrocitnu fazu *P. falciparum* (IC_{50} = 0,94 – 3,40 μM) u odnosu na primakin. Nasuprot tome, njihovi strukturni analozi (primacini) u kojima su primakin i DCK-i bili povezani amidnom poveznicom pokazali su značajno slabije djelovanje (samo jedan od ukupno 11 sintetiziranih hibrida pokazao je učinkovitost na eritrocitnu fazu *P. falciparum* (IC_{50} < 10 μM)). Odabrane su tri ionske tekućine (R = *p*-OMe, *p*-^{i}Pr, *p*-Cl) i njihovi kovalentni analozi te im je ispitano antimalarijsko djelovanje *in vitro* na hepatocitnu fazu *P. berghei*. Sve su odabrane ionske tekućine bile netoksične na Huh7 staničnu liniju pri najvišim ispitivanim koncentracijama, a dvije u kojima je R = *p*-OMe i R = *p*-^{i}Pr su pokazale jače djelovanje na hepatocitnu fazu u usporedbi s primakinom, ali slabije u odnosu na kovalentne analoge. Nadalje, dvjema odabranim ionskim tekućinama ispitano je gametocitno djelovanje *P. falciparum* te su ostvarile jednako ili jače djelovanje u odnosu na primakin i kovalentne analoge. Ova istraživanja pokazuju da su pripravom ionskih tekućina primakina i DCK-a dobiveni spojevi koji su ostvarili trojno djelovanje, na hepatocitnu fazu uz zadržavanje aktivnosti na eritrocitnu fazu i gametocitnu fazu *P. falciparum*, što ih ubraja među vodeće spojeve za razvoj novih potencijalnih antimalarika (137).

1.4. KVANTITATIVNI ODNOS STRUKTURE I DJELOVANJA

Proces razvoja lijeka uključuje identifikaciju mete, pronalazak vodećeg spoja (engl. *lead compound*) koji pokazuje željeni učinak, optimiranje njegove strukture kako bi se poboljšala učinkovitost, sigurnost i farmakokinetička svojstva potencijalnog lijeka, nakon čega slijede pretklinička i klinička ispitivanja. Od deset tisuća sintetiziranih i ispitanih spojeva, približno sto pokazuje željenu aktivnost i sigurnost, od toga ih deset ulazi u klinička ispitivanja, a najčešće je samo jedan odobren za kliničku uporabu. Cijeli proces je dugotrajan i rezultira dobivanjem odobrenja za stavljanje lijeka u promet tek nakon 10-15 godina pri čemu se troškovi razvoja procjenjuju na 2,6 milijardi USD (138, 139).

Različiti su pristupi u otkrivanju lijekova. Neki od lijekova otkriveni su slučajno, a najpoznatiji primjer svakako je otkriće penicilina, lijeka koji je tijekom Drugog svjetskog rata spasio milijune života i za koji su Fleming, Florey i Chain dobili Nobelovu nagradu za fiziologiju i medicinu 1945. godine. Jedan od pristupa otkrivanja lijekova uključuje kemijsku modifikaciju prirodnih produkata ili već poznatih lijekova. Poznati primjer je aspirin, dobiven kemijskom modifikacijom, odnosno acetiliranjem prirodnog produkta salicilne kiseline čime se znatno poboljšala stabilnost i smanjio nadražujući učinak na želučanu sluznicu (138).

U odnosu na tradicionalne pristupe otkrivanja lijekova koji se oslanjaju na testiranje spojeva *in vitro* na kultiviranim staničnim linijama ili *in vivo* na životinjskim modelima metodom pokušaja i pogrešaka, racionalno dizajniranje lijeka podrazumijeva poznavanje biološke mete. Budući da je razvoj lijeka dugotrajan i skup proces, u razvoju lijeka sve se češće koriste *in silico* (računalne) metode, odn. računalno potpomognuto dizajniranje lijekova (engl. *Computer Aided Drug Design*, CADD). *In silico* metode su od izuzetne važnosti, posebno u ranom procesu razvoja lijeka jer skraćuju vrijeme te znatno smanjuju troškove. Dva su osnovna pristupa u CADD-u: 1) dizajniranje lijekova temeljeno na strukturi (engl. *structure-based drug design*, SBDD) i 2) dizajniranje lijekova temeljeno na ligandu (engl. *ligand-based drug design*, LBDD). SBDD se koristi kada je 3D struktura ciljane mete (najčešće proteina) poznata, a ligand se dizajnira da bude komplementaran veznom mjestu. Neke od SBDD metoda uključuju virtualni probir (engl. *virtual screening*) knjižnica spojeva, molekulsko uklapanje (engl. *molecular docking*) i simulacije molekulske dinamike (engl. *molecular dynamics*, MD). LBDD se temelji na ligandima, odnosno na informacijama o aktivnosti molekula za koje je poznato da stupaju u interakciju s biološkom metom, a najčešće korištene metode su kvantitativni odnos strukture i djelovanja (engl. *quantitative structure-activity relationship*, QSAR) i modeliranje farmakofora (138, 139).

QSAR je metoda računalnog ili matematičkog modeliranja koja za cilj ima kvantificirati odnos između biološke aktivnosti i strukturnih svojstva kemijskih spojeva (140). Temelji se na pretpostavci da struktura molekule, tj. njena geometrijska, sterička i elektronska svojstva sadržavaju značajke odgovorne za njezina fizikalna, kemijska i biološka svojstva (141). QSAR je, osim u farmaceutskoj industriji, našao veliku primjenu u brojnim drugim znanstvenim disciplinama uključujući kemiju, biologiju i toksikologiju (142). Također se, osim biološke aktivnosti, bilo koje fizikalno-kemijsko svojstvo može dovesti u kvantitativan odnos sa strukturnim svojstvima molekula (engl. *Quantitative Structure-Property Activity*, QSPR) (143).

Razvoj QSAR-a započeo je još sredinom 19. stoljeća, kada je Cros uočio da postoji povezanost između toksičnosti primarnih alifatskih alkohola i njihove topljivosti u vodi. Nešto

kasnije Crum-Brown i Fraser iznijeli su ideju da postoji povezanost između biološke aktivnosti različitih alkaloida i njihove kemijske strukture, tj. farmakološko djelovanje su definirali kao funkciju njihove kemijske strukture, a upravo se ova jednadžba smatra prvim QSAR modelom:

$$\text{Farmakološko djelovanje} = f(\text{kemijska struktura})$$

Pretpostavka o postojanju odnosa između kemijske strukture molekula i fizikalno-kemijskih svojstava također je iznesena 1874. godine u radu Körnera i suradnika, koji se bavio sintezom disupstituiranih benzena. Pretpostavka je bila da su različite boje disupstituiranih benzena povezane s njihovim razlikama u kemijskoj strukturi. Kvantitativni modeli odnosa svojstva i aktivnosti, koji se smatraju i početcima sustavnih QSAR/QSPR metoda, proizašli su 1899. godine, kada su Meyer, Overton i Baum određivali odnos između učinkovitosti lokalnih anestetika i koeficijenta raspodjele između ulja i vode. Ova, kao i brojne kasnije studije poslužile su kao temelj za Hanschovo istraživanje ovisnosti aktivnosti hormona rasta biljaka o Hammettovim konstantama i hidrofobnosti, objavljeno 1962. godine. Korištenjem sustava oktanol/voda izmjerio je niz koeficijenata razdijeljenja i tako uveo novu mjeru hidrofobnosti – lipofilnost molekule. Njegovim istraživanjem započeo je moderni razvoj QSAR-a (144).

Organizacija za ekonomsku suradnju i razvoj (engl. *Organisation for Economic Cooperation and Development*, OECD) donijela je 2004. godine pet zahtjeva koje bi trebao ispunjavati svaki QSAR model koji se koristi u regulatorne svrhe:

1. jasno definiran cilj,
2. jednoznačan algoritam,
3. definirana domena primjenljivosti,
4. odgovarajuće statističke mjere pristajanja podataka (engl. *goodness of fit*), robusnosti i moći predviđanja,
5. mehanističku interpretaciju.

Prema prvom zahtjevu QSAR model treba biti povezan s definiranim ciljem, pri čemu se cilj odnosi na bilo koje fizikalno-kemijsko svojstvo, biološki učinak ili parametar u okolišu koji se može mjeriti i modelirati. Namjera ovog zahtjeva je osigurati transparentnost u krajnjoj točki koju model predviđa, budući da se dana krajnja točka može odrediti različitim eksperimentalnim protokolima i pod različitim eksperimentalnim uvjetima. Prema drugom zahtjevu, QSAR model treba biti izražen u obliku nedvosmislenog algoritma. Kako bi model

bio reproducibilan, vrlo je važno poznavati korišteni algoritam, tj. potrebno je osim definiranja korištenog početnog skupa podataka definirati i statističke metode, način generiranja i izbor deskriptora. Treći zahtjev QSAR modela povezan je s definiranom domenom primjenjivosti. Potreba za definiranjem domene primjenjivosti izražava činjenicu da su QSAR modeli neizbježno povezani s ograničenjima u pogledu kemijskih struktura, fizikalno-kemijskih svojstava i mehanizama djelovanja za koje modeli mogu generirati pouzdana predviđanja, odn. niti jedan model ne može kvalitetno predvidjeti svojstva svih mogućih kemijskih spojeva. Prema četvrtom zahtjevu kvalitetu QSAR modela treba potvrditi odgovarajućim statističkim mjerama pristajanja podataka, robusnosti i predvidljivosti. Potrebno je osigurati dvije vrste informacija, internu validaciju modela provedenu na skupu za učenje (potvrđena prilagodbom podataka i robusnošću) i predvidljivost modela, određenu korištenjem odgovarajućeg skupa za testiranje. Posljednji zahtjev uključuje mehanističku interpretaciju, odnosno procjenu veze između deskriptora korištenih u modelu i krajnje točke (svojstva ili biološke aktivnosti), što može biti od velike koristi za buduća istraživanja (145).

Razvoj pouzdanog prediktivnog QSAR modela sastoji se od nekoliko koraka (142, 146, 147). Prvi korak uključuje pronalazak grupe kemijskih spojeva s eksperimentalno izmjerenim biološkim aktivnostima. U idealnom slučaju to bi trebao biti kongenerički skup molekula, koji ima zadovoljavajuću razliku u kemijskoj strukturi koja omogućava varijaciju biološke aktivnosti (146).

Drugi korak podrazumijeva generiranje i odabir molekulskih deskriptora. Molekulski deskriptori su numeričke vrijednosti, nastale kao rezultat logičkih i matematičkih transformacija kemijske informacije, a mogu se klasificirati na više načina. Prema načinu generiranja mogu biti teorijski (računski) i eksperimentalni. Teorijski molekulski deskriptori mogu biti izvedeni iz prikaza cjelokupne strukture molekule (globalni) ili opisivati određeni fragment (lokalni) (142).

Prema dimenzionalnosti molekulski deskriptori mogu se podijeliti na:

- 0D - deskriptori koji opisuju svojstva molekula temeljem sažete molekulske formule (npr. broj atoma, broj veza);
- 1D - deskriptori koji opisuju svojstva supstituenata, fragmenata, funkcionalnih skupina;
- 2D - topološki deskriptori koji daju informaciju o vezama između atoma u molekuli (najveća skupina teorijskih molekulskih deskriptora);
- 3D - geometrijski, sterički i volumni parametri koji opisuju konfiguraciju molekule.

Prema svojstvu molekule koje opisuju mogu se podijeliti na

- konstitucijske - broj atoma, broj veza, broj prstenova i dr.;
- fizikalno-kemijske - predstavljaju fizikalna i kemijska svojstva nekog spoja. (log *P*, temperatura tališa, temperatura vrelišta, gustoća i dr.);
- topološki - Plattov indeks, Randićev indeks povezanosti, Balabanov indeks, Hararyjev indeks i dr.;
- geometrijski - topološka polarna površina, površina molekule dostupna otapalu, van der Waalsov volumen, Taftov sterički parametar i dr.;
- elektronski - dielektrična konstanta, dipolni moment, polarizabilnost, ionizacijski potencijal i dr.;
- kvantno-mehanički - izračunati kvantno-kemijskim proračunima (energija HOMO i LUMO orbitala, ukupna energija i dr.).

Danas su dostupni brojni softveri i programski paketi kojima se može vrlo jednostavno i brzo generirati veliki skup molekulskih deskriptora. Međutim, važno je da među generiranim molekulskim deskriptorima ne postoje oni koji nose istu informaciju. Stoga se vrši selekcija, koja se najčešće provodi računanjem korelacijskog koeficijenta pri čemu se sam odabir temelji na mogućnosti, odnosno jednostavnosti interpretacije samog deskriptora (142, 148).

Treći korak uključuje primjenu statističkih metoda kojima se uspostavlja veza između odabranih kemijskih deskriptora i biološke aktivnosti. Iako odnos između molekulskih deskriptora i biološke aktivnosti može biti linearan ili nelinearan, češće se koriste linearne metode, kao što su višestruka linearna regresija (engl. *Multiple Linear Regression*, MLR) ili parcijalna regresija najmanjih kvadrata (engl. *Partial Least Square*, PLS). Za nelinearno modeliranje, koriste se metode umjetne neuronske mreže (engl. *Artificial Neural Network*, ANN) i klasifikacijskih i regresijskih stabla (142).

Kako bi QSAR model bio prihvaćen kao pouzdan potrebno je provesti validacijski postupak. Razlikujemo unutarnju validaciju, koja se provodi na skupu molekula za učenje i vanjsku validaciju, koja se provodi na odvojenom testnom skupu molekula. Najčešći statistički parametri koji se koriste u predviđanju točnosti i prediktivnosti su koeficijent determinacije (R^2), koji definira koliko dobro model pristaje podatcima korištenima za njegova razvoj, prilagođeni koeficijent determinacije (R_a^2), koji u obzir uzima broj prediktorskih varijabli i slučaja, F-vrijednost, *p*-vrijednost, srednja apsolutna pogreška (engl. *Mean Absolute Error*,

MAE) i korijen srednje kvadratne pogreške (engl. *Root Mean Square Error*, RMSE) (142, 143, 149, 150).

Najčešće korištena metoda unutarnje validacije je unakrsna validacija (engl. *Cross-Validation*, CV), a temelji se na iterativnom postupku izostavljanja jednog (engl. *leave one out cross validation*, LOO-CV) ili više spojeva iz skupa (engl. *Leave-Many-Out Cross-Validation*, LMO-CV) pri čemu se model razvija na preostalim spojevima. Tako razvijeni model zatim se koristi za predviđanje svojstava izostavljenih spojeva iz skupa. Prediktivnost modela procjenjuje se pomoću unakrsno validiranog koeficijenta determinacije Q^2, a vrijednosti $Q^2 > 0,5$ prihvaćaju se kao zadovoljavajući rezultat (142, 150).

Na temelju izrgađenog i validiranog QSAR modela provodi se optimiranje strukture aktivnih spojeva kako bi se poboljšala biološka aktivnost. Odgovarajući spojevi se zatim sintetiziraju te se eksperimentalno ispituje željena biološka aktivnost.

Shematski prikaz razvoja QSAR modela prikazan je na Slici 32.

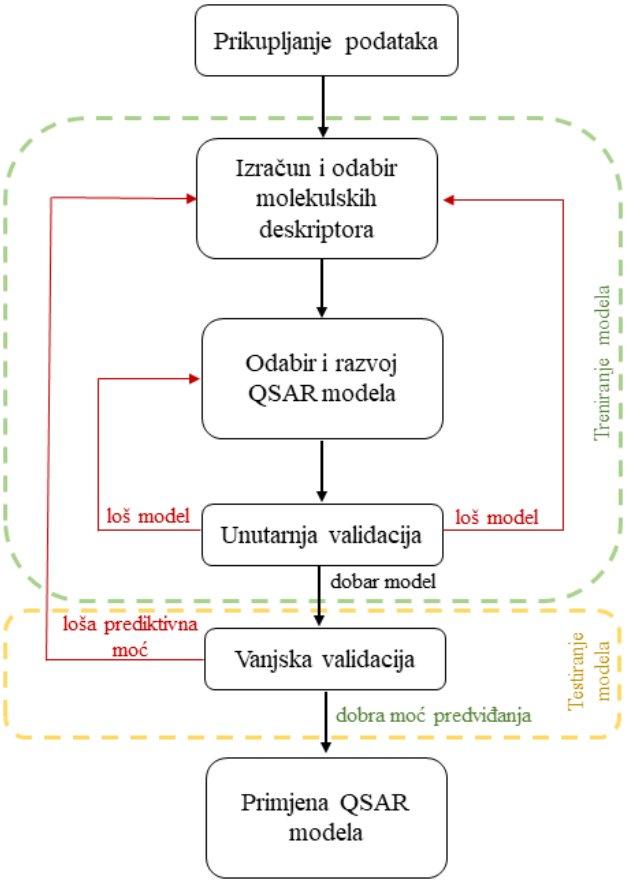

Slika 32. Shematski prikaz razvoja i validacije QSAR modela (prilagođeno prema (151))

QSAR je danas postao neizostavni alat kojim se farmaceutska industrija služi u pronalasku novih lijekova, kao i u optimizaciji postojećih. Korištenjem QSAR metoda u ranom procesu razvoja novoga lijeka mogu se isključiti spojevi koji ne posjeduju fizikalno-kemijska svojstva poželjna za ljekovite tvari (engl. *drug-like properties*) ili oni spojevi za koje se pretpostavi da bi mogli izazvati toksični učinak. Također, predviđanjem biološkog djelovanja novih spojeva može se smanjiti dugotrajan i intenzivan proces sinteze i određivanja biološkog djelovanja ispitivanjima *in vitro* i *in vivo*, čime se znatno skraćuje vrijeme i smanjuju troškovi istraživanja (142).

2. OBRAZLOŽENJE TEME

Malarija je zarazna bolest kojom se godišnje zarazi više od 200 milijuna ljudi. Unatoč dugogodišnjim naporima da se ova bolest iskorijeni ona i dalje ostaje jedan od vodećih uzroka smrtnosti u zemljama u razvoju (1, 2). Nadalje, sve veći problem u suzbijanju ove bolesti predstavlja razvoj rezistencije plazmodija na postojeće lijekove kao i njihovu kombinaciju, što dovodi do potrebe za razvojem novih i učinkovitih antimalarijskih lijekova (1, 2, 20).

Jedan od mogućih pristupa u razvoju novih lijekova je molekulska hibridizacija, a temelji se na kovalentnom povezivanju dviju ili više biološki aktivnih molekula ili njihovih farmakofora, kako bi se dobila jedinstvena hibridna molekula s poboljšanim djelovanjem. Brojne su prednosti primjene hibridnih molekula nad kombiniranom terapijom malarije, a jedna od mogućih prednosti je djelovanje na više bioloških meta, čime bi se mogla povećati učinkovitost pojedinih antimalarika, a ujedno smanjiti toksičnost i vjerojatnost razvoja rezistencije (26, 29).

QSAR je statistički pristup kvantificiranja povezanosti između strukture i farmakološkog učinka neke molekule, pri čemu se taj odnos iskazuje matematičkim modelom (152). Postao je neizostavni alat kojim se farmaceutska industrija danas služi u pronalasku novih lijekova, kao i u optimizaciji postojećih, jer se predviđanjem biološkog djelovanja novih spojeva može smanjiti dugotrajan proces razvoja lijeka čime se znatno smanjuju troškovi i skraćuje vrijeme istraživanja (142).

U okviru ovog doktorskog rada pripravljeni su harmicini amidnoga tipa. Prilikom dizajniranja harmicina primijenjen je pristup molekulske hibridizacije kojim su harmin, β-karbolin s dokazanim antimalarijskim djelovanjem i cimetna kiselina, odn. DCK-i, povezani amidnom vezom u jedinstvenu molekulu. Antiplazmodijsko djelovanje svih harmicina amidnoga tipa ispitano je *in vitro* na eritrocitnu fazu životnog ciklusa *P. falciparum* i hepatocitnu fazu životnog ciklusa *P. berghei*, te citotoksičnost na staničnu liniju HepG2. Na temelju rezultata antiplazmodijskog djelovanja na eritrocitnu fazu provedena je QSAR analiza, kojom je dobiven prediktivni model. U zadnjem dijelu doktorskog rada su, prema dobivenom QSAR modelu, odabrani i sintetizirani novi harmicini amidnoga, karbamatnog i ureidnog tipa te im je ispitano antiplazmodijsko djelovanje *in vitro* na eritrocitnu fazu životnog ciklusa *P. falciparum*.

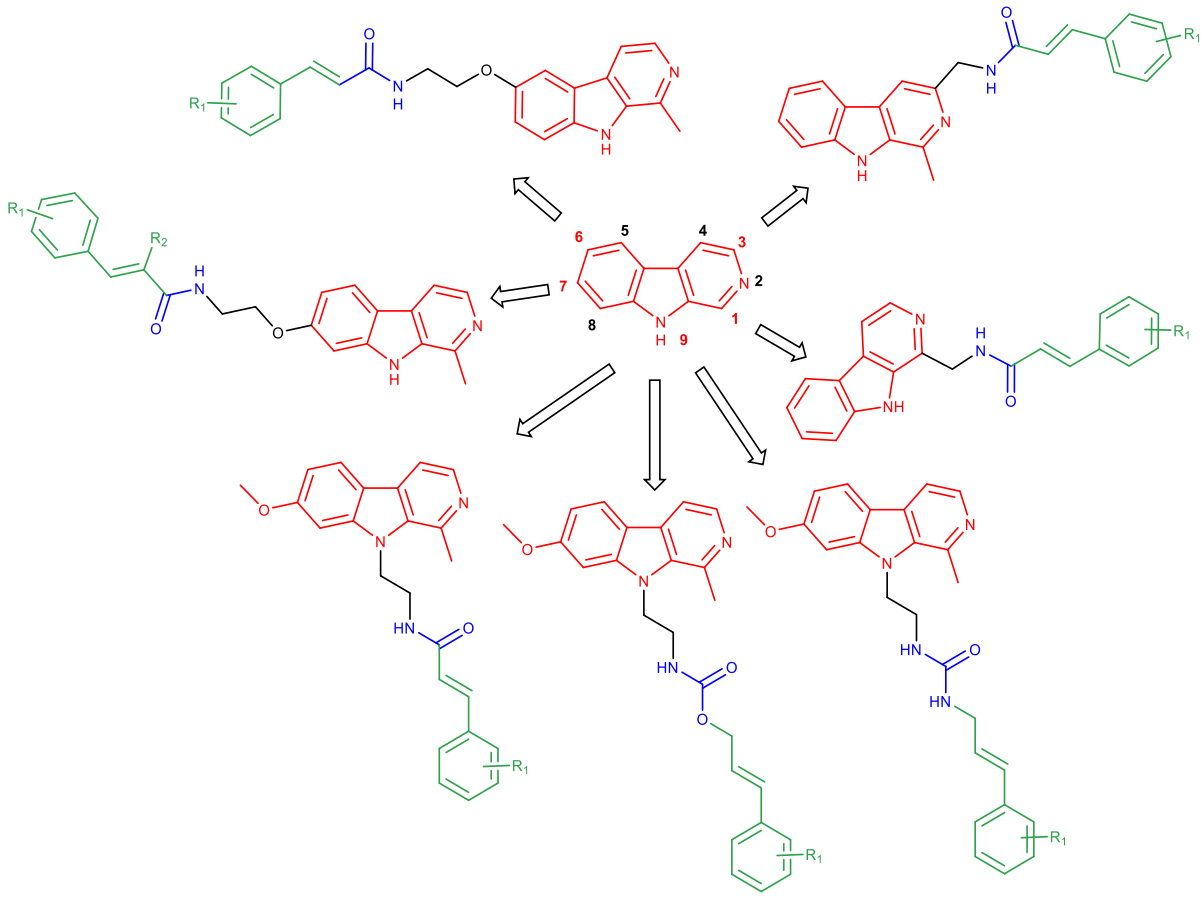

Slika 33. Strukture harmicina amidnoga, karbamatnog i ureidnog tipa

3. MATERIJALI I METODE

3.1. MATERIJALI I INSTRUMENTI

Tijek kemijskih reakcija i čistoća produkata praćeni su tankoslojnom kromatografijom (TLC) na silikagel pločama 60 F254 (Merck, Njemačka) koje su korištene kao nepokretna faza te diklormetan/metanol (95:5, 9:1, 85:15, 8:1, 75:25), etil-acetat/metanol (10:0,5) i/ili cikloheksan/etil-acetat/metanol (1:1:0,5, 3:1:0,5) kao pokretne faze. Za kromatografiju na koloni kao nepokretna faza korišten je silikagel veličine čestica 0,063 – 0,200 mm (Merck, Njemačka) uz iste pokretne faze kao i u TLC-u. Analizirani spojevi detektirani su UV zračenjem (λ = 254 i 366 nm) i parama joda. Iskorištenja nisu optimirana.

CEM Discover mikrovalni reaktor (CEM Corporation, SAD) korišten je u sintezi pomognutoj mikrovalovima (P = 150 W). Tališta (t_t) su određena na Stuart SMP3 instrumentu za određivanje tališta (Barloworld Scientific, UK) u otvorenim kapilarama i nisu korigirana. ^{1}H i ^{13}C NMR spektri snimljeni su na NMR spektrometru Bruker Avance III HD i AV-600 (Bruker, SAD) pri 300, 400 ili 600 MHz za ^{1}H i 75, 101 ili 151 MHz za ^{13}C jezgru. Uzorci su mjereni u DMSO-d_6 otopinama na 20 °C u NMR cjevčicama promjera 5 mm. Kemijski pomaci izraženi su u ppm u odnosu na tetrametilsilan (TMS) ili dimetilsulfoksid (DMSO) kao unutarnji standard u ^{1}H, odnosno signal DMSO-a u ^{13}C spektru (39,52 ppm). Konstante sprezanja (J) izražene su u Hz. Spektri masa snimljeni su na HPLC-MS/MS instrumentima (HPLC, Agilent Technologies 1200; MS, Agilent Technologies 6410 Triple Quad, SAD) (HPLC, Shimadzu SCL-40; MS, Shimadzu LCMS-2020, Japan). Kao tehnika ionizacije korištena je ionizacija elektroraspršenjem (ESI) u pozitivnom i negativnom modu. Pokretne faze sastojale su se od mili Q vode kao komponente A i metanola HPLC stupnja čistoće (J.T. Baker, SAD) kao komponente B. Kao nepokretna faza korištena je obrnuto-fazna kolona Zorbax XDB C18 dimenzija 75 mm × 4,6 mm te veličine čestica 3,5 μm. Odvajanje sastojaka nanesenih na kromatografsku kolonu ostvareno je gradijentnim ispiranjem uz protok pokretne faze 0,5 mL/min, dok je volumen injektiranog uzorka iznosio 5 μL. Početni uvjeti i gradijentni program pokretne faze prilagođavani su prema polarnosti analita. Eluacija sastavnica s kromatografske kolone praćena je primjenom apsorpcijskog detektora s nizom fotosenzitivnih dioda, a rezultati su prikazani kao kromatogram ukupne valne duljine (TWC, engl. *total wavelength chromatogram*,). Kao tehnika ionizacije korištena je ionizacija elektroraspršenjem (ESI) u pozitivnom i negativnom modu, pri čemu je kapilarni napon bio 4,0 kV, a struja 20 nA. Tlak u raspršivaču iznosio je 15 psi, a protok i temperatura plina za sušenje (dušik) bili su 11 L/min odnosno 300 °C. Za analizu MS podataka korišten je program Agilent MassHunter (Agilent Technologies, SAD). IR spektri snimljeni su na Paragon 500 (PerkinElmer, SAD) ili Fourier-

Transform Infrared Attenuated Total Reflection UATR Two (PerkinElmer, SAD) spektrofotometru u području valnih brojeva od 4000 do 450 cm^{-1}.

Harmin, 2,2-dimetoksiacetaldehid, acetaldehid-dimetilacetal, cimetna kiselina, α-metilcimetna kiselina, 2-fluorcimetna kiselina, 3-fluorcimetna kiselina, 4-fluorcimetna kiselina, 4-klorcimetna kiselina, 4-metoksicimetna kiselina, 3-(trifluormetil)cimetna kiselina, 4-(trifluormetl)cimetna kiselina, 3,5-*bis*-(trifluormetil)cimetna kiselina, cimetni alkohol, octena kiselina, 1,8-diazabiciklo[5.4.0]undek-7-en (DBU), 1*H*-benzo[*d*][1,2,3]triazol (benzotriazol, BtH), trifozgen, tionil-klorid, bezvodni metanol, 10 %-tni paladij na aktivnom ugljenu, litijev karbonat, litijev aluminijev hidrid i natrijev hidrid nabavljeni su od tvrtke Sigma-Aldrich (SAD). Triptamin, metilni ester triptofan hidroklorid, 5-metoksitriptamin, trifluoroctena kiselina (TFA), 2-azido-1,3-dimetilimidazolinijev heksafluorofosfat (ADMP), tetrabutilamonijev hidrogensulfat (TBAHS), 2-(*tert*-butoksikarbonilamino)etil bromid, 3-bromcimetna kiselina, 4-propoksicimetna kiselina, 2-klorcimetna kiselina, 3-klorcimetna kiselina, 3-(trifluormetoksi)cimetna kiselina, 4-bromcimetna kiselina, 4-metilcimetna kiselina, 4-nitrocimetna kiselina, 1-(*bis*(dimetilamino)metilen)-1*H*-1,2,3-triazolo(4,5-*b*)piridinijev 3-oksid heksafluorofosfat (HATU), 1,1'-karbonildiimidazol (CDI), cezijev karbonat i *N*,*N*-dimetilformamid (DMF) nabavljeni su od tvrtke TCI Chemicals (Japan). Bromovodična kiselina (47 %) i bezvodni tetrahidrofuran nabavljeni su od tvrtke Merck (Njemačka). Metanol, etil-acetat, cikloheksan, petroleter, toluen, 36 %-tna klorovodična kiselina nabavljeni su od tvrtke Honeywell (SAD). *N*,*N*-diizopropiletilamin (DIEA) i trietilamin (TEA) nabavljeni su od tvrtke Alfa Aesar (Njemačka). 1 M otopina klorovodične kiseline u etil-acetatu, diklormetan i bezvodni dietil-eter nabavljeni su od tvrtke Thermo Fisher Scientific (SAD). Bezvodni etanol je nabavljen od tvrtke Acros Organics (Belgija). Bezvodni natrijev sulfat, natrijev klorid, kalijev permanganat i amonijev klorid nabavljeni su od tvrtke Gram-Mol (Hrvatska). Natrijev hidroksid i natrijev hidrogenkarbonat nabavljeni su od tvrtke Kemika (Hrvatska). Cimetna kiselina i DCK-i nabavljeni su kao *trans* stereoizomeri (≥ 99 %).

U eksperimentalnom dijelu korištena su bezvodna otapala. Bezvodni toluen dobiven je sljedećim postupkom: toluen je ekstrahiran vodom, osušen nad bezvodnim kalcijevim kloridom, destiliran i čuvan nad elementarnim natrijem. Bezvodni dimetilformamid (DMF): smjesa 1 L DMF-a čuvana je nad aktiviranim molekulskim sitima. Bezvodni diklormetan dobiven je na sljedeći način: diklormetan je ekstrahiran vodom, sušen iznad kalcijevog klorida, predestiliran i čuvan nad aktiviranim molekulskim sitima.

Sve kemikalije bile su *p. a.* čistoće.

Harmol je sintetiziran prema prilagođenom ranije objavljenom propisu (75, 153). Spojevi **1**-**3**, **8**-**10** i **15** su pripravljeni prema poznatim propisima (154–156). Spoj **4** je poznat i opisan (157, 158), ali je razvijena alternativna metoda za njegovu pripravu. Fenol **16** je pripravljen prema prilagođenom ranije objavljenom propisu (159). Cinamilni azidi **29b**,**c** su pripravljeni prema prilagođenom ranije objavljenom propisu (75). Amini **6** i **31c**, su komercijalno dostupni, ali je razvijena metoda za njihovu pripravu. Cinamilni alkoholi **27c-g**,**i-k** su poznati spojevi (160–163) i komercijalno su dostupni, ali je razvijena metoda za njihovu sintezu. Klorid 1-benzotriazolkarboksilne kiseline pripravljen je prema poznatom propisu (164).

3.2. SINTEZE

3.2.1. Sinteza derivata u položaju 1 β-karbolinskog prstena (1-7)

*3.2.1.1. Sinteza 1-(dimetoksimetil)-2,3,4,9-tetrahidro-1H-pirido[3,4-b]indola (**1**)*

Suspenzija triptamina (1,0 g, 6,24 mmol) u diklormetanu (9 mL) miješana je na sobnoj temperaturi 5 min, nakon čega je u suspenziju dodan 2,2-dimetoksi acetaldehid (60 %-tna vodena otopina; 1,13 mL, 7,49 mmol), te je polagano, unutar 10 minuta, dokapavana otopina TFA (0,654 mL, 8,80 mmol) u diklormetanu (2,18 mL). Reakcijska smjesa miješana je na sobnoj temperaturi 18 h, nakon čega je reakcija prekinuta dodavanjem 10 %-tne otopine $NaHCO_3$ (40 mL). Reakcijska smjesa zakiseljena je do pH 7,6 te ekstrahirana diklormetanom (3 × 30 mL). Organski slojevi su sakupljeni i isprani vodom (1 × 30 mL), sušeni nad bezvodnim natrijevim sulfatom, filtrirani te je otapalo iz filtrata uklonjeno uparavanjem pod sniženim tlakom. Dobiveno smeđe ulje sirovog produkta **1** (1,21 g) korišteno je u idućem reakcijskom koraku bez dodatnog pročišćavanja.

*3.2.1.2. Sinteza 1-(dimetoksimetil)-9H-pirido[3,4-b]indola (**2**)*

U otopinu spoja **1** (1,21 g, 4,91 mmol) u bezvodnom THF-u (7 mL) dodan je kalijev permangant (3,10 g, 19,64 mmol). Reakcijska smjesa miješana je na sobnoj temperaturi 48 h, zatim profiltrirana kroz celit. Sloj celita ispran je metanolom (10 mL), etil-acetatom (30 mL) i diklormetanom (30 mL). Organska otapala su iz filtrata uklonjena uparavanjem pod sniženim tlakom, a zaostatni talog crne boje otopljen je u diklormetanu (60 mL) i ispran vodom (2 × 40 mL). Organski sloj je sušen nad bezvodnim natrijevim sulfatom, filtriran, a otapalo je iz filtrata uklonjeno uparavanjem pod sniženim tlakom. Sirovi produkt spoja **2** pročišćen je kromatografijom na koloni uz pokretnu fazu etil-acetat:metanol (10:0,5).

Iskorištenje: 0,702 g (59 %).

*3.2.1.3. Sinteza 9H-pirido[3,4-b]indol-1-karbaldehida (**3**)*

Otopina spoja **2** (0,897 g, 3,70 mmol) u smjesi ledene octene kiseline (4,66 mL) i vode (6,99 mL) miješana je 1 h na temperaturi refluksa (100 °C), nakon čega je reakcijska smjesa ohlađena na sobnu temperaturu, zalužena 5 %-tnom otopinom NaOH do pH 8-9, te ekstrahirana etil-acetatom (4 × 50 mL). Organski slojevi su sakupljeni, sušeni nad bezvodnim natrijevim sulfatom, filtrirani, a otapalo je iz filtrata uklonjeno upravanjem pod sniženim tlakom. Pročišćavanjem kromatografijom na koloni uz pokretnu fazu cikloheksan:etil-acetat:metanol (1:1:0,5) dobiven je čist produkt **3**. Iskorištenje: 0,494 g (68 %).

*3.2.1.4. Sinteza (9H-pirido[3,4-b]indol-1-il)metanola (**4**)*

Suspenziji spoja **3** (0,453 g, 2,31 mmol) u bezvodnom THF-u (6 mL) dodavan je $LiAlH_4$ (0,131 g, 3,46 mmol) u malim obrocima. Reakcijska smjesa miješana je 1 h na sobnoj temperaturi pod atmosferom argona. Potom je reakcijska smjesa zakiseljena 10 %-tnom otopinom klorovodične kiseline do pH 8 te ekstrahirana etil-acetatom (4 × 50 mL). Organski slojevi su sakupljeni, sušeni nad bezvodnim natrijevim sulfatom, filtrirani, a otapalo je iz filtrata uklonjeno uparavanjem pod sniženim tlakom. Rastrljavanjem u dietil-eteru dobiven je čist produkt **4**.
Iskorištenje: 0,417 g (91 %).

*3.2.1.5. Sinteza 1-(azidometil)-9H-pirido[3,4-b]indola (**5**)*

Otopina spoja **4** (0,309 g, 1,56 mmol) u bezvodnom THF-u (8 mL) ohlađena je na 0 °C te su joj dodani DBU (0,630 mL, 4,21 mmol) i ADMP (1,11 g, 3,90 mmol). Reakcijska smjesa miješana je 1 h na 0 °C, zatim je daljnji tijek reakcije prekinut dodatkom zasićene otopine amonijeva klorida (40 mL), nakon čega je reakcijska smjesa ekstrahirana diklormetanom (2 × 30 mL). Organski slojevi su sakupljeni te ekstrahirani zasićenom otopinom natrijeva klorida (2 × 30 mL) i vodom (1 × 20 mL), sušeni nad bezvodnim natrijevim sulfatom, filtrirani, a otapalo je iz filtrata uklonjeno uparavanjem pod sniženim tlakom. Sirovi produkt je pročišćen kromatografijom na koloni uz pokretnu fazu cikloheksan:etil-acetat:metanol (1:1:0,5).
Iskorištenje: 0,233 g (67 %).
Ulje.
IR (ATR, ν/cm^{-1}) 3663, 3451, 3288, 3059, 2937, 2855, 2105, 1730, 1631, 1566, 1493, 1428, 1371, 1321, 1248, 1118, 1052, 971, 938, 873, 824, 751, 718, 620, 579, 432.

^{1}H NMR (DMSO-d_6, δ ppm) δ 11,78 (s, 1H, 10), 8,36 (d, 1H, 7, J = 5,2 Hz), 8,29 – 8,23 (m, 1H, 3), 8,13 (d, 1H, 6, J = 5,2 Hz), 7,64 (dt, 1H, 12, J = 8,3, 0,9 Hz), 7,60 – 7,57 (m, 1H, 1), 7,29 – 7,26 (m, 1H, 2), 4,89 (s, 2H, 1').
^{13}C NMR (DMSO-d_6, δ ppm) δ 140,58 (8), 139,19 (11), 137,75 (7), 133,86 (9), 128,50 (5), 128,44 (1), 121,87 (3), 120,74 (4), 119,57 (2), 114,77 (6), 112,02 (12), 51,59 (1').

*3.2.1.6. Sinteza (9H-pirido[3,4-b]indol-1-il)metanamina (**6**)*

Suspenzija spoja **5** (0,191 g, 0,856 mmol) i 10 % Pd/C (0,041 g) u metanolu (5 mL) miješana je 18 h na sobnoj temperaturi u atmosferi vodika. Potom je reakcijska smjesa profiltrirana kroz celit, a otapalo je iz filtrata uklonjeno uparavanjem pod sniženim tlakom. Zaostatni talog je rastrljan u smjesi dietil-etera i petroletera.
Iskorištenje: 0,120 g (71 %).
t_t 201,0 – 205,0 °C (raspad).
IR (ATR, ν/cm^{-1}) 3347, 3282, 3120, 3051, 2955, 2856, 2776, 1625, 1600, 1562, 1501, 1477, 1460, 1430, 1355, 1327, 1316, 1240, 1212, 1163, 1127, 1108, 1071, 960, 896, 848, 829, 772, 747, 671, 595, 564, 516.
^{1}H NMR (DMSO-d_6, δ ppm) δ 8,26 (d, 1H, 7, J = 5,2 Hz), 8,21 (dt, 1H, 3, J = 7,8, 1,0 Hz), 7,97 (d, 1H, 6, J = 5,2 Hz), 7,63 – 7,62 (m, 1H, 12), 7,55 – 7,52 (m, 1H, 1), 7,24 – 7,22 (m, 1H, 2), 4,19 (s, 2H, 1').
^{13}C NMR (DMSO-d_6, δ ppm) δ 146,51 (8), 140,35 (11), 137,18 (7), 133,23 (9), 127,82 (1), 127,42 (5), 121,60 (3), 120,88 (4), 119,15 (2), 113,19 (6), 112,01 (12), 44,59 (1').
ESI-MS: *m/z* 196,0 $(M-1)^-$.

*3.2.1.7. Sinteza harmicina u položaju 1 β-karbolinskog prstena (**7a-h**). Opća metoda*

Otopina odgovarajućeg DCK-a (0,212 mmol), DIEA (0,074 mL, 0,424 mmol) i HATU (0,081 g, 0,212 mmol) u diklormetanu (4 mL) miješana je na sobnoj temperaturi 20 min, nakon čega je u reakcijsku smjesu dodan amin **6** (0,038 g, 0,193 mmol). Reakcijska smjesa miješana je na sobnoj temperaturi 1 h. Novonastali talog je odsisan i pročišćen kromatografijom na koloni uz pokretnu fazu diklormetan:metanol (8:1). Rastrljavanjem u dietil-eteru dobiveni su čisti produkti **7a-h**.

*3.2.1.7.1. N-((9H-pirido[3,4-b]indol-1-il)metil)cinamamid (**7a**)*

Količina reaktanta: 0,031 g *trans*-cimetne kiseline.

Iskorištenje: 0,033 g (52 %).

t_t 225,0 – 227,0 °C.

IR (ATR, ν/cm^{-1}) 3375, 3328, 3226, 3195, 3101, 3060, 2901, 1661, 1623, 1576, 1514, 1435, 1404, 1325, 1243, 1205, 994, 914, 811, 767, 731, 718, 706, 620, 565, 490, 478.

^{1}H NMR (DMSO-d_6, δ ppm) δ 11,62 (s, 1H, 10), 8,78 (t, 1H, 2', J = 5,4 Hz), 8,32 (d, 1H, 7, J = 5,2 Hz), 8,24 (d, 1H, 3, J = 7,9 Hz), 8,06 (d, 1H, 6, J = 5,3 Hz), 7,65 – 7,63 (m, 1H, 12), 7,60 – 7,49 (m, 4H, 1, 5', 7', 11'), 7,45 – 7,34 (m, 3H, 8' – 10'), 7,28 – 7,23 (m, 1H, 2), 6,87 (d, 1H, 4', J = 15,8 Hz), 4,91 (d, 2H, 1', J = 5,3 Hz).

^{13}C NMR (DMSO-d_6, δ ppm) δ 165,43 (3'), 141,41 (8), 140,45 (11), 139,04 (5'), 137,34 (7), 134,92 (9), 133,52 (6'), 129,49 (3), 128,94 (7', 11'), 128,17 (9'), 127,82 (5), 127,58 (8', 10'), 122,10 (1), 121,76 (4'), 120,87 (4), 119,45 (2), 113,96 (6), 112,08 (12), 41,65 (1').

ESI-MS: *m/z* 328,1 $[M+1]^+$.

HPLC čistoća > 99,5 %.

*3.2.1.7.2. (E)-N-((9H-pirido[3,4-b]indol-1-il)metil)-3-(3-fluorfenil)akrilamid (**7b**)*

Količina reaktanta: 0,035 g 3-fluorcimetne kiseline.

Iskorištenje: 0,034 g (51 %).

t_t 224,5 – 225,5 °C.

IR (ATR, ν/cm^{-1}) 3350, 3217, 3149, 3080, 2995, 2905, 2814, 1672, 1627, 1586, 1516, 1448, 1409, 1325, 1273, 1239, 1225, 1146, 1011, 968, 878, 851, 807, 784, 728, 611, 564, 521.

^{1}H NMR (DMSO-d_6, δ ppm) δ 11,63 (s, 1H, 10), 8,78 (t, 1H, 2', J = 5,4 Hz), 8,32 (d, 1H, 7, J = 5,2 Hz), 8,24 (d, 1H, 3, J = 7,8 Hz), 8,07 (d, 1H, 6, J = 5,2 Hz), 7,64 (d, 1H, 12, J = 8,2 Hz), 7,57 (t, 1H, 2, J = 7,6 Hz), 7,52 (d, 1H, 5', J = 15,8 Hz), 7,49 – 7,43 (m, 3H, 1, 10', 11'), 7,26 (t, 1H, 7', J = 7,4 Hz), 7,23 – 7,20 (m, 1H, 9'), 6,94 (d, 1H, 4', J = 15,8 Hz), 4,92 (d, 2H, 1', J = 5,3 Hz).

^{13}C NMR (DMSO-d_6, δ ppm) δ 165,08 (3'), 162,46 (d, 8', J = 244,0 Hz), 141,26 (8), 140,45 (11), 137,71 (d, 5', J = 2,4 Hz), 137,58 (d, 6', J = 7,8 Hz), 137,37 (7), 133,48 (9), 130,90 (d, 10', J = 8,4 Hz), 128,16 (3), 127,80 (5), 123,75 (d, 11', J = 2,5 Hz), 123,70 (1), 121,76 (4'), 120,87 (4), 119,44 (2), 116,14 (d, 9', J = 21,2 Hz), 113,96 (6), 113,96 (d, 7', J = 21,8 Hz), 112,07 (12), 41,65 (1').

ESI-MS: *m/z* 346,1 $[M+1]^+$.

HPLC čistoća 98,2 %.

*3.2.1.7.3. (E)-N-((9H-pirido[3,4-b]indol-1-il)metil)-3-(3-bromfenil)akrilamid (**7c**)*

Količina reaktanta: 0,048 g 3-bromcimetne kiseline.

Iskorištenje: 0,056 g (72 %).

t_t 236,5 – 239,0 °C.

IR (ATR, ν/cm^{-1}) 3191, 3016, 1671, 1626, 1564, 1497, 1471, 1437, 1392, 1328, 1222, 1128, 1078, 971, 929, 820, 778, 722, 667, 584.

^{1}H NMR (DMSO-d_6, δ ppm) δ 11,62 (s, 1H, 10), 8,74 (t, 1H, 2', J = 5,4 Hz), 8,31 (d, 1H, 7, J = 5,2 Hz), 8,23 (d, 1H, 3, J = 7,8 Hz), 8,06 (d, 1H, 6, J = 5,2 Hz), 7,80 (t, 1H, 7', J = 1,9 Hz), 7,63 (d, 1H, 12, J = 8,2 Hz), 7,59 (d, 1H, 11', J = 7,8 Hz), 7,57 – 7,54 (m, 2H, 1, 2), 7,47 (d, 1H, 5', J = 15,8 Hz), 7,37 (t, 1H, 10', J = 7,9 Hz), 7,25 (t, 1H, 9', J = 7,4 Hz), 6,94 (d, 1H, 4', J = 15,8 Hz), 4,91 (d, 2H, 1', J = 5,3 Hz).

^{13}C NMR (DMSO-d_6, δ ppm) δ 165,01 (3'), 141,20 (8), 140,46 (11), 137,53 (6'), 137,34 (5'), 137,30 (7), 133,46 (9), 131,98 (7'), 131,02 (9'), 130,06 (10'), 128,17 (3), 127,82 (5), 126,49 (11'), 123,82 (1), 122,26 (8'), 121,76 (4'), 120,85 (4), 119,44 (2), 113,96 (6), 112,06 (12), 41,62 (1').

ESI-MS: *m/z* 405,9 $[M+1]^+$, 407,9 $[M+1]^+$.

HPLC čistoća 99,4 %.

*3.2.1.7.4. (E)-N-((9H-pirido[3,4-b]indol-1-il)metil)-3-(3-(trifluormetil)fenil)akrilamid (**7d**)*

Količina reaktanta: 0,046 g 3-(trifluormetil)cimetne kiseline.

Iskorištenje: 0,040 g (52 %).

t_t 225,5 – 226,5 °C.

IR (ATR, ν/cm^{-1}) 3197, 3014, 1669, 1628, 1560, 1498, 1438, 1329, 1226, 1177, 1167, 1109, 1077, 972, 885, 804, 742, 721, 691, 581.

^{1}H NMR (DMSO-d_6, δ ppm) δ 11,65 (s, 1H, 10), 8,78 (t, 1H, 2', J = 5,3 Hz), 8,33 (d, 1H, 7, J = 5,2 Hz), 8,24 (dt, 1H, 3, J = 7,9, 1,0 Hz), 8,07 (d, 1H, 6, J = 5,2 Hz), 7,96 (t, 1H, 7', J = 2,0 Hz), 7,90 (d, 1H, 12, J = 7,8 Hz), 7,73 (d, 1H, 11', J = 7,8 Hz), 7,67 – 7,63 (m, 2H, 1, 9'), 7,60 (d, 1H, 5', J = 15,8 Hz), 7,58 – 7,55 (m, 1H, 2), 7,28 – 7,25 (m, 1H, 10'), 7,06 (d, 1H, 4', J = 15,9 Hz), 4,93 (d, 2H, 1', J = 5,3 Hz).

^{13}C NMR (DMSO-d_6, δ ppm) δ 164,96 (3'), 141,19 (8), 140,47 (11), 137,35 (5'), 137,26 (7), 136,19 (6'), 133,47 (9), 131,37 (11'), 130,05 (10'), 129,74 (q, 8', J = 31,7 Hz), 128,15 (3), 127,80 (5), 125,72 (q, 9', J = 2,7 Hz), 124,33 (1), 124,06 (q, 12', J = 273,3 Hz), 123,92 (q, 7', J = 3,6 Hz), 121,75 (4'), 120,87 (4), 119,44 (2), 113,96 (6), 112,07 (12), 41,67 (1').

ESI-MS: *m/z* 396,1 $[M+1]^+$

HPLC čistoća 97,3 %.

*3.2.1.7.5. (E)-N-((9H-pirido[3,4-b]indol-1-il)metil)-3-(4-fluorfenil)akrilamid (**7e**)*

Količina reaktanta: 0,035 g 4-fluorcimetne kiseline.

Iskorištenje: 0,045 g (67 %).

t_t 231,5 – 233,0 °C.

IR (ATR, ν/cm^{-1}) 3380, 3244, 3147, 3075, 2989, 2900, 1655, 1616, 1599, 1556, 1505, 1430, 1426, 1413, 1354, 1325, 1239, 1220, 1161, 1128, 1098, 1010, 977, 828, 755, 734, 628, 508.

^{1}H NMR (DMSO-d_6, δ ppm) δ 11,62 (s, 1H, 10), 8,75 (t, 1H, 2', J = 5,4 Hz), 8,32 (d, 1H, 7, J = 5,2 Hz), 8,24 (d, 1H, 3, J = 7,8 Hz), 8,06 (d, 1H, 6, J = 5,2 Hz), 7,66 – 7,63 (m, 3H, 12, 7', 11'), 7,56 (t, 1H, 1, J = 7,6 Hz), 7,51 (d, 1H, 5', J = 15,8 Hz), 7,27 – 7,24 (m, 3H, 2, 8', 10'), 6,83 (d, 1H, 4', J = 15,8 Hz), 4,91 (d, 2H, 1', J = 5,3 Hz).

^{13}C NMR (DMSO-d_6, δ ppm) δ 165,31 (3'), 162,69 (d, 9', J = 247,0 Hz), 141,39 (8), 140,42 (11), 137,80 (4'), 137,35 (7), 133,49 (9), 131,56 (d, 6', J = 3,0 Hz), 129,71 (d, 7', 11', J = 8,4 Hz), 128,12 (3), 127,77 (5), 122,00 (d, 5', J = 1,7 Hz), 121,73 (1), 120,86 (4), 119,41 (2), 115,89 (d, 8', 10', J = 21,8 Hz), 113,92 (6), 112,05 (12), 41,64 (1').

ESI-MS: *m/z* 346,1 $[M+1]^+$.

*3.2.1.7.6. (E)-N-((9H-pirido[3,4-b]indol-1-il)metil)-3-(4-klorfenil)akrilamid (**7f**)*

Količina reaktanta: 0,039 g 4-klorcimetne kiseline.

Iskorištenje: 0,036 g (52 %).

t_t 241,0 – 243,5 °C (raspad).

IR (ATR, ν/cm^{-1}) 3384, 3275, 3053, 1671, 1627, 1532, 1505, 1494, 1457, 1435, 1405, 1323, 1237, 1219, 1094, 1028, 1013, 972, 819, 732, 609, 589, 573, 495.

^{1}H NMR (DMSO-d_6, δ ppm) δ 11,62 (s, 1H, 10), 8,79 (t, 1H, 2', J = 5,4 Hz), 8,32 (d, 1H, 7, J = 5,2 Hz), 8,24 (d, 1H, 3, J = 7,8 Hz), 8,06 (d, 1H, 6, J = 5,2 Hz), 7,65 – 7,61 (m, 3H, 12, 7', 11'), 7,58 – 7,55 (m, 1H, 1), 7,52 – 7,48 (m, 3H, 5', 8', 10'), 7,26 (t, 1H, 2, J = 7,4 Hz), 6,89 (d, 1H, 4', J = 15,8 Hz), 4,91 (d, 2H, 1', J = 5,4 Hz).

^{13}C NMR (DMSO-d_6, δ ppm) δ 165,20 (3'), 141,35 (8), 140,45 (11), 137,67 (5'), 137,38 (7), 133,92 (9', 9), 133,51 (6'), 129,29 (7', 11'), 128,99 (8', 10'), 128,16 (3), 127,80 (5), 122,93 (1), 121,77 (4'), 120,88 (4), 119,45 (2), 113,96 (6), 112,08 (12), 41,66 (1').

ESI-MS: *m/z* 362,1 $[M+1]^+$, 364,1 $[M+1]^+$.

*3.2.1.7.7. (E)-N-((9H-pirido[3,4-b]indol-1-il)metil)-3-(4-metoksifenil)akrilamid (**7g**)*

Količina reaktanta: 0,038 g 4-metoksicimetne kiseline.

Iskorištenje: 0,034 g (49 %).

t_t 230,5 – 232,0 °C.

IR (ATR, ν/cm^{-1}) 3350, 3173, 3097, 3006, 1662, 1624, 1603, 1511, 1432, 1366, 1325, 1254, 1240, 1174, 1029, 981, 914, 818, 791, 733, 596, 528, 506.

^{1}H NMR (DMSO-d_6, δ ppm) δ 11,59 (s, 1H, 10), 8,68 (t, 1H, 2', J = 5,5 Hz), 8,31 (d, 1H, 7, J = 5,3 Hz), 8,23 (d, 1H, 3, J = 7,8 Hz), 8,06 (d, 1H, 6, J = 4,7 Hz), 7,64 (d, 1H, 12, J = 8,2 Hz), 7,57 – 7,52 (m, 3H, 1, 7', 11'), 7,46 (d, 1H, 5', J = 15,7 Hz), 7,25 (t, 1H, 2, J = 7,5 Hz), 6,97 (d, 2H, 8', 10', J = 8,2 Hz), 6,71 (d, 1H, 4', J = 15,7 Hz), 4,89 (d, 2H, 1', J = 5,5 Hz), 3,78 (s, 3H, 12').

^{13}C NMR (DMSO-d_6, δ ppm) δ 165,82 (3'), 160,39 (9'), 141,57 (8), 140,46 (11), 138,83 (5'), 137,34 (7), 133,54 (9), 129,20 (7', 11'), 128,20 (3), 127,85 (6'), 127,49 (5), 121,78 (1), 120,90 (4), 119,57 (4'), 119,48 (2), 114,42 (8', 10'), 113,98 (6), 112,10 (12), 55,28 (12'), 41,67 (1').

ESI-MS: m/z 358,1 $[M+1]^+$.

HPLC čistoća 99,0 %.

*3.2.1.7.8. (E)-N-((9H-pirido[3,4-b]indol-1-il)metil)-3-(4-(trifluormetil)fenil)akrilamid (**7h**)*

Količina reaktanta: 0,046 g 4-(trifluormetil)cimetne kiseline.

Iskorištenje: 0,050 g (65 %).

t_t 262,5 – 265,0 °C.

IR (ATR, ν/cm^{-1}) 3341, 3236, 1664, 1622, 1504, 1436, 1416, 1323, 1239, 1217, 1155, 1116, 1068, 1013, 988, 826, 755, 740, 572, 532, 494.

^{1}H NMR (DMSO-d_6, δ ppm) δ 11,65 (s, 1H, 10), 8,87 (t, 1H, 2', J = 5,4 Hz), 8,33 (d, 1H, 7, J = 5,3 Hz), 8,25 (d, 1H, 3, J = 7,9 Hz), 8,08 (d, 1H, 6, J = 5,3 Hz), 7,83 – 7,76 (m, 4H, 1, 12, 7', 11'), 7,66 – 7,54 (m, 3H, 5', 8', 10'), 7,29 – 7,24 (m, 1H, 2), 7,03 (d, 1H, 4', J = 15,8 Hz), 4,94 (d, 2H, 1', J = 5,3 Hz).

^{13}C NMR (DMSO-d_6, δ ppm) δ 164,89 (3'), 141,23 (8), 140,46 (11), 139,04 (6'), 137,38 (5'), 137,32 (7), 133,49 (9), 129,21 (q, 9', J = 32,3 Hz), 128,20 (7', 11'), 128,16 (1), 127,81 (5), 125,81 (q, 8', 10', J = 3,0 Hz), 124,95 (3), 124,12 (q, 12', J = 272,7 Hz), 121,76 (2), 120,87 (4), 119,44 (4'), 113,96 (6), 112,07 (12), 41,66 (1').

ESI-MS: m/z 396,1 $[M+1]^+$.

HPLC čistoća 99,4 %.

3.2.2. Sinteza derivata u položaju 3 β-karbolinskog prstena (8-13)

*3.2.2.1. Sinteza metil-1-metil-2,3,4,9-tetrahidro-1H-pirido[3,4-b]indol-3-karboksilata (**8**)*

U suspenziju metilnog estera triptofana hidroklorida (1,0 g, 3,93 mmol) u diklormetanu (8 mL) dodan je acetaldehid-dimetil acetal (95 %-tna vodena otopina; 0,526 mL, 4,71 mmol) te je dokapavana otopina TFA (0,583 mL, 7,85 mmol) u diklormetanu (2 mL). Reakcijska smjesa miješana je na sobnoj temperaturi 18 h. Potom je u reakcijsku smjesu dodana 10 %-tna otopina $NaHCO_3$ (30 mL) do pH 7,6. Reakcijska smjesa je zatim ekstrahirana diklormetanom (3 × 30 mL), a organski slojevi su sakupljeni, isprani vodom (1 × 30 mL), sušeni nad bezvodnim natrijevim sulfatom, filtrirani, a otapalo je iz filtrata uklonjeno uparavanjem pod sniženim tlakom. Dobiveno žuto ulje sirovog produkta **8** (1,04 g) korišteno je u idućem reakcijskom koraku bez dodatnog pročišćavanja.

*3.2.2.2. Sinteza metil-1-metil-9H-pirido[3,4-b]indol-3-karboksilata (**9a**) i etil-1-metil-9H-pirido[3,4-b]indol-3-karboksilata (**9b**)*

U otopinu spoja **8** (0,250 g, 1,02 mmol) u bezvodnom EtOH (4 mL) dodan je 10 %-tni Pd/C (0,083 g). Reakcijska smjesa miješana je u mikrovalnom reaktoru 20 minuta na 130 °C, nakon čega je ohlađena na sobnu temperaturu i profiltrirana kroz celit. Sloj celita ispran je metanolom, a otapala su iz filtrata uklonjena uparavanjem po sniženim tlakom. Smjesa sirovih produktata spojeva **9a**,**b** rastrljana je u smjesi dietil-etera i petroletera.

Iskorištenje: 0,150 g (61 %).

*3.2.2.3. Sinteza (1-metil-9H-pirido[3,4-b]indol-3-il)metanola (**10**)*

Suspenziji spojeva **9a** i **9b** (0,542 g, 2,26 mmol) u bezvodnom THF-u (6 mL) dodan je $LiAlH_4$ (0,172 g, 4,52 mmol). Reakcijska smjesa miješana je 1 h na sobnoj temperaturi pod atmosferom argona. Potom je reakcijska smjesa zakiseljena 10 %-tnom otopinom HCl-a do pH 9 te je ekstrahirana etil-acetatom (4 × 50 mL). Organski slojevi su sakupljeni, sušeni nad bezvodnim natrijevim sulfatom, filtrirani, a otapalo je iz filtrata uklonjeno uparavanjem pod sniženim tlakom. Rastrljavanjem u dietil-eteru dobiven je čist produkt **10**.

Iskorištenje: 0,437 g (91 %).

*3.2.2.4. Sinteza 3-(azidometil)-1-metil-9H-pirido[3,4-b]indola (**11**)*

Spoj je pripravljen analogno spoju **5**.

Količina reaktanta: 0,331 g alkohola **10**.

Iskorištenje: 0,281 g (76 %).

Ulje.

IR (ATR, ν/cm^{-1}) 3671, 3451, 3239, 3051, 2937, 2863, 2447, 2325, 2104, 1689, 1631, 1566, 1509, 1452, 1403, 1354, 1264, 1085, 1036, 971, 848, 759, 718, 644, 579, 431.

^{1}H NMR (DMSO-d_6, δ ppm) δ 11,66 (s, 1H, 10), 8,20 (d, 1H, 3, J = 7,9 Hz), 8,00 (s, 1H, 6), 7,62 – 7,60 (m, 1H, 12), 7,57 – 7,53 (m, 1H, 1), 7,26 – 7,23 (m, 1H, 2), 4,57 (s, 2H, 1'), 2,78 (s, 3H, 13).

^{13}C NMR (DMSO-d_6, δ ppm) δ 143,23 (7), 142,12 (11), 140,74 (8), 133,94 (9), 128,02 (1), 127,56 (5), 121,74 (3), 121,01 (4), 119,39 (2), 112,07 (12), 111,72 (6), 55,30 (1'), 20,41 (13).

*3.2.2.5. Sinteza (1-metil-9H-pirido[3,4-b]indol-3-il)metanamina (**12**)*

Suspenzija spoja **11** (0,203 g, 0,856 mmol) i 10 % Pd/C (0,041 g) u metanolu (5 mL) miješana je 2 h na sobnoj temperaturi u atmosferi vodika. Potom je reakcijska smjesa profiltrirana kroz celit, a otapalo je iz filtrata uklonjeno uparavanjem pod sniženim tlakom. Zaostatni talog je rastrljan u smjesi dietil-etera i petroletera.

Iskorištenje: 0,110 g (61 %).

t_t 176,0 – 178,5 °C.

IR (ATR, ν/cm^{-1}) 3338, 3239, 3130, 3057, 2978, 2940, 2914, 2882, 2850, 2783, 2737, 2690, 2637, 1626, 1606, 1566, 1503, 1453, 1401, 1374, 1344, 1317, 1284, 1250, 1176, 1147, 1103, 1083, 1009, 970, 945, 891, 838, 813, 775, 734, 643, 588, 545.

^{1}H NMR (DMSO-d_6, δ ppm) δ 11,42 (s, 1H, 10), 8,14 (d, 1H, 3, J = 7,6 Hz), 7,91 (s, 1H, 6), 7,57 – 7,47 (m, 2H, 12, 1), 7,20 (t, 1H, 2, J = 6,9 Hz), 3,89 (s, 2H, 1'), 2,73 (s, 3H, 13).

^{13}C NMR (DMSO-d_6, δ ppm) 151,13 (7), 140,89 (11), 140,74 (8), 133,29 (9), 127,76 (5), 127,62 (1), 121,53 (3), 121,19 (4), 118,98 (2), 111,89 (12), 109,01 (6), 47,59 (1'), 20,38 (13).

ESI-MS: m/z 210,0 $(M-1)^-$.

*3.2.2.6. Sinteza harmicina u položaju 3 β-karbolinskog prstena (**13a-h**). Opća metoda*

Otopina odgovarajućeg DCK-a (0,162 mmol), DIEA (0,056 mL, 0,324 mmol) i HATU (0,062 g, 0,162 mmol) u diklormetanu (4 mL) miješana je na sobnoj temperaturi 20 min, nakon čega je u reakcijsku smjesu dodan amin **12** (0,031 g, 0,147 mmol). Reakcijska smjesa miješana je na sobnoj temperaturi 1 h, zatim pročišćena metodom A ili metodom B.

Metoda A: Novonastali talog je odsisan i pročišćen kromatografijom na koloni uz pokretnu fazu diklormetan:metanol (8:1). Rastrljavanjem u dietil-eteru dobiveni su čisti produkti.

Metoda B: Nakon završetka reakcije, otapalo je upareno pod sniženim tlakom te je dodan etil-acetat (10 mL). Stajanjem kristalizira sirovi produkt koji je pročišćen kromatografijom na koloni uz pokretnu fazu diklormetan:metanol (8:1). Rastrljavanjem u dietil-eteru dobiveni su čisti produkti.

*3.2.2.6.1. N-((1-metil-9H-pirido[3,4-b]indol-3-il)metil)cinamamid (**13a**)*

Količina reaktanta: 0,024 g *trans*-cimetne kiseline.

Pročišćavanje: Metoda A.

Iskorištenje: 0,032 g (64 %).

t_t 207,0 – 208,0 °C.

IR (ATR, ν/cm^{-1}) 3352, 3284, 3089, 3048, 2896, 2851, 1659, 1621, 1568, 1510, 1451, 1388, 1354, 1319, 1284, 1246, 1206, 1176, 1075, 1015, 973, 899, 871, 741, 714, 643, 612, 587, 557, 487.

^{1}H NMR (DMSO-d_6, δ ppm) δ 11,54 (s, 1H, 10), 8,69 (t, 1H, 2', J = 5,7 Hz), 8,19 (d, 1H, 3, J = 7,8 Hz), 7,88 (s, 1H, 6), 7,60 – 7,58 (m, 3H, 7', 11', 12), 7,53 – 7,49 (m, 2H, 1, 5'), 7,44 – 7,41 (m, 2H, 8', 10'), 7,39 – 7,37 (m, 1H, 9'), 7,21 (t, 1H, 2, J = 7,4 Hz), 6,81 (d, 1H, 4', J = 15,8 Hz), 4,62 (d, 2H, 1', J = 5,8 Hz), 2,78 (s, 3H, 13).

^{13}C NMR (DMSO-d_6, δ ppm) 164,89 (3'), 146,07 (7), 141,27 (11), 140,79 (8), 138,77 (5'), 134,98 (6'), 133,55 (9), 129,41 (9'), 128,92 (8', 10'), 127,86 (1), 127,79 (5), 127,52 (7', 11'), 122,38 (3), 121,70 (4'), 120,99 (4), 119,17 (2), 111,93 (12), 110,08 (6), 44,64 (1'), 20,26 (13).

ESI-MS: m/z 342,4 $[M+1]^+$.

HPLC čistoća 97,1 %.

*3.2.2.6.2. (E)-3-(3-fluorfenil)-N-((1-metil-9H-pirido[3,4-b]indol-3-il)metil)akrilamid (**13b**)*

Količina reaktanta: 0,027 g 3-fluorcimetne kiseline.

Pročišćavanje: Metoda A.

Iskorištenje: 0,022 g (41 %).

t_t 118,0 – 119,0 °C.

IR (ATR, ν/cm^{-1}) 3242, 3080, 2972, 2907, 2783, 1658, 1620, 1571, 1501, 1451, 1420, 1341, 1247, 1144, 1032, 983, 899, 859, 779, 740, 632, 561, 517.

^{1}H NMR (DMSO-d_6, δ ppm) δ 11,52 (s, 1H, 10), 8,69 (t, 1H, 2', J = 5,5 Hz), 8,18 (d, 1H, 3, J = 7,4 Hz), 7,87 (s, 1H, 6), 7,59 – 7,42 (m, 6H, 1, 2, 12, 5', 10', 11'), 7,24 – 7,19 (m, 2H, 7', 9'), 6,85 (d, 1H, 4', J = 15,7 Hz), 4,61 (d, 2H, 1', J = 4,3 Hz), 2,77 (s, 3H, 13).

^{13}C NMR (DMSO-d_6, δ ppm) δ 164,59 (3'), 162,46 (d, 8', J = 243,9 Hz), 146,03 (7), 141,35 (11), 140,75 (8), 137,63 (d, 6', J = 7,9 Hz), 137,47 (5'), 133,57 (9), 130,89 (d, 10', J = 8,3 Hz), 127,83 (11'), 127,73 (5), 123,97 (1), 123,67 (3), 121,68 (4'), 121,00 (4), 119,15 (2), 116,07 (d, 9', J = 21,4 Hz), 113,92 (d, 7', J = 21,8 Hz), 111,94 (12), 110,07 (6), 44,73 (1'), 20,34 (13).
ESI-MS: *m/z* 360,3 $[M+1]^+$.

*3.2.2.6.3. (E)-3-(3-bromfenil)-N-((1-metil-9H-pirido[3,4-b]indol-3-il)metil)akrilamid (**13c**)*
Količina reaktanta: 0,037 g 3-bromcimetne kiseline.
Pročišćavanje: Metoda A.
Iskorištenje: 0,017 g (28 %).
t_t 121,5 – 123,5 °C.
IR (ATR, ν/cm^{-1}) 3243, 3082, 1743, 1725, 1655, 1617, 1562, 1501, 1452, 1419, 1470, 1396, 1340, 1248, 1234, 1150, 1069, 1029, 984, 899, 863, 779, 741, 697, 666, 638, 609, 561.
^{1}H NMR (DMSO-d_6, δ ppm) δ 11,54 (s, 1H, 10), 8,68 (t, 1H, 2', J = 5,8 Hz), 8,18 (d, 1H, 3, J = 7,9 Hz), 7,87 (s, 1H, 6), 7,80 (t, 1H, 7', J = 1,8 Hz), 7,61 – 7,56 (m, 3H, 12, 9', 11'), 7,52 (t, 1H, 1, J = 7,4 Hz), 7,47 (d, 1H, 5', J = 15,8 Hz), 7,39 (t, 1H, 10', J = 7,9 Hz), 7,21 (t, 1H, 2, J = 7,4 Hz), 6,87 (d, 1H, 4', J = 15,8 Hz), 4,62 (d, 2H, 1', J = 5,8 Hz), 2,78 (s, 3H, 13).
^{13}C NMR (DMSO-d_6, δ ppm) δ 164,53 (3'), 145,98 (7), 141,34 (11), 140,77 (8), 137,60 (6'), 137,13 (5'), 133,57 (9), 131,94 (7'), 131,04 (9'), 130,04 (10'), 127,86 (11'), 127,76 (5), 126,43 (1), 124,08 (3), 122,26 (8'), 121,70 (4'), 121,00 (4), 119,17 (2), 111,95 (12), 110,08 (6), 44,70 (1'), 20,32 (13).
ESI-MS: *m/z* 420,0 $[M+1]^+$, 422,0 $[M+1]^+$.
HPLC čistoća 98,3 %.

*3.2.2.6.4. (E)-N-((1-metil-9H-pirido[3,4-b]indol-3-il)metil)-3-(3-(trifluormetil)fenil)akrilamid (**13d**)*
Količina reaktanta: 0,035 g 4-(trifluormetil)cimetne kiseline.
Pročišćavanje: Metoda B.
Iskorištenje: 0,023 g (39 %).
t_t 235,5 – 237,0 °C (raspad).
IR (ATR, ν/cm^{-1}) 3339, 3251, 3084, 2992, 2950, 2893, 2855, 2786, 1664, 1622, 1570, 1517, 1470, 1451, 1396, 1331, 1284, 1249, 1229, 1165, 1122, 1095, 1072, 1020, 969, 937, 899, 864, 803, 777, 738, 695, 657, 596, 559, 524, 507.

^{1}H NMR (DMSO-d_6, δ ppm) δ 11,53 (s, 1H, 10), 8,70 (t, 1H, 2', J = 5,8 Hz), 8,18 (d, 1H, 3, J = 7,9 Hz), 7,95 (t, 1H, 7', J = 2,0 Hz), 7,90 (d, 1H, 12, J = 7,8 Hz), 7,88 (s, 1H, 6), 7,74 (d, 1H, 11', J = 7,8 Hz), 7,67 (t, 1H, 2, J = 7,8 Hz), 7,61 – 7,58 (m, 2H, 5', 1), 7,54 – 7,51 (m, 1H, 9'), 7,22 – 7,20 (m, 1H, 10'), 6,96 (d, 1H, 4', J = 15,9 Hz), 4,63 (d, 2H, 1', J = 5,8 Hz), 2,78 (s, 3H, 13).

^{13}C NMR (DMSO-d_6, δ ppm) δ 164,49 (3'), 145,97 (7), 141,37 (11), 140,77 (8), 137,06 (5'), 136,23 (6'), 133,58 (9), 131,31 (11'), 130,07 (10'), 129,73 (d, 8', J = 31,7 Hz), 127,85 (1) 127,75 (5), 125,69 (q, 9', J = 3,5 Hz), 124,06 (q, 12', J = 272,8 Hz), 124,56 (3), 123,88 (q, 7', J = 3,5 Hz), 121,69 (4'), 121,01 (4), 119,16 (2), 111,95 (12), 110,07 (6), 44,74 (1'), 20,34 (13).

ESI-MS: m/z 410,1 $[M+1]^+$.

HPLC čistoća 98,4 %.

*3.2.2.6.5. (E)-3-(4-fluorfenil)-N-((1-metil-9H-pirido[3,4-b]indol-3-il)metil)akrilamid (**13e**)*

Količina reaktanta: 0,027 g 4-fluorcimetne kiseline.

Pročišćavanje: Metoda A.

Iskorištenje: 0,018 g (34 %).

t_t 217,5 – 219,5 °C (raspad).

IR (ATR, ν/cm^{-1}) 3243, 3077, 2993, 2950, 2913, 2890, 2851, 2785, 1655, 1620, 1597, 1571, 1553, 1507, 1451, 1416, 1394, 1341, 1318, 1282, 1249, 1226, 1156, 1124, 1094, 1033, 1011, 984, 933, 899, 859, 830, 788, 739, 693, 643, 608, 591, 565, 506, 462.

^{1}H NMR (DMSO-d_6, δ ppm) δ 11,52 (s, 1H, 10), 8,67 (t, 1H, 2', J = 5,1 Hz), 8,18 (d, 1H, 3, J = 7,8 Hz), 7,87 (s, 1H, 6), 7,67 – 7,63 (m, 2H, 7', 11'), 7,59 – 7,48 (m, 3H, 1, 5', 12), 7,26 (t, 2H, 8', 10', J = 8,7 Hz), 7,20 (t, 1H, 2, J = 7,4 Hz), 6,75 (d, 1H, 4', J = 15,8 Hz), 4,61 (d, 2H, 1', J = 5,5 Hz), 2,77 (s, 3H, 13).

^{13}C NMR (DMSO-d_6, δ ppm) δ 164,81 (3'), 162,66 (d, 9', J = 246,9 Hz), 146,14 (7), 141,32 (11), 140,75 (8), 137,57 (5'), 133,56 (9), 131,62 (d, 6', J = 3,2 Hz), 129,66 (d, 7', 11', J = 8,4 Hz), 127,82 (1), 127,72 (5), 122,28 (3), 121,68 (4'), 121,00 (4), 119,14 (2), 115,90 (d, 8', 10', J = 21,7 Hz), 111,93 (12), 110,04 (6), 44,70 (1'), 20,33 (13).

ESI-MS: m/z 360,1 $[M+1]^+$.

HPLC čistoća 98,8 %.

*3.2.2.6.6. (E)-3-(4-klorfenil)-N-((1-metil-9H-pirido[3,4-b]indol-3-il)metil)akrilamid (**13f**)*

Količina reaktanta: 0,030 g 4-klorcimetne kiseline.

Pročišćavanje: Metoda A.

Iskorištenje: 0,012 g (21 %).

t_t 255,0 – 257,5 °C (raspad).

IR (ATR, ν/cm^{-1}) 3649, 3239, 3055, 2918, 2874, 2798, 1982, 1925, 1897, 1662, 1624, 1551, 1502, 1454, 1404, 1318, 1283, 1251, 1220, 1176, 1088, 1044, 1011, 976, 902, 867, 815, 735, 646, 590, 550, 497.

^{1}H NMR (DMSO-d_6, δ ppm) δ 11,53 (s, 1H, 10), 8,70 (t, 1H, 2', J = 5,8 Hz), 8,18 (d, 1H, 3, J = 7,9 Hz), 7,87 (s, 1H, 6), 7,63 – 7,56 (m, 3H, 1, 12, 5'), 7,54 – 7,46 (m, 4H, 7', 8', 10', 11'), 7,23 – 7,18 (m, 1H, 2), 6,81 (d, 1H, 4', J = 15,8 Hz), 4,61 (d, 2H, 1', J = 5,7 Hz), 2,77 (s, 3H, 13).

^{13}C NMR (DMSO-d_6, δ ppm) δ 164,67 (3'), 146,08 (7), 141,33 (11), 140,75 (8), 137,41 (5'), 133,96 (9), 133,82 (9'), 133,56 (6'), 129,22 (8', 10'), 128,97 (7', 11'), 127,82 (1), 127,72 (5), 123,19 (3), 121,68 (4'), 121,00 (4), 119,14 (2), 111,93 (12), 110,06 (6), 44,72 (1'), 20,33 (13).

ESI-MS: *m/z* 374,0 $(M-1)^-$.

*3.2.2.6.7. (E)-3-(4-metoksifenil)-N-((1-metil-9H-pirido[3,4-b]indol-3-il)metil)akrilamid (**13g**)*

Količina reaktanta: 0,029 g 4-metoksicimetne kiseline.

Pročišćavanje: Metoda A.

Iskorištenje: 0,028 g (51 %).

t_t 263,0 – 264,0 °C (raspad).

IR (ATR, ν/cm^{-1}) 3249, 3162, 3079, 2964, 2910, 2835, 2787, 2684, 1652, 1603, 1555, 1512, 1454, 1419, 1345, 1287, 1251, 1175, 1109, 1026, 987, 932, 900, 873, 827, 778, 744, 592, 549, 520.

^{1}H NMR (DMSO-d_6, δ ppm) δ 11,54 (s, 1H, 10), 8,59 (t, 1H, 2', J = 5,6 Hz), 8,18 (d, 1H, 3, J = 7,9 Hz), 7,87 (s, 1H, 6), 7,59 – 7,50 (m, 4H, 1, 12, 8', 10'), 7,45 (d, 1H, 5', J = 15,8 Hz), 7,20 (t, 1H, 2, J = 7,5 Hz), 6,98 (d, 2H, 7', 11', J = 8,2 Hz), 6,66 (d, 1H, 4', J = 15,8 Hz), 4,61 (d, 2H, 1', J = 5,9 Hz), 3,79 (s, 3H, 12'), 2,78 (s, 3H, 13).

^{13}C NMR (DMSO-d_6, δ ppm) δ 165,20 (3'), 160,29 (9'), 146,31 (7), 141,29 (11), 140,75 (8), 138,47 (5'), 133,54 (9), 129,09 (8', 10'), 127,81 (1), 127,73 (5), 127,55 (6'), 121,68 (4'), 121,01 (4), 119,89 (2), 119,14 (3), 114,38 (7', 11'), 111,93 (12), 109,98 (6), 55,25 (12'), 44,66 (1'), 20,33 (13).

ESI-MS: *m/z* 372,3 $[M+1]^+$.

*3.2.2.6.8. (E)-N-((1-metil-9H-pirido[3,4-b]indol-3-il)metil)-3-(4-(trifluormetil)fenil)akrilamid (**13h**)*

Količina reaktanta: 0,035 g 4-(trifluormetil)cimetne kiseline.

Pročišćavanje: Metoda A.

Iskorištenje: 0,026 g (43 %).

t_t 264,5 – 266,5 °C.

IR (ATR, ν/cm^{-1}) 3339, 3263, 3058, 2920, 1666, 1626, 1575, 1496, 1452, 1413, 1324, 1248, 1164, 1120, 1065, 1012, 972, 900, 858, 822, 778, 737, 702, 586, 522, 491.

^{1}H NMR (DMSO-d_6, δ ppm) δ 11,54 (s, 1H, 10), 8,79 (t, 1H, 2', J = 5,8 Hz), 8,18 (d, 1H, 3, J = 7,9 Hz), 7,88 (s, 1H, 6), 7,82 – 7,76 (m, 4H, 12, 1, 7', 11'), 7,59 – 7,49 (m, 3H, 5', 8', 10'), 7,23 – 7,18 (m, 1H, 2), 6,94 (d, 1H, 4', J = 15,8 Hz), 4,63 (d, 2H, 1', J = 5,7 Hz), 2,77 (s, 3H, 13).

^{13}C NMR (DMSO-d_6, δ ppm) δ 164,43 (3'), 145,97 (7), 141,38 (11), 140,77 (8), 139,09 (6'), 137,12 (5'), 133,59 (9), 129,17 (q, 9', J = 31,8 Hz), 128,16 (7', 11'), 127,84 (1), 127,74 (5), 125,81 (q, 8', 10', J = 3,9 Hz), 125,20 (3), 124,13 (q, 12', J = 272,0 Hz), 121,70 (4'), 121,01 (4), 119,16 (2), 111,95 (12), 110,14 (6), 44,78 (1'), 20,34 (13).

ESI-MS: *m/z* 410,1 $[M+1]^+$.

HPLC čistoća 97,3 %.

3.2.3. Sinteza derivata u položaju 6 β-karbolinskog prstena (14-19)

*3.2.3.1. Sinteza 6-metoksi-1-metil-2,3,4,9-tetrahidro-1H-pirido[3,4-b]indol-2-ijevog trifluoracetata (**14**)*

U otopinu 5-metoksitriptamina (0,200 g, 1,05 mmol) u acetonitrilu (4 mL) dodani su acetaldehid-dimetil acetal (0,222 mL, 2,10 mmol) i TFA (0,161 mL, 2,10 mmol). Reakcijska smjesa miješana je u mikrovalnom reaktoru 10 minuta na 110 °C (150 W). Nakon hlađenja na sobnu temperaturu dodan je dietil-eter (40 mL). Nastali talog je odsisan i ispran dietil-eterom (2 × 10 mL). Sirovi produkt **14** korišten je u sljedećem reakcijskom koraku bez dodatnog pročišćavanja.

*3.2.3.2. Sinteza 6-metoksi-1-metil-9H-pirido[3,4-b]indola (**15**)*

Suspenzija spoja **14** (0,200 g, 0,605 mmol), litijevog karbonata (0,89 g, 1,21 mmol) i 10 % Pd/C (0,023 g) u bezvodnom etanolu (4 mL) miješana je u mikrovalnom reaktoru 25 minuta na 150 °C (150 W). Potom je reakcijska smjesa ohlađena na sobnu temperaturu, filtrirana kroz

celit te je sloj celita ispran metanolom. Otapala su iz filtrata uklonjena uparavanjem pod sniženim tlakom. Zaostatni talog je rastrljan prvo u 20 %-tnoj vodenoj otopini natrijevog klorida, a potom u dietil-eteru.

Iskorištenje: 0,113 g (88 %).

*3.2.3.3. Sinteza metil-9H-pirido[3,4-b]indol-6-ola (**16**)*

Suspenzija spoja **15** (0,100 g, 0,471 mmol), 47 % bromovodične kiseline (0,6 mL) i koncentrirane octene kiseline (1,2 mL) miješana je u mikrovalnom reaktoru 25 minuta na 140 °C. Potom je reakcijska smjesa ohlađena na sobnu temperaturu, zalužena 5 %-tnom otopinom NaOH do pH 8 te ekstrahirana etil-acetatom (3 × 40 mL). Organski slojevi su sakupljeni, sušeni nad bezvodnim natrijevim sulfatom, filtrirani, a otapalo je iz filtrata uklonjeno uparavanjem pod sniženim tlakom. Sirovi produkt pročišćen je kromatografijom na koloni uz pokretnu fazu cikloheksan:etil-acetat:metanol (1:1:0,5). Nakon rastrljavanja u smjesi dietil-etera i petroletera dobiven je čist spoj **16**.

Iskorištenje: 0,077 g (83 %).

*3.2.3.4. Sinteza tert-butil-(2-((1-metil-9H-pirido[3,4-b]indol-6-il)oksi)etil)karbamata (**17**)*

Spoj **16** (0,647 g, 3,26 mmol) otopljen je u bezvodnom DMF-u (6 mL) te su u dobivenu otopinu dodani cezijev karbonat (2,98 g, 9,14 mmol) i tetrabutilamonijev hidrogen sulfat (0,887 g, 2,61 mmol). Reakcijska smjesa miješana je 20 min pod atmosferom dušika. Zatim je u reakcijsku smjesu dodan 2-(*tert*-butoksikarbonilamino)etil bromid (2,93 g, 13,06 mmol) te je miješanje nastavljeno na sobnoj temperaturi pod atmosferom dušika tijekom 24 h. Potom je u reakcijsku smjesu dodano 40 mL destilirane vode, a dobivena otopina je ekstrahirana etil-acetatom (3 × 50 mL). Organski slojevi su sakupljeni i isprani vodom (1 × 40 mL), zatim sušeni nad bezvodnim natrijevim sulfatom, filtrirani, a otapalo je iz filtrata uklonjeno uparavanjem pod sniženim tlakom. Sirovi produkt pročišćen je kromatografijom na koloni uz pokretnu fazu diklormetan:metanol (8:1). Nakon rastrljavanja u smjesi dietil-etera i petroletera dobiven je čist spoj **17**.

Iskorištenje: 0,623 g (56 %)

Ulje.

^{1}H NMR (DMSO-d_6, δ ppm) δ 11,42 (s, 1H, 10), 8,16 (d, 1H, 7, J = 5,3 Hz), 7,92 (d, 1H, 6, J = 5,3 Hz), 7,77 (d, 1H, 3, J = 1,7 Hz), 7,51 (d, 1H, 12, J = 8,8 Hz), 7,18 (dd, 1H, 1, J = 8,8, 2,3 Hz), 7,06 (t, 1H, 3', J = 5,0 Hz), 4,05 (t, 2H, 1', J = 5,8 Hz), 3,39 – 3,34 (m, 2H, 2'), 2,75 (s, 3H, 13), 1,40 (s, 9H, 6' – 8').

^{13}C NMR (DMSO-d_6, δ ppm) δ 155,73 (4'), 152,39 (2), 142,04 (8), 136,56 (7), 135,41 (11), 135,03 (9), 126,88 (4), 121,35 (5), 118,42 (1), 112,78 (6), 112,75 (12), 104,68 (3), 77,76 (5'), 67,19 (1'), 39,61 (2'), 28,24 (6' – 8'), 20,23 (13).
ESI-MS (*m/z*): 342,4 $[M+1]^+$.

*3.2.3.5. Sinteza 2-((1-metil-9H-pirido[3,4-b]indol-6-il)oksi)etan-1-amina (**18**)*

Suspenziji spoja **17** (0,550 g, 1,61 mmol) u metanolu (5 mL) dodana je 4 M klorovodična kiselina (4,013 mL, 16,05 mmol). Reakcijska smjesa je miješana 18 h na 50 °C. Potom je metanol uparen pod sniženim tlakom, a zaostatni talog otopljen u 15 mL destilirane vode, zalužen 5 %-tnom otopinom NaOH do pH 12. Novonastali talog je odsisan i rastrljan u dietil-eteru.
Iskorištenje: 0,268 g (69 %).
t_t 170,5 – 172,0 °C.
IR (ATR, ν/cm^{-1}) 3645, 3359, 3241, 3065, 2925, 2869, 1605, 1581, 1566, 1500, 1478, 1458, 1401, 1288, 1234, 1211, 1126, 1071, 1059, 992, 905, 884, 847, 825, 816, 741, 703, 632.
^{1}H NMR (DMSO-d_6, δ ppm) δ 11,36 (s, 1H, 10), 8,15 (d, 1H, 7, J = 5,3 Hz), 7,90 (d, 1H, 6, J = 5.3 Hz), 7,74 (d, 1H, 3, J = 2,3 Hz), 7,50 (d, 1H, 12, J = 8,8 Hz), 7,19 (dd, 1H, 1, J = 8,8, 2,5 Hz), 4,02 (t, 2H, 1', J = 5,8 Hz), 2,94 (t, 2H, 2', J = 5,7 Hz), 2,74 (s, 3H, 13).
^{13}C NMR (DMSO-d_6, δ ppm) δ 152,47 (2), 141,87 (8), 136,70 (7), 135,19 (11), 134,93 (9), 126,54 (4), 121,29 (5), 117,98 (6), 112,34 (1), 112,18 (12), 104,86 (3), 71,06 (1'), 40,87 (2'), 19,97 (13).
ESI-MS (*m/z*): 242,2 $[M+1]^+$.

*3.2.3.6. Sinteza harmicina u položaju 6 β-karbolinskog prstena (**19a-h**). Opća metoda*

Otopina odgovarajućeg DCK-a (0,249 mmol), DIEA (0,087 mL, 0,498 mmol) i HATU (0,095 g, 0,249 mmol) u diklormetanu (4 mL) miješana je na sobnoj temperaturi 20 min, nakon čega je u reakcijsku smjesu dodan amin **18** (0,050 g, 0,208 mmol). Reakcijska smjesa miješana je na sobnoj temperaturi 1 h. Novonastali talog je odsisan i pročišćen kromatografijom na koloni uz pokretnu fazu diklormetan:metanol (8:1). Nakon rastrljavanja u smjesi dietil-etera i petroletera dobiveni su čisti produkti.

*3.2.3.6.1. N-(2-((1-metil-9H-pirido[3,4-b]indol-6-il)oksi)etil)cinamamid (**19a**)*

Količina reaktanta: 0,037 g *trans*-cimetne kiseline.

Iskorištenje: 0,045 g (58 %).

t_t 128,0 – 129,5 °C.

IR (ATR, ν/cm^{-1}) 3640, 3220, 3062, 2986, 2938, 2811, 2609, 1871, 1665, 1622, 1545, 1502, 1458, 1422, 1343, 1286, 1209, 1121, 1074, 970, 897, 808, 766, 714, 659, 630, 574, 512, 483.

^{1}H NMR (DMSO-d_6, δ ppm) δ 11,39 (s, 1H, 10), 8,45 (t, 1H, 3', J = 5,6 Hz), 8,16 (d, 1H, 7, J = 5,3 Hz), 7,91 (d, 1H, 6, J = 5,3 Hz), 7,81 (d, 1H, 3, J = 2,5 Hz), 7,57 (d, 2H, 8', 12', J = 7,3 Hz), 7,53 – 7,46 (m, 2H, 6', 12), 7,44 – 7,36 (m, 3H, 9', 10', 11'), 7,22 (dd, 1H, 1, J = 8,9, 2,6 Hz), 6,73 (d, 1H, 5', J = 15,9 Hz), 4,17 (t, 2H, 1', J = 5,6 Hz), 3,64 (q, 2H, 2', J = 5,6 Hz), 2,74 (s, 3H, 13).

^{13}C NMR (DMSO-d_6, δ ppm) δ 165,27 (4'), 152,37 (2), 142,04 (8), 138,83 (6'), 136,54 (7), 135,46 (11), 135,03 (9), 134,89 (7'), 129,45 (10'), 128,93 (9', 11'), 127,52 (8', 12'), 126,90 (4), 122,07 (5'), 121,37 (5), 118,43 (1), 112,79 (6), 112,77 (12), 104,73 (3), 67,12 (1'), 38,67 (2'), 20,20 (13).

ESI-MS: *m/z* 372,0 $[M+1]^+$.

HPLC čistoća > 99,5 %.

3.2.3.6.2. (E)-3-(3-fluorfenil)-N-(2-((1-metil-9H-pirido[3,4-b]indol-6-il)oksi)etil)akrilamid ***(19b)***

Količina reaktanta: 0,041 g 3-fluorcimetne kiseline.

Iskorištenje: 0,062 g (76 %).

t_t 225,0 – 226,0 °C.

IR (ATR, ν/cm^{-1}) 3658, 3236, 3068, 2974, 2936, 2882, 2822, 2608, 1871, 1666, 1625, 1585, 1551, 1501, 1448, 1344, 1286, 1248, 1207, 1146, 1075, 1037, 974, 902, 856, 807, 738, 666, 630, 573, 519, 467.

^{1}H NMR (DMSO-d_6, δ ppm) δ 11,38 (s, 1H, 10), 8,46 (t, 1H, 3', J = 5,5 Hz), 8,16 (d, 1H, 7, J = 5,4 Hz), 7,91 (d, 1H, 6, J = 5,3 Hz), 7,80 (d, 1H, 3, J = 2,4 Hz), 7,51 (d, 1H, 12, J = 8,9 Hz), 7,50 – 7,40 (m, 4H, 1, 6', 11', 12'), 7,24 – 7,19 (m, 2H, 8', 10'), 6,77 (d, 1H, 5', J = 15,8 Hz), 4,17 (t, 2H, 1', J = 5,5 Hz), 3,64 (q, 2H, 2', J = 5,5 Hz), 2,74 (s, 3H, 13).

^{13}C NMR (DMSO-d_6, δ ppm) δ 164,99 (4'), 162,45 (d, 9', J = 243,8 Hz), 152,32 (2), 142,15 (8), 137,54 (6'), 137,49 (7'), 136,83 (7), 135,37 (11), 135,07 (9), 130,89 (d, 11', J = 8,4 Hz), 126,76 (4), 123,68 (5'), 123,65 (12'), 121,40 (5), 118,29 (1), 116,11 (d, 10', J = 21,2 Hz) 113,93 (d, 8', J = 21,8 Hz), 112,74 (6), 112,72 (12), 104,73 (3), 67,07 (1'), 38,71 (2'), 20,34 (13).

ESI-MS: *m/z* 390,4 $[M+1]^+$.

HPLC čistoća > 99,5 %.

*3.2.3.6.3. (E)-3-(3-bromfenil)-N-(2-((1-metil-9H-pirido[3,4-b]indol-6-il)oksi)etil)akrilamid (**19c**)*

Količina reaktanta: 0,057 g 3-bromcimetne kiseline.

Iskorištenje: 0,072 g (77 %).

t_t 230,5 – 232,5 °C.

IR (ATR, ν/cm^{-1}) 3646, 3171, 3062, 2975, 2939, 2879, 2792, 2613, 1664, 1620, 1566, 1501, 1460, 1384, 1345, 1287, 1199, 1110, 1072, 970, 856, 811, 781, 736, 667, 631, 561.

^{1}H NMR (DMSO-d_6, δ ppm) δ 11,40 (s, 1H, 10), 8,43 (t, 1H, 3', J = 5,5 Hz), 8,16 (d, 1H, 7, J = 5,4 Hz), 7,92 (d, 1H, 6, J = 5,4 Hz), 7,81 (d, 1H, 3, J = 2,3 Hz), 7,79 (t, 1H, 8', J = 1,8 Hz), 7,59 – 7,56 (m, 2H, 10', 11'), 7,52 (d, 1H, 12, J = 8,8 Hz), 7,45 (d, 1H, 6', J = 15,8 Hz), 7,38 (t, 1H, 12', J = 7,9 Hz), 7,22 (dd, 1H, 1, J = 8,8, 2,4 Hz), 6,78 (d, 1H, 5', J = 15,8 Hz), 4,17 (t, 2H, 1', J = 5,5 Hz), 3,64 (q, 2H, 2', J = 5,4 Hz), 2,75 (s, 3H, 13).

^{13}C NMR (DMSO-d_6, δ ppm) δ 164,92 (4'), 152,33 (2), 142,09 (8), 137,50 (7'), 137,19 (6'), 136,68 (7), 135,42 (11), 135,05 (9), 131,97 (8'), 131,02 (10'), 130,04 (11'), 126,83 (4), 126,40 (12'), 123,76 (5'), 122,25 (9'), 121,38 (5), 118,37 (1), 112,76 (6, 12), 104,74 (3), 67,08 (1'), 38,71 (2'), 20,27 (13).

ESI-MS*: m/z* 450,3 $[M+1]^+$, 452,3 $[M+1]^+$.

HPLC čistoća > 99,5%.

*3.2.3.6.4. (E)-N-(2-((1-metil-9H-pirido[3,4-b]indol-6-il)oksi)etil)-3-(3-(trifluormetil)fenil)akrilamid (**19d**)*

Količina reaktanta: 0,054 g 3-(trifluormetil)cimetne kiseline.

Iskorištenje: 0,058 g (64 %).

t_t 216,5 – 218,0 °C.

IR (ATR, ν/cm^{-1}) 3676, 3222, 3100, 3067, 2988, 2937, 2881, 2820, 2611, 1665, 1624, 1545, 1501, 1440, 1331, 1286, 1200, 1167, 1117, 1073, 1031, 971, 863, 805, 738, 691, 658, 630, 574, 465.

^{1}H NMR (DMSO-d_6, δ ppm) δ 11,41 (s, 1H, 10), 8,46 (t, 1H, 3', J = 5,6 Hz), 8,16 (d, 1H, 7, J = 5,4 Hz), 7,93 – 7,88 (m, 3H, 3, 6, 12'), 7,81 (d, 1H, 8', J = 2,6 Hz), 7,73 (d, 1H, 10', J = 7,8 Hz), 7,66 (t, 1H, 11', J = 7,8 Hz), 7,57 (d, 1H, 6', J = 15,8 Hz), 7,52 (d, 1H, 12, J = 8,8 Hz), 7,22 (dd, 1H, 1, J = 8,8, 2,5 Hz), 6,88 (d, 1H, 5', J = 15,9 Hz), 4,18 (t, 2H, 1', J = 5,5 Hz), 3,65 (q, 2H, 2', J = 5,6 Hz), 2,75 (s, 3H, 13).

^{13}C NMR (DMSO-d_6, δ ppm) δ 164,88 (4'), 152,34 (2), 142,10 (8), 137,14 (6'), 136,69 (7), 136,13 (11), 135,43 (7'), 135,06 (9), 131,30 (12'), 130,06 (11'), 129,73 (q, 9', J = 32,3 Hz),

126,83 (4), 125,73 (q, 10', J = 3,0 Hz), 124,23 (5'), 124,04 (q, 13', J = 273,7 Hz), 123,88 (q, 8', J = 3,0 Hz), 121,38 (5), 118,37 (1), 112,76 (6, 12), 104,74 (3), 67,09 (1'), 38,74 (2'), 20,27 (13)
ESI-MS: *m/z* 440,1 $[M+1]^+$.

3.2.3.6.5. (E)-3-(4-fluorfenil)-N-(2-((1-metil-9H-pirido[3,4-b]indol-6-il)oksi)etil)akrilamid ***(19e)***

Količina reaktanta: 0,041 g 4-fluorcimetne kiseline.
Iskorištenje: 0,065 g (80 %).
t_t 226,5 – 227,5 °C.
IR (ATR, ν/cm^{-1}) 3659, 3311, 3225, 3099, 3045, 2990, 2938, 2165, 1870, 1667, 1625, 1542, 1502, 1422, 1347, 1286, 1208, 1160, 1122, 1074, 976, 897, 824, 740, 630, 576, 501, 459.
^{1}H NMR (DMSO-d_6, δ ppm) δ 11,40 (s, 1H, 10), 8,43 (t, 1H, 3', J = 5,4 Hz), 8,16 (d, 1H, 7, J = 5,4 Hz), 7,92 (d, 1H, 6, J = 5,3 Hz), 7,81 (d, 1H, 3, J = 2,2 Hz), 7,66 – 7,62 (m, 2H, 8', 12'), 7,53 – 7,46 (m, 2H, 6', 12), 7,28 – 7,21 (m, 3H, 1, 9', 11'), 6,68 (d, 1H, 5', J = 15,8 Hz), 4,17 (t, 2H, 1', J = 5,5 Hz), 3,64 (q, 2H, 2', J = 5,4 Hz), 2,75 (s, 3H, 13).
^{13}C NMR (DMSO-d_6, δ ppm) δ 165,21 (4'), 162,68 (d, 10', J = 247,0 Hz), 152,35 (2), 142,10 (8), 137,65 (6'), 136,71 (7), 135,41 (11), 135,05 (9), 131,53 (d, 7', J = 2,6 Hz), 129,68 (d, 8', 12', J = 8,4 Hz), 126,82 (4), 121,97 (5'), 121,39 (5), 118,36 (1), 115,90 (d, 9', 11', J = 21,7 Hz), 112,76 (6, 12), 104,72 (3), 67,11 (1'), 38,68 (2'), 20,28 (13).
ESI-MS: *m/z* 390,4 $[M+1]^+$.
HPLC čistoća > 99,5 %.

3.2.3.6.6. (E)-3-(4-klorfenil)-N-(2-((1-metil-9H-pirido[3,4-b]indol-6-il)oksi)etil)akrilamid ***(19f)***

Količina reaktanta: 0,045 g 4-klorcimetne kiseline.
Iskorištenje: 0,071 g (84 %).
t_t 228,5 – 229,5 °C.
IR (ATR, ν/cm^{-1}) 3642, 3231, 3066, 2989, 2939, 2164, 2113, 1872, 1665, 1621, 1548, 1502, 1406, 1342, 1288, 1208, 1075, 976, 938, 897, 809, 742, 630, 575, 490.
^{1}H NMR (DMSO-d_6, δ ppm) δ 11,40 (s, 1H, 10), 8,46 (t, 1H, 3', J = 5,3 Hz), 8,16 (d, 1H, 7, J = 5,3 Hz), 7,91 (d, 1H, 6, J = 5,3 Hz), 7,80 (d, 1H, 3, J = 2,0 Hz), 7,60 (d, 2H, 8', 12', J = 8,4 Hz), 7,51 (d, 1H, 12, J = 8,9 Hz), 7,49 – 7,45 (m, 3H, 6', 9', 11'), 7,22 (dd, 1H, 1, J = 8,8, 2,3 Hz), 6,73 (d, 1H, 5', J = 15,8 Hz), 4,17 (t, 2H, 1', J = 5,4 Hz), 3,64 (q, 2H, 2', J = 5,3 Hz), 2,74 (s, 3H, 13).

^{13}C NMR (DMSO-d_6, δ ppm) δ 165,08 (4'), 152,33 (2), 142,11 (8), 137,49 (6'), 136,72 (7), 135,41 (11), 135,05 (9), 133,87 (7', 10'), 129,22 (8', 12'), 128,97 (9', 11'), 126,81 (4), 122,88 (5'), 121,39 (5), 118,35 (1), 112,76 (6, 12), 104,73 (3), 67,09 (1'), 38,70 (2'), 20,29 (13).
ESI-MS: *m/z* 406,3 $[M+1]^+$, 408,3 $[M+1]^+$.
HPLC čistoća > 97,5 %.

*3.2.3.6.7. (E)-3-(4-metoksifenil)-N-(2-((1-metil-9H-pirido[3,4-b]indol-6-il)oksi)etil)akrilamid (**19g**)*

Količina reaktanta: 0,044 g 4-metoksicimetne kiseline.
Iskorištenje: 0,063 g (75 %).
t_t 241,5 – 242,5 °C.
IR (ATR, ν/cm^{-1}) 3210, 3133, 3058, 2971, 2941, 2873, 2775, 2601, 2164, 1983, 1886, 1651, 1602, 1554, 1514, 1461, 1425, 1353, 1284, 1230, 1205, 1175, 1125, 1064, 1033, 983, 862, 827, 761, 699, 624, 555, 521.
^{1}H NMR (DMSO-d_6, δ ppm) δ 11,39 (s, 1H, 10), 8,34 (t, 1H, 3', J = 5,5 Hz), 8,16 (d, 1H, 7, J = 5,4 Hz), 7,91 (d, 1H, 6, J = 5,3 Hz), 7,80 (d, 1H, 3, J = 2,4 Hz), 7,53 – 7,50 (m, 3H, 12, 8', 12'), 7,43 (d, 1H, 6', J = 15,8 Hz), 7,22 (dd, 1H, 1, J = 8,8, 2,5 Hz), 6,98 (d, 2H, 9', 11', J = 8,8 Hz), 6,58 (d, 1H, 5', J = 15,8 Hz), 4,16 (t, 2H, 1', J = 5,6 Hz), 3,79 (s, 3H, 13'), 3,63 (q, 2H, 2', J = 5,5 Hz), 2,74 (s, 3H, 13).
^{13}C NMR (DMSO-d_6, δ ppm) δ 165,59 (4'), 160,32 (10'), 152,35 (2), 142,13 (8), 138,54 (6'), 136,80 (7), 135,37 (11), 135,06 (9), 129,09 (8', 12'), 127,45 (7'), 126,77 (4), 121,40 (5), 119,58 (5'), 118,30 (1), 114,38 (9', 11'), 112,74 (6, 12), 104,71 (3), 67,16 (1'), 55,24 (13'), 38,63 (2'), 20,33 (13).
ESI-MS: *m/z* 402,4 $[M+1]^+$.
HPLC čistoća > 99,5 %.

*3.2.3.6.8. (E)-N-(2-((1-metil-9H-pirido[3,4-b]indol-6-il)oksi)etil)-3-(4-(trifluormetil)fenil)akrilamid (**19h**)*

Količina reaktanta: 0,054 g 4-(trifluormetil)cimetne kiseline.
Iskorištenje: 0,057 g (62 %).
t_t 231,5 – 233,5 °C.
IR (ATR, ν/cm^{-1}) 3645, 3269, 3061, 2932, 2875, 1667, 1628, 1559, 1501, 1461, 1417, 1384, 1328, 1286, 1234, 1202, 1166, 1119, 1067, 1016, 976, 953, 882, 829, 814, 728, 708, 614, 591, 562, 522, 495.

^{1}H NMR (DMSO-d_6, δ ppm) δ 11,41 (s, 1H, 10), 8,54 (t, 1H, 3', J = 5,5 Hz), 8,16 (d, 1H, 7, J = 5,3 Hz), 7,92 (d, 1H, 6, J = 5,3 Hz), 7,81 – 7,76 (m, 5H, 3, 8', 9', 11', 12'), 7,57 – 7,51 (m, 2H, 6', 12), 7,22 (dd, 1H, 1, J = 8,9, 2,5 Hz), 6,86 (d, 1H, 5', J = 15,8 Hz), 4,18 (t, 2H, 1', J = 5,5 Hz), 3,65 (q, 2H, 2', J = 5,4 Hz), 2,75 (s, 3H, 13).

^{13}C NMR (DMSO-d_6, δ ppm) δ 164,82 (4'), 152,34 (2), 142,09 (8), 139,00 (7'), 137,19 (6'), 136,65 (7), 135,44 (11), 135,05 (9), 129,20 (q, 10', J = 32,3 Hz), 128,16 (8', 12'), 126,85 (4), 125,80 (q, 9', 11', J = 3,0 Hz), 124,87 (5'), 124,11 (q, 13', J = 272,7 Hz), 121,38 (5), 118,39 (1), 112,78 (6, 12), 104,74 (3), 67,06 (1'), 38,75 (2'), 20,25 (13).

ESI-MS: m/z 440,1 $[M+1]^+$.

3.2.4. Sinteza derivata u položaju 7 β-karbolinskog prstena (harmol, 20-22)

3.2.4.1. Sinteza harmola

Suspenzija harmina (0,250 g, 1,18 mmol), octene kiseline (3 mL) i 47 % bromovodične kiseline (1,5 mL) miješana je u mikrovalnom reaktoru 25 minuta na 140 °C. Potom je reakcijska smjesa zalužena 10 %-tnom otopinom NaOH do pH 9 te je ekstrahirana etil-acetatom (3 × 40 mL). Organski slojevi su sakupljeni, sušeni nad bezvodnim natrijevim sulfatom, filtrirani, a otapalo je iz filtrata uklonjeno uparavanjem pod sniženim tlakom. Nakon rastrljavanja u dietil-eteru dobiven je čist spoj harmol.

Iskorištenje: 0,215 g (92 %).

*3.2.4.2. Sinteza tert-butil-(2-((1-metil-9H-pirido[3,4-b]indol-7-il)oksi)etil)karbamata (**20**)*

Otopini harmola (0,431 g, 2,17 mmol) u bezvodnom DMF-u (4 mL) dodani su cezijev karbonat (0,992 g, 3,04 mmol) i 2-(*tert*-butoksikarbonilamino)etil bromid (1,17 g, 5,21 mmol). Reakcijska smjesa je miješana 24 h na 95 °C pod atmosferom dušika. Nakon hlađenja na sobnu temperaturu dodano je 40 mL destilirane vode. Potom je provedena ekstrakcija etil-acetatom (3 × 40 mL). Organski slojevi su sakupljeni i isprani vodom (1 × 40 mL), sušeni nad bezvodnim natrijevim sulfatom, filtrirani, a otapalo je iz filtrata uklonjeno uparavanjem pod sniženim tlakom. Sirovi produkt pročišćen je kromatografijom na koloni uz pokretnu fazu diklormetan:metanol (8:1), a nakon rastrljavanja u smjesi dietil-etera i petroletera dobiven je čist produkt **20**.

Iskorištenje: 0,578 g (78 %).

t_t 189,5 – 190,5 °C.

IR (KBr, ν/cm^{-1}) 3390, 3134, 3052, 2978, 2944, 2872, 2764, 2726, 2582, 2406, 1692, 1634, 1568, 1530, 1480, 1448, 1394, 1368, 1334, 1296, 1260, 1174, 1114, 1052, 1010, 964, 872, 846, 820, 788, 720, 686, 634, 604, 522.

^{1}H NMR (DMSO-d_6, δ ppm) δ 11,42 (s, 1H, 10), 8,15 (d, 1H, 7, J = 5,3 Hz), 8,05 (d, 1H, 3, J = 8,6 Hz), 7,81 (d, 1H, 6, J = 5,3 Hz), 7,06 (t, 1H, 3', J = 5,4 Hz), 7,00 (d, 1H, 12, J = 2,1 Hz), 6,85 (dd, 1H, 2, J = 8,7, 2,2 Hz), 4,08 (t, 2H, 1', J = 5,8 Hz), 3,41 – 3,35 (m, 2H, 2'), 2,73 (s, 3H, 13), 1,40 (s, 9H, 6' – 8').

^{13}C NMR (DMSO-d_6, δ ppm) δ 159,22 (4'), 155,73 (1), 141,92 (8), 141,21 (11), 137,59 (7), 134,55 (9), 127,26 (4), 122,66 (3), 114,96 (5), 111,96 (6), 109,33 (2), 95,39 (12), 77,80 (5'), 66,66 (1'), 28,23 (6' – 8'), 20,26 (13).

ESI-MS: m/z 342,3 [M+1]$^+$.

*3.2.4.3. Sinteza 2-((1-metil-9H-pirido[3,4-b]indol-7-il)oksi)etan-1-amina (**21**)*

Suspenziji spoja **20** (0,550 g, 1,61 mmol) u metanolu (5 mL) dodana je 4 M klorovodična kiselina (4,013 mL, 16,05 mmol). Reakcijska smjesa je miješana 18 h na 50 °C. Potom je metanol uparen pod sniženim tlakom, a zaostatni talog otopljen u 15 mL destilirane vode, zalužen 5 %-tnom otopinom NaOH do pH 12 i ekstrahiran etil-acetatom (3 × 40 mL). Organski slojevi su sakupljeni, sušeni nad bezvodnim natrijevim sulfatom, filtrirani, a otapalo je iz filtrata uklonjeno uparavanjem pod sniženim tlakom. Rastrljavanjem u dietil-eteru dobiven je čist produkt.

Iskorištenje: 0,311 g (80 %).

t_t 172,5 – 173,0 °C.

IR (KBr, ν/cm^{-1}) 3332, 3250, 3156, 3068, 2930, 2864,2774, 2372, 1892, 1756, 1720, 1628, 1568, 1486, 1444, 1326, 1284, 1238, 1180, 1104, 1028, 996, 908, 860, 812, 636, 590.

^{1}H NMR (DMSO-d_6, δ ppm, J/Hz) δ 11,38 (s, 1H, 10), 8,15 (d, 1H, 7, J = 5,2 Hz), 8,04 (d, 1H, 3, J = 8,6 Hz), 7,79 (d, 1H, 6, J = 5,2 Hz), 7,01 (d, 1H, 12, J = 2,2 Hz), 6,85 (dd, 1H, 2, J = 8,6, 2,2 Hz), 4,03 (t, 2H, 1', J = 5,7 Hz), 2,95 (t, 2H, 2', J = 5,7 Hz), 2,73 (s, 3H, 13), 1,58 (s, 2H, 3').

^{13}C NMR (DMSO-d_6, δ ppm) δ 159,46 (1), 141,91 (8), 141,25 (11), 137,73 (7), 134,54 (9), 127,20 (5), 122,57 (3), 114,84 (4), 111,89 (6), 109,37 (2), 95,29 (12), 70,36 (1'), 40,98 (2'), 20,33 (13).

ESI-MS (m/z): 242,2 [M+1]$^+$.

*3.2.4.4. Sinteza harmicina u položaju 7 β-karbolinskog prstena (**22a**-**h**). Opća metoda*

Otopina odgovarajućeg DCK-a (0,200 mmol), DIEA (0,070 mL, 0,400 mmol) i HATU (0,077 g, 0,200 mmol) u diklormetanu (4 mL) miješana je na sobnoj temperaturi 15 min, nakon čega je u reakcijsku smjesu dodan amin **21** (0,049 g, 0,200 mmol). Reakcijska smjesa miješana je na sobnoj temperaturi 1 h. Novonastali talog je odsisan i pročišćen kromatografijom na koloni uz pokretnu fazu diklormetan:metanol (85:15). Nakon rastrljavanja u smjesi dietil-etera i petroletera dobiveni su čisti produkti.

*3.2.4.4.1. N-(2-((1-metil-9H-pirido[3,4-b]indol-7-il)oksi)etil)cinamamid (**22a**)*

Količina reaktanta: 0,030 g *trans*-cimetne kiseline.

Iskorištenje: 0,045 g (60 %).

t_t 151,5 °C (raspad).

IR (KBr, ν/cm^{-1}) 3424, 3222, 3060, 2972, 2932, 2874, 2768, 2372, 1874, 1720, 1664, 1630, 1574, 1544, 1486, 1450, 1392, 1332, 1280, 1234, 1174, 1110, 1056, 976, 812, 764, 684, 596, 528.

^{1}H NMR (DMSO-d_6, δ ppm) δ 11,66 (s, 1H, 10), 8,47 (t, 1H, 3', J = 5,3 Hz), 8,19 (d, 1H, 7, J = 5,4 Hz), 8,11 (d, 1H, 3, J = 8,7 Hz), 7,90 (d, 1H, 6, J = 5,4 Hz), 7,57 (d, 2H, 8', 12', J = 7,0 Hz), 7,48 (d, 1H, 6', J = 15,8 Hz), 7,45 – 7,36 (m, 3H, 9', 10', 11'), 7,07 (d, 1H, 12, J = 1,8 Hz), 6,91 (dd, 1H, 2, J = 8,7, 2,0 Hz), 6,73 (d, 1H, 5', J = 15,8 Hz), 4,20 (t, 2H, 1', J = 5,4 Hz), 3,65 (q, 2H, 2' J = 5,3 Hz), 2,77 (s, 3H, 13).

^{13}C NMR (DMSO-d_6, δ ppm) δ 165,30 (4'), 159,53 (1), 142,39 (8), 140,71 (11), 138,88 (6'), 136,38 (7), 134,88 (9), 134,46 (7'), 129,47 (10'), 128,93 (9', 11'), 127,90 (5), 127,53 (8', 12'), 122,96 (3), 122,03 (5'), 114,85 (4), 112,26 (6), 109,81 (2), 95,40 (12), 66,70 (1'), 38,52 (2'), 19,67 (13).

ESI-MS: m/z 372,2 $[M+1]^+$.

*3.2.4.4.2. (E)-3-(3-fluorfenil)-N-(2-((1-metil-9H-pirido[3,4-b]indol-7-il)oksi)etil)akrilamid (**22b**)*

Količina reaktanta: 0,033 g 3-fluorcimetne kiseline.

Iskorištenje: 0,052 g (67 %).

t_t 210,0 – 212,5 °C.

IR (KBr, ν/cm^{-1}) 3256, 3070, 2940, 2866, 2812, 2370, 1872, 1720, 1670, 1630, 1580, 1486, 1444, 1344, 1250, 1178, 1110, 1060, 1028, 964, 852, 784, 670, 624, 594, 528.

^{1}H NMR (DMSO-d_6, δ ppm) δ 11,47 (s, 1H, 10), 8,47 (t, 1H, 3', J = 5,5 Hz), 8,16 (d, 1H, 7, J = 5,3 Hz), 8,08 (d, 1H, 3, J = 8,7 Hz), 7,83 (d, 1H, 6, J = 5,3 Hz), 7,50 – 7,40 (m, 4H, 6', 8', 11', 12'), 7,24 – 7,19 (m 1H, 10'), 7,05 (d, 1H, 12, J = 2,1 Hz), 6,89 (dd, 1H, 2, J = 8,7, 2,2 Hz), 6,77 (d, 1H, 5', J = 15,8 Hz), 4,19 (t, 2H, 1', J = 5,4 Hz), 3,65 (q, 2H, 2', J = 5,4 Hz), 2,74 (s, 3H, 13).

^{13}C NMR (DMSO-d_6, δ ppm) δ 165,01 (4'), 162,45 (d, 9', J = 243,8 Hz), 159,23 (1), 141,98 (8), 141,17 (11), 137,60 (6'), 137,48 (7'), 137,43 (7), 134,55 (9), 130,89 (d, 11', J = 8,4 Hz), 127,34 (5), 123,66 (12'), 123,61 (3), 122,73 (5'), 116,13 (d, 10', J = 21,3 Hz), 115,01 (4), 113,93 (d, 8', J = 21,8 Hz), 112,02 (6), 109,43 (2), 95,43 (12), 66,63 (1'), 38,59 (2'), 20,18 (13).

ESI-MS: m/z 390,2 $[M+1]^+$.

3.2.4.4.3. (E)-3-(3-bromfenil)-N-(2-((1-metil-9H-pirido[3,4-b]indol-7-il)oksi)etil)akrilamid ***(22c)***

Količina reaktanta: 0,045 g 3-bromcimetne kiseline.

Iskorištenje: 0,042 g (47 %).

t_t 135,0 – 137,5 °C.

IR (ATR, ν/cm^{-1}) 3422, 3206, 3056, 2970, 2932, 2872, 2774, 2374, 2340, 1720, 1664, 1628, 1572, 1450, 1338, 1282, 1236, 1170, 1110, 1054, 974, 848, 786, 738, 668, 634, 602.

^{1}H NMR (DMSO-d_6, δ ppm) δ 11,48 (s, 1H, 10), 8,44 (t, 1H, 3', J = 5,5 Hz), 8,16 (d, 1H, 7, J = 5,3 Hz), 8,08 (d, 1H, 3, J = 8,7 Hz), 7,83 (d, 1H, 6, J = 5,3 Hz), 7,79 (t, 1H, 8', J = 1,5 Hz), 7,60 – 7,56 (m, 2H, 10', 12'), 7,45 (d, 1H, 6', J = 15,8 Hz), 7,38 (t, 1H, 11', J = 7,9 Hz), 7,05 (d, 1H, 12, J = 2,1 Hz), 6,89 (dd, 1H, 2, J = 8,7, 2,2 Hz), 6,78 (d, 1H, 5', J = 15,8 Hz), 4,19 (t, 2H, 1', J = 5,4 Hz), 3,65 (q, 2H, 2', J = 5,4 Hz), 2,74 (s, 3H, 13).

^{13}C NMR (DMSO-d_6, δ ppm) δ 164,94 (4'), 159,22 (1), 141,99 (8), 141,15 (11), 137,48 (7'), 137,40 (6'), 137,23 (7), 134,54 (9), 131,98 (8'), 131,02 (10'), 130,05 (11'), 127,35 (5), 126,41 (12'), 123,73 (3), 122,73 (5'), 122,25 (9'), 115,00 (4), 112,02 (6), 109,43 (2), 95,43 (12), 66,63 (1'), 38,58 (2'), 20,17 (13).

ESI-MS: m/z 450,1 $[M+1]^+$, 452,1 $[M+1]^+$.

3.2.4.4.4. (E)-3-(4-fluorfenil)-N-(2-((1-metil-9H-pirido[3,4-b]indol-7-il)oksi)etil)akrilamid ***(22d)***

Količina reaktanta: 0,033 g 4-fluorcimetne kiseline.

Iskorištenje: 0,057 g (73 %).

t_t 199,5 – 200,0 °C.

IR (KBr, ν/cm^{-1}) 3248, 3072, 2940, 2866, 2812, 2366, 1872, 1720, 1668, 1630, 1576, 1508, 1456, 1344, 1278, 1230, 1178, 1110, 1060, 1030, 964, 876, 796, 740, 674, 626, 594, 506.

^{1}H NMR (DMSO-d_6, δ ppm) δ 11,47 (s, 1H, 10), 8,44 (t, 1H, 3', J = 5,5 Hz), 8,16 (d, 1H, 7, J = 5,3 Hz), 8,08 (d, 3, 1H, J = 8,7 Hz), 7,83 (d, 1H, 6, J = 5,3 Hz), 7,66 – 7,62 (m, 2H, 8', 12'), 7,48 (d, 1H, 6', J = 15,8 Hz), 7,28 – 7,23 (m, 2H, 9', 11'), 7,05 (d, 1H, 12, J = 2,1 Hz), 6,89 (dd, 1H, 2, J = 8,7, 2,2 Hz), 6,68 (d, 1H, 5', J = 15,8 Hz), 4,19 (t, 2H, 1', J = 5,5 Hz), 3,65 (q, 2H, 2', J = 5,4 Hz), 2,74 (s, 3H, 13).

^{13}C NMR (DMSO-d_6, δ ppm) δ 165,24 (4'), 162,70 (d, 10', J = 247,1 Hz), 159,24 (1), 141,99 (8), 141,17 (11), 137,70 (6'), 137,44 (7), 134,55 (9), 131,53 (d, 7', J = 2,7 Hz), 129,69 (d, 8', 12', J = 8,4 Hz), 127,35 (5), 122,74 (3), 121,93 (5'), 115,91 (d, 9', 11', J = 21,7 Hz), 115,00 (4), 112,02 (6), 109,44 (2), 95,43 (12), 66,67 (1'), 38,56 (2'), 20,19 (13).

ESI-MS: m/z 390,3 [M+1]$^+$.

3.2.4.4.5. (E)-3-(4-klorfenil)-N-(2-((1-metil-9H-pirido[3,4-b]indol-7-il)oksi)etil)akrilamid ***(22e)***

Količina reaktanta: 0,037 g 4-klorcimetne kiseline.

Iskorištenje: 0,052 g (64 %).

t_t 230,5 – 234,0 °C.

IR (KBr, ν/cm^{-1}) 3400, 3268, 3046, 2942, 2880, 2772, 2372, 1662, 1624, 1560, 1490, 1450, 1332, 1284, 1234, 1166, 1102, 1012, 982, 874, 818, 738, 692, 656, 606.

^{1}H NMR (DMSO-d_6, δ ppm) δ 11,68 (s, 1H, 10), 8,49 (t, 1H, 3', J = 5,5 Hz), 8,19 (d, 1H, 7, J = 5,5 Hz), 8,11 (d, 1H, 3, J = 8,7 Hz), 7,91 (d, 1H, 6, J = 5,4 Hz), 7,60 (d, 2H, 9', 11', J = 8,5 Hz), 7,49 – 7,45 (m, 3H, 6', 8', 12'), 7,07 (d, 1H, 12, J = 2,1 Hz), 6,91 (dd, 1H, 2, J = 8,7, 2,2 Hz), 6,74 (d, 1H, 5', J = 15,8 Hz), 4,20 (t, 2H, 1', J = 5,4 Hz), 3,65 (q, 2H, 2', J = 5,4 Hz), 2,77 (s, 3H, 13).

^{13}C NMR (DMSO-d_6, δ ppm) δ 165,10 (4'), 159,54 (1), 142,41 (8), 140,67 (11), 137,52 (6'), 136,30 (7), 134,45 (9), 133,88 (10'), 133,85 (7'), 129,23 (9', 11'), 128,96 (8', 12'), 127,93 (5), 122,97 (3), 122,84 (5'), 114,85 (4), 112,27 (6), 109,82 (2), 95,39 (12), 66,67 (1'), 38,54 (2'), 19,64 (13).

ESI-MS: m/z 406,2 [M+1]$^+$, 408,2 [M+1]$^+$.

3.2.4.4.6. (E)-3-(4-metoksifenil)-N-(2-((1-metil-9H-pirido[3,4-b]indol-7-il)oksi)etil)akrilamid ***(22f)***

Količina reaktanta: 0,036 g 4-metoksicimetne kiseline.

Iskorištenje: 0,051 g (63 %).

t_t 191,0 – 194,5 °C.

IR (ATR, ν/cm^{-1}) 3432, 3258, 3070, 3008, 2938, 2842, 2770, 2342, 1720, 1628, 1602, 1574, 1546, 1514, 1448, 1258, 1174, 1108, 1060, 1030, 984, 872, 828, 744, 714, 674, 588, 554, 518.

^{1}H NMR (DMSO-d_6, δ ppm) δ 11,46 (s, 1H, 10), 8,35 (t, 1H, 3', J = 5,5 Hz), 8,16 (d, 1H, 7, J = 5,3 Hz), 8,07 (d, 1H, 3, J = 8,7 Hz), 7,83 (d, 1H, 6, J = 5,3 Hz), 7,52 (d, 2H, 8', 12', J = 8,8 Hz), 7,43 (d, 1H, 6', J = 15,8 Hz), 7,05 (d, 1H, 12, J = 2,1 Hz), 6,98 (d, 2H, 9', 11', J = 8,8 Hz), 6,89 (dd, 1H, 2, J = 8,7, 2,2 Hz), 6,58 (d, 1H, 5', J = 15,8 Hz), 4,18 (t, 2H, 1', J = 5,5 Hz), 3,79 (s, 3H, 13'), 3,64 (q, 2H, 2', J = 5,4 Hz), 2,73 (s, 3H, 13).

^{13}C NMR (DMSO-d_6, δ ppm) δ 165,61 (4'), 160,34 (10'), 159,24 (1), 141,97 (8), 141,19 (11), 138,59 (6'), 137,49 (7), 134,55 (9), 129,11 (9', 11'), 127,44 (7'), 127,32 (5), 122,72 (3), 119,53 (5'), 115,00 (4), 114,39 (8', 12'), 112,01 (6), 109,42 (2), 95,42 (12), 66,71 (1'), 55,25 (13'), 38,51 (2'), 20,22 (13).

ESI-MS: m/z 402,2 [M+1]$^+$.

3.2.4.4.7. (E)-3-(2-fluorfenil)-N-(2-((1-metil-9H-piridо[3,4-b]indol-7-il)oksi)etil)akrilamid ***(22g)***

Količina reaktanta: 0,033 g 2-fluorcimetne kiseline.

Iskorištenje: 0,060 g (77 %).

t_t 241,5 °C (raspad).

IR (KBr, ν/cm^{-1}) 3252, 3066, 2942, 2864, 2818, 2600, 1866, 1668, 1630, 1576, 1486, 1456, 1388, 1344, 1278, 1234, 1180, 1100, 1060, 1022, 976, 850, 812, 750, 676, 626, 594.

^{1}H NMR (DMSO-d_6, δ ppm) δ 11,47 (s, 1H, 10), 8,60 (t, 1H, 3', J = 5,4 Hz), 8,15 (d, 1H, 7, J = 5,3 Hz), 8,07 (d, 1H, 3, J = 8,6 Hz), 7,81 (d, 1H, 6, J = 5,3 Hz), 7,69 – 7,64 (m, 1H, 9'), 7,55 (d, 1H, 6', J = 16,0 Hz), 7,47 – 7,41 (m, 1H, 10'), 7,31 – 7,24 (m, 2H, 11', 12'), 7,06 (d, 1H, 12, J = 2,0 Hz), 6,88 (dd, 1H, 2, J = 8,7, 2,1 Hz), 6,84 (d, 1H, 5', J = 16,0 Hz), 4,19 (t, 2H, 1', J = 5,4 Hz), 3,65 (q, 2H, 2', J = 5,4 Hz), 2,73 (s, 3H, 13).

^{13}C NMR (DMSO-d_6, δ ppm) δ 165,08 (4'), 160,49 (d, 8', J = 250,4 Hz), 159,15 (1), 141,90 (8), 141,35 (11), 137,75 (6'), 134,61 (9), 131,39 (7), 131,26 (12'), 129,13 (d, 11' J = 3,0 Hz), 127,19 (5), 125,02 (d, 5', J = 2,6 Hz), 124,88 (d, 10', J = 6,1 Hz), 122,68 (3), 122,53 (d, 7', J = 11,5 Hz), 116,11 (d, 9', J = 21,8 Hz), 115,06 (4), 111,97 (6), 109,34 (2), 95,47 (12), 66,60 (1'), 38,64 (2'), 20,38 (13).

ESI-MS: m/z 390,3 [M+1]$^+$.

*3.2.4.4.8. (E)-2-metil-N-(2-((1-metil-9H-pirido[3,4-b]indol-7-il)oksi)etil)-3-fenilakrilamid (**22h**)*

Količina reaktanta: 0,032 g α-metilcimetne kiseline.

Iskorištenje: 0,047 g (61 %).

t_t 221,5 – 222,5 °C.

IR (KBr, ν/cm^{-1}) 3432, 3202, 3024, 2940, 2880, 2370, 2342, 1952, 1884, 1720, 1630, 1570, 1538, 1484, 1446, 1324, 1276, 1236, 1174, 1106, 1070, 972, 926, 850, 814, 760, 698, 664, 634, 588, 516.

^{1}H NMR (DMSO-d_6, δ ppm) δ 11,52 (s, 1H, 10), 8,33 (t, 1H, 3', J = 5,3 Hz), 8,17 (d, 1H, 7, J = 5,2 Hz), 8,09 (d, 1H, 3, J = 8,6 Hz), 7,85 (d, 1H, 6, J = 5,1 Hz), 7,43 – 7,36 (m, 4H, 8', 9', 11', 12'), 7,33 – 7,30 (m, 1H, 10'), 7,26 (s, 1H, 6'), 7,07 (s, 1H, 12), 6,90 (d, 1H, 2, J = 8,4 Hz), 4,22 (t, 2H, 1', J = 5,2 Hz), 3,63 (q, 2H, 2', J = 5,4 Hz), 2,75 (s, 3H, 13), 2,04 (s, 3H, 13').

^{13}C NMR (DMSO-d_6, δ ppm) δ 169,16 (4'), 159,43 (1), 142,13 (8), 141,01 (11), 137,11 (7), 136,03 (9), 134,53 (7'), 132,51 (6'), 132,29 (5'), 129,22 (9', 11'), 128,41 (8', 12'), 127,71 (10'), 127,54 (5), 122,80 (3), 114,94 (4), 112,09 (6), 109,57 (2), 95,48 (12), 66,29 (1'), 38,97 (2'), 20,04 (13), 14,30 (13').

ESI-MS: *m/z* 386,3 $[M+1]^+$.

3.2.5. Sinteza derivata u položaju 9 β-karbolinskog prstena (23-25)

*3.2.5.1. Sinteza tert-butil-(2-(7-metoksi-1-metil-9H-pirido[3,4-b]indol-9-il)etil)karbamata (**23**)*

Harmin (0,300 g, 1,41 mmol) je pri 85 °C otopljen u bezvodnom DMF-u (4 mL) te mu je u inertnoj atmosferi argona dodan cezijev karbonat (2,07 g, 6,35 mmol), a nakon 20 min i 2-(*tert*-butoksikarbonilamino)etil bromid (1,27 g, 5,65 mmol). Reakcijska smjesa miješana je 24 h na 90 °C pod atmosferom argona. Nakon hlađenja na sobnu temperaturu dodano je 40 mL destilirane vode te je provedena ekstrakcija etil-acetatom (3 × 40 mL). Organski slojevi su sakupljeni i isprani destiliranom vodom (1 × 40 mL), sušeni nad bezvodnim natrijevim sulfatom, filtrirani, a otapalo je iz filtrata uklonjeno uparavanjem pod sniženim tlakom. Sirovi produkt je pročišćen kromatografijom na koloni uz pokretnu fazu diklormetan:metanol (8:1), a nakon rastrljavanja u smjesi dietil-etera i petroletera dobiven je čist spoj **23**.

Iskorištenje: 0,291 g (58 %).

t_t 197,5 – 199,0 °C.

IR (KBr, ν/cm^{-1}) 3183, 3065, 3013, 2993, 2969, 2937, 1701, 1623, 1567, 1502, 1447, 1409, 1366, 1343, 1330, 1313, 1278, 1247, 1195, 1166, 1146, 1124, 1092, 1048, 1018, 970, 944, 876, 841, 803, 768, 727, 684, 639, 598, 559, 534.

^{1}H NMR (DMSO-d_6, δ ppm) δ 8,15 (d, 1H, 7, J = 5,1 Hz), 8,07 (d, 1H, 3, J = 8,5 Hz), 7,85 (d, 1H, 6, J = 5,0 Hz), 7,22 (s, 1H, 12), 7,02 (t, 1H, 3', J = 5,2 Hz), 6,87 (dd, 1H, 2, J = 8,4, 1,6 Hz), 4,55 (t, 2H, 1', J = 6,6 Hz), 3,92 (s, 3H, 14), 3,33 – 3,31 (m, 2H, 2'), 2,95 (s, 3H, 13), 1,29 (s, 8H, 6' – 8'), 1,01 (s, 1H, 6' – 8').

^{13}C NMR (DMSO-d_6, δ ppm) δ 160,46 (1), 155,63 (4'), 142,85 (8), 140,47 (11), 137,64 (7), 134,71 (9), 128,40 (4), 122,21 (3), 114,35 (5), 112,11 (6), 108,96 (2), 93,81 (12), 77,78 (5'), 55,48 (14), 43,99 (1'), 39,98 (2'), 28,02 (6' – 8'), 23,00 (13).

ESI-MS (*m/z*): 356,2 $[M+1]^+$.

*3.2.5.2. Sinteza 2-(7-metoksi-1-metil-9H-pirido[3,4-b]indol-9-il)etan-1-amina (**24**)*

Suspenziji spoja **23** (0,572 g, 1,61 mmol) u metanolu (5 mL) dodana je 4 M klorovodična kiselina (4,013 mL, 16,05 mmol). Reakcijska smjesa je miješana 18 h na 50 °C. Potom je metanol uparen pod sniženim tlakom, a zaostatni talog otopljen u 15 mL destilirane vode i zalužen 5 %-tnom otopinom NaOH do pH 12. Novonastali talog je odsisan i rastrljan u dietil-eteru.

Iskorištenje: 0,243 g (59 %).

t_t 133,5 – 135,5 °C.

IR (KBr, ν/cm^{-1}) 3354, 3327, 3274, 3054, 3039, 2966, 2932, 2837, 1751, 1621, 1563, 1496, 1443, 1404, 1343, 1302, 1283, 1236, 1219, 1151, 1136, 1117, 1089, 1040, 1021, 973, 941, 922, 887, 848, 815, 768, 723, 643, 599, 551, 528.

^{1}H NMR (DMSO-d_6, δ ppm) δ 8,15 (d, 1H, 7, J = 5,2 Hz), 8,07 (d, 1H, 3, J = 8,6 Hz), 7,86 (d, 1H, 6, J = 5,2 Hz), 7,23 (d, 1H, 12, J = 2,2 Hz), 6,86 (dd, 1H, 2, J = 8,6, 2,2 Hz), 4,52 (t, 2H, 1', J = 7,2 Hz), 3,91 (s, 3H, 14), 2,97 (s, 3H, 13), 2,92 (t, 2H, 2', J = 7,2 Hz), 1,61 (s, 2H, 3').

^{13}C NMR (DMSO-d_6, δ ppm) δ 160,47 (1), 142,93 (11), 140,63 (8), 137,61 (7), 134,78 (9), 128,19 (4), 122,26 (3), 114,15 (5), 112,16 (6), 109,08 (2), 93,80 (12), 55,59 (14), 47,22 (1'), 42,14 (2'), 23,28 (13).

ESI-MS (*m/z*): 256,3 $[M+1]^+$.

*3.2.5.3. Sinteza harmicina u položaju 9 β-karbolinskog prstena (**25a-f**, **i-p**). Opća metoda*

Otopina odgovarajućeg DCK-a (0,180 mmol), DIEA (0,061 mL, 0,350 mmol) i HATU (0,068 g, 0,180 mmol) u diklormetanu (4 mL) miješana je na sobnoj temperaturi 15 min, nakon čega je u reakcijsku smjesu dodan amin **24** (0,042 g, 0,164 mmol). Reakcijska smjesa miješana je na sobnoj temperaturi 2 h, zatim pročišćavana metodom A, B ili C.

Metoda A: Reakcijskoj smjesi dodano je 40 mL diklormetana te je ekstrahirana zasićenom otopinom NaCl (2 × 20 mL) i vodom (1 × 20 mL). Organski sloj je sušen nad bezvodnim natrijevim sulfatom, filtriran, a otapalo je iz filtrata uklonjeno uparavanjem pod sniženim tlakom. Sirovi produkt pročišćen je kromatografijom na koloni uz pokretnu fazu diklormetan:metanol (8:1), a zatim rastrljan u dietil-eteru te su dobiveni čisti produkti.

Metoda B: Novonastali talog je odsisan, a filtrat ekstrahiran zasićenom otopinom NaCl (2 × 20 mL) i vodom (1 × 20 mL). Organski slojevi su sakupljeni, sušeni nad bezvodnim natrijevim sulfatom, filtrirani, a otapalo je iz filtrata uklonjeno uparavanjem pod sniženim tlakom. Zaostatni talog spojen je s prethodno odsisanim talogom, zatim pročišćen kromatografijom na koloni uz pokretnu fazu diklormetan:metanol (8:1). Nakon rastrljavanja u dietil-eteru dobiveni su čisti produkti.

Metoda C: Novonastali talog je odsisan i pročišćen kromatografijom na koloni uz pokretnu fazu diklormetan:metanol (8:1). Nakon rastrljavanja u dietil-eteru dobiveni su čisti produkti.

*3.2.5.3.1. N-(2-(7-metoksi-1-metil-9H-pirido[3,4-b]indol-9-il)etil)cinamamid (**25a**)*

Količina reaktanta: 0,027 g *trans*-cimetne kiseline.

Pročišćavanje: Metoda A.

Iskorištenje: 0,032 g (51 %).

t_t 201,5 – 203,0 °C.

IR (KBr, ν/cm^{-1}) 3202, 3027, 2968, 2926, 2852, 1672, 1622, 1566, 1532, 1496, 1447, 1405, 1340, 1306, 1282, 1247, 1218, 1196, 1175, 1138, 1091, 1043, 1020, 972, 938, 856, 814, 762, 679, 641, 597, 555, 485.

^{1}H NMR (DMSO-d_6, δ ppm) δ 8,41 (t, 1H, 3', J = 5,9 Hz), 8,18 (d, 1H, 7, J = 5,2 Hz), 8,09 (d, 1H, 3, J = 8,6 Hz), 7,88 (d, 1H, 6, J = 5,2 Hz), 7,57 – 7,55 (m, 2H, 8', 12'), 7,48 – 7,36 (m, 4H, 6', 9'–11'), 7,27 (d, 1H, 12, J = 1,9 Hz), 6,87 (dd, 1H, 2, J = 8,6, 2,0 Hz), 6,54 (d, 1H, 5', J = 15,8 Hz), 4,67 (t, 2H, 1', J = 6,8 Hz), 3,90 (s, 3H, 14), 3,59 (q, 2H, 2', J = 6,5 Hz), 2,99 (s, 3H, 13).

^{13}C NMR (DMSO-d_6, δ ppm) δ 165,73 (4'), 160,51 (1), 142,91 (8), 140,65 (11), 139,17 (6'), 137,86 (7), 134,75 (9), 134,65 (7'), 129,57 (10'), 128,95 (9', 11'), 128,47 (4), 127,58 (8', 12'), 122,38 (3), 121,66 (5'), 114,29 (5), 112,26 (6), 109,41 (2), 93,50 (12), 55,39 (14), 43,37 (1'), 39,11 (2'), 23,10 (13).

ESI-MS: *m/z* 386,4 $[M+1]^+$.

*3.2.5.3.2. (E)-3-(3-fluorfenil)-N-(2-(7-metoksi-1-metil-9H-pirido[3,4-b]indol-9-il)etil)akrilamid (**25b**)*

Količina reaktanta: 0,030 g 3-fluorcimetne kiseline.

Pročišćavanje: Metoda A.

Iskorištenje: 0,031 g (47 %).

t_t 226,5 – 228,0 °C.

IR (KBr, ν/cm^{-1}) 3661, 3599, 3182, 3009, 2931, 2838, 1671, 1623, 1584, 1538, 1505, 1445, 1412, 1343, 1295, 1240, 1182, 1141, 1095, 1043, 1017, 976, 848, 808, 783, 729, 668, 556, 517.

^{1}H NMR (DMSO-d_6, δ ppm) δ 8,42 (t, 1H, 3', J = 5,9 Hz), 8,18 (d, 1H, 7, J = 5,2 Hz), 8,09 (d, 1H, 3, J = 8,6 Hz), 7,89 (d, 1H, 6, J = 5,2 Hz), 7,49 – 7,40 (m, 4H, 6', 8', 11', 12'), 7,27 (d, 1H, 12, J = 2,0 Hz), 7,24 – 7,20 (m, 1H, 10'), 6,87 (dd, 1H, 2, J = 8,6, 2,1 Hz), 6,59 (d, 1H, 5', J = 15,8 Hz), 4,67 (t, 2H, 1', J = 6,9 Hz), 3,90 (s, 3H, 14), 3,59 (q, 2H, 2', J = 6,5 Hz), 2,99 (s, 3H, 13).

^{13}C NMR (DMSO-d_6, δ ppm) δ 165,45 (4'), 162,46 (d, 9', J = 243,8 Hz), 160,52 (1), 142,92 (8), 140,63 (11), 137,90 (6'), 137,81 (7), 137,36 (d, 7', J = 7,9 Hz), 134,64 (9), 130,91 (d, 11', J = 8,4 Hz), 128,51 (4), 123,77 (12'), 123,21 (3), 122,41 (5'), 116,24 (d, 10', J = 21,3 Hz), 114,29 (5), 113,98 (d, 8', J = 21,8 Hz), 112,28 (6), 109,41 (2), 93,52 (12), 55,40 (14), 43,34 (1'), 39,11 (2') 23,06 (13).

ESI-MS: *m/z* 404,4 $[M+1]^+$.

*3.2.5.3.3. (E)-3-(3-bromfenil)-N-(2-(7-metoksi-1-metil-9H-pirido[3,4-b]indol-9-il)etil)akrilamid (**25c**)*

Količina reaktanta: 0,041 g 3-bromcimetne kiseline.

Pročišćavanje: Metoda B.

Iskorištenje: 0,053 g (70 %).

t_t 225,0 – 226,0 °C.

IR (ATR, ν/cm^{-1}) 3180, 3051, 3021, 2975, 2932, 2901, 2864, 2792, 2559, 1944, 1875, 1679, 1621, 1565, 1498, 1468, 1450, 1410, 1377, 1345, 1305, 1251, 1223, 1195, 1138, 1106, 1043, 1018, 980, 941, 911, 885, 862, 812, 786, 729, 671, 648, 614, 599, 555, 537, 515.

^{1}H NMR (DMSO-d_6, δ ppm) δ 8,39 (t, 1H, 3', J = 6,0 Hz), 8,18 (d, 1H, 7, J = 5,2 Hz), 8,09 (d, 1H, 3, J = 8,6 Hz), 7,89 (d, 1H, 6, J = 5,2 Hz), 7,77 (t, 1H, 8', J = 1,7 Hz), 7,57 (dd, 2H, 10', 12', J = 8,1, 1,4 Hz), 7,44 – 7,36 (m, 2H, 6', 11'), 7,26 (d, 1H, 12, J = 2,1 Hz), 6,87 (dd, 1H, 2, J = 8,6, 2,2 Hz), 6,59 (d, 1H, 5', J = 15,8 Hz), 4,67 (t, 2H, 1', J = 6,9 Hz), 3,90 (s, 3H, 14), 3,60 (q, 2H, 2', J = 6,5 Hz), 2,99 (s, 3H, 13).

^{13}C NMR (DMSO-d_6, δ ppm) 165,40 (4'), 160,53 (1), 142,93 (8), 140,63 (11), 137,81 (6'), 137,58 (7), 137,33 (7'), 134,65 (9), 132,10 (8'), 131,05 (10'), 130,14 (11'), 128,53 (9'), 126,44 (12'), 123,32 (3), 122,42 (5'), 122,28 (4), 114,30 (5), 112,29 (6), 109,40 (2), 93,55 (12), 55,42 (14), 43,35 (1'), 39,11 (2'), 23,06 (13).

ESI-MS: *m/z* 464,3 $[M+1]^+$, 466,3 $[M+1]^+$.

3.2.5.3.4. (E)-3-(4-fluorfenil)-N-(2-(7-metoksi-1-metil-9H-piridо[3,4-b]indol-9-il)etil)akrilamid ***(25d)***

Količina reaktanta: 0,030 g 4-fluorcimetne kiseline.

Pročišćavanje: Metoda B.

Iskorištenje: 0,022 g (33 %).

t_t 202,5 – 204,0 °C.

IR (KBr, ν/cm^{-1}) 3664, 3583, 3438, 3207, 3083, 2985, 2938, 2756, 2723, 1656, 1622, 1601, 1545, 1508, 1471, 1449, 1416, 1390, 1370, 1345, 1292, 1256, 1223, 1203, 1181, 1163, 1141, 1098, 1045, 1018, 976, 944, 836, 741, 722, 644, 557, 530, 511.

^{1}H NMR (DMSO-d_6, δ ppm) δ 8,40 (t, 1H, 3', J = 6,1 Hz), 8,19 (d, 1H, 7, J = 5,3 Hz), 8,11 (d, 1H, 3, J = 8,6 Hz), 7,92 (d, 1H, 6, J = 5,2 Hz), 7,62 (t, 2H, 8', 12', J = 6,9 Hz), 7,45 (d, 1H, 6', J = 15,8 Hz), 7,27 – 7,23 (m, 3H, 9', 11', 12), 6,88 (d, 1H, 2, J = 8,6 Hz), 6,49 (d, 1H, 5', J = 15,8 Hz), 4,67 (t, 2H, 1', J = 7,0 Hz), 3,90 (s, 3H, 14), 3,59 (q, 2H, 2', J = 6,7 Hz), 3,00 (s, 3H, 13).

^{13}C NMR (DMSO-d_6, δ ppm) δ 165,70 (4'), 162,77 (d, 10', J = 247,0 Hz), 160,68 (1), 143,13 (8), 140,45 (11), 138,02 (6'), 137,35 (7), 134,59 (9), 131,38 (d, 7', J = 2,5 Hz), 129,78 (d, 8', 12', J = 8,3 Hz), 128,78 (4), 122,52 (3), 121,53 (5'), 115,94 (d, 9', 11', J = 21,7 Hz), 114,23 (5), 112,40 (6), 109,62 (2), 93,52 (12), 55,44 (14), 43,41 (1'), 39,10 (2'), 22,77 (13).

ESI-MS: *m/z* 404,2 $[M+1]^+$.

*3.2.5.3.5. (E)-3-(4-klorfenil)-N-(2-(7-metoksi-1-metil-9H-pirido[3,4-b]indol-9-il)etil)akrilamid (**25e**)*

Količina reaktanta: 0,033 g 4-klorcimetne kiseline.

Pročišćavanje: Metoda B.

Iskorištenje: 0,036 g (53 %).

t_t 245,0 °C (raspad).

IR (KBr, ν/cm^{-1}) 3195, 3103, 3025, 2998, 2928, 2835, 1672, 1621, 1558, 1493, 1442, 1407, 1338, 1284, 1254, 1200, 1138, 1086, 1045, 977, 947, 799, 748, 708, 680, 634, 593, 550, 497.

^{1}H NMR (DMSO-d_6, δ ppm) δ 8,41 (t, 1H, 3', J = 5,9 Hz), 8,17 (d, 1H, 7, J = 5,2 Hz), 8,09 (d, 1H, 3, J = 8,6 Hz), 7,88 (d, 1H, 6, J = 5,2 Hz), 7,60 – 7,58 (m, 2H, 8', 12'), 7,49 – 7,43 (m, 3H, 6', 9', 11'), 7,26 (d, 1H, 12, J = 2,0 Hz), 6,87 (dd, 1H, 2, J = 8,6, 2,1 Hz), 6,55 (d, 1H, 5', J = 15,8 Hz), 4,67 (t, 2H, 1', J = 6,8 Hz), 3,89 (s, 3H, 14), 3,59 (q, 2H, 2', J = 6,5 Hz), 2,99 (s, 3H, 13).

^{13}C NMR (DMSO-d_6, δ ppm) δ 165,54 (4'), 160,51 (1), 142,91 (8), 140,64 (11), 137,84 (7, 6'), 134,65 (9), 134,00 (10'), 133,71 (7'), 129,30 (9',11'), 128,99 (8', 12'), 128,49 (4), 122,45 (3), 122,39 (5'), 114,29 (5), 112,27 (6), 109,40 (2), 93,51 (12), 55,40 (14), 43,35 (1'), 39,11 (2'), 23,08 (13).

ESI-MS: *m/z* 420,3 $[M+1]^+$, 422,3 $[M+1]^+$.

*3.2.5.3.6. (E)-N-(2-(7-metoksi-1-metil-9H-pirido[3,4-b]indol-9-il)etil)-3-(4-metoksifenil)akrilamid (**25f**)*

Količina reaktanta: 0,032 g 4-metoksicimetne kiseline.

Pročišćavanje: Metoda A.

Iskorištenje: 0,028 g (41 %).

t_t 216,0 – 217,5 °C.

IR (KBr, ν/cm^{-1}) 3212, 3102, 3040, 2993, 2973, 2940, 2919, 2840, 1667, 1620, 1604, 1558, 1514, 1474, 1443, 1409, 1382, 1338, 1306, 1283, 1254, 1229, 1198, 1173, 1138, 1096, 1033, 979, 949, 827, 801, 780, 731, 701, 684, 635, 592, 541, 521.

^{1}H NMR (DMSO-d_6, δ ppm) δ 8,31 (t, 1H, 3', J = 5,9 Hz), 8,17 (d, 1H, 7, J = 5,2 Hz), 8,09 (d, 1H, 3, J = 8,6 Hz), 7,88 (d, 1H, 6, J = 5,2 Hz), 7,51 (d, 2H, 8', 12', J = 8,8 Hz), 7,41 (d, 1H, 6', J = 15,8 Hz), 7,27 (d, 1H, 12, J = 2,1 Hz), 6,97 (d, 2H, 11', 9', J = 8,8 Hz), 6,87 (dd, 1H, 2, J = 8,6, 2,2 Hz), 6,40 (d, 1H, 5', J = 15,8 Hz), 4,66 (t, 2H, 1', J = 6,9 Hz), 3,90 (s, 3H, 14), 3,79 (s, 3H, 13'), 3,58 (q, 2H, 2', J = 6,6 Hz), 2,99 (s, 3H, 13).

^{13}C NMR (DMSO-d_6, δ ppm) δ 166,03 (4'), 160,50 (10'), 160,40 (1), 142,92 (8), 140,63 (11), 138,88 (6'), 137,80 (7), 134,63 (9), 129,17 (9', 11'), 128,46 (7'), 127,30 (4), 122,37 (3), 119,14 (5'), 114,39 (8', 12'), 114,26 (5), 112,26 (6), 109,42 (2), 93,49 (12), 55,39 (14), 55,26 (13'), 43,43 (1'), 39,10 (2'), 23,07 (13).

ESI-MS: *m/z* 416,3 $[M+1]^+$.

*3.2.5.3.7. (E)-N-(2-(7-metoksi-1-metil-9H-pirido[3,4-b]indol-9-il)etil)-3-(3-(trifluormetil)fenil)akrilamid (**25i**)*

Količina reaktanta: 0,039 g 3-(trifluormetil)cimetne kiseline.

Pročišćavanje: Metoda C.

Iskorištenje: 0,033 g (44 %).

t_t 220,5 – 222,5 °C.

IR (ATR, ν/cm^{-1}) 3177, 2978, 2930, 1679, 1623, 1570, 1500, 1450, 1409, 1377, 1343, 1328, 1281, 1270, 1253, 1221, 1199, 1185, 1169, 1139, 1114, 1096, 1079, 1043, 1018, 991, 981, 803, 694, 659, 556, 530.

^{1}H NMR (DMSO-d_6, δ ppm) δ 8,42 (t, 1H, 3', J = 6,0 Hz), 8,18 (d, 1H, 7, J = 5,2 Hz), 8,09 (d, 1H, 3, J = 8,5 Hz), 7,91 – 7,87 (m, 3H, 6, 8', 12'), 7,74 (dd, 1H, 11', J = 7,7, 1,6 Hz), 7,66 (t, 1H, 10', J = 7,8 Hz), 7,54 (d, 1H, 6', J = 15,8 Hz), 7,27 (d, 1H, 12, J = 2,2 Hz), 6,87 (dd, 1H, 2, J = 8,6, 2,2 Hz), 6,68 (d, 1H, 5', J = 15,8 Hz), 4,68 (t, 2H, 1', J = 7,0 Hz), 3,90 (s, 3H, 14), 3,61 (q, 2H, 2', J = 6,6 Hz), 2,99 (s, 3H, 13).

^{13}C NMR (DMSO-d_6, δ ppm) δ 165,35 (4'), 160,52 (1), 142,92 (8), 140,66 (11), 137,87 (6'), 137,51 (7), 135,98 (9), 134,68 (7'), 131,26 (12'), 130,09 (11'), 129,76 (q, 9', J = 31,7 Hz), 128,51 (4), 125,86 (q, 10', J = 3,6 Hz), 124,06 (q, 8', J = 3,6 Hz), 124,04 (q, 13', J = 272,5 Hz), 123,81 (3), 122,41 (5'), 114,33 (5), 112,29 (6), 109,37 (2), 93,57 (12), 55,41 (14), 43,37 (1'), 39,13 (1'), 23,10 (13).

ESI-MS: *m/z* 454,2 $[M+1]^+$.

HPLC čistoća 98,2 %.

*3.2.5.3.8. (E)-N-(2-(7-metoksi-1-metil-9H-pirido[3,4-b]indol-9-il)etil)-3-(4-(trifluormetil)fenil)akrilamid (**25j**)*

Količina reaktanta: 0,039 g 4-(trifluormetil)cimetne kiseline.

Pročišćavanje: Metoda C.

Iskorištenje: 0,033 g (45 %).

t_t 252,0 – 254,5 °C.

IR (ATR, ν/cm^{-1}) 3188, 3005, 2962, 2844, 1680, 1633, 1569, 1445, 1412, 1321, 1253, 1199, 1165, 1108, 1066, 974, 831, 801, 597, 573.

^{1}H NMR (DMSO-d_6, δ ppm) δ 8,50 (t, 1H, 3', J = 6,0 Hz), 8,18 (d, 1H, 7, J = 5,1 Hz), 8,09 (d, 1H, 3, J = 8,6 Hz), 7,89 (d, 1H, 6, J = 5,2 Hz), 7,78 (s, 4H, 8', 9', 11', 12'), 7,53 (d, 1H, 6', J = 15,8 Hz), 7,27 (d, 1H, 12, J = 2,2 Hz), 6,87 (dd, 1H, 2, J = 8,6, 2,2 Hz), 6,68 (d, 1H, 5', J = 15,8 Hz), 4,68 (t, 2H, 1', J = 6,9 Hz), 3,90 (s, 3H, 14), 3,61 (q, 2H, 2', J = 6,7 Hz), 3,00 (s, 3H, 13).

^{13}C NMR (DMSO-d_6, δ ppm) δ 165,27 (4'), 160,52 (1), 142,92 (8), 140,62 (9), 138,83 (7'), 137,83 (6'), 137,51 (7), 134,64 (11), 129,29 (q, 10', J = 31,8 Hz), 128,52 (4), 128,21 (8', 12'), 125,81 (q, 9', 11', J = 3,5 Hz), 124,44 (3), 124,09 (q, 13', J = 272,0 Hz), 122,40 (5'), 114,30 (5), 112,28 (6), 109,40 (2), 93,51 (12), 55,40 (14), 43,32 (1'), 39,13 (2'), 23,06 (13).

ESI-MS: m/z 454,1 $[M+1]^+$.

HPLC čistoća 99,1 %.

*3.2.5.3.9. (E)-3-(2-klorfenil)-N-(2-(7-metoksi-1-metil-9H-piridо[3,4-b]indol-9-il)etil)akrilamid (**25k**)*

Količina reaktanta: 0,033 g 2-klorcimetne kiseline.

Pročišćavanje: Metoda A.

Iskorištenje: 0,032 g (47 %).

t_t 218,5 – 221,5 °C.

IR (ATR, ν/cm^{-1}) 3285, 3081, 2970, 1741, 1650, 1616, 1556, 1498, 1469, 1454, 1440, 1406, 1380, 1338, 1305, 1228, 1199, 1178, 1138, 1120, 1102, 1092, 1047, 1036, 974, 948, 880, 819, 807, 767, 746, 709, 684, 664, 637, 614, 604, 594, 584, 550, 536, 511, 486.

^{1}H NMR (DMSO-d_6, δ ppm) δ 8,50 (t, 1H, 3', J = 6,0 Hz), 8,18 (d, 1H, 7, J = 5,2 Hz), 8,09 (d, 1H, 3, J = 8,6 Hz), 7,89 (d, 1H, 6, J = 5,2 Hz), 7,76 (d, 1H, 6', J = 15,7 Hz), 7,69 – 7,67 (m, 1H, 9'), 7,55 – 7,53 (m, 1H, 10'), 7,44 – 7,39 (m, 2H, 11', 12'), 7,25 (d, 1H, 12, J = 2,2 Hz), 6,87 (dd, 1H, 2, J = 8,6, 2,1 Hz), 6,58 (d, 1H, 5', J = 15,7 Hz), 4,69 (t, 2H, 1', J = 6,9 Hz), 3,90 (s, 3H, 14), 3,60 (q, 2H, 2', J = 6,6 Hz), 3,00 (s, 3H, 13).

^{13}C NMR (DMSO-d_6, δ ppm) δ 165,23 (4'), 160,54 (1), 142,98 (8), 140,61 (11), 137,79 (7), 134,63 (9), 134,45 (6'), 133,33 (8'), 132,56 (7'), 131,04 (9'), 130,00 (10'), 128,57 (4), 127,80 (12'), 127,62 (11'), 124,75 (5'), 122,41 (3), 114,27 (5), 112,30 (6), 109,45 (2), 93,50 (12), 55,42 (14), 43,30 (1'), 39,22 (2'), 23,04 (13).

ESI-MS: m/z 420,1 $[M+1]^+$, 422,15 $[M+1]^+$.

*3.2.5.3.10. (E)-3-(3-klorfenil)-N-(2-(7-metoksi-1-metil-9H-pirido[3,4-b]indol-9-il)etil)akrilamid (**25l**)*

Količina reaktanta: 0,033 g 3-klorcimetne kiseline.

Pročišćavanje: Metoda A.

Iskorištenje: 0,057 g (83 %).

t_t 210,5 – 213,0 °C.

IR (ATR, ν/cm^{-1}) 3182, 2934, 2975, 1743, 1680, 1622, 1592, 1567, 1499, 1450, 1410, 1377, 1345, 1305, 1281, 1228, 1252, 1197, 1171, 1138, 1125, 1107, 1043, 1018, 910, 893, 862, 825, 812, 799, 788, 730, 672, 649, 636, 614, 599, 576, 556, 5445, 529.

^{1}H NMR (DMSO-d_6, δ ppm) δ 8,40 (t, 1H, 3', J = 6,0 Hz), 8,18 (d, 1H, 7, J = 5,2 Hz), 8,09 (d, 1H, 3, J = 8,6 Hz), 7,89 (d, 1H, 6, J = 5,1 Hz), 7,64 (s, 1H, 8'), 7,54 – 7,52 (m, 1H, 10'), 7,46 – 7,42 (m, 3H, 6', 11', 12'), 7,26 (d, 1H, 12, J = 2,2 Hz), 6,87 (dd, 1H, 2, J = 8,6, 2,2 Hz), 6,60 (d, 1H, 5', J = 15,8 Hz), 4,67 (t, 2H, 1', J = 6,9 Hz), 3,90 (s, 3H, 14), 3,60 (q, 2H, 2', J = 6,7 Hz), 2,99 (s, 3H, 13).

^{13}C NMR (DMSO-d_6, δ ppm) δ 165,40 (4'), 160,51 (1), 142,91 (8), 140,63 (11), 137,83 (7), 137,64 (6'), 137,07 (9'), 134,65 (9), 133,68 (7'), 130,77 (10'), 129,19 (11'), 128,50 (4), 127,27 (8'), 126,06 (12'), 123,33 (5'), 122,40 (3), 114,30 (5), 112,27 (6), 109,38 (2), 93,54 (12), 55,40 (14), 43,34 (1'), 39,11 (2'), 23,07 (13).

ESI-MS: m/z 420,05 $[M+1]^+$, 422,05 $[M+1]^+$.

*3.2.5.3.11. (E)-N-(2-(7-metoksi-1-metil-9H-pirido[3,4-b]indol-9-il)etil)-3-(3-(trifluormetoksi)fenil)akrilamid (**25m**)*

Količina reaktanta: 0,042 g 3-(trifluormetoksi)cimetne kiseline.

Pročišćavanje: Metoda A.

Iskorištenje: 0,062 g (81 %).

t_t 204,5 – 207,0 °C.

IR (ATR, ν/cm^{-1}) 3200, 2981, 2901, 1740, 1675, 1623, 1563, 1497, 1472, 1452, 1410, 1383, 1364, 1340, 1308, 1263, 1254, 1199, 1177, 1107, 1096, 1047, 1024, 991, 978, 948, 938, 881, 827, 802, 787, 698, 670, 633, 605, 596, 569, 528, 550.

^{1}H NMR (DMSO-d_6, δ ppm) δ 8,43 (t, 1H, 3', J = 6,0 Hz), 8,18 (d, 1H, 7, J = 5,2 Hz), 8,09 (d, 1H, 3, J = 8,6 Hz), 7,89 (d, 1H, 6, J = 5,2 Hz), 7,61 – 7,60 (m, 1H, 11'), 7,57 – 7,54 (m, 2H, 8', 12'), 7,48 (d, 1H, 6', J = 15,8 Hz), 7,38 (d, 1H, 10', J = 8,1 Hz), 7,27 (d, 1H, 12, J = 2,3 Hz), 6,87 (dd, 1H, 2, J = 8,6, 2,2 Hz), 6,63 (d, 1H, 5', J = 15,8 Hz), 4,67 (t, 2H, 1', J = 7,0 Hz), 3,90 (s, 3H, 14), 3,60 (q, 2H, 2', J = 6,7 Hz), 2,99 (s, 3H, 13).

^{13}C NMR (DMSO-d_6, δ ppm) δ 165,34 (4'), 160,51 (1), 148,81 (9'), 142,91 (8), 140,64 (11), 137,84 (7), 137,50 (6'), 137,30 (7'), 134,65 (9), 130,94 (11'), 128,50 (4), 126,55 (12'), 123,68 (5'), 122,40 (3), 121,75 (8'), 120,07 (q, 13', J = 230,5 Hz), 119,81 (10'), 114,31 (5), 112,28 (6), 109,38 (2), 93,54 (12), 55,41 (14), 43,34 (1'), 39,11 (2'), 23,08 (13).
ESI-MS: 470,1 *m/z* $[M+1]^+$.

*3.2.5.3.12. (E)-3-(4-bromfenil)-N-(2-(7-metoksi-1-metil-9H-pirido[3,4-b]indol-9-il)etil)akrilamid (**25n**)*

Količina reaktanta: 0,041 g 4-bromcimetne kiseline.
Pročišćavanje: Metoda C.
Iskorištenje: 0,049 g (64 %).
t_t 250,0 – 252,5 °C.
IR (ATR, ν/cm^{-1}) 3292, 1742, 1653, 1621, 1589, 1562, 1548, 1488, 1468, 1455, 1440, 1428, 1404, 1375, 1335, 1280, 1251, 1227, 1198, 1138, 1121, 1101, 1084, 1045, 1024, 1013, 975, 946, 868, 847, 818, 811, 753, 734, 705, 670, 642, 631, 601, 589, 549, 519, 506, 469.
^{1}H NMR (DMSO-d_6, δ ppm) δ 8,42 (t, 1H, 3', J = 6,0 Hz), 8,18 (d, 1H, 7, J = 5,1 Hz), 8,09 (d, 1H, 3, J = 8,6 Hz), 7,89 (d, 1H, 6, J = 5,1 Hz), 7,61 (d, 2H, 9', 11', J = 8,4 Hz), 7,51 (d, 2H, 8', 12', J = 8,5 Hz), 7,43 (d, 1H, 6', J = 15,8 Hz), 7,26 (d, 1H, 12, J = 2,2 Hz), 6,87 (dd, 1H, 2, J = 8,6, 2,2 Hz), 6,56 (d, 1H, 5', J = 15,8 Hz), 4,67 (t, 2H, 1', J = 6,9 Hz), 3,89 (s, 3H, 14), 3,59 (q, 2H, 2', J = 6,7 Hz), 2,99 (s, 3H, 13).
^{13}C NMR (DMSO-d_6, δ ppm) δ 165,52 (4'), 160,53 (1), 142,93 (8), 140,60 (11), 137,92 (7), 137,77 (6'), 134,63 (9), 134,05 (7'), 131,91 (9', 11'), 129,54 (8', 12'), 128,52 (4), 122,74 (10'), 122,50 (5'), 122,41 (3), 114,28 (5), 112,28 (6), 109,42 (2), 93,51 (12), 55,40 (14), 43,35 (1'), 39,11 (2'), 23,04 (13).
ESI-MS*: m/z* 464,05 $[M+1]^+$, 466,0 $[M+1]^+$.

*3.2.5.3.13. (E)-N-(2-(7-metoksi-1-metil-9H-pirido[3,4-b]indol-9-il)etil)-3-(p-tolil)akrilamid (**25o**)*

Količina reaktanta: 0,029 g 4-metilcimetne kiseline.
Pročišćavanje: Metoda A.
Iskorištenje: 0,046 g (70 %).
t_t 216,5 – 219,5 °C.

IR (ATR, ν/cm^{-1}) 3208, 3021, 2904, 1734, 1672, 1622, 1559, 1516, 1499, 1409, 1381, 1340, 1323, 1307, 1283, 1255, 1230, 1200, 1178, 1138, 1123, 1096, 1025, 1046, 980, 948, 865, 832, 812, 803, 723, 703, 681, 635, 603, 593, 552, 516, 498.

^{1}H NMR (DMSO-d_6, δ ppm) δ 8,35 (t, 1H, 3', J = 6,0 Hz), 8,17 (d, 1H, 7, J = 5,2 Hz), 8,09 (d, 1H, 3, J = 8,5 Hz), 7,89 (d, 1H, 6, J = 5,1 Hz), 7,45 – 7,14 (m, 3H, 6', 9', 11'), 7,26 (d, 1H, 12, J = 2,2 Hz), 7,22 (d, 2H, 8', 12', J = 7,7 Hz), 6,87 (dd, 1H, 2, J = 8,6, 2,1 Hz), 6,48 (d, 1H, 5', J = 15,8 Hz), 4,66 (t, 2H, 1', J = 7,0 Hz), 3,89 (s, 3H, 14), 3,58 (q, 2H, 2', J = 6,6 Hz), 2,99 (s, 3H, 13), 2,32 (s, 3H, 13').

^{13}C NMR (DMSO-d_6, δ ppm) δ 165,88 (4'), 160,53 (1), 142,95 (8), 140,61 (11), 139,34 (10'), 139,12 (6'), 137,77 (7), 134,63 (9), 131,99 (7'), 129,54 (9', 11'), 128,51 (4), 127,56 (8', 12'), 122,39 (3), 120,61 (5'), 114,26 (5), 112,28 (6), 109,44 (2), 93,50 (12), 55,39 (14), 43,40 (1'), 39,10 (2'), 23,04 (13), 20,95 (13').

ESI-MS*: m/z* 400,15 $[M+1]^+$.

*3.2.5.3.14. (E)-N-(2-(7-metoksi-1-metil-9H-pirido[3,4-b]indol-9-il)etil)-3-(4-nitrofenil)akrilamid (**25p**)*

Količina reaktanta: 0,035 g 4-nitrocimetne kiseline.

Pročišćavanje: Metoda C.

Iskorištenje: 0,044 g (62 %).

t_t 275,0 – 278,0 °C.

IR (ATR, ν/cm^{-1}) 3184, 3011, 1739, 1669, 1622, 1592, 1555, 1508, 1473, 1446, 1409, 1382, 1363, 1333, 1254, 1225, 1197, 1176, 1119, 1139, 1092, 1044, 980, 846, 822, 799, 754, 739, 705, 671, 632, 601, 591, 548, 512.

^{1}H NMR (DMSO-d_6, δ ppm) δ 8,54 (t, 1H, 3', J = 6,0 Hz), 8,25 (d, 2H, 9', 11', J = 8,7 Hz), 8,18 (d, 1H, 7, J = 5,2 Hz), 8,09 (d, 1H, 3, J = 8,6 Hz), 7,89 (d, 1H, 6, J = 5,1 Hz), 7,83 (d, 2H, 8', 12', J = 8,7 Hz), 7,55 (d, 1H, 6', J = 15,8 Hz), 7,26 (d, 1H, 12, J = 2,1 Hz), 6,87 (dd, 1H, 2, J = 8,6, 2,1 Hz), 6,73 (d, 1H, 5', J = 15,8 Hz), 4,68 (t, 2H, 1', J = 6,9 Hz), 3,89 (s, 3H, 14), 3,61 (q, 2H, 2', J = 6,6 Hz), 2,99 (s, 3H, 13).

^{13}C NMR (DMSO-d_6, δ ppm) δ 165,06 (4'), 160,51 (1), 147,57 (10'), 142,91 (8), 141,33 (7'), 140,62 (11), 137,85 (7), 136,88 (6'), 134,65 (9), 128,65 (8', 12'), 128,52 (4), 125,87 (5'), 124,11 (9', 11'), 122,41 (3), 114,31 (5), 112,28 (6), 109,39 (2), 93,53 (12), 55,41 (14), 43,30 (1'), 39,16 (2'), 23,06 (13).

ESI-MS*: m/z* 431,1 $[M+1]^+$.

3.2.6. Sinteza klorida DCK-a (26b-k). Opća metoda

Otopina odgovarajućeg DCK-a (2,91 mmol), tionil-klorida (17,46 mmol, 1,27 mL) i bezvodnog DMF-u (5 kapi) u bezvodnom toluenu (8 mL) miješana je na sobnoj temperaturi 3 h. Zatim je otapalo upareno pod sniženim tlakom, a reakcijska smjesa naparena toluenom (2 × 6 mL). Sirovi produkti klorida DCK-a **26b-k** korišteni su u idućem reakcijskom koraku bez dodatnog pročišćavanja.

3.2.7. Sinteza cinamilnih alkohola (27b-k). Opća metoda

Otopini klorida DCK-a (2,91 mmol) u bezvodnom otapalu dodan je $NaBH_4$. Reakcijska smjesa miješana je na sobnoj temperaturi u inertnoj atmosferi dušika ili argona uz postepeno dokapavanje bezvodnog metanola (1 mL) unutar 1 h. Reakcija je prekinuta uparavanjem otapala pod sniženim tlakom te je u zaostatni talog dodana 1 M HCl (2,5 mL). Novonastala suspenzija miješana je nekoliko minuta, a zatim pročišćavana metodom A ili B.

Metoda A: U suspenziju je dodan dietil-eter (40 mL) te je provedena ekstrakcija vodom (2 × 30 mL). Organski sloj je sušen nad bezvodnim natrijevim sulfatom, filtriran, a otapalo je iz filtrata uklonjeno uparavanjem pod sniženim tlakom. Sirovi produkt pročišćen je kromatografijom na koloni uz pokretnu fazu cikloheksan:etil-acetat:metanol (3:1:0,5), a spojevi **27b** i **27d** su dodatno pročišćeni rastrljavanjem u cikloheksanu.

Metoda B: U suspenziju je dodana voda (30 mL) te je provedena ekstrakcija dietil-eterom (3 × 30 mL). Organski slojevi sakupljeni, sušeni nad bezvodnim natrijevim sulfatom, filtrirani, a otapalo je iz filtrata uklonjeno uparavanjem pod sniženim tlakom. Sirovi produkt pročišćen je kromatografijom na koloni uz pokretnu fazu cikloheksan:etil-acetat:metanol (3:1:0,5) ili cikloheksan:etil-acetat (3:2). Spojevi **27e** i **27i** dodatno su pročišćeni rastrljavanjem u cikloheksanu.

*3.2.7.1. (E)-3-(4-propoksifenil)prop-2-en-1-ol (**27b**)*

Količina reaktanta: 0,654 g spoja **26b**.

Otapalo: bezvodni THF (8 mL).

Količina $NaBH_4$: 0,220 g, 5,82 mmol.

Trajanje reakcije: 40 min.

Pročišćavanje: Metoda A.

Iskorištenje: 0,436 g (78 %).

t_t 78,5 – 79,5 °C.

IR (ATR, ν/cm^{-1}) 3356, 3037, 2963, 2933, 2877, 1605, 1575, 1510, 1466, 1393, 1306, 1268, 1240, 1174, 1132, 1085, 1024, 1005, 965, 918, 834, 806, 778, 636, 543, 519, 499.

^{1}H NMR (DMSO-d_6, δ ppm) δ 7,33 (d, 2H, 6, 10, J = 8,2 Hz), 6,87 (d, 2H, 7, 9, J = 8,1 Hz), 6,47 (d, 1H, 4, J = 15,9 Hz), 6,20 (dt, 1H, 3, J = 16,1, 5,3 Hz), 4,78 (t, 1H, 1, J = 5,5 Hz), 4,08 (t, 2H, 2, J = 5,4 Hz), 3,91 (t, 2H, 1', J = 6,5 Hz), 1,71 (h, 2H, 2', J = 7,0 Hz), 0,97 (t, 3H, 3', J = 7,4 Hz).

^{13}C NMR (DMSO-d_6, δ ppm) δ 158,02 (8), 129,36 (5), 128,24 (4), 128,19 (3), 127,32 (6, 10), 114,49 (7, 9), 68,88 (1'), 61,65 (2), 22,04 (2'), 10,40 (3').

*3.2.7.2. (E)-3-(3-(trifluormetil)fenil)prop-2-en-1-ol (**27c**)*

Količina reaktanta: 0,683 g spoja **26c**.

Otapalo: bezvodni THF (8 mL).

Količina $NaBH_4$: 0,220 g, 5,82 mmol.

Trajanje reakcije: 2 h.

Pročišćavanje: Metoda A.

Iskorištenje: 0,447 g (76 %).

Ulje.

IR (ATR, ν/cm^{-1}) 3313, 2866, 1740, 1593, 1440, 1332, 1270, 1164, 1124, 1100, 1012, 967, 902, 792, 697, 664, 536, 461, 452.

^{1}H NMR (DMSO-d_6, δ ppm) δ 7,76 – 7,75 (m, 2H, 6, 8), 7,58 – 7,52 (m, 2H, 9, 10), 6,66 (dt, 1H, 4, J = 15,9, 1,8 Hz), 6,56 (dt, 1H, 3, J = 16,0, 4,7 Hz), 4,95 (t, 1H, 1, J = 5,4 Hz), 4,15 (td, 2H, 2, J = 5,1, 1,8 Hz).

^{13}C NMR (DMSO-d_6, δ ppm) δ 138,11 (5), 133,34 (4), 129,88 (q, 9, J = 1,4 Hz), 129,64 (10), 129,51 (q, 7, J = 31,2 Hz), 126,69 (3), 124,23 (q, 1', J = 271,8 Hz), 123,54 (q, 6, J = 3,8 Hz), 122,54 (q, 8, J = 3,8 Hz), 61,24 (2).

*3.2.7.3. (E)-3-(3,5-bis(trifluormetil)fenil)prop-2-en-1-ol (**27d**)*

Količina reaktanta: 0,881 g spoja **26d**.

Otapalo: bezvodni THF (9 mL).

Količina $NaBH_4$: 0,220 g, 5,82 mmol.

Trajanje reakcije: 20 h.

Pročišćavanje: Metoda A.

Iskorištenje: 0,102 g (13 %).

t_t 89,0 – 91,5°C.

IR (ATR, ν/cm^{-1}) 3344, 2927, 1742, 1662, 1616, 1469, 1385, 1368, 1281, 1233, 1203, 1159, 1117, 968, 905, 845, 784, 750, 728, 698, 664, 532, 469.

^{1}H NMR (DMSO-d_6, δ ppm) δ 8,13 (s, 2H, 6, 10), 7,90 (s, 1H, 8), 6,82 – 6,75 (m, 2H, 3, 4), 5,03 (t, 1H, 1, J = 5,4 Hz), 4,19 – 4,18 (m, 2H, 2).

^{13}C NMR (DMSO-d_6, δ ppm) δ 139,89 (5), 135,98 (4), 130,61 (q, 7, 9 J = 32,7 Hz), 126,53 (q, 6, 10, J = 3,5 Hz), 125,15 (3), 123,38 (q, 1', 2', J = 272,6 Hz), 120,07 (dt, 8, J = 7,5, 3,7 Hz), 61,07 (2).

*3.2.7.4. (E)-3-(4-(trifluormetil)fenil)prop-2-en-1-ol (**27e**)*

Količina reaktanta: 0,683 g spoja **26e**.

Otapalo: bezvodni dietil-eter (8 mL).

Količina $NaBH_4$: 0,165 g, 4,37 mmol.

Trajanje reakcije: 22 h.

Pročišćavanje: Metoda B; pokretna faza: cikloheksan:etil-acetat (3:2).

Iskorištenje: 0,059 g (10 %).

t_t 50,5 – 53,0 °C.

IR (ATR, ν/cm^{-1}) 3277, 2931, 2082, 1927, 1740, 1657, 1613, 1577, 1459, 1413, 1318, 1279, 1206, 1167, 1111, 1121, 1092, 1066, 969, 920, 858, 849, 789, 757, 724, 679, 646, 636, 597, 536, 496.

^{1}H NMR (DMSO-d_6, δ ppm) δ 7,68 – 7,64 (m, 4H, 6, 7, 9, 10), 6,66 (dt, 1H, 4, J = 16,0, 1,8 Hz), 6,58 (dt, 1H, 3, J = 16,0, 4,6 Hz), 4,98 (t, 1H, 1, J = 5,4 Hz), 4,16 (td, 2H, 2, J = 5,1, 1,8 Hz).

^{13}C NMR (DMSO-d_6, δ ppm) δ 141,06 (5), 134,27 (4), 129,12 (3), 127,27 (q, 8, J = 31,7 Hz), 126,69 (6, 10), 125,46 (q, 7, 9, J = 3,8 Hz), 124,35 (q, 1', J = 271,8 Hz), 61,22 (2).

*3.2.7.5. (E)-3-(2-klorfenil)prop-2-en-1-ol (**27f**)*

Količina reaktanta: 0,585 g spoja **26f**.

Otapalo: bezvodni dietil-eter (8 mL).

Količina $NaBH_4$: 0,165 g, 4,37 mmol.

Trajanje reakcije: 15 h.

Pročišćavanje: Metoda B; pokretna faza: cikloheksan:etil-acetat:metanol (3:1:0,5).

Iskorištenje: 0,015 g (3 %).

Spoj je korišten u daljnjoj reakciji bez karakterizacije, a njegova struktura je potvrđena neizravno, karakterizacijom spoja **28f**.

*3.2.7.6. (E)-3-(3-klorfenil)prop-2-en-1-ol (**27g**)*

Količina reaktanta: 0,585 g spoja **26g**.

Otapalo: bezvodni dietil-eter (8 mL).

Količina $NaBH_4$: 0,165 g, 4,37 mmol.

Trajanje reakcije: 14 h.

Pročišćavanje: Metoda B; pokretna faza: cikloheksan:etil-acetat:metanol (3:1:0,5).

Iskorištenje: 0,118 g (24 %).

Ulje.

IR (ATR, ν/cm^{-1}) 3312, 2862, 1741, 1658, 1594, 1565, 1475, 1425, 1369, 1202, 1166, 1091, 1076, 997, 962, 930, 882, 767, 702, 680, 568, 522.

^{1}H NMR (DMSO-d_6, δ ppm) δ 7,49 (t, 1H, 6, J = 1,9 Hz), 7,39 (dt, 1H, 8, J = 7,7, 1,4 Hz), 7,34 (t, 1H, 10, J = 7,8 Hz), 7,28 – 7,26 (m, 1H, 9), 6,55 (dt, 1H, 4, J = 15,9, 1,7 Hz), 6,48 (dt, 1H, 3, J = 15,9, 4,6 Hz), 4,92 (t, 1H, 1, J = 5,4 Hz), 4,13 (td, 2H, 2, J = 5,0, 1,7 Hz).

^{13}C NMR (DMSO-d_6, δ ppm) δ 139,26 (5), 133,43 (7), 132,83 (4), 130,38 (10), 126,86 (9), 126,77 (8), 125,74 (3), 124,74 (6), 61,25 (2).

*3.2.7.7. (E)-3-(3-(trifluormetoksi)fenil)prop-2-en-1-ol (**27h**)*

Količina reaktanta: 0,729 g spoja **26h**.

Otapalo: bezvodni dietil-eter (9 mL).

Količina $NaBH_4$: 0,275 g, 7,28 mmol.

Trajanje reakcije: 16 h.

Pročišćavanje: Metoda B; pokretna faza: cikloheksan:etil-acetat (3:2).

Iskorištenje: 0,438 g (69 %).

Ulje.

IR (ATR, ν/cm^{-1}) 3313, 2866, 1741, 1609, 1584, 1491, 1446, 1371, 1253, 1216, 1164, 1096, 1002, 965, 837, 770, 702, 635, 524, 483.

^{1}H NMR (DMSO-d_6, δ ppm) δ 7,48 – 7,44 (m, 2H, 9, 10), 7,41 (s, 1H, 6), 7,21 (d, 1H, 8, J = 7,3 Hz), 6,60 (dt, 1H, 4, J = 16,1, 1,7 Hz), 6,51 (dt, 1H, 3, J = 16,0, 4,7 Hz), 4,94 (t, 1H, 1, J = 5,4 Hz), 4,14 (td, 2H, 2, J = 5,1, 1,8 Hz).

^{13}C NMR (DMSO-d_6, δ ppm) δ 148,83 (7), 139,54 (5), 133,22 (4), 130,48 (9), 126,70 (10), 125,20 (3), 120,01 (q, 1', J = 256,2 Hz), 119,38 (8), 118,39 (6), 61,22 (2).

*3.2.7.8. (E)-3-(4-bromfenil)prop-2-en-1-ol (**27i**)*

Količina reaktanta: 0,714 g spoja **26i**.

Otapalo: bezvodni dietil-eter (9 mL).

Količina $NaBH_4$: 0,165 g, 4,37 mmol.

Trajanje reakcije: 20 h.

Pročišćavanje: Metoda B; pokretna faza: cikloheksan:etil-acetat (3:2).

Iskorištenje: 0,068 g (11 %).

t_t 71,5 – 73,0 °C.

IR (ATR, ν/cm^{-1}) 3232, 2849, 1741, 1656, 1583, 1485, 1397, 1351, 1295, 1219, 1204, 1175, 1084, 1070, 1021, 994, 964, 920, 825, 691, 652, 533, 499.

^{1}H NMR (DMSO-d_6, δ ppm) 7,51 – 7,49 (m, 2H, 7, 9), 7,40 – 7,37 (m, 2H, 6, 10), 6,53 (dt, 1H, 4, J = 15,9, 1,8 Hz), 6,42 (dt, 1H, 3, J = 16,0, 4,9 Hz), 4,89 (t, 1H, 1, J = 5,4 Hz), 4,11 – 4,10 (m, 2H, 2).

^{13}C NMR (DMSO-d_6, δ ppm) δ 136,21 (5), 131,99 (4), 131,45 (7, 9), 128,14 (6, 10), 127,04 (3), 120,02 (8), 61,32 (2).

*3.2.7.9. (E)-3-(p-tolil)prop-2-en-1-ol (**27j**)*

Količina reaktanta: 0,526 g spoja **26j**.

Otapalo: bezvodni dietil-eter (10 mL).

Količina $NaBH_4$: 0,165 g, 4,37 mmol.

Trajanje reakcije: 21 h.

Pročišćavanje: Metoda B; pokretna faza: cikloheksan:etil-acetat (3:2).

Iskorištenje: 0,116 g (27 %).

t_t 48,0 – 50,5 °C.

IR (ATR, ν/cm^{-1}) 3277, 3022, 2919, 2855, 1906, 1742, 1655, 1610, 1570, 1511, 1463, 1412, 1337, 1316, 1270, 1219, 1111, 1011, 998, 970, 849, 834, 793, 708, 565, 523, 472.

^{1}H NMR (DMSO-d_6, δ ppm) δ 7,31 – 7,29 (m, 2H, 6, 10), 7,13 – 7,12 (m, 2H, 7, 9), 6,50 (dt, 1H, 4, J = 16,0, 1,8 Hz), 6,30 (dt, 1H, 3, J = 15,9, 5,2 Hz), 4,82 (t, 1H, 1, J = 5,5 Hz), 4,10 (td, 2H, 2, J = 5,4, 1,8 Hz), 2,28 (s, 3H, 1').

^{13}C NMR (DMSO-d_6, δ ppm) δ 136,46 (5), 134,12 (8), 129,69 (4), 129,21 (6, 10), 128,44 (3), 126,08 (7, 9), 61,58 (2), 20,79 (1').

*3.2.7.10. (E)-3-(4-nitrofenil)prop-2-en-1-ol (**27k**)*

Količina reaktanta: 0,616 g spoja **26k**.

Otapalo: bezvodni dietil-eter (9 mL).

Količina $NaBH_4$: 0,165 g, 4,37 mmol.

Trajanje reakcije: 16 h.

Pročišćavanje: Metoda B; pokretna faza: cikloheksan:etil-acetat:metanol (3:1:0,5).

Spoj je korišten u daljnjoj reakciji bez karakterizacije, a njegova struktura je potvrđena neizravno, karakterizacijom spoja **28k**.

3.2.8. Sinteza harmicina karbamatnog tipa (28a-d). Opća metoda

Otopina CDI-a (0,038 g, 0,235 mmol) u bezvodnom DMF-u (0,8 mL) miješana je 30 minuta na 0 °C. Zatim je u otopinu postepeno dokapavana suspenzija amina **24** (0,050 g, 0,196 mmol) u bezvodnom DMF-u (0,8 mL). Suspenzija odgovarajućeg cinamilnog alkohola (0,235 mmol) i 60 %-tnog natrijevog hidrida (0,0094 g, 0,235 mmol) u bezvodnom DMF-u (0,8 mL) miješana je na sobnoj temperaturi 1 h, a nakon toga je postepeno dokapavana u smjesu CDI-a i amina **24** u bezvodnom DMF-u. Reakcijska smjesa miješana je na sobnoj temperaturi 18 h, nakon čega je u reakcijsku smjesu dodano 40 mL destilirane vode te je ekstrahirana etil-acetatom (2 × 40 mL). Organski slojevi su sakupljeni, isprani vodom (1 × 30 mL), sušeni nad bezvodnim natrijevim sulfatom, filtrirani, a otapalo je iz filtrata uklonjeno uparavanjem pod sniženim tlakom. Sirovi produkt pročišćen je kromatografijom na koloni uz pokretnu fazu diklormetan:metanol ili cikloheksan:etil-acetat:metanol. Nakon rastrljavanja u smjesi dietil-etera i petroletera dobiveni su čisti produkti **28a-d**.

*3.2.8.1. Cinamil (2-(7-metoksi-1-metil-9H-pirido[3,4-b]indol-9-il)etil)karbamat (**28a**)*

Količina reaktanta: 0,032 g cinamilnog alkohola.

Pokretna faza: diklormetan:metanol (8:1).

Iskorištenje: 0,025 g (31 %).

t_t 147,5 – 149,0 °C.

IR (ATR, ν/cm^{-1}) 3193, 2971, 2931, 1713, 1623, 1566, 1496, 1447, 1405, 1345, 1257, 1221, 1197, 1178, 1138, 1122, 1092, 1044, 1020, 964, 948, 814, 733, 690, 598, 551, 529, 500.

^{1}H NMR (DMSO-d_6, δ ppm) δ 8,17 (d, 1H, 7, J = 5,2 Hz), 8,09 (d, 1H, 3, J = 8,6 Hz), 7,88 (d, 1H, 6, J = 5,2 Hz), 7,47 – 7,41 (m, 3H, 3', 9', 13'), 7,35 (t, 2H, 10', 12', J = 7,6 Hz), 7,29 – 7,26 (m, 1H, 11'), 7,21 (d, 1H, 12, J = 2,3 Hz), 6,88 (dd, 1H, 2, J = 8,6, 2,1 Hz), 6,62 (d, 1H, 7', J = 15,9 Hz), 6,30 (dt, 1H, 6', J = 15,9, 6,1 Hz), 4,62 – 4,60 (m, 4H, 1', 5'), 3,90 (s, 3H, 14), 3,41 (q, 2H, 2', J = 6,6 Hz), 2,96 (s, 3H, 13).

^{13}C NMR (DMSO-d_6, δ ppm) δ 160,50 (4'), 156,30 (1), 142,89 (8), 140,54 (11), 137,78 (7), 136,06 (8'), 134,69 (9), 132,39 (7'), 128,66 (10', 12'), 128,48 (4), 127,89 (11'), 126,42 (9', 13'), 124,67 (6'), 122,39 (3), 114,34 (5), 112,26 (6), 109,19 (2), 93,55 (12), 64,35 (5'), 55,48 (14), 43,74 (1'), 40,40 (2'), 23,05 (13).

ESI-MS: *m/z* 416,1 $[M+1]^+$.

*3.2.8.2. (E)-3-(4-propoksifenil)alil(2-(7-metoksi-1-metil-9H-pirido[3,4-b]indol-9-il)etil)karbamat (**28b**)*

Količina reaktanta: 0,045 g spoja **27b**.

Pokretna faza: diklormetan:metanol (9:1).

Iskorištenje: 0,034 g (37 %).

t_t 154,5 – 155,5 °C.

IR (ATR, ν/cm^{-1}) 3198, 2966, 2934, 1714, 1624, 1511, 1446, 1404, 1344, 1307, 1254, 1221, 1197, 1177, 1138, 1123, 1021, 964, 814, 597, 565, 529.

^{1}H NMR (DMSO-d_6, δ ppm) δ 8,17 (d, 1H, 7, J = 5,2 Hz), 8,09 (d, 1H, 3, J = 8,6 Hz), 7,88 (d, 1H, 6, J = 5,2 Hz), 7,43 (t, 1H, 3', J = 6,0 Hz), 7,36 (d, 2H, 9', 13', J = 8,6 Hz), 7,21 (d, 1H, 12, J = 2,2 Hz), 6,92 – 6,87 (m, 3H, 2, 10', 12'), 6,55 (d, 1H, 7', J = 15,9 Hz), 6,12 (dt, 1H, 6', J = 15,9, 6,3 Hz), 4,61 (t, 2H, 1', J = 6,9 Hz), 4,57 (d, 2H, 5', J = 6,2 Hz), 3,92 (t, 2H, 14', J = 6,5 Hz), 3,90 (s, 3H, 14), 3,40 (q, 2H, 2', J = 6,6 Hz), 2,96 (s, 3H, 13), 1,72 (h, 2H, 15', J = 7,1 Hz), 0,97 (t, 3H, 16', J = 7,4 Hz).

^{13}C NMR (DMSO-d_6, δ ppm) δ 160,52 (4'), 158,54 (11'), 156,36 (1), 142,91 (8), 140,52 (11), 137,73 (7), 134,68 (9), 132,48 (7'), 128,51 (8'), 128,50 (4), 127,75 (10', 12'), 122,40 (3), 121,95 (6'), 114,55 (9', 13'), 114,33 (5), 112,27 (6), 109,21 (2), 93,55 (12), 68,93 (14'), 64,63 (5'), 55,48 (14), 43,75 (1'), 40,39 (2'), 23,02 (13), 22,02 (15'), 10,39 (16').

ESI-MS: *m/z* 474,2 $[M+1]^+$.

*3.2.8.3. (E)-3-(3-(trifluormetil)fenil)alil(2-(7-metoksi-1-metil-9H-pirido[3,4-b]indol-9-il)etil)karbamat (**28c**)*

Količina reaktanta: 0,048 g spoja **27c**.

Pokretna faza: cikloheksan:etil-acetat:metanol (1:1:0,5).

Iskorištenje: 0,027 g (28 %).

t_t 176,0 – 178,5°C.

IR (ATR, ν/cm^{-1}) 3191, 2971, 1717, 1625, 1568, 1500, 1449, 1408, 1362, 1336, 1321, 1259, 1225, 1198, 1164, 1110, 1093, 1072, 1045, 988, 970, 951, 911, 796, 694, 666, 635, 597, 551, 530.

^{1}H NMR (DMSO-d_6, δ ppm) δ 8,17 (d, 1H, 7, J = 5,2 Hz), 8,08 (d, 1H, 3, J = 8,6 Hz), 7,87 (d, 1H, 6, J = 5,2 Hz), 7,78 – 7,76 (m, 2H, 12', 13'), 7,64 – 7,62 (m, 1H, 9'), 7,61 – 7,58 (m, 1H, 11'), 7,47 (t, 1H, 3', J = 6,0 Hz), 7,22 (d, 1H, 12, J = 2,2 Hz), 6,87 (dd, 1H, 2, J = 8,6, 2,1 Hz), 6,69 (d, 1H, 7', J = 16,0 Hz), 6,47 (dt, 1H, 6', J = 16,0, 5,8 Hz), 4,64 – 4,61 (m, 4H, 1', 5'), 3,90 (s, 3H, 14), 3,42 (q, 2H, 2', J = 6,6 Hz), 2,96 (s, 3H, 13).

^{13}C NMR (DMSO-d_6, δ ppm) δ 160,48 (4'), 156,20 (1), 142,89 (8), 140,55 (11), 137,80 (7), 137,26 (8'), 134,70 (9), 130,45 (7'), 130,16 (13'), 129,74 (12'), 129,54 (q, 10', J = 31,5 Hz), 128,47 (4), 127,26 (6'), 124,24 (q, 11', J = 3,6 Hz), 124,17 (q, 14', J = 272,3 Hz), 122,94 (q, 9', J = 3,6 Hz), 122,36 (3), 114,35 (5), 112,24 (6), 109,16 (2), 93,56 (12), 64,00 (5'), 55,46 (14), 43,74 (1'), 40,43 (2'), 23,07 (13).

ESI-MS: m/z 484,1 $[M+1]^+$.

*3.2.8.4. (E)-3-(3,5-bis(trifluormetil)fenil)alil(2-(7-metoksi-1-metil-9H-piridо[3,4-b]indol-9-il)etil)karbamat (**28d**)*

Količina reaktanta: 0,063 g spoja **27d**.

Pokretna faza: cikloheksan:etil-acetat:metanol (1:1:0,5).

Iskorištenje: 0,038 g (35 %).

^{1}H NMR (DMSO-d_6, δ ppm) δ 8,16 – 8,15 (m, 3H, 7, 9', 13'), 8,07 (d, 1H, 3, J = 8,6 Hz), 7,98 (s, 1H, 11'), 7,87 (d, 1H, 6, J = 5,1 Hz), 7,48 (t, 1H, 3', J = 6,0 Hz), 7,21 (d, 1H, 12, J = 2,2 Hz), 6,85 (dd, 1H, 2, J = 8,6, 2,1 Hz), 6,75 (d, 1H, 7', J = 16,1 Hz), 6,69 (dt, 1H, 6', J = 16,0, 5,3 Hz), 4,66 – 4,61 (m, 4H, 1', 5'), 3,89 (s, 3H, 14), 3,42 (q, 2H, 2', J = 6,6 Hz), 2,96 (s, 3H,13).

^{13}C NMR (DMSO-d_6, δ ppm) δ 160,45 (4'), 156,41 (1), 142,90 (8), 140,54 (11), 139,01 (9), 137,78 (7), 134,72 (8'), 130,18 (q, 10', 12', J = 32,7 Hz), 129,92 (7'), 129,24 (9', 13'), 128,45 (4), 123,46 (q, 14', 15', J = 272,8 Hz), 122,34 (6'), 122,30 (3), 119,72 (q, 11', J = 4,0 Hz), 114,34 (5), 112,21 (6), 109,08 (2), 93,58 (12), 63,73 (5'), 55,42 (14), 43,77 (1'), 40,33 (2'), 23,08 (13).

ESI-MS: m/z 552,1 $[M+1]^+$.

3.2.9. Sinteza harmicina karbamatnog tipa (28e-k). Opća metoda

Otopini odgovarajućeg alkohola **27e-k** (0,205 mmol) u bezvodnom dietil-eteru (3 mL) dodan je CDI (0,066 g, 0,410 mmol) u inertnoj atmosferi argona. Reakcijska smjesa miješana je na

sobnoj temperaturi 2 h, nakon čega je dodana voda (40 mL) i provedena ekstrakcija dietil-eterom (2 × 40 mL). Organski slojevi su sakupljeni, sušeni nad bezvodnim natrijevim sulfatom, filtrirani, a otapalo je iz filtrata uklonjeno uparavanjem pod sniženim tlakom. Otopini sirovog produkta (ulje) u bezvodnom DMF-u (4 mL) dodan je amin **24** (0,063 g, 0,246 mmol) u inertnoj atmosferi te je reakcijska smjesa miješana 18 h na sobnoj temperaturi. Nakon toga je u reakcijsku smjesu dodana voda (40 mL) te je provedena ekstrakcija etil-acetatom (3 × 30 mL). Organski slojevi su sakupljeni i isprani vodom (1 × 40 mL), zatim sušeni nad bezvodnim natrijevim sulfatom, filtrirani, a otapalo je iz filtrata uklonjeno uparavanjem pod sniženim tlakom. Dobiveni sirovi produkt pročišćen je kromatografijom na koloni uz pokretnu fazu diklormetan:metanol (8:1). Nakon rastrljavanja u smjesi dietil-etera i petroletera dobiveni su čisti produkti **28e-k**.

*3.2.9.1. (E)-3-(4-(trifluormetil)fenil)alil(2-(7-metoksi-1-metil-9H-pirido[3,4-b]indol-9-il)etil)karbamat (**28e**)*

Količina reaktanta: 0,041 g spoja **27e**.

Iskorištenje: 0,035 g (35 %).

t_t 182,0 – 183,0 °C.

IR (ATR, ν/cm^{-1}) 3213, 2938, 1713, 1624, 1566, 1519, 1498, 1446, 1377, 1358, 1323, 1307, 1259, 1222, 1198, 1176, 1152, 1138, 1107, 1045, 1066, 1035, 1017, 986, 966, 954, 936, 851, 814, 785, 724, 641, 611, 594, 541, 510.

^{1}H NMR (DMSO-d_6, δ ppm) δ 8,17 (d, 1H, 7, J = 5,2 Hz), 8,09 (d, 1H, 3, J = 8,5 Hz), 7,88 (d, 1H, 6, J = 5,2 Hz), 7,71 (d, 2H, 10', 12', J = 8,2 Hz), 7,66 (d, 2H, 9', 13', J = 8,2 Hz), 7,50 (t, 1H, 3', J = 6,0 Hz), 7,22 (d, 1H, 12, J = 2,2 Hz), 6,88 (dd, 1H, 2, J = 8,6, 2,2 Hz), 6,70 – 6,67 (m, 1H, 7'), 6,47 (dt, 1H, 6', J = 16,0, 5,8 Hz), 4,65 (d, 2H, 5', J = 5,4 Hz), 4,62 (t, 2H, 1', J = 6,9 Hz), 3,90 (s, 3H, 14), 3,42 (q, 2H, 2', J = 6,6 Hz), 2,96 (s, 3H, 13).

^{13}C NMR (DMSO-d_6, δ ppm) δ 160,49 (4'), 156,20 (1), 142,88 (8), 140,54 (11), 140,20 (8'), 137,81 (7), 134,70 (9), 130,40 (7'), 128,48 (4), 128,12 (6'), 127,90 (q, 11', J = 31,7 Hz), 127,03 (9', 13'), 125,54 (q, 10', 12', J = 3,5 Hz), 124,26 (q, 14', J = 271,8 Hz), 122,39 (3), 114,35 (5), 112,26 (6), 109,18 (2), 93,56 (12), 63,97 (5'), 55,48 (14), 43,74 (1'), 40,41 (2'), 23,07 (13).

ESI-MS: m/z 484,2 $[M+1]^+$.

*3.2.9.2. (E)-3-(2-klorfenil)alil(2-(7-metoksi-1-metil-9H-pirido[3,4-b]indol-9-il)etil)karbamat (**28f**)*

Količina reaktanta: 0,035 g spoja **27f**.

Iskorištenje: 0,035 g (38 %).

t_t 189,0 – 190,0 °C.

IR (ATR, ν/cm^{-1}) 3169, 2953, 1708 1625, 1568, 1527, 1501, 1473, 1408, 1363, 1346, 1267, 1250, 1225, 1197, 1125, 1096, 1044, 1020, 996, 975, 951, 807, 749, 635, 597, 554, 531, 484.

^{1}H NMR (DMSO-d_6, δ ppm) δ 8,16 (d, 1H, 7, J = 5,2 Hz), 8,08 (d, 1H, 3, J = 8,6 Hz), 7,87 (d, 1H, 6, J = 5,2 Hz), 7,68 (dd, 1H, 10', J = 7,8, 1,8 Hz), 7,52 (t, 1H, 3', J = 6,0 Hz), 7,46 (dd, 1H, 13', J = 7,8, 1,4 Hz), 7,35 (td, 1H, 11', J = 7,5, 1,5 Hz), 7,31 (td, 1H, 12', J = 7,6, 1,8 Hz), 7,21 (d, 1H, 12, J = 2,2 Hz), 6,92 (dt, 1H, 7', J = 16,0, 1,8 Hz), 6,87 (dd, 1H, 2, J = 8,6, 2,2 Hz), 6,35 (dt, 1H, 6', J = 15,9, 5,7 Hz), 4,66 (dd, 2H, 5', J = 5,7, 1,6 Hz), 4,61 (t, 2H, 1', J = 7,0 Hz), 3,90 (s, 3H, 14), 3,41 (q, 2H, 2', J = 6,7 Hz), 2,96 (s, 3H, 13).

^{13}C NMR (DMSO-d_6, δ ppm) δ 160,50 (4'), 156,19 (1), 142,87 (8), 140,53 (11), 137,79 (7), 134,67 (9), 133,91 (9'), 131,89 (8'), 129,58 (10'), 129,41 (7'), 128,47 (4), 128,37 (11'), 127,52 (12'), 127,21 (13'), 127,18 (6'), 122,38 (3), 114,33 (5), 112,25 (6), 109,19 (2), 93,53 (12), 64,03 (5'), 55,47 (14), 43,73 (1'), 40,38 (2'), 23,04 (13).

ESI-MS: *m/z* 450,1 $[M+1]^+$, 452,15 $[M+1]^+$.

*3.2.9.3. (E)-3-(3-klorfenil)alil(2-(7-metoksi-1-metil-9H-pirido[3,4-b]indol-9-il)etil)karbamat (**28g**)*

Količina reaktanta: 0,035 g spoja **27g**.

Iskorištenje: 0,031 g (34 %).

t_t 165,0 – 168,0 °C.

IR (ATR, ν/cm^{-1}) 3175, 2931, 1721, 1624, 1522, 1502, 1452, 1410, 1375, 1363, 1347, 1311, 1266, 1254, 1225, 1199, 1160, 1140, 1094, 1068, 1046, 1022, 969, 944, 885, 811, 799, 768, 731, 699, 677, 653, 635, 597, 568, 538, 482.

^{1}H NMR (DMSO-d_6, δ ppm) δ 8,17 (d, 1H, 7, J = 5,2 Hz), 8,08 (d, 1H, 3, J = 8,6 Hz), 7,87 (d, 1H, 6, J = 5,2 Hz), 7,52 (t, 1H, 9', J = 1,8 Hz), 7,47 (t, 1H, 3', J = 6,1 Hz), 7,42 – 7,37 (m, 2H, 12', 13'), 7,34 – 7,32 (m, 1H, 11'), 7,21 (d, 1H, 12, J = 2,3 Hz), 6,88 (dd, 1H, 2, J = 8,6, 2,2 Hz), 6,58 (d, 1H, 7', J = 15,9 Hz), 6,38 (dt, 1H, 6', J = 16,0, 5,9 Hz), 4,63 – 4,60 (m, 4H, 1', 5'), 3,90 (s, 3H, 14), 3,41 (q, 2H, 2', J = 6,6 Hz), 2,96 (s, 3H, 13).

^{13}C NMR (DMSO-d_6, δ ppm) δ 160,48 (4'), 156,21 (1), 142,89 (8), 140,54 (11), 138,38 (10'), 137,79 (7), 134,69 (9), 133,50 (8'), 130,61 (7'), 130,48 (11'), 128,47 (4), 127,58 (9'), 126,04 (13'), 125,08 (12'), 122,37 (3), 114,34, (5) 112,25 (6), 109,18 (2), 93,56 (12), 64,04 (5'), 55,48 (14), 43,74 (1'), 40,42 (2'), 23,07 (13).

ESI-MS: *m/z* 450,1 $[M+1]^+$, 452,15 $[M+1]^+$.

*3.2.9.4. (E)-3-(3-(trifluormetoksi)fenil)alil(2-(7-metoksi-1-metil-9H-pirido[3,4-b]indol-9-il)etil)karbamat (**28h**)*

Količina reaktanta: 0,045 g spoja **27h**.

Iskorištenje: 0,050 g (49 %).

t_t 156,5 – 159,0 °C.

IR (ATR, ν/cm^{-1}) 3173, 2961, 1713, 1624, 1562, 1533, 1502, 1472, 1409, 1376, 1362, 1345, 1299, 1254, 1225, 1201, 1178, 1139, 1126, 1094, 1045, 1029, 1021, 1008, 999, 977, 964, 936, 923, 874, 811, 793, 771, 733, 701, 677, 652, 598, 582, 537, 512.

^{1}H NMR (DMSO-d_6, δ ppm) δ 8,17 (d, 1H, 7, J = 5,2 Hz), 8,08 (d, 1H, 3, J = 8,6 Hz), 7,87 (d, 1H, 6, J = 5,2 Hz), 7,51 – 7,47 (m, 3H, 11' – 13'), 7,45 (s, 1H, 9'), 7,27 (t, 1H, 3', J = 6,0 Hz), 7,21 (d, 1H, 12, J = 2,1 Hz), 6,87 (dd, 1H, 2, J = 8,6, 2,2 Hz), 6,64 (dt, 1H, 7', J = 15,8, 1,5 Hz), 6,42 (dt, 1H, 6', J = 16,0, 5,9 Hz), 4,63 – 4,60 (m, 4H, 1', 5'), 3,90 (s, 3H, 14), 3,41 (q, 2H, 2', J = 6,7 Hz), 2,96 (s, 3H, 13).

^{13}C NMR (DMSO-d_6, δ ppm) δ 160,48 (4'), 156,21 (1), 148,80 (10'), 142,88 (8), 140,55 (11), 138,65 (8'), 137,80 (7), 134,70 (9), 130,59 (7'), 130,45 (11'), 128,47 (4), 127,12 (11'), 125,51 (6'), 122,37 (9'), 120,12 (13'), 120,09 (q, 14', J = 256,2 Hz), 118,75 (12'), 114,35 (5), 112,24 (6), 109,17 (2), 93,56 (12), 63,99 (5'), 55,46 (14), 43,74 (1'), 40,41 (2'), 23,07 (13).

ESI-MS: m/z 500,2 $[M+1]^+$.

*3.2.9.5. (E)-3-(4-bromfenil)alil(2-(7-metoksi-1-metil-9H-pirido[3,4-b]indol-9-il)etil)karbamat (**28i**)*

Količina reaktanta: 0,044 g spoja **27i**.

Iskorištenje: 0,040 g (39 %).

t_t 166,5 – 169,0 °C.

IR (ATR, ν/cm^{-1}) 3192, 2939, 1712, 1623, 1566, 1522, 1488, 1445, 1379, 1359, 1345, 1324, 1306, 1258, 1247, 1221, 1197, 1177, 1154, 1137, 1123, 1092, 1067, 1036, 1007, 967, 942, 813, 773, 723, 640, 611, 596, 566, 528, 499.

^{1}H NMR (DMSO-d_6, δ ppm) δ 8,17 (d, 1H, 7, J = 5,1 Hz), 8,09 (d, 1H, 3, J = 8,5 Hz), 7,87 (d, 1H, 6, J = 5,1 Hz), 7,55 – 7,53 (m, 2H, 10', 12'), 7,46 (t, 1H, 3', J = 6,1 Hz), 7,41 – 7,39 (m, 2H, 9', 13'), 7,21 (d, 1H, 12, J = 2,2 Hz), 6,88 (dd, 1H, 2, J = 8,6, 2,2 Hz), 6,58 (dt, 1H, 7', J = 16,1, 1,6 Hz), 6,33 (dt, 1H, 6', J = 16,0, 6,0 Hz), 4,62 – 4,59 (m, 4H, 1', 5'), 3,90 (s, 3H, 14), 3,40 (q, 2H, 2', J = 6,6 Hz), 2,96 (s, 3H, 13).

^{13}C NMR (DMSO-d_6, δ ppm) δ 160,48 (4'), 156,24 (1), 142,87 (8), 140,55 (11), 137,82 (7), 135,38 (8'), 134,69 (9), 131,56 (10', 12'), 130,99 (7'), 128,45 (9', 13'), 125,85 (6'), 122,38 (3),

120,85 (11'), 114,35 (5), 112,25 (6), 109,17 (2), 93,56 (12), 64,16 (5'), 55,48 (14), 43,74 (1'), 40,40 (2') 23,08 (13).

ESI-MS: *m/z* 494,1 $[M+1]^+$, 496,1 $[M+1]^+$.

*3.2.9.6. (E)-3-(p-tolil)alil(2-(7-metoksi-1-metil-9H-pirido[3,4-b]indol-9-il)etil)karbamat (**28j**)*

Količina reaktanta: 0,030 g spoja **27j**.

Iskorištenje: 0,031 g (31 %).

t_t 158,0 – 160,0 °C.

IR (ATR, ν/cm^{-1}) 3216, 2930, 1714, 1623, 1564, 1514, 1497, 1446, 1404, 1378, 1343, 1324, 1257, 1197, 1179, 1138, 1122, 1043, 1020, 990, 949, 815, 769, 722, 640, 611, 598, 582, 550, 528, 465.

^{1}H NMR (DMSO-d_6, δ ppm) δ 8,17 (d, 1H, 7, J = 5,2 Hz), 8,08 (d, 1H, 3, J = 8,5 Hz), 7,87 (d, 1H, 6, J = 5,1 Hz), 7,44 (t, 1H, 3', J = 6,0 Hz), 7,33 (d, 2H, 9', 13', J = 8,0 Hz), 7,21 (d, 1H, 12, J = 2,2 Hz), 7,16 (d, 2H, 10', 12', J = 7,8 Hz), 6,88 (dd, 1H, 2, J = 8,6, 2,2 Hz), 6,57 (d, 1H, 7', J = 15,9 Hz), 6,23 (dt, 1H, 6', J = 15,9, 6,2 Hz), 4,62 – 4,59 (m, 4H, 1', 5'), 3,40 (q, 2H, 2', J = 6,6 Hz), 3,90 (s, 3H, 14), 2,96 (s, 3H, 13), 2,29 (s, 3H, 14').

^{13}C NMR (DMSO-d_6, δ ppm) δ 160,49 (4'), 156,32 (1), 142,87 (8), 140,55 (11), 137,81 (7), 137,27 (8'), 134,69 (9), 133,28 (11'), 132,50 (7'), 129,24 (9', 13'), 128,46 (4), 126,36 (10', 12'), 123,50 (6'), 122,38 (3), 114,35 (5), 112,25 (6), 109,17 (2), 93,55 (12), 64,47 (5'), 55,47 (14), 43,74 (1'), 40,39 (2'), 23,06 (13), 20,78 (14').

ESI-MS: *m/z* 430,2 $[M+1]^+$.

*3.2.9.7. (E)-3-(4-nitrofenil)alil(2-(7-metoksi-1-metil-9H-pirido[3,4-b]indol-9-il)etil)karbamat (**28k**)*

Količina reaktanta: 0,037 g spoja **27k**.

Iskorištenje: 0,033 g (35 %).

t_t 208,5 – 211,5 °C.

IR (ATR, ν/cm^{-1}) 3179, 2940, 1713, 1626, 1595, 1567, 1540, 1515, 1497, 1446, 1409, 1377, 1340, 1269, 1256, 1198, 1177, 1147, 1139, 1123, 1108, 1065, 1025, 1003, 972, 939, 862, 822, 808, 793, 763, 736, 683, 635, 608, 598, 569, 531, 491.

^{1}H NMR (DMSO-d_6, δ ppm) δ 8,21 (d, 2H, 10', 12', J = 8,7 Hz), 8,17 (d, 1H, 7, J = 5,2 Hz), 8,09 (d, 1H, 3, J = 8,6 Hz), 7,88 (d, 1H, 6, J = 5,2 Hz), 7,71 (d, 2H, 9', 13', J = 8,7 Hz), 7,51 (t, 1H, 3', J = 6,0 Hz), 7,21 (d, 1H, 2, J = 2,3 Hz), 6,88 (dd, 1H, 12, J = 8,6, 2,2 Hz), 6,72 (d, 1H,

7', *J* = 16,0 Hz), 6,57 (dt, 1H, 6', *J* = 16,0, 5,6 Hz), 4,67 (d, 2H, 5', *J* = 5,0 Hz), 4,62 (t, 2H, 1', *J* = 7,0 Hz), 3,90 (s, 3H, 14), 3,42 (q, 2H, 2', *J* = 6,6 Hz), 2,96 (s, 3H, 13).

^{13}C NMR (DMSO-d_6, δ ppm) δ 160,48 (4'), 156,14 (1), 146,56 (11'), 142,86 (8), 140,54 (11), 137,82 (7), 134,70 (9), 130,23 (7'), 129,61 (6'), 128,47 (4), 127,40 (10', 12'), 123,94 (9', 13'), 122,39 (3), 114,36 (5), 112,26 (6), 109,18 (2), 93,57 (12), 63,85 (5'), 55,49 (14), 43,73 (1'), 40,43 (2'), 23,08 (13).

ESI-MS: *m/z* 461,15 $[M+1]^+$.

3.2.10. Sinteza cinamilnih azida (29b,c). Opća metoda

U otopinu odgovarajućeg cinamilnog alkohola **27b,c** (0,936 mmol) u bezvodnom THF-u (5 mL) dodani su ADMP (0,642 g, 2,25 mmol) i DBU (0,363 mL, 2,43 mmol) pri 0 °C. Reakcijska smjesa miješana je 1 h na 0 °C, zatim je dodana zasićena otopina NH_4Cl (20 mL). Dobivena otopina ekstrahirana je diklormetanom (2 × 30 mL). Organski slojevi su sakupljeni i ekstrahirani zasićenom otopinom NaCl-a (1 × 40 mL) i vodom (1 × 40 mL), sušeni nad bezvodnim natrijevim sulfatom, filtrirani, a otapalo je iz filtrata uklonjeno uparavanjem pod sniženim tlakom. Sirovi produkt pročišćen je kromatografijom na koloni uz pokretnu fazu cikloheksan:etil-acetat:metanol (3:1:0,5).

*3.2.10.1. (E)-1-(3-azidoprop-1-en-1-il)-4-propoksibenzen (**29b**)*

Količina reaktanta: 0,180 g spoja **27b**.

Iskorištenje: 0,118 g (58 %).

Ulje.

IR (ATR, ν/cm^{-1}) 3036, 2937, 2966, 2877, 2094, 1651, 1606, 1575, 1510, 1472, 1422, 1350, 1240, 1174, 1163, 1113, 1067, 1047, 1019, 968, 934, 883, 838, 800, 718, 661, 638, 591, 558, 529.

^{1}H NMR (DMSO-d_6, δ ppm) δ 7,42 – 7,40 (m, 2H, 7, 9), 6,91 – 6,89 (m, 2H, 6, 10), 6,64 (dt, 1H, 4, *J* = 15,9, 1,4 Hz), 6,22 (dt, 1H, 3, *J* = 15,8, 6,7 Hz), 3,99 (dd, 2H, 2, *J* = 6,8, 1,3 Hz), 3,93 (t, 2H, 1', *J* = 6,5 Hz), 1,75 – 1,69 (m, 2H, 2'), 0,97 (t, 3H, 3', *J* = 7,4 Hz).

^{13}C NMR (DMSO-d_6, δ ppm) δ 158,66 (8), 133,72 (4), 128,28 (5), 127,87 (7, 9), 120,29 (3), 114,58 (6, 10), 68,94 (1'), 52,35 (2), 21,99 (2'), 10,36 (3').

*3.2.10.2. (E)-1-(3-azidoprop-1-en-1-il)-3-(trifluormetil)benzen (**29c**)*

Količina reaktanta: 0,189 g spoja **27c**.

Iskorištenje: 0,170 g (80 %).

Ulje.

IR (ATR, ν/cm^{-1}) 2931, 2097, 1593, 1487, 1440, 1330, 1274, 1200, 1163, 1071, 1098, 1001, 965, 899, 791, 662, 696, 558, 524, 478.

^{1}H NMR (DMSO-d_6, δ ppm) δ 7,85 – 7,84 (m, 1H, 10), 7,82 – 7,81 (m, 1H, 9), 7,64 – 7,62 (m, 1H, 6), 7,60 – 7,59 (m, 1H, 8), 6,81 (dt, 1H, 4, J = 15,9, 1,5 Hz), 6,58 (dt, 1H, 3, J = 15,9, 6,4 Hz), 4,08 (dd, 2H, 2, J = 6,4, 1,4 Hz).

^{13}C NMR (DMSO-d_6, δ ppm) δ 137,08 (5), 131,80 (10), 130,30 (4), 129,75 (9), 129,57 (q, 7, J = 31,7 Hz), 125,76 (3), 124,38 (q, 6, J = 3,9 Hz), 124,14 (d, 1', J = 271,8 Hz), 123,04 (q, 8, J = 3,8 Hz), 51,93 (2).

3.2.11. Sinteza cinamilnih amina (30b,c). Opća metoda

Otopini odgovarajućeg azida **29** (0,867 mmol) u bezvodnom dietil-eteru (5 mL) na 0 °C u inertnoj atmosferi dušika dodan je $LiAlH_4$ (0,033 g, 0,867 mmol). Reakcijska smjesa miješana je 2 h na 0 °C u inertnoj atmosferi dušika. Potom je dodana voda (15 mL) i 10 %-tna otopina HCl-a (2 mL). Reakcijska smjesa je zatim ekstrahirana dietil-eterom (1 × 30 mL). Organski sloj je bačen, a vodeni sloj zalužen 10 %-tnom otopinom NaOH do pH 12 te ekstrahiran dietil-eterom (2 × 30 mL). Eterski slojevi su sakupljeni i sušeni nad bezvodnim natrijevim sulfatom, filtrirani, a otapalo je iz filtrata uklonjeno uparavanjem pod sniženim tlakom. Nakon rastrljavanja u dietil-eteru dobiveni su čisti produkti **30b,c**.

*3.2.11.1. (E)-3-(4-propoksifenil)prop-2-en-1-amin (**30b**)*

Količina reaktanta: 0,188 g spoja **29b**.

Iskorištenje: 0,114 g (69 %).

^{1}H NMR (DMSO-d_6, δ ppm) δ 7,42 – 7,40 (m, 2H, 7, 9), 6,92 – 6,89 (m, 2H, 6, 10), 6,64 (dd, 1H, 4, J = 15,8, 1,4 Hz), 6,22 (dt, 1H, 3, J = 15,8, 6,7 Hz), 4,00 (dd, 2H, 2, J = 6,8, 1,3 Hz), 3,93 (t, 2H, 1', J = 6,6 Hz), 1,75 – 1,69 (m, 2H, 2'), 0,97 (t, 3H, 3', J = 7,4 Hz).

^{13}C NMR (DMSO-d_6, δ ppm) δ 158,67 (8), 133,73 (4), 128,29 (5), 127,89 (7, 9), 120,30 (3), 114,58 (6, 10), 68,94 (1'), 52,36 (2), 22,00 (2'), 10,37 (3').

*3.2.11.2. (E)-3-(3-(trifluormetil)fenil)prop-2-en-1-amin (**30c**)*

Količina reaktanta: 0,197 g spoja **29c**.

Iskorištenje: 0,122 g (70 %).

IR (ATR, ν/cm^{-1}) 3285, 2967, 2934, 2879, 1741, 1604, 1575, 1510, 1469, 1394, 1377, 1307, 1272, 1241, 1177, 1143, 1115, 1068, 970, 912, 839, 809, 794, 775, 644, 592, 559, 528.
^{1}H NMR (DMSO-d_6, δ ppm) δ 7,72 – 7,70 (m, 2H, 6, 8), 7,59 – 7,56 (m, 2H, 9, 10), 6,66 – 6,63 (m, 1H, 4), 6,54 (dt, 1H, 3, J = 16,0, 5,8 Hz), 3,39 (dd, 2H, 2, J = 5,8, 1,5 Hz).
^{13}C NMR (DMSO-d_6, δ ppm) δ 138,03 (5), 132,51 (4), 129,84 (q, 9, J = 2,0 Hz), 129,71 (10), 129,28 (3), 129,25 (q, 7, J = 32,7 Hz), 124,75 (q, 8, J = 3,8 Hz), 123,70 (q, 6, J = 3,9 Hz), 40,90 (2).

3.2.12. Sinteza klorida 1-benzotriazolkarboksilne kiseline (BtcCl)

Otopina BtH (0,139 g, 1,17 mmol) i trifozgena (0,196 g, 0,661 mmol) u bezvodnom toluenu (7 mL) refluksirana je 3 h na 118 °C. Otapalo je upareno pod sniženim tlakom te je reakcijska smjesa nekoliko puta naparena bezvodnim toluenom. Dobiveni klorid 1-benzotriazolkarboksilne kiseline (BtcCl) upotrijebljen je bez pročišćavanja u sljedećem reakcijskom koraku.

3.2.13. Sinteza *N*-(2-(7-metoksi-1-metil-9*H*-pirido[3,4-*b*]indol-9-il)etil)-1*H*-benzo[*d*][1,2,3]triazol-1-karboksamida (31)

Otopini BtcCl (0,070 g, 0,384 mmol) u bezvodnom diklormetanu (3 mL) uz miješanje je dokapana otopina TEA (0,053 mL, 0,384 mmol) i amina **24** (0,070 g, 0,274 mmol) u bezvodnom diklormetanu (3 mL) tijekom 15 min. Nakon dokapavanja je reakcijska smjesa miješana 1 h na sobnoj temperaturi. Novonastali talog je odsisan i rastrljan u metanolu čime je dobiven čist produkt **31**.
Iskorištenje: 0,061 g (56 %).
t_t 238,0 – 240,0 °C.
IR (ATR, ν/cm^{-1}) 3010, 2966, 1728, 1621, 1563, 1486, 1460, 1445, 1413, 1381, 1365, 1343, 1330, 1294, 1256, 1227, 1196, 1179, 1127, 1114, 1065, 1043, 1010, 979, 953, 918, 852, 839, 784, 770, 748, 707, 656, 635, 600, 584, 555, 529.
^{1}H NMR (DMSO-d_6, δ ppm) δ 9,51 (t, 1H, 3', J = 6,1 Hz), 8,20 – 8,17 (m, 2H, 3, 7), 8,10 (d, 1H, 6', J = 8,3 Hz), 8,05 (d, 1H, 9', J = 8,6 Hz), 7,88 (d, 1H, 6, J = 5,2 Hz), 7,70 (t, 1H, 7', J = 7,7 Hz), 7,55 (t, 1H, 8', J = 7,7 Hz), 7,31 (d, 1H, 12, J = 2,3 Hz), 6,79 (dd, 1H, 2, J = 8,5, 2,2 Hz), 4,81 (t, 2H, 1', J = 7,0 Hz), 3,83 – 3,76 (m, 5H, 14, 2'), 3,05 (s, 3H, 13).

^{13}C NMR (DMSO-d_6, δ ppm) δ 160,45 (4'), 149,20 (1), 145,40 (10'), 142,93 (8), 140,61 (9), 137,94 (7), 134,64 (11), 131,15 (5'), 130,00 (7'), 128,60 (4), 125,56 (8'), 122,34 (3), 119,76 (9'), 114,31 (5), 113,49 (6'), 112,25 (6), 109,29 (2), 93,40 (12), 55,25 (14), 43,32 (1'), 39,94 (2'), 23,12 (13).

3.2.14. Sinteza harmicina ureidnog tipa (32b-c). Opća metoda

Suspenzija odgovarajućeg amina **30** (0,299 mmol), spoja **31** (0,075 g, 0,187 mmol) i TEA (0,042 mL, 0,299 mmol) u diklormetanu miješana je u mikrovalnom reaktoru 35 min na 60 °C. Reakcijska smjesa ohlađena je na sobnu temperaturu te je dodan diklormetan (30 mL). Dobivena otopina ekstrahirana je vodom (2 × 20 mL). Organski sloj sušen je nad bezvodnim natrijevim sulfatom, filtriran, a otapalo je iz filtrata uklonjeno uparavanjem pod sniženim tlakom. Sirovi produkt pročišćen je kromatografijom na koloni uz pokretnu fazu diklormetan:metanol (9:1).

*3.2.14.1. (E)-1-(2-(7-metoksi-1-metil-9H-pirido[3,4-b]indol-9-il)etil)-3-(3-(4-propoksifenil)alil)urea (**32b**)*

Količina reaktanta: 0,057 g spoja **30b**.

Iskorištenje: 0,061 g (69 %).

t_t 174,0 – 177,0 °C.

IR (ATR, ν/cm^{-1}) 3328, 2966, 2931, 1739, 1623, 1572, 1511, 1447, 1407, 1345, 1281, 1248, 1202, 1090, 1023, 1047, 805, 635, 600, 546, 519.

^{1}H NMR (DMSO-d_6, δ ppm) δ 8,17 (d, 1H, 7, J = 5,2 Hz), 8,08 (d, 1H, 3, J = 8,5 Hz), 7,88 (d, 1H, 6, J = 5,2 Hz), 7,32 – 7,30 (m, 2H, 10', 14'), 7,29 (d, 1H, 12, J = 2,2 Hz), 6,89 – 6,86 (m, 3H, 2, 11', 13'), 6,37 (dt, 1H, 8', J = 15,9, 1,7 Hz), 6,22 (t, 1H, 5', J = 5,8 Hz), 6,13 (t, 1H, 3', J = 6,0 Hz), 6,05 (dt, 1H, 7', J = 15,9, 5,9 Hz), 4,59 (t, 2H, 1', J = 6,9 Hz), 3,92 – 3,90 (m, 5H, 14, 15'), 3,78 (td, 2H, 6', J = 5,8, 1,6 Hz), 3,42 (q, 2H, 2', J = 6,6 Hz), 2,98 (s, 3H, 13), 1,71 (h, 2H, 16', J = 7,3 Hz), 0,97 (t, 3H, 17', J = 7,4 Hz).

^{13}C NMR (DMSO-d_6, δ ppm) δ 160,52 (4'), 158,07 (1), 158,04 (12'), 142,99 (8), 140,72 (11), 137,60 (7), 134,71 (9), 129,19 (7'), 128,37 (4), 127,30 (10', 14'), 125,79 (8'), 122,29 (3), 114,50 (11', 13'), 114,21 (5), 112,22 (6), 109,28 (2), 93,78 (12), 68,89 (15'), 55,49 (14), 44,40 (1'), 41,40 (6'), 39,61 (2'), 23,09 (13), 22,04 (16'), 10,40 (17').

ESI-MS: m/z 473,2 $[M+1]^+$.

*3.2.14.2. (E)-1-(2-(7-metoksi-1-metil-9H-pirido[3,4-b]indol-9-il)etil)-3-(3-(3-(trifluormetil)fenil)alil)urea (**32c**)*

Količina reaktanta: 0,060 g spoja **30c**.

Iskorištenje: 0,042 g (46 %).

^{1}H NMR (DMSO-d_6, δ ppm) δ 8,16 (d, 1H, 7, J = 5,3 Hz), 8,08 (d, 1H, 3, J = 8,7 Hz), 7,87 (d, 1H, 6, J = 5,2 Hz), 7,74 – 7,72 (m, 2H, 10', 12'), 7,60 – 7,56 (m, 2H, 13', 14'), 7,29 (d, 1H, 12, J = 2,2 Hz), 6,87 (dd, 1H, 2, J = 8,6, 2,1 Hz), 6,53 (dt, 1H, 8', J = 16,0, 1,7 Hz), 6,40 (dt, 1H, 7', J = 16,0, 5,5 Hz), 6,30 (t, 1H, 5', J = 5,8 Hz), 6,18 (t, 1H, 3', J = 5,9 Hz), 4,60 (t, 2H, 1', J = 6,9 Hz), 3,90 (s, 3H, 14), 3,84 (td, 2H, 6', J = 5,7, 1,6 Hz), 3,43 (q, 2H, 2', J = 6,7 Hz), 2,98 (s, 3H, 13).

^{13}C NMR (DMSO-d_6, δ ppm) δ 160,47 (4'), 158,02 (1), 142,95 (8), 140,76 (11), 137,90 (9'), 137,69 (7), 134,75 (9), 132,55 (q, 13', J = 1,5 Hz), 131,14 (7'), 129,67 (14'), 129,50 (q, 11', J = 30,7 Hz), 129,27 (8'), 128,32 (4), 124,76 (q, 12', J = 3,7 Hz), 124,23 (q, 15', J = 271,8 Hz), 123,66 (q, 10', J = 3,6 Hz), 122,26 (3), 114,24 (5), 112,19 (6), 109,21 (2), 93,78 (12), 55,46 (14), 44,38 (6'), 41,17 (1'), 39,62 (2'), 23,14 (13).

ESI-MS: *m/z* 483,3 $[M+1]^+$.

3.3. BIOLOŠKA ISPITIVANJA

Ispitivanja antiplazmodijskog djelovanja na eritrocitnu fazu *P. falciparum* i ispitivanja citotoksičnosti provedena su na Institutu za tropsku medicinu, Sveučilišta u Tübingenu, Njemačka, a ispitivanja djelovanja na hepatocitnu fazu plazmodija provedena su na Institutu za molekularnu medicinu, Medicinski fakultet, Sveučilište u Lisabonu, Portugal.

3.3.1. Ispitivanja antiplazmodijskog djelovanja *in vitro*

Ispitivanje djelovanja harmicina na eritrocitnu fazu *P. falciparum* provedena su *in vitro* na dva soja: *Pf*3D7 (soj osjetljiv na klorokin) i *Pf*Dd2 (soj otporan na klorokin), korištenjem HRP2 testa (engl. *histidine-rich protein 2*). Mikrotitarska pločica s 96 bunarića tretirana je ispitivanim spojevima te je potom u bunariće dodana stanična kultura plazmodija u stadiju prstena (hematokrit 1,5 %, parazitemija 0,05 %). Nakon trodnevne inkubacije na 37 °C, pri 5 % CO_2 i 5 % O_2 uzorci su analizirani HRP2-ELISA metodom. Sva ispitivanja provedena su u duplikatu, u najmanje dva neovisna eksperimenta. IC_{50} vrijednost je određena iz krivulje ovisnosti vijabilnosti stanica o koncentraciji ispitivanog spoja primjenom nelinearne regresijske analize u programu R v2.6.1 pomoću programskog paketa drc v0.9.0. Pojedini rezultati prikazani su u obliku srednjih vrijednosti s pripadajućim standardnim devijacijama (165–167).

Ispitivanje djelovanja harmicina na hepatocitnu fazu *P. berghei* povedena su *in vitro* testom bioluminiscencije. Stanična linija Huh7 uzgajana je u mediju RPMI 1640, obogaćenim 10 %-tnim fetalnim govođim serumom, 1 %-tnim glutaminom, antibioticima (penicilin/streptomicin), 1 %-tnim neesencijalnim aminokiselinama i 10 mM 2-[4-(2-hidroksietil)piperazin-1-il]etan-1-sulfonskoj kiselini (HEPES). Stanice su nasađene na mikrotitarsku pločicu s 96 bunarića te inkubirane na 37 °C pri 5 % CO_2 tijekom noći. Idući dan je stanični medij zamijenjen serijski razrijeđenim otopinama ispitivanih spojeva, a mikrotitarske pločice inkubirane na 37 °C pri 5 % CO_2 tijekom 1 h. Nakon toga su stanične kulture u bunarićima tretirane sporozoitima *P. berghei* koji eksprimiraju luciferazu. Stanice su zatim centrifugirane i inkubirane na 37 °C pri 5 % CO_2 tijekom 46 h, nakon čega su inkubirane s bojom Alamar Blue (Invitrogen, SAD) te je proveden test bioluminiscencije (Biotium, Fremont, CA, SAD). IC_{50} vrijednost je određena iz krivulje ovisnosti vijabilnosti stanica o koncentraciji ispitivanog spoja primjenom nelinearne regresijske analize u programu GraphPad Prism 6 (168, 169).

3.3.2. Ispitivanja citotoksičnosti *in vitro*

Citotoksičnost spojeva ispitana je *in vitro* na humanoj staničnoj liniji hepatocelularnog karcinoma (HepG2). Stanice su nasađene na mikrotitarsku pločicu s 96 bunarića te su inkubirane tijekom 24 h. Sljedeći dan stanice su tretirane otopinama ispitivanih spojeva odgovarajućih koncentracija te ponovno inkubirane tijekom 24 h. Po isteku vremena stanice su tretirane bojom Neutral Red te je izmjerena absorbancija koja je proporcionalna broju živih stanica. IC_{50} vrijednost je određena iz krivulje ovisnosti vijabilnosti stanica o koncentraciji ispitivanog spoja primjenom nelinearne regresijske analize u programu R v2.6.1 pomoću programskog paketa drc v0.9.0. Pojedini rezultati prikazani su u obliku srednjih vrijednosti s pripadajućim standardnim devijacijama (170). Indeksi selektivnosti (SI) pojedinih spojeva izračunati su kao omjer IC_{50} vrijednosti spoja za HepG2 i IC_{50} vrijednosti za *Pf*3D7.

3.4. QSAR ANALIZA

QSAR analiza je provedena za skup od 40 harmicina amidnoga tipa (**7a-h**, **13a-h**, **19a-h**, **22a-h** i **25a-f**,**i**,**j**). Zavisna varijabla bila je eksperimentalno određena vrijednost antiplazmodijskog djelovanja navedenih harmicina na *Pf*3D7 soj (Y_{eksp}), dok je nezavisne varijable činio skup generiranih molekulskih deskriptora (3.4.1.).

Statistički izračuni, vizualizacija, matematičko modeliranje i validacija provedeni su u programskom jeziku R verzija 4.0.3. (R Foundation, Austrija) koristeći RStudio 1.3.1093 program i programske pakete „tidyverse", „ggplot2", „readxl" i „caret" (167).

Za izračunavanje molekulskih deskriptora korišteni su programi i mrežne aplikacije:

- ACD/ChemSketch verzija 2019.2.1 (Freeware) (Advanced Chemistry Development, Inc., Kanada) (171)
- MarvinSketch verzija 19.21.5 (ChemAxon, Mađarska) (172)
- ChemBioDraw Ultra 14.0 (PerkinElmer, Inc, SAD) (173)
- MNova verzija 12.0.0. (Mestrelab Research, Španjolska) (174)
- *chemicalize.com* (ChemAxon, Mađarska) (101)
- *swissadme.ch* (SwissADME; Švicarski institut za bioinformatiku, Švicarska). (175)

3.4.1. Molekulski deskriptori

Na temelju strukture harmicina amidnoga tipa (**7a-h**, **13a-h**, **19a-h**, **22a-h** i **25a-f**,**i**,**j**) nacrtanih u programu ACD/ChemSketch, izračunati su deskriptori supstituenata: masa supstituenta (M_S), volumen supstituenta (V_S) i hidrofobna konstanta po Hanschu (πs).

3.4.1.1. Fizikalno-kemijski deskriptori

Relativna molekulska masa (M_r), logaritam koeficijenta razdjeljenja (log P_{chem}, log P_{dr}, log P_{swiss}, log P_{mestr}), računski logaritam koeficijenta razdjeljenja između oktanola i vode (Clog *P*), logaritam intrizične topljivosti (log S_{chem}, log S_{dr}, log S_{swiss}, log S_{mestr}), topljivost (*s*), molarna topljivost (s_M), preuzeti su s mrežnih stranica *chemicalize.com* i *swissadme.ch* i/ili generirani u programima ChemBioDraw Ultra, MNova. Temperatura tališta (t_t) određena je eksperimentalno te predviđena (t_{tmestr}) programom MNova. Površinska napetost (σ), gustoća (ρ) i parahor (p) izračunati su u programu ACD/ChemSketch. Logaritam koeficijenta permeabilnosti kroz kožu (logK_p) preuzet je s mrežne stranice *swissadme.ch*. Henryjeve konstante (K_h, H^{cc}) izračunate su programima ChemBioDraw Ultra i MNova, a hidrofilno-lipofilne ravnoteže ($HLB_{chemaxon}$, HLB_{Davies}, $HLB_{Griffin}$) izračunate su u programu MarvinSketch. Abrahamov deskriptor A (Abr A), Abrahamov deskriptor B (Abr B), Abrahamov dekriptor E (Abr E), Abrahamov deskriptor S (Abr S), Abrahamov deskriptor V (Abr V), tlak para (p_V), temperatura vrelišta (t_B), logaritam koeficijenta razdjeljenja između oktanola i vode pri pH 7,4 (log *D*), logaritam konstante vezanja za kiseli α-glikoprotein (logK_{aAGP}), logaritam konstante vezanja za humani serumski albumin (logK_{aHSA}), logaritam konstante vezanja za membrane (logK_{aMemb}), logaritam koeficijenta razdjeljenja između krvno-moždane barijere (log *BB*), slobodna frakcija lijeka u plazmi (fu_p), slobodna frakcija lijeka u mozgu (fu_b), postotak vezanja za proteine plazme (*PPB*), napad hidroksilnih radikala (*HRA*) izračunati su programom MNova.

3.4.1.2. 0D i 1D-deskriptori, deskriptori vodikove veze i indeksi fleksibilnosti

Sljedeći deskriptori preuzeti su i izračunati pomoću mrežnih stranica *chemicalize.com*, *swissadme.ch* i programom MarvinSketch: udio atoma ugljika u strukturi (W_C), udio atoma vodika u strukturi (W_H), udio atoma dušika u strukturi (W_N), broj atoma (NA), broj teških atoma (NHA), broj veza u molekuli koje mogu slobodno rotirati oko vlastite osi (B_{FRchem}, $B_{FRswiss}$), omjer sp^3-hibridiziranih ugljikovih atoma i ukupnog broja ugljikovih atoma (Fsp^3), broj donorskih skupina vodikove veze (HBD_{chem}, HBD_{swiss}), broj akceptorskih skupina vodikove veze (HBA_{chem}, HBA_{swiss}), broj veza (NB), broj asimetričnih atoma (AAC), broj atoma u

alifatskim vezama (AlAC), broj alifatskih veza (AlBC), broj atoma u aromatskim vezama (ArAC), broj aromatskih veza (ArBC), broj prstenova (RC), broj zasićenih prstenova (AlRC), broj aromatskih prstenova (ArRC), broj atoma u prstenovima (RAC), broj veza u prstenovma (RBC), broj aromatskih prstenova s ugljikovim kosturom (CArC), broj prstena s ugljikovim kosturom (CRC), broj heterocikala (HRC), broj aromatskih heterocikala (HArC), broj heteroaromatsih prstenova (HArRC), broj teških aromatskih atoma (NArHA), broj fuzioniranih zasićenih prstenova (FAlRC), broj fuzioniranih aromatskih prstenova (FArRC), broj fuzioniranih prstenova (FRC), veličina najvećeg prstena (LRS), veličina najmanjeg prstena (SRS), ciklomatski broj (CN). Na temelju strukture harmicina određeni su slijedeći deskriptori: broj teških atoma u linearnoj poveznici (CAC), broj veza u linearnoj poveznici (CBC), broj atoma u supstitucijskom lancu (ACC), broj atoma izvan β-karbolina (ACOR), supstitucija u položaju 1 β-karbolina (pol. 1), supstitucija u položaju 3 β-karbolina (pol. 3), supstitucija u položaju 6 β-karbolina (pol. 6), supstitucija u položaju 7 β-karbolinskog prstena (pol. 7), supstitucija u položaju 9 β-karbolina (pol. 9), prisutnost supstituenta u *orto*-položaju DCK-a (fenil 2'), prisutnost supstituenta u *meta*-položaju DCK-a (fenil 3'), prisutnost supstituenta u *para*-položaju DCK-a (fenil 4'), prisutnost metoksi skupine u položaju 7 β-karbolinskog prstena (OCH_3 pol. 7), prisutnost metilne skupine u položaju 1 β-karbolina (CH_3 pol. 1), prisutnost metilne skupine u α-položaju DCK-a (CH_3 pol. 5').

3.4.1.3. Topološki deskriptori

Topološki deskriptori računaju se iz grafa (G) koji predstavlja kemijsku strukturu molekule. Vrhovi grafa predstavljaju atome, a bridovi grafa predstavljaju veze među atomima (176). U programu MarvinSketch izračunati su sljedeći topološki molekulski deskriptori: Plattov indeks *F*(G), Randićev indeks povezanosti χ(G), Balabanov indeks *J*(G), Hararyjev indeks *H*(G), hiper-Wienerov indeks *WW*(G), Szeged-indeks *Sz*(G), Wienerov indeks *W*(G), Wienerov indeks polarnosti *Wp*(G).

3.4.1.4. Geometrijski i sterički molekulski deskriptori

Topološka polarna površina ($TPSA_{chem}$, $TPSA_{dr}$, $TPSA_{swiss}$), površina molekule dostupna otapalu (*SASA*), van der Waalsov volumen (V_w, $V_{wmarvin}$), van der Waalsova površina (A_W), minimalna projekcijska površina (A_{min}, $A_{minmarvin}$), maksimalna projekcijska površina ($A_{max,}$ $A_{maxmarvin}$), polumjer minimalne projekcijske površine ($r_{min,}$ $r_{minmarvin}$) polumjer maksimalne projekcijske površine (r_{max}, $r_{maxmarvin}$), Dreidingova energija (E_D), Merck molekularno polje sila (MMFF94), dužina okomita na maksimalnu površinu ($LP_{max}A$), dužina okomita na minimalnu

površinu ($LP_{min}A$) preuzeti su s mrežnih stranica *chemicalize.com* i *swissadme.ch* i/ili izračunati u programima ChemBioDraw Ultra i MarvinSketch. Vrijednosti kontaktne polarne površine (CSP_{HBD}, CSP_{HBA}, CSP_n, CSP_t) izračunate su u programu MNova.

3.4.1.5. Elektronski deskriptori

Polarizabilnost (P_{chem}, P_{sk}), molarna refraktivnost (MR_{chem}, MR_{dr}, MR_{sk}, MR_{swiss}), izoelektrična točka (pI, pI_{marvin}), indeks loma svjetlosti (n) i molarni volumen (V_M) izračunati su u programima MarvinSketch, ACD/ChemSketch i/ili preuzeti s mrežnih stranica *swissadme.ch* i *chemicalize.com*.

3.4.2. QSAR model

U svrhu određivanja kvalitete izgrađenog QSAR modela primijenjene su određene statističke veličine:

- R^2 - koeficijent determinacije
- R_a^2 - prilagođeni koeficijent determinacije
- F - omjer varijanci stvarnih i izračunatih vrijednosti
- *p*-vrijednost - razina značajnosti
- Q^2 - koeficijent determinacije unakrsne validacije
- MAE - srednja apsolutna pogreška
- RMSE - korijen srednje kvadratne pogreške

Pouzdanost izgrađenog QSAR modela procijenjena je metodom unutarnje i vanjske validacije.

Statistički parametri korišteni za evaluaciju izgrađenog QSAR modela i jednadžbe za izračun dane su u Tablici 3.

Tablica 3. Statistički parametri korišteni u evaluaciji QSAR modela

Statistički parametar	Jednadžba
R^2	$R^2 = 1 - \frac{\sum(Y_{eksp} - Y_{pred})^2}{\sum(Y_{eksp} - \bar{Y}_{eksp})^2}$
R_a^2	$R_a^2 = 1 - \frac{(1 - R^2)(N-1)}{N-p-1}$
F	$F = \frac{\frac{\sum(Y_{pred} - \bar{Y}_{eksp})^2}{p}}{\frac{\sum(Y_{eksp} - Y_{pred})^2}{N-1-p}}$
Q^2	$Q^2 = 1 - \frac{\sum(Y_{\text{eksp }(tr)} - Y_{pred\ (tr)})^2}{\sum(Y_{\text{eksp }(tr)} - \bar{Y}_{\text{eksp }(tr)})^2}$
MAE	$MAE = \frac{1}{N}\sum\lvert Y_{eksp} - Y_{pred}\rvert$
RMSE	$RMSE = \sqrt{\frac{1}{N}\sum(Y_{eksp} - Y_{pred})^2}$

Y_{eksp} - eksperimentalno dobivena vrijednost biološke aktivnosti

Y_{pred} - vrijednost biološke aktivnosti predviđena QSAR modelom

$\bar{Y}_{eksp}$ - prosječna eksperimentalno dobivena vrijednost biološke aktivnosti

$Y_{\text{eksp }(tr)}$ - eksperimentalno dobivena vrijednost biološke aktivnosti u skupu za učenje

$\bar{Y}_{\text{eksp }(tr)}$ - prosječna eksperimentalno dobivena vrijednost biološke aktivnosti u skupu za učenje

$Y_{pred(tr)}$ - vrijednost biološke aktivnosti u skupu za učenje predviđena QSAR modelom

N - ukupan broj spojeva

p - broj prediktorskih varijabli (molekulskih deskriptora

4. REZULTATI I RASPRAVA

4.1. SINTEZE

U okviru ovog doktorskog rada sintetizirani su hibridni spojevi β-karbolina i DCK-a: harmicini amidnoga **7a-h**, **13a-h**, **19a-h**, **22a-h**, **25a-f**, **i-p**, karbamatnog **28a-k** i ureidnog **32b**,**c** tipa te pripadajući prekursori.

4.1.1. Sinteza harmicina amidnoga tipa

Harmicini amidnoga tipa sintetizirani su u položajima 1, 3, 6, 7 i 9 β-karbolinskog prstena reakcijom povezivanja prethodno sintetiziranih amina **6**, **12**, **18**, **21** i **24** i cimetne kiseline odn. odabranih DCK-a. Za sintezu amina u položajima 1, 3 i 6 prvotno su sintetizirani β-karbolinski prstenovi Pictet-Spenglerovom kondenzacijom, dok su amini u položajima 7 i 9 sintetizirani iz harmina.

4.1.1.1. Sinteza harmicina amidnoga tipa u položaju C-1 β-karbolina

Početni spoj u sintezi amina **6** u položaju C-1 β-karbolina bio je triptamin. Pictet-Spenglerovom kondenzacijom triptamina i 2,2-dimetoksi acetaldehida u diklormetanu uz prisutnost TFA kao kiselog katalizatora dolazi do stvaranja iminijevog iona te posljedično do zatvaranja šesteročlanog prstena pri čemu nastaje THβC **1**, supstituiran acetalnom skupinom u položaju 1. Budući da je TFA korištena u suvišku (ukupno 1,4 ekvivalenta), reakcija je prekinuta dodavanjem baze, odn. 10 %-tne otopine $NaHCO_3$. Postepenim zakiseljavanjem 10 %-tnom HCl do pH 7,6 novonastali produkt je preveden iz oblika soli u neionizirani oblik amina. Prednosti ove reakcije su mogućnost provođenja na gramskoj skali u blagim uvjetima (miješanje 18 h na sobnoj temperaturi) te minimalno stvaranje nusprodukata koje ne zahtijeva pročišćavanje kromatografijom na koloni.

U sljedećem reakcijskom koraku je novosintetizirani THβC **1** podvrgnut reakciji oksidacije, pri čemu je kao oksidans korišten kalijev permanganat. Reakcija oksidacije prvotno je provođena u aprotičnom polarnom otapalu, DMF-u, no zbog iznimno egzotermnog karaktera ove reakcije DMF je zamijenjen THF-om. Zamjenom otapala i produljenjem vremena miješanja na sobnoj temperaturi (do 48 h) uočeno je povećanje iskorištenja reakcije i jednostavnost pročišćivanja željenog produkta. Budući da je kalijev permanganat korišten u suvišku (4 ekvivalenta), neizreagirani $KMnO_4$ te novonastali manganov (IV) oksid uklonjeni su filtracijom reakcijske smjese kroz sloj celita, a dobiveni β-karbolin **2** dodatno je pročišćen ispiranjem otopine spoja u diklormetanu vodom te kromatografijom na koloni.

Nadalje, kiselom hidrolizom u smjesi ledene octene kiseline i vode na temperaturi refluksa (100 °C) tijekom 1 h uklonjena je zaštitna acetalna skupina i dobiven aldehid **3**. Suvišak kiseline neutraliziran je zaluživanjem reakcijske smjese 5 %-tnom otopinom NaOH do pH 8-9, pri kojemu se novosintetizirani aldehid **3** nalazi u neioniziranom obliku. Nakon ekstrakcije aldehida **3** u etil-acetat, spoj je dodatno pročišćen kromatografijom na koloni.

U sljedećem reakcijskom koraku novosintetizirani aldehid **3** je upotrebom $LiAlH_4$, snažnog redukcijskog sredstva, reduciran u primarni alkohol **4**, uz vrlo visoki prinos reakcije od 91 %. Reakcija je provedena u THF-u, koji je uz dietil-eter najpoželjnije otapalo u reakcijama redukcije uz $LiAlH_4$. Budući da $LiAlH_4$ burno reagira s vodom pri čemu se stvara vodik, reakcijski uvjeti su strogo kontrolirani te je u tu svrhu korišten bezvodni THF, a reakcija je provedena u inertnim uvjetima pod strujom argona. Redukcijom aldehida uz $LiAlH_4$ dolazi do stvaranja aluminijeva alkoksida kojega je potrebno naknadno hidrolizirati kako bi se nastali alkoksid preveo u željeni alkohol te mogao izolirati. Stoga je, po završetku, u reakcijsku smjesu dodana 10 %-tna vodena otopina HCl-a i provedena ekstrakcija etil-acetatom u pH području u kojem se novosintetizirani alkohol **4** nalazi u neioniziranom obliku (pH 8), a zatim je dodatno pročišćen rastrljavanjem u dietil-eteru.

Reakcija direktnog prevođenja primarnog alkohola **4** u azid **5** korištenjem ADMP-a kao donora azidne skupine i DBU-a kao baze pokazala se jednostavnom i sigurnom. Reakcija je provedena u bezvodnom THF-u pri 0 °C kako bi se mogućnost raspada ADMP-a i novosintetiziranog azida pri višim temperaturama svela na minimum. Reakcija je brza (unutar 1 h), a nastali azid **5** lako se pročišćava. S obzirom da su heksafluorofosfatna sol DBU-a i 1,3-dimetilimidazolidin-2-on, koji nastaju kao nusprodukti ove reakcije, topljivi u vodi, lako su uklonjeni ekstrakcijom. No, zbog velikog suviška ADMP-a (2,5 ekvivalenta) i DBU-a (2,7 ekvivalenta) korištenih u ovoj reakciji, bilo je potrebno dodatno pročistiti azid **5**, a njegov izuzetno lipofilni karakter omogućio je brzo i jednostavno pročišćavanje kromatografijom na koloni.

Za redukciju azida **5** u amin **6** odabrana je metoda katalitičkog hidrogeniranja. Reakcija je provedena u blagim uvjetima, na sobnoj temperaturi u metanolu pod atmosferom vodika, a kao katalizator korišten je paladij na aktivnom ugljenu (Pd/C). U odnosu na druge, često korištene metode redukcije azida u amin, poput Staudingerove redukcije pomoću Ph_3P ili redukcije pomoću $LiAlH_4$, ova reakcija ne zahtijeva korištenje toksičnih reagensa kao ni dodatne metode pročišćavanja. Katalizator je jednostavno uklonjen filtracijom reakcijske smjese kroz sloj celita, a novosintetizirani amin **6** pročišćen je rastrljavanjem u smjesi dietil-

etera i petroletera dajući čist spoj uz visoki prinos od 71 %. Sintetski put priprave amina **6** prikazan je na Shemi 1.

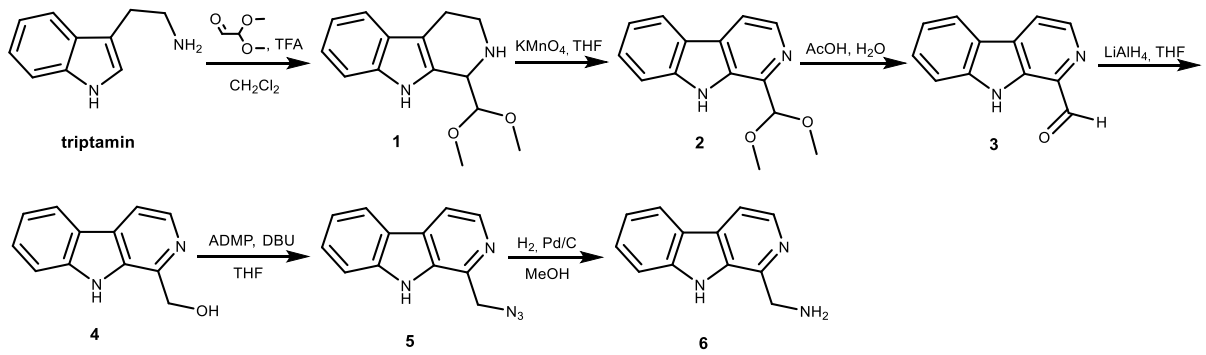

Shema 1 Sinteza amina **6** u položaju C-1 β-karbolina

Odabrana metoda u sintezi ciljanih amida **7a-h**, **13a-h**, **19a-h**, **22a-h**, **25a-f**, **i-p** uključivala je aktivaciju cimetne kiseline i odabranih DCK-a *coupling* reagensom HATU u prisutnosti DIEA.

Harmicini amidnoga tipa **7a-h** u položaju C-1 β-karbolina pripravljeni su reakcijama povezivanja prethodno sintetiziranog amina **6** i cimetne kiseline, odn. sedam odabranih DCK-a (*m*-F-, *m*-Br-, *m*-CF_3-, *p*-F-, *p*-Cl-, *p*-OCH_3-, *p*-CF_3-cimetna kiselina) u 10 %-tnom suvišku u prisutnosti HATU i DIEA-a (Shema 2). DCK-i korišteni u reakcijama povezivanja odabrani su na temelju literaturnih podataka (75, 133, 136) i komercijalne dostupnosti. Cimetna kiselina/DCK-i prvotno su miješani 20 minuta na sobnoj temperaturi u prisutnosti HATU i DIEA-a u diklormetanu, kako bi se omogućilo stvaranje reaktivnog intermedijera prije dodatka amina **6**. DIEA je tercijarni amin koji je u reakcijama povezivanja korišten kao baza pri čemu je jedan ekvivalent baze korišten za deprotoniranje cimetne kiseline/DCK-a, a drugi za deprotoniranje amina **6**. Mehanizam *in situ* aktivacije uz HATU započinje deprotoniranjem cimetne kiseline/DCK-a, pri čemu nastaje karboksilatni anion koji napada elektrofilni ugljikov atom HATU-a, što dovodi do stvaranja aniona i aktivirane kiseline. Nadalje, novonastali anion reagira s aktiviranom kiselinom stvarajući tako aktivni ester, a kao nusprodukt nastaje tetrametilurea. Dodatkom amina **6** u reakcijsku smjesu dolazi do nukleofilnog napada dušika amina na elektrofilni karbonilni ugljik aktiviranog estera te dolazi do stvaranja amidne veze pri čemu nastaju amidi **7a-h**.

Reakcije su provedene na sobnoj temperaturi tijekom sat vremena. Svi novosintetizirani amidi taložili su se u reakcijskoj smjesi te su vrlo lako izolirani filtracijom, a zatim pročišćeni

kromatografijom na koloni i rastrljavanjem u dietil-eteru, čime su dobiveni čisti spojevi (HPLC čistoća **7a-d**, **7g**,**h** > 97 %) u umjerenim do visokim iskorištenjima (51 – 72 %).

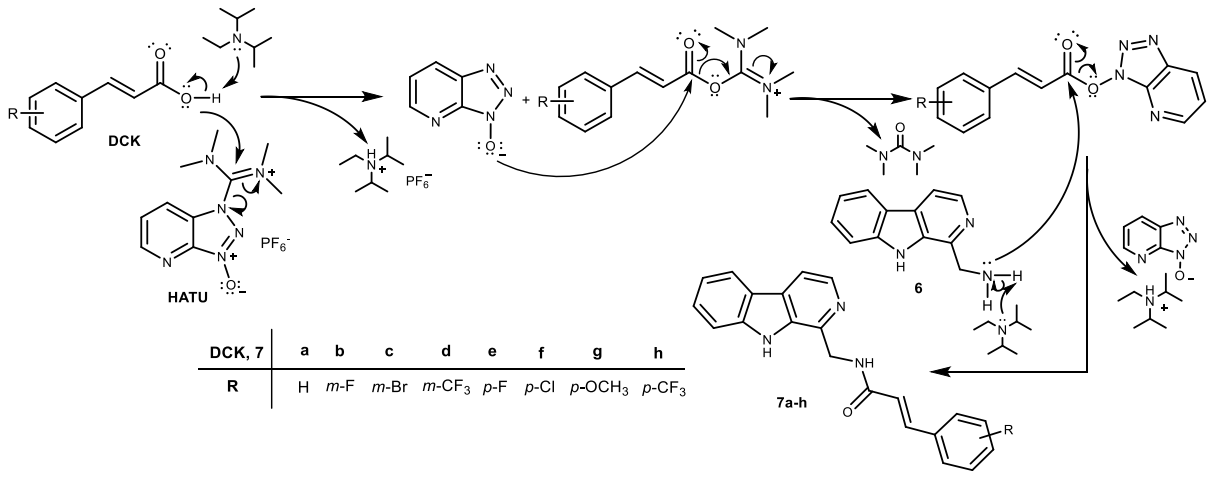

Shema 2. Mehanizam aktivacije DCK-a *coupling* reagensom HATU u sintezi harmicina amidnoga tipa **7a-h** u položaju C-1 β-karbolina

U položaju C-1 β-karbolina sintetizirani su sljedeći novi spojevi:

1-(azidometil)-9*H*-pirido[3,4-*b*]indol (**5**),

(9*H*-pirido[3,4-*b*]indol-1-il)metanamin (**6**),

N-((9*H*-pirido[3,4-*b*]indol-1-il)metil)cinamamid (**7a**),

(*E*)-*N*-((9*H*-pirido[3,4-*b*]indol-1-il)metil)-3-(3-fluorfenil)akrilamid (**7b**),

(*E*)-*N*-((9*H*-pirido[3,4-*b*]indol-1-il)metil)-3-(3-bromfenil)akrilamid (**7c**),

(*E*)-*N*-((9*H*-pirido[3,4-*b*]indol-1-il)metil)-3-(3-(trifluormetil)fenil)akrilamid (**7d**),

(*E*)-*N*-((9*H*-pirido[3,4-*b*]indol-1-il)metil)-3-(4-fluorfenil)akrilamid (**7e**),

(*E*)-*N*-((9*H*-pirido[3,4-*b*]indol-1-il)metil)-3-(4-klorfenil)akrilamid (**7f**),

(*E*)-*N*-((9*H*-pirido[3,4-*b*]indol-1-il)metil)-3-(4-metoksifenil)akrilamid (**7g**),

(*E*)-*N*-((9*H*-pirido[3,4-*b*]indol-1-il)metil)-3-(4-(trifluormetil)fenil)akrilamid (**7h**).

4.1.1.2. Sinteza harmicina amidnoga tipa u položaju C-3 β-karbolina

Za pripravu harmicina amidnoga tipa **13a-h** u položaju C-3 β-karbolina potrebno je bilo sintetizirati β-karbolinski prsten. Stoga je kao početni spoj u sintezi harmicina amidnoga tipa **13a-h** odabran metilni ester triptofana hidroklorida, a kako bi se uvela metilna skupina u položaj C-1, umjesto acetaldehida koji je izuzetno reaktivan te ima nisko vrelište (20,2 °C), korišten je zaštićeni aldehid, acetaldehid-dimetil acetal. Kondenzacijom metilnog estera triptofana hidroklorida s acetaldehid-dimetil acetalom u kiselim uvjetima dolazi do stvaranja iminijevog

iona, a zatim ciklizacijom do zatvaranja šesteročlanog prstena pri čemu nastaje THβC **8**, supstituiran esterom u položaju C-3 i metilnom skupinom u položaju C-1. Reakcija je provedena u diklormetanu miješanjem na sobnoj temperaturi, a kako bi se poboljšao prinos reakcije acetaldehid-dimetil acetal korišten je u 20 %-tnom suvišku. Kao kiseli katalizator upotrijebljena je TFA, a korišteno je ukupno 2 ekvivalenta čime je omogućeno *in situ* uklanjanje zaštitne acetalne skupine acetaldehid-dimetil acetala. Reakcija je nakon 18 h prekinuta zaluživanjem 10 %-tnom otopinom $NaHCO_3$ do pH područja u kojem se novosintetizirani THβC **8** nalazi u neioniziranom obliku (7,6). Ekstrakcijom tekuće-tekuće preveden je u diklormetan koji se lako uklanja pod sniženim tlakom, a zatim je korišten u idućem reakcijskom koraku bez dodatnog pročišćavanja.

U odnosu na reakciju oksidacije THβC **1** u položaju C-1, oksidacija THβC **8** provedena je pod utjecajem mikrovalnog zračenja, u bezvodnom etanolu u prisutnosti 10 %-tnog Pd/C koji je korišten kao oksidacijsko sredstvo. Reakcija je brza (20 min), a katalizator je jednostavno uklonjen filtracijom kroz sloj celita. Zbog korištenja bezvodnog etanola nastala je smjesa etilnog i metilnog estera s većim udjelom metilnog estera (potvrđeno NMR-om). Međutim, zbog provođenja redukcije novonastalih estera u idućem reakcijskom koraku, nije bilo potrebno optimirati uvjete oksidacije kao ni razdvajati nastale estere **9a**,**b**.

Nadalje, dobiveni esteri β-karbolina **9a**,**b** reducirani su u primarni alkohol **10** upotrebom $LiAlH_4$ u bezvodnom THF-u. Reakcija je provedena na sobnoj temperaturi pod strujom argona, a dobiveni alkohol **10** pročišćavan je analogno alkoholu **4** u položaju C-1 (4.1.1.1.) te je dobiven u vrlo visokom iskorištenju od 91 %.

U sljedećem reakcijskom koraku alkohol **10** je, analogno pripravi azida **5** u položaju C-1, upotrebom ADMP-a i DBU-a u bezvodnom THF-u preveden u azid **11**. Pročišćavanjem ekstrakcijom te kromatografijom na koloni izoliran je kao ulje u 76 %-tnom iskorištenju, a zatim, analogno redukciji azida **5**, katalitičkim hidrogeniranjem reduciran u primarni amin **12**. Reakcija redukcije provedena je miješanjem 2 h na sobnoj temperaturi u metanolu u atmosferi vodika. Katalizator je uklonjen filtracijom kroz sloj celita, a sirovi produkt je nakon rastrljavanja u dietil-eteru i petroleteru izoliran u 61 %-tnom iskorištenju.

Zadnji korak u sintezi harmicina amidnoga tipa **13a-h** u položaju C-3 β-karbolina uključivao je reakcije povezivanja prethodno sintetiziranog amina **12** i cimetne kiseline odn. DCK-a. Analogno sintezi harmicina amidnoga tipa **7a-h** u položaju C-1 β-karbolina, odabrani DCK-i bilu su: *m*-F-, *m*-Br-, *m*-CF_3-, *p*-F-, *p*-Cl-, *p*-OCH_3-, *p*-CF_3-cimetna kiselina, a reakcije su provedene na sobnoj temperaturi u diklormetanu. Cimetna kiselina i DCK-i također su korišteni u 10 %-tnom suvišku, a prvotno su miješani 20 minuta u prisutnosti HATU i DIEA-

a. Novosintetizirani amidi **13a-c** te **13e-h** taložili su se u reakcijskoj smjesi te su vrlo lako izolirani filtracijom, zatim pročišćeni kromatografijom na koloni i rastrljavanjem u dietil-eteru, dok je harmicin **13d** koji se nije taložio u reakcijskoj smjesi, istaložen dodatkom etil-acetata, a zatim filtriran te pročišćen kromatografijom na koloni i rastrljavanjem u dietil-eteru.

Većina međuprodukata dobivena je provođenjem reakcija u blagim uvjetima bez dodatnog pročišćavanja kromatografijom na koloni, a ukupno osam novosintetiziranih amida **13a-h** pripravljeno je uz nešto niža iskorištenja (21 – 64 %) u odnosu na harmicine amidnoga tipa **7a-h**. Sintetski put u pripravi harmicina amidnoga tipa **13a-h** u položaju C-3 β-karbolina prikazan je na Shemi 3.

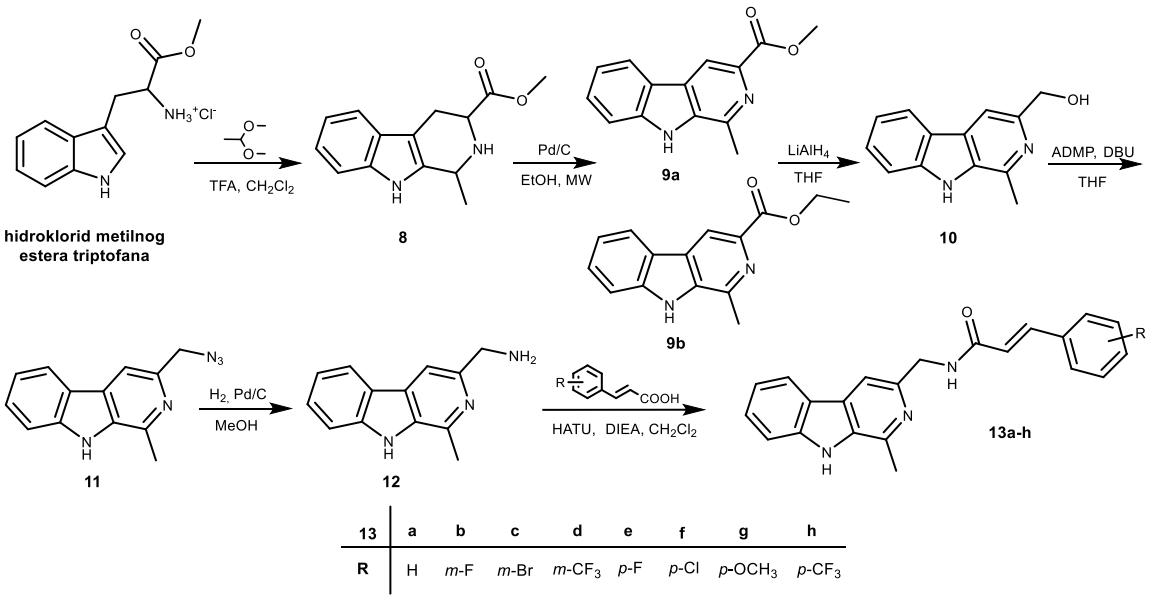

Shema 3. Sinteza harmicina amidnoga tipa u položaju C-3 β-karbolina

U položaju C-3 β-karbolina sintetizirani su sljedeći novi spojevi:

3-(azidometil)-1-metil-9*H*-pirido[3,4-*b*]indol (**11**),

(1-metil-9*H*-pirido[3,4-*b*]indol-3-il)metanamin (**12**),

N-((1-metil-9*H*-pirido[3,4-*b*]indol-3-il)metil)cinamamid (**13a**),

(*E*)-3-(3-fluorfenil)-*N*-((1-metil-9*H*-pirido[3,4-*b*]indol-3-il)metil)akrilamid (**13b**),

(*E*)-3-(3-bromfenil)-*N*-((1-metil-9*H*-pirido[3,4-*b*]indol-3-il)metil)akrilamid (**13c**),

(*E*)-*N*-((1-metil-9*H*-pirido[3,4-*b*]indol-3-il)metil)-3-(3-(trifluormetil)fenil)akrilamid (**13d**),

(*E*)-3-(4-fluorfenil)-*N*-((1-metil-9*H*-pirido[3,4-*b*]indol-3-il)metil)akrilamid (**13e**),

(*E*)-3-(4-klorfenil)-*N*-((1-metil-9*H*-pirido[3,4-*b*]indol-3-il)metil)akrilamid (**13f**),

(*E*)-3-(4-metoksifenil)-*N*-((1-metil-9*H*-pirido[3,4-*b*]indol-3-il)metil)akrilamid (**13g**),

(*E*)-*N*-((1-metil-9*H*-pirido[3,4-*b*]indol-3-il)metil)-3-(4-(trifluormetil)fenil)akrilamid (**13h**).

4.1.1.3. Analitički i spektroskopski podaci novosintetiziranih spojeva u položajima C-1 i C-3 β-karbolina

Tijek kemijskih reakcija i čistoća produkata praćeni su tankoslojnom kromatografijom. Strukture spojeva **5**, **6**, **11**, **12**, **7a-h** te **13a-h** potvrđene su uobičajenim spektroskopskim i analitičkim metodama (IR, ^{1}H i ^{13}C NMR i MS). Aminima **6** i **12** te harmicinima amidnoga tipa **7a-h** i **13a-h** određena su tališta, dok su azidi **5** i **11** izolirani kao ulja. Harmicinima **7a-d**, **7g**,**h**, **13a**, **13c-e** i **13h** određena je relativna čistoća.

IR spektar 1-(azidometil)-9*H*-pirido[3,4-*b*]indola (**5**) pokazuje oštru vrpcu jakog intenziteta na valnom broju 2105 cm^{-1} karakterističnu za N=N=N istezanje azidne (-N_3) skupine, dok se ta vrpca u IR spektru 3-(azidometil)-1-metil-9*H*-pirido[3,4-*b*]indola (**11)** nalazi na valnom broju 2104 cm^{-1}. U IR spektrima (9*H*-pirido[3,4-*b*]indol-1-il)metanamina (**6**) i (1-metil-9*H*-pirido[3,4-*b*]indol-3-il)metanamina (**12**) uočene su oštre vrpce srednjeg intenziteta na valnim brojevima 3347 cm^{-1} (**6**) i 3338 cm^{-1} (**12**), koje odgovaraju N–H istezanju primarne amino skupine te široke vrpce slabog intenziteta N–H istezanja sekundarnog (indolskog) amina na valnim brojevima 3282 cm^{-1} (**6**) i 3239 cm^{-1} (**12**). Zatim su vidljive oštre vrpce srednjeg intenziteta na 1625 cm^{-1} i 1600 cm^{-1} (**6**) te 1626 cm^{-1} i 1606 cm^{-1} (**12**) koje odgovaraju N–H savijanju.

U ^{1}H NMR spektrima azida **5** i **11** te amina **12** uočeni su signali za indolski proton H-10 na kemijskim pomacima od 11,78 ppm (**5**), 11,66 ppm (**11**) i 11,42 ppm (**12**), dok u ^{1}H spektru amina **6** nije uočen taj pik. Također, analizom ^{1}H spektara amina **6** i **12** nisu uočeni signali za protone primarne amino skupine H-2', stoga su njihove strukture izravno potvrđene MS analizom kojom je vidljiv pik molekulskog iona pri *m/z* 196,0 sniman u negativnom modu (**6**) te pri *m/z* 210,0 (snimano u negativnom modu) i *m/z* 212,1 (snimano u pozitivnom modu) (**12**), te neizravno daljnjim reakcijama povezivanja koje su provedene u blagim uvjetima dajući harmicine amidnoga tipa **7a-h** i **13a-h** čije su strukture također potvrđene uobičajenim spektroskopskim i analitičkim metodama. Zatim su u ^{1}H spektrima spojeva **11** i **12** vidljivi pikovi singleta s relativnim integralom 3H na kemijskim pomacima od 2,78 ppm (**11)** odn. 2,73 ppm (**12**), a koji odgovaraju signalima protona metilne skupine H-13. U ^{13}C spektrima azida **11** i amina **12** vidljiv su pikovi ugljikovog atoma metilne skupine C-13 na 20,41 ppm (**11**), odn. 20,38 ppm (**12**).

Analitički i spektroskopski podaci spojeva **5**, **6**, **11** i **12** dani su u Tablicama 4 i 5.

Tablica 4. Analitički i IR spektroskopski podaci azida **5** i **11** i amina **6** i **12**

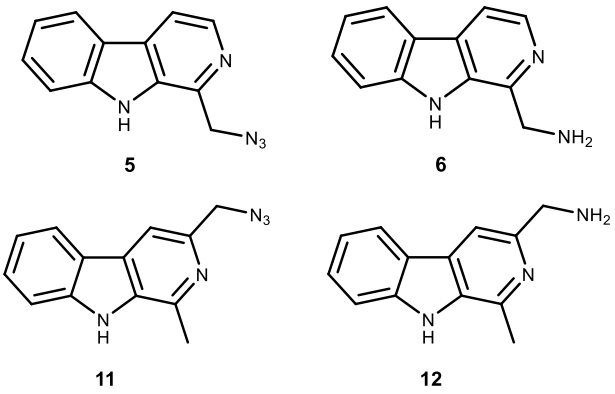

Spoj	Iskorištenje (%)	t_t (°C)	Molekulska formula (M_r)	MS [*m/z*]	IR (ATR, ν/cm^{-1})
5	67	ulje	$C_{12}H_9N_5$ (223,24)	n.s.[a]	3663, 3451, 3288, 3059, 2937, 2855, 2105, 1730, 1631, 1566, 1493, 1428, 1371, 1321, 1248, 1118, 1052, 971, 938, 873, 824, 751, 718, 620, 579, 432
6	71	201,0 – 205,0 (raspad)	$C_{12}H_{11}N_3$ (197,24)	196,0 $[M-1]^-$	3347, 3282, 3120, 3051, 2955, 2856, 2776, 1625, 1600, 1562, 1501, 1477, 1460, 1430, 1355, 1327, 1316, 1240, 1212, 1163, 1127, 1108, 1071, 960, 896, 848, 829, 772, 747, 671, 595, 564, 516
11	76	ulje	$C_{13}H_{11}N_5$ (237,27)	n.s.	3671, 3451, 3239, 3051, 2937, 2863, 2447, 2325, 2104, 1689, 1631, 1566, 1509, 1452, 1403, 1354, 1264, 1085, 1036, 971, 848, 759, 718, 644, 579, 431
12	61	176,0 – 178,5	$C_{13}H_{13}N_3$ (211,27)	210,0 $[M-1]^-$ 212,2 $[M+1]^+$	3338, 3239, 3130, 3057, 2978, 2940, 2914, 2882, 2850, 2783, 2737, 2690, 2637, 1626, 1606, 1566, 1503, 1453, 1401, 1374, 1344, 1317, 1284, 1250, 1176, 1147, 1103, 1083, 1009, 970, 945, 891, 838, 813, 775, 734, 643, 588, 545

[a] n.s. - nije sniman

Tablica 5. ^{1}H i ^{13}C NMR spektroskopski podaci azida **5**, **11** i amina **6**, **12**

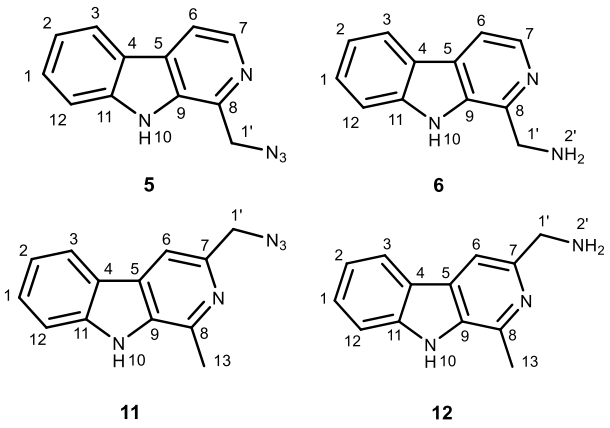

Spoj	^{1}H NMR (DMSO-d_6, δ ppm, J/Hz)	^{13}C NMR (DMSO-d_6, δ ppm)
5	11,78 (s, 1H, 10), 8,36 (d, 1H, 7, J = 5,2 Hz), 8,29 – 8,23 (m, 1H, 3), 8,13 (d, 1H, 6, J = 5,2 Hz), 7,64 (dt, 1H, 12, J = 8,3, 0,9 Hz), 7,60 – 7,57 (m, 1H, 1), 7,29 – 7,26 (m, 1H, 2), 4,89 (s, 2H, 1')	140,58 (8), 139,19 (11), 137,75 (7), 133,86 (9), 128,50 (5), 128,44 (1), 121,87 (3), 120,74 (4), 119,57 (2), 114,77 (6), 112,02 (12), 51,59 (1')
6	8,26 (d, 1H, 7, J = 5,2 Hz), 8,21 (dt, 1H, 3, J = 7,8, 1,0 Hz), 7,97 (d, 1H, 6, J = 5,2 Hz), 7,63 – 7,62 (m, 1H, 12), 7,55 – 7,52 (m, 1H, 1), 7,24 – 7,22 (m, 1H, 2), 4,19 (s, 2H, 1')	146,51 (8), 140,35 (11), 137,18 (7), 133,23 (9), 127,82 (1), 127,42 (5), 121,60 (3), 120,88 (4), 119,15 (2), 113,19 (6), 112,01 (12), 44,59 (1')
11	11,66 (s, 1H, 10), 8,20 (d, 1H, 3, J = 7,9 Hz), 8,00 (s, 1H, 6), 7,62 – 7,60 (m, 1H, 12), 7,57 – 7,53 (m, 1H, 1), 7,26 – 7,23 (m, 1H, 2), 4,57 (s, 2H, 1'), 2,78 (s, 3H, 13)	143,23 (7), 142,12 (11), 140,74 (8), 133,94 (9), 128,02 (1), 127,56 (5), 121,74 (3), 121,01 (4), 119,39 (2), 112,07 (12), 111,72 (6), 55,30 (1'), 20,41 (13)
12	11,42 (s, 1H, 10), 8,14 (d, 1H, 3, J = 7,6 Hz), 7,91 (s, 1H, 6), 7,57 – 7,47 (m, 2H, 12, 1), 7,20 (t, 1H, 2, J = 6,9 Hz), 3,89 (s, 2H, 1'), 2,73 (s, 3H, 13)	151,13 (7), 140,89 (11), 140,74 (8), 133,29 (9), 127,76 (5), 127,62 (1), 121,53 (3), 121,19 (4), 118,98 (2), 111,89 (12), 109,01 (6), 47,59 (1'), 20,38 (13)

Analizom IR spektara harmicina amidnoga tipa **7a-h** i **13a-h** uočeno je nekoliko karakterističnih apsorpcijskih vrpci:

- Oštre vrpce srednjeg do slabog intenziteta N–H istezanja indolskog amina u području valnih brojeva 3300 – 3400 cm^{-1} (**7a**, 3375 cm^{-1}; **7b**, 3350 cm^{-1}; **7e**, 3380 cm^{-1}; **7f**, 3384 cm^{-1}; **7g**, 3350 cm^{-1}; **7h**, 3341cm^{-1}; **13a**, 3352 cm^{-1}; **13d**, 3339 cm^{-1}; **13h**, 3339 cm^{-1}). Vrpce N–H istezanja amida **7c** i **7d** te **13b**,**c**,**e-g** preklopile su se s vrpcama istezanja aromatskih C–H veza te su u IR spektrima vidljive široke vrpce s maksimumima apsorpcije na valnim brojevima 3191 cm^{-1} (**7c**), 3197 cm^{-1} (**7d**), 3242 cm^{-1} (**13b**), 3243 cm^{-1} (**13c**), 3243 cm^{-1} (**13e**), 3239 cm^{-1} (**13f**) i 3249 cm^{-1} (**13g**).

- Oštre vrpce srednjeg intenziteta u području valnih brojeva 1680 – 1640 cm^{-1} koje odgovaraju C=O istezanju karbonilne skupine sekundarnog amida (**7a**, 1661 cm^{-1}; **7b**, 1672 cm^{-1}; **7c**, 1671 cm^{-1}; **7d**, 1669 cm^{-1}; **7e,** 1655 cm^{-1}; **7f**, 1671 cm^{-1}; **7g**, 1662 cm^{-1}; **7h**, 1664 cm^{-1}; **13a**, 1659 cm^{-1}; **13b**, 1658 cm^{-1}; **13c**, 1655 cm^{-1}; **13d**, 1664 cm^{-1}; **13e**, 1655 cm^{-1}; **13f**, 1662 cm^{-1}; **13g**, 1652 cm^{-1}; **13h**, 1666 cm^{-1}).
- Nekoliko oštrih vrpci srednjeg intenziteta u području valnih brojeva 1501 –1630 cm^{-1} koje odgovaraju N–H savijanju indolskog amina te istezanju aromatskih C=C veza.

Masenom spektrometrijom harmicina amidnoga tipa **7a-h** i **13a-h** dobiveni su spektri koji pokazuju signale najvećeg intenziteta protoniranih molekulskih iona $[M+1]^+$ pojedinih harmicina: **7a**, *m/z* 328,1; **7b**, *m/z* 346,1; **7d**, *m/z* 396,1; **7e**, *m/z* 346,1; **7g**, *m/z* 358,1; **7h**, *m/z* 396,1; **13a**, *m/z* 342,4; **13b**, *m/z* 360,3; **13d**, *m/z* 410,1; **13e**, *m/z* 360,1; **13g**, *m/z* 372,3; **13h**, *m/z* 410,1.

Budući da harmicini **7c** i **13c** sadrže u strukturi *m*-Br-supstituiranu cimetnu kiselinu odn. atom broma čiji su izotopi ^{79}Br i ^{81}Br stabilni i prisutni u prirodi u gotovo jednakim omjerima, u MS spektru spojeva **7c** i **13c** vidljiva su dva pika podjednakog intenziteta pri *m/z* 405,9 i 407,9 (**7c**) te pri *m/z* 420,0 i 422,0 (**13c**) koji odgovaraju protoniranim molekulskim ionima $[M+1]^+$. U MS spektrima harmicina **7f** i **13f** koji u svojoj strukturi sadrže *p*-Cl-supstituiranu cimetnu kiselinu prisutna su dva pika protoniranih molekulskih iona pri *m/z* 362,1 i 364,1 (**7f**) koji odgovaraju protoniranim molekulskim ionima $[M+1]^+$ i *m/z* 398,3 i 400,3 (**13f**) koji odgovaraju ionima adukta s natrijem $[M+Na]^+$, a čiji intenziteti signala u približnim omjerima 1:3 odgovaraju izotopnoj raspodjeli izotopa ^{35}Cl i ^{37}Cl.

Analitički i IR spektroskopski podaci harmicina amidnoga tipa **7a-h** i **13a-h** dani su u Tablicama 6 i 7.

Tablica 6. Analitički i IR spektroskopski podaci harmicina amidnoga tipa **7a-h**

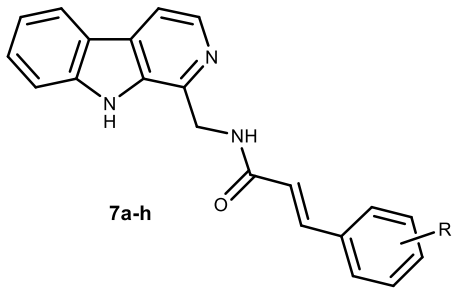

7a-h

Spoj	R	Iskorištenje (%)	t_t (°C)	Molekulska formula (M_r)	MS [*m/z*]	IR (ATR, ν/cm^{-1})
7a	H	52	225,0 – 227,0	$C_{21}H_{17}N_3O$ (327,39)	328,1 $[M+1]^+$	3375, 3328, 3226, 3195, 3101, 3060, 2901, 1661, 1623, 1576, 1514, 1435, 1404, 1325, 1243, 1205, 994, 914, 811, 767, 731, 718, 706, 620, 565, 490, 478
7b	*m*-F	51	224,5 – 225,5	$C_{21}H_{16}FN_3O$ (345,38)	346,1 $[M+1]^+$	3350, 3217, 3149, 3080, 2995, 2905, 2814, 1672, 1627, 1586, 1516, 1448, 1409, 1325, 1273, 1239, 1225, 1146, 1011, 968, 878, 851, 807, 784, 728, 611, 564, 521
7c	*m*-Br	72	236,5 – 239,0	$C_{21}H_{16}BrN_3O$ (406,28)	405,9 $[M+1]^+$ 407,9 $[M+1]^+$	3191, 3016, 1671, 1626, 1564, 1497, 1471, 1437, 1392, 1328, 1222, 1128, 1078, 971, 929, 820, 778, 722, 667, 584
7d	*m*-CF_3	52	225,5 – 226,5	$C_{22}H_{16}F_3N_3O$ (395,39)	396,1 $[M+1]^+$	3197, 3014, 1669, 1628, 1560, 1498, 1438, 1329, 1226, 1177, 1167, 1109, 1077, 972, 885, 804, 742, 721, 691, 581

7e	*p*-F	67	231,5 – 233,0	$C_{21}H_{16}FN_3O$ (345,38)	346,1 $[M+1]^+$	3380, 3244, 3147, 3075, 2989, 2900, 1655, 1616, 1599, 1556, 1505, 1430, 1426, 1413, 1354, 1325, 1239, 1220, 1161, 1128, 1098, 1010, 977, 828, 755, 734, 628, 508
7f	*p*-Cl	52	241,0 – 243,5 (raspad)	$C_{21}H_{16}ClN_3O$ (361,83)	362,1 $[M+1]^+$ 364,1 $[M+1]^+$	3384, 3275, 3053, 1671, 1627, 1532, 1505, 1494, 1457, 1435, 1405, 1323, 1237, 1219, 1094, 1028, 1013, 972, 819, 732, 609, 589, 573, 495
7g	*p*-OCH_3	49	230,5 – 232,0	$C_{22}H_{19}N_3O_2$ (357,41)	358,1 $[M+1]^+$	3350, 3173, 3097, 3006, 1662, 1624, 1603, 1511, 1432, 1366, 1325, 1254, 1240, 1174, 1029, 981, 914, 818, 791, 733, 596, 528, 506
7h	*p*-CF_3	65	262,5 – 265,0 (raspad)	$C_{22}H_{16}F_3N_3O$ (395,39)	396,1 $[M+1]^+$	3341, 3236, 1664, 1622, 1504, 1436, 1416, 1323, 1239, 1217, 1155, 1116, 1068, 1013, 988, 826, 755, 740, 572, 532, 494

Tablica 7. Analitički i IR spektroskopski podaci harmicina amidnoga tipa **13a-h**

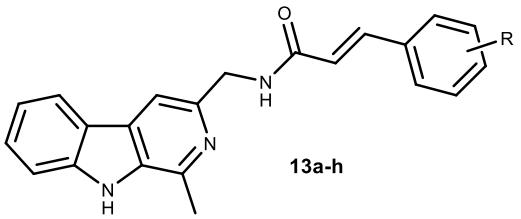

Spoj	R	Iskorištenje (%)	t_t (°C)	Molekulska formula (M_r)	MS [*m*/*z*]	IR (ATR, ν/cm^{-1})
13a	H	64	207,0 – 208,0	$C_{22}H_{19}N_3O$ (341,41)	342,4 $[M+1]^+$	3352, 3284, 3089, 3048, 2896, 2851, 1659, 1621, 1568, 1510, 1451, 1388, 1354, 1319, 1284, 1246, 1206, 1176, 1075, 1015, 973, 899, 871, 741, 714, 643, 612, 587, 557, 487
13b	*m*-F	41	118,0 – 119,0	$C_{22}H_{18}FN_3O$ (359,40)	360,3 $[M+1]^+$	3242, 3080, 2972, 2907, 2783, 1658, 1620, 1571, 1501, 1451, 1420, 1341, 1247, 1144, 1032, 983, 899, 859, 779, 740, 632, 561, 517
13c	*m*-Br	28	121,5 – 123,5	$C_{22}H_{18}BrN_3O$ (420,31)	420,0 $[M+1]^+$ 422,0 $[M+1]^+$	3243, 3082, 1743, 1725, 1655, 1617, 1562, 1501, 1452, 1419, 1470, 1396, 1340, 1248, 1234, 1150, 1069, 1029, 984, 899, 863, 779, 741, 697, 666, 638, 609, 561
13d	*m*-CF_3	39	235,5 – 237,0	$C_{23}H_{18}F_3N_3O$ (409,41)	410,1 $[M+1]^+$	3339, 3251, 3084, 2992, 2950, 2893, 2855, 2786, 1664, 1622, 1570, 1517, 1470, 1451, 1396, 1331, 1284, 1249, 1229, 1165, 1122, 1095, 1072, 1020, 969, 937, 899, 864, 803, 777, 738, 695, 657, 596, 559, 524, 507

13e	*p*-F	34	217,5 – 219,5	$C_{22}H_{18}FN_3O$ (359,40)	360,1 $[M+1]^+$	3243, 3077, 2993, 2950, 2913, 2890, 2851, 2785, 1655, 1620, 1597, 1571, 1553, 1507, 1451, 1416, 1394, 1341, 1318, 1282, 1249, 1226, 1156, 1124, 1094, 1033, 1011, 984, 933, 899, 859, 830, 788, 739, 693, 643, 608, 591, 565, 506, 462
13f	*p*-Cl	21	255,0 – 257,5	$C_{22}H_{18}ClN_3O$ (375,86)	398,3 $[M+Na]^+$ 400,3 $[M+Na]^+$	3649, 3239, 3055, 2918, 2874, 2798, 1982, 1925, 1897, 1662, 1624, 1551, 1502, 1454, 1404, 1318, 1283, 1251, 1220, 1176, 1088, 1044, 1011, 976, 902, 867, 815, 735, 646, 590, 550, 497
13g	*p*-OCH_3	51	263,0 – 264,0	$C_{23}H_{21}N_3O_2$ (371,44)	372,3 $[M+1]^+$	3249, 3162, 3079, 2964, 2910, 2835, 2787, 2684, 1652, 1603, 1555, 1512, 1454, 1419, 1345, 1287, 1251, 1175, 1109, 1026, 987, 932, 900, 873, 827, 778, 744, 592, 549, 520
13h	*p*-CF_3	43	264,5 – 266,5	$C_{23}H_{18}F_3N_3O$ (409,41)	410,1 $[M+1]^+$	3339, 3263, 3058, 2920, 1666, 1626, 1575, 1496, 1452, 1413, 1324, 1248, 1164, 1120, 1065, 1012, 972, 900, 858, 822, 778, 737, 702, 586, 522, 491

Kemijski pomaci protona u ^{1}H, odnosno ugljika u ^{13}C NMR spektrima te multipletnosti odgovarajućih signala harmicina amidnoga tipa **7a-h** i **13a-h** u skladu su s predloženim strukturama.

- U ^{1}H spektrima se signal za indolski proton (H-10) vidi kao singlet u području kemijskih pomaka 11,52 – 11,65 ppm (**7a**, 11,62 ppm; **7b**, 11,63 ppm; **7c**, 11,62 ppm; **7d**, 11,65 ppm; **7e**, 11,62 ppm; **7f**, 11,62 ppm; **7g**, 11,59 ppm; **7h**, 11,65 ppm; **13a**, 11,54 ppm; **13b**, 11,52 ppm; **13c**, 11,54 ppm; **13d**, 11,53 ppm; **13e**, 11,52 ppm; **13f**, 11,53 ppm; **13g**, 11,54 ppm; **13h**, 11,54 ppm).
- Signal za proton amidne veze H-2' u svim ^{1}H spektrima je zbog sprezanja sa susjednim H-1' protonima vidljiv kao triplet u rasponu kemijskih pomaka 8,59 – 8,87 ppm s

konstantama sprege J = 5,1 Hz (**13e**), J = 5,3 Hz (**7d**), J = 5,4 Hz (**7a-c**,**e**,**f**,**h**), J = 5,5 Hz (**7g**, **13b**), J = 5,6 Hz (**13g**), J = 5,7 Hz (**13a**), J = 5,8 Hz (**13c**,**d**,**f**,**h**).

- Budući da su cimetna kiselina i DCK-i korišteni kao *trans* izomeri izračunate su konstante sprege protona *trans* veze H-4' i H-5' i u skladu su s teorijskim podacima, a iznose J = 15,8 Hz, odn. 15,7 Hz za spoj **7g** i **13b** te 15,9 Hz za spoj **13d**.
- Protoni metilne skupine H-13 vidljivi su u svim ^{1}H spektrima harmicina **13a-h** kao singlet na kemijskom pomaku od 2,78 ppm (**13a**, **13c**,**d**, **13g**) odn. 2,77 ppm (**13b**,**e**,**f**,**h**) s relativnim integralom od 3H.
- ^{13}C spektri snimani su APT (engl. *attached proton test*) tehnikom te su svi signali za ugljikove atome za koje je izravno vezan paran broj vodikovih atoma (C-H_2), signali kvaternih ugljikovih atoma i signali ugljikovih atoma karbonilne skupine vidljivi na istoj strani, dok su signali za ugljikove atome za koje je izravno vezan neparan broj vodika (C-H, C-H_3) vidljivi na suprotnoj strani.
- Signal za karbonilni ugljikov atom amidne veze C-3' je u ^{13}C spektrima vidljiv u rasponu kemijskih pomaka od 164 – 165 ppm (**7a**, 165,43 ppm; **7b**, 165,08 ppm; **7c**, 165,01 ppm; **7d**, 164,96 ppm; **7e**, 165,31 ppm; **7f**, 165,20 ppm; **7g**, 165,82 ppm; **7h**, 164,89 ppm **13a**, 164,89 ppm; **13b**, 164,59 ppm; **13c**, 164,53 ppm; **13d**, 164,49 ppm; **13e**, 164,81 ppm; **13f**, 164,67 ppm; **13g**, 165,20 ppm; **13h**, 164,43 ppm).
- Signal za ugljikov atom metilne skupine C-13 je u svim ^{13}C spektrima harmicina **13a-h** vidljiv na kemijskom pomaku od 20 ppm (**13a**, 20,26 ppm; **13b**, 20,34 ppm; **13c**, 20,32 ppm; **13d**, 20,34 ppm; **13e**, 20,33 ppm; **13f**, 20,33 ppm; **13g**, 20,33 ppm; **13h**, 20,34 ppm).
- Zbog 100 %-tne prirodne zastupljenosti izotopa ^{19}F u ^{13}C spektrima jasno se vide sprezanja signala ugljikovih atoma s fluorom te se tako u spektrima amida **7b**, **13b**, **7e** i **13e**, koji u svojoj strukturi sadrže atom fluora, signali ugljikovih atoma koji se sprežu s fluorom vide kao dubleti dok se u spektrima spojeva **7d**, **13d**, **7h** i **13h**, koji u svojoj strukturi sadrže CF_3 skupinu, vide kao kvarteti.
- Signali za ugljikove atome spojeva **7b**, **13b**, **7e** i **13e** za koje je izravno vezan atom flora C-8' (**7b**, **13b**) i C-9' (**7e**, **13e**) nalaze se na kemijskim pomacima 162,5 ppm s pripadajućim konstantama sprege od 244 Hz (**7b**, **13b**), odn. na 162,7 ppm (**7e**, **13e**) s konstantama sprege od 247 Hz, dok se signali za ugljikove atome za koje su izravno vezani atomi fluora u spektrima spojeva **7d**, **13d**, **7h** i **13h** (C-12') nalaze na nižim kemijskim pomacima od 124 ppm, ali su sprezanja jača (**7d**, J = 273,3 Hz; **13d**, J = 272,8 Hz; **7h**, J = 272,7 Hz; **13h**, J = 272,0 Hz).

- U ^{13}C spektrima spojeva **7b**, **13b**, **7e** i **13e** uočena su C-F sprezanja kroz dvije kovalentne veze, a vidljiva su na kemijskim pomacima od 116 ppm (C-9') i 114 ppm (C-7') u spektrima spojeva **7b** i **13b** te na 115,9 ppm (C-8', C-10') u spektrima spojeva **7e** i **13e**, s konstantama sprege od 21 Hz.
- C-F sprezanja kroz dvije kovalentne veze u spektrima spojeva **7d** i **13d** i vidljiva su na kemijskom pomaku od 129,7 ppm (C-8') s pripadajućim konstantama sprege J = 31,7 Hz te na 129,2 ppm (C-9') s konstantom sprezanja J = 32 Hz u spektrima spojeva **7h** i **13h**.
- Sprezanja signala ugljikovih atoma s fluorom u ^{13}C spektrima vidljiva su kroz tri kovalentne veze, pa se tako u spektru spoja **7b** i **13b** signal za C-6' atom nalazi na kemijskom pomaku od 137,6 ppm, a izračunata konstanta sprezanja iznosi 7,8 Hz (**7b**), odn. 7,9 Hz (**13b**), dok se signal za C-10' atom nalazi na 130,9 ppm s pripadajućom konstantom sprezanja od 8,4 Hz (**7b**) odn. 8,3 Hz (**13b**). U spektrima spojeva **7e** i **13e** su sprezanja kroz tri kovalentne veze vidljiva na kemijskom pomaku od 129,7 ppm s pripadajućom konstantom sprezanja od 8,4 Hz, a odgovaraju ekvivalentnim C-7' i C-11' atomima.
- Sprezanja C atoma s atomima fluora CF_3 skupine kroz tri kovalentne veze vidljiva su u spektrima spojeva **7d** i **13d** na kemijskim pomacima 125,7 ppm (C-9') čije konstante sprega iznose 2,7 Hz (**7d**) odn. 3,5 Hz (**13d**) i 123,9 ppm (C-7') s konstantama sprezanja od 3,6 Hz (**7d**) i 3,5 Hz (**13d**), dok su atomi C-8' i C-10' spojeva **7h** i **13h** ekvivalenti i nalaze se na kemijskom pomaku od 125,8 ppm, a s atomima fluora CF_3 skupine sprežu se s konstantom sprezanja od 3,0 Hz (**7h**) i 3,9 Hz (**13h**).
- Sprege dalekog dosega, kroz četiri kovalentne veze, uočene su u spektru spoja **7b** pri čemu se signal za atom C-5' nalazi na 137,71 ppm, a izračunata konstanta sprege iznosi $^4J_{CF}$ = 2,4 Hz, dok se signal za atom C-11' nalazi na kemijskom pomaku 123,75 ppm s konstantom sprezanja $^4J_{CF}$ = 2,5 Hz. U ^{13}C spektrima spojeva **7e** i **13e** sprezanja C-6' atoma kroz četiri kovalentne veze vidljiva su na kemijskom pomaku od 131,6 ppm, a izračunata konstanta sprezanja iznosi 3,0 Hz (**7e**) odn. 3,2 Hz (**13e**). Također je, u odnosu na spektar spoja **7b**, uočeno sprezanje C-5' atoma s fluorom kroz pet kovalentnih veza, s pripadajućom konstantom sprezanja $^5J_{CF}$ = 1,7 Hz.

^{1}H i ^{13}C spektroskopski podaci harmicina **7a-h** i **13a-h** nalaze se u Tablicama 8 i 9.

Tablica 8. ^{1}H i ^{13}C NMR spektroskopski podaci harmicina amidnoga tipa **7a-h**

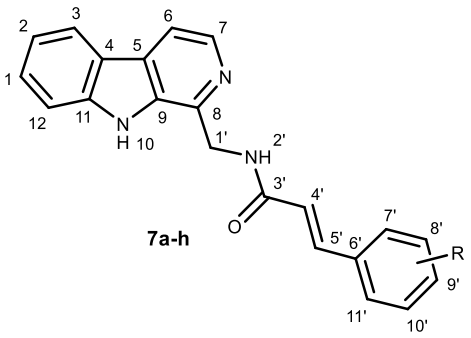

Spoj	R	^{1}H NMR (DMSO-d_6, δ ppm, J/Hz)	^{13}C NMR (DMSO-d_6, δ ppm)
7a	H	11,62 (s, 1H, 10), 8,78 (t, 1H, 2', J = 5,4 Hz), 8,32 (d, 1H, 7, J = 5,2 Hz), 8,24 (d, 1H, 3, J = 7,9 Hz), 8,06 (d, 1H, 6, J = 5,3 Hz), 7,65 – 7,63 (m, 1H, 12), 7,60 – 7,49 (m, 4H, 1, 5', 7', 11'), 7,45 – 7,34 (m, 3H, 8' – 10'), 7,28 – 7,23 (m, 1H, 2), 6,87 (d, 1H, 4', J = 15,8 Hz), 4,91 (d, 2H, 1', J = 5,3 Hz)	165,43 (3'), 141,41 (8), 140,45 (11), 139,04 (5'), 137,34 (7), 134,92 (9), 133,52 (6'), 129,49 (3), 128,94 (7', 11'), 128,17 (9'), 127,82 (5), 127,58 (8', 10'), 122,10 (1), 121,76 (4'), 120,87 (4), 119,45 (2), 113,96 (6), 112,08 (12), 41,65 (1')
7b	*m*-F	11,63 (s, 1H, 10), 8,78 (t, 1H, 2', J = 5,4 Hz), 8,32 (d, 1H, 7, J = 5,2 Hz), 8,24 (d, 1H, 3, J = 7,8 Hz), 8,07 (d, 1H, 6, J = 5,2 Hz), 7,64 (d, 1H, 12, J = 8,2 Hz), 7,57 (t, 1H, 2, J = 7,6 Hz), 7,52 (d, 1H, 5', J = 15,8 Hz), 7,49 – 7,43 (m, 3H, 1, 10', 11'), 7,26 (t, 1H, 7', J = 7,4 Hz), 7,23 – 7,20 (m, 1H, 9'), 6,94 (d, 1H, 4', J = 15,8 Hz), 4,92 (d, 2H, 1', J = 5,3 Hz)	165,08 (3'), 162,46 (d, 8', J = 244,0 Hz), 141,26 (8), 140,45 (11), 137,71 (d, 5', J = 2,4 Hz), 137,58 (d, 6', J = 7,8 Hz), 137,37 (7), 133,48 (9), 130,90 (d, 10', J = 8,4 Hz), 128,16 (3), 127,80 (5), 123,75 (d, 11', J = 2,5 Hz), 123,70 (1), 121,76 (4'), 120,87 (4), 119,44 (2), 116,14 (d, 9', J = 21,2 Hz), 113,96 (6), 113,96 (d, 7', J = 21,8 Hz), 112,07 (12), 41,65 (1')
7c	*m*-Br	11,62 (s, 1H, 10), 8,74 (t, 1H, 2', J = 5,4 Hz), 8,31 (d, 1H, 7, J = 5,2 Hz), 8,23 (d, 1H, 3, J = 7,8 Hz), 8,06 (d, 1H, 6, J = 5,2 Hz), 7,80 (t, 1H, 7', J = 1,9 Hz), 7,63 (d, 1H, 12, J = 8,2 Hz), 7,59 (d, 1H, 11', J = 7,8 Hz), 7,57 – 7,54 (m, 2H, 1, 2), 7,47 (d, 1H, 5', J = 15,8 Hz), 7,37 (t, 1H, 10', J = 7,9 Hz), 7,25 (t, 1H, 9', J = 7,4 Hz), 6,94 (d, 1H, 4', J = 15,8 Hz), 4,91 (d, 2H, 1', J = 5,3 Hz)	165,01 (3'), 141,20 (8), 140,46 (11), 137,53 (6'), 137,34 (5'), 137,30 (7), 133,46 (9), 131,98 (7'), 131,02 (9'), 130,06 (10'), 128,17 (3), 127,82 (5), 126,49 (11'), 123,82 (1), 122,26 (8'), 121,76 (4'), 120,85 (4), 119,44 (2), 113,96 (6), 112,06 (12), 41,62 (1')
7d	12' *m*-CF_3	11,65 (s, 1H, 10), 8,78 (t, 1H, 2', J = 5,3 Hz), 8,33 (d, 1H, 7, J = 5,2 Hz), 8,24 (dt, 1H, 3, J = 7,9, 1,0 Hz), 8,07 (d, 1H, 6, J = 5,2 Hz), 7,96 (t, 1H, 7', J = 2,0 Hz), 7,90 (d, 1H, 12, J = 7,8 Hz), 7,73 (d, 1H, 11', J = 7,8 Hz), 7,67 – 7,63 (m, 2H, 1, 9'), 7,60 (d, 1H, 5', J = 15,8 Hz), 7,58 – 7,55 (m, 1H, 2), 7,28 – 7,25 (m, 1H, 10'), 7,06 (d, 1H, 4', J = 15,9 Hz), 4,93 (d, 2H, 1', J = 5,3 Hz)	164,96 (3'), 141,19 (8), 140,47 (11), 137,35 (5'), 137,26 (7), 136,19 (6'), 133,47 (9), 131,37 (11'), 130,05 (10'), 129,74 (q, 8', J = 31,7 Hz), 128,15 (3), 127,80 (5), 125,72 (q, 9', J = 2,7 Hz), 124,33 (1), 124,06 (q, 12', J = 273,3 Hz), 123,92 (q, 7', J = 3,6 Hz), 121,75 (4'), 120,87 (4), 119,44 (2), 113,96 (6), 112,07 (12), 41,67 (1')

7e	*p*-F	11,62 (s, 1H, 10), 8,75 (t, 1H, 2', *J* = 5,4 Hz), 8,32 (d, 1H, 7, *J* = 5,2 Hz), 8,24 (d, 1H, 3, *J* = 7,8 Hz), 8,06 (d, 1H, 6, *J* = 5,2 Hz), 7,66 – 7,63 (m, 3H, 12, 7', 11'), 7,56 (t, 1H, 1, *J* = 7,6 Hz), 7,51 (d, 1H, 5', *J* = 15,8 Hz), 7,27 – 7,24 (m, 3H, 2, 8', 10'), 6,83 (d, 1H, 4', *J* = 15,8 Hz), 4,91 (d, 2H, 1', *J* = 5,3 Hz)	165,31 (3'), 162,69 (d, 9', *J* = 247,0 Hz), 141,39 (8), 140,42 (11), 137,80 (4'), 137,35 (7), 133,49 (9), 131,56 (d, 6', *J* = 3,0 Hz), 129,71 (d, 7', 11', *J* = 8,4 Hz), 128,12 (3), 127,77 (5), 122,00 (d, 5', *J* = 1,7 Hz), 121,73 (1), 120,86 (4), 119,41 (2), 115,89 (d, 8', 10', *J* = 21,8 Hz), 113,92 (6), 112,05 (12), 41,64 (1')
7f	*p*-Cl	11,62 (s, 1H, 10), 8,79 (t, 1H, 2', *J* = 5,4 Hz), 8,32 (d, 1H, 7, *J* = 5,2 Hz), 8,24 (d, 1H, 3, *J* = 7,8 Hz), 8,06 (d, 1H, 6, *J* = 5,2 Hz), 7,65 – 7,61 (m, 3H, 12, 7', 11'), 7,58 – 7,55 (m, 1H, 1), 7,52 – 7,48 (m, 3H, 5', 8', 10'), 7,26 (t, 1H, 2, *J* = 7,4 Hz), 6,89 (d, 1H, 4', *J* = 15,8 Hz), 4,91 (d, 2H, 1', *J* = 5,4 Hz)	165,20 (3'), 141,35 (8), 140,45 (11), 137,67 (5'), 137,38 (7), 133,92 (9', 9), 133,51 (6'), 129,29 (7', 11'), 128,99 (8', 10'), 128,16 (3), 127,80 (5), 122,93 (1), 121,77 (4'), 120,88 (4), 119,45 (2), 113,96 (6), 112,08 (12), 41,66 (1').
7g	$^{12'}$ *p*-OCH_3	11,59 (s, 1H, 10), 8,68 (t, 1H, 2', *J* = 5,5 Hz), 8,31 (d, 1H, 7, *J* = 5,3 Hz), 8,23 (d, 1H, 3, *J* = 7,8 Hz), 8,06 (d, 1H, 6, *J* = 4,7 Hz), 7,64 (d, 1H, 12, *J* = 8,2 Hz), 7,57 – 7,52 (m, 3H, 1, 7', 11'), 7,46 (d, 1H, 5', *J* = 15,7 Hz), 7,25 (t, 1H, 2, *J* = 7,5 Hz), 6,97 (d, 2H, 8', 10', *J* = 8,2 Hz), 6,71 (d, 1H, 4', *J* = 15,7 Hz), 4,89 (d, 2H, 1', *J* = 5,5 Hz), 3,78 (s, 3H, 12')	165,82 (3'), 160,39 (9'), 141,57 (8), 140,46 (11), 138,83 (5'), 137,34 (7), 133,54 (9), 129,20 (7', 11'), 128,20 (3), 127,85 (6'), 127,49 (5), 121,78 (1), 120,90 (4), 119,57 (4'), 119,48 (2), 114,42 (8', 10'), 113,98 (6), 112,10 (12), 55,28 (12'), 41,67 (1')
7h	$^{12'}$ *p*-CF_3	11,65 (s, 1H, 10), 8,87 (t, 1H, 2', *J* = 5,4 Hz), 8,33 (d, 1H, 7, *J* = 5,3 Hz), 8,25 (d, 1H, 3, *J* = 7,9 Hz), 8,08 (d, 1H, 6, *J* = 5,3 Hz), 7,83 – 7,76 (m, 4H, 1, 12, 7', 11'), 7,66 – 7,54 (m, 3H, 5', 8', 10'), 7,29 – 7,24 (m, 1H, 2), 7,03 (d, 1H, 4', *J* = 15,8 Hz), 4,94 (d, 2H, 1', *J* = 5,3 Hz)	164,89 (3'), 141,23 (8), 140,46 (11), 139,04 (6'), 137,38 (5'), 137,32 (7), 133,49 (9), 129,21 (q, 9', *J* = 32,3 Hz), 128,20 (7', 11'), 128,16 (1), 127,81 (5), 125,81 (q, 8', 10', *J* = 3,0 Hz), 124,95 (3), 124,12 (q, 12', *J* = 272,7 Hz), 121,76 (2), 120,87 (4), 119,44 (4'), 113,96 (6), 112,07 (12), 41,66 (1')

Tablica 9. ^{1}H i ^{13}C NMR spektroskopski podaci harmicina amidnoga tipa **13a-h**

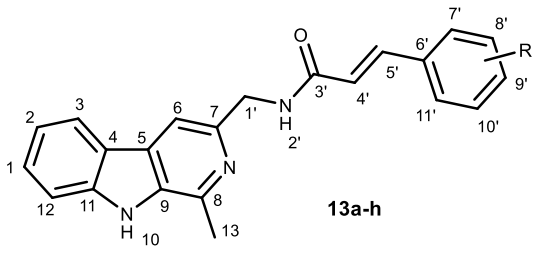

Spoj	R	^{1}H NMR (DMSO-d_6, δ ppm, J/Hz)	^{13}C NMR (DMSO-d_6, δ ppm)
13a	H	11,54 (s, 1H, 10), 8,69 (t, 1H, 2', J = 5,7 Hz), 8,19 (d, 1H, 3, J = 7,8 Hz), 7,88 (s, 1H, 6), 7,60 – 7,58 (m, 3H, 7', 11', 12), 7,53 – 7,49 (m, 2H, 1, 5'), 7,44 – 7,41 (m, 2H, 8', 10'), 7,39 – 7,37 (m, 1H, 9'), 7,21 (t, 1H, 2, J = 7,4 Hz), 6,81 (d, 1H, 4', J = 15,8 Hz), 4,62 (d, 2H, 1', J = 5,8 Hz), 2,78 (s, 3H, 13)	164,89 (3'), 146,07 (7), 141,27 (11), 140,79 (8), 138,77 (5'), 134,98 (6'), 133,55 (9), 129,41 (9'), 128,92 (8', 10'), 127,86 (1), 127,79 (5), 127,52 (7', 11'), 122,38 (3), 121,70 (4'), 120,99 (4), 119,17 (2), 111,93 (12), 110,08 (6), 44,64 (1'), 20,26 (13)
13b	*m*-F	11,52 (s, 1H, 10), 8,69 (t, 1H, 2', J = 5,5 Hz), 8,18 (d, 1H, 3, J = 7,4 Hz), 7,87 (s, 1H, 6), 7,59 – 7,42 (m, 6H, 1, 2, 12, 5', 10', 11'), 7,24 – 7,19 (m, 2H, 7', 9'), 6,85 (d, 1H, 4', J = 15,7 Hz), 4,61 (d, 2H, 1', J = 4,3 Hz), 2,77 (s, 3H, 13)	164,59 (3'), 162,46 (d, 8', J = 243,9 Hz), 146,03 (7), 141,35 (11), 140,75 (8), 137,63 (d, 6', J = 7,9 Hz), 137,47 (5'), 133,57 (9), 130,89 (d, 10', J = 8,3 Hz), 127,83 (11'), 127,73 (5), 123,97 (1), 123,67 (3), 121,68 (4'), 121,00 (4), 119,15 (2), 116,07 (d, 9', J = 21,4 Hz), 113,92 (d, 7', J = 21,8 Hz), 111,94 (12), 110,07 (6), 44,73 (1'), 20,34 (13)
13c	*m*-Br	11,54 (s, 1H, 10), 8,68 (t, 1H, 2', J = 5,8 Hz), 8,18 (d, 1H, 3, J = 7,9 Hz), 7,87 (s, 1H, 6), 7,80 (t, 1H, 7', J = 1,8 Hz), 7,61 – 7,56 (m, 3H, 12, 9', 11'), 7,52 (t, 1H, 1, J = 7,4 Hz), 7,47 (d, 1H, 5', J = 15,8 Hz), 7,39 (t, 1H, 10', J = 7,9 Hz), 7,21 (t, 1H, 2, J = 7,4 Hz), 6,87 (d, 1H, 4', J = 15,8 Hz), 4,62 (d, 2H, 1', J = 5,8 Hz), 2,78 (s, 3H, 13)	164,53 (3'), 145,98 (7), 141,34 (11), 140,77 (8), 137,60 (6'), 137,13 (5'), 133,57 (9), 131,94 (7'), 131,04 (9'), 130,04 (10'), 127,86 (11'), 127,76 (5), 126,43 (1), 124,08 (3), 122,26 (8'), 121,70 (4'), 121,00 (4), 119,17 (2), 111,95 (12), 110,08 (6), 44,70 (1'), 20,32 (13)
13d	$^{12'}$ *m*-CF_3	11,53 (s, 1H, 10), 8,70 (t, 1H, 2', J = 5,8 Hz), 8,18 (d, 1H, 3, J = 7,9 Hz), 7,95 (t, 1H, 7', J = 2,0 Hz), 7,90 (d, 1H, 12, J = 7,8 Hz), 7,88 (s, 1H, 6), 7,74 (d, 1H, 11', J = 7,8 Hz), 7,67 (t, 1H, 2, J = 7,8 Hz), 7,61 – 7,58 (m, 2H, 5', 1), 7,54 – 7,51 (m, 1H, 9'), 7,22 – 7,20 (m, 1H, 10'), 6,96 (d, 1H, 4', J = 15,9 Hz), 4,63 (d, 2H, 1', J = 5,8 Hz), 2,78 (s, 3H, 13)	164,49 (3'), 145,97 (7), 141,37 (11), 140,77 (8), 137,06 (5'), 136,23 (6'), 133,58 (9), 131,31 (11'), 130,07 (10'), 129,73 (d, 8', J = 31,7 Hz), 127,85 (1) 127,75 (5), 125,69 (q, 9', J = 3,5 Hz), 124,06 (q, 12', J = 272,8 Hz), 124,56 (3), 123,88 (q, 7', J = 3,5 Hz), 121,69 (4'), 121,01 (4), 119,16 (2), 111,95 (12), 110,07 (6), 44,74 (1'), 20,34 (13)
13e	*p*-F	11,52 (s, 1H, 10), 8,67 (t, 1H, 2', J = 5,1 Hz), 8,18 (d, 1H, 3, J = 7,8 Hz), 7,87 (s, 1H, 6), 7,67 – 7,63 (m, 2H, 7', 11'), 7,59	164,81 (3'), 162,66 (d, 9', J = 246,9 Hz), 146,14 (7), 141,32 (11), 140,75 (8), 137,57 (5'), 133,56 (9), 131,62 (d, 6', J

		– 7,48 (m, 3H, 1, 5', 12), 7,26 (t, 2H, 8', 10', *J* = 8,7 Hz), 7,20 (t, 1H, 2, *J* = 7,4 Hz), 6,75 (d, 1H, 4', *J* = 15,8 Hz), 4,61 (d, 2H, 1', *J* = 5,5 Hz), 2,77 (s, 3H, 13)	= 3,2 Hz), 129,66 (d, 7', 11', *J* = 8,4 Hz), 127,82 (1), 127,72 (5), 122,28 (3), 121,68 (4'), 121,00 (4), 119,14 (2), 115,90 (d, 8', 10', *J* = 21,7 Hz), 111,93 (12), 110,04 (6), 44,70 (1'), 20,33 (13)
13f	*p*-Cl	11,53 (s, 1H, 10), 8,70 (t, 1H, 2', *J* = 5,8 Hz), 8,18 (d, 1H, 3, *J* = 7,9 Hz), 7,87 (s, 1H, 6), 7,63 – 7,56 (m, 3H, 1, 12, 5'), 7,54 – 7,46 (m, 4H, 7', 8', 10', 11'), 7,23 – 7,18 (m, 1H, 2), 6,81 (d, 1H, 4', *J* = 15,8 Hz), 4,61 (d, 2H, 1', *J* = 5,7 Hz), 2,77 (s, 3H, 13)	164,67 (3'), 146,08 (7), 141,33 (11), 140,75 (8), 137,41 (5'), 133,96 (9), 133,82 (9'), 133,56 (6'), 129,22 (8', 10'), 128,97 (7', 11'), 127,82 (1), 127,72 (5), 123,19 (3), 121,68 (4'), 121,00 (4), 119,14 (2), 111,93 (12), 110,06 (6), 44,72 (1'), 20,33 (13)
13g	$\overset{12'}{p\text{-}OCH_3}$	11,54 (s, 1H, 10), 8,59 (t, 1H, 2', *J* = 5,6 Hz), 8,18 (d, 1H, 3, *J* = 7,9 Hz), 7,87 (s, 1H, 6), 7,59 – 7,50 (m, 4H, 1, 12, 8', 10'), 7,45 (d, 1H, 5', *J* = 15,8 Hz), 7,20 (t, 1H, 2, *J* = 7,5 Hz), 6,98 (d, 2H, 7', 11', *J* = 8,2 Hz), 6,66 (d, 1H, 4', *J* = 15,8 Hz), 4,61 (d, 2H, 1', *J* = 5,9 Hz), 3,79 (s, 3H, 12'), 2,78 (s, 3H, 13)	165,20 (3'), 160,29 (9'), 146,31 (7), 141,29 (11), 140,75 (8), 138,47 (5'), 133,54 (9), 129,09 (8', 10'), 127,81 (1), 127,73 (5), 127,55 (6'), 121,68 (4'), 121,01 (4), 119,89 (2), 119,14 (3), 114,38 (7', 11'), 111,93 (12), 109,98 (6), 55,25 (12'), 44,66 (1'), 20,33 (13)
13h	$\overset{12'}{p\text{-}CF_3}$	11,54 (s, 1H, 10), 8,79 (t, 1H, 2', *J* = 5,8 Hz), 8,18 (d, 1H, 3, *J* = 7,9 Hz), 7,88 (s, 1H, 6), 7,82 – 7,76 (m, 4H, 12, 1, 7', 11'), 7,59 – 7,49 (m, 3H, 5', 8', 10'), 7,23 – 7,18 (m, 1H, 2), 6,94 (d, 1H, 4', *J* = 15,8 Hz), 4,63 (d, 2H, 1', *J* = 5,7 Hz), 2,77 (s, 3H, 13)	164,43 (3'), 145,97 (7), 141,38 (11), 140,77 (8), 139,09 (6'), 137,12 (5'), 133,59 (9), 129,17 (q, 9', *J* = 31,8 Hz), 128,16 (7', 11'), 127,84 (1), 127,74 (5), 125,81 (q, 8', 10', *J* = 3,9 Hz), 125,20 (3), 124,13 (q, 12', *J* = 272,0 Hz), 121,70 (4'), 121,01 (4), 119,16 (2), 111,95 (12), 110,14 (6), 44,78 (1'), 20,34 (13)

4.1.1.4. Sinteza harmicina amidnoga tipa u položaju O-6 β-karbolina

Sinteza harmicina amidnoga tipa **19a-h** u položaju C-6 β-karbolina započinje Pictet-Spenglerovom kondenzacijom. Kao početni spoj odabran je 5-metoksitriptamin čime se uvodi metoksi skupina u strukturu β-karbolina i omogućava daljnja derivatizacija O-6 položaja β-karbolina. Kako bi se smanjile neželjene sporedne reakcije i izbjeglo korištenje acetaldehida u velikom suvišku, za uvođenje metilne skupine u položaj C-1 β-karbolina, analogno sintezi harmicina amidnoga tipa **13a-h**, korišten je zaštićeni aldehid (acetaldehid-dimetil acetal). Reakcija je provedena pod utjecajem mikrovalova u polarnom aprotičnom otapalu acetonitrilu u prisustvu TFA koja služi kao kiseli katalizator. Prednosti ove reakcije su kratko reakcijsko vrijeme od samo 10 minuta te taloženje trifluoracetatne soli spoja **14** dodatkom dietil-etera, što omogućava jednostavnu izolaciju novosintetiziranog THβC **14** filtracijom, bez potrebe za podešavanjem pH reakcijske smjese i provođenjem ekstrakcije.

Upotrebom 10 %-tnog Pd/C novosintetizirani THβC **14** je oksidiran u β-karbolin **15**, a reakcija je provedena u EtOH pod utjecajem mikrovalova. Budući da je THβC **14**, zbog suviška TFA korištene u prvom reakcijskom koraku (2 ekvivalenta), izoliran u obliku trifluoracetatne soli, reakcija oksidacije provedena je u prisutnosti baze. Dodatkom 2 ekvivalenta Li_2CO_3 u reakciji oksidacije omogućeno je *in situ* prevođenje THβC **14** iz oblika soli u neionizirani oblik amina. Dobiveni β-karbolin **15** pročišćen je filtracijom reakcijske smjese kroz sloj celita čime je uklonjen katalizator (Pd/C), dok je višak Li_2CO_3 uklonjen rastrljavanjem sirovog produkta **15** u 20 %-tnoj otopini NaCl-a. Rastrljavanjem u dietil-eteru dodatno je pročišćen te izoliran u visokom iskorištenju od 88 %.

U sljedećem reakcijskom koraku kiselom hidrolizom u prisutnosti bromovodične i koncentrirane octene kiseline β-karbolin **15** preveden je u fenol **16**, a reakcija je provedena pod utjecajem mikrovalova pri povišenoj temperaturi od 140 °C. Suvišak kiseline neutraliziran je dodatkom 5 %-tne otopine NaOH do pH područja u kojem se novosintetizirani fenol **16** nalazi u neioniziranom obliku (pH 8). Upravo je u tom pH području topljivost fenola **16** u vodi izuzetno niska stoga je lako preveden u etil-acetatni sloj ekstrakcijom, a zatim pročišćen kromatografijom na koloni.

Daljnjim alikliranjem novosintetiziranog fenola **16** 2-(*tert*-butoksikarbonilamino)etil bromidom dobiven je eter **17**. Budući da je u strukturi fenola **16** prisutna i sekundarna amino skupina u položaju 9 β-karbolina potrebno je bilo, uz odabir odgovarajućih reagensa, optimirati reakcijske uvjete kako bi se postiglo selektivno O-alkiliranje. Stoga je u tu svrhu odabrana baza bila cezijev karbonat. Naime, brojne su prednosti cezijevog karbonata u odnosu na druge, često korištene baze u reakcijama alkiliranja (177). Veliki radijus Cs^+ kationa omogućava bolju solvataciju u raznim otapalima pa je tako na sobnoj temperaturi topljivost cezijevog karbonata u DMF-u znatno veća u odnosu na topljivost kalijevog karbonata. Također, smatra se srednje jakom bazom, što ga čini pogodnim za selektivno deprotoniranje u reakcijama alkiliranja jer mu je bazični karakter znatno slabiji od hidroksida ili alkoksida, a jači od ostalih karbonata. Kao otapalo u reakciji alkiliranja odabran je DMF – aprotično polarno otapalo koje je uz aceton, DMSO i THF najpogodnije za provođenje S_N2 reakcija nukleofilne supstitucije. Budući da je 2-(*tert*-butoksikarbonilamino)etil bromid osjetljiv na vlagu reakcija je provedena u inertnim uvjetima pod strujom dušika, a korišteni DMF bio je bezvodan. Kako bi se reakcija mogla provesti u blagim uvjetima, na sobnoj temperaturi uz zadovoljavajući prinos, upotrijebljen je katalizator faznog prijelaza TBAHS. Reakcija je provedena na sobnoj temperaturi tijekom 24 h, a dobiveni eter **17** je pročišćen ekstrakcijom (voda-etil-acetat) kako bi se u što većoj mjeri uklonio DMF, koji u odnosu na druga organska otapala ima izuzetno visoko vrelište (153 °C)

te se znatno teže uklanja uparavanjem pod sniženim tlakom. Također su ekstrakcijom uklonjene i soli novonastale u kemijskoj reakciji, kao i zaostatne soli koje su korištene u suvišku. Budući da nije postignuta potpuna selektivnost O-alkiliranja, željeni eter **17** izoliran je kromatografijom na koloni, a nakon rastrljavanja u smjesi dietil-etera i petroletera dobiven je čist u 56 %-tnom iskorištenju.

Obzirom na to da je u pripravi etera **17**, s ciljem izbjegavanja neželjenih sporednih reakcija, korišten zaštićeni amin 2-(*tert*-butoksikarbonilamino)etil bromid, daljnji reakcijski korak u sintezi harmicina **19a-h** uključivao je uklanjanje zaštitne Boc skupine kako bi se dobio željeni amin **18**. Reakcija uklanjanja zaštitne Boc skupine etera **17** provedena je u kiselim uvjetima u prisutnosti 10 ekvivalenata 4 M otopine HCl-a u metanolu pri blago povišenoj temperaturi od 50 °C. U reakciji najprije dolazi do protoniranja kisika *tert*-butoksi skupine vodikom HCl-a, nakon čega dolazi do gubitka *tert*-butilnog karbokationa, pri čemu nastaje karbamatna kiselina. Nadalje, dekarboksilacijom karbamatne kiseline nastaje amin **18**, koji se zbog suviška korištene kiseline dobiva u obliku kloridne soli. Zaluživanjem reakcijske smjese 5 %-tnom otopinom NaOH do pH 12 dolazi do taloženja novosintetiziranog amina **18**, koji se vrlo jednostavno izolira filtracijom. Daljnjim rastrljavanjem u dietil-eteru dobiven je čisti amin **18** u 69 %-tnom iskorištenju. Mehanizam uklanjanja Boc zaštitne skupine u prisutnosti HCl-a u pripravi amina **18** prikazan je na Shemi 4.

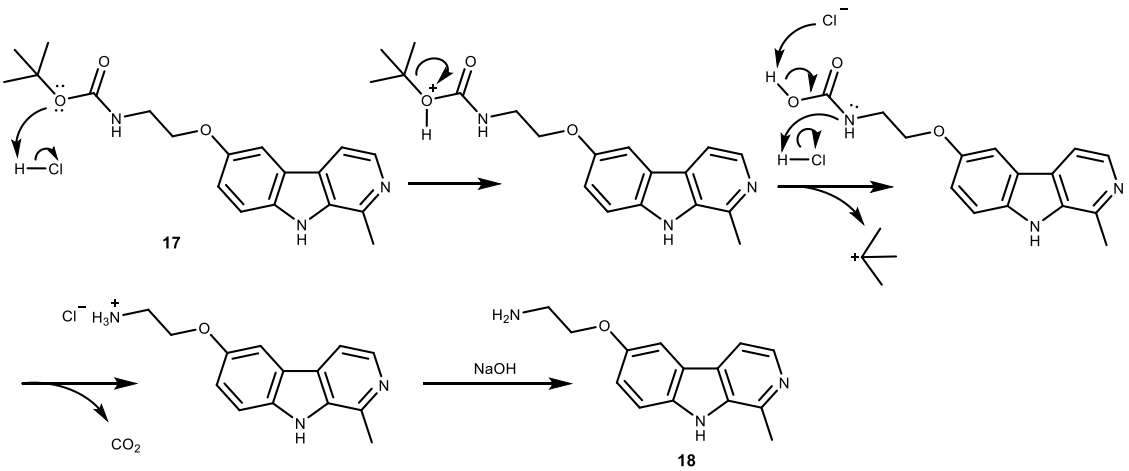

Shema 4. Mehanizam reakcije uklanjanja Boc zaštitne skupine u prisutnosti HCl-a u sintezi amina **18**

Novosintetizirani amin **18** korišten je u reakcijama povezivanja s cimetnom kiselinom/DCK-ima kako bi se pripravili željeni harmicini amidnoga tipa **19a-h** u položaju O-6 β-karbolina. Analogno sintezi harmicina **7a-h** u položaju C-1 β-karbolina te harmicina **13a-**

h u položaju C-3 β-karbolina odabrani su isti DCK-i (*m*-F-, *m*-Br-, *m*-CF_3-, *p*-F-, *p*-Cl-, *p*-OCH_3-, *p*-CF_3-cimetna kiselina), a metoda priprave također je bila ista. Novosintetizirani amidi **19a-h** taložili su se u reakcijskoj smjesi te su vrlo lako izolirani filtracijom, zatim pročišćeni kromatografijom na koloni i rastrljavanjem u dietil-eteru te su dobiveni u rasponu iskorištenja 58 – 84 %. Sinteza harmicina amidnoga tipa **19a-h** u položaju O-6 β-karbolina prikazana je na Shemi 5.

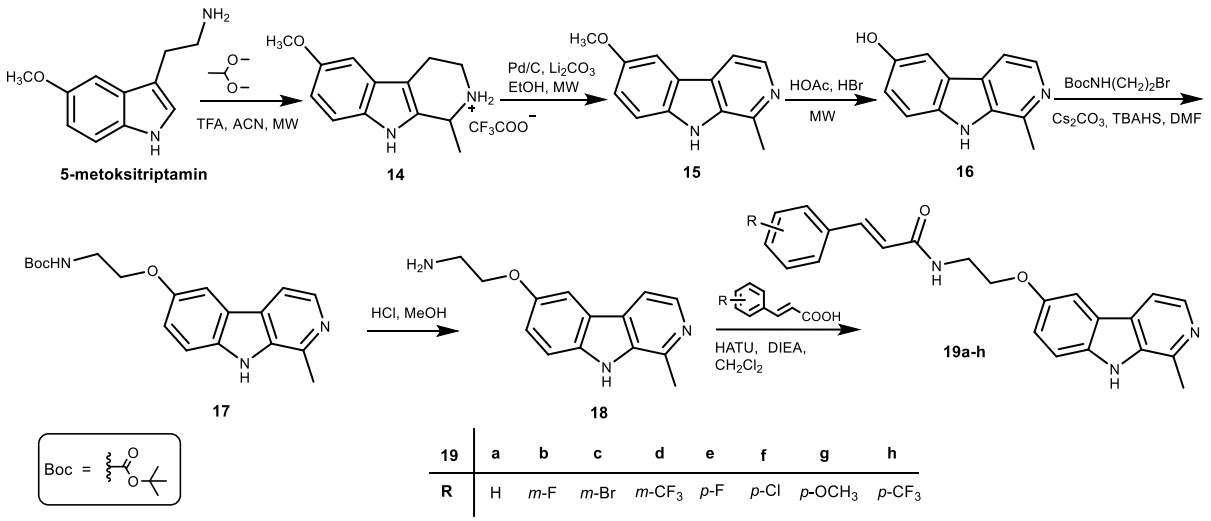

Shema 5. Sinteza harmicina amidnoga tipa u položaju O-6 β-karbolina

U položaju O-6 β-karbolina sintetizirani su sljedeći novi spojevi:

tert-butil-(2-((1-metil-9*H*-pirido[3,4-*b*]indol-6-il)oksi)etil)karbamat (**17**),

2-((1-metil-9*H*-pirido[3,4-*b*]indol-6-il)oksi)etan-1-amin (**18**),

N-(2-((1-metil-9*H*-pirido[3,4-*b*]indol-6-il)oksi)etil)cinamamid (**19a**),

(E)-3-(3-fluorfenil)-*N*-(2-((1-metil-9*H*-pirido[3,4-*b*]indol-6-il)oksi)etil)akrilamid (**19b**),

(*E*)-3-(3-bromfenil)-*N*-(2-((1-metil-9*H*-pirido[3,4-*b*]indol-6-il)oksi)etil)akrilamid (**19c**),

(*E*)-*N*-(2-((1-metil-9*H*-pirido[3,4-*b*]indol-6-il)oksi)etil)-3-(3-trifluormetil)fenil)akrilamid (**19d**),

(*E*)-3-(4-fluorfenil)-*N*-(2-((1-metil-9*H*-pirido[3,4-*b*]indol-6-il)oksi)etil)akrilamid (**19e**),

(*E*)-3-(4-klorfenil)-*N*-(2-((1-metil-9*H*-pirido[3,4-*b*]indol-6-il)oksi)etil)akrilamid (**19f**),

(*E*)-3-(4-metoksifenil)-*N*-(2-((1-metil-9*H*-pirido[3,4-*b*]indol-6-il)oksi)etil)akrilamid (**19g**),

(*E*)-*N*-(2-((1-metil-9*H*-pirido[3,4-*b*]indol-6-il)oksi)etil)-3-(4-(trifluormetil)fenil)akrilamid (**19h**).

4.1.1.5. Sinteza harmicina amidnoga tipa u položaju O-7 i N-9 β-karbolina

Harmicini amidnoga tipa **22a-h** u položaju O-7 β-karbolina te **25a-f**, **i-p** u položaju N-9 β-karbolina sintetizirani su iz harmina. Kako bi se omogućila derivatizacija položaja O-7 β-karbolina, metoksi skupina harmina hidrolizirana je analogno metoksi skupini spoja **15** u položaju O-6 β-karbolina – zagrijavanjem harmina na 140 °C u prisutnosti ledene octene i koncentrirane bromovodične kiseline pod utjecajem mikrovalova pri čemu je dobiven harmol. Dobiveni harmol pročišćavan je na isti način kao i spoj **16** (4.1.1.4.). Međutim, prednost u sintezi harmola je što dodatno pročišćavanje kromatografijom na koloni nije bilo potrebno, a izoliran je kao krutina žute boje u vrlo visokom iskorištenju od 92 %.

Harmol je zatim alkiliran pomoću 2-(*tert*-butoksikarbonilamino)etil bromida u prisutnosti cezijevog karbonata pri čemu je dobiven spoj **20**. Analogno alkiliranju spoja **16** u položaju O-6 β-karbolina reakcijski uvjeti su optimirani kako bi se u što većoj mjeri spriječilo provođenje sporedne reakcije N-9 alkiliranja. Stoga je u tu svrhu korišteno 1,4 ekvivalenta cezijevog karbonata i 2,4 ekvivalenta 2-(*tert*-butoksikarbonilamino)etil bromida, gotovo u pola manje količine u odnosu na količine reagensa korištenih u reakciji alkiliranja spoja **16**. Reakcija je također provedena u bezvodnom DMF-u u inertnim uvjetima pod strujom dušika. Međutim, reakcija je provedena zagrijavanjem na 95 °C bez upotrebe katalizatora faznog prijelaza TBAHS. Novosintetizirani eter **20** pročišćavan je na isti način kao i spoj **17** (4.1.1.4.), a dobiven je u nešto većem iskorištenju (78 %) u odnosu na spoj **17** (56 %).

Nadalje, zaštitna Boc skupina novosintetiziranog etera **20** uklonjena je u kiselim uvjetima upotrebom 4 M HCl u metanolu zagrijavanjem na 50 °C, a mehanizam uklanjanja zaštitne Boc skupine analogan je mehanizmu prikazanom na Shemi 4. Budući da se novosintetizirani amin **21** nije taložio zaluživanjem reakcijske smjese, izoliran je ekstrakcijom upotrebom etil-acetata, a rastrljavanjem u dietil-eteru dodatno je pročišćen i dobiven u visokom 80 %-tom iskorištenju.

S druge strane, harmicini amidnoga tipa **25a-f**, **i-p** dobiveni su iz amina **24** koji je pripravljen alkiliranjem harmina u položaju N-9 β-karbolina. Harmin je najprije otopljen u bezvodnom DMF-u pri temperaturi od 85 °C nakon čega su mu dodani cezijev karbonat i 2-(*tert*-butoksikarbonilamino)etil bromid. Budući da u ovom slučaju nije bilo kompetitivnih reakcija reagensi su korišteni u velikom suvišku (cezijev karbonat 4,5 ekvivalenata; 2-(*tert*-butoksikarbonilamino)etil bromid 4 ekvivalenta). Reakcija je također provedena u inertnim uvjetima pod strujom argona, pri 90 °C i bez upotrebe katalizatora faznog prijelaza. Novosintetizirani spoj **23** pročišćavan je na isti način kao i spoj **17** (4.1.1.4.) te je izoliran čist u 58 %-tnom iskorištenju.

Uklanjanje Boc zaštitne skupine spoja **23** provedeno je, analogno uklanjanju zaštitne skupine spoja **17**, u kiselim uvjetima pri 50 °C pri čemu je dobiven amin **24** uz iskorištenje reakcije od 59 %.

Novosintetizirani amini **21** i **23** dalje su korišteni u reakcijama povezivanja s cimetnom kiselinom i odabranim DCK-ima u pripravi željenih harmicina amidnoga tipa **22a-h** i **25a-f**, **i-p**.

U sintezi harmicina amidnoga tipa **22a-h** u položaju O-7 β-karbolina odabrani su nešto drugačiji DCK-i u odnosu na DCK-e korištene u sintezi harmicina amidnoga tipa **7a-h**, **13a-h** i **19a-h**, a odabrani DCK-i bili su sljedeći: *m*-F-, *m*-Br-, *p*-F-, *p*-Cl-, *p*-OCH_3-, *o*-F- i α-CH_3-cimetna kiselina. Cimetna kiselina i odabrani DCK-i nisu korišteni u suvišku, a miješani su 15 minuta u prisutnosti HATU i DIEA prije dodatka amina **21**. Nakon miješanja 1 h na sobnoj temperaturi u diklormetanu svi su se novonastali harmicini amidnoga tipa **22a-h** taložili u reakcijskoj smjesi te su lako izolirani filtracijom, a zatim su pročišćeni kromatografijom na koloni i rastrljavanjem u dietil-eteru. U položaju O-7 β-karbolina pripravljeno je ukupno osam harmicina amidnoga tipa **22a-h** u rasponu iskorištenja od 60 do 77 %, izuzev spoja **22c** koji je izoliran u iskorištenju od 47 %.

U položaju N-9 β-karbolina sintetizirano je ukupno 14 harmicina amidnoga tipa pri čemu su uz cimetnu kiselinu odabrani sljedeći DCK-i: *m*-F-, *m*-Br-, *m*-CF_3-, *p*-F-, *p*-Cl-, *p*-OCH_3-, *p*-CF_3-, *o*-Cl-, *m*-Cl-, *m*-OCF_3-, *p*-Br-, *p*-CH_3, *p*-NO_2-cimetna kiselina. Reakcije su provedene na sobnoj temperaturi u diklormetanu, a cimetna kiselina i DCK-i prvotno su aktivirani miješanjem 15 minuta u prisutnosti HATU i DIEA. Nakon miješanja na sobnoj temperaturi tijekom 2 sata novosintetizirani harmicni amidnoga tipa **25a-f**, **i-p** pročišćavani su na tri različita načina. U prvom slučaju reakcijskoj smjesi harmicina **25a**,**b**,**f**, **25k-m** i **25o** dodan je diklormetan te je reakcijska smjesa pročišćena ekstrakcijom pomoću zasićene otopine NaCl-a kako bi se uklonile soli i tetrametilurea, koje nastaju kao nusprodukti ovih reakcija. Pročišćavanjem kromatografijom na koloni i rastrljavanjem u dietil-eteru dobiveni su harmicini amidnoga tipa u rasponu iskorištenja 41 – 83 %. Nasuprot tome, u reakcijskim smjesama spojeva **25c-e** novonastali talog je odsisan, a filtrat je pročišćavan ekstrakcijom zasićenom otopinom NaCl-a i vodom, analogno pročišćavanju spojeva **25a**,**b**,**f**, **25k-m** i **25o**. Zatim su pročišćeni filtrat i prethodno odsisani talog spojeni i pročišćeni kromatografijom na koloni i rastrljavanjem u dietil-eteru čime su dobiveni harmicini **25c-e** u iskorištenju od 70 % (**25c**), 33 % (**25d**) i 53 % (**25e**). Konačno, spojevi **25i**,**j**,**n**,**p** taložili su se u reakcijskoj smjesi te su odsisani i pročišćeni kromatografijom na koloni i rastrljavanjem u dietil-eteru te su izolirani u rasponu iskorištenja 44 do 64 %.

Sinteza harmicina amidnoga tipa **22a-h** u položaju O-7 β-karbolina i **25a-f**, **i-p** u položaju N-9 β-karbolina prikazana je na Shemi 6.

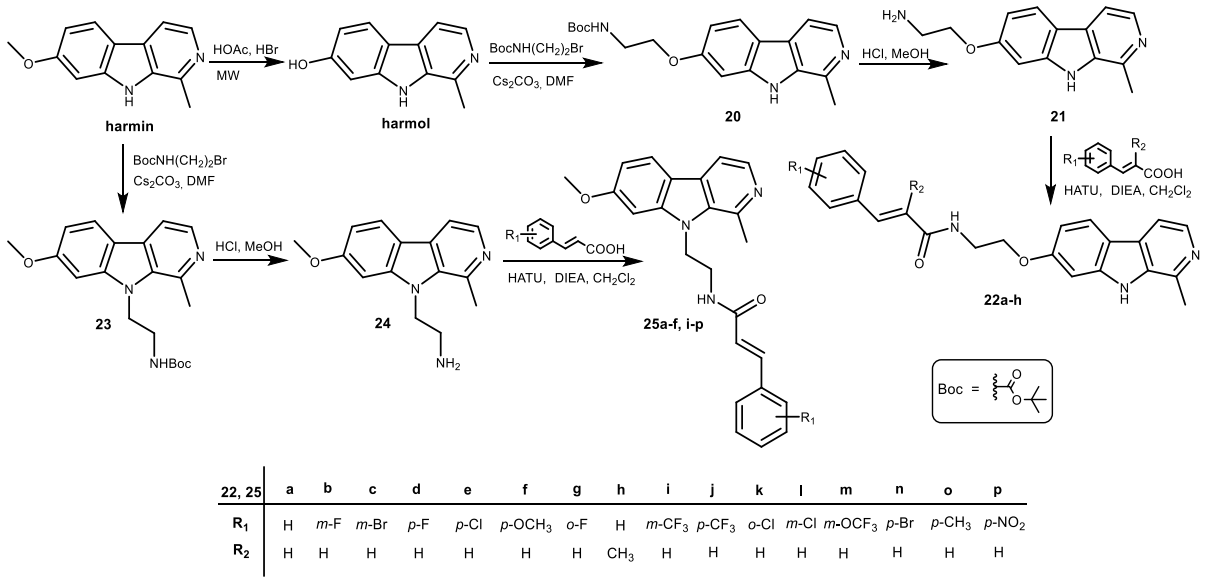

22, 25	a	b	c	d	e	f	g	h	i	j	k	l	m	n	o	p
R_1	H	*m*-F	*m*-Br	*p*-F	*p*-Cl	*p*-OCH_3	*o*-F	H	*m*-CF_3	*p*-CF_3	*o*-Cl	*m*-Cl	*m*-OCF_3	*p*-Br	*p*-CH_3	*p*-NO_2
R_2	H	H	H	H	H	H	H	CH_3	H	H	H	H	H	H	H	H

Shema 6. Sinteza harmicina amidnoga tipa u položajima O-7 i N-9 β-karbolina

U položaju O-7 β-karbolina sintetizirani su sljedeći novi spojevi:

tert-butil-(2-((1-metil-9*H*-pirido[3,4-*b*]indol-7-il)oksi)etil)karbamat (**20**),

2-((1-metil-9*H*-pirido[3,4-*b*]indol-7-il)oksi)etan-1-amin (**21**),

N-(2-((1-metil-9*H*-pirido[3,4-*b*]indol-7-il)oksi)etil)cinamamid (**22a**),

(*E*)-3-(3-fluorfenil)-*N*-(2-((1-metil-9*H*-pirido[3,4-*b*]indol-7-il)oksi)etil)akrilamid (**22b**),

(*E*)-3-(3-bromfenil)-*N*-(2-((1-metil-9*H*-pirido[3,4-*b*]indol-7-il)oksi)etil)akrilamid (**22c**),

(*E*)-3-(4-fluorfenil)-*N*-(2-((1-metil-9*H*-pirido[3,4-*b*]indol-7-il)oksi)etil)akrilamid (**22d**),

(*E*)-3-(4-klorfenil)-*N*-(2-((1-metil-9*H*-pirido[3,4-*b*]indol-7-il)oksi)etil)akrilamid (**22e**),

(*E*)-3-(4-metoksifenil)-*N*-(2-((1-metil-9*H*-pirido[3,4-*b*]indol-7-il)oksi)etil)akrilamid (**22f**),

(*E*)-3-(2-fluorfenil)-*N*-(2-((1-metil-9*H*-pirido[3,4-*b*]indol-7-il)oksi)etil)akrilamid (**22g**),

(*E*)-2-metil-*N*-(2-((1-metil-9*H*-pirido[3,4-*b*]indol-7-il)oksi)etil)-3-fenilakrilamid (**22h**).

U položaju N-9 β-karbolina sintetizirani su sljedeći novi spojevi:

tert-butil-(2-(7-metoksi-1-metil-9*H*-pirido[3,4-*b*]indol-9-il)etil)karbamat (**23**),

2-(7-metoksi-1-metil-9*H*-pirido[3,4-*b*]indol-9-il)etan-1-amin (**24**),

N-(2-(7-metoksi-1-metil-9*H*-pirido[3,4-*b*]indol-9-il)etil)cinamamid (**25a**),

(*E*)-3-(3-fluorfenil)-*N*-(2-(7-metoksi-1-metil-9*H*-pirido[3,4-*b*]indol-9-il)etil)akrilamid (**25b**),

(*E*)-3-(3-bromfenil)-*N*-(2-(7-metoksi-1-metil-9*H*-pirido[3,4-*b*]indol-9-il)etil)akrilamid (**25c**),

(*E*)-3-(4-fluorfenil)-*N*-(2-(7-metoksi-1-metil-9*H*-pirido[3,4-*b*]indol-9-il)etil)akrilamid (**25d**),
(*E*)-3-(4-klorfenil)-*N*-(2-(7-metoksi-1-metil-9*H*-pirido[3,4-*b*]indol-9-il)etil)akrilamid (**25e**),
(*E*)-*N*-(2-(7-metoksi-1-metil-9*H*-pirido[3,4-*b*]indol-9-il)etil)-3-(4-metoksifenil)akrilamid (**25f**),
(*E*)-*N*-(2-(7-metoksi-1-metil-9*H*-pirido[3,4-*b*]indol-9-il)etil)-3-(3-(trifluormetil)fenil)akrilamid (**25i**),
(*E*)-*N*-(2-(7-metoksi-1-metil-9*H*-pirido[3,4-*b*]indol-9-il)etil)-3-(4-(trifluormetil)fenil)akrilamid (**25j**),
(*E*)-3-(2-klorfenil)-*N*-(2-(7-metoksi-1-metil-9*H*-pirido[3,4-*b*]indol-9-il)etil)akrilamid (**25k**),
(*E*)-3-(3-klorfenil)-*N*-(2-(7-metoksi-1-metil-9*H*-pirido[3,4-*b*]indol-9-il)etil)akrilamid (**25l**),
(*E*)-*N*-(2-(7-metoksi-1-metil-9*H*-pirido[3,4-*b*]indol-9-il)etil)-3-(3-(trifluormetoksi)fenil)akrilamid (**25m**),
(*E*)-3-(4-bromfenil)-*N*-(2-(7-metoksi-1-metil-9*H*-pirido[3,4-*b*]indol-9-il)etil)akrilamid (**25n**),
(*E*)-*N*-(2-(7-metoksi-1-metil-9*H*-pirido[3,4-*b*]indol-9-il)etil)-3-(*p*-tolil)akrilamid (**25o**),
(*E*)-*N*-(2-(7-metoksi-1-metil-9*H*-pirido[3,4-*b*]indol-9-il)etil)-3-(4-nitrofenil)akrilamid (**25p**).

4.1.1.6. Analitički i spektroskopski podaci novosintetiziranih spojeva u položajima O-6, O-7 i N-9 β-karbolina

Tijek kemijskih reakcija i čistoća produkata praćeni su tankoslojnom kromatografijom, a strukture spojeva **17**, **18**, **20**, **21**, **23**, **24** te **19a-h**, **22a-h** i **25a-f**, **i-p** potvrđene su uobičajenim spektroskopskim i analitičkim metodama (IR, ^{1}H i ^{13}C NMR i MS). Novosintetiziranim spojevima određeno je talište, dok je spoj **17** izoliran kao ulje. Čistoća harmicina **19a-g** i **25i**,**j** dodatno je potvrđena određivanjem relativne čistoće.

Analizom IR spektara spojeva **20** i **23** uočena je karakteristična apsorpcijska vrpca istezanja C=O veze karbamatne skupine na valnim brojevima 1692 cm^{-1} (**20**) i 1701 cm^{-1} (**23**). U IR spektrima amina **18**, **21** i **24** uočene su oštre vrpce slabog intenziteta na valnim brojevima 3359 cm^{-1} (**18**), 3332 cm^{-1} (**21**) i 3354 cm^{-1} (**24**), koje odgovaraju N–H istezanju primarne amino skupine. Vrpca N–H istezanja sekundarnog (indolskog) amina u IR spektru spoja **21** vidljiva je na 3250 cm^{-1} dok su se vrpce C–H istezanja aromatskih veza i N–H istezanja sekundarnog (indolskog) amina spoja **18** preklopile u široku vrpcu čiji su maksimumi vidljivi na valnim brojevima 3241 cm^{-1} i 3065 cm^{-1}. Zatim su vidljive oštre vrpce slabog intenziteta na 1605 cm^{-1} (**18**), na 1628 cm^{-1} (**21**) te na 1621 cm^{-1} (**24**) koje odgovaraju N–H savijanju.

Signali za indolske protone H-10 nalaze se u ^{1}H NMR spektrima spojeva **17**, **18**, **20** i **21** na kemijskim pomacima od 11,42 ppm (**17**), 11,36 ppm (**18**), 11,42 ppm (**20**), odn. 11,38 ppm

(**21**), dok ti signali u spektrima spojeva **23** i **24** nisu vidljivi zbog derivatizacije položaja N-9. Pikovi singleta s relativnim integralom 3H na kemijskim pomacima od 2,75 ppm (**17**), odn. 2,74 ppm (**18**), odgovaraju signalima protona H-13 metilne skupine. Također, u spektrima spojeva **23** i **24** vidljivi su pikovi protona metoksi skupine H-14, koji su zbog prisutnosti elektronegativnog kisikovog atoma odsjenjeni te se nalaze na višim kemijskim pomacima od 3,92 ppm (**23**) odn. 3,91 ppm (**24**), dok se u spektrima spojeva **20** i **21** ti signali ne vide zbog derivatizacije O-7 položaja. Pikovi protona *tert*-butilne skupine s relativnim integralom 9H se u ^{1}H spektrima spojeva **17** i **20** zbog zasjenjenosti nalazi pri nižim kemijskim pomacima, a vidljivi su na kemijskom pomaku od 1,40 ppm, međutim u spektru spoja **23** vidljiva su dva pika na kemijskom pomaku od 1,29 ppm s relativnim integralom 8H i na 1,01 ppm s integralom 1H. Analizom ^{1}H spektra amina **18** nije uočen signal za protone primarne amino skupine H-3' te je njegova struktura izravno potvrđena MS analizom kojom je uočen pik protoniranog molekulskog iona pri *m/z* 242,2 te neizravno provođenjem daljnjih reakcija povezivanja pri čemu su sintetizirani harmicini amidnoga tipa **19a-h** čije su strukture također potvrđene uobičajenim spektroskopskim i analitičkim metodama. Analizom ^{1}H spektra amina **21** i **24** uočeni su signali za protone primarne amino skupine H-3' i u spektru spoja **21** se nalaze na kemijskom pomaku od 1,58 ppm, a u spektru spoja **24** na 1,61 ppm s relativnim integralom 2H.

U ^{13}C spektrima spojeva **17** i **18** pikovi ugljikovih atoma metilne skupine C-13 vidljivi su na kemijskim pomacima 20,23 ppm (**17**), odn. 19,97 ppm (**18**). Budući da su ugljikovi atomi *tert*-butilne skupine kemijski ekvivalentni, u spektru spoja **17** vidljiv je samo jedan signal za ugljikove atome C-6', C-7', C-8' na kemijskom pomaku od 28,24 ppm dok se u ^{13}C spektru spoja **20** njihovi signali nalaze na kemijskom pomaku od 28,23 ppm, a u spektru spoja **23** na 28,02 ppm. U ^{13}C spektru spoja **20** nije uočen signal za C-2' atom, a njegova struktura je izravno potvrđena MS analizom te neizravno daljnjim reakcijama, te je tako već u spektru spoja **21** uočen signal za C-2' atom na 40,98 ppm.

MS analizom spojeva **20**, **21**, **23** i **24** dobiveni su maseni spektri u kojima su vidljivi pikovi najvećeg intenziteta, a koji odgovaraju protoniranim molekulskim ionima: *m/z* 342,3 (**20**), *m/z* 242,2 (**21**), *m/z* 356,2 (**23**), *m/z* 256,3 (**24**).

Analitički i spektroskopski podaci spojeva **17**, **18**, **20**, **21**, **23** i **24** dani su u Tablicama 10 i 11.

Tablica 10. Analitički i IR spektroskopski podaci spojeva **17**, **18**, **20**, **21**, **23** i **24**

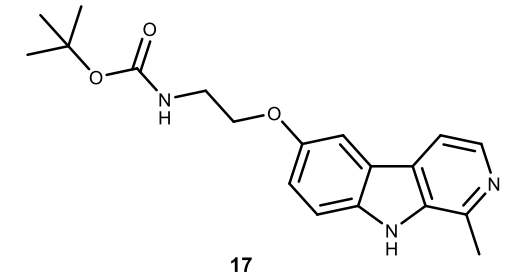

17

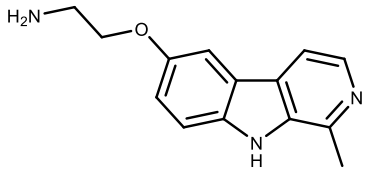

18

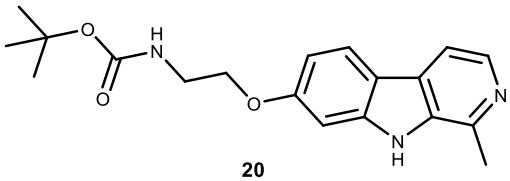

20

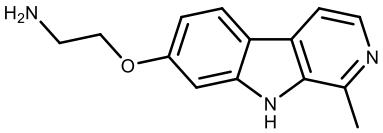

21

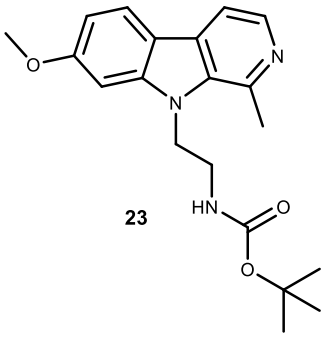

23

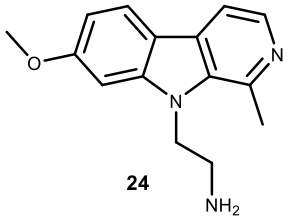

24

Spoj	Iskorištenje (%)	t_t (°C)	Molekulska formula (M_r)	MS [*m*/*z*]	IR (ATR, ν/cm^{-1})
17	56	ulje	$C_{19}H_{23}N_3O_3$ (341,41)	342,4 $[M+1]^+$	n.s.[a]
18	69	170,5 – 172,0	$C_{14}H_{15}N_3O$ (241,29)	242,2 $[M+1]^+$	3645, 3359, 3241, 3065, 2925, 2869, 1605, 1581, 1566, 1500, 1478, 1458, 1401, 1288, 1234, 1211, 1126, 1071, 1059, 992, 905, 884, 847, 825, 816, 741, 703, 632
20	78	189,5 – 190,5	$C_{19}H_{23}N_3O_3$ (341,41)	342,3 $[M+1]^+$	3390, 3134, 3052, 2978, 2944, 2872, 2764, 2726, 2582, 2406, 1692, 1634, 1568, 1530, 1480, 1448, 1394, 1368, 1334, 1296, 1260, 1174, 1114, 1052, 1010, 964, 872, 846, 820, 788, 720, 686, 634, 604, 522
21	80	172,5 – 173,0	$C_{14}H_{15}N_3O$ (241,29)	242,2 $[M+1]^+$	3332, 3250, 3156, 3068, 2930, 2864,2774, 2372, 1892, 1756, 1720, 1628, 1568, 1486, 1444, 1326, 1284, 1238, 1180, 1104, 1028, 996, 908, 860, 812, 636

23	58	197,5 – 199,0	$C_{20}H_{25}N_3O_3$ (355,44)	356,2 $[M+1]^+$	3183, 3065, 3013, 2993, 2969, 2937, 1701, 1623, 1567, 1502, 1447, 1409, 1366, 1343, 1330, 1313, 1278, 1247, 1195, 1166, 1146, 1124, 1092, 1048, 1018, 970, 944, 876, 841, 803, 768, 727, 684, 639, 598, 559, 534
24	59	133,5 – 135,5	$C_{15}H_{17}N_3O$ (255,32)	256,3 $[M+1]^+$	3354, 3327, 3274, 3054, 3039, 2966, 2932, 2837, 1751, 1621, 1563, 1496, 1443, 1404, 1343, 1302, 1283, 1236, 1219, 1151, 1136, 1117, 1089, 1040, 1021, 973, 941, 922, 887, 848, 815, 768, 723, 643, 599, 551, 528

[a] n.s. - nije sniman

Tablica 11. ^{1}H i ^{13}C NMR spektroskopski podaci spojeva **17**, **18**, **20**, **21**, **23** i **24**

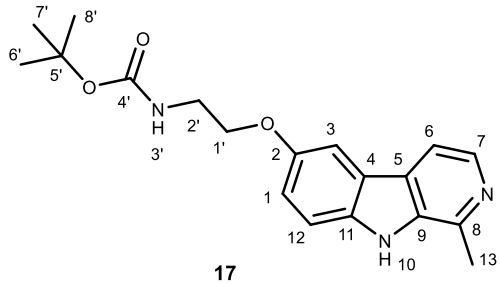

17

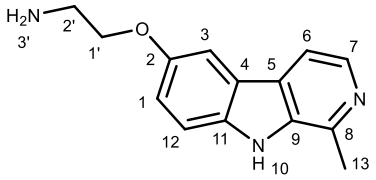

18

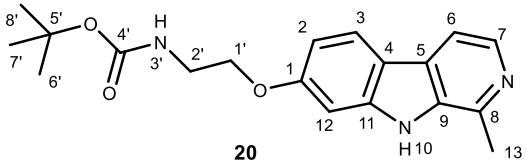

20

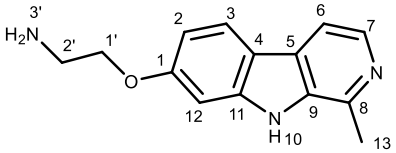

21

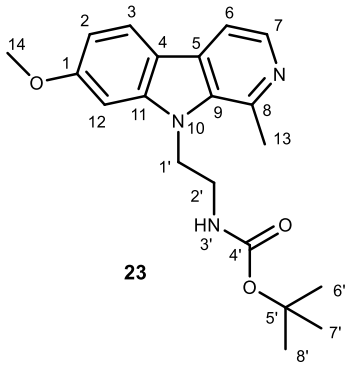

23

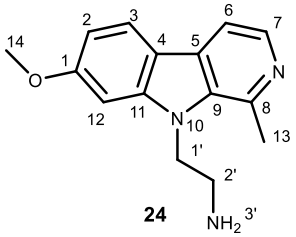

24

Spoj	^{1}H NMR (DMSO-d_6, δ ppm, J/Hz)	^{13}C NMR (DMSO-d_6, δ ppm)
17	11,42 (s, 1H, 10), 8,16 (d, 1H, 7, J = 5,3 Hz), 7,92 (d, 1H, 6, J = 5,3 Hz), 7,77 (d, 1H, 3, J = 1,7 Hz), 7,51 (d, 1H, 12, J = 8,8 Hz), 7,18 (dd, 1H, 1, J = 8,8, 2,3 Hz), 7,06 (t, 1H, 3', J = 5,0 Hz), 4,05 (t, 2H, 1', J = 5,8 Hz), 3,39 – 3,34 (m, 2H, 2'), 2,75 (s, 3H, 13), 1,40 (s, 9H, 6' – 8')	155,73 (4'), 152,39 (2), 142,04 (8), 136,56 (7), 135,41 (11), 135,03 (9), 126,88 (4), 121,35 (5), 118,42 (1), 112,78 (6), 112,75 (12), 104,68 (3), 77,76 (5'), 67,19 (1'), 39,61 (2'), 28,24 (6' – 8'), 20,23 (13)
18	11,36 (s, 1H, 10), 8,15 (d, 1H, 7, J = 5,3 Hz), 7,90 (d, 1H, 6, J = 5.3 Hz), 7,74 (d, 1H, 3, J = 2,3 Hz), 7,50 (d, 1H, 12, J = 8,8 Hz), 7,19 (dd, 1H, 1, J = 8,8, 2,5 Hz), 4,02 (t, 2H, 1', J = 5,8 Hz), 2,94 (t, 2H, 2', J = 5,7 Hz), 2,74 (s, 3H, 13)	152,47 (2), 141,87 (8), 136,70 (7), 135,19 (11), 134,93 (9), 126,54 (4), 121,29 (5), 117,98 (6), 112,34 (1), 112,18 (12), 104,86 (3), 71,06 (1'), 40,87 (2'), 19,97 (13)
20	11,42 (s, 1H, 10), 8,15 (d, 1H, 7, J = 5,3 Hz), 8,05 (d, 1H, 3, J = 8,6 Hz), 7,81 (d, 1H, 6, J = 5,3 Hz), 7,06 (t, 1H, 3', J = 5,4 Hz), 7,00 (d, 1H, 12, J = 2,1 Hz), 6,85 (dd, 1H, 2, J = 8,7, 2,2 Hz), 4,08 (t, 2H, 1', J = 5,8 Hz), 3,41 – 3,35 (m, 2H, 2'), 2,73 (s, 3H, 13), 1,40 (s, 9H, 6' – 8')	159,22 (4'), 155,73 (1), 141,92 (8), 141,21 (11), 137,59 (7), 134,55 (9), 127,26 (4), 122,66 (3), 114,96 (5), 111,96 (6), 109,33 (2), 95,39 (12), 77,80 (5'), 66,66 (1'), 28,23 (6' – 8'), 20,26 (13)
21	11,38 (s, 1H, 10), 8,15 (d, 1H, 7, J = 5,2 Hz), 8,04 (d, 1H, 3, J = 8,6 Hz), 7,79 (d, 1H, 6, J = 5,2 Hz), 7,01 (d, 1H, 12, J = 2,2 Hz), 6,85 (dd, 1H, 2, J = 8,6, 2,2 Hz), 4,03 (t, 2H, 1', J = 5,7 Hz), 2,95 (t, 2H, 2', J = 5,7 Hz), 2,73 (s, 3H, 13), 1,58 (s, 2H, 3')	159,46 (1), 141,91 (8), 141,25 (11), 137,73 (7), 134,54 (9), 127,20 (5), 122,57 (3), 114,84 (4), 111,89 (6), 109,37 (2), 95,29 (12), 70,36 (1'), 40,98 (2'), 20,33 (13)
23	8,15 (d, 1H, 7, J = 5,1 Hz), 8,07 (d, 1H, 3, J = 8,5 Hz), 7,85 (d, 1H, 6, J = 5,0 Hz), 7,22 (s, 1H, 12), 7,02 (t, 1H, 3', J = 5,2 Hz), 6,87 (dd, 1H, 2, J = 8,4, 1,6 Hz), 4,55 (t, 2H, 1', J = 6,6 Hz), 3,92 (s, 3H, 14), 3,33 – 3,31 (m, 2H, 2'), 2,95 (s, 3H, 13), 1,29 (s, 8H, 6' – 8'), 1,01 (s, 1H, 6' – 8')	160,46 (1), 155,63 (4'), 142,85 (8), 140,47 (11), 137,64 (7), 134,71 (9), 128,40 (4), 122,21 (3), 114,35 (5), 112,11 (6), 108,96 (2), 93,81 (12), 77,78 (5'), 55,48 (14), 43,99 (1'), 39,98 (2'), 28,02 (6' – 8'), 23,00 (13)
24	8,15 (d, 1H, 7, J = 5,2 Hz), 8,07 (d, 1H, 3, J = 8,6 Hz), 7,86 (d, 1H, 6, J = 5,2 Hz), 7,23 (d, 1H, 12, J = 2,2 Hz), 6,86 (dd, 1H, 2, J = 8,6, 2,2 Hz), 4,52 (t, 2H, 1', J = 7,2 Hz), 3,91 (s, 3H, 14), 2,97 (s, 3H, 13), 2,92 (t, 2H, 2', J = 7,2 Hz), 1,61 (s, 2H, 3')	160,47 (1), 142,93 (11), 140,63 (8), 137,61 (7), 134,78 (9), 128,19 (4), 122,26 (3), 114,15 (5), 112,16 (6), 109,08 (2), 93,80 (12), 55,59 (14), 47,22 (1'), 42,14 (2'), 23,28 (13)

U IR spektrima harmicina amidnoga tipa **19a-h**, **22a-h** i **25a-f**, **i-p** vidljive su karakteristične apsorpcijske vrpce:

- Oštre vrpce srednjeg intenziteta C=O istezanja karbonilne skupine sekundarnog amida u području valnih brojeva 1650 – 1680 cm^{-1}: **19a**, 1665 cm^{-1}; **19b**, 1666 cm^{-1}; **19c**, 1664 cm^{-1}; **19d**, 1665 cm^{-1}; **19e**, 1667 cm^{-1}; **19f**, 1665 cm^{-1}; **19g**, 1651 cm^{-1}; **19h**, 1667 cm^{-1}; **22a**, 1664 cm^{-1}; **22b**, 1670 cm^{-1}; **22c**, 1664 cm^{-1}; **22d**, 1668 cm^{-1}; **22e**, 1662 cm^{-1}; **22g**, 1668 cm^{-1}; **25a**, 1672 cm^{-1}; **25b**, 1671 cm^{-1}; **25c**, 1679 cm^{-1}; **25d**, 1656 cm^{-1}; **25e**, 1672 cm^{-1}; **25f**, 1667 cm^{-1}; **25i**, 1679 cm^{-1}; **25j**, 1680 cm^{-1}; **25k**, 1650 cm^{-1}, **25l**, 1680 cm^{-1}; **25m**, 1675 cm^{-1}; **25n**, 1653 cm^{-1}; **25o**, 1672 cm^{-1}; **25p**, 1669 cm^{-1}. U spektrima spojeva **22f** i **22h** te su se vrpce preklopile s vrpcama karakterističnim za N–H savijanje indolskog amina te istezanju aromatskih C=C veza pri čemu se maksimumi apsorpcije nalaze na valnim brojevima 1628 cm^{-1} (**22f**) i 1630 cm^{-1} (**22h**).

Masenom spektrometrijom harmicina amidnoga tipa **19a-h**, **22a-h**, **25a-f**, **i-p** dobiveni su maseni spektri koji pokazuju signale najvećeg intenziteta koji odgovaraju protoniranim molekulskim ionima $[M+1]^+$ pojedinih harmicina: **19a**, *m/z* 372,0; **19b**, *m/z* 390,4; **19d**, *m/z* 440,1; **19e**, *m/z* 390,4; **19g**, *m/z* 402,4; **19h**, *m/z* 440,1; **22a**, *m/z* 372,2; **22b**, *m/z* 390,2; **22d**, *m/z* 390,3; **22f**, *m/z* 402,2; **22g**, *m/z* 390,3; **22h**, *m/z* 386,3; **25a**, *m/z* 386,4; **25b**, *m/z* 404,4; **25d**, *m/z* 404,2; **25f**, *m/z* 416,3; **25i**, *m/z* 454,2; **25j**, *m/z* 454,3; **25m**, *m/z* 470,1; **25o**, *m/z* 400,15; **25p**, *m/z* 431,1.

Zbog izotopne raspodjele izotopa ^{79}Br i ^{81}Br u MS spektrima harmicina **19c**, **22c**, **25c** i **25n** vidljiva su dva pika podjednakog intenziteta pri *m/z* 450,3 i 452,3 (**19c**), *m/z* 450,1 i 452,1 (**22c**), *m/z* 464,3 i 466,3 (**25c**), *m/z* 464,05 i *m/z* 466,0 (**25n**) koji odgovaraju protoniranim molekulskim ionima $[M+1]^+$. Signali najvećeg intenziteta u MS spektrima harmicina **19f**, **22e**, **25e**,**k**,**l** odgovaraju protoniranim molekulskim ionima $[M+1]^+$ pojedinih harmicina, a zbog izotopne raspodjele izotopa ^{35}Cl i ^{37}Cl prisutna su dva pika pri *m/z* 406,3 i 408,3 (**19f**), *m/z* 406,2 i 408,2 (**22e**), *m/z* 420,3 i 422,3 (**25e**), *m/z* 420,1 i 422,15 (**25k**), *m/z* 420,05 i 422,05 (**25l**) čiji su intenziteti u približnim relativnim omjerima 1:3.

Analitički i IR spektroskopski podaci harmicina amidnoga tipa **19a-h**, **22a-h** i **25a-f**, **i-p** dani su u Tablicama 12 – 14.

Tablica 12. Analitički i IR spektroskopski podaci harmicina amidnoga tipa **19a-h**

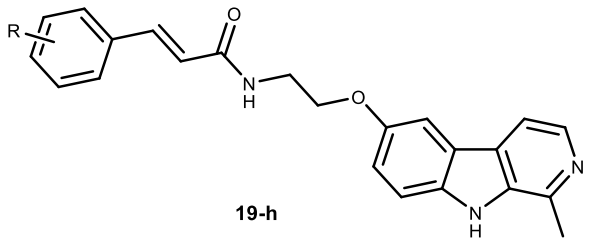

19-h

Spoj	R	Iskorištenje (%)	t_t (°C)	Molekulska formula (M_r)	MS [*m/z*]	IR (ATR, ν/cm^{-1})
19a	H	58	128,0 – 129,5	$C_{23}H_{21}N_3O_2$ (371,44)	372,0 $[M+1]^+$	3640, 3220, 3062, 2986, 2938, 2811, 2609, 1871, 1665, 1622, 1545, 1502, 1458, 1422, 1343, 1286, 1209, 1121, 1074, 970, 897, 808, 766, 714, 659, 630, 574, 512, 483
19b	*m*-F	76	225,0 – 226,0	$C_{23}H_{20}FN_3O$ (389,43)	390,4 $[M+1]^+$	3658, 3236, 3068, 2974, 2936, 2882, 2822, 2608, 1871, 1666, 1625, 1585, 1551, 1501, 1448, 1344, 1286, 1248, 1207, 1146, 1075, 1037, 974, 902, 856, 807, 738, 666, 630, 573, 519, 467
19c	*m*-Br	77	230,5 – 232,5	$C_{23}H_{20}BrN_3O_2$ (450,34)	450,3 $[M+1]^+$ 452,3 $[M+1]^+$	3646, 3171, 3062, 2975, 2939, 2879, 2792, 2613, 1664, 1620, 1566, 1501, 1460, 1384, 1345, 1287, 1199, 1110, 1072, 970, 856, 811, 781, 736, 667, 631, 561
19d	*m*-CF_3	64	216,5 – 218,0	$C_{24}H_{20}F_3N_3O_2$ (439,44)	440,1 $[M+1]^+$	3676, 3222, 3100, 3067, 2988, 2937, 2881, 2820, 2611, 1665, 1624, 1545, 1501, 1440, 1331, 1286, 1200, 1167, 1117, 1073, 1031, 971, 863, 805, 738, 691, 658, 630, 574, 465

19e	*p*-F	80	226,5 – 227,5	$C_{23}H_{20}FN_3O$ (389,43)	390,4 $[M+1]^+$	3659, 3311, 3225, 3099, 3045, 2990, 2938, 2165, 1870, 1667, 1625, 1542, 1502, 1422, 1347, 1286, 1208, 1160, 1122, 1074, 976, 897, 824, 740, 630, 576, 501, 459
19f	*p*-Cl	84	228,5–229,5	$C_{23}H_{20}ClN_3O_2$ (405,88)	406,3 $[M+1]^+$ 408,3 $[M+1]^+$	3642, 3231, 3066, 2989, 2939, 2164, 2113, 1872, 1665, 1621, 1548, 1502, 1406, 1342, 1288, 1208, 1075, 976, 938, 897, 809, 742, 630, 575, 490
19g	*p*-OCH_3	75	241,5 – 242,5	$C_{24}H_{23}N_3O_3$ (401,47)	402,4 $[M+1]^+$	3210, 3133, 3058, 2971, 2941, 2873, 2775, 2601, 2164, 1983, 1886, 1651, 1602, 1554, 1514, 1461, 1425, 1353, 1284, 1230, 1205, 1175, 1125, 1064, 1033, 983, 862, 827, 761, 699, 624, 555, 521
19h	*p*-CF_3	62	231,5 – 233,5	$C_{24}H_{20}F_3N_3O_2$ (439,44)	440,1 $[M+1]^+$	3645, 3269, 3061, 2932, 2875, 1667, 1628, 1559, 1501, 1461, 1417, 1384, 1328, 1286, 1234, 1202, 1166, 1119, 1067, 1016, 976, 953, 882, 829, 814, 728, 708, 614, 591, 562, 522, 495

Tablica 13. Analitički i IR spektroskopski podaci harmicina amidnoga tipa **22a-h**

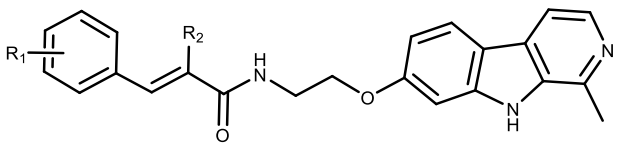

22a-h

Spoj	**R_1**	**R_2**	**Iskorištenje (%)**	**t_t (°C)**	**Molekulska formula (M_r)**	**MS [*m*/*z*]**	**IR (KBr, ν/cm^{-1})**
22a	H	H	60	151,5 (raspad)	$C_{23}H_{21}N_3O_2$ (371,44)	372,2 $[M+1]^+$	3424, 3222, 3060, 2972, 2932, 2874, 2768, 2372, 1874, 1720, 1664, 1630,

							1574, 1544, 1486, 1450, 1392, 1332, 1280, 1234, 1174, 1110, 1056, 976, 812, 764, 684, 596, 528
22b	*m*-F	H	67	210,0 – 212,5	$C_{23}H_{20}FN_3O_2$ (389,43)	390,2 $[M+1]^+$	3256, 3070, 2940, 2866, 2812, 2370, 1872, 1720, 1670, 1630, 1580, 1486, 1444, 1344, 1250, 1178, 1110, 1060, 1028, 964, 852, 784, 670, 624, 594, 528
22c	*m*-Br	H	47	135,0 – 137,5	$C_{23}H_{20}BrN_3O_2$ (450,34)	450,1 $[M+1]^+$ 452,1 $[M+1]^+$	3422, 3206, 3056, 2970, 2932, 2872, 2774, 2374, 2340, 1720, 1664, 1628, 1572, 1450, 1338, 1282, 1236, 1170, 1110, 1054, 974, 848, 786, 738, 668, 634, 602
22d	*p*-F	H	73	199,5 – 200,0	$C_{23}H_{20}FN_3O_2$ (389,43)	390,3 $[M+1]^+$	3248, 3072, 2940, 2866, 2812, 2366, 1872, 1720, 1668, 1630, 1576, 1508, 1456, 1344, 1278, 1230, 1178, 1110, 1060, 1030, 964, 876, 796, 740, 674, 626, 594, 506
22e	*p*-Cl	H	64	230,5 – 234,0	$C_{23}H_{20}ClN_3O_2$ (405,88)	406,2 $[M+1]^+$ 408,2 $[M+1]^+$	3400, 3268, 3046, 2942, 2880, 2772, 2372, 1662, 1624, 1560, 1490, 1450, 1332, 1284, 1234, 1166, 1102, 1012, 982, 874, 818, 738,692, 656, 606
22f	*p*-OCH_3	H	63	191,0 – 194,5	$C_{24}H_{23}N_3O_3$ (401,47)	402,2 $[M+1]^+$	3432, 3258, 3070, 3008, 2938, 2842, 2770, 2342, 1720, 1628, 1602, 1574, 1546, 1514, 1448, 1258, 1174, 1108, 1060, 1030, 984, 872, 828, 744, 714, 674, 588, 554, 518
22g	*o*-F	H	77	241,5 (raspad)	$C_{23}H_{20}FN_3O_2$ (389,43)	390,3 $[M+1]^+$	3252, 3066, 2942, 2864, 2818, 2600, 1866, 1668, 1630, 1576, 1486, 1456, 1388, 1344, 1278, 1234, 1180, 1100, 1060, 1022, 976, 850, 812, 750, 676, 626, 594

22h	H	CH_3	61	221,5 – 222,5	$C_{24}H_{23}N_3O_2$ (385,47)	386,3 $[M+1]^+$	3432, 3202, 3024, 2940, 2880, 2370, 2342, 1952, 1884, 1720, 1630, 1570, 1538, 1484, 1446, 1324, 1276, 1236, 1174, 1106, 1070, 972, 926, 850, 814, 760, 698, 664, 634, 588, 516

Tablica 14. Analitički i IR spektroskopski podaci harmicina amidnoga tipa **25a-f**, **i-p**

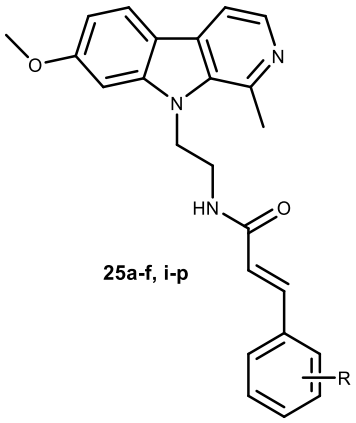

25a-f, i-p

Spoj	**R**	**Iskorištenje (%)**	**t_t (°C)**	**Molekulska formula (M_r)**	**MS [*m*/*z*]**	**IR (ν/cm^{-1})[a]**
25a	H	51	201,5 – 203,0	$C_{24}H_{23}N_3O_2$ (385,47)	386,4 $[M+1]^+$	3202, 3027, 2968, 2926, 2852, 1672, 1622, 1566, 1532, 1496, 1447, 1405, 1340, 1306, 1282, 1247, 1218, 1196, 1175, 1138, 1091, 1043, 1020, 972, 938, 856, 814, 762, 679, 641, 597, 555, 485
25b	*m*-F	47	226,5 – 228,0	$C_{24}H_{22}FN_3O_2$ (403,46	404,4 $[M+1]^+$	3661, 3599, 3182, 3009, 2931, 2838, 1671, 1623, 1584, 1538, 1505, 1445, 1412, 1343, 1295, 1240, 1182, 1141, 1095, 1043, 1017, 976, 848, 808, 783, 729, 668, 556, 517
25c	*m*-Br	70	225,0 – 226,0	$C_{24}H_{22}BrN_3O_2$ (464,36)	464,3 $[M+1]^+$ 466,3 $[M+1]^+$	3180, 3051, 3021, 2975, 2932, 2901, 2864, 2792, 2559, 1944, 1875, 1679, 1621, 1565, 1498,

						1468, 1450, 1410, 1377, 1345, 1305, 1251, 1223, 1195, 1138, 1106, 1043, 1018, 980, 941, 911, 885, 862, 812, 786, 729, 671, 648, 614, 599, 555, 537, 515
25d	*p*-F	33	202,5 – 204,0	$C_{24}H_{22}FN_3O_2$ (403,46)	404,2 $[M+1]^+$	3664, 3583, 3438, 3207, 3083, 2985, 2938, 2756, 2723, 1656, 1622, 1601, 1545, 1508, 1471, 1449, 1416, 1390, 1370, 1345, 1292, 1256, 1223, 1203, 1181, 1163, 1141, 1098, 1045, 1018, 976, 944, 836, 741, 722, 644, 557, 530, 511
25e	*p*-Cl	53	245,0 (raspad)	$C_{24}H_{22}ClN_3O_2$ (419,91)	420,3 $[M+1]^+$ 422,3 $[M+1]^+$	3195, 3103, 3025, 2998, 2928, 2835, 1672, 1621, 1558, 1493, 1442, 1407, 1338, 1284, 1254, 1200, 1138, 1086, 1045, 977, 947, 799, 748, 708, 680, 634, 593, 550, 497
25f	*p*-OCH_3	41	216,0 – 217,5	$C_{25}H_{25}N_3O_3$ (415,49)	416,3 $[M+1]^+$	3212, 3102, 3040, 2993, 2973, 2940, 2919, 2840, 1667, 1620, 1604, 1558, 1514, 1474, 1443, 1409, 1382, 1338, 1306, 1283, 1254, 1229, 1198, 1173, 1138, 1096, 1033, 979, 949, 827, 801, 780, 731, 701, 684, 635, 592, 541, 521
25i	*m*-CF_3	44	220,5 – 222,5	$C_{25}H_{22}F_3N_3O_2$ (453,47)	454,2 $[M+1]^+$	3177, 2978, 2930, 1679, 1623, 1570, 1500, 1450, 1409, 1377, 1343, 1328, 1281, 1270, 1253, 1221, 1199, 1185, 1169, 1139, 1114, 1096, 1079, 1043, 1018, 991, 981, 803, 694, 659, 556, 530
25j	*p*-CF_3	45	252,0 – 254,5	$C_{25}H_{22}F_3N_3O_2$ (453,47)	454,3 $[M+1]^+$	3188, 3005, 2962, 2844, 1680, 1633, 1569, 1445, 1412, 1321, 1253, 1199, 1165, 1108, 1066, 974, 831, 801, 597, 573

25k	*o*-Cl	47	218,5 – 221,5	$C_{24}H_{22}ClN_3O_2$ (419,91)	420,1 $[M+1]^+$ 422,15 $[M+1]^+$	3285, 3081, 2970, 1741, 1650, 1616, 1556, 1498, 1469, 1454, 1440, 1406, 1380, 1338, 1305, 1228, 1199, 1178, 1138, 1120, 1102, 1092, 1047, 1036, 974, 948, 880, 819, 807, 767, 746, 709, 684, 664, 637, 614, 604, 594, 584, 550, 536, 511, 486
25l	*m*-Cl	83	210,5 – 213,0	$C_{24}H_{22}ClN_3O_2$ (419,91)	420,05 $[M+1]^+$ 422,05 $[M+1]^+$	3182, 2934, 2975, 1743, 1680, 1622, 1592, 1567, 1499, 1450, 1410, 1377, 1345, 1305, 1281, 1228, 1252, 1197, 1171, 1138, 1125, 1107, 1043, 1018, 910, 893, 862, 825, 812, 799, 788, 730, 672, 649, 636, 614, 599, 576, 556, 545, 529
25m	*m*-OCF_3	81	204,5 – 207,0	$C_{25}H_{22}F_3N_3O_3$ (469,46)	470,1 $[M+1]^+$	3200, 2981, 2901, 1740, 1675, 1623, 1563, 1497, 1472, 1452, 1410, 1383, 1364, 1340, 1308, 1263, 1254, 1199, 1177, 1107, 1096, 1047, 1024, 991, 978, 948, 938, 881, 827, 802, 787, 698, 670, 633, 605, 596, 569, 528, 550
25n	*p*-Br	64	250,0 – 252,5	$C_{24}H_{22}BrN_3O_2$ (464,36)	464,05 $[M+1]^+$, 466,0 $[M+1]^+$	3292, 1742, 1653, 1621, 1589, 1562, 1548, 1488, 1468, 1455, 1440, 1428, 1404, 1375, 1335, 1280, 1251, 1227, 1198, 1138, 1121, 1101, 1084, 1045, 1024, 1013, 975, 946, 868, 847, 818, 811, 753, 734, 705, 670, 642, 631, 601, 589, 549, 519, 506, 469
25o	*p*-CH_3	70	216,5 – 219,5	$C_{25}H_{25}N_3O_2$ (399,49)	400,15 $[M+1]^+$	3208, 3021, 2904, 1734, 1672, 1622, 1559, 1516, 1499, 1409, 1381, 1340, 1323, 1307, 1283, 1255, 1230, 1200, 1178, 1138, 1123, 1096, 1025, 1046,

						980, 948, 865, 832, 812, 803, 723, 703, 681, 635, 603, 593, 552, 516, 498
25p	*p*-NO_2	62	275,0 – 278,0	$C_{24}H_{22}N_4O_4$ (430,46)	431,1 $[M+1]^+$	3184, 3011, 1739, 1669, 1622, 1592, 1555, 1508, 1473, 1446, 1409, 1382, 1363, 1333, 1254, 1225, 1197, 1176, 1119, 1139, 1092, 1044, 980, 846, 822, 799, 754, 739, 705, 671, 632, 601, 591, 548, 512

[a] Spojevi **25a-f** - IR (ATR); Spojevi **25i-p** - IR (KBr)

Kemijski pomaci protona u ^{1}H, odnosno ugljika u ^{13}C NMR spektrima harmicina amidnoga tipa **19a-h**, **22a-h**, **25a-f**, **i-p** u skladu su s predloženim strukturama.

- Budući da susjedni C atomi (C-11 i C-9) nemaju za sebe vezan niti jedan proton, signali za indolski proton (H-10) se u ^{1}H spektrima harmicina **19a-h** i **22a-h** vide kao singleti s relativnim integralom 1H na sljedećim kemijskim pomacima: **19a**, 11,39 ppm; **19b**, 11,38 ppm; **19c**, 11,40 ppm; **19d**, 11,41 ppm; **19e**, 11,40 ppm; **19f**, 11,40 ppm; **19g**, 11,39 ppm; **19h**, 11,41 ppm; **22a**, 11,66 ppm; **22b**, 11,47 ppm; **22c**, 11,48 ppm; **22d**, 11,47 ppm; **22e**, 11,68 ppm; **22f**, 11,46 ppm; **22g**, 11,47 ppm; **22h**, 11,52 ppm. Signal za H-10 (indolski) proton nije prisutan u spektrima harmicina **25a-f**, **i-p** zbog derivatizacije položaja N-9.
- Signal za protone amidne veze H-3' je zbog sprezanja sa susjednim H-2' protonima u svim ^{1}H spektrima vidljiv kao triplet, a nalazi se u rasponu kemijskih pomaka od 8,34 – 8,60 ppm s pripadajućim konstantama sprege u rasponu od 5,2 Hz do 6,1 Hz.
- Konstante sprega protona *trans* veze H-5' i H-6' u skladu su s teorijskim podacima i iznose J = 15,8 Hz, odn. 15,7 Hz za spoj **25k**, 15,9 Hz za spojeve **19a**,**d** i 16,0 Hz za spoj **22g**.
- Signal za protone metilne skupine H-13 s relativnim integralom od 3H vidljiv je u svim ^{1}H spektrima harmicina **19a-h** kao singlet na kemijskom pomaku od 2,74 ppm (**19a**,**b**,**f**,**g**), odn. 2,75 ppm (**19c-e**, **19h**).
- Signal na kemijskom pomaku od 2,04 ppm s relativnim integralom od 3H u ^{1}H spektru spoja **22h** odgovara signalu za protone α-metilne skupine H-13'.
- Unatoč prisutnosti jednog H-3' i dva H-1' susjednih protona signal za protone H-2' je u svim ^{1}H spektrima vidljiv kao kvartet.

- Signal za karbonilni ugljikov atom amidne veze C-4' je vidljiv u svim ^{13}C spektrima u rasponu kemijskih pomaka od 165 – 166 ppm, izuzev spoja **22h** čiji se signal nalazi na 169,16 ppm.
- Signal za ugljikov atom metilne skupine C-13 se u svim ^{13}C spektrima harmicina **19a-h** javlja na kemijskom pomaku od 20 ppm (**19a**, 20,20 ppm; **19b**, 20,34 ppm; **19c**, 20,27 ppm; **19d**, 20,27 ppm; **19e**, 20,28 ppm; **19f**, 20,29 ppm; **19g**, 20,33 ppm; **19h**, 20,25 ppm).
- Signali za C-6 i C-12 atome se u ^{13}C spektrima spojeva **19a**,**b** javljaju na vrlo bliskim pomacima s razlikom od 0,02 ppm, dok su u spektrima spojeva **19c-h** vidljivi na istom kemijskom pomaku (**19c-f**, 112,76 ppm; **19g**, 112,74 ppm; **19h**, 112,78 ppm).
- Signal za ugljikov atom α-CH_3 skupine je u ^{13}C spektru spoja **22h** uočen na 14,30 ppm.
- Također su u ^{13}C spektrima prisutna cijepanja signala ugljikovih atoma s fluorom. U spektrima harmicina **19b**, **19e**, **22b**, **22d**, **22g**, **25b** i **25d**, koji u svojoj strukturi sadrže atom fluora, signali ugljikovih atoma koji se sprežu s fluorom vidljivi su kao dubleti, dok se u spektrima spojeva **19d**, **19h**, **25i**, **25j** i **25m** koji u svojoj strukturi sadrže CF_3 skupinu, sprežu u kvartet.
- Signali za ugljikove atome spojeva **19b**, **22b** i **25b** za koje je izravno vezan atom fluora (C-9') nalaze se na kemijskom pomaku od 162,5 ppm s pripadajućim konstantama sprege od 243,8 Hz, dok se u ^{13}C spektrima spojeva **19e**, **22d** i **25d** signal za C-10' atom za koji je izravno vezan atom fluora nalazi na 162,7 ppm (**19e**, **22d**) odn. 162,8 ppm (**25d**) s pripadajućim konstantama sprege od 247 Hz. Signal za C-8' atom u spektru spoja **22g**, koji u svojoj strukturi sadrži *o*-F-supstituiranu cimetnu kiselinu, nalazi se na kemijskom pomaku od 160,49 ppm s konstantom sprege od 250,4 Hz.
- Signali za ugljikove atome za koje su izravno vezani atomi fluora u spektrima spojeva **19d**, **19h**, **25i**, **25j** (C-13') nalaze na nižim kemijskim pomacima od 124 ppm, ali su sprezanja jača (J = 272 – 274 Hz). Signal za C-13' atom se u ^{13}C spektru spoja **25m**, koji u svojoj strukturi zadrži *m*-OCF_3-supstituiranu cimetnu kiselinu, nalazi na kemijskom pomaku od 120 ppm s pripadajućom konstantom sprege od 231 Hz.
- C-F sprezanja kroz dvije kovalentne veze uočena su u ^{13}C spektrima spojeva **19b**, **22b** i **25b**, a vidljiva su na kemijskim pomacima od 116 ppm (C-10') i 113,9 ppm (C-8') s pripadajućim konstantama sprege od 21,3 Hz (C-10') odn. 21,8 Hz (C-8'). Atomi C-9' i C-11' spojeva **19e**, **22d** i **25d**, koji u svojoj strukturi sadrže *p*-F-supstituiranu cimetnu kiselinu, kemijski su ekvivalentni stoga je njihov signal u ^{13}C spektrima vidljiv na kemijskom pomaku od 115,9 ppm, a s atomom fluora sprežu se s konstantom sprege od

21,7 Hz. Također se u ^{13}C spektru spoja **22g**, koji u svojoj strukturi sadrži *o*-F-supstituiranu cimetnu kiselinu, vide C-F sprezanja kroz dvije kovalentne veze, a nalaze se na sljedećim kemijskim pomacima: 122,53 ppm (C-7') i 116,11 ppm (C-9') s pripadajućim konstantama sprege od 11,5 Hz i 21,8 Hz.

- U ^{13}C spektrima spojeva koji sadrže *m*-CF_3- (**19d**, **25i**) i *p*-CF_3-supstituiranu cimetnu kiselinu (**19h**, **25j**) također su vidljiva sprezanja kroz dvije kovalentne veze te se tako u spektrima spojeva **19d** i **25i** signali za C-9' atom nalaze na kemijskom pomaku od 129,7 ppm s pripadajućim konstantama sprege od 32 Hz, a u spektrima spojeva **19h** i **25j** se signali za C-10' atom nalaze na kemijskim pomacima od 129,2 ppm (**19h**), odn. 129,3 ppm (**25j**) s konstantama sprezanja 32 Hz.
- Sprezanja signala ugljikovih atoma s fluorom u ^{13}C spektrima spojeva **19b**, **22b** i **25b** vidljiva su kroz tri kovalentne veze te se signali za C-11' atom nalazi na kemijskom pomaku od 130,89 ppm s izračunatim konstantama sprege od 8,4 Hz (**19b**, **22b**), dok su u ^{13}C spektru spoja **25b** vidljiva sprezanja atoma C-7' i C-11' s atomom fluora kroz tri kovalentne veze, a nalaze se na kemijskom pomaku od 137,36 ppm (C-7') s izračunatom konstantom sprege od 7,9 Hz, te 130,91 ppm (C-11') s konstantom sprege J = 8,4 Hz.
- U ^{13}Cspektrima spojeva **19e** i **22d**, koji u svojoj strukturi sadrže *p*-F-supstituiranu kiselinu, sprezanja kroz tri kovalentne veze vidljiva su na kemijskom pomaku od 129,7 ppm s konstantama sprege od 8,4 Hz, a odgovaraju ekvivalentnim C-8' i C-12' atomima, dok su u spektru spoja **25d** vidljiva na kemijskom pomaku od 129,8 ppm s konstantom sprege od 8,3 Hz.
- U spektru spoja koji sadrži *o*-F-supstituiranu cimetnu kiselinu u svojoj strukturi (**22g**) uočena su sprezanja signala ugljikovih atoma kroz tri (C-10') i četiri (C-11') kovalentne veze, a nalaze se na kemijskim pomacima od 124,88 ppm (C-10') s konstantom sprege 6,1 Hz te 129,13 ppm (C-11') s konstantom sprege 3,0 Hz.
- Sprezanja C atoma s atomima fluora CF_3 skupine kroz tri kovalentne veze vidljiva su u spektru spoja **19d**, a nalaze se na kemijskim pomacima 125,73 ppm (C-10') i 123,88 ppm (C-8') s izračunatim konstantama sprege od 3,0 Hz, dok su u spektru spoja **25i** vidljiva na kemijskim pomacima 125,86 ppm (C-10') i 124,06 ppm (C-8') s izračunatim konstantama sprege od 3,6 Hz. Atomi C-9' i C-11' spojeva **19h** i **25j**, koji u svojim strukturama sadrže *p*-CF_3-supstituiranu cimetnu kiselinu, kemijski su ekvivalenti i nalaze se na pomaku od 125,8 ppm, a pripadajuće konstante sprezanja iznose 3,0 Hz (**19h**), odn. 3,5 Hz (**25j**).

- Sprezanja signala ugljikovih atoma s atomima fluora kroz dvije ili tri kovalentne veze u ^{13}C spektru spoja **25m**, koji u svojoj strukturi sadrži *m*-OCF_3-supstituiranu cimetnu kiselinu, nisu uočena.
- Sprege dalekog dosega, kroz četiri kovalentne veze, uočene su u spektrima spojeva koji u svojim strukturama sadrže *p*-F-supstituiranu cimetnu kiselinu **19e**, **22d** i **25d**, pri čemu se signal za atom C-7' nalazi na 131,53 ppm, a izračunata konstanta sprege iznosi $^4J_{CF}$ = 2,6 Hz (**19e**), odn. 2,7 Hz (**22d**), dok se taj signal u spektru spoja **25d** nalazi na 131,38 ppm, a izračunata konstanta sprege iznosi 2,5 Hz. Zatim se u spektru spoja **22g** (*o*-F cimetna kiselina) signal za C-5' atom spreže s fluorom s konstantom sprege $^4J_{CF}$ = 2,6 Hz, a nalazi se na kemijskom pomaku od 125,02 ppm.

^{1}H i ^{13}C spektroskopski podaci harmicina **19a-h**, **22a-h** i **25a-f**, **i-p** nalaze se u Tablicama 15 – 17.

Tablica 15. ^{1}H i ^{13}C NMR spektroskopski podaci harmicina amidnoga tipa **19a-h**

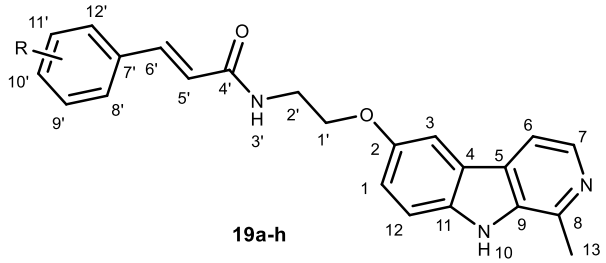

Spoj	R	^{1}H NMR (DMSO-d_6, δ ppm, J/Hz)	^{13}C NMR (DMSO-d_6, δ ppm)
19a	H	11,39 (s, 1H, 10), 8,45 (t, 1H, 3', J = 5,6 Hz), 8,16 (d, 1H, 7, J = 5,3 Hz), 7,91 (d, 1H, 6, J = 5,3 Hz), 7,81 (d, 1H, 3, J = 2,5 Hz), 7,57 (d, 2H, 8', 12', J = 7,3 Hz), 7,53 – 7,46 (m, 2H, 6', 12), 7,44 – 7,36 (m, 3H, 9', 10', 11'), 7,22 (dd, 1H, 1, J = 8,9, 2,6 Hz), 6,73 (d, 1H, 5', J = 15,9 Hz), 4,17 (t, 2H, 1', J = 5,6 Hz), 3,64 (q, 2H, 2', J = 5,6 Hz), 2,74 (s, 3H, 13)	165,27 (4'), 152,37 (2), 142,04 (8), 138,83 (6'), 136,54 (7), 135,46 (11), 135,03 (9), 134,89 (7'), 129,45 (10'), 128,93 (9', 11'), 127,52 (8', 12'), 126,90 (4), 122,07 (5'), 121,37 (5), 118,43 (1), 112,79 (6), 112,77 (12), 104,73 (3), 67,12 (1'), 38,67 (2'), 20,20 (13)
19b	*m*-F	11,38 (s, 1H, 10), 8,46 (t, 1H, 3', J = 5,5 Hz), 8,16 (d, 1H, 7, J = 5,4 Hz), 7,91 (d, 1H, 6, J = 5,3 Hz), 7,80 (d, 1H, 3, J = 2,4 Hz), 7,51 (d, 1H, 12, J = 8,9 Hz), 7,50 – 7,40 (m, 4H, 1, 6', 11', 12'), 7,24 – 7,19 (m, 2H, 8', 10'), 6,77 (d, 1H, 5', J = 15,8 Hz), 4,17 (t, 2H, 1', J = 5,5 Hz), 3,64 (q, 2H, 2', J = 5,5 Hz), 2,74 (s, 3H, 13)	164,99 (4'), 162,45 (d, 9', J = 243,8 Hz), 152,32 (2), 142,15 (8), 137,54 (6'), 137,49 (7'), 136,83 (7), 135,37 (11), 135,07 (9), 130,89 (d, 11', J = 8,4 Hz), 126,76 (4), 123,68 (5'), 123,65 (12'), 121,40 (5), 118,29 (1), 116,11 (d, 10', J = 21,2 Hz) 113,93 (d, 8', J = 21,8 Hz), 112,74 (6), 112,72 (12), 104,73 (3), 67,07 (1'), 38,71 (2'), 20,34 (13)

19c	*m*-Br	11,40 (s, 1H, 10), 8,43 (t, 1H, 3', *J* = 5,5 Hz), 8,16 (d, 1H, 7, *J* = 5,4 Hz), 7,92 (d, 1H, 6, *J* = 5,4 Hz), 7,81 (d, 1H, 3, *J* = 2,3 Hz), 7,79 (t, 1H, 8', *J* = 1,8 Hz), 7,59 – 7,56 (m, 2H, 10', 11'), 7,52 (d, 1H, 12, *J* = 8,8 Hz), 7,45 (d, 1H, 6', *J* = 15,8 Hz), 7,38 (t, 1H, 12', *J* = 7,9 Hz), 7,22 (dd, 1H, 1, *J* = 8,8, 2,4 Hz), 6,78 (d, 1H, 5', *J* = 15,8 Hz), 4,17 (t, 2H, 1', *J* = 5,5 Hz), 3,64 (q, 2H, 2', *J* = 5,4 Hz), 2,75 (s, 3H, 13)	164,92 (4'), 152,33 (2), 142,09 (8), 137,50 (7'), 137,19 (6'), 136,68 (7), 135,42 (11), 135,05 (9), 131,97 (8'), 131,02 (10'), 130,04 (11'), 126,83 (4), 126,40 (12'), 123,76 (5'), 122,25 (9'), 121,38 (5), 118,37 (1), 112,76 (6, 12), 104,74 (3), 67,08 (1'), 38,71 (2'), 20,27 (13)
19d	$^{13'}$*m*-CF_3	11,41 (s, 1H, 10), 8,46 (t, 1H, 3', *J* = 5,6 Hz), 8,16 (d, 1H, 7, *J* = 5,4 Hz), 7,93 – 7,88 (m, 3H, 3, 6, 12'), 7,81 (d, 1H, 8', *J* = 2,6 Hz), 7,73 (d, 1H, 10', *J* = 7,8 Hz), 7,66 (t, 1H, 11', *J* = 7,8 Hz), 7,57 (d, 1H, 6', *J* = 15,8 Hz), 7,52 (d, 1H, 12, *J* = 8,8 Hz), 7,22 (dd, 1H, 1, *J* = 8,8, 2,5 Hz), 6,88 (d, 1H, 5', *J* = 15,9 Hz), 4,18 (t, 2H, 1', *J* = 5,5 Hz), 3,65 (q, 2H, 2', *J* = 5,6 Hz), 2,75 (s, 3H, 13)	164,88 (4'), 152,34 (2), 142,10 (8), 137,14 (6'), 136,69 (7), 136,13 (11), 135,43 (7'), 135,06 (9), 131,30 (12'), 130,06 (11'), 129,73 (q, 9', *J* = 32,3 Hz), 126,83 (4), 125,73 (q, 10', *J* = 3,0 Hz), 124,23 (5'), 124,04 (q, 13', *J* = 273,7 Hz), 123,88 (q, 8', *J* = 3,0 Hz), 121,38 (5), 118,37 (1), 112,76 (6, 12), 104,74 (3), 67,09 (1'), 38,74 (2'), 20,27 (13)
19e	*p*-F	11,40 (s, 1H, 10), 8,43 (t, 1H, 3', *J* = 5,4 Hz), 8,16 (d, 1H, 7, *J* = 5,4 Hz), 7,92 (d, 1H, 6, *J* = 5,3 Hz), 7,81 (d, 1H, 3, *J* = 2,2 Hz), 7,66 – 7,62 (m, 2H, 8', 12'), 7,53 – 7,46 (m, 2H, 6', 12), 7,28 – 7,21 (m, 3H, 1, 9', 11'), 6,68 (d, 1H, 5', *J* = 15,8 Hz), 4,17 (t, 2H, 1', *J* = 5,5 Hz), 3,64 (q, 2H, 2', *J* = 5,4 Hz), 2,75 (s, 3H, 13)	165,21 (4'), 162,68 (d, 10', *J* = 247,0 Hz), 152,35 (2), 142,10 (8), 137,65 (6'), 136,71 (7), 135,41 (11), 135,05 (9), 131,53 (d, 7', *J* = 2,6 Hz), 129,68 (d, 8', 12', *J* = 8,4 Hz), 126,82 (4), 121,97 (5'), 121,39 (5), 118,36 (1), 115,90 (d, 9', 11', *J* = 21,7 Hz), 112,76 (6, 12), 104,72 (3), 67,11 (1'), 38,68 (2'), 20,28 (13)
19f	*p*-Cl	11,40 (s, 1H, 10), 8,46 (t, 1H, 3', *J* = 5,3 Hz), 8,16 (d, 1H, 7, *J* = 5,3 Hz), 7,91 (d, 1H, 6, *J* = 5,3 Hz), 7,80 (d, 1H, 3, *J* = 2,0 Hz), 7,60 (d, 2H, 8', 12', *J* = 8,4 Hz), 7,51 (d, 1H, 12, *J* = 8,9 Hz), 7,49 – 7,45 (m, 3H, 6', 9', 11'), 7,22 (dd, 1H, 1, *J* = 8,8, 2,3 Hz), 6,73 (d, 1H, 5', *J* = 15,8 Hz), 4,17 (t, 2H, 1', *J* = 5,4 Hz), 3,64 (q, 2H, 2', *J* = 5,3 Hz), 2,74 (s, 3H, 13)	165,08 (4'), 152,33 (2), 142,11 (8), 137,49 (6'), 136,72 (7), 135,41 (11), 135,05 (9), 133,87 (7', 10'), 129,22 (8', 12'), 128,97 (9', 11'), 126,81 (4), 122,88 (5'), 121,39 (5), 118,35 (1), 112,76 (6, 12), 104,73 (3), 67,09 (1'), 38,70 (2'), 20,29 (13)
19g	$^{13'}$*p*-OCH_3	11,39 (s, 1H, 10), 8,34 (t, 1H, 3', *J* = 5,5 Hz), 8,16 (d, 1H, 7, *J* = 5,4 Hz), 7,91 (d, 1H, 6, *J* = 5,3 Hz), 7,80 (d, 1H, 3, *J* = 2,4 Hz), 7,53 – 7,50 (m, 3H, 12, 8', 12'), 7,43 (d, 1H, 6', *J* = 15,8 Hz), 7,22 (dd, 1H, 1, *J* = 8,8, 2,5 Hz), 6,98 (d, 2H, 9', 11', *J* = 8,8 Hz), 6,58 (d, 1H, 5', *J* = 15,8 Hz), 4,16 (t, 2H, 1', *J* = 5,6 Hz), 3,79 (s, 3H, 13'), 3,63 (q, 2H, 2', *J* = 5,5 Hz), 2,74 (s, 3H, 13)	165,59 (4'), 160,32 (10'), 152,35 (2), 142,13 (8), 138,54 (6'), 136,80 (7), 135,37 (11), 135,06 (9), 129,09 (8', 12'), 127,45 (7'), 126,77 (4), 121,40 (5), 119,58 (5'), 118,30 (1), 114,38 (9', 11'), 112,74 (6, 12), 104,71 (3), 67,16 (1'), 55,24 (13'), 38,63 (2'), 20,33 (13)
19h	$^{13'}$*p*-CF_3	11,41 (s, 1H, 10), 8,54 (t, 1H, 3', *J* = 5,5 Hz), 8,16 (d, 1H, 7, *J* = 5,3 Hz), 7,92 (d, 1H, 6, *J* = 5,3 Hz), 7,81 – 7,76 (m, 5H, 3, 8', 9', 11', 12'), 7,57 – 7,51 (m, 2H, 6', 12), 7,22 (dd, 1H, 1, *J* = 8,9, 2,5 Hz), 6,86 (d, 1H, 5', *J* = 15,8 Hz), 4,18 (t, 2H, 1', *J* = 5,5 Hz), 3,65 (q, 2H, 2', *J* = 5,4 Hz), 2,75 (s, 3H, 13)	164,82 (4'), 152,34 (2), 142,09 (8), 139,00 (7'), 137,19 (6'), 136,65 (7), 135,44 (11), 135,05 (9), 129,20 (q, 10', *J* = 32,3 Hz), 128,16 (8', 12'), 126,85 (4), 125,80 (q, 9', 11', *J* = 3,0 Hz), 124,87 (5'), 124,11 (q, 13', *J* = 272,7 Hz), 121,38 (5), 118,39 (1), 112,78 (6, 12), 104,74 (3), 67,06 (1'), 38,75 (2'), 20,25 (13)

Tablica 16. ^{1}H i ^{13}C NMR spektroskopski podaci harmicina amidnoga tipa **22a-h**

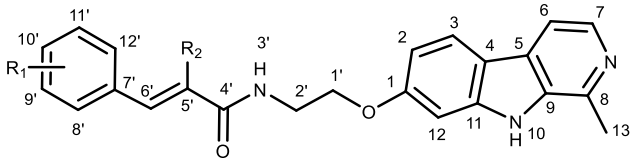

22a-h

Spoj	R_1	R_2	^{1}H NMR (DMSO-d_6, δ ppm, J/Hz)	^{13}C NMR (DMSO-d_6, δ ppm)
22a	H	H	11,66 (s, 1H, 10), 8,47 (t, 1H, 3', J = 5,3 Hz), 8,19 (d, 1H, 7, J = 5,4 Hz), 8,11 (d, 1H, 3, J = 8,7 Hz), 7,90 (d, 1H, 6, J = 5,4 Hz), 7,57 (d, 2H, 8', 12', J = 7,0 Hz), 7,48 (d, 1H, 6', J = 15,8 Hz), 7,45 – 7,36 (m, 3H, 9', 10', 11'), 7,07 (d, 1H, 12, J = 1,8 Hz), 6,91 (dd, 1H, 2, J = 8,7, 2,0 Hz), 6,73 (d, 1H, 5', J = 15,8 Hz), 4,20 (t, 2H, 1', J = 5,4 Hz), 3,65 (q, 2H, 2' J = 5,3 Hz), 2,77 (s, 3H, 13)	165,30 (4'), 159,53 (1), 142,39 (8), 140,71 (11), 138,88 (6'), 136,38 (7), 134,88 (9), 134,46 (7'), 129,47 (10'), 128,93 (9', 11'), 127,90 (5), 127,53 (8', 12'), 122,96 (3), 122,03 (5'), 114,85 (4), 112,26 (6), 109,81 (2), 95,40 (12), 66,70 (1'), 38,52 (2'), 19,67 (13)
22b	*m*-F	H	11,47 (s, 1H, 10), 8,47 (t, 1H, 3', J = 5,5 Hz), 8,16 (d, 1H, 7, J = 5,3 Hz), 8,08 (d, 1H, 3, J = 8,7 Hz), 7,83 (d, 1H, 6, J = 5,3 Hz), 7,50 – 7,40 (m, 4H, 6', 8', 11', 12'), 7,24 – 7,19 (m 1H, 10'), 7,05 (d, 1H, 12, J = 2,1 Hz), 6,89 (dd, 1H, 2, J = 8,7, 2,2 Hz), 6,77 (d, 1H, 5', J = 15,8 Hz), 4,19 (t, 2H, 1', J = 5,4 Hz), 3,65 (q, 2H, 2', J = 5,4 Hz), 2,74 (s, 3H, 13)	165,01 (4'), 162,45 (d, 9', J = 243,8 Hz), 159,23 (1), 141,98 (8), 141,17 (11), 137,60 (6'), 137,48 (7'), 137,43 (7), 134,55 (9), 130,89 (d, 11', J = 8,4 Hz), 127,34 (5), 123,66 (12'), 123,61 (3), 122,73 (5'), 116,13 (d, 10', J = 21,3 Hz), 115,01 (4), 113,93 (d, 8', J = 21,8 Hz), 112,02 (6), 109,43 (2), 95,43 (12), 66,63 (1'), 38,59 (2'), 20,18 (13)
22c	*m*-Br	H	11,48 (s, 1H, 10), 8,44 (t, 1H, 3', J = 5,5 Hz), 8,16 (d, 1H, 7, J = 5,3 Hz), 8,08 (d, 1H, 3, J = 8,7 Hz), 7,83 (d, 1H, 6, J = 5,3 Hz), 7,79 (t, 1H, 8', J = 1,5 Hz), 7,60 – 7,56 (m, 2H, 10', 12'), 7,45 (d, 1H, 6', J = 15,8 Hz), 7,38 (t, 1H, 11', J = 7,9 Hz), 7,05 (d, 1H, 12, J = 2,1 Hz), 6,89 (dd, 1H, 2, J = 8,7, 2,2 Hz), 6,78 (d, 1H, 5', J = 15,8 Hz), 4,19 (t, 2H, 1', J = 5,4 Hz), 3,65 (q, 2H, 2', J = 5,4 Hz), 2,74 (s, 3H, 13)	164,94 (4'), 159,22 (1), 141,99 (8), 141,15 (11), 137,48 (7'), 137,40 (6'), 137,23 (7), 134,54 (9), 131,98 (8'), 131,02 (10'), 130,05 (11'), 127,35 (5), 126,41 (12'), 123,73 (3), 122,73 (5'), 122,25 (9'), 115,00 (4), 112,02 (6), 109,43 (2), 95,43 (12), 66,63 (1'), 38,58 (2'), 20,17 (13)
22d	*p*-F	H	11,47 (s, 1H, 10), 8,44 (t, 1H, 3', J = 5,5 Hz), 8,16 (d, 1H, 7, J = 5,3 Hz), 8,08 (d, 3, 1H, J = 8,7 Hz), 7,83 (d, 1H, 6, J = 5,3 Hz), 7,66 – 7,62 (m, 2H, 8', 12'), 7,48 (d, 1H, 6', J = 15,8 Hz), 7,28 – 7,23 (m, 2H, 9', 11'), 7,05 (d, 1H, 12, J = 2,1 Hz), 6,89 (dd, 1H, 2, J = 8,7, 2,2 Hz), 6,68 (d, 1H, 5', J = 15,8 Hz), 4,19 (t, 2H, 1', J = 5,5	165,24 (4'), 162,70 (d, 10', J = 247,1 Hz), 159,24 (1), 141,99 (8), 141,17 (11), 137,70 (6'), 137,44 (7), 134,55 (9), 131,53 (d, 7', J = 2,7 Hz), 129,69 (d, 8', 12', J = 8,4 Hz), 127,35 (5), 122,74 (3), 121,93 (5'), 115,91 (d, 9', 11', J = 21,7 Hz), 115,00 (4), 112,02 (6), 109,44 (2),

			Hz), 3,65 (q, 2H, 2', *J* = 5,4 Hz), 2,74 (s, 3H, 13).	95,43 (12), 66,67 (1'), 38,56 (2'), 20,19 (13)
22e	*p*-Cl	H	11,68 (s, 1H, 10), 8,49 (t, 1H, 3', *J* = 5,5 Hz), 8,19 (d, 1H, 7, *J* = 5,5 Hz), 8,11 (d, 1H, 3, *J* = 8,7 Hz), 7,91 (d, 1H, 6, *J* = 5,4 Hz), 7,60 (d, 2H, 9', 11', *J* = 8,5 Hz), 7,49 – 7,45 (m, 3H, 6', 8', 12'), 7,07 (d, 1H, 12, *J* = 2,1 Hz), 6,91 (dd, 1H, 2, *J* = 8,7, 2,2 Hz), 6,74 (d, 1H, 5', *J* = 15,8 Hz), 4,20 (t, 2H, 1', *J* = 5,4 Hz), 3,65 (q, 2H, 2', *J* = 5,4 Hz), 2,77 (s, 3H, 13)	165,10 (4'), 159,54 (1), 142,41 (8), 140,67 (11), 137,52 (6'), 136,30 (7), 134,45 (9), 133,88 (10'), 133,85 (7'), 129,23 (9', 11'), 128,96 (8', 12'), 127,93 (5), 122,97 (3), 122,84 (5'), 114,85 (4), 112,27 (6), 109,82 (2), 95,39 (12), 66,67 (1'), 38,54 (2'), 19,64 (13)
22f	$^{13'}$ *p*-OCH_3	H	11,46 (s, 1H, 10), 8,35 (t, 1H, 3', *J* = 5,5 Hz), 8,16 (d, 1H, 7, *J* = 5,3 Hz), 8,07 (d, 1H, 3, *J* = 8,7 Hz), 7,83 (d, 1H, 6, *J* = 5,3 Hz), 7,52 (d, 2H, 8', 12', *J* = 8,8 Hz), 7,43 (d, 1H, 6', *J* = 15,8 Hz), 7,05 (d, 1H, 12, *J* = 2,1 Hz), 6,98 (d, 2H, 9', 11', *J* = 8,8 Hz), 6,89 (dd, 1H, 2, *J* = 8,7, 2,2 Hz), 6,58 (d, 1H, 5', *J* = 15,8 Hz), 4,18 (t, 2H, 1', *J* = 5,5 Hz), 3,79 (s, 3H, 13'), 3,64 (q, 2H, 2', *J* = 5,4 Hz), 2,73 (s, 3H, 13)	165,61 (4'), 160,34 (10'), 159,24 (1), 141,97 (8), 141,19 (11), 138,59 (6'), 137,49 (7), 134,55 (9), 129,11 (9', 11'), 127,44 (7'), 127,32 (5), 122,72 (3), 119,53 (5'), 115,00 (4), 114,39 (8', 12'), 112,01 (6), 109,42 (2), 95,42 (12), 66,71 (1'), 55,25 (13'), 38,51 (2'), 20,22 (13)
22g	*o*-F	H	11,47 (s, 1H, 10), 8,60 (t, 1H, 3', *J* = 5,4 Hz), 8,15 (d, 1H, 7, *J* = 5,3 Hz), 8,07 (d, 1H, 3, *J* = 8,6 Hz), 7,81 (d, 1H, 6, *J* = 5,3 Hz), 7,69 – 7,64 (m, 1H, 9'), 7,55 (d, 1H, 6', *J* = 16,0 Hz), 7,47 – 7,41 (m, 1H, 10'), 7,31 – 7,24 (m, 2H, 11', 12'), 7,06 (d, 1H, 12, *J* = 2,0 Hz), 6,88 (dd, 1H, 2, *J* = 8,7, 2,1 Hz), 6,84 (d, 1H, 5', *J* = 16,0 Hz), 4,19 (t, 2H, 1', *J* = 5,4 Hz), 3,65 (q, 2H, 2', *J* = 5,4 Hz), 2,73 (s, 3H, 13)	165,08 (4'), 160,49 (d, 8', *J* = 250,4 Hz), 159,15 (1), 141,90 (8), 141,35 (11), 137,75 (6'), 134,61 (9), 131,39 (7), 131,26 (12'), 129,13 (d, 11' *J* = 3,0 Hz), 127,19 (5), 125,02 (d, 5', *J* = 2,6 Hz), 124,88 (d, 10', *J* = 6,1 Hz), 122,68 (3), 122,53 (d, 7', *J* = 11,5 Hz), 116,11 (d, 9', *J* = 21,8 Hz), 115,06 (4), 111,97 (6), 109,34 (2), 95,47 (12), 66,60 (1'), 38,64 (2'), 20,38 (13)
22h	H	$^{13'}$ CH_3	11,52 (s, 1H, 10), 8,33 (t, 1H, 3', *J* = 5,3 Hz), 8,17 (d, 1H, 7, *J* = 5,2 Hz), 8,09 (d, 1H, 3, *J* = 8,6 Hz), 7,85 (d, 1H, 6, *J* = 5,1 Hz), 7,43 – 7,36 (m, 4H, 8', 9', 11', 12'), 7,33 – 7,30 (m, 1H, 10'), 7,26 (s, 1H, 6'), 7,07 (s, 1H, 12), 6,90 (d, 1H, 2, *J* = 8,4 Hz), 4,22 (t, 2H, 1', *J* = 5,2 Hz), 3,63 (q, 2H, 2', *J* = 5,4 Hz), 2,75 (s, 3H, 13), 2,04 (s, 3H, 13')	169,16 (4'), 159,43 (1), 142,13 (8), 141,01 (11), 137,11 (7), 136,03 (9), 134,53 (7'), 132,51 (6'), 132,29 (5'), 129,22 (9', 11'), 128,41 (8', 12'), 127,71 (10'), 127,54 (5), 122,80 (3), 114,94 (4), 112,09 (6), 109,57 (2), 95,48 (12), 66,29 (1'), 38,97 (2'), 20,04 (13), 14,30 (13')

Tablica 17. ^{1}H i ^{13}C NMR spektroskopski podaci harmicina amidnoga tipa **25a-f**, **i-p**

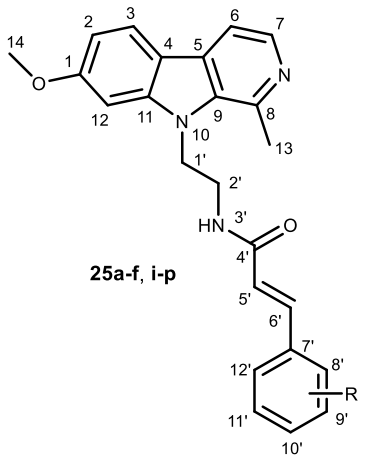

Spoj	R	^{1}H NMR (DMSO-d_6, δ ppm, J/Hz)	^{13}C NMR (DMSO-d_6, δ ppm)
25a	H	8,41 (t, 1H, 3', J = 5,9 Hz), 8,18 (d, 1H, 7, J = 5,2 Hz), 8,09 (d, 1H, 3, J = 8,6 Hz), 7,88 (d, 1H, 6, J = 5,2 Hz), 7,57 – 7,55 (m, 2H, 8', 12'), 7,48 – 7,36 (m, 4H, 6', 9'–11'), 7,27 (d, 1H, 12, J = 1,9 Hz), 6,87 (dd, 1H, 2, J = 8,6, 2,0 Hz), 6,54 (d, 1H, 5', J = 15,8 Hz), 4,67 (t, 2H, 1', J = 6,8 Hz), 3,90 (s, 3H, 14), 3,59 (q, 2H, 2', J = 6,5 Hz), 2,99 (s, 3H, 13)	165,73 (4'), 160,51 (1), 142,91 (8), 140,65 (11), 139,17 (6'), 137,86 (7), 134,75 (9), 134,65 (7'), 129,57 (10'), 128,95 (9', 11'), 128,47 (4), 127,58 (8', 12'), 122,38 (3), 121,66 (5'), 114,29 (5), 112,26 (6), 109,41 (2), 93,50 (12), 55,39 (14), 43,37 (1'), 39,11 (2'), 23,10 (13)
25b	*m*-F	8,42 (t, 1H, 3', J = 5,9 Hz), 8,18 (d, 1H, 7, J = 5,2 Hz), 8,09 (d, 1H, 3, J = 8,6 Hz), 7,89 (d, 1H, 6, J = 5,2 Hz), 7,49 – 7,40 (m, 4H, 6', 8', 11', 12'), 7,27 (d, 1H, 12, J = 2,0 Hz), 7,24 – 7,20 (m, 1H, 10'), 6,87 (dd, 1H, 2, J = 8,6, 2,1 Hz), 6,59 (d, 1H, 5', J = 15,8 Hz), 4,67 (t, 2H, 1', J = 6,9 Hz), 3,90 (s, 3H, 14), 3,59 (q, 2H, 2', J = 6,5 Hz), 2,99 (s, 3H, 13)	165,45 (4'), 162,46 (d, 9', J = 243,8 Hz), 160,52 (1), 142,92 (8), 140,63 (11), 137,90 (6'), 137,81 (7), 137,36 (d, 7', J = 7,9 Hz), 134,64 (9), 130,91 (d, 11', J = 8,4 Hz), 128,51 (4), 123,77 (12'), 123,21 (3), 122,41 (5'), 116,24 (d, 10', J = 21,3 Hz), 114,29 (5), 113,98 (d, 8', J = 21,8 Hz), 112,28 (6), 109,41 (2), 93,52 (12), 55,40 (14), 43,34 (1'), 39,11 (2') 23,06 (13)
25c	*m*-Br	8,39 (t, 1H, 3', J = 6,0 Hz), 8,18 (d, 1H, 7, J = 5,2 Hz), 8,09 (d, 1H, 3, J = 8,6 Hz), 7,89 (d, 1H, 6, J = 5,2 Hz), 7,77 (t, 1H, 8', J = 1,7 Hz), 7,57 (dd, 2H, 10', 12', J = 8,1, 1,4 Hz), 7,44 – 7,36 (m, 2H, 6', 11'), 7,26 (d, 1H, 12, J = 2,1 Hz), 6,87 (dd, 1H, 2, J = 8,6, 2,2 Hz), 6,59 (d, 1H, 5', J = 15,8 Hz), 4,67 (t, 2H, 1', J = 6,9 Hz), 3,90 (s, 3H, 14), 3,60 (q, 2H, 2', J = 6,5 Hz), 2,99 (s, 3H, 13)	165,40 (4'), 160,53 (1), 142,93 (8), 140,63 (11), 137,81 (6'), 137,58 (7), 137,33 (7'), 134,65 (9), 132,10 (8'), 131,05 (10'), 130,14 (11'), 128,53 (9'), 126,44 (12'), 123,32 (3), 122,42 (5'), 122,28 (4), 114,30 (5), 112,29 (6), 109,40 (2), 93,55 (12), 55,42 (14), 43,35 (1'), 39,11 (2'), 23,06 (13)

25d	*p*-F	8,40 (t, 1H, 3', *J* = 6,1 Hz), 8,19 (d, 1H, 7, *J* = 5,3 Hz), 8,11 (d, 1H, 3, *J* = 8,6 Hz), 7,92 (d, 1H, 6, *J* = 5,2 Hz), 7,62 (t, 2H, 8', 12', *J* = 6,9 Hz), 7,45 (d, 1H, 6', *J* = 15,8 Hz), 7,27 – 7,23 (m, 3H, 9', 11', 12), 6,88 (d, 1H, 2, *J* = 8,6 Hz), 6,49 (d, 1H, 5', *J* = 15,8 Hz), 4,67 (t, 2H, 1', *J* = 7,0 Hz), 3,90 (s, 3H, 14), 3,59 (q, 2H, 2', *J* = 6,7 Hz), 3,00 (s, 3H, 13)	165,70 (4'), 162,77 (d, 10', *J* = 247,0 Hz), 160,68 (1), 143,13 (8), 140,45 (11), 138,02 (6'), 137,35 (7), 134,59 (9), 131,38 (d, 7', *J* = 2,5 Hz), 129,78 (d, 8', 12', *J* = 8,3 Hz), 128,78 (4), 122,52 (3), 121,53 (5'), 115,94 (d, 9', 11', *J* = 21,7 Hz), 114,23 (5), 112,40 (6), 109,62 (2), 93,52 (12), 55,44 (14), 43,41 (1'), 39,10 (2'), 22,77 (13)
25e	*p*-Cl	8,41 (t, 1H, 3', *J* = 5,9 Hz), 8,17 (d, 1H, 7, *J* = 5,2 Hz), 8,09 (d, 1H, 3, *J* = 8,6 Hz), 7,88 (d, 1H, 6, *J* = 5,2 Hz), 7,60 – 7,58 (m, 2H, 8', 12'), 7,49 – 7,43 (m, 3H, 6', 9', 11'), 7,26 (d, 1H, 12, *J* = 2,0 Hz), 6,87 (dd, 1H, 2, *J* = 8,6, 2,1 Hz), 6,55 (d, 1H, 5', *J* = 15,8 Hz), 4,67 (t, 2H, 1', *J* = 6,8 Hz), 3,89 (s, 3H, 14), 3,59 (q, 2H, 2', *J* = 6,5 Hz), 2,99 (s, 3H, 13)	165,54 (4'), 160,51 (1), 142,91 (8), 140,64 (11), 137,84 (7, 6'), 134,65 (9), 134,00 (10'), 133,71 (7'), 129,30 (9',11'), 128,99 (8', 12'), 128,49 (4), 122,45 (3), 122,39 (5'), 114,29 (5), 112,27 (6), 109,40 (2), 93,51 (12), 55,40 (14), 43,35 (1'), 39,11 (2'), 23,08 (13)
25f	$^{13'}$*p*-OCH_3	8,31 (t, 1H, 3', *J* = 5,9 Hz), 8,17 (d, 1H, 7, *J* = 5,2 Hz), 8,09 (d, 1H, 3, *J* = 8,6 Hz), 7,88 (d, 1H, 6, *J* = 5,2 Hz), 7,51 (d, 2H, 8', 12', *J* = 8,8 Hz), 7,41 (d, 1H, 6', *J* = 15,8 Hz), 7,27 (d, 1H, 12, *J* = 2,1 Hz), 6,97 (d, 2H, 11', 9', *J* = 8,8 Hz), 6,87 (dd, 1H, 2, *J* = 8,6, 2,2 Hz), 6,40 (d, 1H, 5', *J* = 15,8 Hz), 4,66 (t, 2H, 1', *J* = 6,9 Hz), 3,90 (s, 3H, 14), 3,79 (s, 3H, 13'), 3,58 (q, 2H, 2' *J* = 6,6 Hz), 2,99 (s, 3H, 13)	166,03 (4'), 160,50 (10'), 160,40 (1), 142,92 (8), 140,63 (11), 138,88 (6'), 137,80 (7), 134,63 (9), 129,17 (9', 11'), 128,46 (7'), 127,30 (4), 122,37 (3), 119,14 (5'), 114,39 (8', 12'), 114,26 (5), 112,26 (6), 109,42 (2), 93,49 (12), 55,39 (14), 55,26 (13'), 43,43 (1'), 39,10 (2'), 23,07 (13)
25i	$^{13'}$*m*-CF_3	8,42 (t, 1H, 3', *J* = 6,0 Hz), 8,18 (d, 1H, 7, *J* = 5,2 Hz), 8,09 (d, 1H, 3, *J* = 8,5 Hz), 7,91 – 7,87 (m, 3H, 6, 8', 12'), 7,74 (dd, 1H, 11', *J* = 7,7, 1,6 Hz), 7,66 (t, 1H, 10', *J* = 7,8 Hz), 7,54 (d, 1H, 6', *J* = 15,8 Hz), 7,27 (d, 1H, 12, *J* = 2,2 Hz), 6,87 (dd, 1H, 2, *J* = 8,6, 2,2 Hz), 6,68 (d, 1H, 5', *J* = 15,8 Hz), 4,68 (t, 2H, 1', *J* = 7,0 Hz), 3,90 (s, 3H, 14), 3,61 (q, 2H, 2', *J* = 6,6 Hz), 2,99 (s, 3H, 13)	165,35 (4'), 160,52 (1), 142,92 (8), 140,66 (11), 137,87 (6'), 137,51 (7), 135,98 (9), 134,68 (7'), 131,26 (12'), 130,09 (11'), 129,76 (q, 9', *J* = 31,7 Hz), 128,51 (4), 125,86 (q, 10', *J* = 3,6 Hz), 124,06 (q, 8', *J* = 3,6 Hz), 124,04 (q, 13', *J* = 272,5 Hz), 123,81 (3), 122,41 (5'), 114,33 (5), 112,29 (6), 109,37 (2), 93,57 (12), 55,41 (14), 43,37 (1'), 39,13 (1'), 23,10 (13)
25j	$^{13'}$*p*-CF_3	8,50 (t, 1H, 3', *J* = 6,0 Hz), 8,18 (d, 1H, 7, *J* = 5,1 Hz), 8,09 (d, 1H, 3, *J* = 8,6 Hz), 7,89 (d, 1H, 6, *J* = 5,2 Hz), 7,78 (s, 4H, 8', 9', 11', 12'), 7,53 (d, 1H, 6', *J* = 15,8 Hz), 7,27 (d, 1H, 12, *J* = 2,2 Hz), 6,87 (dd, 1H, 2, *J* = 8,6, 2,2 Hz), 6,68 (d, 1H, 5', *J* = 15,8 Hz), 4,68 (t, 2H, 1', *J* = 6,9 Hz), 3,90 (s, 3H, 14), 3,61 (q, 2H, 2', *J* = 6,7 Hz), 3,00 (s, 3H, 13)	165,27 (4'), 160,52 (1), 142,92 (8), 140,62 (9), 138,83 (7'), 137,83 (6'), 137,51 (7), 134,64 (11), 129,29 (q, 10', *J* = 31,8 Hz), 128,52 (4), 128,21 (8', 12'), 125,81 (q, 9', 11', *J* = 3,5 Hz), 124,44 (3), 124,09 (q, 13', *J* = 272,0 Hz), 122,40 (5'), 114,30 (5), 112,28 (6), 109,40 (2), 93,51 (12), 55,40 (14), 43,32 (1'), 39,13 (2'), 23,06 (13)
25k	*o*-Cl	8,50 (t, 1H, 3', *J* = 6,0 Hz), 8,18 (d, 1H, 7, *J* = 5,2 Hz), 8,09 (d, 1H, 3, *J* = 8,6 Hz), 7,89 (d, 1H, 6, *J* = 5,2 Hz), 7,76 (d, 1H, 6', *J* = 15,7 Hz), 7,69 – 7,67 (m, 1H,	165,23 (4'), 160,54 (1), 142,98 (8), 140,61 (11), 137,79 (7), 134,63 (9), 134,45 (6'), 133,33 (8'), 132,56 (7'), 131,04 (9'), 130,00 (10'), 128,57 (4),

		9'), 7,55 – 7,53 (m, 1H, 10'), 7,44 – 7,39 (m, 2H, 11', 12'), 7,25 (d, 1H, 12, *J* = 2,2 Hz), 6,87 (dd, 1H, 2, *J* = 8,6, 2,1 Hz), 6,58 (d, 1H, 5', *J* = 15,7 Hz), 4,69 (t, 2H, 1', *J* = 6,9 Hz), 3,90 (s, 3H, 14), 3,60 (q, 2H, 2', *J* = 6,6 Hz), 3,00 (s, 3H, 13)	127,80 (12'), 127,62 (11'), 124,75 (5'), 122,41 (3), 114,27 (5), 112,30 (6), 109,45 (2), 93,50 (12), 55,42 (14), 43,30 (1'), 39,22 (2'), 23,04 (13)
25l	*m*-Cl	8,40 (t, 1H, 3', *J* = 6,0 Hz), 8,18 (d, 1H, 7, *J* = 5,2 Hz), 8,09 (d, 1H, 3, *J* = 8,6 Hz), 7,89 (d, 1H, 6, *J* = 5,1 Hz), 7,64 (s, 1H, 8'), 7,54 – 7,52 (m, 1H, 10'), 7,46 – 7,42 (m, 3H, 6', 11', 12'), 7,26 (d, 1H, 12, *J* = 2,2 Hz), 6,87 (dd, 1H, 2, *J* = 8,6, 2,2 Hz), 6,60 (d, 1H, 5', *J* = 15,8 Hz), 4,67 (t, 2H, 1', *J* = 6,9 Hz), 3,90 (s, 3H, 14), 3,60 (q, 2H, 2', *J* = 6,7 Hz), 2,99 (s, 3H, 13)	165,40 (4'), 160,51 (1), 142,91 (8), 140,63 (11), 137,83 (7), 137,64 (6'), 137,07 (9'), 134,65 (9), 133,68 (7'), 130,77 (10'), 129,19 (11'), 128,50 (4), 127,27 (8'), 126,06 (12'), 123,33 (5'), 122,40 (3), 114,30 (5), 112,27 (6), 109,38 (2), 93,54 (12), 55,40 (14), 43,34 (1'), 39,11 (2'), 23,07 (13)
25m	*m*-$^{13'}OCF_3$	8,43 (t, 1H, 3', *J* = 6,0 Hz), 8,18 (d, 1H, 7, *J* = 5,2 Hz), 8,09 (d, 1H, 3, *J* = 8,6 Hz), 7,89 (d, 1H, 6, *J* = 5,2 Hz), 7,61 – 7,60 (m, 1H, 11'), 7,57 – 7,54 (m, 2H, 8', 12'), 7,48 (d, 1H, 6', *J* = 15,8 Hz), 7,38 (d, 1H, 10', *J* = 8,1 Hz), 7,27 (d, 1H, 12, *J* = 2,3 Hz), 6,87 (dd, 1H, 2, *J* = 8,6, 2,2 Hz), 6,63 (d, 1H, 5', *J* = 15,8 Hz), 4,67 (t, 2H, 1', *J* = 7,0 Hz), 3,90 (s, 3H, 14), 3,60 (q, 2H, 2', *J* = 6,7 Hz), 2,99 (s, 3H, 13)	165,34 (4'), 160,51 (1), 148,81 (9'), 142,91 (8), 140,64 (11), 137,84 (7), 137,50 (6'), 137,30 (7'), 134,65 (9), 130,94 (11'), 128,50 (4), 126,55 (12'), 123,68 (5'), 122,40 (3), 121,75 (8'), 120,07 (q, 13', *J* = 230,5 Hz), 119,81 (10'), 114,31 (5), 112,28 (6), 109,38 (2), 93,54 (12), 55,41 (14), 43,34 (1'), 39,11 (2'), 23,08 (13)
25n	*p*-Br	8,42 (t, 1H, 3', *J* = 6,0 Hz), 8,18 (d, 1H, 7, *J* = 5,1 Hz), 8,09 (d, 1H, 3, *J* = 8,6 Hz), 7,89 (d, 1H, 6, *J* = 5,1 Hz), 7,61 (d, 2H, 9', 11', *J* = 8,4 Hz), 7,51 (d, 2H, 8', 12', *J* = 8,5 Hz), 7,43 (d, 1H, 6', *J* = 15,8 Hz), 7,26 (d, 1H, 12, *J* = 2,2 Hz), 6,87 (dd, 1H, 2, *J* = 8,6, 2,2 Hz), 6,56 (d, 1H, 5', *J* = 15,8 Hz), 4,67 (t, 2H, 1', *J* = 6,9 Hz), 3,89 (s, 3H, 14), 3,59 (q, 2H, 2', *J* = 6,7 Hz), 2,99 (s, 3H, 13)	165,52 (4'), 160,53 (1), 142,93 (8), 140,60 (11), 137,92 (7), 137,77 (6'), 134,63 (9), 134,05 (7'), 131,91 (9', 11'), 129,54 (8', 12'), 128,52 (4), 122,74 (10'), 122,50 (5'), 122,41 (3), 114,28 (5), 112,28 (6), 109,42 (2), 93,51 (12), 55,40 (14), 43,35 (1'), 39,11 (2'), 23,04 (13)
25o	*p*-$^{13'}CH_3$	8,35 (t, 1H, 3', *J* = 6,0 Hz), 8,17 (d, 1H, 7, *J* = 5,2 Hz), 8,09 (d, 1H, 3, *J* = 8,5 Hz), 7,89 (d, 1H, 6, *J* = 5,1 Hz), 7,45 – 7,14 (m, 3H, 6', 9', 11'), 7,26 (d, 1H, 12, *J* = 2,2 Hz), 7,22 (d, 2H, 8', 12', *J* = 7,7 Hz), 6,87 (dd, 1H, 2, *J* = 8,6, 2,1 Hz), 6,48 (d, 1H, 5', *J* = 15,8 Hz), 4,66 (t, 2H, 1', *J* = 7,0 Hz), 3,89 (s, 3H, 14), 3,58 (q, 2H, 2', *J* = 6,6 Hz), 2,99 (s, 3H, 13), 2,32 (s, 3H, 13')	165,88 (4'), 160,53 (1), 142,95 (8), 140,61 (11), 139,34 (10'), 139,12 (6'), 137,77 (7), 134,63 (9), 131,99 (7'), 129,54 (9', 11'), 128,51 (4), 127,56 (8', 12'), 122,39 (3), 120,61 (5'), 114,26 (5), 112,28 (6), 109,44 (2), 93,50 (12), 55,39 (14), 43,40 (1'), 39,10 (2'), 23,04 (13), 20,95 (13')
25p	*p*-NO_2	8,54 (t, 1H, 3', *J* = 6,0 Hz), 8,25 (d, 2H, 9', 11', *J* = 8,7 Hz), 8,18 (d, 1H, 7, *J* = 5,2 Hz), 8,09 (d, 1H, 3, *J* = 8,6 Hz), 7,89 (d, 1H, 6, *J* = 5,1 Hz), 7,83 (d, 2H, 8', 12', *J* = 8,7 Hz), 7,55 (d, 1H, 6', *J* = 15,8	165,06 (4'), 160,51 (1), 147,57 (10'), 142,91 (8), 141,33 (7'), 140,62 (11), 137,85 (7), 136,88 (6'), 134,65 (9), 128,65 (8', 12'), 128,52 (4), 125,87 (5'), 124,11 (9', 11'), 122,41 (3),

	Hz), 7,26 (d, 1H, 12, *J* = 2,1 Hz), 6,87 (dd, 1H, 2, *J* = 8,6, 2,1 Hz), 6,73 (d, 1H, 5', *J* = 15,8 Hz), 4,68 (t, 2H, 1', *J* = 6,9 Hz), 3,89 (s, 3H, 14), 3,61 (q, 2H, 2', *J* = 6,6 Hz), 2,99 (s, 3H, 13)	114,31 (5), 112,28 (6), 109,39 (2), 93,53 (12), 55,41 (14), 43,30 (1'), 39,16 (2'), 23,06 (13)

4.1.2. Sinteza harmicina karbamatnog tipa

Harmicini karbamatnog tipa **28a-k** pripravljeni su u položaju N-9 β-karbolina reakcijom amina **24** i cinamilnih alkohola **27a-k** na dva načina. Za pripravu harmicina karbamatnog tipa sintetizirani su cinamilni alkoholi **27b-k**, dok je cinamilni alkohol **27a** nabavljen iz komercijalnih izvora (3.1.). Priprava amina **24** u položaju N-9 β-karbolina prethodno je opisana (4.1.1.5.).

*4.1.2.1. Sinteza cinamilnih alkohola **27b-k***

Cinamilni alkoholi **27b-k** opisani su spojevi, ali je razvijena metoda za njihovu pripravu. Budući da je u strukturi DCK-a prisutna α,β-nezasićena dvostruka veza koja je izravno vezana za benzenski prsten, redukcija DCK-a jakim redukcijskim sredstvom poput $LiAlH_4$ ili katalitičkim hidrogeniranjem nije bila moguća. Stoga su ciljani cinamilni alkoholi **27b-k** pripravljeni iz odabranih DCK-a putem kiselinskih klorida **26b-k**. Cimetna kiselina i deset odabranih DCK-a (*p*-$O(CH_2)_2CH_3$-, *m*-CF_3-, *m*,*m*-di-CF_3-, *p*-CF_3-, *o*-Cl-, *m*-Cl-, *m*-OCF_3-, *p*-Br-, *p*-CH_3-, *p*-NO_2-cimetna kiselina) prevedeni su prvo u reaktivnije acil-kloride pomoću tionil-klorida prema prilagođenom ranije objavljenom propisu (75). Tioni-klorid je vrlo reaktivan, a s vodom brzo reagira dajući SO_2 i HCl, zbog čega je korišten u suvišku (6 ekvivalenata), a reakcija je provedena u bezvodnom aprotičnom otapalu toluenu u kojem je tionil-klorid topljiv. Također je korištena i katalitička količina DMF-a, jer se reakcijom tionil-klorida i DMF-a stvara kompleks koji je zbog svoje polarnosti reaktivniji od samog tionil-klorida što u konačnici omogućava provođenje reakcije u blagim uvjetima na sobnoj temperaturi (178). Budući da su novosintetizirani kloridi **26b-k** izuzetno reaktivni, nakon naparavanja toluenom korišteni su u idućem reakcijskom koraku bez dodatnog pročišćavanja.

Kako bi se spriječila djelomična redukcija dvostruke veze kiselinski kloridi **26e-k** reducirani su upotrebom $NaBH_4$ koji je u odnosu na $LiAlH_4$ znatno slabije redukcijsko sredstvo. U reakcijama redukcije korištena su dva različita otapala, THF (**27b-d**) i dietil-eter (**27e-k**), a zbog mogućnosti hidrolize novosintetiziranih acil-klorida korištena otapala bila su bezvodna. Također je, ovisno o prirodi DCK-a, varirana i količina dodanog $NaBH_4$, uz maksimalno dodanu količinu od 2,5 ekvivalenta u pripravi alkohola **27h**. U pripravi alkohola **27b-d**

korišteno je ukupno 2 ekvivalenta $NaBH_4$, a u pripravi alkohola **27e-g**, **i-k** ukupno 1,5 ekvivalent. S obzirom na to da je $NaBH_4$ slabije redukcijsko sredstvo, u reakcijsku smjesu postepeno je dokapavan bezvodni metanol koji vodikovim vezama s karbonilnim kisikovim atomom acil-klorida stvara kompleks i na taj način čini karbonilni ugljikov atom elektrofilnijim za adiciju hidridnog aniona $NaBH_4$. Analogno reakciji redukcije spoja **3** uz $LiAlH_4$ (4.1.1.1.), mehanizam redukcije uz $NaBH_4$ uključuje stvaranje alkoksida kojeg je potrebno hidrolizom prevesti u željene alkohole. Stoga je po završetku u reakcijsku smjesu dodana 1 M HCl. Novosintetizirani alkoholi **27b-k** pročišćavani su ekstrakcijom na dva načina: 1) dodatkom dietil-etera te ispiranjem vodom kako bi se uklonile novonastali natrijev borohidrd i suvišak HCl-a (**27b-d**), 2) dodatkom vode te izolacijom produkta dietil-eterom (**27e-k**). Svi su novosintetizirani alkoholi pročišćavani kromatografijom na koloni, a alkoholi **27b**,**d**,**e**,**i** koji su izolirani kao krutine, dodatno su pročišćeni rastrljavanjem u dietil-eteru.

Sinteza cinamilnih alkohola **27b-k** prikazana je na Shemi 7.

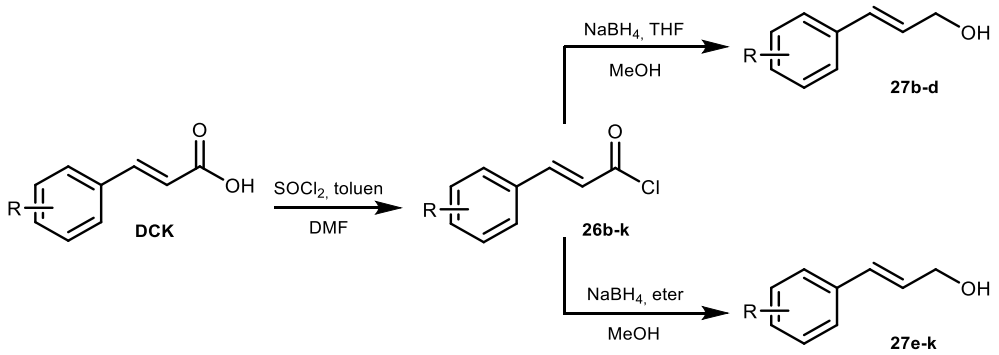

DCK, 26, 27	b	c	d	e	f	g	h	i	j	k
R	*p*-$O(CH_2)_2CH_3$	*m*-CF_3	*m,m*-di-CF_3	*p*-CF_3	*o*-Cl	*m*-Cl	*m*-OCF_3	*p*-Br	*p*-CH_3	*p*-NO_2

Shema 7. Sinteza cinamilnih alkohola **27b-k**

Alkohol **27f** pripravljen je u vrlo niskom iskorištenju od samo 3 % te njegova karakterizacija uobičajenim analitičkim i spektroskopskim metodama nije provedena, već je neizravno potvrđena analizom spoja **28f**. Alkohol **27k** nije izoliran čist, stoga njegovi spektroskopski podaci nisu navedeni, a struktura je neizravno potvrđena analizom spoja **28k**.

Analizom IR spektara cinamilnih alkohola **27b-e**,**g-j** uočena je karakteristična široka vrpca jakog intenziteta koja odgovara O–H istezanju hidroksilne skupine, koja je povezana vodikovim vezama, a nalaze se na sljedećim valnim brojevima: 3356 cm^{-1} (**27b**), 3313 cm^{-1} (**27c**), 3344 cm^{-1} (**27d**), 3277 cm^{-1} (**27e**), 3312 cm^{-1} (**27g**), 3313 cm^{-1} (**27h**), 3232 cm^{-1} (**27i**), 3277 cm^{-1} (**27j**).

Analitički i spektroskopski podaci alkohola **27b-k** dani su u tablicama 18 i 19.

Tablica 18. Analitički i IR spektroskopski podaci alkohola **27b-k**

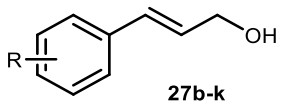

27b-k

Spoj	R	Iskorištenje (%)	t_t (°C)	Molekulska formula (M_r)	IR (ATR, ν/cm^{-1})
27b	*p*-O(CH$_2$)$_2$CH$_3$	78	78,5 – 79,5	$C_{12}H_{16}O_2$ (192,26)	3356, 3037, 2963, 2933, 2877, 1605, 1575, 1510, 1466, 1393, 1306, 1268, 1240, 1174, 1132, 1085, 1024, 1005, 965, 918, 834, 806, 778, 636, 543, 519, 499
27c	*m*-CF$_3$	76	ulje	$C_{10}H_9F_3O$ (202,18)	3313, 2866, 1740, 1593, 1440, 1332, 1270, 1164, 1124, 1100, 1012, 967, 902, 792, 697, 664, 536, 461, 452
27d	*m*,*m*-di-CF$_3$	13	89,0 – 91,5	$C_{11}H_8F_6O$ (270,17)	3344, 2927, 1742, 1662, 1616, 1469, 1385, 1368, 1281, 1233, 1203, 1159, 1117, 968, 905, 845, 784, 750, 728, 698, 664, 532, 469
27e	*p*-CF$_3$	10	50,5 – 53,0	$C_{10}H_9F_3O$ (202,18)	3277, 2931, 2082, 1927, 1740, 1657, 1613, 1577, 1459, 1413, 1318, 1279, 1206, 1167, 1111, 1121, 1092, 1066, 969, 920, 858, 849, 789, 757, 724, 679, 646, 636, 597, 536, 496
27f	*o*-Cl	3	n.o.[b]	C_9H_9ClO (168,62)	n.s.[a]
27g	*m*-Cl	24	ulje	C_9H_9ClO (168,62)	3312, 2862, 1741, 1658, 1594, 1565, 1475, 1425, 1369, 1202, 1166, 1091, 1076, 997, 962, 930, 882, 767, 702, 680, 568, 522
27h	*m*-OCF$_3$	69	ulje	$C_{10}H_9F_3O_2$ (218,18)	3313, 2866, 1741, 1609, 1584, 1491, 1446, 1371, 1253, 1216, 1164, 1096, 1002, 965, 837, 770, 702, 635, 524, 483

27i	*p*-Br	11	71,5 – 73,0	C_9H_9BrO (213,07)	3232, 2849, 1741, 1656, 1583, 1485, 1397, 1351, 1295, 1219, 1204, 1175, 1084, 1070, 1021, 994, 964, 920, 825, 691, 652, 533, 499
27j	*p*-CH_3	27	48,0 – 50,5	$C_{10}H_{12}O$ (148,21)	3277, 3022, 2919, 2855, 1906, 1742, 1655, 1610, 1570, 1511, 1463, 1412, 1337, 1316, 1270, 1219, 1111, 1011, 998, 970, 849, 834, 793, 708, 565, 523, 472
27k	*p*-NO_2	n.o.	n.o.	$C_9H_9NO_3$ (179,18)	n.s.

[a] n.s. - nije sniman; [b] n.o. - nije određen

Kemijski pomaci protona u ^{1}H, odnosno ugljika u ^{13}C NMR spektrima alkohola **27b-e**, **g-j** u skladu su s predloženim strukturama.

- Signal za proton OH skupine H-1 je u svim ^{1}H spektrima, zbog sprezanja sa susjednim H-2 protonima, vidljiv kao triplet, a nalazi se na sljedećim kemijskim pomacima s pripadajućim konstantama sprega: **27b**, 4,78 ppm, *J* = 5,5 Hz; **27c**, 4,95 ppm, *J* = 5,4 Hz; **27d**, 5,03 ppm, *J* = 5,4 Hz; **27e**, 4,98 ppm, *J* = 5,4 Hz; **27g**, 4,92 ppm, *J* =5,4 Hz; **27h**, 4,94 ppm, *J* = 5,4 Hz; **27i**, 4,89 ppm, *J* = 5,4 Hz; **27j**, 4,82 ppm, *J* = 5,5 Hz.
- Signal za proton H-2 s relativnim integralom 2H se u ^{1}H spektrima najčešće spreže u triplet dubleta, a zbog prisutnosti kisikovog atoma protoni su odsjenjeni i nalaze se na višim kemijskim pomacima: **27c**, 4,15 ppm, *J* = 5,1 Hz, 1,8 Hz; **27e**, 4,16 ppm, *J* = 5,1 Hz, 1,8 Hz; **27g**, 4,13 ppm, *J* = 5,0 Hz, 1,7 Hz; **27h**, 4,14 ppm, *J* = 5,1 Hz, 1,8 Hz; **27j**, 4,10 ppm, *J* = 5,4 Hz, 1,8 Hz. Signal za H-2 proton je u spektrima alkohola **27d** i **27i** vidljiv kao multiplet, a nalaze se u rasponu kemijskih pomaka 4,18 – 4,19 ppm (**27d**) te 4,10 – 4,11 (**27i**). Jedino je u spektru spoja **27b** ovaj signal vidljiv kao triplet na kemijskom pomaku od 4, 08 ppm s konstantom sprege od 5,4 Hz.
- Zbog utjecaja elektronegativnosti kisika signal za C-2 atom se u ^{13}C spektrima također nalazi na višim kemijskim pomacima: 61,65 ppm (**27b**), 61,24 ppm (**27c**), 61,07 (**27d**), 61,22 (**27e**), 61,25 ppm (**27g**), 61,22 ppm (**27h**), 61,32 (**27i**), 61,58 (**27j**).
- U ^{13}C spektrima spojeva **27c-e**,**h** također su uočena sprezanja signala C atoma s fluorom, a zbog prisutnosti CF_3 skupine sprezanja su vidljiva kao kvartet.

Tablica 19. ^{1}H i ^{13}C NMR spektroskopski podaci alkohola **27b-k**

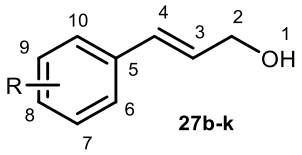

27b-k

Spoj	R	^{1}H NMR (DMSO-d_6, δ ppm, J/Hz)	^{13}C NMR (DMSO-d_6, δ ppm)
27b	p-O($\overset{1',2'}{CH_2}$)$_2\overset{3'}{CH_3}$	7,33 (d, 2H, 6, 10, J = 8,2 Hz), 6,87 (d, 2H, 7, 9, J = 8,1 Hz), 6,47 (d, 1H, 4, J = 15,9 Hz), 6,20 (dt, 1H, 3, J = 16,1, 5,3 Hz), 4,78 (t, 1H, 1, J = 5,5 Hz), 4,08 (t, 2H, 2, J = 5,4 Hz), 3,91 (t, 2H, 1', J = 6,5 Hz), 1,71 (h, 2H, 2', J = 7,0 Hz), 0,97 (t, 3H, 3', J = 7,4 Hz)	158,02 (8), 129,36 (5), 128,24 (4), 128,19 (3), 127,32 (6, 10), 114,49 (7, 9), 68,88 (1'), 61,65 (2), 22,04 (2'), 10,40 (3')
27c	$\overset{1'}{m}$-CF_3	7,76 – 7,75 (m, 2H, 6, 8), 7,58 – 7,52 (m, 2H, 9, 10), 6,66 (dt, 1H, 4, J = 15,9, 1,8 Hz), 6,56 (dt, 1H, 3, J = 16,0, 4,7 Hz), 4,95 (t, 1H, 1, J = 5,4 Hz), 4,15 (td, 2H, 2, J = 5,1, 1,8 Hz)	138,11 (5), 133,34 (4), 129,88 (q, 9, J = 1,4 Hz), 129,64 (10), 129,51 (q, 7, J = 31,2 Hz), 126,69 (3), 124,23 (q, 1', J = 271,8 Hz), 123,54 (q, 6, J = 3,8 Hz), 122,54 (q, 8, J = 3,8 Hz), 61,24 (2)
27d	$\overset{1',2'}{m,m}$-di-CF_3	8,13 (s, 2H, 6, 10), 7,90 (s, 1H, 8), 6,82 – 6,75 (m, 2H, 3, 4), 5,03 (t, 1H, 1, J = 5,4 Hz), 4,19 – 4,18 (m, 2H, 2)	139,89 (5), 135,98 (4), 130,61 (q, 7, 9 J = 32,7 Hz), 126,53 (q, 6, 10, J = 3,5 Hz), 125,15 (3), 123,38 (q, 1', 2', J = 272,6 Hz), 120,07 (dt, 8, J = 7,5, 3,7 Hz), 61,07 (2)
27e	$\overset{1'}{p}$-CF_3	7,68 – 7,64 (m, 4H, 6, 7, 9, 10), 6,66 (dt, 1H, 4, J = 16,0, 1,8 Hz), 6,58 (dt, 1H, 3, J = 16,0, 4,6 Hz), 4,98 (t, 1H, 1, J = 5,4 Hz), 4,16 (td, 2H, 2, J = 5,1, 1,8 Hz)	141,06 (5), 134,27 (4), 129,12 (3), 127,27 (q, 8, J = 31,7 Hz), 126,69 (6, 10), 125,46 (q, 7, 9, J = 3,8 Hz), 124,35 (q, 1', J = 271,8 Hz), 61,22 (2)
27f	o-Cl	n.s.[a]	n.s.
27g	m-Cl	7,49 (t, 1H, 6, J = 1,9 Hz), 7,39 (dt, 1H, 8, J = 7,7, 1,4 Hz), 7,34 (t, 1H, 10, J = 7,8 Hz), 7,28 – 7,26 (m, 1H, 9), 6,55 (dt, 1H, 4, J = 15,9, 1,7 Hz), 6,48 (dt, 1H, 3, J = 15,9, 4,6 Hz), 4,92 (t, 1H, 1, J = 5,4 Hz), 4,13 (td, 2H, 2, J = 5,0, 1,7 Hz)	139,26 (5), 133,43 (7), 132,83 (4), 130,38 (10), 126,86 (9), 126,77 (8), 125,74 (3), 124,74 (6), 61,25 (2)
27h	$\overset{1'}{m}$-OCF_3	7,48 – 7,44 (m, 2H, 9, 10), 7,41 (s, 1H, 6), 7,21 (d, 1H, 8, J = 7,3 Hz), 6,60 (dt, 1H, 4, J = 16,1, 1,7 Hz), 6,51 (dt, 1H, 3, J = 16,0, 4,7 Hz), 4,94 (t, 1H, 1, J = 5,4 Hz), 4,14 (td, 2H, 2, J = 5,1, 1,8 Hz)	148,83 (7), 139,54 (5), 133,22 (4), 130,48 (9), 126,70 (10), 125,20 (3), 120,01 (q, 1', J = 256,2 Hz), 119,38 (8), 118,39 (6), 61,22 (2)
27i	p-Br	7,51 – 7,49 (m, 2H, 7, 9), 7,40 – 7,37 (m, 2H, 6, 10), 6,53 (dt, 1H, 4, J = 15,9, 1,8 Hz), 6,42 (dt, 1H, 3, J = 16,0, 4,9 Hz), 4,89 (t, 1H, 1, J = 5,4 Hz), 4,11 – 4,10 (m, 2H, 2)	136,21 (5), 131,99 (4), 131,45 (7, 9), 128,14 (6, 10), 127,04 (3), 120,02 (8), 61,32 (2)

27j	p-CH_3 (1')	7,31 – 7,29 (m, 2H, 6, 10), 7,13 – 7,12 (m, 2H, 7, 9), 6,50 (dt, 1H, 4, *J* = 16,0, 1,8 Hz), 6,30 (dt, 1H, 3, *J* = 15,9, 5,2 Hz), 4,82 (t, 1H, 1, *J* = 5,5 Hz), 4,10 (td, 2H, 2, *J* = 5,4, 1,8 Hz), 2,28 (s, 3H, 1')	136,46 (5), 134,12 (8), 129,69 (4), 129,21 (6, 10), 128,44 (3), 126,08 (7, 9), 61,58 (2), 20,79 (1')
27k	p-NO_2	n.s.	n.s.

[a] n.s. - nije sniman

*4.1.2.2. Sinteza harmicina karbamatnog tipa **28a-d** u položaju N-9 β-karbolina*

Prva metoda koja je odabrana za sintezu harmicina karbamatnog tipa **28a-d** uključivala je aktivaciju amina **24** s prethodno sintetiziranim BtcCl te nukleofilni napad odgovarajućeg cinamilnog alkohola u prisutnosti TEA. Međutim, ovom metodom nisu pripravljeni željeni harmicini, stoga je kao alternativna metoda odabrana sinteza pomoću CDI-a. Reakcijom amina **24** s CDI-om u DMF-u pri 0 °C nastaje N-supstituirani karbonilimidazolid, koji *in situ* reagira s cinamilnim alkoholima **27a-d** na sobnoj temperaturi dajući željene karbamate **28a-d**. Budući da je CDI nestabilan u vodi, u reakcijama je korišten bezvodni DMF, a cinamilni alkoholi **27a-d** prethodno su deprotonirani u prisutnosti jake baze NaH u bezvodnom DMF-u, kako bi se dobili alkoksidi, koji su u odnosu na cinamilne alkohole znatno jači nukleofili. Reakcijske smjese miješane su 18 h na sobnoj temperaturi, a novonastali karbamati pročišćavani su ekstrakcijom u smjesi etil-acetat-voda s ciljem uklanjanja DMF-a. Svi su karbamati dodatno pročišćeni kromatografijom na koloni i rastrljavanjem u dietil-eteru te su izolirani čisti u rasponu iskorištenja 28 – 37 %.

Sinteza harmicina karbamatnog tipa **28a-d** prikazana je na Shemi 8.

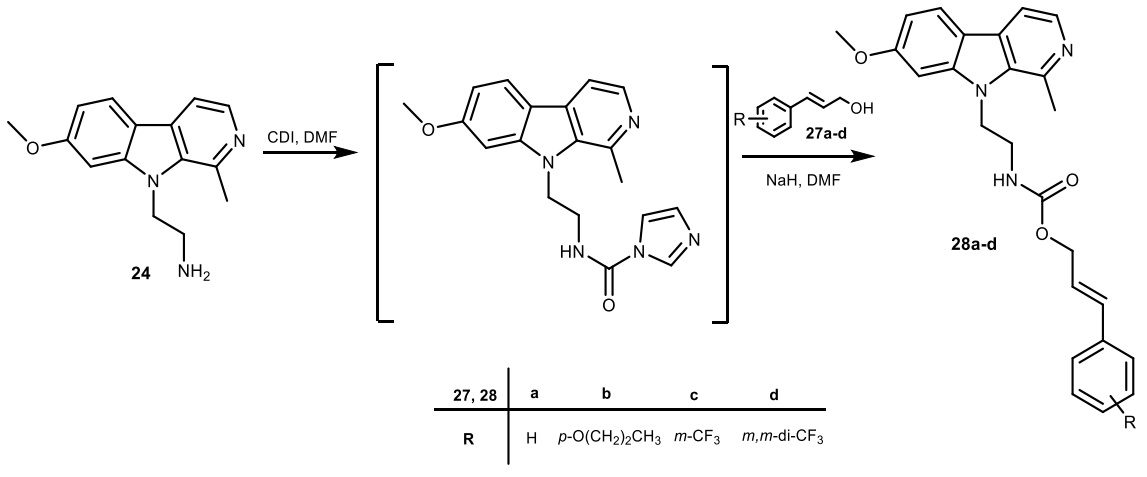

Shema 8. Sinteza harmicina karbamatnog tipa **28a-d** u položaju N-9 β-karbolina

U IR spektrima harmicina karbamatnog tipa **28a-c** uočene su karakteristične oštre vrpce jakog intenziteta koje odgovaraju C=O istezanju karbamatne karbonilne skupine koje se nalaze na sljedećim valnim brojevima: 1713 cm^{-1} (**28a**), 1714 cm^{-1} (**28b**), 1717 cm^{-1} (**28c**).

Analizom masenih spektara harmicina karbamatnog tipa **28a-d** uočeni su pikovi najvećeg intenziteta koji odgovaraju protoniranim molekulskim ionima $[M+1]^+$ pojedinih harmicina: **28a**, *m/z* 416,1; **28b**, *m/z* 474,2; **28c**, *m/z* 484,1; **28d**, *m/z* 552,1.

Analitički i IR spektroskopski podaci harmicina karbamatnog tipa **28a-d** dani su u Tablici 20.

Tablica 20. Analitički i IR spektroskopski podaci harmicina karbamatnog tipa **28a-d**

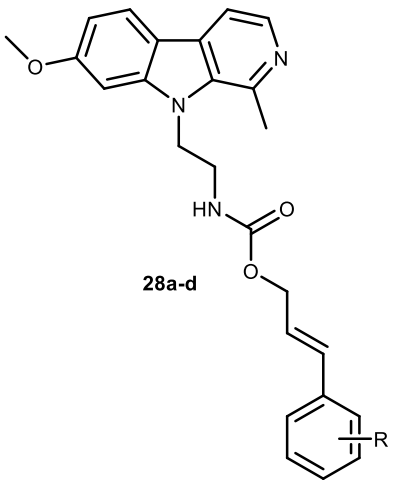

28a-d

Spoj	R	Iskorištenje (%)	t_t (°C)	Molekulska formula (M_r)	MS [*m/z*]	IR (ATR, ν/cm^{-1})
28a	H	31	147,5 – 149,0	$C_{25}H_{25}N_3O_3$ (415,49)	416,1 $[M+1]^+$	3193, 2971, 2931, 1713, 1623, 1566, 1496, 1447, 1405, 1345, 1257, 1221, 1197, 1178, 1138, 1122, 1092, 1044, 1020, 964, 948, 814, 733, 690, 598, 551, 529, 500
28b	*p*-$O(CH_2)_2CH_3$	37	154,5 – 155,5	$C_{28}H_{31}N_3O_4$ (473,57)	474,2 $[M+1]^+$	3198, 2966, 2934, 1714, 1624, 1511, 1446, 1404, 1344, 1307, 1254, 1221, 1197, 1177, 1138, 1123, 1021, 964, 814, 597, 565, 529

28c	*m*-CF_3	28	176,0 – 178,5	$C_{26}H_{24}F_3N_3O_3$ (483,49)	484,1 $[M+1]^+$	3191, 2971, 1717, 1625, 1568, 1500, 1449, 1408, 1362, 1336, 1321, 1259, 1225, 1198, 1164, 1110, 1093, 1072, 1045, 988, 970, 951, 911, 796, 694, 666, 635, 597, 551
28d	*m*,*m*-di-CF_3	35	n.o.[b]	$C_{27}H_{23}F_6N_3O_3$ (551,49)	552,1 $[M+1]^+$	n.s.[a]

[a] n.s. - nije sniman; [b] n.o. - nije određen

Kemijski pomaci protona u ^{1}H, odnosno ugljika u ^{13}C NMR spektrima harmicina karbamatnog tipa **28a-d** u skladu su s predloženim strukturama.

- Signal za proton karbamatne veze H-3' je zbog sprezanja sa susjednim H-2' protonima u svim ^{1}H spektrima spojeva **28a-d** vidljiv kao triplet, a nalazi se na sljedećim kemijskim pomacima: **28b**, 7,43 ppm; **28c**, 7,47 ppm; **28d**, 7,48 ppm, s pripadajućim konstantama sprezanja od 6,0 Hz, dok je u ^{1}H spektru spoja **28a** signal upao u multiplet u rasponu kemijskih pomaka 7,41 – 7,47 ppm.
- Signal za proton H-5' je u spektru spoja **28b** vidljiv kao dublet na kemijskom pomaku od 4,57 ppm s konstantom sprege od 6,2 Hz i relativnim integralom 2H, dok je u spektrima spojeva **28a**,**c**,**d** upao u signal protona H-1' te su vidljivi kao multiplet u rasponu kemijskih pomaka od 4,60 do 4,66 ppm.
- Proton *trans* veze H-7' se u svim ^{1}H spektrima spreže u dublet, a vidljiv je na sljedećim kemijskim pomacima s pripadajućim konstantama sprege: 6,62 ppm, J = 15,9 Hz (**28a**), 6,55 ppm, J = 15,9 Hz (**28b**), 6,69 ppm, J = 16,0 Hz (**28c**), 6,75 ppm, J = 16,1 Hz (**28d**), dok se proton H-6' spreže s protonom H-7' i protonima H-5' u dublet tripleta, a vidljivi su na sljedećim kemijskim pomacima s pripadajućim konstantama sprege: **28a**, 6,30 ppm, J = 15,9 Hz, 6,1 Hz; **28b**, 6,12 ppm, J = 15,9 Hz, 6,3 Hz; **28c**, 6,47 ppm, J = 16,0 Hz, 5,8 Hz; **28d**, 6,69 ppm, J = 16,0 Hz, 5,3 Hz.
- Unatoč prisutnosti jednog H-3' i dva H-1' susjednih protona signal za protone H-2' je u svim ^{1}H spektrima vidljiv kao kvartet.
- Signal za karbonilni ugljikov atom karbamatne veze C-4' se u ^{13}C spektrima nalazi na kemijskom pomaku od 160 ppm (**28a**, 160,50 ppm; **28b**, 160,52 ppm; **28c**, 160,48 ppm; **28d**, 160,45 ppm).

- U ^{13}C spektrima također su prisutna cijepanja signala ugljikovih atoma s fluorom te se tako u spektrima spojeva **28c** i **28d** signali ugljikovih atoma koji se sprežu s atomima fluora CF_3 skupine sprežu u kvartet.
- Signal za ugljikov atom na koji su izravno vezani atomi fluora C-14' se u ^{13}C spektru spoja **28c** nalazi na kemijskom pomaku od 124,17 ppm s pripadajućom konstantom sprege od 272,3 Hz, dok su ugljikovi atomi C-14' i C-15' ekvivalentni te se u ^{13}C spektru spoja **28d** njihov signal nalazi na kemijskom pomaku 123,46 ppm s izračunatom konstantom sprege od 272,8 Hz.
- Zatim su vidljiva C-F sprezanja kroz dvije kovalentne veze te se u ^{13}C spektru spoja **28c** nalazi na kemijskom pomaku od 129,54 ppm (C-10') s konstantom sprege od 31,5 Hz, dok se u spektru spoja **28d** nalazi na kemijskom pomaku od 130,18 ppm (C-10', C-12') s konstantom sprege od 32,7 Hz.
- Također su uočena sprezanja signala ugljikovih atoma s fluorom kroz tri kovalentne veze, a vidljiva su u ^{13}C spektru spoja **28c** na kemijskim pomacima 124,24 ppm (C-11') i 122,94 ppm (C-9') s pripadajućim konstantama sprege od 3,6 Hz, dok je u ^{13}C spektru spoja **28d** signal za C-11' proton uočen na kemijskom pomaku od 119,72 ppm s konstantom sprege od 4,0 Hz.

^{1}H i ^{13}C spektroskopski podaci harmicina karbamatnog tipa **28a-d** dani su u Tablici 21.

Tablica 21. ^{1}H i ^{13}C NMR spektroskopski podaci harmicina karbamatnog tipa **28a-d**

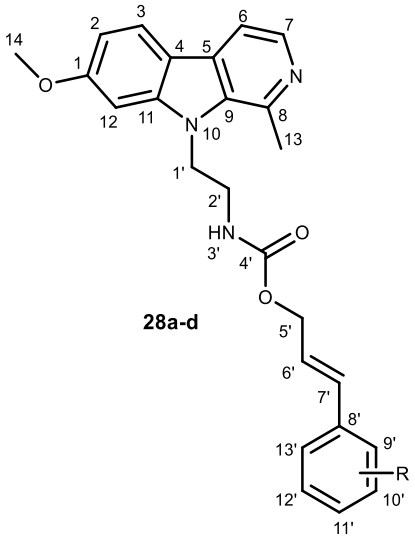

28a-d

Spoj	R	^{1}H NMR (DMSO-d_6, δ ppm, J/Hz)	^{13}C NMR (DMSO-d_6, δ ppm)
28a	H	8,17 (d, 1H, 7, J = 5,2 Hz), 8,09 (d, 1H, 3, J = 8,6 Hz), 7,88 (d, 1H, 6, J = 5,2 Hz), 7,47 – 7,41 (m, 3H, 3', 9', 13'), 7,35 (t, 2H, 10', 12', J = 7,6 Hz), 7,29 – 7,26 (m, 1H, 11'), 7,21 (d, 1H, 12, J = 2,3 Hz), 6,88 (dd, 1H, 2, J = 8,6, 2,1 Hz), 6,62 (d, 1H, 7', J = 15,9 Hz), 6,30 (dt, 1H, 6', J = 15,9, 6,1 Hz), 4,62 – 4,60 (m, 4H, 1', 5'), 3,90 (s, 3H, 14), 3,41 (q, 2H, 2', J = 6,6 Hz), 2,96 (s, 3H, 13)	160,50 (4'), 156,30 (1), 142,89 (8), 140,54 (11), 137,78 (7), 136,06 (8'), 134,69 (9), 132,39 (7'), 128,66 (10', 12'), 128,48 (4), 127,89 (11'), 126,42 (9', 13'), 124,67 (6'), 122,39 (3), 114,34 (5), 112,26 (6), 109,19 (2), 93,55 (12), 64,35 (5'), 55,48 (14), 43,74 (1'), 40,40 (2'), 23,05 (13)
28b	$^{14',15'}$ $^{16'}$ p-O(CH_2)$_2$$CH_3$	8,17 (d, 1H, 7, J = 5,2 Hz), 8,09 (d, 1H, 3, J = 8,6 Hz), 7,88 (d, 1H, 6, J = 5,2 Hz), 7,43 (t, 1H, 3', J = 6,0 Hz), 7,36 (d, 2H, 9', 13', J = 8,6 Hz), 7,21 (d, 1H, 12, J = 2,2 Hz), 6,92 – 6,87 (m, 3H, 2, 10', 12'), 6,55 (d, 1H, 7', J = 15,9 Hz), 6,12 (dt, 1H, 6', J = 15,9, 6,3 Hz), 4,61 (t, 2H, 1', J = 6,9 Hz), 4,57 (d, 2H, 5', J = 6,2 Hz), 3,92 (t, 2H, 14', J = 6,5 Hz), 3,90 (s, 3H, 14), 3,40 (q, 2H, 2', J = 6,6 Hz), 2,96 (s, 3H, 13), 1,72 (h, 2H, 15', J = 7,1 Hz), 0,97 (t, 3H, 16', J = 7,4 Hz)	160,52 (4'), 158,54 (11'), 156,36 (1), 142,91 (8), 140,52 (11), 137,73 (7), 134,68 (9), 132,48 (7'), 128,51 (8'), 128,50 (4), 127,75 (10', 12'), 122,40 (3), 121,95 (6'), 114,55 (9', 13'), 114,33 (5), 112,27 (6), 109,21 (2), 93,55 (12), 68,93 (14'), 64,63 (5'), 55,48 (14), 43,75 (1'), 40,39 (2'), 23,02 (13), 22,02 (15'), 10,39 (16')
28c	$^{14'}$ m-CF_3	8,17 (d, 1H, 7, J = 5,2 Hz), 8,08 (d, 1H, 3, J = 8,6 Hz), 7,87 (d, 1H, 6, J = 5,2 Hz), 7,78 – 7,76 (m, 2H, 12', 13'), 7,64 – 7,62 (m, 1H, 9'), 7,61 – 7,58 (m, 1H, 11'), 7,47 (t, 1H, 3', J = 6,0 Hz), 7,22 (d, 1H, 12, J = 2,2 Hz), 6,87 (dd, 1H, 2, J = 8,6, 2,1 Hz), 6,69 (d, 1H, 7', J = 16,0	160,48 (4'), 156,20 (1), 142,89 (8), 140,55 (11), 137,80 (7), 137,26 (8'), 134,70 (9), 130,45 (7'), 130,16 (13'), 129,74 (12'), 129,54 (q, 10', J = 31,5 Hz), 128,47 (4), 127,26 (6'), 124,24 (q, 11', J = 3,6 Hz), 124,17 (q, 14', J = 272,3 Hz), 122,94 (q, 9', J = 3,6 Hz),

		Hz), 6,47 (dt, 1H, 6', *J* = 16,0, 5,8 Hz), 4,64 – 4,61 (m, 4H, 1', 5'), 3,90 (s, 3H, 14), 3,42 (q, 2H, 2', *J* = 6,6 Hz), 2,96 (s, 3H, 13)	122,36 (3), 114,35 (5), 112,24 (6), 109,16 (2), 93,56 (12), 64,00 (5'), 55,46 (14), 43,74 (1'), 40,43 (2'), 23,07 (13)
28d	$^{14',15'}$ *m,m*-di-CF_3	8,16 – 8,15 (m, 3H, 7, 9', 13'), 8,07 (d, 1H, 3, *J* = 8,6 Hz), 7,98 (s, 1H, 11'), 7,87 (d, 1H, 6, *J* = 5,1 Hz), 7,48 (t, 1H, 3', *J* = 6,0 Hz), 7,21 (d, 1H, 12, *J* = 2,2 Hz), 6,85 (dd, 1H, 2, *J* = 8,6, 2,1 Hz), 6,75 (d, 1H, 7', *J* = 16,1 Hz), 6,69 (dt, 1H, 6', *J* = 16,0, 5,3 Hz), 4,66 – 4,61 (m, 4H, 1', 5'), 3,89 (s, 3H, 14), 3,42 (q, 2H, 2', *J* = 6,6 Hz), 2,96 (s, 3H, 13)	160,45 (4'), 156,41 (1), 142,90 (8), 140,54 (11), 139,01 (9), 137,78 (7), 134,72 (8'), 130,18 (q, 10', 12', *J* = 32,7 Hz), 129,92 (7'), 129,24 (9', 13'), 128,45 (4), 123,46 (q, 14', 15', *J* = 272,8 Hz), 122,34 (6'), 122,30 (3), 119,72 (q, 11', *J* = 4,0 Hz), 114,34 (5), 112,21 (6), 109,08 (2), 93,58 (12), 63,73 (5'), 55,42 (14), 43,77 (1'), 40,33 (2'), 23,08 (13)

*4.1.2.3. Sinteza harmicina karbamatnog tipa **28e-k** u položaju N-9 β-karbolina*

Harmicini karbamatnog tipa **28e-k** pripravljeni su u položaju N-9 β-karbolina u dva reakcijska koraka. Sinteze cinamilnih alkohola **27b-k** (4.1.2.1.) i amina **24** (4.1.1.5.) prethodno su opisane. Obzirom da cinamilni alkoholi **27e-k** lako reagiraju s CDI-em (unutar 2 h na sobnoj temperaturi) dajući odgovarajuće alkoksi-karbonil-imidazole te da je amin **24** jači nukleofil u odnosu na cinamilne alkohole, u sintezi harmicina karbamatnog tipa **28e-k** promijenjen je reakcijski slijed. U prvom reakcijskom koraku odgovarajući cinamilni alkoholi **27e-k** su aktivirani reakcijom s CDI-em, a zatim su reakcijom nukleofilne supstitucije s aminom **24** dobiveni ciljani harmicini karbamatnog tipa **28e-k**. U pripravi harmicina karbamatnog tipa **28e-k** također je zamijenjeno otapalo, te je umjesto aprotičnog polarnog otapala DMF-a korišteno nepolarno otapalo bezvodni dietil-eter, čija je velika prednost nisko vrelište što omogućava lako uklanjanje uparavanjem pod sniženim tlakom. U odnosu na sintezu harmicina karbamatnog tipa **28a-d** u kojoj aktivirani amin *in situ* reagira s deprotoniranim cinamilnim alkoholima **27a-d** kao nukleofilima, u sintezi harmicina karbamatnog tipa **28e-k** aktivirani cinamilni alkoholi pročišćavani su ekstrakcijom tekuće-tekuće u smjesi voda dietil-eter kako bi se uklonio suvišak CDI-a, te imidazol koji nastaje kao nusprodukt ove reakcije te su zatim su korišteni u sljedećem reakcijskom koraku bez dodatnog pročišćavanja. Reakcijom s aminom **24** na sobnoj temperaturi u bezvodnom DMF-u dolazi do stvaranja karbamatne veze pri čemu imidazol kao izlazna skupina napušta molekulu odgovarajućeg alkoksi-karbonil-imidazola. Reakcije su provedene na sobnoj temperaturi u inertnoj atmosferi argona, a novosintetizirani harmicni karbamatnog tipa **28e-k** pročišćavani su ekstrakcijom tekuće-tekuće u smjesi voda-etil-acetat kako bi se u što većoj mjeri uklonio DMF. Zatim su pročišćavani kromatografijom na koloni te rastrljavanjem u smjesi dietil-etera i petroletera i izolirani čisti u rasponu iskorištenja od 31 – 49 %.

Reakcije su provedene miješanjem na sobnoj temperaturi (18 h), a napredak reakcije nije uočen zagrijavanjem reakcijske smjese do 70 °C.

Sinteza harmicina karbamatnog tipa **28e-k** prikazana je na Shemi 9.

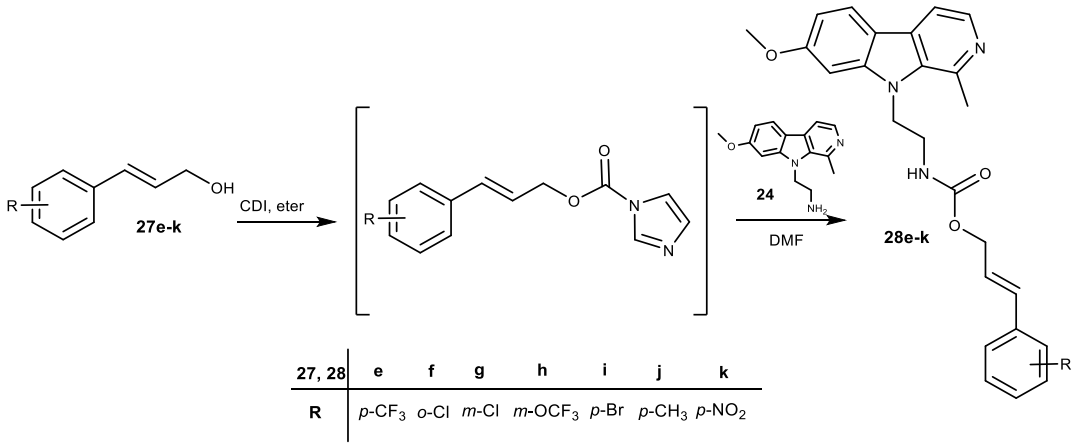

Shema 9. Sinteza harmicina karbamatnog tipa **28e-k** u položaju N-9 β-karbolina

U IR spektrima harmicina karbamatnog tipa **28e-k** vidljive su karakteristične oštre vrpce jakog intenziteta koje odgovaraju C=O istezanju karbamatne karbonilne skupine, a nalaze se na sljedećim valnim brojevima: 1713 cm^{-1} (**28e**), 1708 cm^{-1} (**28f**), 1721 cm^{-1} (**28g**), 1713 cm^{-1} (**28h**), 1712 cm^{-1} (**28i**), 1714 cm^{-1} (**28j**), 1713 cm^{-1} (**28k**).

U masenim spektrima harmicina karbamatnog tipa **28e-k** uočeni su pikovi najvećeg intenziteta koji odgovaraju protoniranim molekulskim ionima $[M+1]^+$ pojedinih harmicina: **28e**, *m/z* 484,2; **28h**, *m/z* 500,2; **28j**, *m/z* 430,2; **28k** *m/z* 461,15. Zbog izotopne raspodjele izotopa ^{79}Br i ^{81}Br u MS spektru harmicina **28i** koji u svojoj strukturi sadrži *p*-Br-supstituiranu cimetnu kiselinu vidljiva su dva pika podjednakog intenziteta pri *m/z* 494,1 i 496,1 koji odgovaraju protoniranim molekulskim ionima $[M+1]^+$. Također se zbog izotopne raspodjele izotopa ^{35}Cl i ^{37}Cl u MS spektrima harmicina **28f** i **28g** vide dva signala najvećeg intenziteta koji odgovaraju protoniranom molekulskom ionu $[M+1]^+$. Nalaze se pri *m/z* 450,1 i 452,15 (**28f**), *m/z* 450,1 i 452,15 (**28g**), a relativni intenziteti su u približnim omjerima 1:3.

Analitički i IR spektroskopski podaci harmicina karbamatnog tipa **28e-k** dani su u Tablici 22.

Tablica 22. Analitički i IR spektroskopski podaci harmicina karbamatnog tipa **28e-k**

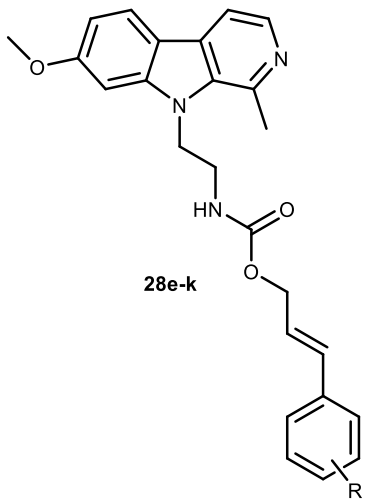

28e-k

Spoj	R	Iskorištenje (%)	t_t (°C)	Molekulska formula (M_r)	MS [*m*/*z*]	IR (ATR, ν/cm^{-1})
28e	*p*-CF_3	35	182,0 – 183,0	$C_{26}H_{24}F_3N_3O_3$ (483,49)	484,2 $[M+1]^+$	3213, 2938, 1713, 1624, 1566, 1519, 1498, 1446, 1377, 1358, 1323, 1307, 1259, 1222, 1198, 1176, 1152, 1138, 1107, 1045, 1066, 1035, 1017, 986, 966, 954, 936, 851, 814, 785, 724, 641, 611, 594, 541, 510
28f	*o*-Cl	38	189,0 – 190,0	$C_{25}H_{24}ClN_3O_3$ (449,94)	450,1 $[M+1]^+$ 452,15 $[M+1]^+$	3169, 2953, 1708 1625, 1568, 1527, 1501, 1473, 1408, 1363, 1346, 1267, 1250, 1225, 1197, 1125, 1096, 1044, 1020, 996, 975, 951, 807, 749, 635, 597, 554, 531, 484
28g	*m*-Cl	34	165,0 – 168,0	$C_{25}H_{24}ClN_3O_3$ (449,94)	450,1 $[M+1]^+$ 452,15 $[M+1]^+$	3175, 2931, 1721, 1624, 1522, 1502, 1452, 1410, 1375, 1363, 1347, 1311, 1266, 1254, 1225, 1199, 1160, 1140, 1094, 1068, 1046, 1022, 969, 944, 885, 811, 799, 768, 731, 699, 677, 653, 635, 597, 568, 538, 482

28h	*m*-OCF_3	49	156,5 – 159,0	$C_{26}H_{24}F_3N_3O_4$ (499,49)	500,2 $[M+1]^+$	3173, 2961, 1713, 1624, 1562, 1533, 1502, 1472, 1409, 1376, 1362, 1345, 1299, 1254, 1225, 1201, 1178, 1139, 1126, 1094, 1045, 1029, 1021, 1008, 999, 977, 964, 936, 923, 874, 811, 793, 771, 733, 701, 677, 652, 598, 582, 537, 512
28i	*p*-Br	39	166,5 – 169,0	$C_{25}H_{24}BrN_3O_3$ (494,39)	494,1 $[M+1]^+$ 496,1 $[M+1]^+$	3192, 2939, 1712, 1623, 1566, 1522, 1488, 1445, 1379, 1359, 1345, 1324, 1306, 1258, 1247, 1221, 1197, 1177, 1154, 1137, 1123, 1092, 1067, 1036, 1007, 967, 942, 813, 773, 723, 640, 611, 596, 566, 528, 499
28j	*p*-CH_3	31	158,0 – 160,0	$C_{26}H_{27}N_3O_3$ (429,52)	430,2 $[M+1]^+$	3216, 2930, 1714, 1623, 1564, 1514, 1497, 1446, 1404, 1378, 1343, 1324, 1257, 1197, 1179, 1138, 1122, 1043, 1020, 990, 949, 815, 769, 722, 640, 611, 598, 582, 550, 528, 465
28k	*p*-NO_2	35	208,5 – 211,5	$C_{25}H_{24}N_4O_5$ (460,49)	461,15 $[M+1]^+$	3179, 2940, 1713, 1626, 1595, 1567, 1540, 1515, 1497, 1446, 1409, 1377, 1340, 1269, 1256, 1198, 1177, 1147, 1139, 1123, 1108, 1065, 1025, 1003, 972, 939, 862, 822, 808, 793, 763, 736, 683, 635, 608, 598, 569, 531, 491

Kemijski pomaci protona u ^1H, odnosno ugljika u ^{13}C NMR spektrima harmicina karbamatnog tipa **28e-k** u skladu su s predloženim strukturama.

- Signal za proton karbamatne veze H-3' se zbog utjecaja susjednih H-2' protona u svim ^1H spektrima spojeva **28e-k** spreže u triplet, a nalazi se na sljedećim kemijskim pomacima s pripadajućim konstantama sprege: **28e**, 7,50 ppm, J = 6,0 Hz; **28f**, 7,52 ppm, J = 6,0 Hz;

28g, 7,47 ppm, *J* = 6,1 Hz; **28h**, 7,27 ppm, *J* =6,0 Hz; **28i**, 7,46 ppm, *J* = 6,1 Hz; **28j**, 7,44 ppm, *J* = 6,0 Hz; **28k**, 7,51 ppm, *J* = 6,0 Hz.

- Signal za protone H-5' je u spektrima spojeva **28e** i **28k** vidljiv kao dublet na kemijskim pomacima 4,65 ppm (**28e**) i 4,67 ppm (**28k**) s konstantom sprege od 5,4 Hz (**28e**), odn. 5,0 Hz (**28k**), dok je u spektru spoja **28f** taj signal vidljiv kao dublet dubleta na kemijskom pomaku od 4,66 ppm i konstantama sprega od 5,7 Hz i 1,6 Hz, a u spektrima spojeva **28g-j** je ovaj signal upao u signal H-1' protona te su vidljivi kao multipleti u rasponu kemijskih pomaka 4,59 – 4,63 ppm.
- Proton *trans* veze H-7' se u ^{1}H spektrima spojeva **28g**,**j**,**k** spreže kao dublet, a vidljiv je na sljedećim kemijskim pomacima: 6,58 ppm (**28g**), 6,57 ppm (**28j**), 6,72 ppm (**28k**), s pripadajućim konstantama sprege od *J* = 15,9 Hz (**28g**,**j**) i *J* = 16,0 Hz (**28k**). U spektrima spojeva **28e**,**f**,**i**,**j** je signal za H-7' protone vidljiv kao dublet tripleta na sljedećim kemijskim pomacima s pripadajućim konstantama sprega: 6,92 ppm, *J* = 16,0 Hz, 1,8 Hz (**28f**); 6,64 ppm, *J* = 15,8 Hz, 1,5 Hz (**28h**); 6,58 ppm, *J* = 16,1 Hz, 1,6 Hz (**28i**), dok je taj signal u spektru spoja **28e** vidljiv kao multiplet u rasponu kemijskih pomaka 6,67 – 6,70 ppm.
- Signal za proton H-6' spreže s protonom H-7' i protonima H-5' u dublet tripleta, a u ^{1}H spektrima je vidljiv na sljedećim kemijskim pomacima s odgovarajućim konstantama sprega: **28e**, 6,47 ppm, *J* = 16,0 Hz, 5,8 Hz; **28f**, 6,35 ppm, *J* = 15,9 Hz, 5,7 Hz; **28g**, 6,38 ppm, *J* = 16,0 Hz, 5,9 Hz; **28h**, 6,42 ppm, *J* = 16,0 Hz, 5,9 Hz; **28i**, 6,33 ppm, *J* = 16,0 Hz, 6,0 Hz; **28j**, 6,23 ppm, *J* = 15,9 Hz, 6,2 Hz; **28k**, 6,57 ppm, *J* = 16,0 Hz, 5,6 Hz.
- Također , signal za protone H-2' u svim ^{1}H spektrima vidljiv kao kvartet.
- Signal za karbonilni ugljikov atom karbamatne veze C-4' se u ^{13}C spektrima nalazi na kemijskom pomaku od 160 ppm (**28e**, 160,49 ppm; **28f**, 160,50 ppm; **28g**, 160,48 ppm; **28h**, 160,48 ppm; **28i**, 160,48 ppm; **28j**, 160,49 ppm; **28k**, 160,48 ppm).
- U ^{13}C spektrima također su prisutna cijepanja signala ugljikovih atoma s fluorom te se tako u spektrima spojeva **28e** i **28h** signali ugljikovih atoma koji se sprežu s atomima fluora CF_3 skupine sprežu u kvartet.
- Signal za ugljikov atom na koji su izravno vezani atomi fluora C-14' se u ^{13}C spektru spoja **28e** nalazi na kemijskom pomaku od 124,26 ppm s pripadajućom konstantom sprege od 271,8 Hz, dok se u spektru spoja **28h** nalazi na kemijskom pomaku od 120,09 ppm s izračunatom konstantom sprege od 256,2 Hz.

- U ^{13}C spektru spoja **28e** vidljiva su C-F sprezanja kroz dvije kovalentne veze te se nalaze na kemijskom pomaku od 127,90 ppm (C-11') s konstantom sprege od 31,7 Hz, dok su sprezanja kroz tri kovalentne veze vidljiva na kemijskom pomaku od 125,54 ppm (C-10', C-12') s izračunatom konstantom sprege od 3,5 Hz.
- Sprezanja C-F kroz dvije i tri kovalentne veze u ^{13}C spektru spoja **28h** nisu uočena.

^{1}H i ^{13}C spektroskopski podaci harmicina karbamatnog tipa **28e-k** dani su u Tablici 23.

Tablica 23. ^{1}H i ^{13}C NMR spektroskopski podaci harmicina karbamatnog tipa **28e-k**

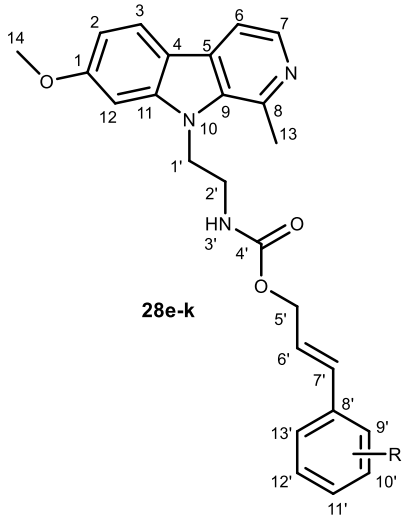

Spoj	R	^{1}H NMR (DMSO-d_6, δ ppm, J/Hz)	^{13}C NMR (DMSO-d_6, δ ppm)
28e	$^{14'}$ *p*-CF_3	8,17 (d, 1H, 7, J = 5,2 Hz), 8,09 (d, 1H, 3, J = 8,5 Hz), 7,88 (d, 1H, 6, J = 5,2 Hz), 7,71 (d, 2H, 10', 12', J = 8,2 Hz), 7,66 (d, 2H, 9', 13', J = 8,2 Hz), 7,50 (t, 1H, 3', J = 6,0 Hz), 7,22 (d, 1H, 12, J = 2,2 Hz), 6,88 (dd, 1H, 2, J = 8,6, 2,2 Hz), 6,70 – 6,67 (m, 1H, 7'), 6,47 (dt, 1H, 6', J = 16,0, 5,8 Hz), 4,65 (d, 2H, 5', J = 5,4 Hz), 4,62 (t, 2H, 1', J = 6,9 Hz), 3,90 (s, 3H, 14), 3,42 (q, 2H, 2', J = 6,6 Hz), 2,96 (s, 3H, 13)	160,49 (4'), 156,20 (1), 142,88 (8), 140,54 (11), 140,20 (8'), 137,81 (7), 134,70 (9), 130,40 (7'), 128,48 (4), 128,12 (6'), 127,90 (q, 11', J = 31,7 Hz), 127,03 (9', 13'), 125,54 (q, 10', 12', J = 3,5 Hz), 124,26 (q, 14', J = 271,8 Hz), 122,39 (3), 114,35 (5), 112,26 (6), 109,18 (2), 93,56 (12), 63,97 (5'), 55,48 (14), 43,74 (1'), 40,41 (2'), 23,07 (13)
28f	*o*-Cl	8,16 (d, 1H, 7, J = 5,2 Hz), 8,08 (d, 1H, 3, J = 8,6 Hz), 7,87 (d, 1H, 6, J = 5,2 Hz), 7,68 (dd, 1H, 10', J = 7,8, 1,8 Hz), 7,52 (t, 1H, 3', J = 6,0 Hz), 7,46 (dd, 1H, 13', J = 7,8, 1,4 Hz), 7,35 (td, 1H, 11', J = 7,5, 1,5 Hz), 7,31 (td, 1H, 12', J = 7,6, 1,8 Hz), 7,21 (d, 1H, 12, J = 2,2 Hz), 6,92 (dt, 1H, 7', J = 16,0, 1,8 Hz), 6,87 (dd, 1H, 2, J = 8,6, 2,2 Hz), 6,35 (dt, 1H, 6', J = 15,9, 5,7 Hz), 4,66 (dd, 2H,	160,50 (4'), 156,19 (1), 142,87 (8), 140,53 (11), 137,79 (7), 134,67 (9), 133,91 (9'), 131,89 (8'), 129,58 (10'), 129,41 (7'), 128,47 (4), 128,37 (11'), 127,52 (12'), 127,21 (13'), 127,18 (6'), 122,38 (3), 114,33 (5), 112,25 (6), 109,19 (2), 93,53 (12), 64,03 (5'), 55,47 (14), 43,73 (1'), 40,38 (2'), 23,04 (13)

		5', *J* = 5,7, 1,6 Hz), 4,61 (t, 2H, 1', *J* = 7,0 Hz), 3,90 (s, 3H, 14), 3,41 (q, 2H, 2', *J* = 6,7 Hz), 2,96 (s, 3H, 13)	
28g	*m*-Cl	8,17 (d, 1H, 7, *J* = 5,2 Hz), 8,08 (d, 1H, 3, *J* = 8,6 Hz), 7,87 (d, 1H, 6, *J* = 5,2 Hz), 7,52 (t, 1H, 9', *J* = 1,8 Hz), 7,47 (t, 1H, 3', *J* = 6,1 Hz), 7,42 – 7,37 (m, 2H, 12', 13'), 7,34 – 7,32 (m, 1H, 11'), 7,21 (d, 1H, 12, *J* = 2,3 Hz), 6,88 (dd, 1H, 2, *J* = 8,6, 2,2 Hz), 6,58 (d, 1H, 7', *J* = 15,9 Hz), 6,38 (dt, 1H, 6', *J* = 16,0, 5,9 Hz), 4,63 – 4,60 (m, 4H, 1', 5'), 3,90 (s, 3H, 14), 3,41 (q, 2H, 2', *J* = 6,6 Hz), 2,96 (s, 3H, 13)	160,48 (4'), 156,21 (1), 142,89 (8), 140,54 (11), 138,38 (10'), 137,79 (7), 134,69 (9), 133,50 (8'), 130,61 (7'), 130,48 (11'), 128,47 (4), 127,58 (9'), 126,04 (13'), 125,08 (12'), 122,37 (3), 114,34, (5) 112,25 (6), 109,18 (2), 93,56 (12), 64,04 (5'), 55,48 (14), 43,74 (1'), 40,42 (2'), 23,07 (13)
28h	$^{14'}$ *m*-OCF_3	8,17 (d, 1H, 7, *J* = 5,2 Hz), 8,08 (d, 1H, 3, *J* = 8,6 Hz), 7,87 (d, 1H, 6, *J* = 5,2 Hz), 7,51 – 7,47 (m, 3H, 11' – 13'), 7,45 (s, 1H, 9'), 7,27 (t, 1H, 3', *J* = 6,0 Hz), 7,21 (d, 1H, 12, *J* = 2,1 Hz), 6,87 (dd, 1H, 2, *J* = 8,6, 2,2 Hz), 6,64 (dt, 1H, 7', *J* = 15,8, 1,5 Hz), 6,42 (dt, 1H, 6', *J* = 16,0, 5,9 Hz), 4,63 – 4,60 (m, 4H, 1', 5'), 3,90 (s, 3H, 14), 3,41 (q, 2H, 2', *J* = 6,7 Hz), 2,96 (s, 3H, 13)	160,48 (4'), 156,21 (1), 148,80 (10'), 142,88 (8), 140,55 (11), 138,65 (8'), 137,80 (7), 134,70 (9), 130,59 (7'), 130,45 (11'), 128,47 (4), 127,12 (11'), 125,51 (6'), 122,37 (9'), 120,12 (13'), 120,09 (q, 14', *J* = 256,2 Hz), 118,75 (12'), 114,35 (5), 112,24 (6), 109,17 (2), 93,56 (12), 63,99 (5'), 55,46 (14), 43,74 (1'), 40,41 (2'), 23,07 (13)
28i	*p*-Br	8,17 (d, 1H, 7, *J* = 5,1 Hz), 8,09 (d, 1H, 3, *J* = 8,5 Hz), 7,87 (d, 1H, 6, *J* = 5,1 Hz), 7,55 – 7,53 (m, 2H, 10', 12'), 7,46 (t, 1H, 3', *J* = 6,1 Hz), 7,41 – 7,39 (m, 2H, 9', 13'), 7,21 (d, 1H, 12, *J* = 2,2 Hz), 6,88 (dd, 1H, 2, *J* = 8,6, 2,2 Hz), 6,58 (dt, 1H, 7', *J* = 16,1, 1,6 Hz), 6,33 (dt, 1H, 6', *J* = 16,0, 6,0 Hz), 4,62 – 4,59 (m, 4H, 1', 5'), 3,90 (s, 3H, 14), 3,40 (q, 2H, 2', *J* = 6,6 Hz), 2,96 (s, 3H, 13)	160,48 (4'), 156,24 (1), 142,87 (8), 140,55 (11), 137,82 (7), 135,38 (8'), 134,69 (9), 131,56 (10', 12'), 130,99 (7'), 128,45 (9', 13'), 125,85 (6'), 122,38 (3), 120,85 (11'), 114,35 (5), 112,25 (6), 109,17 (2), 93,56 (12), 64,16 (5'), 55,48 (14), 43,74 (1'), 40,40 (2') 23,08 (13)
28j	$^{14'}$ *p*-CH_3	8,17 (d, 1H, 7, *J* = 5,2 Hz), 8,08 (d, 1H, 3, *J* = 8,5 Hz), 7,87 (d, 1H, 6, *J* = 5,1 Hz), 7,44 (t, 1H, 3', *J* = 6,0 Hz), 7,33 (d, 2H, 9', 13', *J* = 8,0 Hz), 7,21 (d, 1H, 12, *J* = 2,2 Hz), 7,16 (d, 2H, 10', 12', *J* = 7,8 Hz), 6,88 (dd, 1H, 2, *J* = 8,6, 2,2 Hz), 6,57 (d, 1H, 7', *J* = 15,9 Hz), 6,23 (dt, 1H, 6', *J* = 15,9, 6,2 Hz), 4,62 – 4,59 (m, 4H, 1', 5'), 3,40 (q, 2H, 2', *J* = 6,6 Hz), 3,90 (s, 3H, 14), 2,96 (s, 3H, 13), 2,29 (s, 3H, 14')	160,49 (4'), 156,32 (1), 142,87 (8), 140,55 (11), 137,81 (7), 137,27 (8'), 134,69 (9), 133,28 (11'), 132,50 (7'), 129,24 (9', 13'), 128,46 (4), 126,36 (10', 12'), 123,50 (6'), 122,38 (3), 114,35 (5), 112,25 (6), 109,17 (2), 93,55 (12), 64,47 (5'), 55,47 (14), 43,74 (1'), 40,39 (2'), 23,06 (13), 20,78 (14')
28k	*p*-NO_2	8,21 (d, 2H, 10', 12', *J* = 8,7 Hz), 8,17 (d, 1H, 7, *J* = 5,2 Hz), 8,09 (d, 1H, 3, *J* = 8,6 Hz), 7,88 (d, 1H, 6, *J* = 5,2 Hz), 7,71 (d, 2H, 9', 13', *J* = 8,7 Hz), 7,51 (t, 1H, 3', *J* = 6,0 Hz), 7,21 (d, 1H, 2, *J* = 2,3 Hz), 6,88 (dd, 1H, 12, *J* = 8,6, 2,2 Hz), 6,72 (d, 1H, 7', *J* = 16,0 Hz), 6,57 (dt, 1H, 6', *J* = 16,0, 5,6 Hz), 4,67 (d, 2H, 5', *J* = 5,0 Hz), 4,62 (t, 2H, 1', *J* = 7,0 Hz), 3,90 (s, 3H, 14), 3,42 (q, 2H, 2', *J* = 6,6 Hz), 2,96 (s, 3H, 13)	160,48 (4'), 156,14 (1), 146,56 (11'), 142,86 (8), 140,54 (11), 137,82 (7), 134,70 (9), 130,23 (7'), 129,61 (6'), 128,47 (4), 127,40 (10', 12'), 123,94 (9', 13'), 122,39 (3), 114,36 (5), 112,26 (6), 109,18 (2), 93,57 (12), 63,85 (5'), 55,49 (14), 43,73 (1'), 40,43 (2'), 23,08 (13)

4.1.3. Sinteza harmicina ureidnog tipa

Harmicini ureidnog tipa **32b**,**c** pripravljeni su reakcijom spoja **31** i cinamilnih amina **30b**,**c** u položaju N-9 β-karbolina. Za pripravu željenih harmicina ureidnog tipa sintetizirani su cinamilni amini **30b**,**c** (4.1.3.2.) i spoj **31** (4.1.3.3.).

*4.1.3.1. Sinteza cinamilnih azida **29b**,**c***

Cinamilni azidi pripravljeni su iz cinamilnih alkohola **27b**,**c** analogno pripravi azida u položajima C-1 (4.1.1.1.) i C-3 β–karbolina (4.1.1.2.). Reakcijom odgovarajućeg cinamilnog alkohola s ADMP-om i DBU-om u THF-u pri 0 °C pripravljeni su ciljani azidi **29b**,**c**, a pročišćavani su na isti način kao i azidi **5** i **11**. Izolirani su kao ulja u iskorištenjima od 58 % (**29b**) i 80 % (**29c**).

Sinteza cinamilnih azida **29b**,**c** prikazana je na Shemi 10.

U IR spektrima cinamilnih azida **29b**,**c** vidljive su oštre vrpce jakog intenziteta na valnim brojevima 2094 cm^{-1} (**29b**) i 2097 cm^{-1} (**29c**) koje odgovaraju N=N=N istezanju azidne skupine.

Analitički i IR spektroskopski podaci cinamilnih azida **29b**,**c** dani su u Tablici 24.

Tablica 24. Analitički i IR spektroskopski podaci cinamilnih azida **29b**,**c**

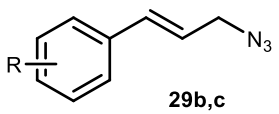

29b,c

Spoj	R	Iskorištenje (%)	t_t (°C)	Molekulska formula (M_r)	IR (ATR, ν/cm^{-1})
29b	*p*-$O(CH_2)_2CH_3$	58	ulje	$C_{12}H_{15}N_3O$ (217,27)	3036, 2937, 2966, 2877, 2094, 1651, 1606, 1575, 1510, 1472, 1422, 1350, 1240, 1174, 1163, 1113, 1067, 1047, 1019, 968, 934, 883, 838, 800, 718, 661, 638, 591, 558, 529
29c	*m*-CF_3	80	ulje	$C_{10}H_8F_3N_3$ (227,19)	2931, 2097, 1593, 1487, 1440, 1330, 1274, 1200, 1163, 1071, 1098, 1001, 965, 899, 791, 662, 696, 558, 524, 478

Kemijski pomaci protona u ^{1}H, odnosno ugljika u ^{13}C NMR spektrima azida **29b**,**c** u skladu su s predloženim strukturama.

- U ^{1}H spektrima azida **29b** i **29c** nisu vidljivi pikovi za OH protone koji se u spektrima alkohola nalaze na kemijskim pomacima 4,78 ppm (**27b**) i 4,95 ppm (**27c**).
- U ^{13}C spektru azida **29c** vidljiva su sprezanja signala atoma ugljika s fluorom, a zbog prisutnosti CF_3 skupine vidljivi su kao kvarteti.

  ^{1}H i ^{13}C NMR spektroskopski podaci cinamilnih azida **29b**,**c** dani su u Tablici 25.

Tablica 25. ^{1}H i ^{13}C NMR spektroskopski podaci cinamilnih azida **29b**,**c**

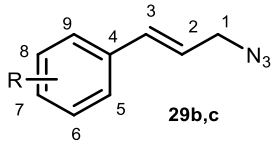

29b,c

Spoj	R	^{1}H NMR (DMSO-d_6, δ ppm, J/Hz)	^{13}C NMR (DMSO-d_6, δ ppm)
29b	p-O($\overset{1',2'}{CH_2}$)$_2\overset{3'}{CH_3}$	7,42 – 7,40 (m, 2H, 7, 9), 6,91 – 6,89 (m, 2H, 6, 10), 6,64 (dt, 1H, 4, J = 15,9, 1,4 Hz), 6,22 (dt, 1H, 3, J = 15,8, 6,7 Hz), 3,99 (dd, 2H, 2, J = 6,8, 1,3 Hz), 3,93 (t, 2H, 1', J = 6,5 Hz), 1,75 – 1,69 (m, 2H, 2'), 0,97 (t, 3H, 3', J = 7,4 Hz)	158,66 (8), 133,72 (4), 128,28 (5), 127,87 (7, 9), 120,29 (3), 114,58 (6, 10), 68,94 (1'), 52,35 (2), 21,99 (2'), 10,36 (3')
29c	$\overset{1'}{m}$-CF_3	7,85 – 7,84 (m, 1H, 10), 7,82 – 7,81 (m, 1H, 9), 7,64 – 7,62 (m, 1H, 6), 7,60 – 7,59 (m, 1H, 8), 6,81 (dt, 1H, 4, J = 15,9, 1,5 Hz), 6,58 (dt, 1H, 3, J = 15,9, 6,4 Hz), 4,08 (dd, 2H, 2, J = 6,4, 1,4 Hz)	137,08 (5), 131,80 (10), 130,30 (4), 129,75 (9), 129,57 (q, 7, J = 31,7 Hz), 125,76 (3), 124,38 (q, 6, J = 3,9 Hz), 124,14 (d, 1', J = 271,8 Hz), 123,04 (q, 8, J = 3,8 Hz), 51,93 (2)

*4.1.3.2. Sinteza cinamilnih amina **30b**,**c***

Cinamilni amini **30b**,**c** pripravljeni su iz odgovarajućih azida **29b**,**c** reakcijom redukcije. Reakcije su provedene u bezvodnom dietil-eteru u inertnoj atmosferi dušika, a kao redukcijsko sredstvo odabran je $LiAlH_4$. Zbog mogućnosti redukcije dvostruke veze $LiAlH_4$ je korišten u stehiometrijskoj količini, a reakcija je nakon miješanja 2 h na 0 °C prekinuta. Neizreagirani azid uklonjen je ekstrakcijom dietil-eterom, a novonastali amini izolirani su zaluživanjem vodenog sloja te posljedično ekstrakcijom tekuće-tekuće u smjesi voda-dietil-eter. Amini **30b**,**c** dodatno su pročišćavani rastrljavanjem u dietil-eteru te izolirani u iskorištenjima od 69 % (**30b**) i 70 % (**30c**).

Sinteza cinamilnih amina **30b**,**c** prikazana je na Shemi 10, a analitički i spektroskopski podaci dani su u Tablicama 26 i 27.

U IR spektru cinamilnog amina **30c** vidljiva je široka vrpca slabog intenziteta koja odgovara N–H istezanju primarnog amina na valnim broju 3285 cm^{-1}.

Tablica 26. Analitički i IR spektroskopski podaci cinamilnih amina **30b**,**c**

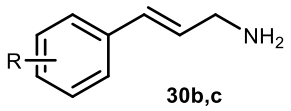

30b,**c**

Spoj	R	Iskorištenje (%)	t_t (°C)	Molekulska formula (Mr)	IR (ATR, ν/cm^{-1})
30b	*p*-$O(CH_2)_2CH_3$	69	n.o.[b]	$C_{12}H_{17}NO$ (191,27)	n.s.[a]
30c	*m*-CF_3	70	194, 5 – 197,0	$C_{10}H_{10}F_3N$ (201,19)	3285, 2967, 2934, 2879, 1741, 1604, 1575, 1510, 1469, 1394, 1377, 1307, 1272, 1241, 1177, 1143, 1115, 1068, 970, 912, 839, 809, 794, 775, 644, 592, 559, 528

[a] n.s. - nije sniman; [b] n.o. - nije određen

U ^{1}H spektrima cinamilnih amina **30b**,**c** nisu vidljivi signali za protone primarne amino skupine H-1, također u ^{13}C spektru amina **30c** nije vidljiv signal za ugljikov atom CF_3 skupine C-1' stoga su njihove strukture potvrđene neizravno analizom spojeva **32b**,**c**.

Tablica 27. ^{1}H i ^{13}C NMR spektroskopski podaci cinamilnih amina **30b**,**c**

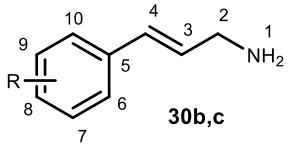

30b,**c**

Spoj	R	^{1}H NMR (DMSO-d_6, δ ppm, J/Hz)	^{13}C NMR (DMSO-d_6, δ ppm)
30b	*p*-$O(\overset{1',2'}{CH_2})_2\overset{3'}{CH_3}$	7,42 – 7,40 (m, 2H, 7, 9), 6,92 – 6,89 (m, 2H, 6, 10), 6,64 (dd, 1H, 4, J = 15,8, 1,4 Hz), 6,22 (dt, 1H, 3, J = 15,8, 6,7 Hz), 4,00 (dd, 2H, 2, J = 6,8, 1,3	158,67 (8), 133,73 (4), 128,29 (5), 127,89 (7, 9), 120,30 (3), 114,58 (6, 10), 68,94 (1'), 52,36 (2), 22,00 (2'), 10,37 (3')

		Hz), 3,93 (t, 2H, 1', *J* = 6,6 Hz), 1,75 – 1,69 (m, 2H, 2'), 0,97 (t, 3H, 3', *J* = 7,4 Hz)	
30c		7,72 – 7,70 (m, 2H, 6, 8), 7,59 – 7,56 (m, 2H, 9, 10), 6,66 – 6,63 (m, 1H, 4), 6,54 (dt, 1H, 3, *J* = 16,0, 5,8 Hz), 3,39 (dd, 2H, 2, *J* = 5,8, 1,5 Hz)	138,03 (5), 132,51 (4), 129,84 (q, 9, *J* = 2,0 Hz), 129,71 (10), 129,28 (3), 129,25 (q, 7, *J* = 32,7 Hz), 124,75 (q, 8, *J* = 3,8 Hz), 123,70 (q, 6, *J* = 3,9 Hz), 40,90 (2)

4.1.3.3. Sinteza N-(2-(7-metoksi-1-metil-9H-pirido[3,4-b]indol-9-il)etil)-1H-benzo[d][1,2,3]triazol-1-karboksamida (**31**)

BtcCl je pripravljen prema ranije objavljenom propisu (164). Sinteza amina **24** prethodno je opisana (4.1.1.5.). Spoj **31** pripravljen je reakcijom nukleofilne supstitucije prethodno pripravljenog BtcCl-a i amina **24** u prisutnosti TEA. Reakcija je, zbog mogućnosti hidrolize BtcCl-a, provedena u bezvodnom diklormetanu. Novosintetizirani spoj **31** taložio se u reakcijskoj smjesi te je izoliran odsisavanjem, a dodatnim rastrljavanjem u metanolu uklonjen je neizreagirani amin **24**. Sinteza spoja **31** prikazana je na Shemi 10.

U IR spektru spoja **31** vidljiva je karakteristična oštra vrpca jakog intenziteta na valnom broju 1728 cm^{-1} koja odgovara C=O istezanju karbonilne skupine.

Kemijski pomaci protona u ^{1}H, odnosno ugljika u ^{13}C NMR spektru spoja **31** u skladu su s predloženom strukturom.

U ^{1}H spektru je signal za H-3' proton vidljiv kao triplet na kemijskom pomaku od 9,51 ppm s izračunatom konstantom sprege *J* = 6,1 Hz. U ^{13}C spektru se signal za karbonilni ugljikov atom C-4' nalazi na kemijskom pomaku 160,45 ppm.

Analitički i spektroskopski podaci spoja **31** dani su u Tablici 28.

Tablica 28. Analitički i spektroskopski podaci spoja **31**

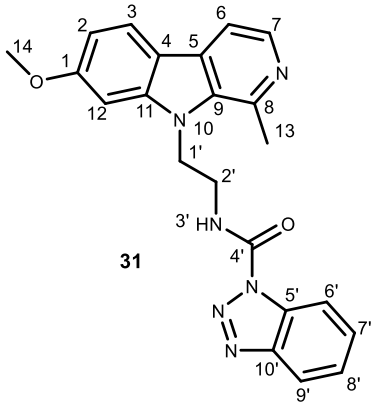

31

Spoj	**31**
Iskorištenje (%)	56
t_t (°C)	238,0 – 240,0
Molekulska formula (M_r)	$C_{22}H_{20}N_6O_2$ (400,44)
IR (ATR, ν/cm^{-1})	3010, 2966, 1728, 1621, 1563, 1486, 1460, 1445, 1413, 1381, 1365, 1343, 1330, 1294, 1256, 1227, 1196, 1179, 1127, 1114, 1065, 1043, 1010, 979, 953, 918, 852, 839, 784, 770, 748, 707, 656, 635, 600, 584, 555, 529
^{1}H NMR (DMSO-d_6, δ ppm, J/Hz)	9,51 (t, 1H, 3', J = 6,1 Hz), 8,20 – 8,17 (m, 2H, 3, 7), 8,10 (d, 1H, 6', J = 8,3 Hz), 8,05 (d, 1H, 9', J = 8,6 Hz), 7,88 (d, 1H, 6, J = 5,2 Hz), 7,70 (t, 1H, 7', J = 7,7 Hz), 7,55 (t, 1H, 8', J = 7,7 Hz), 7,31 (d, 1H, 12, J = 2,3 Hz), 6,79 (dd, 1H, 2, J = 8,5, 2,2 Hz), 4,81 (t, 2H, 1', J = 7,0 Hz), 3,83 – 3,76 (m, 5H, 14, 2'), 3,05 (s, 3H, 13)
^{13}C NMR (DMSO-d_6, δ ppm)	160,45 (4'), 149,20 (1), 145,40 (10'), 142,93 (8), 140,61 (9), 137,94 (7), 134,64 (11), 131,15 (5'), 130,00 (7'), 128,60 (4), 125,56 (8'), 122,34 (3), 119,76 (9'), 114,31 (5), 113,49 (6'), 112,25 (6), 109,29 (2), 93,40 (12), 55,25 (14), 43,32 (1'), 39,94 (2'), 23,12 (13)

*4.1.3.4. Sinteza harmicina ureidnog tipa **32b**,**c** u položaju N-9 β-karbolina*

Reakcijom amina **24** s BtcCl sintetiziran je spoj **31** čime je u strukturu amina uvedena karbonilna skupina te benzotriazol, koji služi kao dobra izlazeća skupina u reakcijama nukleofilne supstitucije. Reakcijom spoja **31** s odgovarajućim cinamilnim aminom **30b**,**c** u prisutnosti TEA u diklormetanu pripravljeni su harmicini ureidnog tipa **32b**,**c**. Reakcije su provedene pod utjecajem mikrovalnog zračenja pri temperaturi od 60 °C. Novosintetizirani harmicini ureidnog tipa **32b**,**c** pročišćavani su ekstrakcijom u smjesi diklormetan-voda kako bi se uklonio benzotriazol, koji nastaje kao nusprodukt u ovim reakcijama, i suvišak TEA. Zatim su novosintetizirani harmicini pročišćeni kromatografijom na koloni te izolirani čisti s iskorištenjem reakcija od 69 % (**32b**) i 46 % (**32c**).

Sinteza harmicina ureidnog tipa **32b**,**c** prikazana je na Shemi 10.

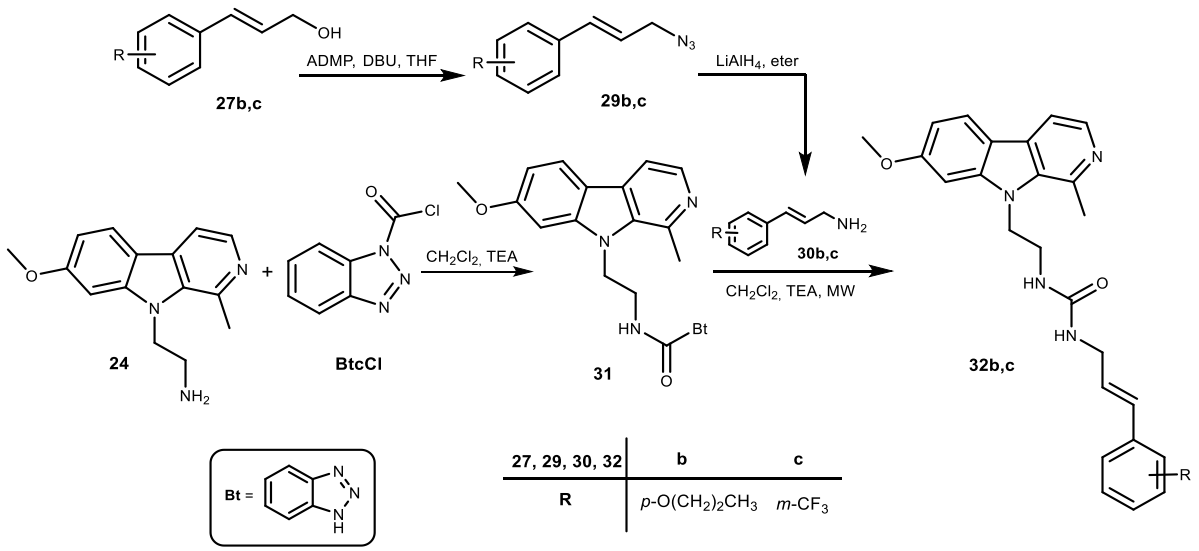

Shema 10. Sinteza harmicina ureidnog tipa u položaju N-9 β-karbolina

U IR spektru harmicina **32b** vidljiva je karakteristična oštra vrpca jakog intenziteta, koja odgovara C=O istezanju karbonilne skupine, a nalazi se na valnom broju 1623 cm^{-1} te široka vrpca slabog intenziteta koja odgovara N–H istezanju na valnom broju 3328 cm^{-1}.

U masenim spektrima harmicina ureidnog tipa **32b**,**c** uočeni su pikovi najvećeg intenziteta koji odgovaraju protoniranim molekulskim ionima $[M+1]^+$ pojedinih harmicina: **32b**, *m/z* 473,2 i **32c**, *m/z* 483,3.

Analitički i spektroskopski podaci harmicina **32b**,**c** dani su u Tablicama 29 i 30.

Tablica 29. Analitički i IR spektroskopski podaci harmicina ureidnog tipa **32b**,**c**

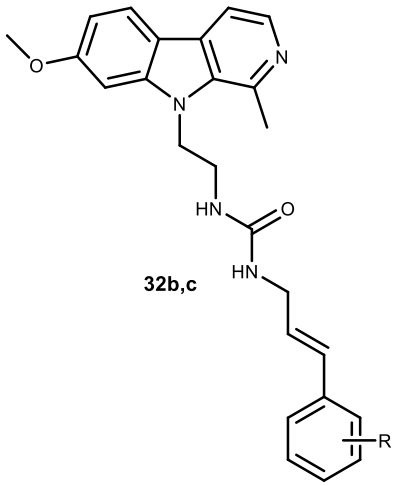

Spoj	R	Iskorištenje (%)	t_t (°C)	Molekulska formula (M_r)	MS [*m*/*z*]	IR (ATR, ν/cm^{-1})
32b	*p*-O(CH$_2$)$_2$CH$_3$	69	174,0 – 177,0	$C_{28}H_{32}N_4O_3$ (472,59)	473,2 $[M+1]^+$	3328, 2966, 2931, 1739, 1623, 1572, 1511, 1447, 1407, 1345, 1281, 1248, 1202, 1090, 1023, 1047, 805, 635, 600, 546, 519
32c	*m*-CF$_3$	46	n.o.[b]	$C_{26}H_{25}F_3N_4O_2$ (482,51)	483,3 $[M+1]^+$	n.s.[a]

[a] n.s. – nije sniman; [b] n.o. – nije određen.

Tablica 30. ^{1}H i ^{13}C NMR spektroskopski podaci za harmicine ureidnog tipa **32b**,**c**

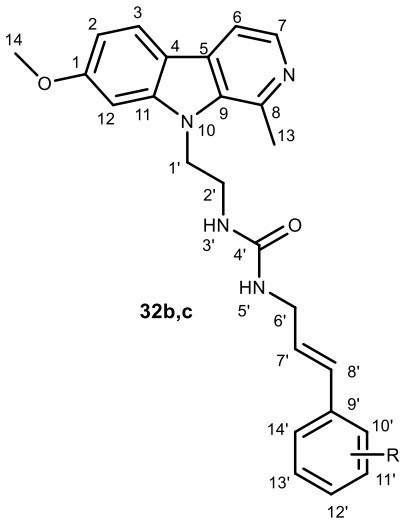

Spoj	R	^{1}H NMR (DMSO-d_6, δ ppm, J/Hz)	^{13}C NMR (DMSO-d_6, δ ppm)
32b	$^{15',16'}$ $^{17'}$ p-O(CH$_2$)$_2$CH$_3$	8,17 (d, 1H, 7, J = 5,2 Hz), 8,08 (d, 1H, 3, J = 8,5 Hz), 7,88 (d, 1H, 6, J = 5,2 Hz), 7,32 – 7,30 (m, 2H, 10', 14'), 7,29 (d, 1H, 12, J = 2,2 Hz), 6,89 – 6,86 (m, 3H, 2, 11', 13'), 6,37 (dt, 1H, 8', J = 15,9, 1,7 Hz), 6,22 (t, 1H, 5', J = 5,8 Hz), 6,13 (t, 1H, 3', J = 6,0 Hz), 6,05 (dt, 1H, 7', J = 15,9, 5,9 Hz), 4,59 (t, 2H, 1', J = 6,9 Hz), 3,92 – 3,90 (m, 5H, 14, 15'), 3,78 (td, 2H, 6', J = 5,8, 1,6 Hz), 3,42 (q, 2H, 2', J = 6,6 Hz), 2,98 (s, 3H, 13), 1,71 (h, 2H, 16', J = 7,3 Hz), 0,97 (t, 3H, 17', J = 7,4 Hz)	160,52 (4'), 158,07 (1), 158,04 (12'), 142,99 (8), 140,72 (11), 137,60 (7), 134,71 (9), 129,19 (7'), 128,37 (4), 127,30 (10', 14'), 125,79 (8'), 122,29 (3), 114,50 (11', 13'), 114,21 (5), 112,22 (6), 109,28 (2), 93,78 (12), 68,89 (15'), 55,49 (14), 44,40 (1'), 41,40 (6'), 39,61 (2'), 23,09 (13), 22,04 (16'), 10,40 (17')
32c	$^{15'}$ m-CF$_3$	8,16 (d, 1H, 7, J = 5,3 Hz), 8,08 (d, 1H, 3, J = 8,7 Hz), 7,87 (d, 1H, 6, J = 5,2 Hz), 7,74 – 7,72 (m, 2H, 10', 12'), 7,60 – 7,56 (m, 2H, 13', 14'), 7,29 (d, 1H, 12, J = 2,2 Hz), 6,87 (dd, 1H, 2, J = 8,6, 2,1 Hz), 6,53 (dt, 1H, 8', J = 16,0, 1,7 Hz), 6,40 (dt, 1H, 7', J = 16,0, 5,5 Hz), 6,30 (t, 1H, 5', J = 5,8 Hz), 6,18 (t, 1H, 3', J = 5,9 Hz), 4,60 (t, 2H, 1', J = 6,9 Hz), 3,90 (s, 3H, 14), 3,84 (td, 2H, 6', J = 5,7, 1,6 Hz), 3,43 (q, 2H, 2', J = 6,7 Hz), 2,98 (s, 3H, 13)	160,47 (4'), 158,02 (1), 142,95 (8), 140,76 (11), 137,90 (9'), 137,69 (7), 134,75 (9), 132,55 (q, 13', J = 1,5 Hz), 131,14 (7'), 129,67 (14'), 129,50 (q, 11', J = 30,7 Hz), 129,27 (8'), 128,32 (4), 124,76 (q, 12', J = 3,7 Hz), 124,23 (q, 15', J = 271,8 Hz), 123,66 (q, 10', J = 3,6 Hz), 122,26 (3), 114,24 (5), 112,19 (6), 109,21 (2), 93,78 (12), 55,46 (14), 44,38 (6'), 41,17 (1'), 39,62 (2'), 23,14 (13)

Kemijski pomaci protona u ^{1}H, odnosno ugljika u ^{13}C NMR spektrima harmicina ureidnog tipa **32b**,**c** u skladu su s predloženim strukturama.

- Signal za protone urea skupine H-3' i H-5' se zbog utjecaja susjednih H-2' i H-5' protona u ^{1}H spektrima sprežu u triplet, a nalaze se na sljedećim kemijskim pomacima s pripadajućim konstantama sprege: **32b**, 6,22 ppm, J = 5,8 Hz (H-5'); 6,13 ppm, J = 6,0 Hz (H-3'); **32c**, 6,30 ppm, J = 5,8 Hz (H-5'); 6,18 ppm, J = 5,9 Hz (H-3').
- Signali za karbonilni ugljikov atom C-4' se u ^{13}C spektrima nalazi na kemijskim pomacima 160,52 ppm (**32b**) i 160,47 (**32c**).
- Signal za atom C-9' u spektru spoja **32b** nije vidljiv, a njegova struktura izravno je potvrđena masenom spektrometrijom u kojoj je vidljiv pik protoniranog molekulskog iona.
- Zbog prisutnosti CF_3 skupine u strukturi spoja **32c** u ^{13}C spektru su uočene sprege signala ugljikovih atoma s fluorom, a vidljive su kao kvartet.
- Signal za ugljikov atom na koji su izravno vezani atomi fluora C-15' nalazi se na kemijskom pomaku 124,23 ppm s konstantom sprege od 271,8 Hz. Sprezanja kroz dvije

kovalentne veze vidljiva su na kemijskom pomaku od 129,50 ppm (C-11') s konstantom sprege od 30,7 Hz, dok su sprezanja kroz tri kovalentne veze vidljiva na pomaku 124,76 ppm koji odgovara ugljikovom atomu C-12' s konstantom sprege od 3,7 Hz te na 123,66 ppm (C-10') s konstantom sprege od 3,6 Hz. Signal na kemijskom pomaku od 132,55 ppm ogovara atomu C-13', a s atomom fluora se spreže kroz četiri kovalentne veze s konstantom sprezanja od 1,5 Hz.

4.2. BIOLOŠKA DJELOVANJA

Harmicinima amidnoga **7a-h**, **13a-h**, **19a-h**, **22a-h**, **25a-f**, **i-p**, karbamatnog **28a-k** i ureidnog **32b**,**c** tipa ispitano je antiplazmodijsko djelovanje *in vitro* na eritrocitnu fazu životnog ciklusa *P. falciparum*, dok je harmicinima amidnoga tipa **7a-h**, **13a-h**, **19a-h**, **22a-h**, **25a-f**, **i-j** dodatno ispitano antiplazmodijsko djelovanje *in vitro* na hepatocitnu fazu životnog ciklusa *P. berghei*. Također je ispitano antiproliferativno djelovanje *in vitro* novosintetiziranih harmicina **13a-h**, **19a-h**, **22a-h**, **25a-f**,**i**,**j**, **28a-d** te **32b**,**c** na humanu staničnu liniju hepatocelularnog karcinoma (HepG2) te su im izračunati pripadajući indeksi selektivnosti.

4.2.1. Antiplazmodijsko djelovanje

4.2.1.1. Ispitivanje in vitro antiplazmodijskog djelovanja harmicina na eritrocitnu fazu životnog ciklusa P. falciparum

Ispitivanje djelovanja harmicina amidnoga, karbamatnog i ureidnog tipa na eritrocitnu fazu *P. falciparum* provedena su *in vitro* na dva soja: *Pf*3D7 (soj osjetljiv na klorokin) i *Pf*Dd2 (soj otporan na klorokin), pri čemu su klorokin i harmin korišteni kao pozitivne kontrole.

Ispitani harmicini **13a-h**, **22a-h**, **25a-f**, **i-p**, **28a-k** i **32b**,**c** pokazali su jače antiplazmodijsko djelovanje u odnosu na harmin (IC_{50} = 8,25 ± 2,83 μM), u mikromolarnim (**13a-h**, **19a**,**b**,**g**, **22b**,**h**, **25p**, **28f**,**j**) i submikromolarnim (**19c-f**,**h**, **22a**, **22c-g**, **25a-f**, **i-o**, **28a-e**, **g-i**,**k**, **32b**,**c**) koncentracijama, dok su harmicini amidnoga tipa u položaju C-1 β-karbolina **7a-h** bili inaktivni u najvišim ispitivanim koncentracijama.

Svi harmicini pokazali su snažnije djelovanje na soj osjetljiv na klorokin (*Pf*3D7) u odnosu na soj otporan na klorokin (*Pf*Dd2), izuzev harmicina amidnoga tipa **25o** koji je pokazao slabije djelovanje na *Pf*3D7 soj, s izračunatom IC_{50} vrijednosti od 0,98 ± 0,37 μM u odnosu na *Pf*Dd2 soj (IC_{50} = 0,64 ± 0,10 μM), dok su harmicini karbamatnog tipa **28e** i **28k** pokazali podjednako djelovanje na oba soja (**28e**, IC_{50} = 0,79 ± 0,23 μM (*Pf*3D7), IC_{50} = 0,70 ± 0,25 μM (*Pf*Dd2); **28k**, IC_{50} = 0,36 ± 0,001 μM (*Pf*3D7), IC_{50} = 0,33 ± 0,04 μM (*Pf*Dd2)).

Među aktivnim spojevima najbolje djelovanje na *Pf*3D7 pokazali su harmicini amidnoga tipa u položaju N-9 β-karbolina **25b-e**,**i**,**j** s rasponom IC_{50} vrijednosti od 0,04 do 0,09 μM, dok su harmicini amidnoga tipa u C-3 položaju β-karbolina **13a-c**, **e-g** pokazali najslabije djelovanje u rasponu IC_{50} vrijednosti od 2,92 do 6,50 μM. Međutim, najmanje učinkovit spoj s pripadajućom IC_{50} vrijednosti od 6,78 ± 0,72 μM bio je **22h**.

Harmicini amidnoga tipa u položaju N-9 β-karbolina **25d**,**e**,**i**,**j** (IC_{50} = 0,17 – 0,33 μM) i u položaju O-6 β-karbolina **19d**,**h** i karbamat **28k** (IC_{50} = 0,32 – 0,35 μM) pokazali su najsnažnije djelovanje na *Pf*Dd2. Harmicini amidnoga tipa u položaju C-3 β-karbolina **13a-h** ponovno su bili najmanje učinkoviti (IC_{50} = 5,97 – 14,8 μM), dok je najneučinkovitiji spoj s IC_{50} vrijednosti od 19,53 ± 11,83 μM također bio spoj **22h**.

Utjecaj vrste poveznice na djelovanje harmicina uočen je uspoređivanjem antiplazmodijskih djelovanja harmicina amidnoga tipa u položaju N-9 β-karbolina **25a**, **25i** i **25j**, analognih harmicina karbamatnog tipa **28a**, **28c** i **28e** te harmicina ureidnog tipa **32c** na oba soja. Spojevi s amidnom poveznicom pokazali su najsnažnije djelovanje. Harmicin amidnoga tipa koji sadrži *p*-CF_3-supstituiranu cimetnu kiselinu u svojoj strukturi (**25j**) pokazao je gotovo 20 puta jače djelovanje na *Pf*3D7 soj (IC_{50} = 0,04 ± 0,003 μM) te četiri puta jače djelovanje na *Pf*Dd2 soj (IC_{50} = 0,17 ± 0,01 μM) u odnosu na analogni harmicin karbamatnog tipa **28e** (IC_{50} = 0,79 ± 0,23 μM (*Pf*3D7), IC_{50} = 0,70 ± 0,25 μM (*Pf*Dd2)). Nadalje, među *m*-CF_3-supstituiranim harmicinima najsnažnije djelovanje na *Pf*3D7 pokazao je harmicin amidnoga tipa **25i** (IC_{50} = 0,06 ± 0,003 μM), zatim harmicin ureidnog **32c** (IC_{50} = 0,22 ± 0,04 μM) te harmicin karbamatnog tipa **28c** (IC_{50} = 0,50 ± 0,11 μM). Djelovanja navedenih spojeva na *Pf*Dd2 pratila su isti slijed te je tako harmicin amidnoga tipa **25i** s IC_{50} = 0,33 ± 0,06 μM bio najaktivniji, zatim harmicin ureidnog tipa **32c** (IC_{50} = 1,07 ± 0,06 μM) te harmicin karbamatnog tipa **28c** (IC_{50} = 1,92 ± 0,34 μM). Harmicini amidnoga tipa **25a** i karbamatnog tipa **28a**, koji u svojoj strukturi sadrže nesupstituiranu cimetnu kiselinu bili su podjednako učinkoviti na oba soja (**25a**, IC_{50} = 0,49 ± 0,25 μM (*Pf*3D7), IC_{50} = 1,11 ± 0,15 μM (*Pf*Dd2); **28a**, IC_{50} = 0,55 ± 0,01μM (*Pf*3D7), IC_{50} = 1,37 ± 0,06 μM (*Pf*Dd2).

Utjecaj poveznice na djelovanje također je uočen među harmicinima amidnoga tipa u položaju N-9 β-karbolina koji u svojim strukturama sadrže *o*-Cl- (**25k**), *m*-Cl- (**25l**), *m*-OCF_3- (**25m**), *p*-Br- (**25n**), *p*-CH_3- (**25o**) i *p*-NO_2- (**25p**) supstituiranu cimetnu kiselinu i analognih harmicina karbamatnog tipa **28f** (*o*-Cl), **28g** (*m*-Cl), **28h** (*m*-OCF_3), **28i** (*p*-Br), **28j** (*p*-CH_3), **28k** (*p*-NO_2). Najučinkovitiji spojevi na *Pf*3D7 soj bili su harmicini amidnoga tipa **25k-m**,**o**. Harmicini **25n** i **28i** bili su podjednako djelotvorni (**25n**, IC_{50} = 0,41 ± 0,13 μM; **28i**, 0,42 ± 0,03 μM), dok je harmicin karbamatnog tipa **28k** (IC_{50} = 0,36 ± 0,001 μM) pokazao 3,8 puta jače djelovanje u odnosu na harmicin amidnoga tipa **25p** (IC_{50} = 1,36 ± 0,39 μM). Djelovanja navedenih harmicina amidnoga i karbamatnog tipa na *Pf*Dd2 pratili su isti slijed, izuzev harmicina karbamatnog tipa **28h** koji je s IC_{50} = 1,78 ± 0,23 μM pokazao jače djelovanje u odnosu na harmicin amidnoga tipa **25m** (IC_{50} = 2,11 ± 0,97 μM).

Utjecaj vrste supstituenta na antiplazmodijsko djelovanje harmicina vidljiv je među harmicinima amidnoga tipa među kojima su harmicini s CF_3-supstituiranom cimetnom kiselinom **13d**,**h**, **19d**,**h**, **25i**,**j** bili najaktivniji na oba soja. Među harmicinima karbamatnog tipa poželjni supstituenti bili su *p*-NO_2 i *p*-propoksi, dok je među harmicinima ureidnog tipa harmicin **32c** s *m*-CF_3-supstituiranom cimetnom kiselinom pokazao jače djelovanje u odnosu na *p*-propoksi-supstituiran harmicin **32b**.

4.2.1.1.1. Ispitivanje in vitro antiplazmodijskog djelovanja harmicina amidnoga tipa na eritrocitnu fazu životnog ciklusa P. falciparum

Ispitivanja antiplazmodijskog djelovanja harmicina amidnoga tipa na eritrocitnu fazu životnog ciklusa *P. falciparum* (oba soja) pokazuju da položaj supstitucije β-karbolina utječe na djelovanje, te su tako harmicini u položaju C-1 β-karbolina bili inaktivni. Među aktivnim spojevima, harmicini u položaju N-9 pokazali su najučinkovitije djelovanje, dok su se harmicini u položaju C-3 pokazali najmanje djelotvornima. Harmicini u položajima O-6 i O-7 pokazali su podjednaka djelovanja, izuzev spoja **22h**, harmicina amidnoga tipa u položaju O-7 β-karbolina koji u svojoj strukturi sadrži α-CH_3-supstituiranu cimetnu kiselinu, a koji je među svim harmicinima pokazao najslabije djelovanje na oba soja. Stoga je u daljnjim istraživanjima α-CH_3-supstituirana cimetna kiselina zamijenjena *p*-CF_3-supstituiranom cimetnom kiselinom što je rezultiralo spojevima **13h**, **19h** i **25j** koji su u pojedinim serijama harmicina amidnoga tipa bili među najdjelotvornijima. Također je i *o*-F-supstituirana cimetna kiselina zamijenjena *m*-CF_3-supstituiranom kiselinom te su dobiveni spojevi **13d**, **19d** i **25i**, koji su također pokazali jaka antiplazmodijska djelovanja.

Među harmicinima amidnoga tipa u položajima C-3 (**13a-h**) i O-6 (**19a-h**), harmicini **13b-e**,**f**,**h** te **19b-e**,**f**,**h** s elektron-odvlačećim supstituentom u *m*- ili *p*-položaju pokazali su bolja djelovanja na *Pf*3D7 soj u odnosu na **13a** i **19a** koji u svojoj strukturi sadrže nesupstituiranu cimetnu kiselinu te *p*-OCH_3-supstituirane harmicine **13g** i **19g**, dok je na djelovanje na *Pf*Dd2 ovaj utjecaj uočen samo u seriji O-6 harmicina **19a-h**. Djelovanja harmicina ovisno o vrsti supstituenta u *m*-položaju pratila su slijed: *m*-CF_3 > *m*-Br > *m*-F, dok je u *p*-položaju niz bio sljedeći: *p*-CF_3 > *p*-Cl > *p*-F > *p*-OCH_3. Iznimka su bili *p*-F- i *m*-Br-supstituirani harmicini u položaju C-3 koji su na *Pf*Dd2 soj pokazali najslabija djelovanja. Najaktivniji spojevi na oba soja bili su *m*-CF_3 (**13d**, **19d**) i *p*-CF_3 (**13h**, **19h**) supstituirani harmicini, pri čemu su harmicini **19d** i **19h** s IC_{50} = 0,12 ± 0,02 μM bili jednako učinkoviti na *Pf*3D7, dok su na *Pf*Dd2 ispoljili približno jednaka djelovanja (**19d**, IC_{50} = 0,32 ± 0,08 μM; **19h**, IC_{50} = 0,35 ± 0,06 μM). U odnosu na to, u seriji C-3 harmicina najsnažnije djelovanje na *Pf*3D7 pokazao je **13d** (IC_{50} =

2,01 ± 0,10 μM;), dok je na *Pf*Dd2 soj značajno djelotvorniji bio *p*-CF_3-supstituirani harmicin **13h** (IC_{50} = 5,97 ± 1,33 μM). Harmicin 19d, odnosno *m*-Br-supstituirani hibrid pokazao je slično djelovanje na *Pf*3D7 soj (IC_{50} = 0,19 ± 0,02 μM).

U seriji O-7 harmicina poželjan položaj supstitucije, neovisno o vrsti supstituenta, bio je *para*. Zamjenom vodika u strukturi harmicina **22a** s izosterom fluorom u *para* položaju dobiven je spoj **22d** koji je s IC_{50} = 0,15 ± 0,06 μM u seriji O-7 harmicina pokazao najjače djelovanje. Uvođenje fluora u *meta* položaj dovelo je do značajnog smanjenja učinkovitosti (**22b**), dok je *o*-F-supstituirani harmicin **22g** pokazao usporedno djelovanje (**22a**, IC_{50} = 0,98 ± 0,12 μM; **22b**, IC_{50} = 2,75 ± 1,6 μM; **22g**, IC_{50} = 0,93 ± 0,28 μM). Nasuprot tome, djelovanja na *Pf*Dd2 soj ukazuju na to da je, neovisno o položaju, fluor bio poželjan supstituent, pri čemu je učinkovitiji spoj bio *o*-F-supstituirani harmicin **22e** (IC_{50} = 0,4 ± 0,24 μM), zatim *m*-F-supstituirani harmicin **22c** (IC_{50} = 0,48 ± 0,24 μM) te *p*-F-supstituirani harmicin **22d** (IC_{50} = 0,69 ± 0,18 μM).

Harmicini u položaju N-9 β-karbolina **25b-e**, **25i**,**j** ostvarili su za dva reda veličine jače djelovanje na *Pf*3D7 soj u odnosu na harmin. Najučinkovitiji su bili *p*-CF_3-supstituirani harmicin **25j** (IC_{50} = 0,04 ± 0,003 μM), *p*-Cl-supstituirani harmicin **25e** (IC_{50} = 0,04 ± 0,02 μM) i *m*-CF_3-supstituirani harmicin **25i** (IC_{50} = 0,04 ± 0,003 μM). Navedeni harmicini također su bili najučinkovitiji na *Pf*Dd2 soj, izuzev *m*-F-supstituiranog harmicina **25b** koji je pokazao znatno slabije djelovanje (IC_{50} = 0,78 ± 0,32 μM). Antiplazmodijsko djelovanje *para*-supstituiranih harmicina u položaju N-9 na oba soja pratilo je niz: *p*-CF_3 > *p*-Cl > *p*-F > *p*-OCH_3 > *p*-Br > *p*-CH_3 > *p*-NO_2. Utjecaj položaja supstitucije na djelovanje vidljiv je među Cl-supstituiranim harmicinima pri čemu je *para*-položaj dao spoj s najsnažnijim djelovanjem (**25e**) dok su se *o*-Cl- (**25k**) i *m*-Cl- (**25l**) supstituirani harmicini pokazali manje učinkovitima na oba soja. Harmicin **25c** koji u svojoj strukturi sadrži *m*-Br-supstituiranu cimetnu kiselinu pokazao je gotovo 6 puta jače djelovanje u odnosu na *p*-Br-supstituirani derivat **25n**. Nasuprot tome, položaj supstitucije u CF_3- i F-supstituiranim harmicinima nije imao značajan utjecaj.

4.2.1.1.2. Ispitivanje in vitro djelovanja harmicina karbamatnog tipa na eritrocitnu fazu životnog ciklusa P. falciparum

Antiplazmodijska djelovanja harmicina karbamatnog tipa **28a-k** na *Pf*3D7 te na *Pf*Dd2 ne prate isti slijed, međutim najaktivniji spoj s pripadajućim IC_{50} vrijednostima bio je *p*-NO_2-supstituirani harmicin **28k**: IC_{50} = 0,36 ± 0,001 μM (*Pf*3D7) i IC_{50} = 0,33 ± 0,04 μM (*Pf*Dd2), dok je *p*-CH_3-supstituirani harmicin **28j** bio među najmanje djelotvornima (IC_{50} = 1,13 ± 0,04 μM (*Pf*3D7), IC_{50} = 2,28 ± 0,24 μM (*Pf*Dd2)).

Usporedno jaka djelovanja s harmicinom **28k** na *Pf*3D7 ispoljili su *p*-propoksi (**28b**) i *p*-Br- (**28i**) supstituirani harmicini s izračunatim IC_{50} vrijednostima: **28b**, IC_{50} = 0,39 ± 0,03 μM; **28i**, IC_{50} = 0,42 ± 0,03 μM.

Utjecaj položaja supstituenta na djelovanje vidljiv je uspoređivanjem djelovanja *m*-CF_3-supstituiranog harmicina **28c**, *m*,*m*-di-CF_3-supstituiranog harmicina **28d** te *p*-CF_3-supstituiranog harmicina **28e** na oba soja. Redoslijed aktivnosti na *Pf*3D7 soj bio je sljedeći: **28c** (IC_{50} = 0,50 ± 0,11 μM) > **28d** (IC_{50} = 0,65 ± 0,003 μM) > **28e** (IC_{50} = 0,79 ± 0,23 μM). Redoslijed djelovanja navedenih harmicina na *Pf*Dd2 soj se razlikovao te je tako *p*-CF_3-supstituirani harmicin **28e** bio najaktivniji (IC_{50} = 0,70 ± 0,25 μM), dok su **28c** i **28d** pokazali znatno slabija djelovanja (**28c**, IC_{50} = 1,92 ± 0,34 μM; **28d**, IC_{50} = 2,63 ± 0,38 μM) pri čemu je *m*,*m*-di-CF_3-supstituirani harmicin **28d** bio najslabije djelotvoran među svim harmicinima karbamatnog tipa. Također, *m*-Cl-supstituirani harmicin **28g** s IC_{50} = 0,97 ± 0,07 μM (*Pf*3D7) i IC_{50} = 1,19 ± 0,16 μM (*Pf*Dd2) pokazao se učinkovitijim na oba soja u odnosu na *o*-Cl-supstituirani harmicin **28f** koji je s IC_{50} = 1,24 ± 0,13 μM bio najmanje učinkovit spoj na *Pf*3D7.

4.2.1.1.3. Ispitivanje in vitro djelovanja harmicina ureidnog tipa na eritrocitnu fazu životnog ciklusa P. falciparum

Između harmicina ureidnog tipa **32b**, koji u svojoj strukturi sadrži *p*-propoksi-supstituiranu cimetnu kiselinu i **32c**, koji sadrži *m*-CF_3-supstituiranu cimetnu kiselinu, gotovo dva puta jače djelovanje na *Pf*3D7 s IC_{50} = 0,22 ± 0,04 μM pokazao je *m*-CF_3-supstituirani harmicin **32c**, dok su se na *Pf*Dd2 s IC_{50} = 1,12 ± 0,05 μM (**32b**) i IC_{50} = 1,07± 0,06 μM (**32c**) pokazali podjednako učinkovitima.

Rezultati antiplazmodijskog djelovanja harmicina amidnoga **7a-h**, **13a-h**, **19a-h**, **22a-h**, **25a-f**, **i-p**, karbamatnog **28a-k** i ureidnog **32b**,**c** tipa dani su u Tablici 31.

Tablica 31. *In vitro* antiplazmodijsko djelovanje harmicina amidnoga (**7**, **13**, **19**, **22**, **25**), karbamatnog (**28**) i ureidnog tipa (**32**) na eritrocitnu fazu životnog ciklusa *P. falciparum*

Spoj	Položaj supstitucije β-karbolina	Vrsta poveznice	Supstituent	IC_{50}[a] (μM)	
				*Pf*3D7	*Pf*Dd2
7a	**C-1**	**AMID**	–	> 55,56	> 55,56
7b			*m*-F	> 27,78	> 27,78
7c			*m*-Br	> 27,78	> 27,78
7d			*m*-CF_3	> 27,78	> 27,78
7e			*p*-F	> 13,89	> 13,89
7f			*p*-Cl	> 27,78	> 27,78
7g			*p*-OCH_3	> 27,78	> 27,78
7h			*p*-CF_3	> 55,56	> 55,56
13a	**C-3**	**AMID**	–	5,78 ± 1,05	10,18 ± 1,68
13b			*m*-F	5,74 ± 0,33	12,71 ± 1,76
13c			*m*-Br	3,23 ± 0,32	14,8 ± 0,35
13d			*m*-CF_3	2,01 ± 0,10	7,40 ± 0,75
13e			*p*-F	4,13 ± 0,61	13,30 ± 7,41
13f			*p*-Cl	2,92 ± 0,03	8,38 ± 3,16
13g			*p*-OCH_3	6,50 ± 0,29	10,72 ± 3,18
13h			*p*-CF_3	2,30 ± 0,41	5,97 ± 1,33
19a	**O-6**	**AMID**	–	1,55 ± 0,45	2,47 ± 0,25
19b			*m*-F	1,11 ± 0,14	1,30 ± 0,09
19c			*m*-Br	0,19 ± 0,02	0,63 ± 0,22
19d			*m*-CF_3	0,12 ± 0,02	0,32 ± 0,08
19e			*p*-F	0,95 ± 0,06	1,67 ± 0,76
19f			*p*-Cl	0,36 ± 0,02	0,92 ± 0,06
19g			*p*-OCH_3	1,17 ± 0,03	2,86 ± 0,52
19h			*p*-CF_3	0,12 ± 0,02	0,35 ± 0,06
22a	**O-7**	**AMID**	–	0,98 ± 0,12	4,7 ± 2,65
22b			*m*-F	2,75 ± 1,6	5,01 ± 0,83
22c			*m*-Br	0,37 ± 0,22	0,48 ± 0,28
22d			*p*-F	0,15 ± 0,06	0,69 ± 0,18
22e			*p*-Cl	0,32 ± 0,03	0,4 ± 0,24
22f			*p*-OCH_3	0,21 ± 0,14	1,09 ± 0,49
22g			*o*-F	0,93 ± 0,28	3,92 ± 1,35
22h			α-CH_3	6,78 ± 0,72	19,53 ± 11,83
25a	**N-9**	**AMID**	–	0,49 ± 0,25	1,11 ± 0,15
25b			*m*-F	0,07 ± 0,03	0,78 ± 0,32

25c			*m*-Br	0,07 ± 0,03	0,41 ± 0,01
25d			*p*-F	0,09 ± 0,06	0,33 ± 0,11
25e			*p*-Cl	0,04 ± 0,02	0,17 ± 0,01
25f			*p*-OCH_3	0,26 ± 0,001	0,49 ± 0,24
25i			*m*-CF_3	0,06 ± 0,02	0,33 ± 0,06
25j	**N-9**	**AMID**	*p*-CF_3	0,04 ± 0,003	0,17 ± 0,01
25k			*o*-Cl	0,32 ± 0,06	0,5 ± 0,06
25l			*m*-Cl	0,33 ± 0,10	0,68 ± 0,20
25m			*m*-OCF_3	0,35 ± 0,02	2,11 ± 0,97
25n			*p*-Br	0,41 ± 0,14	n.o.[b]
25o			*p*-CH_3	0,98 ± 0,37	0,64 ± 0,10
25p			*p*-NO_2	1,36 ± 0,39	2,05 ± 0,80
28a			–	0,55 ± 0,01	1,37 ± 0,06
28b			*p*-$O(CH_2)_2CH_3$	0,39 ± 0,03	0,83 ± 0,002
28c			*m*-CF_3	0,50 ± 0,11	1,92 ± 0,34
28d			*m,m*-di-CF_3	0,65 ± 0,003	2,63 ± 0,38
28e			*p*-CF_3	0,79 ± 0,23	0,70 ± 0,25
28f	**N-9**	**KARBAMAT**	*o*-Cl	1,24 ± 0,13	1,33 ± 0,15
28g			*m*-Cl	0,97 ± 0,07	1,19 ± 0,16
28h			*m*-OCF_3	0,68 ± 0,04	1,78 ± 0,23
28i			*p*-Br	0,42 ± 0,03	1,09 ± 0,01
28j			*p*-CH_3	1,13 ± 0,04	2,28 ± 0,24
28k			*p*-NO_2	0,36 ± 0,001	0,33 ± 0,04
32b	**N-9**	**UREA**	*p*-$O(CH_2)_2CH_3$	0,42 ± 0,0004	1,12 ± 0,05
32c			*m*-CF_3	0,22 ± 0,04	1,07 ± 0,06
CQ[c]				0,003 ± 0,002	0,20 ± 0,10
Harmin				8,25 ± 2,83	> 27,7

[a] IC_{50} - koncentracija spoja koja inhibira rast za 50 %; [b] n.o. - nije određeno; [c] CQ - klorokin

4.2.1.2. Ispitivanje in vitro antiplazmodijskog djelovanja harmicina na hepatocitnu fazu životnog ciklusa P. berghei

Antiplazmodijsko djelovanje harmicina amidnoga tipa **7a-h**, **13a-h**, **19a-h**, **22a-h**, **25a-f**,**i-j** na hepatocitnu fazu životnog ciklusa plazmodija ispitano je *in vitro* na stanicama hepatocelularnog karcinoma Huh7 koje su inficirane s *P. berghei*. Svi su navedeni harmicini testirani pri koncentracijama 1 μM i 10 μM. Harmin i primakin korišteni su kao pozitivna kontrola dok je DMSO bio negativna kontrola. Citotoksičnost spojeva procijenjena je mjerenjem konfluentnosti Huh7 stanica.

Svi su ispitani harmicini, izuzev harmicina **7a** i **7b**, pokazali jače djelovanje na hepatocitnu fazu *P. berghei* pri koncentraciji od 10 μM.

Najaktivniji spojevi pri koncentraciji od 1 μM bili su harmicini u položaju N-9 β-karbolina, pri čemu su jače djelovanje u odnosu na primakin i harmin ostvarili *m*-Br- (**25c**) i *p*-CF_3- (**25j)** supstituirani harmicini. Međutim, najjače djelovanje među svim harmicinima pokazao je *o*-F-supstituirani harmicin u položaju O-7 β-karbolina (**22g**). Među ostalim ispitanim harmicinima jače djelovanje od primakina te usporedno djelovanje s harminom pokazali su *p*-Cl-supstituirani harmicin u položaju C-1 β-karbolina (**7f**) i *p*-F-supstituirani harmicin u položaju O-7 β-karbolina (**22d**).

Pri koncentraciji od 10 μM svi su harmicini u položaju C-1 β-karbolina ispoljili slabije djelovanje u odnosu na referentni lijek primakin (PQ). Harmicin **7f** pokazao je usporedno djelovanje s harminom, a svi ostali harmicini bili su nedjelotvorni.

U seriji C-3- i O-6-supstituiranih harmicina spojevi **13b-f**,**h** te **19a-h** su pri koncentraciji od 10 μM pokazali jače djelovanje od PQ i harmina. Najdjelotvorniji spojevi u seriji O-6-supstituiranih harmicina čije su konfluentnosti iznosile 86 % (**19d**) i 91 % (**19e**) bili su *m*-CF_3-supstituirani harmicin **19d** i *p*-F-supstituirani harmicin **19e**. Zbog visoke citotoksičnosti na Huh7 stanice (konfluentnost = 24 – 80 %) IC_{50} vrijednosti antiplazmodijskog djelovanja ovih harmicina nisu određivane.

Harmicini amidnoga tipa u položaju O-7 β-karbolina **22a-h** i harmicini amidnoga tipa u N-9 položaju **25a-c**,**e**,**f**,**i**,**j** su pri koncentraciji od 10 μM pokazali jača djelovanja u odnosu na PQ i harmin. Najaktivniji među O-7 harmicinima bio je *p*-F-supstituirani harmicin **22d**. Međutim, zbog visoke citotoksičnosti aktivnost se ne može pripisati isključivo antiplazmodijskom djelovanju. Harmicinu amidnoga tipa u položaju N-9 β-karbolina koji u svojoj strukturi sadrži *m*-CF_3-supstituiranu cimetnu kiselinu **25i** određena je IC_{50} vrijednost na hepatocitnu fazu, te je u usporedbi s primakinom pokazao 4,3 puta jače djelovanje (**25i**, IC_{50} = 1,94 ± 0,68 μM; PQ, IC_{50} = 8,4 ± 3,4 μM).

Rezultati antiplazmodijskog djelovanja harmicina amidnoga tipa na hepatocitnu fazu životnog ciklusa *P. berghei* prikazani su na Slikama 34 – 38.

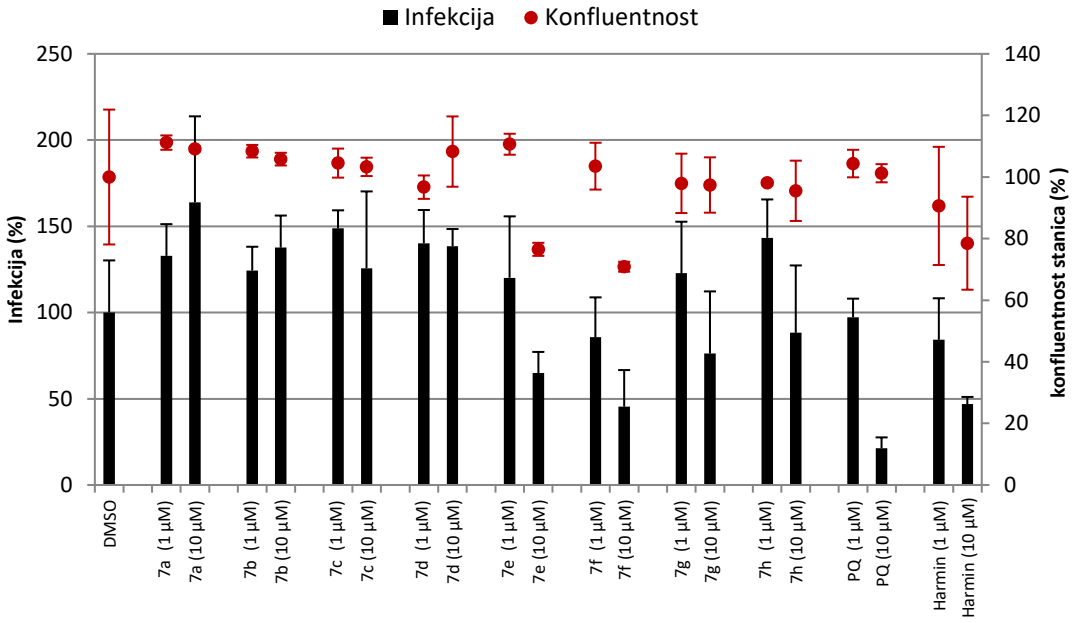

Slika 34. *In vitro* antiplazmodijsko djelovanje harmicina **7a-h** na hepatocitnu fazu životnog ciklusa *P. berghei*. Ukupna količina parazita predstavljena je kao postotak infekcije (stupci), a vijabilnost stanica kao konfluentnost (točke); PQ – primakin

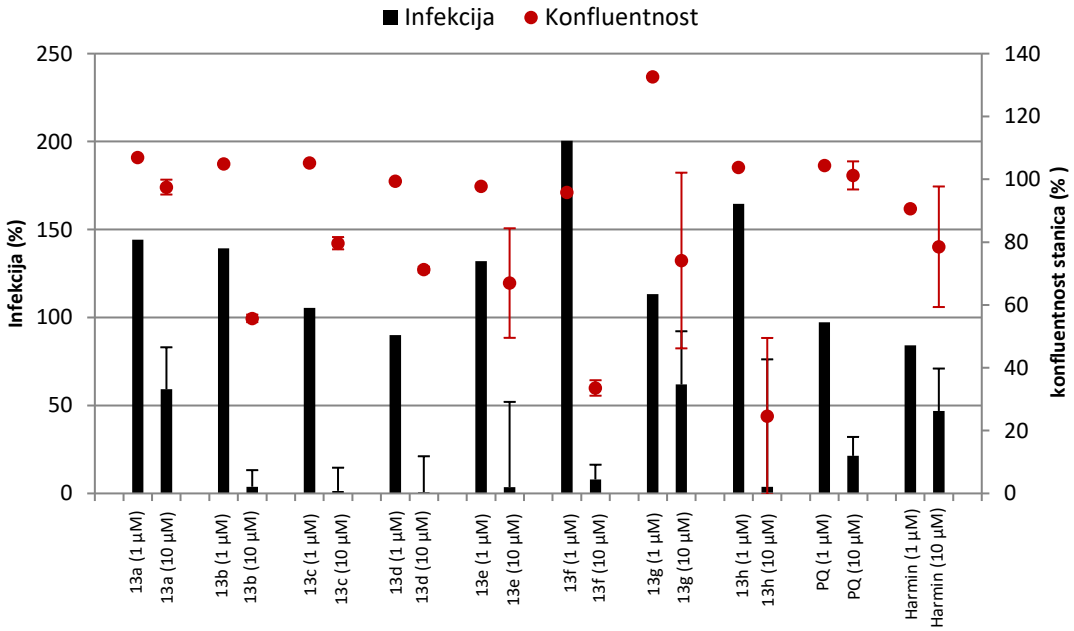

Slika 35. *In vitro* antiplazmodijsko djelovanje harmicina **13a-h** na hepatocitnu fazu životnog ciklusa *P. berghei*. Ukupna količina parazita predstavljena je kao postotak infekcije (stupci), a vijabilnost stanica kao konfluentnost (točke); PQ – primakin

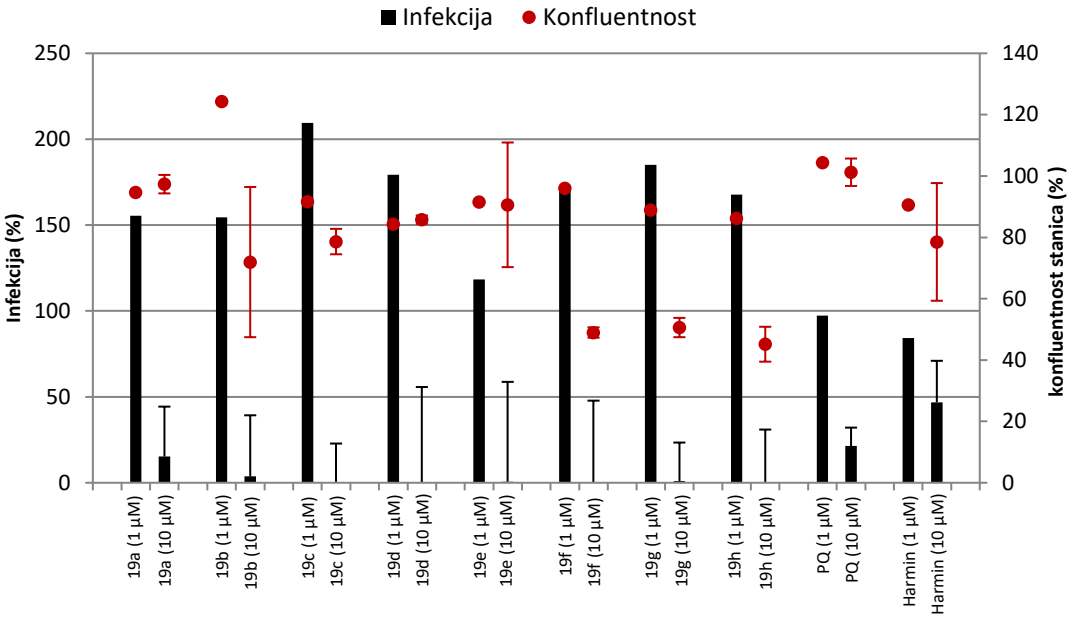

Slika 36. *In vitro* antiplazmodijsko djelovanje harmicina **19a-h** na hepatocitnu fazu životnog ciklusa *P. berghei*. Ukupna količina parazita predstavljena je kao postotak infekcije (stupci), a vijabilnost stanica kao konfluentnost (točke); PQ – primakin

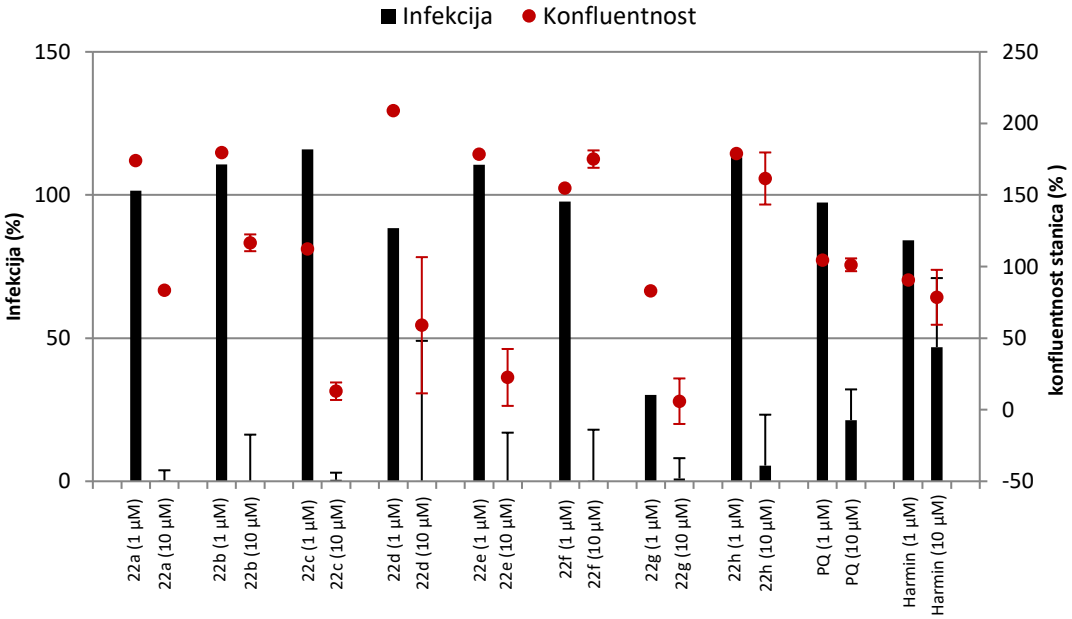

Slika 37. *In vitro* antiplazmodijsko djelovanje harmicina **22a-h** na hepatocitnu fazu životnog ciklusa *P. berghei*. Ukupna količina parazita predstavljena je kao postotak infekcije (stupci), a vijabilnost stanica kao konfluentnost (točke); PQ – primakin

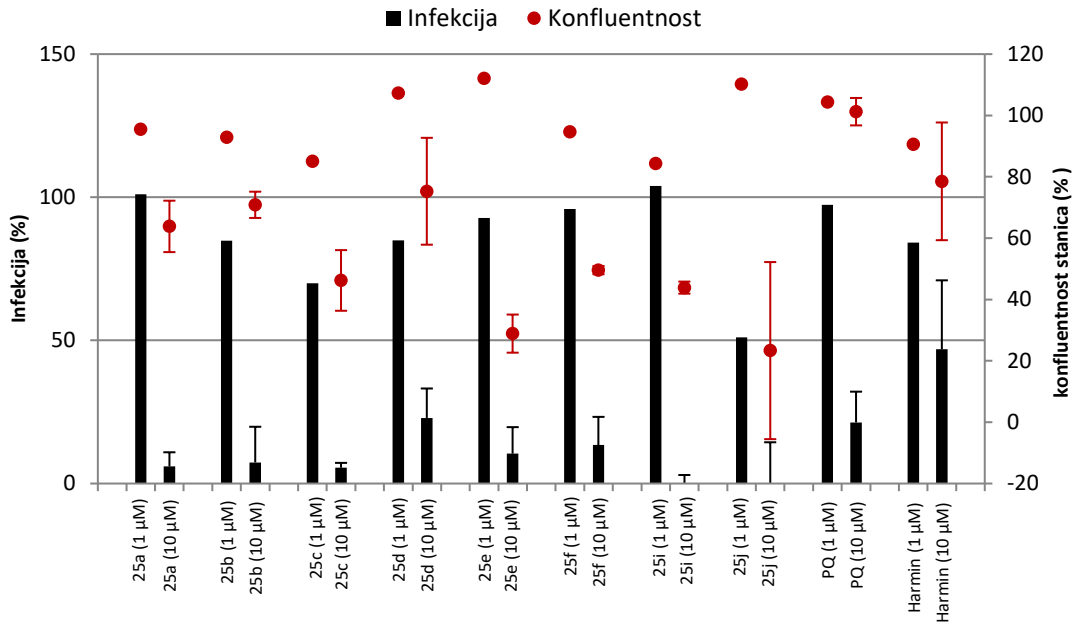

Slika 38. *In vitro* antiplazmodijsko djelovanje harmicina **25a-f**,**i**,**j** na hepatocitnu fazu životnog ciklusa *P. berghei*. Ukupna količina parazita predstavljena je kao postotak infekcije (stupci), a vijabilnost stanica kao konfluentnost (točke); PQ – primakin

4.2.2. *In vitro* antiproliferativno djelovanje harmicina

Antiproliferativno djelovanje harmicina (**13a-h**, **19a-h**, **22a-h**, **25a-f**,**i**,**j**, **28a-d**, **32b**,**c**) ispitano je *in vitro* na HepG2 staničnoj liniji metodom *Neutral red*.

Harmicini amidnoga tipa u položaju O-6 β-karbolina **19e-g** i harmicini karbamatnog tipa **28a**,**c** nisu bili citotoksični pri najvišim ispitivanim koncentracijama (**19e-g**, IC_{50} > 250 µM; **28a**,**c**, IC_{50} > 125 µM). Najmanju citotoksičnost s rasponom IC_{50} vrijednosti od 21 do 75 µM pokazali su harmicini amidnoga tipa u položaju N-9 β-karbolina **25b**,**d**,**i**,**f**, C-3 harmicin **13h**, O-6 harmicin **19b**, zatim harmicini karbamatnog tipa **28b**,**d** te harmicin ureidnog tipa **32b**. U seriji O-7-supstituiranih harmicina najmanju citotoksičnost pokazao je α-CH_3-supstituirani harmicin **22h**, dok je nesupstituirani harmicin amidnoga tipa u položaju N-9 β-karbolina **25a** s IC_{50} = 350,31 ± 13,02 µM bio najmanje citotoksičan spoj među svim testiranim harmicinima.

Nasuprot tome, najcitotoksičniji spojevi, u rasponu IC_{50} vrijednosti od 2,88 do 5,84 µM, bili su harmicini amidnoga tipa u položaju N-9 β-karbolina **25c**,**e**,**j** te O-6 harmicin **19h**.

Prema izračunatim indeksima selektivnosti harmicini amidnoga tipa u položaju N-9 β-karbolina, **25b**,**d**,**i,** koji su ujedno bili među najdjelotvornijim spojevima, imali su najveće indekse selektivnosti, pri čemu je *m*-CF_3-supstituirani harmicin **25i** bio najselektivniji spoj s

indeksom selektivnosti od 1105,33. Najučinkovitiji spojevi **25e**,**j** su zbog visoke citotoksičnosti imali niže indekse selektivnosti (**25e**, SI = 72,75; **25j**, SI = 146,00). Nasuprot tome, harmicini amidnoga tipa u položaju N-9 β-karbolina **25a**,**f**, koji su ispoljili umjereno antiplazmodijsko djelovanje na *Pf*3D7 soj, zbog svoje niske citotoksičnosti, imali su visoke indekse selektivnosti: **25a**, SI = 714,92; **25f**, SI = 287,27. Također, harmicini karbamatnog tipa **28a-d** te ureidnog tipa **32b**,**c** ispoljili su nisku citotoksičnost te su, sukladno tome, imali umjerene indekse selektivnosti (**28b**, SI = 113,49; **28d**, SI = 93,17; **32b**, SI = 53,79; **32c**, SI = 68,00).

Niske indekse selektivnosti (SI < 30) pokazali su O-7-supstituirani harmicini **22a-c**,**e**,**g**,**h** te O-6-supstituirani harmicini **19a**,**h**, dok su spojevi s najnižim indeksima selektivnosti (SI < 5) bili harmicini amidnoga tipa u položaju C-3 β-karbolina **13a-g** i harmicin **22b**.

Rezultati citotoksičnosti i indeksi selektivnosti harmicina amidnoga **7a-h**, **13a-h**, **19a-h**, **22a-h**, **25a-f**, **i-p**, karbamatnog **28a-d** i ureidnog **32b**,**c** tipa dani su u Tablici 32.

Tablica 32. *In vitro* antiproliferativno djelovanje harmicina amidnoga (**13**, **19**, **22**, **25**), karbamatnog (**28a-d**) i ureidnog tipa (**32**) na HepG2 i indeksi selektivnosti

Spoj	Položaj supstitucije β-karbolina	Vrsta poveznice	Supstituent	IC_{50}[a] (μM)	SI
				HepG2	
13a	**C-3**	**AMID**	–	7,05 ± 0,11	1,22
13b			*m*-F	15,83 ± 3,23	2,76
13c			*m*-Br	9,64 ± 4,71	2,98
13d			*m*-CF_3	9,37 ± 4,90	4,66
13e			*p*-F	12,46 ± 5,26	3,02
13f			*p*-Cl	11,33 ± 0,65	3,88
13g			*p*-OCH_3	10,38 ± 4,15	1,60
13h			*p*-CF_3	33,26 ± 1,66	14,46
19a	**O-6**	**AMID**	–	12,02 ± 4,95	7,75
19b			*m*-F	37,57 ± 3,10	33,85
19c			*m*-Br	7,57 ± 2,56	39,84
19d			*m*-CF_3	6,14 ± 0,11	51,17
19e			*p*-F	> 250	> 263,16
19f			*p*-Cl	> 250	> 694,44
19g			*p*-OCH_3	> 250	> 213,68
19h			*p*-CF_3	3,59 ± 1,26	29,92
22a	**O-7**	**AMID**	–	12,74 ± 0,66	13
22b			*m*-F	12,86 ± 3,31	4,68

22c	**O-7**	**AMID**	*m*-Br	6,11 ± 2,07	16,51
22d			*p*-F	7,63 ± 2,47	50,87
22e			*p*-Cl	7,72 ± 3,04	24,13
22f			*p*-OCH_3	10,53 ± 0,43	50,14
22g			*o*-F	16,17 ± 1,86	17,39
22h			α-CH_3	61,28 ± 2,75	9,04
25a	**N-9**	**AMID**	–	350,31 ± 13,02	714,92
25b			*m*-F	54,11 ± 13,36	773
25c			*m*-Br	2,88 ± 0,42	41,14
25d			*p*-F	20,99 ± 0,88	233,22
25e			*p*-Cl	2,91 ± 1,75	72,75
25f			*p*-OCH_3	74,69 ± 7,61	287,27
25i			*m*-CF_3	66,32 ± 3,79	1105,33
25j			*p*-CF_3	5,84 ± 1,67	146
28a	**N-9**	**KARBAMAT**	–	> 125	> 227,27
28b			*p*-$O(CH_2)_2CH_3$	44,26 ± 12,04	113,49
28c			*m*-CF_3	> 125	> 250
28d			*m*,*m*-di-CF_3	60,56 ± 23,44	93,17
32b	**N-9**	**UREA**	*p*-$O(CH_2)_2CH_3$	22,59 ± 11,60	53,79
32c			*m*-CF_3	14,96 ± 5,44	68
CQ[c]				n.o.[b]	n.o.
Harmin				> 250	> 30

[a] IC_{50} - koncentracija spoja koja inhibira rast za 50 %; [b] n.o. - nije određeno; [c] CQ - klorokin

4.3. KVANTITATIVNI ODNOS STRUKTURE I DJELOVANJA

U svrhu kvantificiranja odnosa strukture i djelovanja harmicina amidnoga tipa korišteni su generirani molekulski deskriptori (3.4.1.) i metode statističkog učenja.

4.3.1. Odabir molekulskih deskriptora

Za izradu QSAR modela korišten je skup od 40 novosintetiziranih harmicina amidnoga tipa (**7a-h**, **13a-h**, **19a-h**, **22a-h** i **25a-f**,**i**,**j**) te je generirano ukupno 133 pripadajuća molekulska deskriptora.

Proces odabira deskriptora započeo je izostavljanjem deskriptora, odn. varijabli koje za cijeli skup spojeva imaju konstantnu vrijednost. Popis izostavljenih deskriptora i njihovih vrijednosti dan je u Tablici 33.

Tablica 33. Deskriptori s konstantnim vrijednostima izostavljeni u izradi QSAR modela

Deskriptor	Vrijednost
broj asimetričnih atoma (AAC)	0
broj atoma u aromatskim vezama (ArAC)	19
broj aromatskih veza (ArBC)	21
broj prstenova (RC)	4
broj zasićenih prstenova (AlRC)	0
broj aromatskih prstenova (ArRC)	4
broj atoma u prstenovima (RAC)	19
broj veza u prstenovima (RBC)	21
broj aromatskih prstenova s ugljikovim kosturom (CArC)	2
broj alifatskih prstenova s ugljikovim kosturom (CRC)	0
broj heterocikala (HRC)	0
broj aromatskih heterocikala (HArC)	2
broj heteroaromatskih prstenova (HArRC)	2
broj teških aromatskih atoma (NArHA)	2
broj fuzioniranih zasićenih prstenova (FAlRC)	0
broj fuzioniranih aromatskih prstenova (FArRC)	3
broj fuzioniranih prstenova (FRC)	0
veličina najvećeg prstenova (LRS)	6
veličina najmanjeg prstena (SRS)	5
ciklomatski broj (CN)	4

Za opisivanje supstituenata izračunati su lokalni molekulski deskriptori: masa supstituenta (M_S), volumen supstituenta (V_S) i hidrofobna konstanta po Hanschu (πs), a njihove vrijednosti dane su u Tablici 34.

Tablica 34. Vrijednosti mase supstituenta (M_S), volumena supstituenta (V_S) i hidrofobne konstante po Hanschu (πs) harmicina amidnoga tipa **7a-h**, **13a-h**, **19a-h**, **22a-h**, **25a-f**,**i**,**j**.

Deskriptor / Harmicin	M_S	V_S	π_S	Deskriptor / Harmicin	M_S	V_S	π_S
7a	0	0	0	**19e**	18,998	4,2	0,14
7b	18,998	4,2	0,14	**19f**	35,45	11,55	0,6
7c	79,9	16,1	0,77	**19g**	31,03	24	-0,16
7d	69,01	33,5	0,88	**19h**	69,01	33,5	0,88
7e	18,998	4,2	0,14	**22a**	0	0	0
7f	35,45	11,55	0,6	**22b**	18,998	4,2	0,14
7g	31,03	24	-0,16	**22c**	79,9	16,1	0,77
7h	69,01	33,5	0,88	**22d**	18,998	4,2	0,14
13a	0	0	0	**22e**	35,45	11,55	0,6
13b	18,998	4,2	0,14	**22f**	31,03	24	-0,16
13c	79,9	16,1	0,77	**22g**	18,998	4,2	0,14
13d	69,01	33,5	0,88	**22h**	0	0	0
13e	18,998	4,2	0,14	**25a**	0	0	0
13f	35,45	11,55	0,6	**25b**	18,998	4,2	0,14
13g	31,03	24	-0,16	**25c**	79,9	16,1	0,77
13h	69,01	33,5	0,88	**25d**	18,99	4,2	0,14
19a	0	0	0	**25e**	35,45	11,55	0,6
19b	18,998	4,2	0,14	**25f**	31,03	24	-0,16
19c	79,9	16,1	0,77	**25i**	69,01	33,5	0,88
19d	69,01	33,5	0,88	**25j**	69,01	33,5	0,88

Fizikalno-kemijska svojstva navedenih harmicina amidnoga tipa opisana su pomoću 39 molekulskih deskriptora. Posebnu važnost ima lipofilnost i topljivost spojeva, stoga su koeficijenti razdjeljenja log *P* te logaritam intrizične topljivosti log *S* izračunati u više korištenih programa i mrežnih stranica. Također je, osim izračunate temperature tališta u programu MNova (t_{tmestr}), korištena i eksperimentalno određena temperatura tališta (t_t). Vrijednosti fizikalno-kemijskih deskriptora harmicina amidnoga tipa **7a-h**, **13a-h**, **19a-h**, **22a-h** i **25a-f**,**i**,**j** dani su Tablicama 35 – 37.

Tablica 35. Vrijednosti fizikalno-kemijskih deskriptora harmicina amidnoga tipa **7a-h**, **13a-h**, **19a-h**, **22a-h**, **25a-f**,**i**,**j**

Deskriptor / Harmicin	M_r	log P_{chem}	log P_{dr}	log P_{swiss}	log P_{mestr}	Clog P	log S_{chem}	log S_{dr}	log S_{swiss}	log S_{mestr}	s	s_M	t_t
7a	327,39	3,26	2,93	3,35	2,51	3,99	-5,57	-5,19	-4,45	-4,38	$1,17 \times 10^{-2}$	$3,56\times 10^{-2}$	226,1
7b	345,38	3,40	3,09	3,70	2,68	4,13	-5,83	-5,39	-4,55	-4,73	$9,68 \times 10^{-3}$	$2,80 \times 10^{-5}$	225,1
7c	406,28	4,03	2,96	3,97	3,41	3,68	-6,50	-5,05	-5,16	-5,53	$2,78 \times 10^{-3}$	$6,85 \times 10^{-6}$	238,1
7d	395,39	4,14	3,85	4,37	3,47	4,87	-6,52	-6,16	-5,36	-5,22	$1,72 \times 10^{-3}$	$4,35 \times 10^{-6}$	226
7e	345,38	3,40	3,09	3,73	2,68	4,13	-5,83	-5,41	-4,55	-4,73	$9,68 \times 10^{-3}$	$2,80 \times 10^{-5}$	232,3
7f	361,83	3,86	3,49	3,95	3,24	4,70	-6,26	-5,88	-5,10	-5,21	$2,86 \times 10^{-3}$	$7,90 \times 10^{-6}$	242,2
7g	357,41	3,10	2,80	3,41	2,45	3,91	-5,53	-5,24	-4,61	-4,46	$8,75 \times 10^{-3}$	$2,45 \times 10^{-5}$	231,1
7h	395,39	4,14	3,85	4,34	3,47	4,87	-6,52	-6,14	-5,36	-5,22	$1,72 \times 10^{-3}$	$4,35 \times 10^{-6}$	263,5
13a	341,41	3,39	3,63	3,66	2,80	4,49	-5,71	-5,46	-4,86	-4,52	$4,67 \times 10^{-3}$	$1,37 \times 10^{-5}$	207,7
13b	359,4	3,53	3,79	3,99	3,70	4,63	-5,97	-5,67	-4,97	-5,68	$3,88 \times 10^{-3}$	$1,08 \times 10^{-5}$	114,8
13c	420,31	4,16	4,46	4,37	3,70	5,35	-6,63	-6,27	-5,58	-5,68	$1,11 \times 10^{-3}$	$2,63 \times 10^{-6}$	122,5
13d	409,41	4,27	4,56	4,78	3,75	5,37	-6,65	-6,43	-5,78	-5,37	$6,85 \times 10^{-4}$	$1,67 \times 10^{-6}$	236,4
13e	359,4	3,53	3,79	4,04	2,96	4,63	-5,97	-5,69	-4,97	-4,81	$3,88 \times 10^{-3}$	$1,08 \times 10^{-5}$	218,9
13f	375,86	3,99	4,19	4,25	3,53	5,20	-6,39	-6,16	-5,52	-5,36	$1,14 \times 10^{-3}$	$3,04 \times 10^{-6}$	256,3
13g	371,44	3,23	3,51	3,72	2,74	4,41	-5,67	-5,51	-5,03	-4,60	$3,50 \times 10^{-3}$	$9,41 \times 10^{-6}$	263,5
13h	409,41	4,27	4,56	4,78	3,75	5,37	-6,65	-6,42	-5,78	-5,37	$6,85 \times 10^{-4}$	$1,67 \times 10^{-6}$	265,5
19a	371,44	3,23	3,14	3,71	3,83	4,82	-5,75	-5,50	-5,20	-4,87	$2,33 \times 10^{-3}$	$6,27 \times 10^{-6}$	130
19b	389,43	3,37	3,30	4,03	3,99	4,96	-6,00	-5,72	-5,31	-5,23	$1,92 \times 10^{-3}$	$4,94 \times 10^{-6}$	225,5
19c	450,34	4,00	3,97	4,31	4,73	5,68	-6,63	-6,31	-5,92	-6,02	$5,43 \times 10^{-4}$	$1,21 \times 10^{-6}$	231,5
19d	439,44	4,11	4,06	4,75	4,78	5,70	-6,66	-6,49	-6,12	-5,72	$3,37 \times 10^{-4}$	$7,66 \times 10^{-7}$	217,3
19e	389,43	3,37	3,30	4,01	3,99	4,96	-6,00	-5,74	-5,31	-5,23	$1,92 \times 10^{-3}$	$4,94 \times 10^{-6}$	227
19f	405,88	3,83	3,70	4,23	4,56	5,53	-6,42	-6,20	-5,85	-5,71	$5,79 \times 10^{-4}$	$1,43 \times 10^{-6}$	229
19g	401,47	3,07	3,02	3,73	3,77	4,38	-5,70	-5,57	-5,37	-4,95	$1,73 \times 10^{-3}$	$4,31 \times 10^{-6}$	242
19h	439,44	4,11	4,06	4,76	4,78	5,70	-6,66	-6,47	-6,12	-5,72	$3,37 \times 10^{-4}$	$7,66 \times 10^{-7}$	232,5
22a	371,44	3,23	3,14	3,70	3,83	4,82	-5,75	-5,52	-5,20	-4,87	$2,33 \times 10^{-3}$	$6,27 \times 10^{-6}$	151,6
22b	389,43	3,37	3,30	4,01	3,92	5,13	-6,00	-5,74	-5,31	-5,23	$1,92 \times 10^{-3}$	$4,94 \times 10^{-6}$	211,3
22c	450,34	4,00	3,97	4,32	4,73	4,96	-6,63	-6,32	-5,92	-6,02	$5,43 \times 10^{-4}$	$1,21 \times 10^{-6}$	136,2

22d	389,43	3,37	3,30	4,01	3,92	4,96	-6,00	-5,76	-5,31	-5,23	$1,92 \times 10^{-3}$	$4,94 \times 10^{-6}$	200,1
22e	405,88	3,83	3,70	4,22	4,56	5,68	-6,42	-6,21	-5,85	-5,71	$5,79 \times 10^{-4}$	$1,43 \times 10^{-6}$	232,4
22f	401,47	3,07	3,02	3,69	3,77	4,96	-5,70	-5,58	-5,37	-4,95	$1,73 \times 10^{-3}$	$4,31 \times 10^{-6}$	192,7
22g	389,43	3,37	3,30	4,04	3,96	5,53	-6,00	-5,75	-5,31	-5,32	$1,92 \times 10^{-3}$	$4,94 \times 10^{-6}$	241,6
22h	385,47	3,62	3,49	3,97	4,17	4,74	-5,69	-5,65	-5,59	-5,15	$9,99 \times 10^{-4}$	$2,59 \times 10^{-6}$	221,9
25a	385,47	3,45	3,38	3,70	3,97	4,96	-4,89	-5,66	-4,85	-4,93	$5,44 \times 10^{-3}$	$1,41 \times 10^{-5}$	202,5
25b	403,46	3,60	3,54	3,97	4,13	5,10	-5,13	-5,89	-4,95	-5,29	$4,49 \times 10^{-3}$	$1,11 \times 10^{-5}$	227,1
25c	464,36	4,22	4,21	4,23	4,87	5,82	-5,75	-6,47	-5,57	-6,09	$1,26 \times 10^{-3}$	$2,72 \times 10^{-6}$	225,4
25d	403,46	3,60	3,54	4,03	4,13	5,84	-5,13	-5,91	-4,95	-5,29	$4,49 \times 10^{-3}$	$1,11 \times 10^{-5}$	203,1
25e	419,91	4,06	3,94	4,17	4,69	5,10	-5,55	-6,36	-5,50	-5,77	$1,32 \times 10^{-3}$	$3,13 \times 10^{-6}$	245
25f	415,49	3,29	3,25	3,71	3,90	5,67	-4,83	-5,73	-5,01	-5,01	$4,03 \times 10^{-3}$	$9,71 \times 10^{-6}$	217
25i	453,47	4,33	4,30	4,63	4,92	4,87	-5,78	-6,65	-5,77	-5,78	$7,64 \times 10^{-4}$	$1,68 \times 10^{-6}$	221,4
25j	453,47	4,33	4,30	4,68	4,92	5,84	-5,78	-6,63	-5,77	-5,78	$7,64 \times 10^{-4}$	$1,68 \times 10^{-6}$	253,4

M_r - relativna molekulska masa; log *P* - koeficijent razdjeljenja; Clog *P* - računski logaritam koeficijenta razdjeljenja; log *S* - logaritam intrizične topljivosti; *s* - topljivost; s_M - molarna topljivost; t_t - temperatura tališta

Tablica 36. Vrijednosti fizikalno-kemijskih deskriptora harmicina amidnoga tipa **7a-h**, **13a-h**, **19a-h**, **22a-h**, **25a-f**,**i**,**j**

Deskriptor / Harmicin	t_{tmestr}	σ	ρ	p	logK_p	K_h	H^{rcc}	$HLB_{chemaxon}$	HLB_{Davies}	$HLB_{Griffin}$	Abr A	Abr B	Abr E
7a	250,65	64,0	1,29	716,16	-5,78	-13,41	15,88	4,49	1,98	8,26	0,47	1,49	2,62
7b	248,83	62,3	1,34	723,7	-5,82	-12,81	15,82	4,88	2,45	8,52	0,49	1,47	2,87
7c	287,3	65,6	1,51	767	-5,77	-13,83	14,32	4,37	2,45	7,24	0,49	1,45	2,92
7d	237,91	52,9	1,38	773,8	-5,57	-11,70	14,95	4,16	1,98	7,44	0,51	1,42	2,97
7e	248,83	62,3	1,34	723,7	-5,82	-12,81	15,82	4,88	2,45	8,52	0,49	1,47	2,87
7f	270,71	64,7	1,36	752,4	-5,54	-13,60	16,01	4,72	2,45	8,13	0,40	1,45	2,87
7g	267,82	60,4	1,29	773,2	-5,98	-14,53	17,11	6,24	3,75	9,97	0,48	1,69	2,78
7h	237,91	52,9	1,38	773,8	-5,57	-11,70	14,95	4,16	1,98	7,44	0,51	1,42	2,97
13a	257,21	61,2	1,27	754,2	-5,58	-13,85	15,84	4,04	1,5	7,86	0,47	1,51	2,57
13b	293,88	59,7	1,31	761,3	-5,62	-14,26	15,77	4,44	1,98	8,13	0,48	1,46	2,87
13c	293,88	62,8	1,47	804,7	-5,57	-14,26	16,24	3,97	1,98	6,95	0,48	1,46	2,87
13d	244,47	51,3	1,35	811,4	-5,37	-12,13	14,9	3,76	1,5	7,14	0,50	1,44	2,91
13e	255,38	59,7	1,31	761,3	-5,62	-13,24	15,77	4,44	1,98	8,13	0,48	1,49	2,81
13f	277,27	62	1,33	790,1	-5,34	-14,03	15,97	4,3	1,98	7,78	0,48	1,47	2,82
13g	274,37	58,1	1,27	810,9	-5,78	-14,96	17,07	5,78	3,28	9,54	0,48	1,71	2,73
13h	244,47	51,3	1,35	811,4	-5,37	-12,13	14,9	3,76	1,5	7,14	0,50	1,44	2,91
19a	255,25	58,8	1,26	813,8	-5,66	-16,17	16,99	5,78	3,27	9,54	0,45	1,66	2,72
19b	253,42	57,6	1,31	821	-5,7	-15,57	16,92	6,14	3,75	9,72	0,47	1,64	2,97
19c	291,89	60,4	1,45	864,3	-5,65	-16,58	17,39	5,61	3,75	8,4	0,47	1,62	3,02
19d	242,51	50,1	1,34	871	-5,45	-14,46	16,05	5,41	3,27	8,61	0,48	1,60	3,07
19e	253,42	57,6	1,31	821	-5,7	-15,57	16,92	6,14	3,75	9,72	0,47	1,64	2,97
19f	275,3	59,6	1,33	849,7	-5,43	-16,35	17,12	5,98	3,75	9,32	0,47	1,62	2,97
19g	272,41	56,3	1,26	870,5	-5,87	-17,28	18,22	7,42	5,05	10,97	0,46	1,86	2,88
19h	242,51	50,1	1,34	871	-5,45	-14,46	16,05	5,41	3,27	8,61	0,48	1,60	3,07
22a	255,25	58,8	1,26	813,8	-5,66	-16,17	16,99	5,78	3,27	9,54	0,45	1,66	2,72
22b	253,42	57,6	1,31	821	-5,7	-15,57	16,92	6,14	3,75	9,72	0,47	1,64	2,97

22c	291,89	60,4	1,45	864,3	-5,65	-16,58	17,39	5,61	3,75	8,4	0,47	1,62	3,02
22d	253,42	57,6	1,31	821	-5,7	-15,57	16,92	6,14	3,75	9,72	0,47	1,64	2,97
22e	257,3	59,6	1,33	849,7	-5,43	-16,35	17,12	5,98	3,75	9,32	0,47	1,62	2,97
22f	272,41	56,3	1,26	870,5	-5,87	-17,28	18,22	7,42	5,05	10,97	0,46	1,86	2,88
22g	257,21	57,6	1,31	821	-5,7	-15,93	16,92	6,14	3,75	9,72	0,45	1,64	2,83
22h	244,36	56,4	1,24	849,8	-5,48	-15,46	16,79	5,36	2,8	9,19	0,42	1,59	2,61
25a	214,12	44,6	1,17	845,2	-5,83	-13,01	3,19	5,93	3,27	9,2	0,22	1,66	2,45
25b	212,3	43,1	1,22	845,4	-5,87	-12,40	3,19	6,28	3,75	10,07	0,23	1,64	2,69
25c	250,77	47	1,36	888,8	-5,82	-13,42	3,19	5,75	3,75	8,75	0,23	1,62	2,75
25d	212,3	43,1	1,22	845,4	-5,87	-12,40	3,19	6,28	3,75	10,07	0,23	1,64	2,69
25e	234,18	45,6	1,24	874,1	-5,6	-13,19	3,19	6,12	3,75	9,68	0,23	1,63	2,70
25f	231,3	43,5	1,19	895,5	-6,04	-14,12	3,19	7,54	5,05	11,28	0,23	1,86	2,61
25i	201,38	40,3	1,27	899,2	-5,62	-11,29	3,19	5,55	3,27	8,96	0,25	1,60	2,80
25j	201,38	40,3	1,27	899,2	-5,62	-11,29	3,19	5,55	3,27	8,96	0,25	1,60	2,80

t_{tmestr} - temperatura tališta; σ - površinska napetost; ρ - gustoća; p - parahor; logK_p - logaritam koeficijenta permeabilnosti kroz kožu; K_h, H^{cc} - Henryjeve konstante; *HLB* - hidrofilno-lipofilne ravnoteže; Abr A - Abrahamov deskriptor A; Abr B - Abrahamov deskriptor B; Abr E - Abrahamov deskriptor E

Tablica 37. Vrijednosti fizikalno-kemijskih deskriptora harmicina amidnoga tipa **7a-h**, **13a-h**, **19a-h**, **22a-h**, **25a-f**,**i**,**j**

Deskriptor / Harmicin	Abr S	Abr V	p_V	t_B	log *D*	$\log K_{aAGP}$	$\log K_{aHSA}$	$\log K_{aMemb}$	log *BB*	fu_p	fu_b	*PPB*	*HRA*
7a	2,76	2,37	-12,43	513,03	2,62	5,70	4,59	5,37	0,314	0,035	3,246	96,536	-8,008
7b	2,87	2,42	-12,35	481,75	2,74	5,77	4,58	5,53	0,48	0,038	2,299	96,167	-8,478
7c	2,89	2,54	-13,62	553,75	3,63	5,98	4,76	6,30	0,485	0,027	0,341	97,336	-8,356
7d	2,88	2,64	-12,83	477,46	3,53	5,80	4,74	5,76	0,421	0,025	1,466	97,511	-9,192
7e	2,87	2,42	-12,35	481,04	2,74	5,77	4,58	5,53	0,48	0,038	2,299	96,167	-8,478
7f	2,86	2,51	-13,15	522,5	3,39	6,23	4,84	5,83	0,349	0,019	1,206	98,091	-8,482
7g	3,07	2,56	-13,38	541,05	2,52	5,71	4,58	5,40	0,355	0,037	3,018	96,339	-7,707
7h	2,88	2,64	-12,83	477,46	3,53	5,80	4,74	5,76	0,421	0,025	1,466	97,511	-9,192
13a	2,73	2,50	-12,46	527,21	2,93	5,88	4,71	5,54	0,391	0,031	2,209	96,911	-7,887
13b	2,86	2,68	-13,65	567,93	3,94	6,17	4,88	6,47	0,562	0,024	0,23	97,627	-8,235
13c	2,86	2,68	-13,65	567,93	3,94	6,17	4,88	6,47	0,562	0,024	0,23	97,627	-8,235
13d	2,85	2,78	-12,86	491,64	3,84	5,99	4,86	5,93	0,498	0,022	0,992	97,783	-9,071
13e	2,84	2,56	-12,38	495,22	3,08	5,96	4,69	5,70	0,557	0,034	1,559	96,581	-8,357
13f	2,83	2,64	-13,18	536,66	3,70	6,41	4,95	6,00	0,426	0,017	0,815	98,301	-8,361
13g	3,03	2,70	-13,41	555,23	2,83	5,90	4,69	5,57	0,431	0,033	2,052	96,735	-7,586
13h	2,85	2,78	-12,86	491,64	3,84	5,99	4,86	5,93	0,498	0,022	0,992	97,783	-9,071
19a	2,97	2,70	-13,79	525,41	4,03	5,94	4,65	5,49	0,23	0,034	2,582	96,649	-7,432
19b	3,08	2,75	-13,71	493,42	4,14	6,01	4,63	5,64	0,397	0,037	1,825	96,292	-7,902
19c	3,10	2,88	-14,98	566,13	5,03	6,22	4,82	6,41	0,401	0,026	0,27	97,424	-7,78
19d	3,08	2,97	-14,19	489,84	4,94	6,04	4,80	5,88	0,337	0,024	1,162	97,593	-8,616
19e	3,08	2,75	-13,71	493,42	4,14	6,01	4,63	5,64	0,397	0,037	1,825	96,292	-7,902
19f	3,07	2,84	-14,51	534,88	4,79	6,47	4,89	5,94	0,265	0,018	0,955	98,154	-7,906
19g	3,27	2,89	-14,74	553,43	3,93	5,95	4,63	5,51	0,271	0,035	2,4	96,458	-7,131
19h	3,08	2,97	-14,19	489,84	4,94	6,04	4,80	5,88	0,337	0,024	1,162	97,593	-8,616
22a	2,97	2,70	-13,79	525,41	4,03	5,94	4,65	5,49	0,23	0,034	2,582	96,649	-7,432
22b	3,08	2,75	-13,71	493,42	4,14	6,01	4,63	5,64	0,397	0,037	1,825	96,292	-7,902
22c	3,10	2,88	-14,98	566,13	5,03	6,22	4,82	6,41	0,401	0,026	0,27	97,424	-7,78

22d	3,08	2,75	-13,71	493,42	4,14	6,01	4,63	5,64	0,397	0,037	1,825	96,292	-7,902
22e	3,07	2,84	-14,51	534,88	4,79	6,47	4,89	5,94	0,265	0,018	0,955	98,154	-7,906
22f	3,27	2,89	-14,74	553,43	3,93	5,95	4,63	5,51	0,271	0,035	2,4	96,458	-7,131
22g	3,02	2,73	-14,04	505,81	4,17	5,89	4,56	5,34	0,182	0,041	3,504	95,893	-7,756
22h	2,84	2,88	-13,43	501,58	4,49	6,09	4,67	5,75	0,326	0,034	1,786	96,631	-7,235
25a	2,81	2,76	-11,68	465,69	4,64	5,90	4,83	5,68	0,37	0,025	1,39	97,538	-7,832
25b	2,92	2,82	-11,59	433,69	4,76	5,98	4,81	5,92	0,536	0,027	0,979	97,273	-8,301
25c	2,94	2,94	-12,87	506,41	5,65	6,18	5,00	6,69	0,541	0,019	0,144	98,111	-8,719
25d	2,92	2,82	-11,59	433,69	4,76	5,98	4,81	5,92	0,536	0,027	0,979	97,273	-8,301
25e	2,92	2,90	-12,39	475,15	5,41	6,43	5,07	6,22	0,405	0,014	0,51	98,65	-8,305
25f	3,12	2,96	-12,63	493,71	4,54	5,92	4,81	5,79	0,41	0,026	1,291	97,397	-7,531
25i	2,93	3,04	-12,08	430,12	5,55	6,01	4,98	6,16	0,477	0,018	0,621	98,236	-9,015
25j	2,93	3,04	-12,08	430,12	5,55	6,01	4,98	6,16	0,477	0,018	0,621	98,236	-9,015

Abr S - Abrahamov deskriptor S; Abr V - Abrahamov deskriptor V; p_V - tlak para; t_B - temperatura vrelišta; log *D* - logaritam koeficijenta razdjeljenja pri pH 7,4; logK_{aAGP} - logaritam konstante vezanja za kiseli α-glikoprotein; logK_{aHSA} - logaritam konstante vezanja za humani serumski albumin; logK_{aMemb} - logaritam konstante vezanja za membrane; log *BB* - logaritam koeficijenta razdjeljenja između krvno-moždane barijere; fu_p - slobodna frakcija lijeka u plazmi; fu_b - slobodna frakcija lijeka u mozgu; *PPB* - postotak vezanja za proteine plazme; *HRA* - napad hidroksilnih radikala

Također, generirani su molekulski deskriptori koji se prema dimenzionalnosti svrstavaju u 0D i 1D deskriptore, među kojima se nalaze jednostavni topološki indeksi koji su dobiveni prebrojavanjem atoma, veza i prstenova. Zatim su određeni molekulski deskriptori vodikove veze poput broja akceptorskih i donorskih skupina vodikovih veza (HBA, HBD) i indeksi fleksibilnosti kao što su broj veza u molekuli koje mogu slobodno rotirati oko vlastite osi (B_{FR}). Vrijednosti navedenih deskriptora dane su u Tablici 38.

Na temelju struktura harmicina amidnoga tipa **7a-h**, **13a-h**, **19a-h**, **22a-h**, **25a-f**,**i**,**j** definiran je niz indikatorskih varijabli koje označavaju prisutnost supstitucijskog lanca odn. koji je od navedenih položaja β-karbolina derivatiziran (pol. 1, pol. 3, pol. 6, pol. 7, pol. 9). Nadalje, definirana je i prisutnost supstituenta u *orto*, *meta* ili *para* položaju benzenskog prstena DCK-a (fenil 2', fenil 3', fenil 4'), prisutnost metoksi skupine u položaju 7 β-karbolina (OCH_3 pol. 7), te metilne skupine u položaju 1 β-karbolina (CH_3 pol. 1). Budući da je u sintezi harmicina **22h** korištena α-metil-supstituirana cimetna kiselina definirana je i indikatorska varijabla koja označuje prisutnost/odsutnost supstituenta u α-položaju DCK-a navedenih harmicina amidnoga tipa (CH_3 pol. 5'). Vrijednost 1 u indikatorskim varijablama označuje prisutnost supstitucijskog lanca ili navedenih supstituenata u definiranim položajima β-karbolina, dok vrijednost 0 određuje odsustvo. Vrijednosti indikatorskih varijabli dane su u Tablici 39.

Osim jednostavnih topoloških deskriptora izračunati su i globalni topološki deskriptori: Plattov indeks F(G), Randićev indeks povezanosti χ(G), Balabanov indeks J(G), Hararyjev indeks H(G), hiper-Wienerov indeks WW(G), Szeged-indeks Sz(G), Wienerov indeks W(G), Wienerov indeks polarnosti Wp(G), a njihove vrijednosti dane su u Tablici 40.

Tablica 38. Vrijednosti 0D i 1D-deskriptora, deskriptora vodikove veze i indeksi fleksibilnosti harmicina amidnoga tipa **7a-h**, **13a-h**, **19a-h**, **22a-h**, **25a-f**,**i**,**j**

Deskriptor / Harmicin	W_C	W_H	W_N	NA	NHA	B_{FRchem}	$B_{FRswiss}$	Fsp^3	HBD_{chem}	HBD_{swiss}	HBA_{chem}	HBA_{swiss}	NB	AlAC	AlBC	CAC	CBC	ACC	ACOR
7a	77,04	5,23	12,84	42	25	4	5	0,05	2	2	2	2	45	6	7	1	2	22	22
7b	73,03	4,67	12,17	42	26	4	5	0,05	2	2	2	3	45	7	8	1	2	22	22
7c	62,08	3,97	10,34	42	26	4	5	0,05	2	2	2	2	45	7	8	1	2	22	22
7d	66,83	4,08	10,63	45	29	4	6	0,09	2	2	2	5	48	10	11	1	2	25	25
7e	73,03	4,67	12,17	42	26	4	5	0,05	2	2	2	3	45	7	8	1	2	22	22
7f	69,71	4,46	11,61	42	26	4	5	0,05	2	2	2	2	45	7	8	1	2	22	22
7g	73,93	5,36	11,76	46	27	5	6	0,09	2	2	3	3	49	8	9	1	2	26	26
7h	66,83	4,08	10,63	45	29	5	6	0,09	2	2	2	5	48	1	11	1	2	25	25
13a	77,4	5,61	12,31	45	26	4	5	0,09	2	2	2	2	48	7	8	1	2	22	26
13b	73,52	5,05	11,69	45	27	4	5	0,09	2	2	2	3	48	8	9	1	2	22	26
13c	62,87	4,32	10	45	27	4	5	0,09	2	2	2	2	48	8	9	1	2	22	26
13d	67,48	4,43	10,26	48	30	5	6	0,13	2	2	2	5	51	11	12	1	2	25	29
13e	73,52	5,05	11,69	45	27	4	5	0,09	2	2	2	3	48	8	9	1	2	22	26
13f	70,3	4,83	11,18	45	27	4	5	0,09	2	2	2	2	48	8	9	1	2	22	26
13g	74,37	5,7	11,31	49	28	5	6	0,13	2	2	3	3	52	9	10	1	2	26	30
13h	67,48	4,43	10,26	48	30	5	6	0,13	2	2	2	5	51	11	12	1	2	25	29
19a	74,37	5,7	11,31	49	28	6	7	0,13	2	2	3	3	52	9	10	3	4	26	30
19b	70,94	5,18	10,79	49	29	6	7	0,13	2	2	3	4	52	10	11	3	4	26	30
19c	61,34	4,48	9,33	49	29	6	7	0,13	2	2	3	3	52	10	11	3	4	26	30
19d	65,6	4,59	9,56	52	32	7	8	0,17	2	2	3	6	55	13	14	3	4	29	33
19e	70,94	5,18	10,79	49	29	6	7	0,13	2	2	3	4	52	10	11	3	4	26	30
19f	68,06	4,97	10,35	49	29	6	7	0,13	2	2	3	3	52	10	11	3	4	26	30
19g	71,8	5,77	10,47	53	30	7	8	0,17	2	2	4	4	56	11	12	3	4	30	34
19h	65,6	4,59	9,56	52	32	7	8	0,17	2	2	3	6	55	13	14	3	4	29	33
22a	74,37	5,7	11,31	49	28	6	7	0,13	2	2	3	3	52	9	10	3	4	26	30

22b	70,94	5,18	10,79	49	29	6	7	0,13	2	2	3	4	52	10	11	3	4	26	30
22c	61,34	4,48	9,33	49	29	6	7	0,13	2	2	3	3	52	10	11	3	4	26	30
22d	70,94	5,18	10,79	49	29	6	7	0,13	2	2	3	4	52	10	11	3	4	26	30
22e	68,06	4,97	10,35	49	29	6	7	0,13	2	2	3	3	52	10	11	3	4	26	30
22f	71,8	5,77	10,47	53	30	7	8	0,17	2	2	4	4	56	11	12	3	4	30	34
22g	70,94	5,18	10,79	49	29	6	7	0,13	2	2	3	4	52	10	11	3	4	26	30
22h	74,78	6,01	10,9	52	29	6	7	0,17	2	2	3	3	55	10	11	3	4	29	33
25a	74,78	6,01	10,9	52	29	6	7	0,17	1	1	3	3	55	10	11	2	3	25	34
25b	71,45	5,5	10,42	52	30	6	7	0,17	1	1	3	4	55	11	12	2	3	25	34
25c	62,08	4,78	9,05	52	30	6	7	0,17	1	1	3	3	55	11	12	2	3	25	34
25d	71,45	5,5	10,42	52	30	6	7	0,17	1	1	3	4	55	11	12	2	3	25	34
25e	68,65	5,28	10,01	52	30	6	7	0,17	1	1	3	3	55	11	12	2	3	25	34
25f	72,27	6,07	10,11	56	31	7	8	0,2	1	1	4	4	59	12	13	2	3	29	38
25i	66,22	4,89	9,27	55	33	7	8	0,2	1	1	3	6	58	14	15	2	3	28	37
25j	66,22	4,89	9,27	55	33	7	8	0,2	1	1	3	6	58	14	15	2	3	28	37

W_C - udio atoma ugljika u strukturi; W_H - udio atoma vodika u strukturi; W_N - udio atoma dušika u strukturi; NA - broj atoma; NHA - broj teških atoma; B_{FR} - broj veza u molekuli koje mogu slobodno rotirati oko vlastite osi; Fsp^3 - omjer sp^3-hibridiziranih ugljikovih atoma i ukupnog broja ugljikovih atoma; HBD - broj donorskih skupina vodikove veze; HBA - broj akceptorskih skupina vodikove veze; NB - broj veza; AlAC - broj atoma u alifatskim vezama; AlBC - broj alifatskih veza; CAC - broj teških atoma u linearnoj poveznici; CBC - broj veza u linearnoj poveznici; ACC - broj atoma u supstitucijskom lancu; ACOR - broj atoma izvan β-karbolina

Tablica 39. Indikatorske varijable harmicina amidnoga tipa **7a-h**, **13a-h**, **19a-h**, **22a-h**, **25a-f**,**i**,**j**

Deskriptor / Harmicin	pol. 1	pol. 3	pol. 6	pol. 7	pol. 9	fenil 2'	fenil 3'	fenil 4'	OCH_3 pol. 7	CH_3 pol. 1	CH_3 pol. 5'
7a	1	0	0	0	0	0	0	0	0	0	0
7b	1	0	0	0	0	0	1	0	0	0	0
7c	1	0	0	0	0	0	1	0	0	0	0
7d	1	0	0	0	0	0	1	0	0	0	0
7e	1	0	0	0	0	0	0	1	0	0	0
7f	1	0	0	0	0	0	0	1	0	0	0
7g	1	0	0	0	0	0	0	1	0	0	0
7h	1	0	0	0	0	0	0	1	0	0	0
13a	0	1	0	0	0	0	0	0	0	1	0
13b	0	1	0	0	0	0	1	0	0	1	0
13c	0	1	0	0	0	0	1	0	0	1	0
13d	0	1	0	0	0	0	1	0	0	1	0
13e	0	1	0	0	0	0	0	1	0	1	0
13f	0	1	0	0	0	0	0	1	0	1	0
13g	0	1	0	0	0	0	0	1	0	1	0
13h	0	1	0	0	0	0	0	1	0	1	0
19a	0	0	1	0	0	0	0	0	0	1	0
19b	0	0	1	0	0	0	1	0	0	1	0
19c	0	0	1	0	0	0	1	0	0	1	0
19d	0	0	1	0	0	0	1	0	0	1	0
19e	0	0	1	0	0	0	0	1	0	1	0
19f	0	0	1	0	0	0	0	1	0	1	0
19g	0	0	1	0	0	0	0	1	0	1	0
19h	0	0	1	0	0	0	0	1	0	1	0
22a	0	0	0	1	0	0	0	0	0	1	0
22b	0	0	0	1	0	0	1	0	0	1	0
22c	0	0	0	1	0	0	1	0	0	1	0
22d	0	0	0	1	0	0	0	1	0	1	0
22e	0	0	0	1	0	0	0	1	0	1	0
22f	0	0	0	1	0	0	0	1	0	1	0
22g	0	0	0	1	0	1	0	0	0	1	0
22h	0	0	0	1	0	0	0	0	0	1	1
25a	0	0	0	0	1	0	0	0	1	1	0
25b	0	0	0	0	1	0	1	0	1	1	0
25c	0	0	0	0	1	0	1	0	1	1	0
25d	0	0	0	0	1	0	0	1	1	1	0
25e	0	0	0	0	1	0	0	1	1	1	0
25f	0	0	0	0	1	0	0	1	1	1	0
25i	0	0	0	0	1	0	1	0	1	1	0
25j	0	0	0	0	1	0	0	1	1	1	0

Tablica 40. Vrijednosti topoloških deskriptora harmicina amidnoga tipa **7a-h**, **13a-h**, **19a-h**, **22a-h**, **25a-f**,**i**,**j**

Deskriptor / Harmicin	*F*(G)	χ(G)	*J*(G)	*H*(G)	*WW*(G)	*Sz*(G)	*W*(G)	*Wp*(G).
7a	76	12,31	1,09	89,3	7406	2468	1697	37
7b	80	12,7	1,04	94,37	8552	2750	1901	39
7c	80	12,7	1,04	94,37	8552	2750	1901	39
7d	92	13,91	1,12	110,2	12689	3680	2597	45
7e	80	12,7	1,03	94,12	8760	2788	1920	39
7f	80	12,7	1,03	94,12	8760	2788	1920	39
7g	82	13,24	1,18	98,71	10363	3134	2169	41
7h	92	13,91	1,1	109,38	13578	3832	2673	45
13a	80	12,7	1,04	94,4	8620	2824	1905	39
13b	84	13,1	1,2	99,52	9911	3134	2126	41
13c	84	13,1	1,2	99,52	9911	3134	2126	41
13d	96	14,31	1,08	115,5	14537	4151	2876	47
13e	84	13,1	1,19	99,27	10137	3174	2146	41
13f	84	13,1	1,19	99,27	10137	3174	2146	41
13g	86	13,64	1,14	103,91	11922	3551	2414	43
13h	96	14,31	1,06	114,67	15501	4311	2956	47
19a	84	13,7	1,07	101,76	13385	3611	2552	41
19b	88	14,1	1,03	106,91	15204	3978	2823	43
19c	88	14,1	1,03	106,91	15204	3978	2823	43
19d	100	15,31	1,1	122,98	21570	5172	3729	49
19e	88	14,1	1,03	106,67	15482	4022	2845	43
19f	88	14,1	1,03	106,67	15482	4022	2845	43
19g	90	14,64	0,98	111,33	17901	4462	3167	45
19h	100	15,31	1,07	122,17	22748	5348	3817	49
22a	84	13,7	1,06	101,48	13721	3625	2580	41
22b	88	14,1	1,02	106,62	15573	3993	2853	43
22c	88	14,1	1,02	106,62	15573	3993	2853	43
22d	88	14,1	1,01	106,38	15853	4037	2875	43
22e	88	14,1	1,01	106,38	15853	4037	2875	43
22f	90	14,64	0,97	111,04	18309	4478	3199	45
22g	88	14,11	1,03	106,95	15315	3949	2831	44
22h	88	14,11	1,05	107,55	14724	3875	2779	44
25a	88	14,17	1,2	111,41	11391	3479	2474	46
25b	92	14,56	1,16	116,74	12992	3832	2737	48
25c	92	14,56	1,16	116,74	12992	3832	2737	48
25d	92	14,56	1,15	116,48	13263	3878	2760	48
25e	92	14,56	1,15	116,48	13263	3878	2760	48
25f	94	15,1	1,1	121,3	15451	4307	3076	55
25i	104	15,77	1,22	133,31	18683	4987	3622	54
25j	104	15,77	1,19	132,43	19836	5171	3714	54

F(G) - Plattov indeks; χ(G) - Randićev indeks povezanosti; *J*(G) - Balabanov indeks; *H*(G) - Hararyjev indeks; *WW*(G) - hiper-Wienerov indeks; *Sz*(G) - Szeged-indeks; *W*(G) - Wienerov indeks; *Wp*(G) -Wienerov indeks polarnosti

Geometrijski i sterički molekulski deskriptori izvedeni su iz trodimenzionalne strukture harmicina amidnoga tipa **7a-h**, **13a-h**, **19a-h**, **22a-h**, **25a-f**,**i**,**j**, a uključuju deskriptore koji opisuju volumen molekule (van der Waalsov volumen, V_w, $V_{wmarvin}$), deskriptore koji opisuju površinu dostupnu otapalu (*SASA*), topološku polarnu površinu (*TPSA*) te kontaktnu polarnu površinu (*CSP*), deskriptore koji opisuju površinu: van der Waalsova površina (A_W), minimalna projekcijska površina (A_{min}, $A_{minmarvin}$), maksimalna projekcijska površina ($A_{max,}$ $A_{maxmarvin}$), polumjer minimalne projekcijske površine ($r_{min,}$ $r_{minmarvin}$), polumjer maksimalne projekcijske površine (r_{max}, $r_{maxmarvin}$), dužina okomita na maksimalnu površinu ($LP_{max}A$), dužina okomita na minimalnu površinu ($LP_{min}A$). Nadalje, izračunate su Dreidingove energije (E_D) te Merckovo molekularno polje sila (MMFF94) navedenih harmicina amidnoga tipa. Vrijednosti geometrijskih i steričkih molekulskih deskriptora dane su u Tablicama 41 i 42.

Elektronska svojstva harmicina amidnoga tipa **7a-h**, **13a-h**, **19a-h**, **22a-h**, **25a-f**,**i**,**j** opisana su s ukupno 10 elektronskih molekulskih deskriptora: polarizabilnost (P_{chem}, P_{sk}), molarna refraktivnost (MR_{chem}, MR_{dr}, MR_{sk}, MR_{swiss}), izoelektrična točka (p*I*, pI_{marvin}), indeks loma svjetlosti (n) i molarni volumen (V_M), a njihove vrijednosti dane su u Tablici 43.

Tablica 41. Vrijednosti geometrijskih i steričkih molekulskih deskriptora harmicina amidnoga tipa **7a-h**, **13a-h**, **19a-h**, **22a-h**, **25a-f,i,j**

Deskriptor / Harmicin	$TPSA_{chem}$	$TPSA_{dr}$	$TPSA_{swiss}$	*SASA*	V_w	$V_{wmarvin}$	A_W	A_{min}	$A_{minmarvin}$	A_{max}	$A_{maxmarvin}$
7a	57,78	53,49	57,78	562,83	292,55	292,23	446,74	50,18	53,8	109,41	98,13
7b	57,78	53,49	57,78	569,61	297,35	297,09	453,89	51,34	56,21	112,47	99,72
7c	57,78	53,49	57,78	584,13	310,8	310,49	466,98	52,05	59,36	116,94	103,37
7d	57,78	53,49	57,78	614,89	324,42	324,15	496,6	54,14	59,79	118,3	106,09
7e	57,78	53,49	57,78	570,46	297,39	297,09	454,12	50,79	54,74	112,19	99,27
7f	57,78	53,49	57,78	580,9	306,48	306,16	463,28	50,41	55,37	115,3	102,09
7g	67,01	62,72	67,01	629,35	318,33	318,21	495,34	49,93	55,56	118,75	106,24
7h	57,78	53,49	57,78	615,8	324,22	324,07	496,69	53,66	55,89	119,73	106
13a	57,78	53,49	57,78	613,4	308,92	309	479,27	55,21	54,7	103,24	102,37
13b	57,78	53,49	57,78	618,99	313,78	313,9	486,02	56,8	56,86	105,29	104,63
13c	57,78	53,49	57,78	635,26	327,23	327,36	499,72	60,74	61,45	108,85	108,22
13d	57,78	53,49	57,78	665,58	340,92	340,96	529,07	63,5	63,22	111,95	110,36
13e	57,78	53,49	57,78	619,99	313,78	313,89	486,23	55,74	54,96	104,62	103,82
13f	57,78	53,49	57,78	631,00	322,86	323,04	495,63	56,45	55,84	106,97	106,01
13g	67,01	62,72	67,01	674,48	335,1	335,14	527,12	60,97	58,45	110,17	110,05
13h	57,78	53,49	57,78	666,36	340,95	340,85	529,19	61,9	60,83	110,66	110,05
19a	67,01	62,72	67,01	663,16	335,11	335,19	525,81	49,29	55,58	113,5	113,3
19b	67,01	62,72	67,01	669,94	339,95	340,16	533,06	54,40	56,04	115,24	114,58
19c	67,01	62,72	67,01	684,98	353,52	353,59	546,25	56,97	60,58	119,46	118,55
19d	67,01	62,72	67,01	714,89	367,08	367,19	575,63	60,06	61,64	122,31	122,21
19e	67,01	62,72	67,01	670,1	340,05	340,2	533,08	51,62	54,66	114,06	113,51
19f	67,01	62,72	67,01	680,67	349,1	349,13	542,21	54,07	55,92	117,33	115,9
19g	76,24	71,95	76,24	730,66	361,39	361,34	574,66	55,58	60,11	117,44	116,22
19h	67,01	62,72	67,01	717,41	367,13	367,18	576,1	56,76	60,32	121,94	122,43
22a	67,01	62,72	67,01	664,98	335,12	335,43	526,47	50,21	53,71	112,88	112,18
22b	70,94	62,72	67,01	670,1	340,16	340,11	532,84	52,28	53,83	113,8	113,86
22c	67,01	62,72	67,01	686,28	353,38	353,67	546,62	56,78	57,68	117,61	117,65

22d	67,01	62,72	67,01	670,42	340,07	340,04	532,94	51,81	52,9	113,75	113,46
22e	67,01	62,72	67,01	683,03	349,13	349,06	543,13	52,73	54,33	116,43	115,83
22f	76,24	71,95	76,24	728,28	361,34	361,41	574,17	55,18	59,19	117,06	115,42
22g	70,94	62,72	67,01	666,44	340,19	340,29	532,01	51,26	51,41	113,72	114,03
22h	67,01	62,72	67,01	687,04	352,2	352,11	559,62	55,9	56,52	115,04	114,56
25a	56,15	53,93	56,15	661,15	352,94	353,01	559,68	52,7	49,68	119,27	120,39
25b	56,15	53,93	56,15	667,02	357,69	357,83	566,56	52,89	57,58	120,93	122,31
25c	56,15	53,93	56,15	681,35	371,23	371,29	579,94	56,2	61,19	124,33	125,48
25d	56,15	53,93	56,15	668,13	357,91	357,94	566,66	53,45	52,17	120,54	122,16
25e	56,15	53,93	56,15	676,19	366,82	366,94	576,1	53,35	52,12	124,23	124,97
25f	65,38	63,16	65,38	723,39	379,03	379,06	608,05	56,96	53,37	126,29	128,93
25i	56,15	53,93	56,15	714,16	384,86	384,9	609,54	60,03	58,33	126,42	129,74
25j	56,15	53,93	56,15	713,31	384,96	384,77	609,65	53,51	52,4	126,8	128,81

TPSA - topološka polarna površina; *SASA* - površinu dostupnu otapalu; *V*w - van der Waalsov volumen; A_W - van der Waalsova površina; A_{min} - minimalna projekcijska površina; A_{max} - maksimalna projekcijska površina

Tablica 42. Vrijednosti geometrijskih i steričkih molekulskih deskriptora harmicina amidnoga tipa **7a-h**, **13a-h**, **19a-h**, **22a-h**, **25a-f,i,j**

Deskriptor / Harmicin	r_{min}	$r_{minmarvin}$	r_{max}	$r_{maxmarvin}$	E_D	MMFF94	$LP_{min}A$	$LP_{max}A$	CSP_{HBD}	CSP_{HBA}	CSP_n	CSP_t
7a	5,46	5,46	7,47	8,82	74,61	110,37	17,73	9,97	12,271	25,657	318,748	357,152
7b	6,2	6,2	7,78	8,82	74,8	103,81	17,73	9,97	12,962	26,039	328,38	368,542
7c	5,52	5,52	8,23	8,9	74,36	106,14	17,27	9,97	12,219	24,951	339,685	377,097
7d	5,41	5,41	8,4	8,89	80,42	140,08	17,25	9,97	13,984	24,922	350,972	391,87
7e	5,82	5,82	7,91	9,16	74,84	106,37	17,76	9,97	12,962	26,039	328,38	368,542
7f	5,82	5,82	8,24	9,48	74,92	107,19	18,45	9,97	12,724	25,211	337,848	374,968
7g	5,73	5,73	8,66	9,93	80,5	114,9	19,11	9,97	12,545	30,864	342,833	386,405
7h	5,74	5,74	8,46	9,63	80,08	143,97	18,8	9,97	13,984	24,922	350,972	391,87
13a	5,48	5,48	9,46	9,46	77,4	104,17	18,84	9,97	11,564	26,348	334,237	372,532
13b	5,48	5,48	9,46	9,46	77,63	97,23	18,84	9,97	11,511	25,642	355,174	392,477
13c	5,49	5,49	9,47	9,47	76,94	99	18,85	9,97	11,511	25,642	355,174	392,477
13d	5,63	5,63	9,47	9,46	82,83	113,48	17,64	9,97	13,276	25,613	366,41	407,25
13e	5,48	5,48	9,58	9,57	77,5	99,81	19,06	9,97	12,255	26,73	343,87	383,92
13f	5,48	5,48	9,87	9,86	77,46	100,45	19,65	9,97	12,016	25,902	353,337	390,348
13g	5,49	5,49	10,35	10,33	83,01	108,19	20,27	9,97	11,837	31,555	358,322	401,785
13h	5,49	5,49	10,26	10,08	82,78	137,69	20,11	9,97	13,276	25,613	366,41	407,25
19a	4,87	4,87	10,87	11,13	81,05	116,27	21,82	9,97	11,732	29,034	359,809	399,478
19b	4,97	4,97	10,73	11,1	81,27	109,28	22,07	9,97	12,423	29,416	369,442	410,868
19c	5,33	5,33	10,74	11,1	80,76	111,28	22,07	9,97	11,679	28,328	380,746	419,423
19d	5,45	5,45	10,88	11,12	86,7	145,2	22	9,97	13,444	28,299	392,033	434,196
19e	5,12	5,12	10,96	11,3	81,21	111,84	22,23	9,97	12,423	29,416	369,442	410,868
19f	5,38	5,38	11,25	11,54	81,3	112,86	22,79	9,97	12,185	28,588	378,909	417,294
19g	5,01	5,01	11,12	11,54	86,67	120,6	23,13	9,97	12,005	34,241	383,894	428,731
19h	5,16	5,16	11,38	11,92	86,48	149,08	23,04	9,97	13,444	28,299	392,033	434,196
22a	4,62	4,62	10,91	10,9	80,93	116,82	21,88	9,97	11,732	29,034	359,809	399,478
22b	4,86	4,86	10,95	10,79	81,18	110,38	21,9	9,97	12,423	29,416	369,442	410,868
22c	5,33	5,33	10,94	10,8	80,62	112,25	21,92	9,97	11,679	28,328	380,746	419,423

22d	5,12	5,12	10,94	10,93	81,14	113,36	21,42	9,97	12,423	29,416	369,442	410,868
22e	5,39	5,39	11,29	11,19	81,22	114,35	21,99	9,97	12,185	28,588	378,909	417,294
22f	5,01	5,01	11,5	11,5	86,76	121,54	22,65	9,97	12,005	34,241	383,894	428,731
22g	4,6	4,6	10,85	10,81	82,47	124,03	21,94	9,97	11,724	27,712	366,361	408,652
22h	5,15	5,15	10,04	9,98	92,71	120,67	20,31	9,97	11,247	28,079	369,036	405,839
25a	6,33	6,33	9,42	9,15	92,81	126,53	17,99	9,97	3,973	31,164	374,309	406,346
25b	6,03	6,03	9,39	9,22	92,58	120,69	18,36	9,97	4,664	31,547	383,942	417,736
25c	6,32	6,32	9,43	9,33	92,25	122,43	18,32	9,97	3,921	30,459	395,246	426,291
25d	6,17	6,17	9,65	9,44	92,78	122,23	18,68	9,97	4,664	31,547	383,942	417,736
25e	6,22	6,22	10,04	9,78	92,66	123,55	19,38	9,97	4,426	30,719	393,409	424,163
25f	5,9	5,9	10,17	10,2	98,5	130,36	20,39	9,97	4,247	36,372	398,394	435,6
25i	5,91	5,91	9,55	9,52	96,79	155,88	19,23	9,97	5,686	30,43	406,533	441,064
25j	5,95	5,95	10	9,94	99,14	160,25	19,35	9,97	5,686	30,43	406,533	441,064

r_{min} - polumjer minimalne projekcijske površine; r_{max} - polumjer maksimalne projekcijske površin;, E_D - Dreidingova energija; MMFF94 - Merckovo molekularno polje sila; $LP_{min}A$ - dužina okomita na minimalnu površinu; $LP_{max}A$ - dužina okomita na maksimalnu površinu; *CSP* - kontaktna polarna površina

Tablica 43. Vrijednosti elektronskih molekulskih deskriptora harmicina amidnoga tipa **7a-h**, **13a-h**, **19a-h**, **22a-h**, **25a-f**,**i**,**j**

Deskriptor / Harmicin	P_{chem}	P_{sk}	MR_{chem}	MR_{dr}	MR_{sk}	MR_{swiss}	p*I*	pI_{marvin}	n	V_M
7a	40,29	40,87	99,13	99,76	103,09	100,79	8,64	8,63	1,748	253,3
7b	39,83	40,86	99,34	100,17	103,09	100,75	8,64	8,63	1,732	257,5
7c	42,78	43,91	106,75	107,11	110,78	108,49	8,64	8,63	1,758	269,5
7d	41,03	42,84	105,1	106,27	108,07	105,8	8,64	8,63	1,677	286,8
7e	39,83	40,86	99,34	100,17	103,09	100,75	8,64	8,63	1,732	257,5
7f	42,06	42,81	103,93	104,37	107,99	105,8	8,64	8,63	1,749	265,2
7g	42,75	43,51	105,59	107,01	109,77	107,29	8,64	8,63	1,722	277,3
7h	41,03	42,84	105,1	106,27	108,07	105,8	8,64	8,63	1,677	286,8
13a	42,05	42,78	103,72	104,7	107,92	105,76	9,31	9,31	1,732	269,6
13b	41,6	42,78	103,93	105,11	107,91	105,72	9,3	9,31	1,717	273,8
13c	44,55	45,83	111,34	112,39	115,61	113,46	9,3	9,31	1,743	285,7
13d	42,79	44,75	109,69	111,21	112,9	110,76	9,3	9,3	1,667	303,1
13e	41,6	42,78	103,93	105,11	107,91	105,72	9,3	9,31	1,717	273,8
13f	43,83	44,72	108,52	109,31	112,81	110,77	9,3	9,31	1,733	281,5
13g	44,51	45,43	110,18	111,95	114,6	112,25	9,31	9,31	1,708	293,6
13h	42,79	44,75	109,69	111,21	112,9	110,76	9,3	9,3	1,667	303,1
19a	44,51	45,31	110,18	111,81	114,31	112,09	10,06	10,05	1,706	293,8
19b	44,09	45,31	110,4	112,22	114,31	112,05	10,05	10,05	1,693	298
19c	47,07	48,36	117,8	119,51	122	119,79	10,05	10,04	1,716	309,9
19d	45,32	47,29	116,15	118,32	119,29	117,09	10,04	10,03	1,649	327,3
19e	44,09	45,31	110,4	112,22	114,31	112,05	10,05	10,05	1,693	298
19f	46,31	47,25	114,98	116,42	119,21	117,1	10,05	10,05	1,707	305,7
19g	46,99	47,96	116,64	119,06	120,99	118,58	10,06	10,05	1,686	317,8
19h	45,32	47,29	116,15	118,32	119,29	117,09	10,04	10,03	1,649	327,3
22a	44,51	45,31	110,18	111,81	114,31	112,09	9,84	9,85	1,706	293,8
22b	44,09	45,31	110,4	112,22	114,31	112,05	9,84	9,84	1,693	298
22c	47,07	48,36	117,8	119,51	122	119,79	9,83	9,84	1,716	309,9
22d	44,09	45,31	110,4	112,22	114,31	112,05	9,84	9,84	1,693	298
22e	46,31	47,25	114,98	116,42	119,21	117,1	9,84	9,84	1,707	305,7
22f	46,99	47,96	116,64	119,06	120,99	118,58	9,84	9,85	1,686	317,8
22g	44,09	45,31	110,4	112,22	114,31	112,05	9,84	9,84	1,693	298
22h	46,36	47,09	114,54	115,85	118,79	116,09	9,84	9,85	1,691	310,1
25a	46,36	45,54	115,08	116,81	114,89	116,99	10,94	10,49	1,62	326,9
25b	45,94	45,49	115,29	117,22	114,76	116,95	10,8	10,8	1,612	329,7
25c	48,91	48,54	122,7	124,51	122,45	124,69	10,76	10,76	1,641	339,4
25d	45,93	45,49	115,29	117,22	114,76	116,95	10,8	10,8	1,612	329,7
25e	48,16	47,37	119,88	121,42	119,49	122	10,79	10,79	1,629	336,1
25f	48,84	47,85	121,54	124,06	120,7	123,49	10,85	10,86	1,609	348,5
25i	47,16	47,43	121,05	123,32	119,64	122	10,65	10,64	1,585	356,9
25j	47,16	47,43	121,05	123,32	119,64	122	10,65	10,64	1,585	356,9

P - polarizabilnost; MR - molarna refraktivnost; p*I* - izoelektrična točka; n - indeks loma svjetlosti; V_M - molarni volumen

Idući korak u odabiru molekulskih deskriptora uključivao je određivanje međusobnog odnosa svih parova dvaju varijabli (molekulskih deskriptora) kako bi se utvrdila njihova međusobna korelacija. U tu svrhu izrađena je matrica međusobnih korelacija te su uklonjeni deskriptori s koeficijentom korelacije $r > 0{,}95$ i $r < -0{,}95$ (Slika 39), odn. između visoko koreliranih deskriptora zadržani su oni koji se jednostavnije interpretiraju.

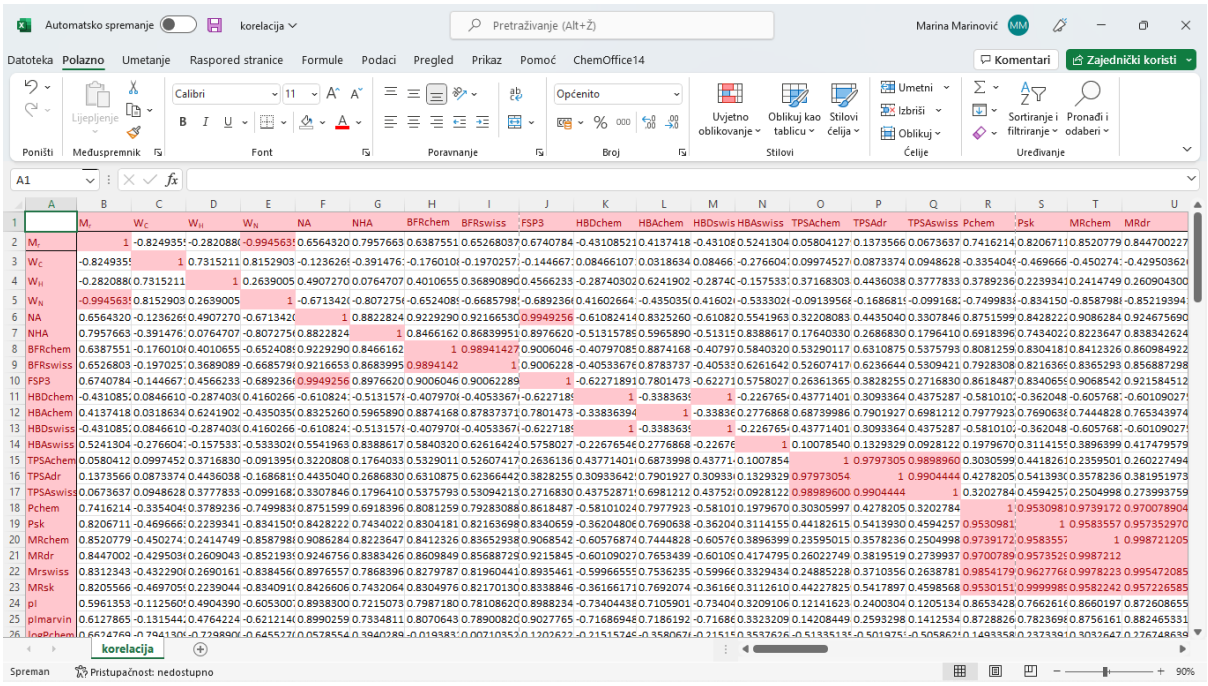

Slika 39. Prikaz dijela matrice korelacije

Matrica korelacije između molekulskih deskriptora je nakon uklanjanja visoko koreliranih varijabli reducirana na ukupno 67 molekulskih deskriptora, koji su odabrani za daljnju QSAR analizu, a navedeni su u Tablici 44.

Tablica 44. Popis molekulskih deskriptora korištenih u izradi QSAR modela

Simbol	Molekulski deskriptor
Abr. E	Abrahamov deskriptor E
Abr. S	Abrahamov deskriptor S
Abr. V	Abrahamov deskriptor V
ACC	broj atoma u supstitucijskom lancu
AlAC	broj atoma u alifatskim vezama
A_{max}	maksimalna projekcijska površina (*chemicalize.com*)

$A_{maxmarvin}$	maksimalna projekcijska površina (MarvinSketch)
A_{min}	minimalna projekcijska površina (*chemicalize.com*)
$A_{minmarvin}$	minimalna projekcijska površina (MarvinSketch)
B_{FR}	broj veza u molekuli koje mogu slobodno rotirati oko vlastite osi
CAC	broj teških atoma u linearnoj poveznici
CH_3 pol. 5'	prisutnost metilne skupine u α-položaju DCK-a
Clog *P*	računski logaritam koeficijenta razdjeljena (ChemDraw)
CSP_{HBA}	kontaktna polarna površina
E_D	Dreidingova energija
fu_b	slobodna frakcija lijeka u mozgu
fenil 2'	prisutnost supstituenta u *orto*-položaju DCK-a
fenil 3'	prisutnost supstituenta u *meta*-položaju DCK-a
fenil 4'	prisutnost supstituenta u *para*-položaju DCK-a
HBA_{chem}	broj akceptorskih skupina vodikove veze (*chemicalize.com)*
HBA_{swiss}	broj akceptorskih skupina vodikove veze (*swissadme.ch)*
HBD_{chem}	broj donorskih skupina vodikove veze (*chemicalize.com)*
HLB	hidrofilno-lipofilna ravnoteža
HRA	napad hidroksilnih radikala
J(G)	Balabanov indeks
K_h	Henryjeva konstanta
log *BB*	logaritam koeficijenta razdjeljenja između krvno-moždane barijere
$\log K_{aAGP}$	logaritam konstante vezanja za kiseli α-glikoprotein
$\log K_{aHSA}$	logaritam konstante vezanja za humani serumski albumin
$\log K_{aMemb}$	logaritam konstante vezanja za membrane
$\log K_p$	logaritam koeficijenta permeabilnosti kroz kožu
log P_{chem}	logaritam koeficijenta razdjeljenja (*chemicalize.com)*
log P_{dr}	logaritam koeficijenta razdjeljenja (ChemDraw)
log P_{mestr}	logaritam koeficijenta razdjeljenja (MNova)
log P_{swiss}	logaritam koeficijenta razdjeljenja (*swissadme.ch*)
log S_{chem}	logaritam intrizične topljivosti (*chemicalize.com)*
log S_{dr}	logaritam intrizične topljivosti (ChemDraw)
log S_{mestr}	logaritam intrizične topljivosti (MNova)

log S_{swiss}	logaritam intrizične topljivosti (*swissadme.ch*)
$LP_{max}A$	dužina okomita na maksimalnu površinu
MMFF94	Merck molekularno polje sila
M_r	relativna molekulska masa
M_S	masa supstituenta
n	indeks loma svjetlosti
NA	broj atoma
NHA	broj teških atoma
P	polarizabilnost
p*I*	izoelektrična točka
pol. 1	supstitucija u položaju 1 β-karbolina
pol. 3	supstitucija u položaju 3 β-karbolina
pol. 6	supstitucija u položaju 6 β-karbolina
pol. 7	supstitucija u položaju 7 β-karbolina
p_V	tlak para
r_{max}	polumjer minimalne projekcijske površine
$r_{maxmarvin}$	polumjer maksimalne projekcijske površine (MarvinSketch)
r_{min}	polumjer minimalne projekcijske površine
$r_{minmarvin}$	polumjer minimalne projekcijske površine (MarvinSketch)
SASA	površina molekule dostupna otapalu
s_M	molarna topljivost
TPSA	topološka polarna površina
t_t	temperatura tališta
t_{tmestr}	temperatura tališta (MNova)
W_C	udio C atoma u strukturi
W_H	udio H atoma u strukturi
Wp(G)	Wienerov indeks polarnosti
WW(G)	hiper-Wienerov indeks
σ	površinska napetost

4.3.2. Izrada QSAR modela

QSAR analiza 40 harmicina amidnoga tipa provedena je na temelju odabranog skupa molekulskih deskriptora (Tablica 44) tehnikom višestruke linearne regresije. Budući da su svi navedeni harmicini amidnoga tipa pokazali jače djelovanje na *Pf*3D7 soj, u odabrani skup molekulskih deskriptora, kao zavisna varijabla, uvedene su eksperimentalno određene vrijednosti antiplazmodijskog djelovanja harmicina amidnoga tipa (**7a-h**, **13a-h**, **19a-h**, **22a-h** i **25a-f**,**i**,**j**) na *Pf*3D7 soj (Y_{eksp}) izražene u nanomolarnim koncentracijama bez pripadajućih standardnih devijacija, a zbog velike razlike u djelovanju pojedinih harmicina rezultati biološkog djelovanja prevedeni su u logaritamsku skalu (log IC_{50}) i dani su Tablici 45.

Tablica 45. IC_{50} i log IC_{50} vrijednosti antiplazmodijskog djelovanja harmicina amidnoga tipa (**7a-h**, **13a-h**, **19a-h**, **22a-h** i **25a-f**,**i**,**j**) na soj *Pf*3D7

Spoj	Y_{eksp}[a] (µM)	Y_{eksp} (nM)	log Y_{eksp} (nM)	**Spoj**	Y_{eksp} (µM)	Y_{eksp} (nM)	log Y_{eksp} (nM)
7a	55,56	55555	4,74	**19e**	0,95	945,8	2,98
7b	27,78	27777	4,44	**19f**	0,36	355,7	2,55
7c	27,78	27777	4,44	**19g**	1,17	1166	3,07
7d	27,78	27777	4,44	**19h**	0,12	123,5	2,09
7e	13,89	13888	4,14	**22a**	0,98	983,1	2,99
7f	27,78	27777	4,44	**22b**	2,75	2753	3,44
7g	27,78	27777	4,44	**22c**	0,37	373,9	2,57
7h	55,56	55555	4,74	**22d**	0,15	145,1	2,16
13a	5,78	5782,5	3,76	**22e**	0,32	320	2,51
13b	5,74	5740,5	3,76	**22f**	0,21	205,1	2,31
13c	3,23	3233,9	3,51	**22g**	0,93	932,2	2,97
13d	2,01	2008	3,30	**22h**	6,78	6784	3,83
13e	4,13	4126	3,62	**25a**	0,49	485,2	2,69
13f	2,92	2915,5	3,46	**25b**	0,07	73,5	1,87
13g	6,50	6501,8	3,81	**25c**	0,07	71,6	1,85
13h	2,30	2297,2	3,36	**25d**	0,09	86,6	1,94
19a	1,55	1549,4	3,19	**25e**	0,04	41,6	1,62
19b	1,11	1113,8	3,05	**25f**	0,26	264,4	2,42
19c	0,19	194,6	2,29	**25i**	0,06	60,6	1,78
19d	0,12	118,6	2,07	**25j**	0,04	38,7	1,59

[a] Y_{eksp} - vrijednost IC_{50} (*Pf*3D7)

Za odabir statistički značajnih varijabli (molekulskih deskriptora) i izradu modela, skup odabranih molekulskih deskriptora podvrgnut je stepenastoj regresiji odabirom unaprijed (engl. *forward stepwise regression*). Kao rezultat dobiven je preliminarni QSAR model s ukupno 11 varijabli (p*I*, Abr E, pol. 6, AlAC, CH_3 pol. 5', Clog *P*, fenil 3', W_p(G), $A_{minmarvin}$, s_M, log P_{mestr}). Preliminarni model je podvrgnut daljnjem optimiranju s ciljem isključivanja manje značajnih deskriptora u statističkom i kemijskom smislu. U svakom koraku provjeravali su se statistički parametri modela, koeficijenti u modelu te broj i vrsta molekulskih deskriptora. Na kraju tog postupka kao najbolji odabran je QSAR model ovisnosti log IC_{50} (koncentracije iskazane u nM) o dvije varijable: izoelektričnoj točki (p*I*) i Abrahamovom deskriptoru E (Abr E). Jednadžba izgrađenog QSAR modela dana je u nastavku:

$$\log IC_{50} = 20{,}591 - 1{,}266 \cdot \mathrm{p}I - 1{,}826 \cdot \text{Abr E} \qquad (1)$$

Prema izgrađenom QSAR modelu, najveći utjecaj na antiplazmodijsko djelovanje (*Pf*3D7) harmicina amidnoga tipa imaju izoelektrična točka koja predstavlja pH otopine pri kojem je neto naboj molekule jednak nuli (179) i Abrahamov deskriptor E (Abr E) koji predstavlja specifičnu mjeru molarne refraktivnosti molekule (kao otopljene tvari pri 293 K) iskazane u $cm^3mol^{-1}/10$ (180, 181).

S obzirom na postavljenu granicu statističke značajnosti (p = 0,05) izračunate *p*-vrijednosti koeficijenata (Tablica 46) ukazuju na to da su statistički značajni. Također, F-omjer s izračunatom *p*-vrijednosti $p < 2 \times 10^{-16}$ statistički je značajan, a iznosio je 148,4 s 2 i 37 stupnjeva slobode.

Kvaliteta prilagodbe podataka modela (engl. *goodness of fit*) kvantificirana je koeficijentom determinacije R^2, a iznosio je približno 0,89. Međutim, u višestrukoj linearnoj regresiji vrlo je bitno uzeti u obzir prilagođeni koeficijent determinacije R_a^2 kako bi se spriječila pretjerana prilagodba modela (engl. *overfitting*). Izračunati prilagođeni koeficijent determinacije R_a^2 daje nam informaciju koliki je postotak varijacije zavisne varijable (log IC_{50}) opisan dobivenim modelom uzimajući u obzir broj nezavisnih varijabli (molekulskih deskriptora) i broj promatranih slučajeva (spojeva), a njegova vrijednost iznosila je 0,88. Visoke vrijednosti R^2 i R_a^2 (> 0,7) ukazuju na to da je izgrađeni QSAR model reprezentativan.

Deskriptori, pripadajući koeficijenti i statistički parametri regresijskih koeficijenata izgrađenog QSAR modela dani su u Tablici 46.

Tablica 46. Varijable, vrijednosti regresijskih koeficijenata u modelu i statističkih parametara i pogrešaka regresijskih koeficijenata QSAR modela

Odsječak/ Molekulski deskriptor	Koeficijent	Standardna pogreška koeficijenta	*p*-vrijednost
odsječak	20,591	1,42	$< 2 \times 10^{-16}$
p*I*	-1,266	0,073	$< 2 \times 10^{-16}$
Abr E	-1,826	0,37	$1,74 \times 10^{-5}$

4.3.3. Validacija QSAR modela

Kvaliteta izgrađenog QSAR modela procijenjena je unutarnjom i vanjskom validacijom.

4.3.3.1. Unutarnja validacija

Unutarnja validacija provedena je na skupu za učenje harmicina amidnoga tipa 10-strukom unakrsnom validacijom. Eksperimentalno dobivene vrijednosti IC_{50} (Y_{eksp}), vrijednosti IC_{50} predviđene izgrađenim modelom ($Y_{pred\_prilag.}$), vrijednosti IC_{50} predviđene 10-strukom unakrsnom validacijom ($Y_{pred\_10\text{-}CV}$) dane su u Tablici 47.

Tablica 47. Eksperimentalno dobivene vrijednosti IC_{50} (Y_{eksp}), vrijednosti IC_{50} predviđene izgrađenim modelom ($Y_{pred\_prilag.}$), vrijednosti IC_{50} predviđene 10-strukom unakrsnom validacijom ($Y_{pred\_10\text{-}CV}$)

Spoj	log Y_{eksp}[a] (nM)	log $Y_{pred\_prilag.}$[b] (nM)	log $Y_{pred\_10\text{-}CV}$[c] (nM)	**Spoj**	log Y_{eksp}[a] (nM)	log $Y_{pred\_prilag.}$[b] (nM)	log $Y_{pred\_10\text{-}CV}$[c] (nM)
7a	4,74	4,87	4,83	**19e**	2,98	2,45	2,42
7b	4,44	4,42	4,44	**19f**	2,55	2,44	2,41
7c	4,44	4,32	4,32	**19g**	3,07	2,59	2,59
7d	4,44	4,24	4,22	**19h**	2,09	2,28	2,33
7e	4,14	4,42	4,42	**22a**	2,99	3,17	3,18
7f	4,44	4,41	4,40	**22b**	3,44	2,72	2,70
7g	4,44	4,57	4,59	**22c**	2,57	2,64	2,68
7h	4,74	4,24	4,48	**22d**	2,16	2,72	2,75
13a	3,76	4,12	4,18	**22e**	2,51	2,71	2,71
13b	3,76	3,59	3,60	**22f**	2,31	2,87	3,17
13c	3,51	3,59	3,58	**22g**	2,97	2,96	2,95
13d	3,30	3,50	3,52	**22h**	3,83	3,36	3,32
13e	3,62	3,68	3,68	**25a**	2,69	2,27	2,13
13f	3,46	3,67	3,68	**25b**	1,87	2,00	2,03

13g	3,81	3,82	4,09	**25c**	1,85	1,95	1,99
13h	3,36	3,50	3,49	**25d**	1,94	2,00	2,04
19a	3,19	2,89	2,88	**25e**	1,62	2,00	2,35
19b	3,05	2,45	2,42	**25f**	2,42	2,08	2,11
19c	2,29	2,36	2,39	**25i**	1,78	2,00	1,98
19d	2,07	2,28	2,25	**25j**	1,59	2,00	2,03

[a] log Y_{eksp} - logaritam eksperimentalno dobivenih vrijednosti IC_{50}; [b] log Y_{pred_prilag} - logaritam vrijednosti IC_{50} predviđenih QSAR modelom; [c] log $Y_{pred\_10\text{-}CV}$ - logaritam vrijednosti IC_{50} predviđenih 10-strukom unakrsnom validacijom

Nakon provedene validacije izračunat je koeficijent determinacije 10-struke unakrsne validacije (Q^2), a njegova vrijednost iznosila je 0,854.

Točnost predviđanja modela procijenjena je računanjem statističkih mjera pogreške modela. Izračunate su srednja apsolutna pogreška (MAE) koja se definira kao prosjek apsolutnih razlika između stvarnih vrijednosti i vrijednosti predviđenih modelom te je izračunat korijen srednje kvadratne pogreške (RMSE) kao pokazatelj standardne devijacije pogreške predviđanja, a njihove vrijednosti iznosile su dane su u Tablici 48.

Tablica 48. Vrijednosti statističkih parametara izgrađenog QSAR modela

	Unutarnja validacija (10-CV)			**Višestruka linearna regresija (MLR)**			
Parametar	**Q^2**	**MAEcv**	**RMSEcv**	**R^2**	**R_a^2**	**MAE_{MLR}**	**$RMSE_{MLR}$**
Vrijednost	0,854	0,282	0,355	0,889	0,883	0,248	0,310

Vrijednost Q^2 izgrađenog QSAR modela znatno je veća od preporučene vrijednosti prema smjernicama koje je izdala Organizacija za ekonomsku suradnju i razvoj ($Q^2 > 0,5$) (145) što ukazuje na to da izgrađeni model ima veliku prediktivnu moć. Upravo velika vrijednost koeficijenata determinacije unakrsne validacije Q^2 i male vrijednosti MAE i RMSE ukazuju na dobro podudaranje stvarnih i predviđenih vrijednosti log IC_{50}, te se prema tome izgrađeni QSAR model može smatrati predvidljivim.

Zadnji korak u provjeri valjanosti i pouzdanosti izgrađenog QSAR modela uključivao je analizu grafičkog prikaza predviđenih u odnosu na eksperimentalno dobivene vrijednosti log IC_{50} ispitivanih harmicina amidnoga tipa (Slika 40).

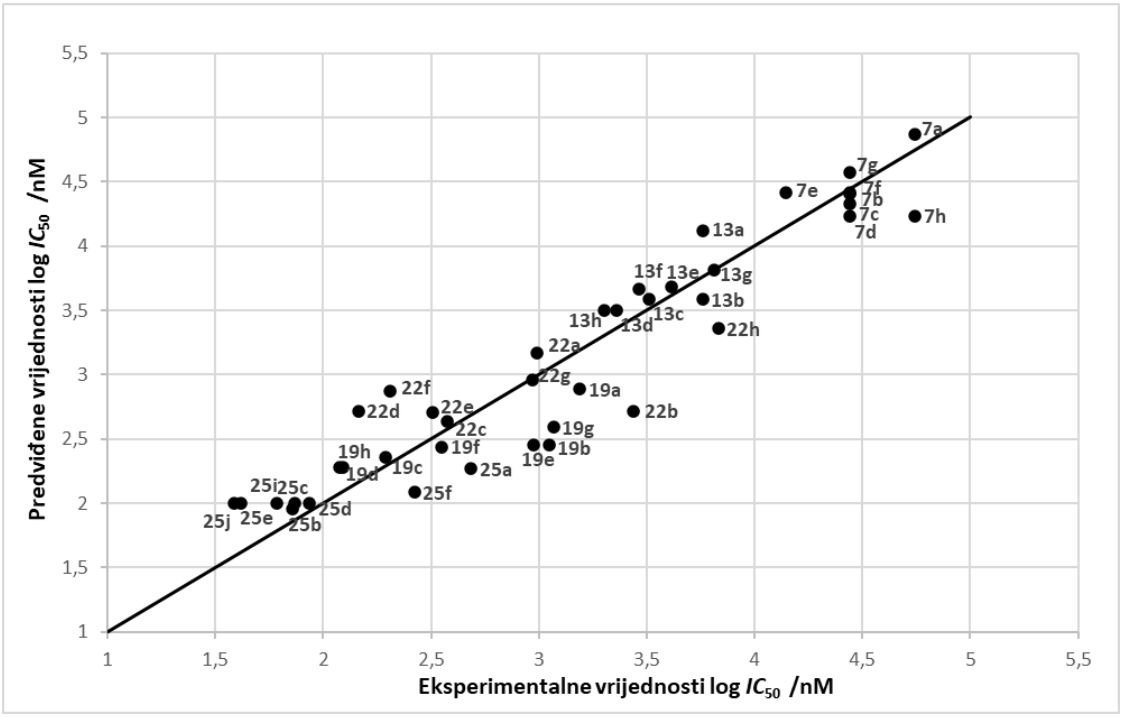

Slika 40. Ovisnost predviđenih o eksperimentalnim vrijednostima log IC_{50} harmicina amidnoga tipa **7a-h**, **13a-h**, **19a-h**, **22a-h** i **25a-f**,**i**,**j**

Iz grafičkog prikaza vidljivo je da se među najaktivnijim spojevima, harmicinima amidnoga tipa u položaju N-9 β-karbolina (**25b-e**,**i**,**j**), najveća odstupanja u predviđanju log IC_{50} vrijednosti u odnosu na eksperimentalno određene vrijednosti log IC_{50} javljaju pri vrijednostima log IC_{50} < 1,78 nM (IC_{50} < 0,06 μM). Pri tome je razlika predviđene i eksperimentalno određene vrijednosti biološke aktivnosti za najaktivniji spoj **25j** iznosila ΔIC_{50} = 0,06 μM, odn. modelom je predviđeno približno 2,6 puta slabije djelovanje (IC_{50eksp} = 0,04 μM, IC_{50pred} = 0,10 μM). Također, za spojeve **25e** (log IC_{50} = 1,62 nM) i **25i** (log IC_{50} = 1,78 nM) razlike u predviđenoj i eksperimentalnoj vrijednosti biološke aktivnosti iznosile su: $|\Delta IC_{50}|$ = 0,06 μM, **25e** i $|\Delta IC_{50}|$ = 0,04 μM, **25i**. Za preostale najaktivnije spojeve **25b-d** model se pokazao pouzdanijim u predviđanju te su razlike između predviđenih i eksperimentalnih vrijednosti IC_{50} bile znatno manje: $|\Delta IC_{50}|$ = 0,03 μM, **25b**; $|\Delta\ IC_{50}|$ = 0,018 μM, **25c**; $|\Delta\ IC_{50}|$ = 0,013, **25d**.

Izgrađeni QSAR model nije pouzdan u predviđanju biološkog djelovanja najaktivnijih spojeva, stoga je prilikom provedbe vanjske validacije ova informacija uzeta u obzir.

4.3.3.2. Vanjska validacija

S ciljem provođenja vanjske validacije izgrađenog QSAR modela dizajnirano je ukupno 356 novih harmicina. Na temelju SAR-a odabrani položaj derivatizacije β-karbolina bio je N-9, a u strukturi harmicina varirani su:

- Vrsta i položaj supstituenta DCK-a
- Duljina poveznice
- Vrsta supstituenta u položaju O-6 β-karbolina
- Vrsta supstituenta u položaju O-7 β-karbolina
- Vrsta supstituenta u položaju C-1 β-karbolina
- Vrsta poveznice.

Dizajniranim harmicinima izračunati su pripadajući molekulski deskriptori (p*I* i ABr E) te su im prema jednadžbi izgrađenog QSAR modela (1) izračunate predviđene vrijednosti antiplazmodijskog djelovanja (log IC_{50}). Ukupno 56 dizajniranih harmicina izostavljeno je iz odabira za provođenje vanjske validacije jer podaci za p*I* na mrežnoj stranici *chemicalize.com* s koje je preuzet navedeni deskriptor nisu bili dostupni za ove spojeve. Nadalje, izostavljeni su oni spojevi čija je predviđena vrijednost log IC_{50} bila veća od 4,1 nM (IC_{50} > 12,6 μM) jer bi, uzimajući u obzir i pogrešku predviđanja modela, IC_{50} vrijednosti ovih spojeva bile visoke, odn. pokazali bi se slabo učinkovitima.

Stoga su među dizajniranim spojevima odabrani spojevi **25k-m**, **28c**,**e**,**g**,**i** i **32b**,**c**, čije su predviđene log IC_{50} bile u rasponu od 1,8 do 2,15 nM (IC_{50} = 0,063 – 0,141 μM), a prema strukturi to su bili harmicini amidnoga (*o*-Cl-supstituirani, **25k**; *m*-Cl-supstituirani, **25l**; *m*-OCF_3-supstituirani, **25m**), karbamatnog (*m*-CF_3-supstituirani, **28c**; *p*-CF_3-supstituirani, **28e**; *m*-Cl-supstituirani, **28g**; *p*-Br-supstituirani, **28i**) i ureidnog tipa (*p*-propoksi-supstituirani, **32b** i *m*-CF_3-supstituirani, **32c**). Unatoč tome što se izgrađeni QSAR model pokazao nepouzdanim pri vrijednostima log IC_{50} nižim od 1,8 nM, za provođenje vanjske validacije odabrano je ukupno četiri spoja čije su predviđene vrijednosti bile niže od navedene granične vrijednosti. Kako bi se ujedno dobio uvid u utjecaj vrste poveznice na djelovanje harmicina, među dizajniranim spojevima s vrijednostima log IC_{50} < 1,8 nM odabrani spojevi bili su: *p*-Br-supstituirani harmicin amidnoga tipa (**25n**) i *p*-NO_2-supstituirani harmicin amidnoga (**25p**), zatim *m*-OCF_3-supstituirani harmicin karbamatnog tipa (**28h**) i *p*-NO_2-supstituirani harmicin karbamatnog tipa (**28k**). Također su odabrani spojevi s nešto većim predviđenim vrijednosti log IC_{50} (2,19 – 2,49 nM), a među njima su bili *p*-CH_3-supstituirani harmicin amidnoga tipa (**25o**), zatim harmicini

karbamatnog tipa (nesupstituirani, **28a**; *p*-propoksi-suptituirani, **28b**; *m*,*m*-di-CF_3-supstituirani, **28d**; *o*-Cl-supstituirani, **28f**; *p*-CH_3-supstituirani, **28j**). Vrijednosti deskriptora (p*I* i Abr E) te predviđene vrijednosti IC_{50} odabranih harmicina amidnoga (**25k-p**), karbamatnog (**28a-k**) i ureidnog (**32b**,**c**) tipa dane su u Tablici 49.

Tablica 49.Vrijednosti deskriptora p*I* i Abr E i predviđene vrijednosti IC_{50} harmicina amidnoga (**25k-p**), karbamatnog (**28a-k**) i ureidnog (**32b**,**c**) tipa

Spoj	p*I*	Abr E	log Y_{pred}
25k	10,79	2,549	2,28
25l	10,79	2,701	2,00
25m	10,60	2,908	1,86
25n	10,93	2,746	1,74
25o	10,96	2,443	2,25
25p	10,68	2,998	1,60
28a	10,52	2,645	2,44
28b	10,41	2,858	2,19
28c	10,25	2,992	2,15
28d	9,63	3,339	2,30
28e	10,50	2,992	1,83
28f	10,39	2,746	2,42
28g	10,39	2,898	2,15
28h	10,45	3,105	1,69
28i	10,52	2,943	1,90
28j	10,49	2,640	2,49
28k	10,30	3,195	1,72
32b	10,43	2,927	2,04
32c	10,28	3,061	1,99

[a] log Y_{pred} - logaritam vrijednosti IC_{50} predviđenih QSAR modelom

Sinteze odabranih spojeva prethodno su opisane (4.1.1.5., 4.1.2.2., 4.1.2.3., 4.1.3.4) te im je ispitano antiplazmodijsko djelovanje na *Pf*3D7 (3.3.1., 4.2.1.). Predviđene i eksperimentalne vrijednosti odabranih harmicina dane su u Tablici 50, a grafički prikaz ovisnosti eksperimentalnih i predviđenih vrijednosti log IC_{50} harmicina amidnoga (**25k-p**), karbamatnog (**28a-k**) i ureidnog tipa (**32b**,**c**) prikazan je na Slici 41.

Tablica 50. Eksperimentalne i predviđene vrijednosti log IC_{50} harmicina amidnoga (**25k-p**), karbamatnog (**28a-k**) i ureidnog tipa (**32b**,**c**)

Spoj	Eksperimentalna vrijednost log IC_{50} (nM)	Predviđena vrijednost log IC_{50} (nM)	Eksperimentalna vrijednost IC_{50} (μM)	Predviđena vrijednost IC_{50} (μM)	ΔIC_{50} (μM) (eksp. IC_{50} – pred. IC_{50}|)
25k	2,51	2,28	0,32	0,19	0,13
25l	2,52	2,00	0,33	0,10	0,23
25m	2,54	1,86	0,35	0,07	0,28
25n	2,61	1,74	0,41	0,05	0,36
25o	2,99	2,25	0,98	0,18	0,80
25p	3,13	1,60	1,36	0,04	1,32
28a	2,74	2,44	0,55	0,28	0,27
28b	2,59	2,19	0,39	0,15	0,24
28c	2,70	2,15	0,5	0,14	0,36
28d	2,81	2,30	0,65	0,20	0,45
28e	2,90	1,83	0,79	0,07	0,72
28f	3,09	2,42	1,24	0,26	0,98
28g	2,99	2,15	0,97	0,14	0,83
28h	2,83	1,69	0,68	0,05	0,63
28i	2,62	1,90	0,42	0,08	0,34
28j	3,05	2,49	1,13	0,31	0,82
28k	2,56	1,72	0,36	0,05	0,31
32b	2,62	2,04	0,42	0,11	0,31
32c	2,34	1,99	0,22	0,10	0,12

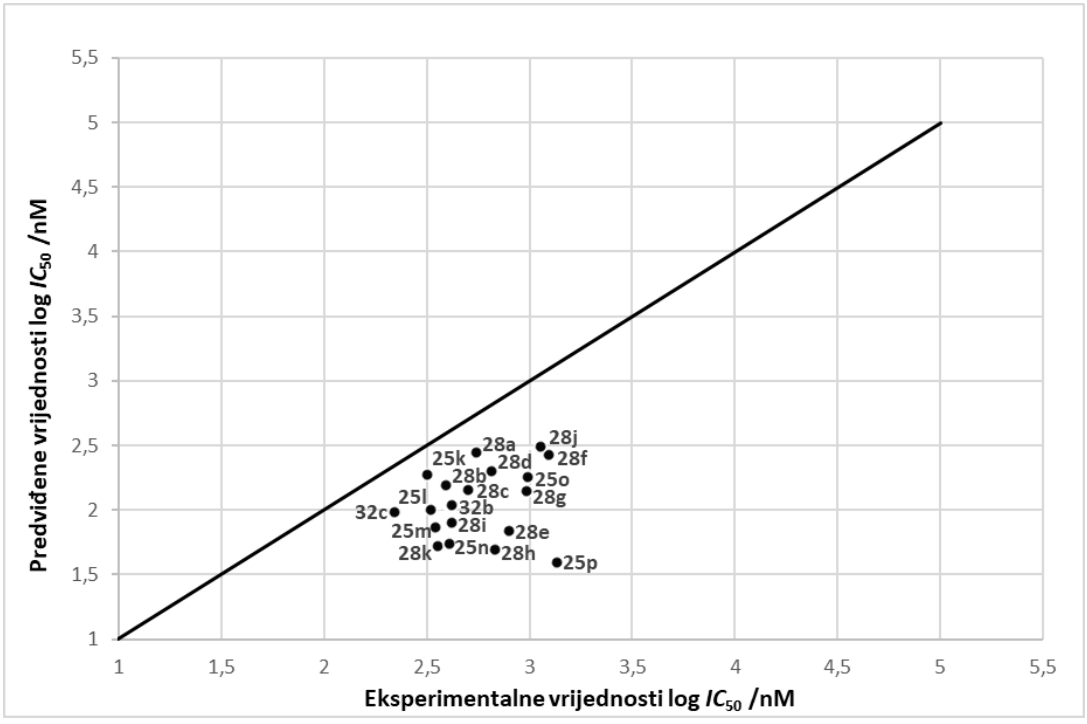

Slika 41. Ovisnost predviđenih o eksperimentalnim vrijednostima log IC_{50} harmicina amidnoga **25k-p**, karbamatnog **28a-k** i ureidnog **32b**,**c** tipa

Prema podacima navedenim u Tablici 50 vidljivo je da je QSAR model izgrađen u okviru ovoga istraživanja predvidio bolja djelovanja za sve harmicine. Izračunata srednja apsolutna pogreška predviđanja (MAE) iznosila je 0,69, a korijen srednje kvadratne pogreške 0,756. Odstupanja u predviđanju djelovanja *p*-NO_2-supstituiranog harmicina amidnoga tipa **25p** bila su najveća, pri čemu je razlika eksperimentalne i predviđene vrijednosti IC_{50} iznosila 1,32 μM, a njegova predviđena vrijednost log IC_{50} (1,6 nM) bila je znatno niža od granične vrijednosti 1,8 nM. Najmanja odstupanja u predviđanju uočena je kod *m*-CF_3-supstituiranog harmicina ureidnog tipa **32c** (ΔIC_{50} = 0,12 μM) i *o*-Cl-supstituiranog harmicina amidnoga tipa (ΔIC_{50} = 0,13 μM).

5. ZAKLJUČCI

U ovom doktorskom radu sintetizirano je ukupno 59 harimicina, hibridnih spojeva harmina/β-karbolina i cimetne kiseline/DCK-a: 46 harmicina amidnoga tipa (**7a-h**, **13a-h**, **19a-h**, **22a-h**, **25a-f**, **i-p**), 11 harmicina karbamatnog tipa (**28a-k**) i dva harmicina ureidnog tipa (**32b**,**c**). Za sintezu ciljanih harmicina pripravljeni su prekursori

a) β-karbolinski amini pripravljeni u 5 položaja β-karbolina: C-1 (**6**), C-3 (**12**), O-6 (**18**), O-7 (**21**) i N-9 (**24**).
b) cinamilni alkoholi **27b-k** – korišteni u pripravi harmicina karbamatnog tipa
c) cinamilni azidi **29b**,**c** – korišteni u pripravi cinamilnih amina
d) cinamilni amini **30b**,**c** – korišteni u pripravi harmicina ureidnog tipa
e) spoj **31** – benzotriazolid harmina korišten u pripravi harmicina ureidnog tipa.

Harmicini amidnoga tipa **7a-h**, **13a-h**, **19a-h**, **22a-h**, **25a-f**, **i-p** pripravljeni su reakcijama povezivanja prethodno sintetiziranih β-karbolinskih amina **6**, **12**, **18**, **21** i **24** i cimetne kiseline/odabranih DCK-a korištenjem standardnih uvjeta (HATU/DIEA). Harmicini karbamatnog tipa (**28a-k**) pripravljeni su u položaju N-9 β-karbolina reakcijom cinamilnih alkohola **27a-k** i β-karbolinskog amina **24** uz CDI. Sinteza ciljanih karbamata provedena je na dva načina. Harmicini karbamatnog tipa **28a-d** pripravljeni su reakcijom amina **24** s CDI-em te cinamilnim alkoholima **27a-d** *in situ*, dok su harmicini karbamatnog tipa **28e-k** pripravljeni reakcijom cinamilnih alkohola **27e-k** s CDI-em, te naknadnom reakcijom s aminom **24**. Harmicini ureidnog tipa **32b**,**c** sintetizirani su u položaju N-9 β-karbolina reakcijom prethodno pripravljenih cinamilnih amina **30b**,**c** i spoja **31**, a reakcije su provedene pod utjecajem mikrovalova.

Strukture novosintetiziranih spojeva potvrđene su spektroskopskim (^{1}H- i ^{13}C-NMR, IR) i spektrometrijskim (MS) tehnikama te im je određeno talište.

Antiplazmodijsko djelovanje svih novosintetiziranih harmicina ispitano je *in vitro* na eritrocitnu fazu životnog ciklusa na dva soja *P. falciparum*: soj osjetljiv na klorokin (*Pf*3D7) i soj otporan na klorokin (*Pf*Dd2). Dodatno je ispitano *in vitro* antiplazmodijsko djelovanje harmicina amidnoga tipa **7a-h**, **13a-h**, **19a-h**, **22a-h**, **25a-f**,**i-j** na hepatocitnu fazu životnog ciklusa *P. berghei*. Nadalje, ispitana je citotoksičnost harmicina **13a-h**, **19a-h**, **22a-h**, **25a-f**,**i**,**j**, **28a-d** te **32b**,**c** na humanu staničnu liniju hepatocelularnog karcinoma (HepG2) te su im izračunati pripadajući indeksi selektivnosti.

Svi harmicini pokazali su jače djelovanje u odnosu na harmin, u submikromolarnim i mikromolarnim koncentracijama, izuzev harmicina u položaju C-1 β-karbolina **7a-h** koji su se pokazali nedjelotvornima pri najvišim ispitivanim koncentracijama. Gotovo su svi harmicini pokazali jače djelovanje na *Pf*3D7 soj. Među aktivnim spojevima najbolje djelovanje na *Pf*3D7 ostvarili su harmicini amidnoga tipa u položaju N-9 β-karbolina **25b-e**,**i**,**j**, čije je djelovanje bilo za dva reda veličine snažnije od harmina (IC_{50} = 0,04 – 0,09 μM). Harmicini amidnoga tipa u položaju C-3 β-karbolina (**13a-h**) pokazali su najslabija djelovanja na oba soja, dok su se harmicini amidnoga tipa u položaju O-6 i O-7 pokazali srednje učinkovitima, izuzev α-CH_3-supstituiranog harmicina u položaju O-7 (**22h**) koji je bio najmanje djelotvoran na oba soja. Među harmicinima karbamatnog tipa najjače djelovanje na oba soja ostvario je *p*-NO_2-supstituirani harmicin **28k**, a među harmicinima ureidnog tipa *m*-CF_3-supstituirani harmicin **32c**.

Svi su ispitani harmicini amidnoga tipa, izuzev harmicina **7a** i **7b**, pokazali jače djelovanje na hepatocitnu fazu *P. berghei* pri 10 μM. Zbog visoke citotoksičnosti na Huh7 staničnu liniju, aktivnost pojedinih harmicina ne može se pripisati isključivo antiplazmodijskom djelovanju. Određena je IC_{50} vrijednost harmicina **25i**, a u odnosu na primakin pokazao je 4,3 puta jače djelovanje (**25i**, IC_{50} = 1,94 ± 0,68 μM; primakin, IC_{50} = 8,4 ± 3,4 μM).

Harmicini u položaju O-6 β-karbolina **19e-g** i harmicini karbamatnog tipa **28a**,**c** nisu bili citotoksični pri najvišim ispitivanim koncentracijama, a najmanje citotoksičan spoj među svim ispitanim harmicinima bio je α-CH_3-supstituirani harmicin **22h**. Najveće indekse selektivnosti imali su harmicini amidnoga tipa u položaju N-9 β-karbolina, **25b**,**d**,**i**, pri čemu je najselektivniji spoj s indeksom selektivnosti od 1105,33 bio *m*-CF_3-supstituirani harmicin **25i**.

Provedena je analiza kvantitativnog odnosa strukture i antiplazmodijskog djelovanja (*Pf*3D7) harmicina amidnoga tipa **7a-h**, **13a-h**, **19a-h**, **22a-h**, **25a-f**,**i**,**j** na eritrocitnu fazu *Pf*3D7. Na temelju reduciranog skupa generiranih molekulskih deskriptora primjenom višestruke linearne regresije izgrađen je prediktivni model ovisnosti log IC_{50} vrijednosti harmicina (koncentracije iskazane u nM) o dvije varijable (p*I* i AbrE). Dobiveni model potvrđen je izračunatim statističkim parametrima (R = 0,89; R_a^2 = 0,88) i validiran unutarnjom 10-strukom unakrsnom validacijom (Q^2 = 0,85). Izgrađeni QSAR model omogućio je previđanje, odabir i sintezu novih harmicina amidnoga **25k-p**, karbamatnog tipa **28a-k** i ureidnog **32b**,**c** tipa.

Prema dobivenim rezultatima najbolja djelovanja s visokim indeksima selektivnosti ostvarili su harmicini amidnoga tipa u položaju N-9 β-karbolina (**25b**,**d**,**i**) što ih čini dobrim spojevima uzorima za daljnji razvoj novih i učinkovitijih harmicina.

6. LITERATURA

1. Mishra M, Mishra VK, Kashaw V, Iyer AK, Kashaw SK. Comprehensive review on various strategies for antimalarial drug discovery. Eur J Med Chem 2017;125:1300–1320.
2. World Health Organization. World malaria report 2021. Preuzeto s: https://www.who.int/publications/i/item/9789240040496 (pristupljeno: 2. svibnja 2022.)
3. World Health Organization. Malaria. Preuzeto s: https://www.who.int/news-room/fact-sheets/detail/malaria (pristupljeno: 28. listopada 2022.)
4. Price RN, Commons RJ, Battle KE, Thriemer K, Mendis K. *Plasmodium vivax* in the era of the shrinking *P. falciparum* map. Trends Parasitol 2020;36:560–570.
5. Alanazi A, Almusailhi BAH, Bamousa GK, Alhawashim NH, Alotaibi NM, AlShamekh S, et al. A decade of travel-associated malaria at King Fahad Hospital of the University in the Eastern Province of Saudi Arabia. Sci Rep 2022;12:966.
6. Shahinas D, Folefoc A, Pillai DR. Targeting *Plasmodium falciparum* Hsp90: towards reversing antimalarial resistance. Pathogens 2013;2:33–54.
7. Fernández-Álvaro E, Hong WD, Nixon GL, O'Neill PM, Calderón F. Antimalarial chemotherapy: natural product inspired development of preclinical and clinical candidates with diverse mechanisms of action. J Med Chem 2016;59:5587−5603.
8. Mishra M, Mishra VK, Kashaw V, Kashaw SK. Molecular approaches for malaria therapy. In: Tyagi RK, editor. *Plasmodium* species and drug resistance. London: IntechOpen, 2021.
9. Centers for Disease Control and Prevention. Malaria - About Malaria - Biology. Preuzeto s: https://www.cdc.gov/malaria/about/biology/ (pristupljeno: 25. listopada 2022.)
10. Maier AG, Matuschewski K, Zhang M, Rug M. *Plasmodium falciparum*. Trends Parasitol 2017;35:481–482.
11. Centers for disease control and prevention. Malaria - about malaria – disease. Preuzeto s: https://www.cdc.gov/malaria/about/disease.html (pristupljeno: 29. listopada 2022.)
12. Brasil P, de Pina Costa A, Pedro RS, Silveira Bressan C, Silva S, Tauil PL, et al. Unexpectedly long incubation period of *Plasmodium vivax* malaria, in the absence of chemoprophylaxis, in patients diagnosed outside the transmission area in Brazil. Malar J 2011;10:122.
13. Laurens MB. RTS,S/AS01 vaccine (Mosquirix™): an overview. Hum Vaccines Immunother. 2020;16:480–489.
14. Tse EG, Korsik M, Todd MH. The past, present and future of anti-malarial medicines. Malaria J 2019;18:93.

15. Sharma C, Awasthi SK. Recent advances in antimalarial drug discovery – challenges and opportunities. In: Samie A, editor. An overview of tropical diseases. London: IntechOpen, 2015.
16. Pinheiro LCS, Feitosa LM, Da Silveira FF, Boechat N. Current antimalarial therapies and advances in the development of semi-synthetic artemisinin derivatives. An Acad Bras Cienc 2018;90:1251–1271.
17. World Health Organization. WHO model list of essential medicines - 22nd list, 2021. Preuzeto s: https://www.who.int/publications/i/item/WHO-MHP-HPS-EML-2021.02 (pristupljeno: 30. listopada 2022.)
18. Drug bank online. Tafenoquine. Preuzeto s: https://go.drugbank.com/drugs/DB06608 (pristupljeno: 28. listopada 2022.)
19. Drug bank online. Primaquine. Preuzeto s: https://go.drugbank.com/drugs/DB01087 (pristupljeno: 28. listopada 2022.)
20. Belete TM. Recent progress in the development of new antimalarial drugs with novel targets. Drug Des Devel Ther 2020;14:3875–3889.
21. W van der Pluijm R, Amaratunga C, Dhorda M, Dondorp AM. Triple artemisinin-based combinationt for malaria – a new paradigm? Trends parasitol 2021;37:15–24.
22. Arnou B, Montigny C, Morth JP, Nissen P, Jaxel C, Jesper V, et al. The *Plasmodium* falciparum Ca^{2+}-ATPase PfATP6: insensitive to artemisinin, but a potential drug target. Biochem Soc Trans 2011;39:823–831.
23. Gaillard T, Dormoi J, Madamet M, Pradines B. Macrolides and associated antibiotics based on similar mechanism of action like lincosamides in malaria. Malar J 2016;15:85.
24. Sinha S, Medhi B, Sehga R. Challenges of drug-resistant malaria. Parasite 2014;21:61.
25. Teixeira C, Vale N, Pérez B, Gomes A, Gomes JRB, Gomes P. "Recycling" classical drugs for malaria. Chem Rev 2014;114:11164−11220.
26. Agarwal D, Gupt RD, Awasthia SK. Are antimalarial hybrid molecules a close reality or a distant dream? Antimicrob Agents Chemother 2017;61:e00249–17.
27. Muregi FW, Ishih A. Next-generation antimalarial drugs: hybrid molecules as a new strategy in drug design. Drug Dev Res 2010;71:20–32.
28. Sunil RJ, Sarbani Pal, Jayashree A. Molecular hybridization - an emanating tool in drug design. Med Chem (Los Angeles) 2019;9:93–95.
29. Walsh JJ, Bell A. Hybrid drugs for malaria. Curr Pharm Des 2009;15:2970–2985.

30. Rasul A, Millimouno FM, Eltayb WA, Ali M, Li J, Li X. Pinocembrin: a novel natural compound with versatile pharmacological and biological activities. BioMed Res Int 2013;2013:379850.
31. Calixto JB. The role of natural products in modern drug discovery. An Acad Bras Ciênc 2019;91:e20190105.
32. Veeresham C. Natural products derived from plants as a source of drugs. J Adv Pharm Technol Res 2012;3:200–201.
33. Newman DJ, Cragg GM. Natural products as sources of new drugs over the nearly four decades from 01/1981 to 09/2019. J Nat Prod 2020;83:770–803.
34. Mathur S, Hoskins C. Drug development: lessons from nature (review). Biomed Rep 2017;6:612–614.
35. Atanasov AG, Zotchev SB, Dirsch VM, the International Natural Product Sciences Taskforce, Supuran CT. Natural products in drug discovery: advances and opportunities. Nat Rev Drug Discov 2021;20:200–216.
36. Lopez V. Are traditional medicinal plants and ethnobotany still valuable approaches in pharmaceutical research? Bol Latinoam Caribe Plantas Med Aromat 2011;10:3–10.
37. Chevallier A. Encyclopedia of Herbal Medicine. 3rd. ed. New York: DK Publishing; 2016.
38. Hrvatska enciklopedija. Velebilje. Preuzeto s: https://www.enciklopedija.hr/natuknica.aspx?ID=64105 (pristupljeno: 27. listopada 2022.)
39. Halmed. Baza lijekova. Preuzeto s: https://www.halmed.hr/Lijekovi/Baza-lijekova/Acopair-18-mikrograma-prasak-inhalata-tvrde-kapsule/15086/ (pristupljeno: 27. listopada 2022.)
40. Hrvatska enciklopedija. Mak. Preuzeto s: https://www.enciklopedija.hr/natuknica.aspx?id=38221 (pristupljeno: 27. listopada 2022.)
41. Halmed. Baza lijekova. Preuzeto s: https://www.halmed.hr/Lijekovi/Baza-lijekova/Dacepton-10-mg-ml-otopina-za-injekciju-u-ulosku/13533/ (pristupljeno: 26. listopada 2022.)
42. Hrvatska enciklopedija. Kalistemon. Preuzeto s: https://www.enciklopedija.hr/natuknica.aspx?id=29963 (pristupljeno: 27. listopada 2022.)

43. Halmed. Baza lijekova. Preuzeto s: https://www.halmed.hr/Lijekovi/Baza-lijekova/Orfadin/9840/ (pristupljeno: 27. listopada 2022.)
44. Das AM. Clinical utility of nitisinone for the treatment of hereditary tyrosinemia type-1 (HT-1). Appl Clin Genet. 2017;10:43–48.
45. Hrvatska enciklopedija. Visibaba. Preuzeto s: https://www.enciklopedija.hr/natuknica.aspx?ID=64817 (pristupljeno 27. listopada 2022.)
46. Drug bank online. Galantamine. Preuzeto s: https://go.drugbank.com/drugs/DB00674 (pristupljeno 27. listopada 2022.)
47. Halmed. Baza lijekova. Preuzeto s: https://www.halmed.hr/Lijekovi/Baza-lijekova/Paklitaksel-Kabi-6-mg-ml-koncentrat-za-otopinu-za-infuziju/8493/ (pristupljeno 28. listopada 2022.)
48. Halmed. Baza lijekova. Preuzeto s: https://www.halmed.hr/Lijekovi/Baza-lijekova/Topotecan-Teva/10023/ (pristupljeno 28. listopada 2022.)
49. Halmed. Baza lijekova. Preuzeto s: https://www.halmed.hr/Lijekovi/Baza-lijekova/Campto-20-mg-ml-koncentrat-za-otopinu-za-infuziju/13002/ (pristupljeno 28. listopada 2022.)
50. Zhao D, Hamilton JP, Pham GM, Crisovan E, Wiegert-Rininger K, Vaillancourt B, et al. *De novo* genome assembly of *Camptotheca acuminata*, a natural source of the anti-cancer compound camptothecin. Gigascience 2017;6:1–7.
51. Halmed. Baza lijekova. Preuzeto s: https://www.halmed.hr/Lijekovi/Baza-lijekova/Etoposide-Sandoz-20-mg-ml-koncentrat-za-otopinu-za-infuziju/14778/ (pristupljeno 29. listopada 2022.)
52. Csupor D, Csorbaa A, Hohmanna J. Recent advances in the analysis of flavonolignans of *Silybum marianum* J Pharm Biomed Anal 2016;130:301–317.
53. Hrvatska enciklopedija. Konoplja. Preuzeto s: https://www.enciklopedija.hr/natuknica.aspx?ID=32842 (pristupljeno 28. listopada 2022.)
54. Drug bank online. Dronabinol. Preuzeto s: https://go.drugbank.com/drugs/DB00470 (pristupljeno 27. listopada 2022.)
55. Halmed. Baza lijekova. Preuzeto s: https://www.halmed.hr/Lijekovi/Baza-lijekova/Epidyolex/15646/ (pristupljeno 28. listopada 2022)
56. Hrvatska enciklopedija. Paprika. Preuzeto s:

https://www.enciklopedija.hr/natuknica.aspx?id=46554 (pristupljeno: 29. listopada 2022.)

57. Halmed. Baza lijekova. Preuzeto s: https://www.halmed.hr/Lijekovi/Baza-lijekova/Qutenza/9901/ (pristupljeno: 29. listopada 2022.)
58. Halmed. Baza lijekova. Preuzeto s: https://www.halmed.hr/Lijekovi/Baza-lijekova/Kodeinfosfat-Alkaloid-30-mg-tablete/13270/ (pristupljeno: 29. listopada 2022.)
59. Drug bank online. Cocaine. Preuzeto s: https://go.drugbank.com/drugs/DB00907 (pristupljeno 29. listopada 2022.)
60. Hrvatska enciklopedija. Mrazovac. Preuzeo s: https://www.enciklopedija.hr/Natuknica.aspx?ID=42211 (pristupljeno 29. listopada 2022.)
61. Halmed. Baza lijekova. Preuzeto s: https://www.halmed.hr/Lijekovi/Baza-lijekova/Colcamexx-05-mg-tablete/16402/ (pristupljeno 29. listopada 2022.)
62. Hrvatska enciklopedija. Naprstak. Preuzeto s: https://www.enciklopedija.hr/natuknica.aspx?id=42939 (pristupljeno 29. listopada 2022.)
63. Halmed. Baza lijekova. Preuzeto s: https://www.halmed.hr/Lijekovi/Baza-lijekova/Lanitop-01-mg-tablete/6250/ (pristupljeno 29. listopada 2022.)
64. Olimat S. Pilocarpine Alkaloid A Review. EAS J Pharm Pharmacol 2020;2:161–165.
65. Halmed. Baza lijekova. Preuzeto s: https://www.halmed.hr/Lijekovi/Baza-lijekova/Alleofta-20-mg-ml-kapi-za-oko-otopina-u-jednodoznom-spremniku/11049/ (pristupljeno 29. listopada 2022.)
66. Pandita D, Pandita A, Wani SH, Abdelmohsen SAM, Alyousef HA, Abdelbacki AMM, et al. Crosstalk of multi-omics platforms with plants of therapeutic importance. Cells 2021;10:1296.
67. Breijyeh Z, Jubeh B, Bufo SA, Karaman R, Scrano L. Cannabis: a toxin-producing plant with potential therapeutic uses. Toxins 2021;13:117.
68. Mohamed F, Salih Mohamed M, Intisar F, Wadah JA, Malik SM. The role of natural products in drug discovery and development. World J Pharm Res 2015;4:22–33.
69. Achan J, Talisuna AO, Erhart A, Yeka A, Tibenderana JK, Baliraine FN, et al. Quinine, an old anti-malarial drug in a modern world: role in the treatment of malaria. Malar J 2011;10:144.

70. Wang J, Xu C, Wong YK, Li Y, Liao F, Jiang T, et al. Artemisinin, the magic drug discovered from traditional chinese medicine. Engineering 2019;5:32–39.
71. Cruz LR, Spangenberg T, Lacerda MVG, Wells TNC. Malaria in South America: a drug discovery perspective. Malar J 2013;12:168.
72. Borghi AA, Mauri Sergio Alves Palma MSA. Tetracycline: production, waste treatment and environmental impact assessment. Braz J Pharm Sci 2014;50:1.
73. Jelić D, Antolović R. From erythromycin to azithromycin and new potential ribosome-binding antimicrobials. Antibiotics 2016;5:29.
74. Spížek J, Řezanka T. Lincomycin, clindamycin and their applications. Appl Microbiol Biotechnol 2004;64:455–464.
75. Perković I, Raić-Malić S, Fontinha D, Prudêncio M, Pessanha de Carvalho L, Held J, et al. Harmicines - harmine and cinnamic acid hybrids as novel antiplasmodial hits. Eur J Med Chem 2020;187:111927.
76. Dai J, Dan W, Schneider U, Wang J. β-Carboline alkaloid monomers and dimers: occurrence, structural diversity, and biological activities. Eur J Med Chem 2018;157:622–655.
77. Ashok P, Ganguly S, Murugesan S. Review on *in-vitro* anti-malarial activity of natural β-carboline alkaloids. Mini Rev Med Chem 2013;13:1778–1791.
78. Puerto Galvis CE, Kouznetsov VV, Novel approaches in the synthesis of natural and synthetic fused aza-polycycles toward the development of new bioactive compounds. In: Atta-ur-Rahman, editor. Studies in natural products chemistry. Amsterdam: Elsevier, 2018:1–51.
79. Kamboj A, Sihag B, Brar DS, Kaur A, Salunke DB. Structure activity relationship in β-carboline derived anti-malarial agents. Eur J Med Chem 2021;221:113536.
80. Cao R, Peng W, Wang Z, Xu A. β-Carboline alkaloids: biochemical and pharmacological functions. Curr Med Chem 2007;14:479–500.
81. Goebel F. Über das harmalin. Eur J Organic Chem 1841;38:363–366.
82. Mayer AMS, Hall ML, Lynch SM, Gunasekera SP, Sennett SH and Pomponi SA. Differential modulation of microglia superoxide anion and thromboxane B2 generation by the marine manzamines. BMC Pharmacol 2005;5:6.
83. Hamann MT. The manzamines as an example of the unique structural classes available for the discovery and optimization of infectious disease controls based on marine natural products. Curr Pharm Des 2007;13:653–660.

84. Stachel SJ, Stockwell SA, Van Vrankenl DL. The fluorescence of scorpions and cataractogenesis. Chem Biol 1999;8:531–539.
85. Piechowska P, Zawirska-Wojtasiak R, Mildner-Szkudlarz S. Bioactive β-carbolines in food: a review. Nutrients 2019;11:814.
86. Herraiz T. Relative exposure to β-carbolines norharman and harman from foods and tobacco smoke. Food Addit Contam 2004;11:1041–1050.
87. Dalpozzo R. The chiral pool in the Pictet–Spengler reaction for the synthesis of β-carbolines. Molecules 2016;21:699.
88. Love BE. Synthesis of β-carbolines. A review. Org Prep Proced Int 1996;28:1–64.
89. Laine AE, Lood C, Koskinen AMP. Pharmacological importance of optically active tetrahydro-β-carbolines and synthetic approaches to create the C1 stereocenter. Molecules 2014;19:1544–1567.
90. Cox ED, Cook JM. The Pictet-Spengler condensation: a new direction for an old reaction. Chem Rev 1995;95:1797–1842.
91. Rao RN, Maiti B, Chanda K. Application of Pictet−Spengler reaction to indole-based alkaloids containing tetrahydro-β-carboline scaffold in combinatorial chemistry. ACS Comb Sci 2017;19:199−228.
92. Dalpozzo R. The chiral pool in the Pictet–Spengler reaction for the synthesis of β-carbolines. Molecules 2016;21:699.
93. Guan H, Liu X, Peng W, Cao R, Ma Y, Chen H, Xu A. β-Carboline derivatives: novel photosensitizers that intercalate into DNA to cause direct DNA damage in photodynamic therapy. Biochem Biophys Res Commun 2006;342:894–901.
94. Szabó T, Volk, Milen M. Recent advances in the synthesis of β-carboline alkaloids. Molecules 2021;26:663.
95. Abinaya R, Srinath S, Soundarya S, Sridhar R, Balasubramanian KK, Baskar B. Recent developments on synthesis strategies, SAR studies and biological activities of β-carboline derivatives – an update. J Mol Struct 2022;1261:132750.
96. Drug bank online. Rescinnamine. Preuzeto s: https://go.drugbank.com/drugs/DB01180 (pristupljeno 30. listopada 2022)
97. Drug bank online. Ajmaline. Preuzeto s: https://go.drugbank.com/drugs/DB01426 (pristupljeno: 30. listopada 2022.)
98. Drug bank online. Lurbinectedin. Preuzeto s: https://go.drugbank.com/drugs/DB12674 (pristupljeno: 30. listopada 2022.)

99. Gorki V, Walter NS, Singh R, Chauhan M, Dhingra N, Salunke NB, et al. β-Carboline derivatives tackling malaria: biological evaluation and docking analysis. ACS Omega 2020;5:17993−18006.
100. PubChem. Harmine. Preuzeto s: https://pubchem.ncbi.nlm.nih.gov/compound/Harmine (pristupljeno: 23. listopada 2022.)
101. Chemicalize - Instant Cheminformatics Solutions. Preuzeto s: https://chemicalize.com/app/calculation (pristupljeno 23. listopada 2022.)
102. Shahrajabian MH, Sun W, Cheng Q. Improving health benefits with considering traditional and modern health benefits of *Peganum harmala*. Clin Phytoscience 2021;7:18.
103. Doskaliyev A, Seidakhmetova RB, Tutai DS, Goldaeva K, Surov VK, Adekenov SM. Alkaloids of *Peganum harmala* L. and their pharmacological activity. Open Access Maced J Med Sci 2021;9:766–775.
104. Zhang L, Li D, Yu D. Pharmacological effects of harmine and its derivatives: a review. Arch Pharm Res 2020;43:1259–1275.
105. Cao R, Fan W, Guo L, Ma Q, Zhang G, Li J, et al. Synthesis and structure activity relationships of harmine derivatives as potential antitumor agents. Eur J Med Chem 2013;60:135–143.
106. Javeed M, Rasul A, Hussain G, Jabeen F, Rasool B, Shafiq N. Harmine and its derivatives: biological activities and therapeutic potential in human diseases. Bangladesh J Pharmacol 2018;13:203–213.
107. Dubey A, Prajapati KS, Swamy M, Pachauri V. Heat shock proteins: a therapeutic target worth to consider. Vet World 2015;8:46–51.
108. Miller DJ, Fort PE. Heat shock proteins regulatory role in neurodevelopment. Front Neurosci 2018;12:821.
109. Dubrez L, Causse S, Bonan NB, Dumétier B, Garrido C. Heat-shock proteins: chaperoning DNA repair. Oncogene 2020;39:516–529.
110. Posfai D, Eubanks AL, Keim AI, Lu KY, Wang GZ, Hughes PF, et al. Identification of Hsp90 inhibitors with anti-*Plasmodium a*ctivity. Antimicrob Agents Chemother 2018;62:e01799-17.
111. Shahinas D, MacMullin G, Benedict C, Crandall I, Pillai DR. Harmine is a potent antimalarial targeting Hsp90 and synergizes with chloroquine and artemisinin. Antimicrob Agents Chemother 2012;56:4207–4213.

112. Marinović M, Poje G, Perković I, Fontinha D, Prudêncio M, Held J, et al. Further investigation of harmicines as novel antiplasmodial agents: synthesis, structure-activity relationship and insight into the mechanism of action. Eur J Med Chem 2021;224:113687.
113. Poje G, Marinović M, Pavić K, Mioč M, Kralj M, de Carvalho LP. Harmicens, novel harmine and ferrocene hybrids: design, synthesis and biological activity. Int J Mol Sci 2022;23:9315.
114. Poje G, de Carvalho PL, Held J, Moita D, Prudêncio M, Perković I, et al. Design and synthesis of harmiquins, harmine and chloroquine hybrids as potent antiplasmodial agents. E J Med Chem 2022;238:114408.
115. Silva AT, Bento CM, Pena AC, Figueiredo LM, Prudêncio C, Aguiar L, et al. Cinnamic acid conjugates in the rescuing and repurposing of classical antimalarial drugs. Molecules 2020;25:66.
116. Ruwizhi N, Aderibigbe BA. Cinnamic acid derivatives and their biological efficacy. Int J Mol Sci 2020;21:5712.
117. Adisakwattana S. Cinnamic acid and its derivatives: mechanisms for prevention and management of diabetes and its complications. Nutrients 2017;9:163.
118. De P, Bedos-Belval F, Vanucci-Bacqué C, Baltas M. Cinnamic acid derivatives in tuberculosis, malaria and cardiovascular diseases - a review. Curr Org Chem 2012;16:747–768.
119. Gottardi M, Knudsen D, Prado L, Oreb M, Branduardi P, Bole E. De novo biosynthesis of *trans*-cinnamic acid derivatives in *Saccharomyces cerevisiae*. Appl Microbiol Biotechnol 2017;101:4883–4893.
120. Gunia-Krzyzak A, Słoczyńska K, Popioł J, Koczurkiewicz P, Marona H, Pękala E. Cinnamic acid derivatives in cosmetics: current use and future prospects. Int J Cosmet Sci 2018;40:356–366.
121. El-Seedi HR, Taher EA, Sheikh BY, Anjum S, Saeed A, AlAjmi MF, et al. Hydroxycinnamic acids: natural sources, biosynthesis, possible biological activities, and roles in islamic medicine. In: Atta-ur-Rahman, editor. Studies in natural products chemistry. Amsterdam: Elsevier, 2018:269–292.
122. França SB, dos Santos Correia PR, de Castro IBD, da Silva Júnior EF, de Sá Barreto Barros ME, da Paz Lima DJ. Synthesis, applications and structure-activity relationship (SAR) of cinnamic acid derivatives: a review. Res Soc Dev 2021;10: e28010111691.

123. Sharma P. Cinnamic acid derivatives: a new chapter of various pharmacological activities. J Chem Pharm Res 2011;3:403–423.
124. Sova M. Antioxidant and antimicrobial activities of cinnamic acid derivatives. Mini-Rev Med Chem 2012;12:749–767.
125. Pavić K, Perković I, Gilja P, Kozlina F, Ester K, Kralj M, et al. Design, synthesis and biological evaluation of novel primaquine-cinnamic acid conjugates of the amide and acylsemicarbazide type. Molecules 2016;21:1629.
126. Mabeta P, Pavić K, Zorc B. Insights into the mechanism of antiproliferative effects of primaquine-cinnamic acid conjugates on MCF-7 cells. Acta Pharm 2018;68:337–348.
127. Kanaani J, Ginsburg H. Effects of cinnamic acid derivatives on *in vitro* growth of *Plasmodium falciparum* and on the permeability of the membrane of malaria-infected erythrocytes. Antimicrob Agents Chemother 1992;36:1102–1108.
128. Bouyer G, Egée S, Thomas SL. Three types of spontaneously active anionic channels in malaria-infected human red blood cells. Blood Cells Mol Dis 2006;36:248–254.
129. Pérez BC, Teixeira C, Albuquerque IS, Figueiras M, Gut J, Rosenthal PJ, Gomes JRB, Gomes P. Novel cinnamic acid/4-aminoquinoline conjugates bearing non-proteinogenic amino acids: towards the development of potential dual action antimalarials. Eur J Med Chem 2012;54:887–899.
130. Pérez B, Teixeira C, Gut J, Rosenthal PJ, Gomes JR, Gomes P. Cinnamic acid/chloroquinoline conjugates as potent agents against chloroquine-resistant Plasmodium falciparum. ChemMedChem 2012;7:1537–1540.
131. Pérez BC, Teixeira C, Albuquerque IS, Gut J, Rosenthal PJ, Gomes JRB, Prudêncio M, Gomes P. N-cinnamoylated chloroquine analogues as dual-stage antimalarial leads. J Med Chem 2013;56:556–567.
132. Gayam V, Ravi S. Cinnamoylated chloroquine analogues: a new structural class of antimalarial agents. E J Med Chem 2017;135:382–391.
133. Pérez B, Teixeira C, Albuquerque IS, Gut J, Rosenthal PJ, Prudêncio M, Gomes P. PRIMACINS, N-cinnamoyl-primaquine conjugates, with improved liver-stage antimalarial activity. Med Chem Commun 2012;3:1170–1172.
134. Levatić J, Pavić K, Perković I, Uzelac L, Ester K, Kralj M, et al. Machine learning prioritizes synthesis of primaquine ureidoamides with high antimalarial activity and attenuated cytotoxicity. Eur J Med Chem 2018;146:651–667.

135. Pérez B, Teixeira C, Gomes AS, Albuquerque IS, Gut J, Rosenthal PJ et al. *In vitro* efficiency of 9-(*N*-cinnamoylbutyl)aminoacridines against blood- and liver-stage malaria parasites. Bioorg Med Chem Lett 2013;23:610–613.
136. Gomes A, Pérez B, Albuquerque IS, Machado M, Prudêncio M, Nogueira F, et al. N-cinnamoylation of antimalarial classics: quinacrine analogues with decreased toxicity and dual-stage activity. ChemMedChem 2014;9:305–310.
137. Ferraz R, Noronha J, Murtinheira F, Nogueira F, Machado M, Prudêncio M, et al. Primaquine-based ionic liquids as a novel class of antimalarial hits. RSC Adv 2016;6:56134–56138.
138. Doytchinova I. Drug design – past, present, future. Molecules 2022;27:1496.
139. Hamad ON, Amran SIB, Sabbah AM. Drug discovery - yesterday and tomorrow: the common approaches in drug design and cancer. Cell Cellular Lif Sci J 2018;3:000119.
140. Kwon S, Bae H, Jo J, Yoon S. Comprehensive ensemble in QSAR prediction for drug discovery. BMC Bioinform 2019;20:521.
141. Jhanwar B, Sharma V, Singla RK, Shrivastava B. QSAR - Hansch analysis and related approaches in drug design. Pharmacologyonline 2011;1:306–344.
142. Perkins R, Fang H, Tong W, Welsh WJ. Quantitative structure-activity relationship methods: perspectives on drug discovery and toxicology. Environ Toxicol Chem 2003;22:1666–1679.
143. Muhammad U, Uzairu A, Arthur DE. Review on: quantitative structure activity relationship (QSAR) modeling. J Anal Pharm Res 2018;7:240–242.
144. Todeschini R, Consonni V, Gramatica P. Chemometrics in QSAR. In: Brown ST, Tauler R, Walczak B, editors. Comprehensive Chemometrics. Amsterdam: Elsevier, 2009:129–172.
145. OECD. Validation of (Q)SAR Models. Preuzeto s: https://www.oecd.org/chemicalsafety/risk-assessment/validationofqsarmodels.htm (pristupljeno: 25. listopada 2022.)
146. Acharya C, Coop A, Polli JE, MacKerell Jr AD. Recent advances in ligand-based drug design: relevance and utility of the conformationally sampled pharmacophore approach. Curr Comput Aided Drug Des. 2011;7:10–22.
147. Golbraikh A, Wang XS, Zhu H, Tropsha A. Predictive QSAR modeling: methods and applications in drug discovery and risk assessment. In: Leszczynski J, Kaczmarek-

Kedziera A, Puzyn TG, Papadopoulos M, Reis H, Shukla M, editors. Handbook of computational chemistry. Berlin: Springer, 2017:2303–2340.

148. Abuhammad A, Tah MO. QSAR studies in the discovery of novel type-II diabetic therapies. Expert Opin Drug Discov. 2016;11:197–214.
149. Alexander DLJ, Tropsha A, Winkler DA. Beware of R^2: simple, unambiguous assessment of the prediction accuracy of QSAR and QSPR models. J Chem Inf Model. 2015;55:1316–1322.
150. Gramatica P. On the development and validation of QSAR models. In: Reisfeld B, Mayeno A, editors. Computational toxicology. Methods in molecular biology. Totowa: Humana Press, 2013:499–526.
151. Myint KZ, Xie X-Q. Recent advances in fragment-based QSAR and multi-dimensional QSAR methods. Int J Mol Sci 2010;11:3846–3866.
152. Debeljak Ž, Bojić M, Rimac H, Medić-Šarić M. Uvod u računalnu kemiju i dizajn lijekova, 1. izdanje. Zagreb: Medicinska naklada; 2020.
153. Frederick R, Bruyere C, Vancraeynest C, Reniers J, Meinguet C, Pochet L, et al. Novel trisubstituted harmine derivatives with original *in vitro* anticancer activity, J Med Chem 2012;55:6489–6501.
154. Devi N, Singh D, Honey, Mor S, Chaudhary S, Rawal RK, et al. $In(OTf)_3$ catalysed an expeditious synthesis of β-carboline-imidazo[1,2-*a*] pyridine and imidazo[1,2-*a*]pyrazine conjugates. RSC Adv 2016;6:43881–43891.
155. Eagon S, Anderson MO. Microwave-assisted synthesis of tetrahydro-β-carbolines and β-carbolines. Eur J Org Chem 2014;2014:1653–1665.
156. Singh D, Hazra CK, Malakar CC, Pandey SK, Kaith BS, Singh V. Indium mediated domino allylation-lactonisation approach: diastereoselective synthesis of β-carboline C-3 tethered α methylene γ-butyrolactones. ChemistrySelect 2018;3:4859–4864.
157. Szabó T, Hazai V, Volk B, Simig G, Milen M. First total synthesis of the β-carboline alkaloids trigonostemine A, trigonostemine B and a new synthesis of pityriacitrin and hyrtiosulawesine. Tetrahedron Lett 2019;60:1471–1475.
158. Lin G, Wang Y, Zhou Q, Tang W, Wang J, Lu T. A facile synthesis of 1-substituted β-carboline derivatives via minisci-reaction. Synth Commun 2011;41:3541–3550.
159. Schott Y, Decker M, Rommelspacher H, Lehmann J. 6-Hydroxy- and 6-methoxy-β-carbolines as acetyl-and butyrylcholinesterase inhibitors. Bioorg Med Chem Lett 2006;16:5840–5843.

160. Cowles RS, Miller JR, Hollingworth RM, Abdel-AAl MT, Szurdoki F, Bauer K, et al. Cinnamyl derivatives and monoterpenoids as nonspecific ovipositional deterrnets of the onion fly. J Chem Ecol 1990;16:2410–2428.
161. Ambrogio I, Cacchi S, Fabrizi G, Goggiamani A, Sgalla S. Regio- and stereoselective Heck α-arylation of cinnamyl alcohols. Synlett 2009;4:620–624.
162. Shao PP, Ye F, Vachal P. 2017. U.S. Patent 9,663,534.
163. Takale BS, Wang S, Zhang X, Feng X, Yu X, Jin T, Bao M, Yamamoto Y. Chemoselective reduction of α,β- unsaturated aldehydes using unsupported anoporous gold catalyst. Chem Commun 2014;50:14401–14404.
164. Butula I, Proštenik MV, Vela V. Reactions with 1-benzotriazolecarboxylic acid chloride. I. Synthesis of the 2,6-*bis*(hydroxymethyl)pyridinedicarbamates. Croat Chem Acta 1977;49:837–842.
165. Held J, Gebru T, Kalesse M, Jansen R, Gerth K, Müller R, Mordmüller B. Antimalarial activity of the myxobacterial macrolide chlorotonil a. Antimicrob Agents Chemother 2014;58:6378–6384.
166. Noedl H, Bronnert J, Yingyuen K, Attlmayr B, Kollaritsch H, Fukuda M. Simple histidine-rich protein 2 double-site sandwich enzyme-linked immunosorbent assay for use in malaria drug sensitivity testing. Antimicrob Agents Chemother 2005;49:3575–3577.
167. The R Project for Statistical Computing. Preuzeto s: https://www.R-project.org/ (pristupljeno: 20. prosinca 2021.)
168. Machado M, Sanches-Vaz M, Cruz JP, Mendes AM, Prudêncio M. Inhibition of Plasmodium hepatic infection by antiretroviral compounds, Front Cell Infect Microbiol 2017;7:329.
169. Ploemen IHJ, Prudêncio M, Douradinha BG, Ramesar J, Fonager J, van Gemert G-J, et al. Visualisation and quantitative analysis of the rodent malaria liver stage by real time imaging. PloS One 2009:4:e7881.
170. Borenfreund E, Puerner JA. A simple quantitative procedure using monolayer cultures for cytotoxicity assays (HTD/NR-90). J Tissue Cult Methods 1985;9:7–9.
171. ACD/Labs. Software for R&D. Chemistry Software. Preuzeto s: https://www.acdlabs.com/resources/free-chemistry-software-apps/chemsketch-freeware/ (pristupljeno 15. travnja 2020.)
172. Chemaxon. Preuzeto s: https://chemaxon.com/marvin (pristupljeno: 10. lipnja 2020.)

173. CambridgeSoft. Preuzeto s: https://perkinelmerinformatics.com/products/research/chemdraw (pristupljeno: 20 veljače 2020.)
174. Mestrelab Research S.L. - Analytical Chemistry Software. Preuzeto s: https://mestrelab.com/download/mnova/ (pristupljeno 24. siječnja 2020.)
175. SwissADME. Preuzeto s: http://www.swissadme.ch/ (pristupljeno 14. veljače 2020.)
176. Trinajstić N. Chemical graph theory. 2nd edition. Boca Raton: CRC Press; 1992.
177. Hammouda MM, Elattar KM, Rabie R. Cesium carbonate as a mediated inorganic base in some organic transformations. Res Chem Intermed 2017;43:1979–2015.
178. Vinogradova SV, Pankratov VA, Korshak VV, Komarova LI. Investigation of the reaction of thionyl chloride with dimethylformamide. Russ Chem Bull. 1971;20:450–455.
179. Wikipedia. Isoelectric point. Preuzeto s: https://en.wikipedia.org/wiki/Isoelectric_point#cite_note-1 (pristupljeno 11. prosinca 2022.)
180. Abraham MH, Whiting GS, Doherty RM, Shuely WJ. Hydrogen bonding. Part 13. A new method for the characterisation of GLC stationary phases—the laffort data set. J Chem Soc Perkin Trans 2 1990:1451–1460.
181. Bradley JC, Abraham MH, Acree Jr WE, Lang ASID, Beck SN, Bulger DA, et al. Determination of Abraham model solute descriptors for the monomeric and dimeric forms of trans-cinnamic acid using measured solubilities from the Open Notebook Science Challenge. Chem Cent J 2015;9:11.

7. ŽIVOTOPIS

Marina Marinović rođena je 2. travnja 1993. godine u Slavonskom Brodu. Osnovnu i srednju školu završila je u Orahovici. Preddiplomski studij na Fakultetu kemijskog inženjerstva i tehnologije u Zagrebu, smjer primijenjena kemija upisala je 2011 godine, te završila 2014. godine visokim prosjekom (4,7) i javnom obranom završnog rada pri čemu je stekla akademski naziv prvostupnica primijenjene kemije. Iste godine upisuje diplomski studij na Fakultetu kemijskog inženjerstva i tehnologije, smjer primijenjena kemija, modul primijenjena organska kemija. Godine 2015. nagrađena je Dekanovom nagradom za zapažen studentski znanstveni rad. Eksperimentalni dio diplomskog rada izradila je u sklopu ERASMUS+ projekta na Češkom Tehničkom Sveučilištu u Pragu, a diplomski studij završila je 2016. godine izvrsnim prosjekom (4,9) i javnom obranom diplomskog rada čime je stekla akademski naziv magistra primijenjene kemije.

Od rujna 2018. zaposlena je kao asistent/doktorand na projektu na Farmaceutsko-biokemijskom fakultetu Sveučilišta u Zagrebu u Zavodu za farmaceutsku kemiju, u okviru projekta „Projekt razvoja karijera mladih istraživača – izobrazba novih doktora znanosti". Suradnica je na uspostavnom istraživačkom projektu „Derivati harmina kao potencijalni antimalarici" Hrvatske zaklade za znanost (UIP-2017-05-5160). Poslijediplomski doktorski studij Farmaceutsko-biokemijske znanosti na Farmaceutsko-biokemijskom fakultetu upisala je akademske godine 2018./19. Dobitnica je stipendije Sveučilišta u Zagrebu za akademsku mobilnost u 2022. godini i stipendije za sudjelovanje na 9. međunarodnom kongresu farmaceuta u Ljubljani koju je dodjeljivao Lek Pharmaceuticals d.d. (Sandoz).

Objavila je tri znanstvena rada u časopisima zastupljenima u bazi *Web of Science Core Collection* kao prva autorica i jedan stručni rad. Neposredna je voditeljica pet diplomskih radova i dva rada dobitnika Rektorove nagrade. Održala je tri usmena predavanja sudjelovala na zimskim i ljetnim školama te na domaćim i međunarodnim kongresima s ukupno dvanaest posterskih priopćenja.

Popis znanstvenih radova:

1. **Marinović M**, Perković I, Fontinha D, Prudêncio M, Held J, Pessanha de Carvalho L, Tandarić T, Vianello R, Zorc B, Rajić Z. Novel harmicines with improved potency against *Plasmodium*. Molecules 2020;25:4376.

2. **Marinović M**, Poje G, Perković I, Fontinha D, Prudêncio M, Held J, Pessanha de Carvalho L, Tandarić T, Vianello R, Rajić Z. Further investigation of harmicines as novel antiplasmodial

agents: synthesis, structure-activity relationship and insight into the mechanism of action. Eur J Med Chem 2021;224:113687.

3. Poje G, **Marinović M**, Pavić K, Mioč M, Kralj M, Pessanha de Carvalho L, Held J, Perković I, Rajić Z. Harmicens, novel harmine and ferrocene hybrids: design, synthesis and biological activity. Int J Mol Sci. 2022;23:9315.

PRILOG A

Prilog sadrži IR, MS, ^{1}H i ^{13}C NMR spektre i HPLC kromatograme harmicina amidnoga, karbamatnog i ureidnog tipa opisanih u ovom doktorskom radu.

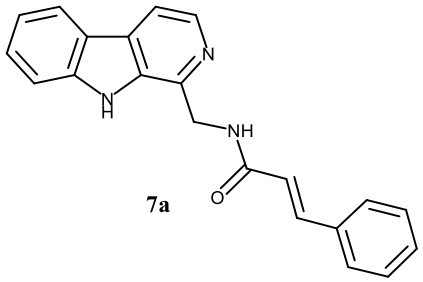
N
H
NH
O

7a

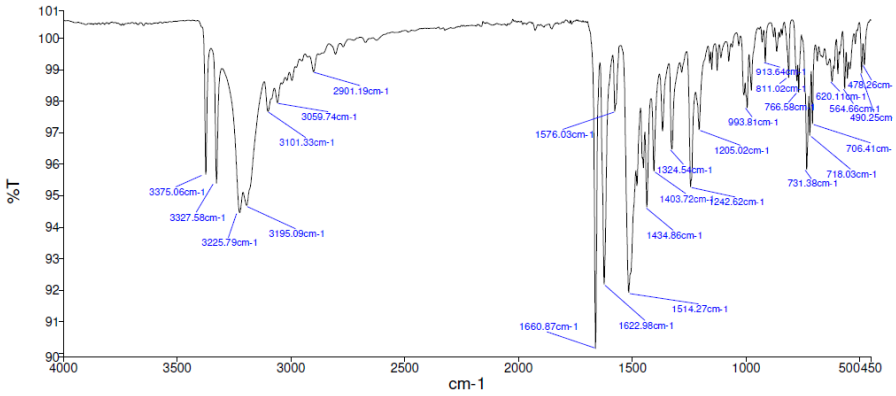
%T
cm-1
3375.06cm-1
3327.58cm-1
3225.79cm-1
3195.09cm-1
3101.33cm-1
3059.74cm-1
2901.19cm-1
1660.87cm-1
1622.98cm-1
1576.03cm-1
1514.27cm-1
1434.86cm-1
1403.72cm-1
1324.54cm-1
1242.62cm-1
1205.02cm-1
993.81cm-1
913.64cm-1
811.02cm-1
766.59cm-1
731.38cm-1
718.03cm-1
706.41cm-1
620.11cm-1
564.66cm-1
490.25cm
479.26cm-

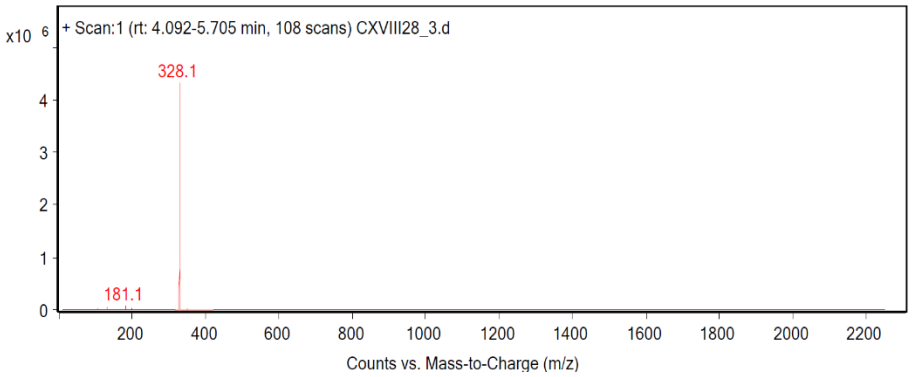
x10 6
+ Scan:1 (rt: 4.092-5.705 min, 108 scans) CXVIII28_3.d
328.1
181.1
Counts vs. Mass-to-Charge (m/z)

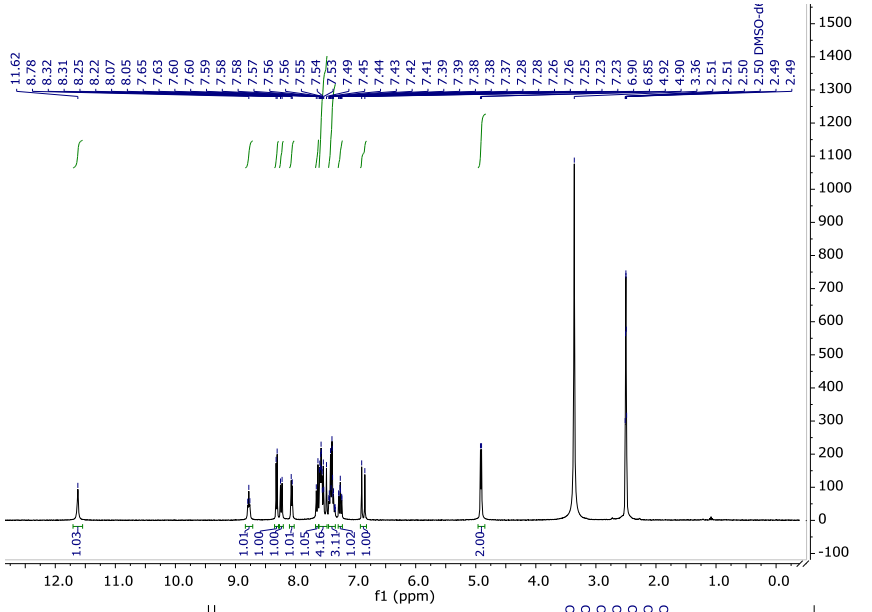
11.62
8.78
8.32
8.31
8.25
8.22
8.07
8.05
7.65
7.63
7.60
7.60
7.59
7.58
7.58
7.57
7.56
7.56
7.55
7.54
7.53
7.49
7.45
7.44
7.43
7.42
7.41
7.39
7.39
7.38
7.38
7.37
7.28
7.28
7.26
7.26
7.25
7.23
7.23
6.90
6.85
4.92
4.90
3.36
2.51
2.51
2.50
2.50 DMSO-d6
2.49
2.49
1.03
1.01
1.00
1.00
1.01
1.05
4.16
3.11
1.02
1.00
2.00
f1 (ppm)

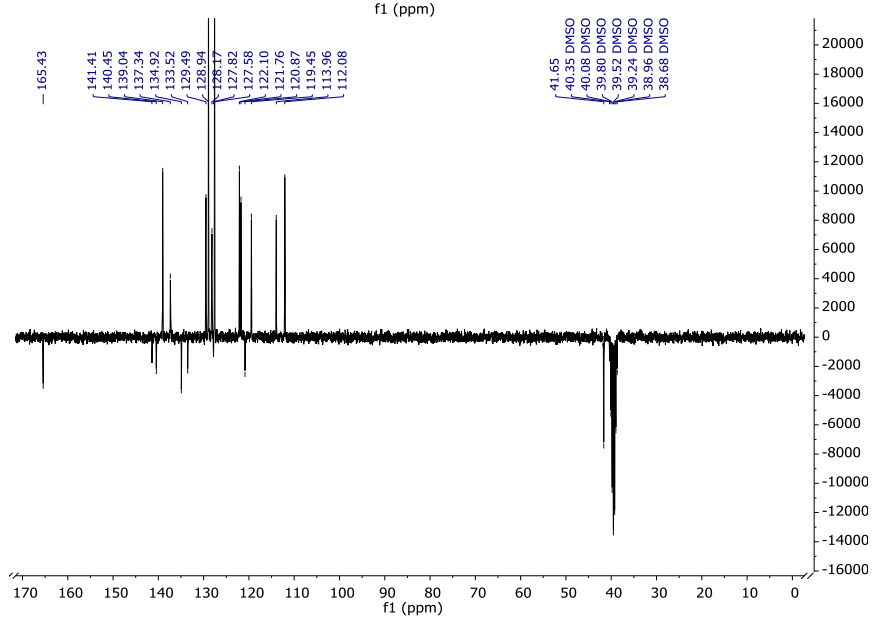
165.43
141.41
140.45
139.04
137.34
134.92
133.52
129.49
128.94
128.17
127.82
127.58
122.10
121.76
120.87
119.45
113.96
112.08
41.65
40.35 DMSO
40.08 DMSO
39.80 DMSO
39.52 DMSO
39.24 DMSO
38.96 DMSO
38.68 DMSO
f1 (ppm)

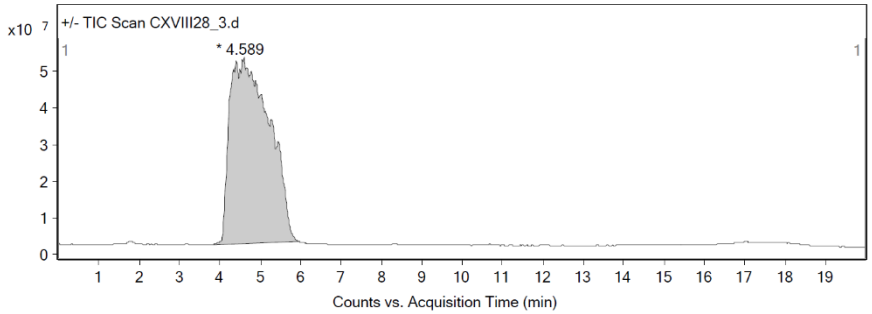

Integration Peak List

Peak	Start	RT	End	Height	Area	Area %
1	3.836	4.589	5.961	50934705.47	3491199962.29	100

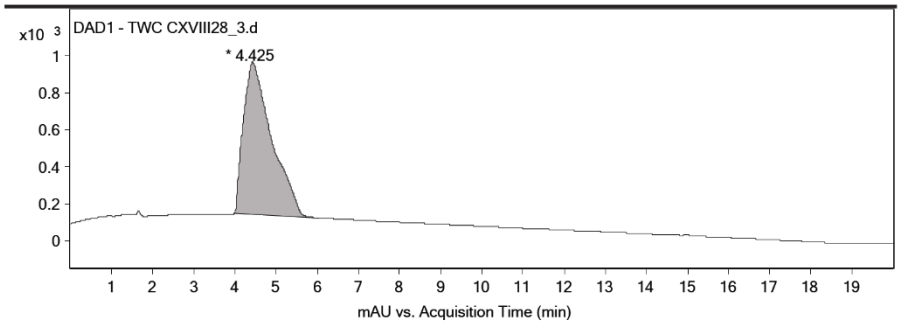

Integration Peak List

Peak	Start	RT	End	Height	Area	Area %
1	3.971	4.425	6.045	821.04	39188.98	100

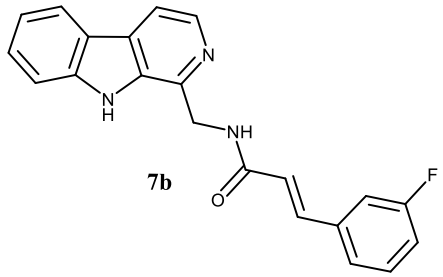
N
H
NH
O
F

7b

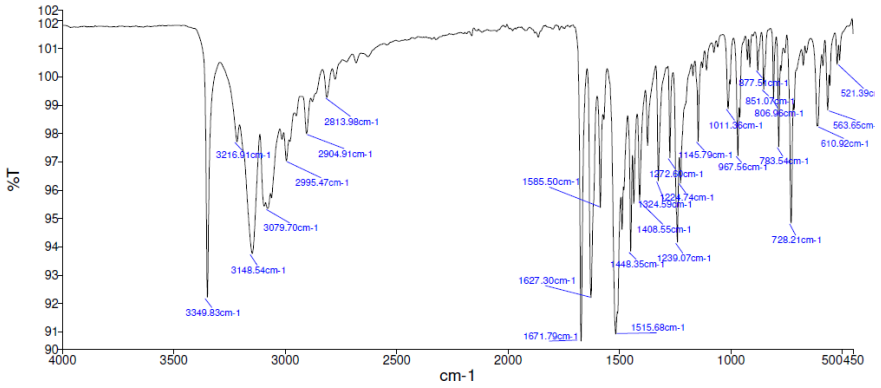
%T
cm-1
3349.83cm-1
3216.31cm-1
3148.54cm-1
3079.70cm-1
2995.47cm-1
2904.91cm-1
2813.98cm-1
1671.79cm-1
1627.30cm-1
1585.50cm-1
1515.68cm-1
1448.35cm-1
1408.55cm-1
1324.59cm-1
1272.88cm-1
1239.07cm-1
1224.74cm-1
1145.79cm-1
1011.35cm-1
967.56cm-1
877.56cm-1
851.07cm-1
806.06cm-1
783.54cm-1
728.21cm-1
610.92cm-1
563.65cm
521.39c

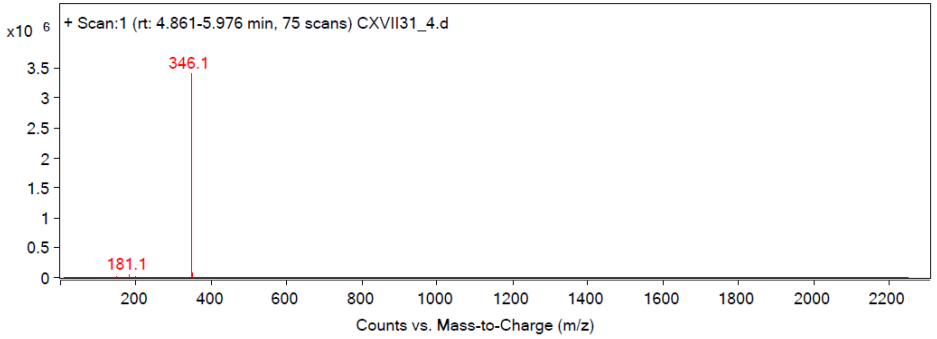
x10 6
+ Scan:1 (rt: 4.861-5.976 min, 75 scans) CXVII31_4.d
346.1
181.1
Counts vs. Mass-to-Charge (m/z)

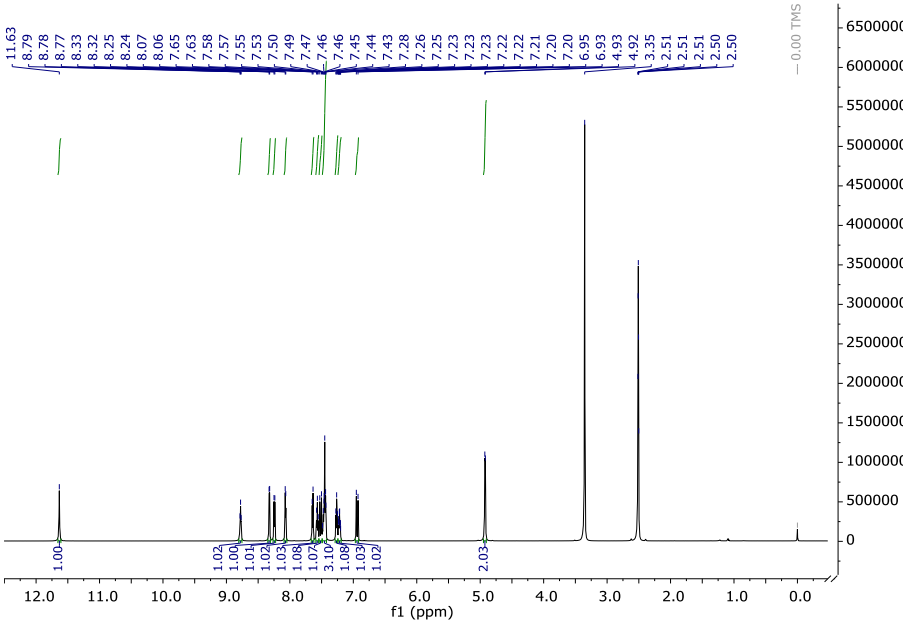
11.63
8.79
8.78
8.77
8.33
8.32
8.25
8.24
8.07
8.06
7.65
7.63
7.58
7.57
7.55
7.53
7.50
7.49
7.47
7.46
7.46
7.45
7.44
7.43
7.28
7.26
7.25
7.23
7.23
7.22
7.22
7.21
7.20
7.20
6.95
6.93
4.93
4.92
3.35
2.51
2.51
2.51
2.50
2.50
0.00 TMS
1.00
1.02
1.00
1.01
1.02
1.03
1.08
1.07
3.10
1.08
1.03
1.02
2.03
f1 (ppm)

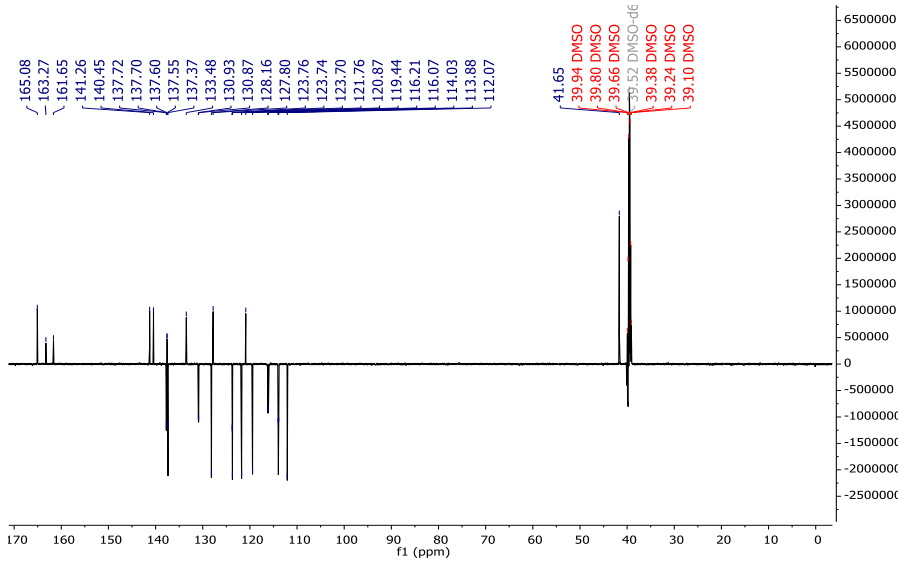
165.08
163.27
161.65
141.26
140.45
137.72
137.70
137.60
137.55
137.37
133.48
130.93
130.87
128.16
127.80
123.76
123.74
123.70
121.76
120.87
119.44
116.21
116.07
114.03
113.88
112.07
41.65
39.94 DMSO
39.80 DMSO
39.66 DMSO
39.52 DMSO-d6
39.38 DMSO
39.24 DMSO
39.10 DMSO
f1 (ppm)

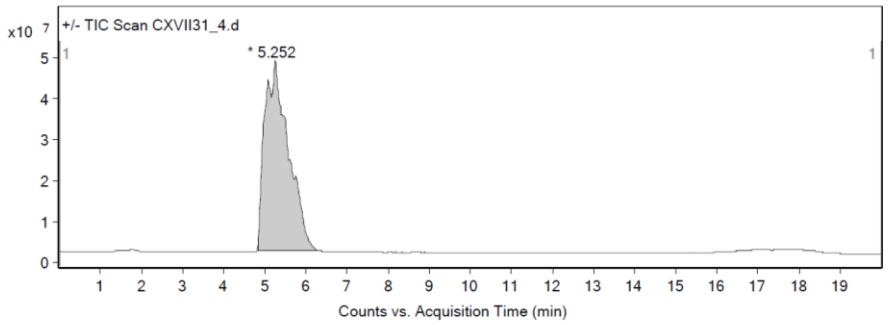

Integration Peak List

Peak	Start	RT	End	Height	Area	Area %
1	4.83	5.252	6.337	46318906.54	1853564809.65	100

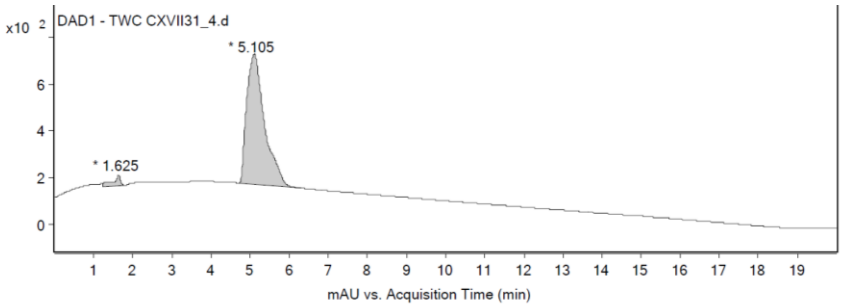

Integration Peak List

Peak	Start	RT	End	Height	Area	Area %
1	1.239	1.625	1.765	45.74	633.7	3.6
2	4.732	5.105	6.305	556.32	17595.03	100

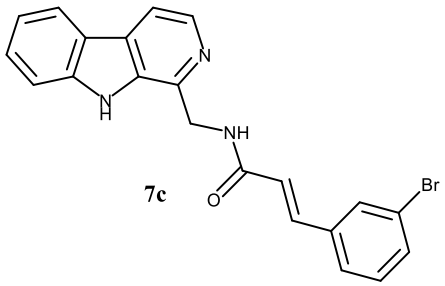

7c

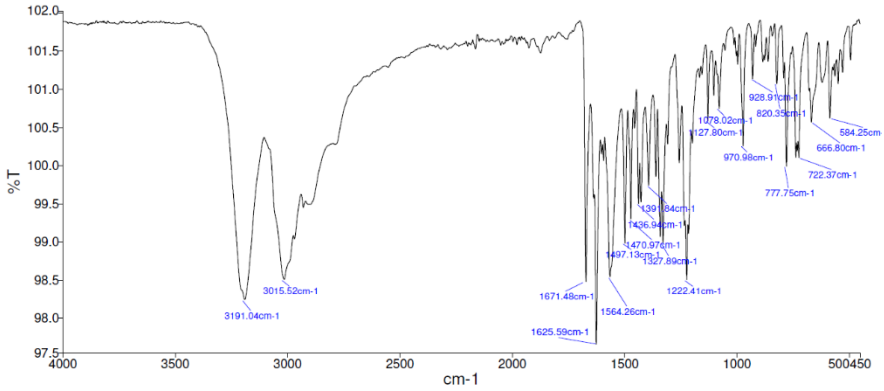

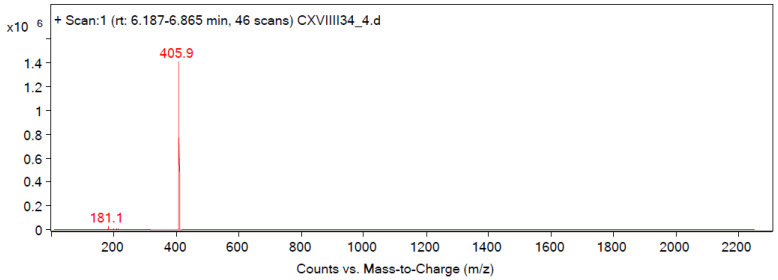

Peak List

m/z	z	Abund
181.1		27370.79
405.9	1	1412220.88
407	1	323633.78
407.9	1	1289329.25
409	1	336270.09
410	1	35611.3

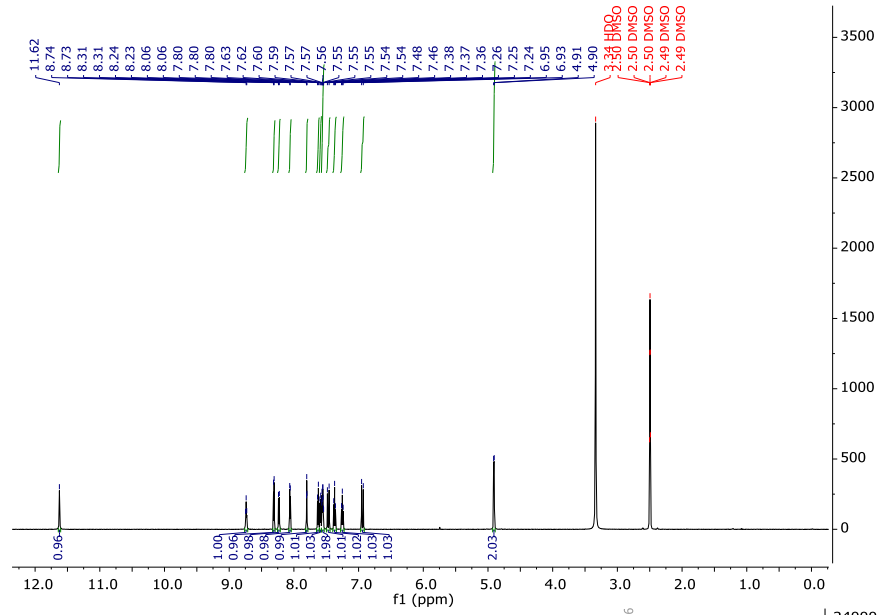

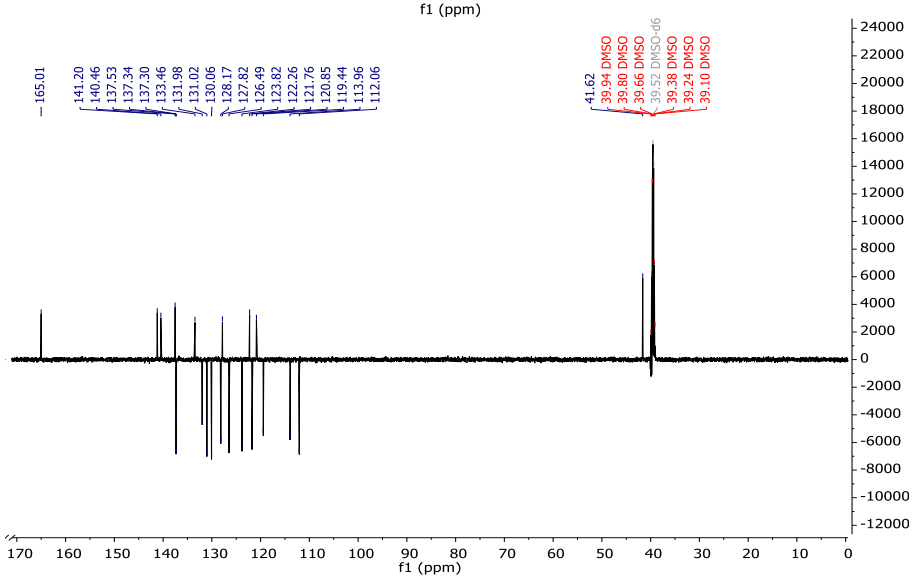

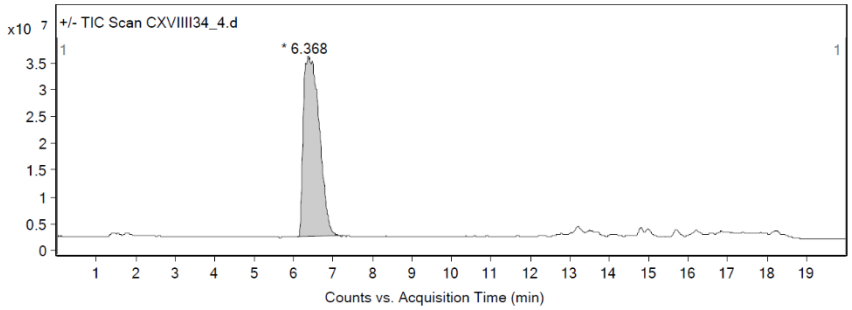

Integration Peak List

Peak	Start	RT	End	Height	Area	Area %
1	6.096	6.368	7.257	33671013.3	937078912.39	100

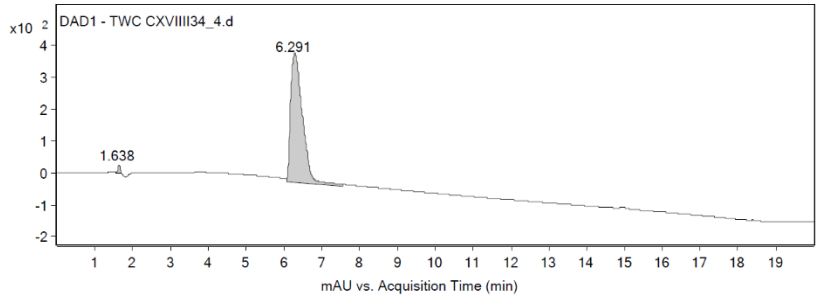

Integration Peak List

Peak	Start	RT	End	Height	Area	Area %
1	1.558	1.638	1.699	24.74	101.66	1.14
2	6.065	6.291	7.538	405.63	8933.15	100

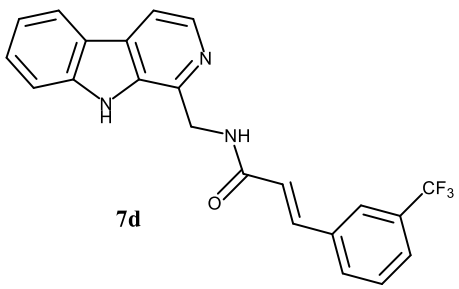
N
H
NH
O
CF3

7d

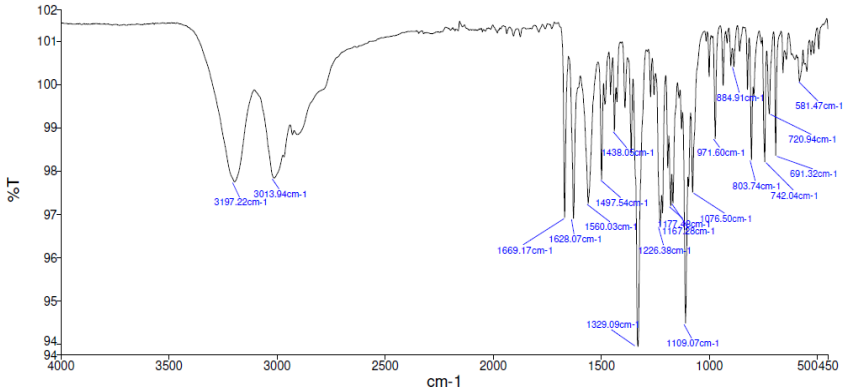
%T
cm-1
3197.22cm-1
3013.94cm-1
1669.17cm-1
1628.07cm-1
1560.03cm-1
1497.54cm-1
1438.05cm-1
1329.09cm-1
1226.38cm-1
1167.28cm-1
1109.07cm-1
1076.50cm-1
971.60cm-1
884.91cm-1
803.74cm-1
742.04cm-1
691.32cm-1
720.94cm-1
581.47cm-1

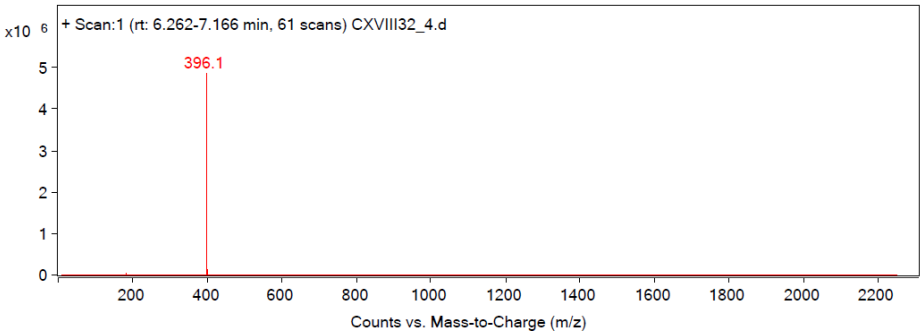
x10 6
+ Scan:1 (rt: 6.262-7.166 min, 61 scans) CXVIII32_4.d
396.1
Counts vs. Mass-to-Charge (m/z)

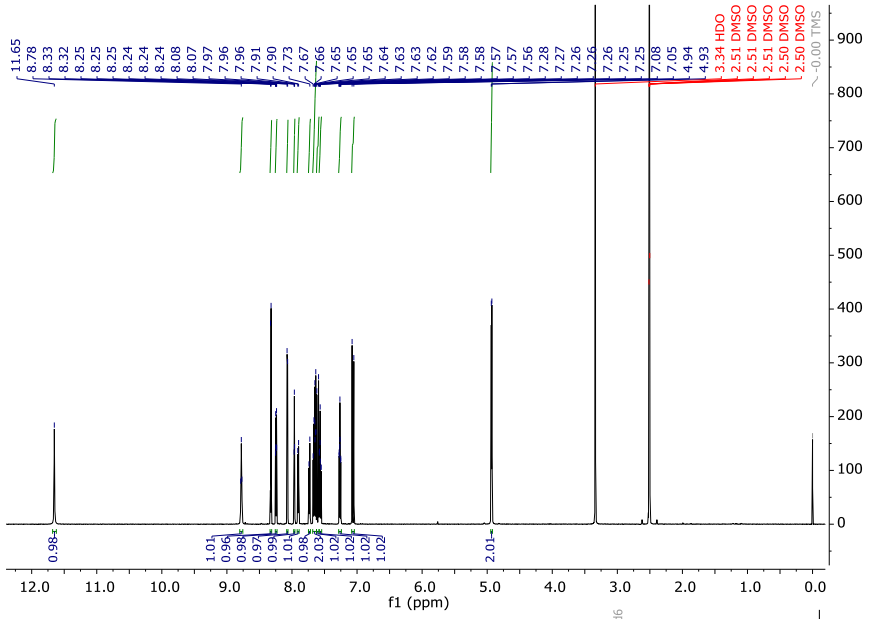
f1 (ppm)
0.98
1.01
0.96
0.98
0.97
0.99
1.01
0.98
2.03
1.02
1.02
1.02
2.01

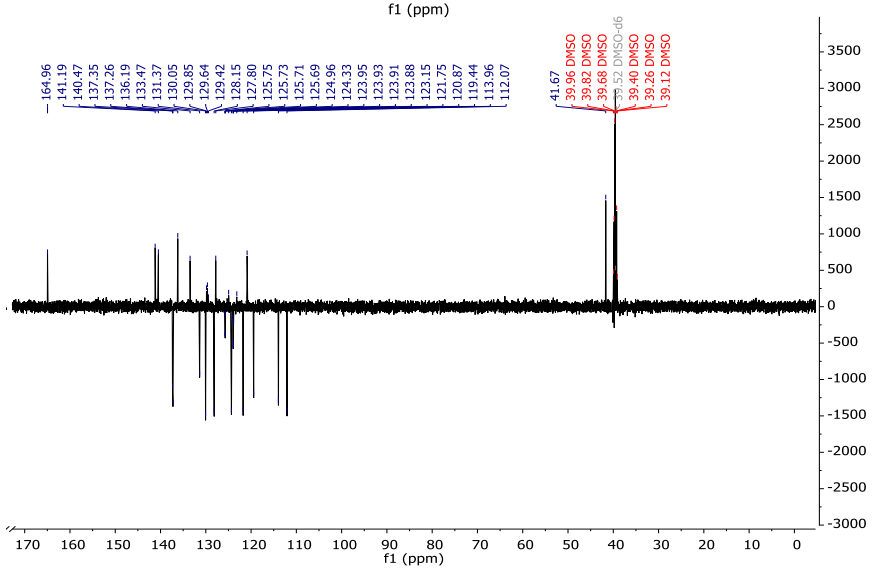
f1 (ppm)
41.67
39.96 DMSO
39.82 DMSO
39.68 DMSO
39.52 DMSO-d6
39.40 DMSO
39.26 DMSO
39.12 DMSO

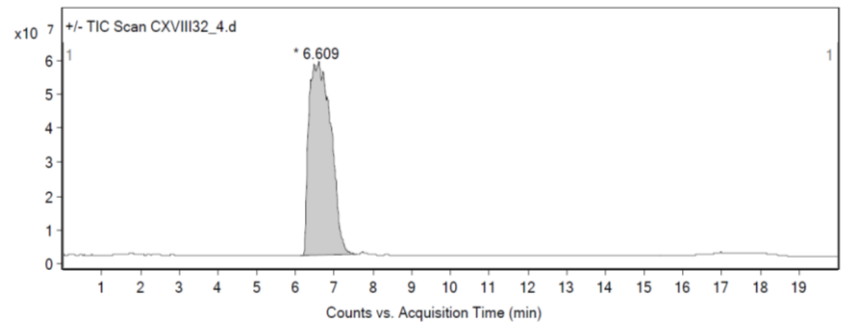

Integration Peak List

Peak	Start	RT	End	Height	Area	Area %
1	6.126	6.609	7.573	56905325.33	2247474068.37	100

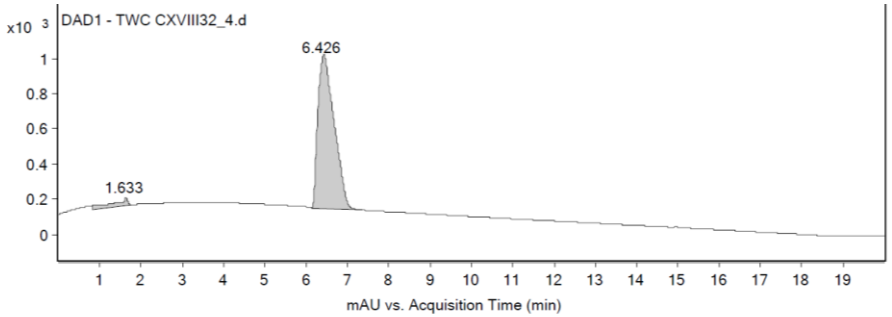

Integration Peak List

Peak	Start	RT	End	Height	Area	Area %
1	0.82	1.633	1.766	45.6	1347.08	5.59
2	6.133	6.426	7.346	878.2	24099.94	100

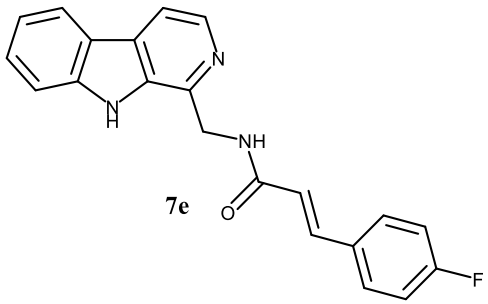
N
H
NH
O
F

7e

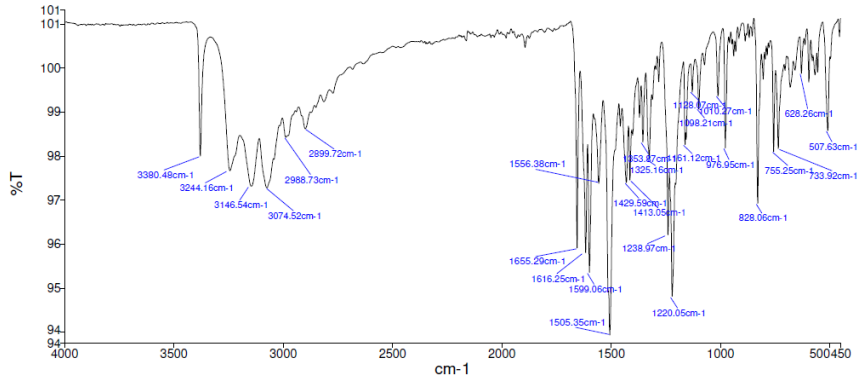
%T
cm-1
3380.48cm-1
3244.16cm-1
3146.54cm-1
3074.52cm-1
2988.73cm-1
2899.72cm-1
1655.29cm-1
1616.25cm-1
1599.06cm-1
1556.38cm-1
1505.35cm-1
1429.59cm-1
1413.05cm-1
1325.16cm-1
1238.97cm-1
1220.05cm-1
1098.21cm-1
976.95cm-1
828.06cm-1
755.25cm-1
733.92cm-1
628.26cm-1
507.63cm-1

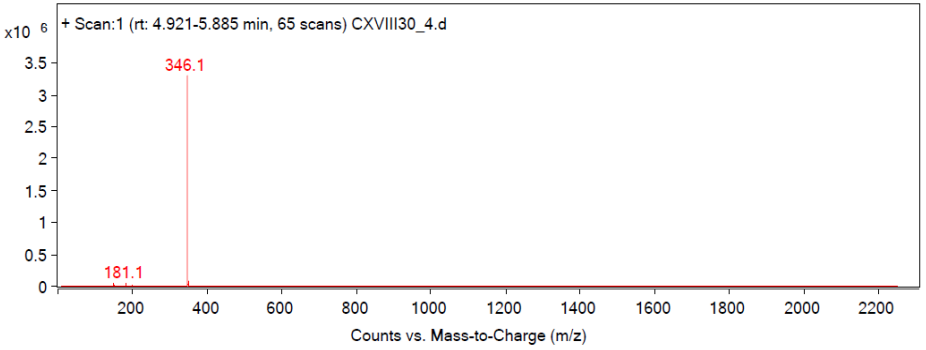
+ Scan:1 (rt: 4.921-5.885 min, 65 scans) CXVIII30_4.d
x10 6
346.1
181.1
Counts vs. Mass-to-Charge (m/z)

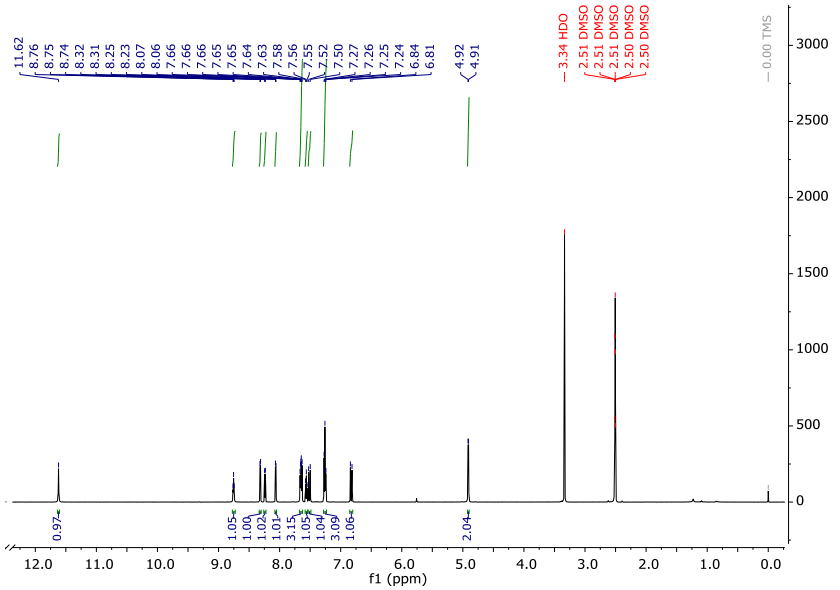
11.62
8.76
8.75
8.74
8.32
8.31
8.25
8.23
8.07
8.06
7.66
7.66
7.66
7.65
7.65
7.64
7.63
7.58
7.56
7.55
7.52
7.50
7.27
7.26
7.25
7.24
6.84
6.81
4.92
4.91
3.34 HDO
2.51 DMSO
2.51 DMSO
2.51 DMSO
2.50 DMSO
2.50 DMSO
0.00 TMS
0.97
1.05
1.00
1.02
1.01
3.15
1.05
1.04
3.09
1.06
2.04
f1 (ppm)

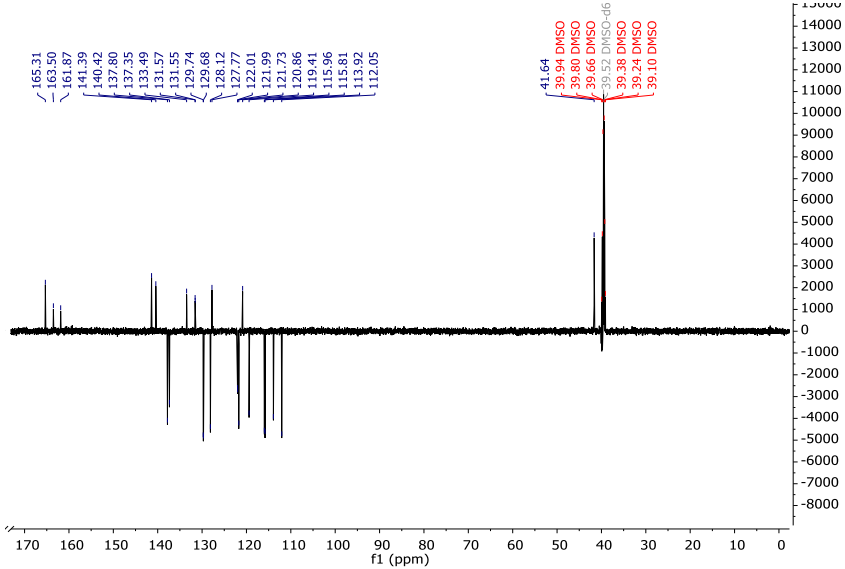
165.31
163.50
161.87
141.39
140.42
137.80
137.35
133.49
131.57
131.55
129.74
129.68
128.12
127.77
122.01
121.99
121.73
120.86
119.41
115.96
115.81
113.92
112.05
41.64
39.94 DMSO
39.80 DMSO
39.66 DMSO
39.52 DMSO-d6
39.38 DMSO
39.24 DMSO
39.10 DMSO
f1 (ppm)

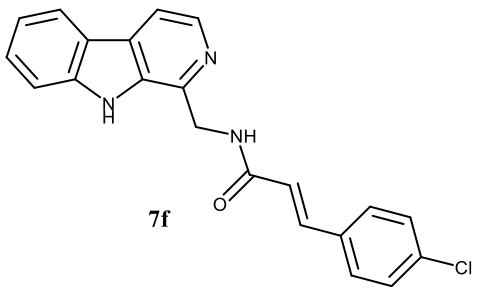
N
H
NH
O
Cl

7f

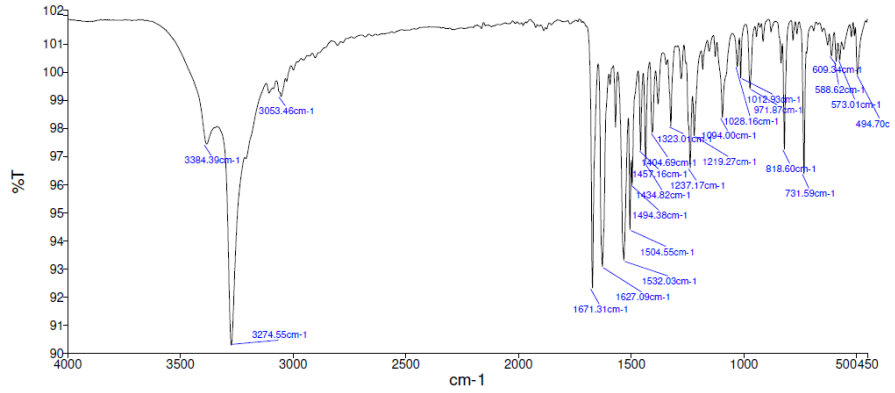
%T
cm-1
3384.39cm-1
3053.46cm-1
3274.55cm-1
1671.31cm-1
1627.09cm-1
1532.03cm-1
1504.55cm-1
1494.38cm-1
1457.16cm-1
1434.82cm-1
1404.69cm-1
1323.01cm-1
1237.17cm-1
1219.27cm-1
1028.16cm-1
994.00cm-1
971.87cm-1
818.60cm-1
731.59cm-1
609.34cm-1
588.62cm-1
573.01cm-1
494.70c

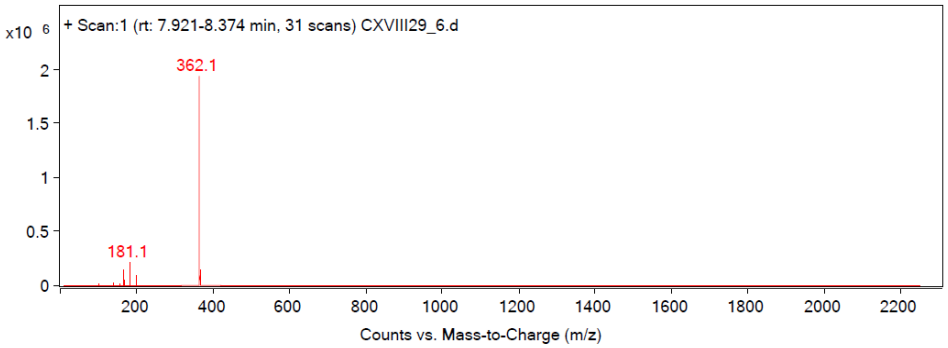
x10 6
+ Scan:1 (rt: 7.921-8.374 min, 31 scans) CXVIII29_6.d
362.1
181.1
Counts vs. Mass-to-Charge (m/z)

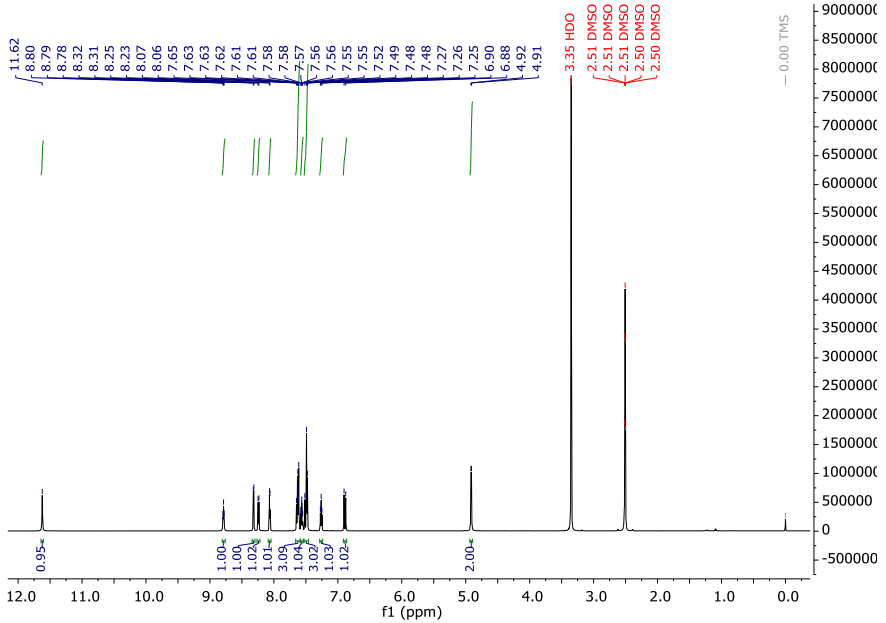
11.62
8.80
8.79
8.78
8.32
8.31
8.25
8.23
8.07
8.06
7.65
7.63
7.63
7.62
7.61
7.61
7.58
7.58
7.57
7.56
7.56
7.55
7.55
7.52
7.49
7.48
7.48
7.27
7.26
7.25
6.90
6.88
4.92
4.91
3.35 HDO
2.51 DMSO
2.51 DMSO
2.51 DMSO
2.50 DMSO
2.50 DMSO
0.00 TMS
0.95
1.00
1.00
1.02
1.01
3.09
1.04
3.02
1.03
1.02
2.00
f1 (ppm)

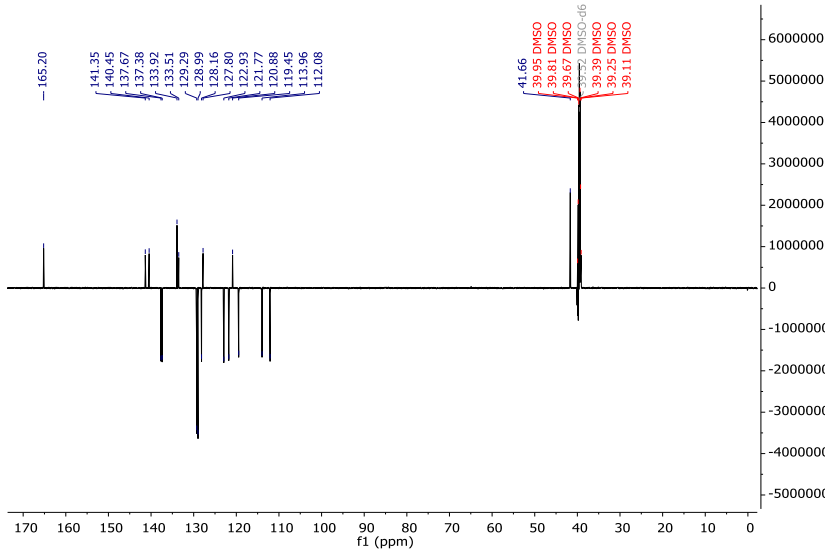
165.20
141.35
140.45
137.67
137.38
133.92
133.51
129.29
128.99
128.16
127.80
122.93
121.77
120.88
119.45
113.96
112.08
41.66
39.95 DMSO
39.81 DMSO
39.67 DMSO
39.53 DMSO-d6
39.39 DMSO
39.25 DMSO
39.11 DMSO
f1 (ppm)

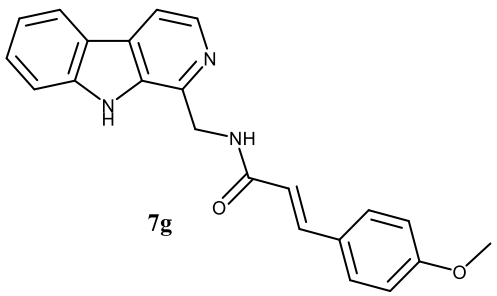
N
H
NH
O
O

7g

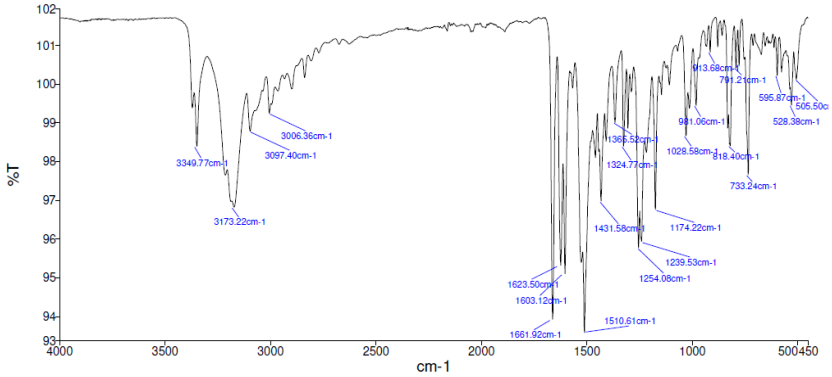
%T
cm-1
3349.77cm-1
3173.22cm-1
3097.40cm-1
3006.36cm-1
1623.50cm-1
1603.12cm-1
1661.92cm-1
1510.61cm-1
1431.58cm-1
1324.77cm-1
1254.08cm-1
1239.53cm-1
1174.22cm-1
1028.58cm-1
981.06cm-1
818.40cm-1
791.21cm-1
733.24cm-1
595.87cm-1
528.38cm-1

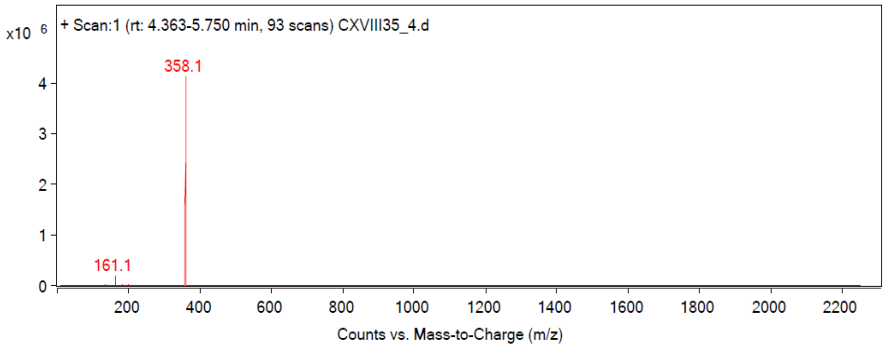
x10 6
+ Scan:1 (rt: 4.363-5.750 min, 93 scans) CXVIII35_4.d
358.1
161.1
Counts vs. Mass-to-Charge (m/z)

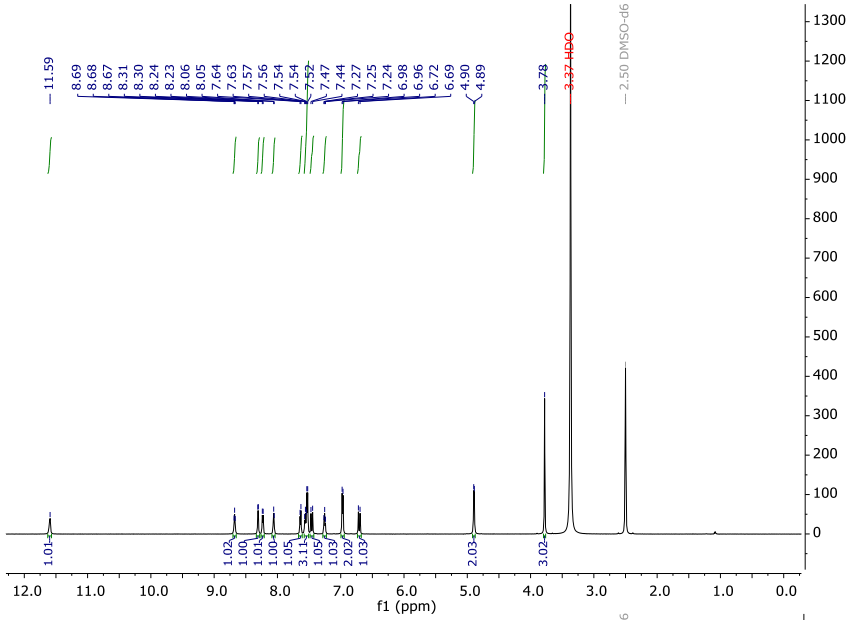
11.59
8.69
8.68
8.67
8.31
8.30
8.24
8.23
8.06
8.05
7.64
7.63
7.57
7.56
7.54
7.54
7.52
7.47
7.44
7.27
7.25
7.24
6.98
6.96
6.72
6.69
4.90
4.89
3.78
3.37 HDO
2.50 DMSO-d6
f1 (ppm)

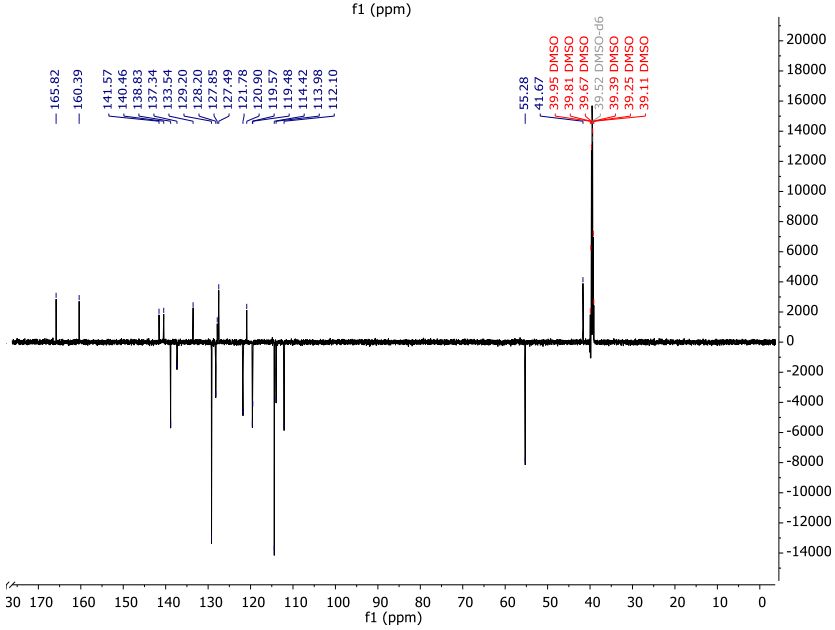
165.82
160.39
141.57
140.46
138.83
137.34
133.54
129.20
128.20
127.85
127.49
121.78
120.90
119.57
119.48
114.42
113.98
112.10
55.28
41.67
39.95 DMSO
39.81 DMSO
39.67 DMSO
39.52 DMSO-d6
39.39 DMSO
39.25 DMSO
39.11 DMSO
f1 (ppm)

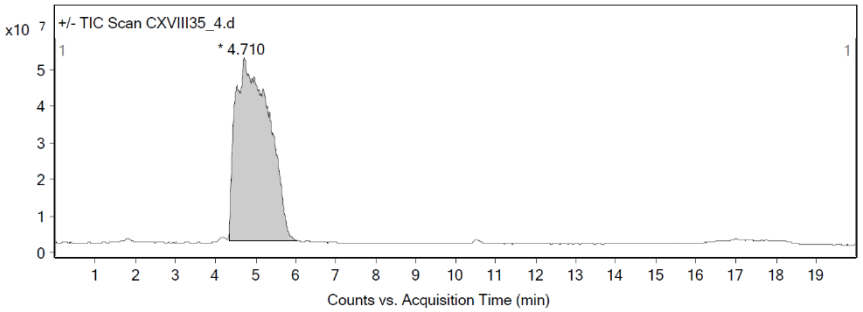

Integration Peak List

Peak	Start	RT	End	Height	Area	Area %
1	4.333	4.71	6.021	50136127.72	2913809484.99	100

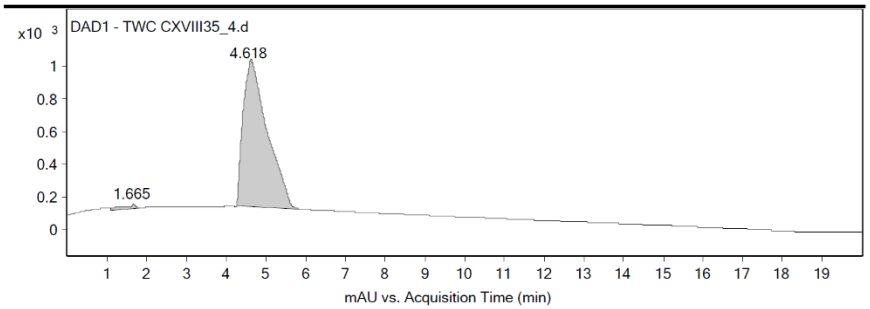

Integration Peak List

Peak	Start	RT	End	Height	Area	Area %
1	1.071	1.665	1.798	31.8	743.41	1.97
2	4.246	4.618	5.845	897.89	37801.61	100

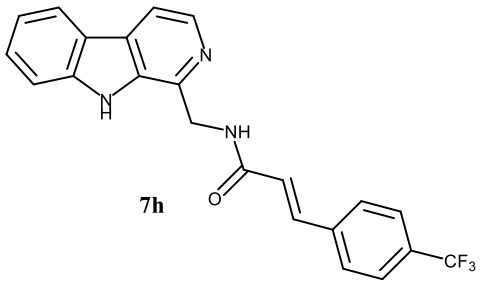
7h
N
H
NH
O
CF3

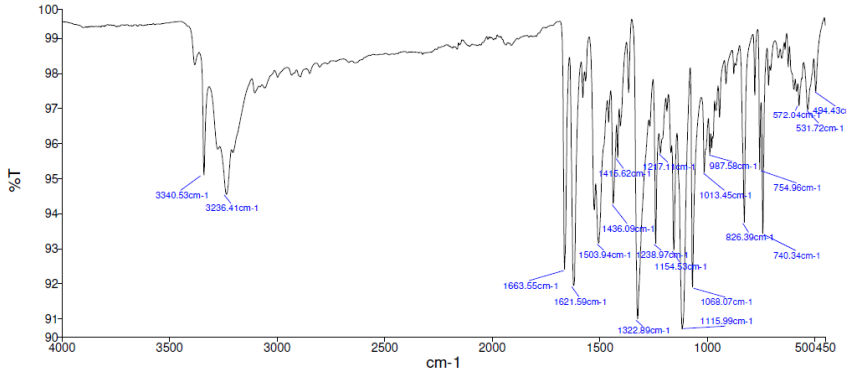
%T
cm-1
3340.53cm-1
3236.41cm-1
1663.55cm-1
1621.59cm-1
1503.94cm-1
1436.09cm-1
1322.89cm-1
1154.53cm-1
1068.07cm-1
1013.45cm-1
987.58cm-1
826.39cm-1
754.96cm-1
740.34cm-1
572.04cm-1
531.72cm-1

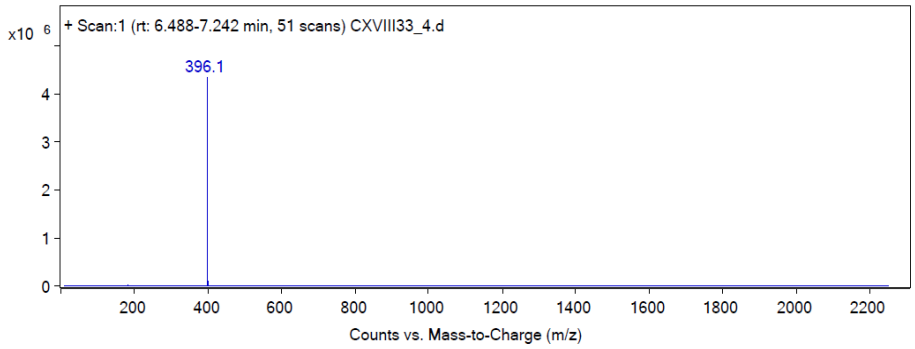
x10
+ Scan:1 (rt: 6.488-7.242 min, 51 scans) CXVIII33_4.d
396.1
Counts vs. Mass-to-Charge (m/z)

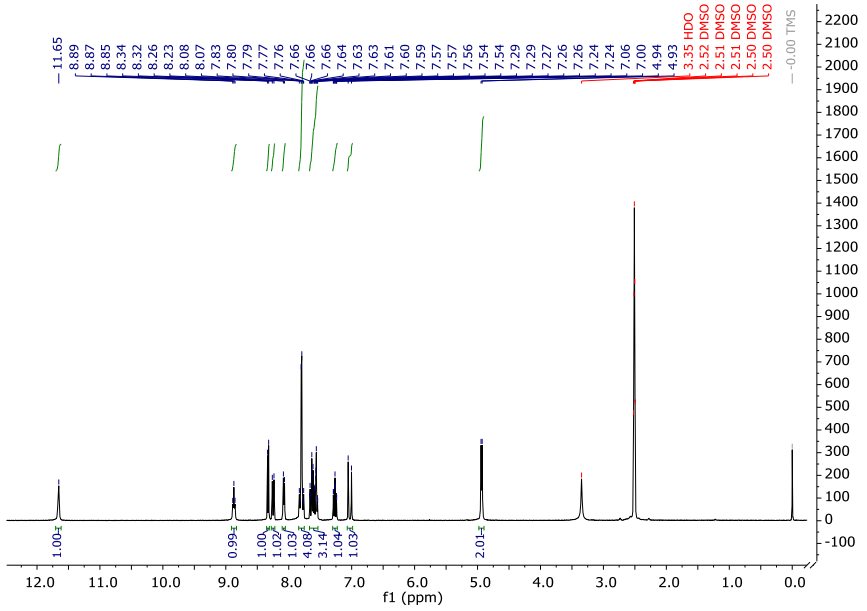
11.65
8.89
8.87
8.85
8.34
8.32
8.26
8.23
8.08
8.07
7.83
7.80
7.79
7.77
7.76
7.66
7.66
7.64
7.63
7.61
7.60
7.59
7.57
7.57
7.56
7.54
7.54
7.29
7.29
7.27
7.26
7.26
7.24
7.24
7.06
7.00
4.94
4.93
3.35 HDO
2.52 DMSO
2.51 DMSO
2.51 DMSO
2.50 DMSO
2.50 DMSO
-0.00 TMS
1.00
0.99
1.00
1.02
1.02
4.08
3.14
1.04
1.03
2.01
f1 (ppm)

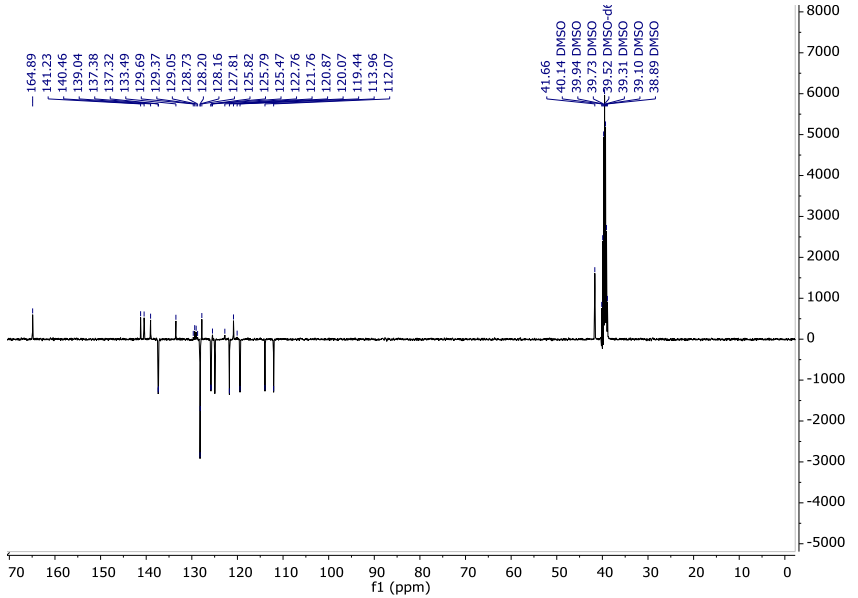
164.89
141.23
140.46
139.04
137.38
137.32
133.49
129.69
129.37
129.05
128.73
128.20
128.16
127.81
125.82
125.79
125.47
122.76
121.76
120.87
120.07
119.44
113.96
112.07
41.66
40.14 DMSO
39.94 DMSO
39.73 DMSO
39.52 DMSO-d6
39.31 DMSO
39.10 DMSO
38.89 DMSO
f1 (ppm)

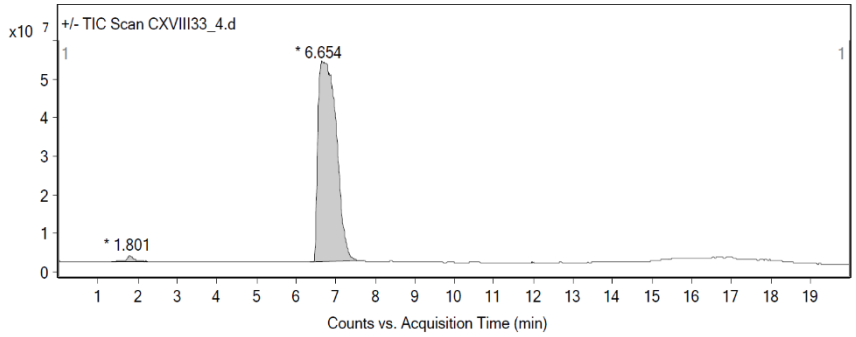

Integration Peak List

Peak	Start	RT	End	Height	Area	Area %
1	1.334	1.801	2.238	1470906.8	19815278.48	1.18
2	6.337	6.654	7.724	52176663.03	1681015500.43	100

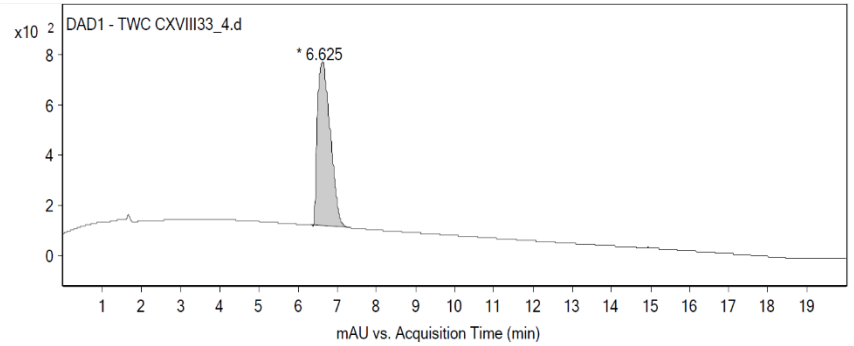

Integration Peak List

Peak	Start	RT	End	Height	Area	Area %
1	6.331	6.625	7.305	654.38	14953.29	100

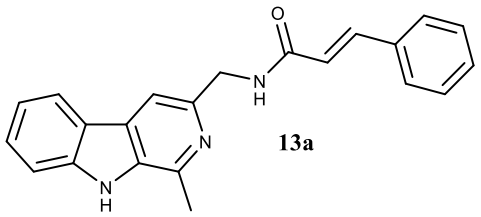

13a

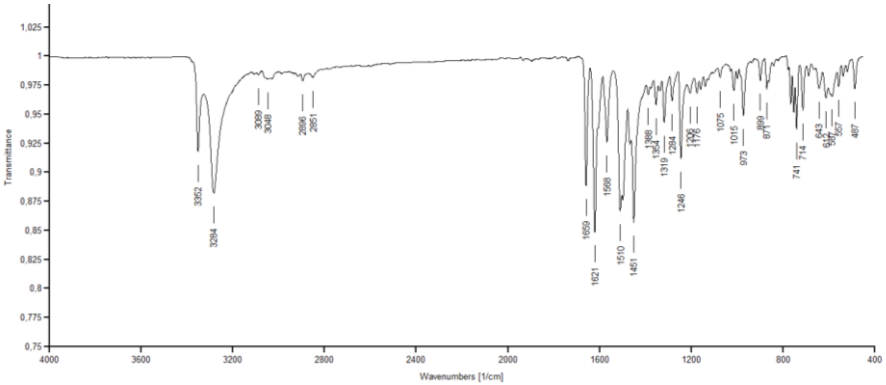
Transmittance
Wavenumbers [1/cm]
3352
3294
3069
3048
2896
2851
1659
1621
1588
1510
1451
1390
1354
1316
1284
1246
1176
1075
1015
973
899
871
741
714
643
557
487

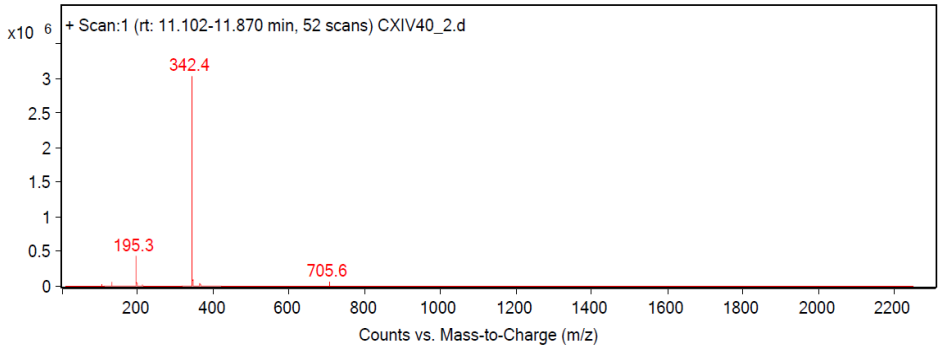
x10 6
+ Scan:1 (rt: 11.102-11.870 min, 52 scans) CXIV40_2.d
342.4
195.3
705.6
Counts vs. Mass-to-Charge (m/z)

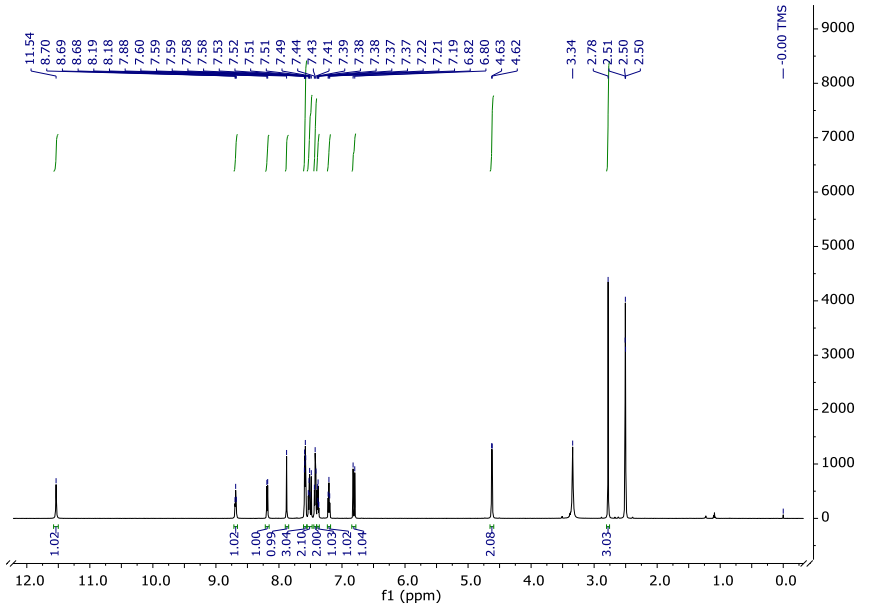
11.54
8.70
8.69
8.68
8.19
8.18
7.88
7.60
7.59
7.59
7.58
7.58
7.53
7.52
7.51
7.51
7.49
7.44
7.43
7.41
7.39
7.38
7.38
7.37
7.37
7.22
7.21
7.19
6.82
6.80
4.63
4.62
3.34
2.78
2.51
2.50
2.50
-0.00 TMS
1.02
1.02
1.00
0.99
3.04
2.10
2.00
1.03
1.02
1.04
2.08
3.03
f1 (ppm)

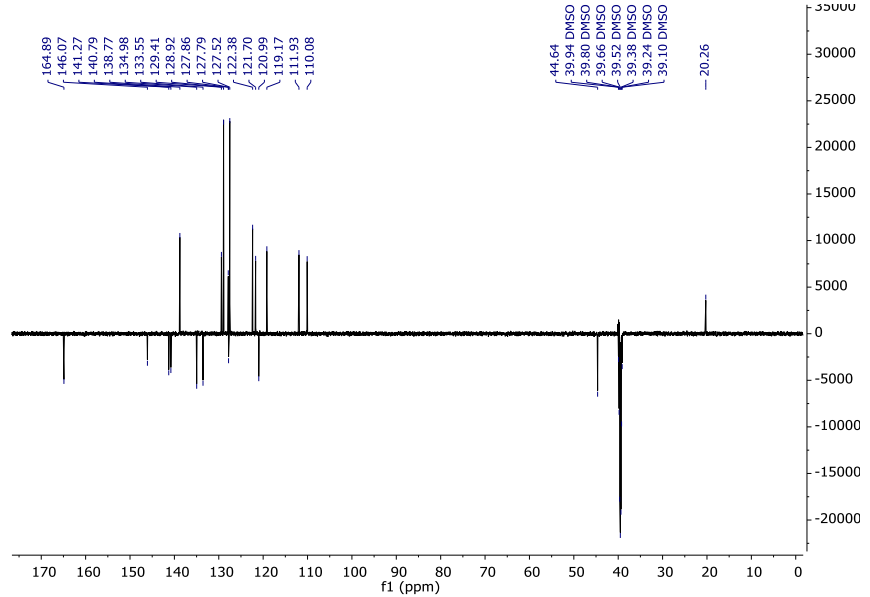
164.89
146.07
141.27
140.79
138.77
134.98
133.55
129.41
128.92
127.86
127.79
127.52
122.38
121.70
120.99
119.17
111.93
110.08
44.64
39.94 DMSO
39.80 DMSO
39.66 DMSO
39.52 DMSO
39.38 DMSO
39.24 DMSO
39.10 DMSO
20.26
f1 (ppm)

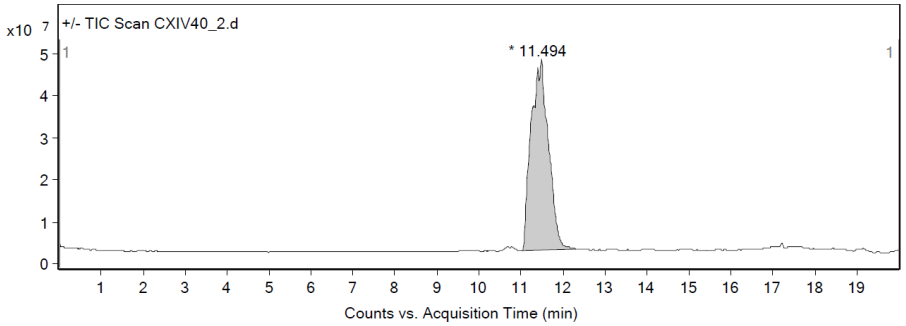

Integration Peak List

Peak	Start	RT	End	Height	Area	Area %
1	11.011	11.494	12.307	45591767.76	1304660971.89	100

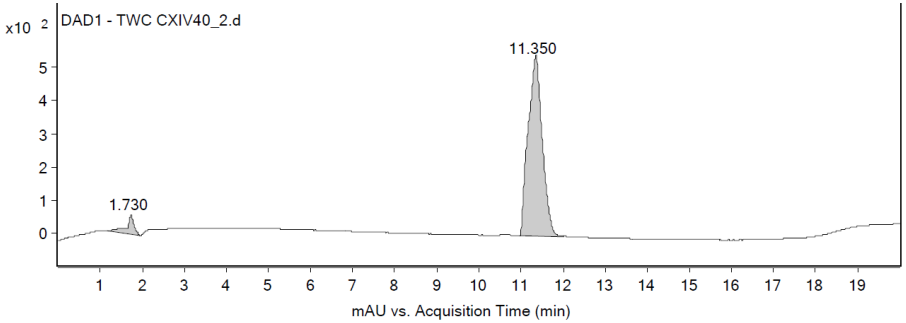

Integration Peak List

Peak	Start	RT	End	Height	Area	Area %
1	1.172	1.73	1.942	59.13	767.93	6.05
2	10.97	11.35	12.004	545.2	12701.28	100

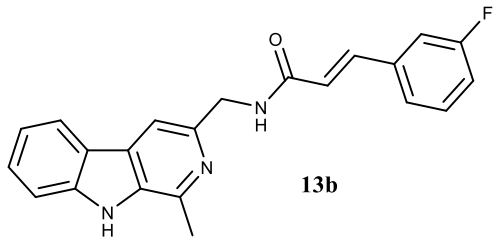
F
O
N
H
N
N
H

13b

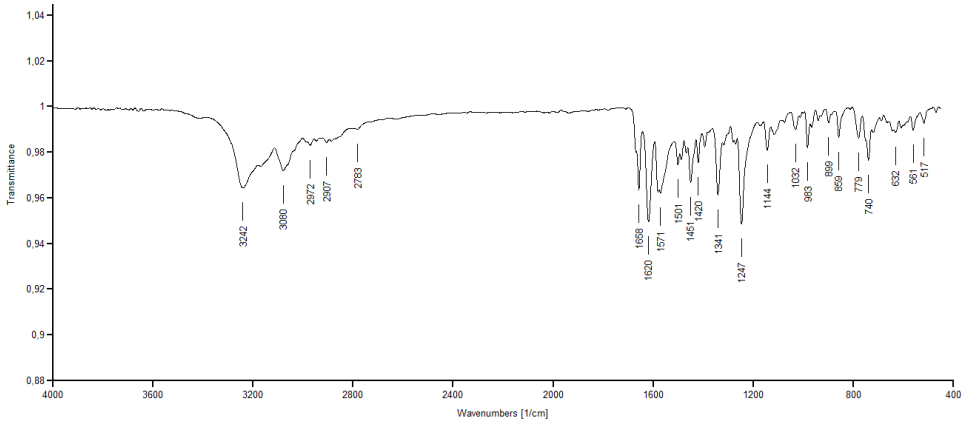
Transmittance
Wavenumbers [1/cm]
3242
3080
2972
2907
2783
1658
1620
1571
1501
1451
1420
1341
1247
1144
1032
983
899
859
779
740
632
561
517

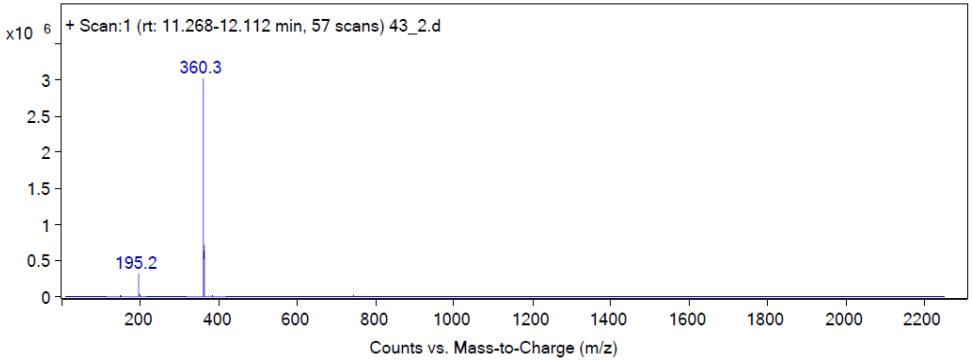
x10 6
+ Scan:1 (rt: 11.268-12.112 min, 57 scans) 43_2.d
360.3
195.2
Counts vs. Mass-to-Charge (m/z)

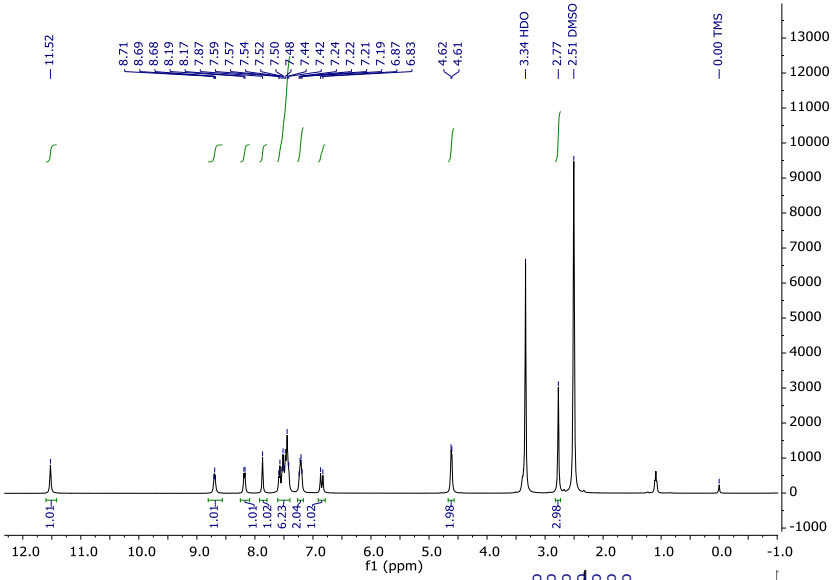
11.52
8.71
8.69
8.68
8.19
8.17
7.87
7.59
7.57
7.54
7.52
7.50
7.48
7.44
7.42
7.24
7.22
7.21
7.19
6.87
6.83
4.62
4.61
3.34 HDO
2.77
2.51 DMSO
0.00 TMS
f1 (ppm)

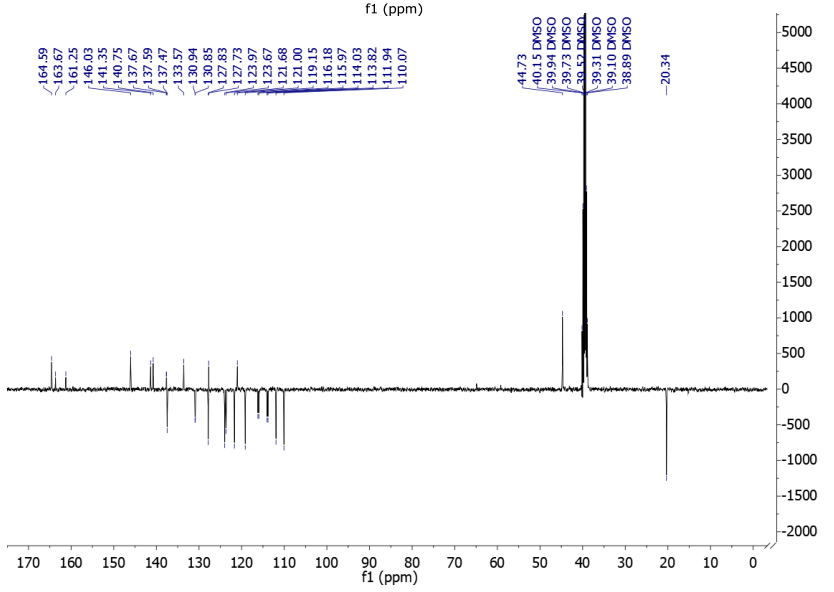
164.59
163.67
161.25
146.03
141.35
140.75
137.67
137.59
137.47
133.57
130.94
130.85
127.83
127.73
123.97
123.67
121.68
121.00
119.15
116.18
115.97
114.03
113.82
111.94
110.07
44.73
40.15 DMSO
39.94 DMSO
39.73 DMSO
39.52 DMSO
39.31 DMSO
39.10 DMSO
38.89 DMSO
20.34
f1 (ppm)

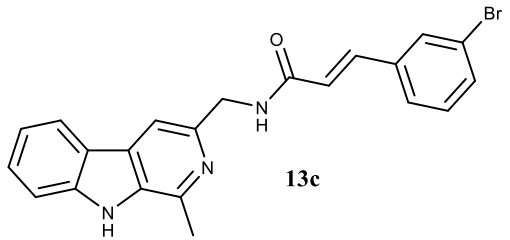
Br
O
N
H
N
N
H

13c

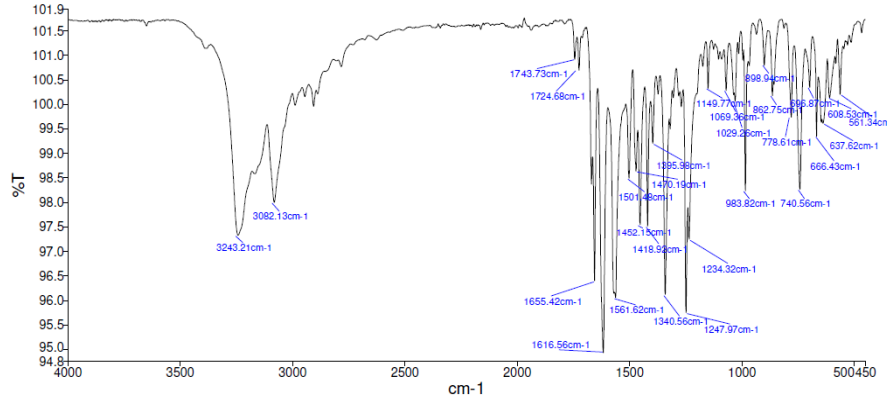
%T
cm-1
3243.21cm-1
3082.13cm-1
1743.73cm-1
1724.68cm-1
1655.42cm-1
1616.56cm-1
1561.62cm-1
1452.15cm-1
1418.93cm-1
1340.56cm-1
1247.97cm-1
1234.32cm-1
1501.48cm-1
1470.19cm-1
1395.38cm-1
1149.77cm-1
1069.36cm-1
1029.26cm-1
983.82cm-1
898.94cm-1
862.75cm-1
778.61cm-1
740.56cm-1
666.43cm-1
637.62cm-1
608.59cm-1

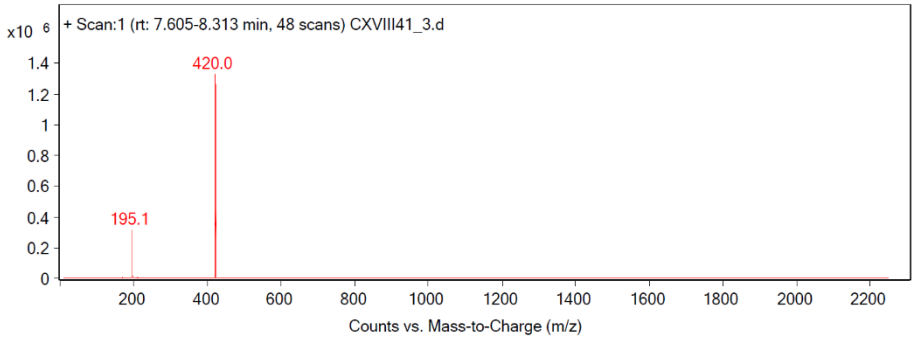
x10 6
+ Scan:1 (rt: 7.605-8.313 min, 48 scans) CXVIII41_3.d
420.0
195.1
Counts vs. Mass-to-Charge (m/z)

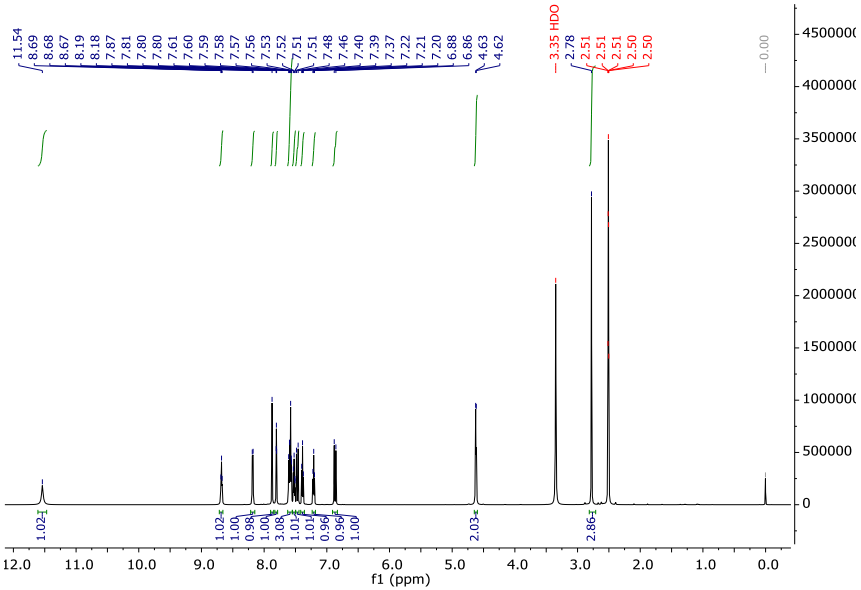
3.35 HDO
f1 (ppm)

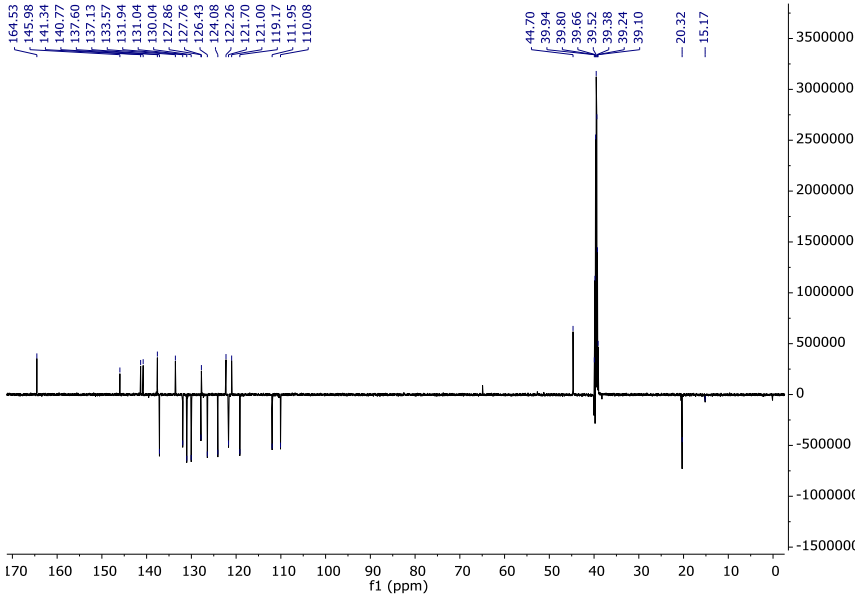
f1 (ppm)

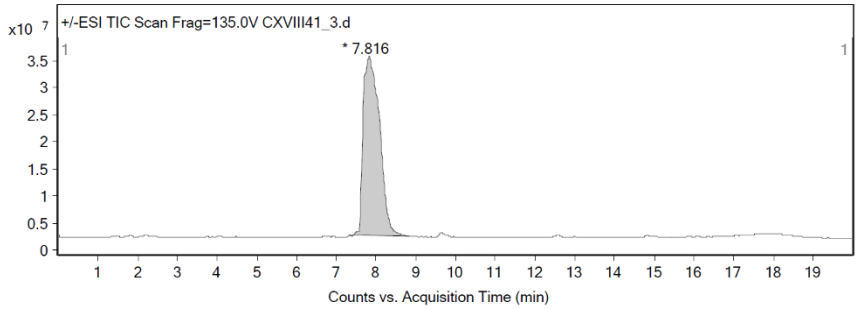

Integration Peak List

Peak	Start	RT	End	Height	Area	Area %
1	7.318	7.816	8.841	33134438.15	955981259.09	100

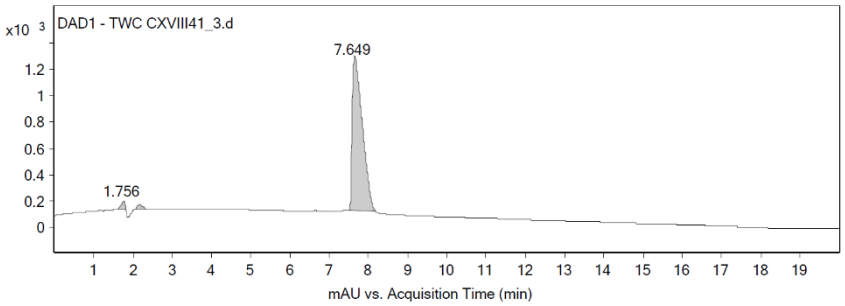

Integration Peak List

Peak	Start	RT	End	Height	Area	Area %
1	1.609	1.756	1.811	61.78	402.58	1.9
2	2.043	2.143	2.323	34.95	321.43	1.52
3	7.508	7.649	8.183	1172.85	21173.21	100

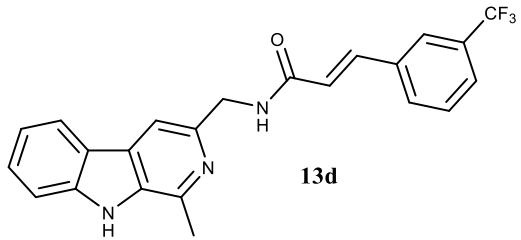
CF3
O
N
H
N
N
H

13d

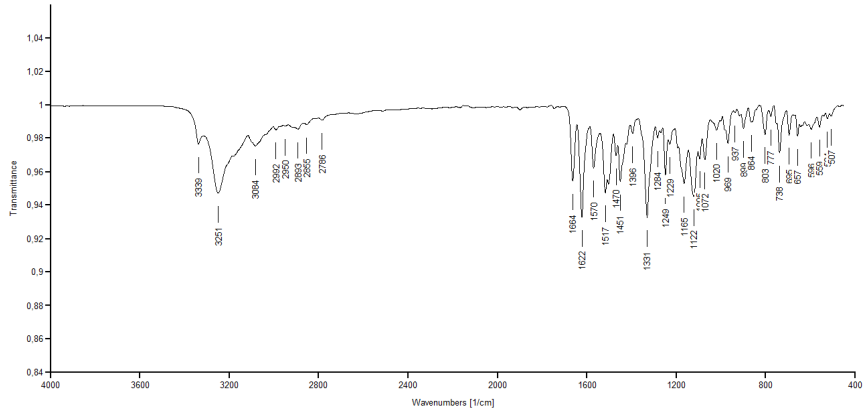
Transmittance
Wavenumbers [1/cm]
3339
3251
3084
2992
2950
2895
2786
1664
1622
1570
1517
1470
1451
1396
1331
1284
1249
1229
1165
1122
1072
1020
969
937
899
864
803
777
738
697
657
596
564
507

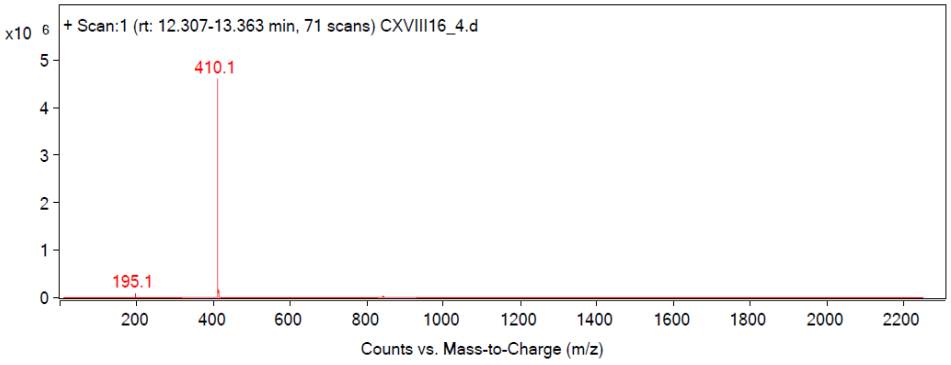
x10 6
+ Scan:1 (rt: 12.307-13.363 min, 71 scans) CXVIII16_4.d
410.1
195.1
Counts vs. Mass-to-Charge (m/z)

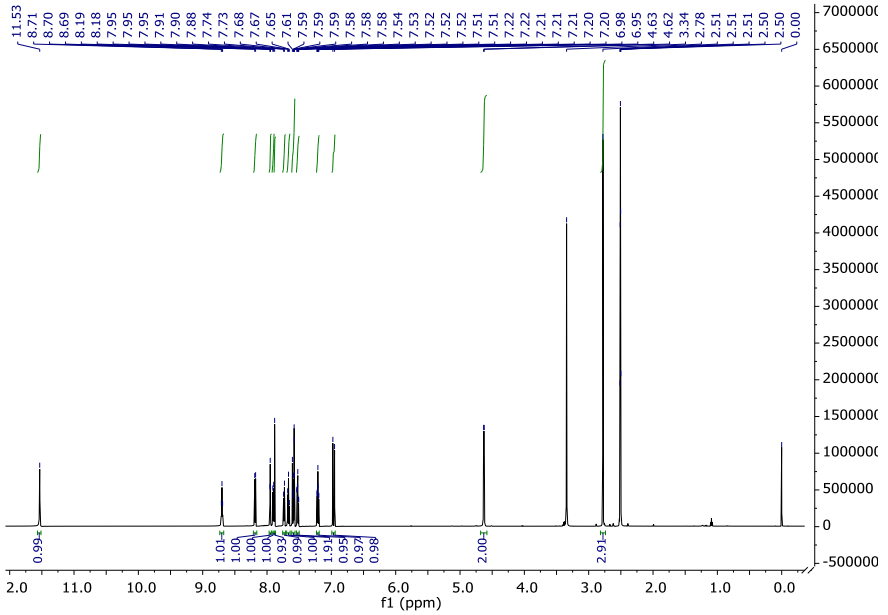
11.53
8.71
8.70
8.69
8.19
8.18
7.95
7.95
7.95
7.91
7.90
7.88
7.74
7.73
7.68
7.67
7.65
7.61
7.59
7.59
7.59
7.58
7.58
7.58
7.54
7.53
7.52
7.52
7.52
7.51
7.51
7.22
7.21
7.21
7.21
7.20
7.20
6.98
6.95
4.63
4.62
3.34
2.78
2.51
2.51
2.51
2.50
2.50
2.50
0.00
0.99
1.01
1.00
1.00
1.00
1.00
0.99
0.99
1.00
1.91
0.95
0.97
0.98
2.00
2.91
f1 (ppm)

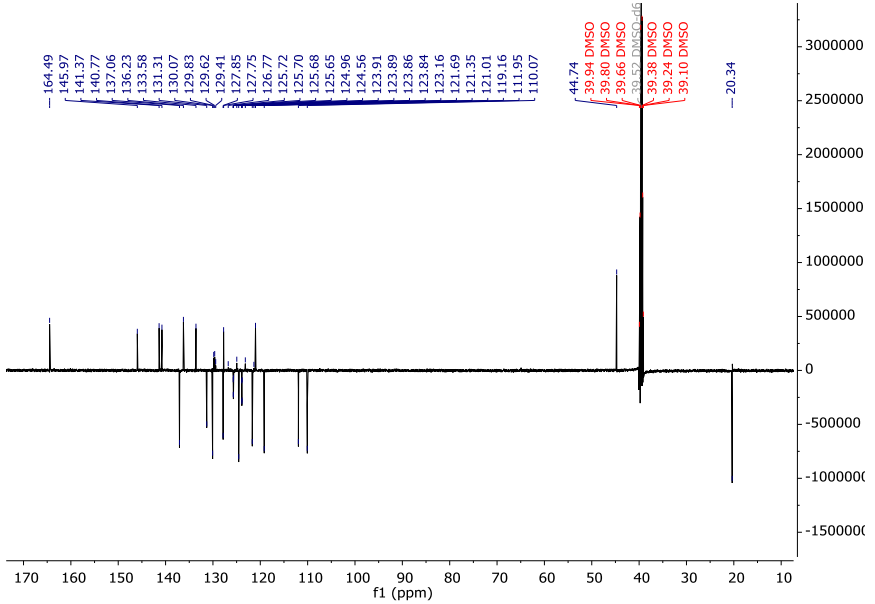
164.49
145.97
141.37
140.77
137.06
136.23
133.58
131.31
130.07
129.83
129.62
129.41
127.85
127.75
126.77
125.72
125.70
125.68
125.65
124.96
124.56
123.91
123.89
123.86
123.84
123.16
121.69
121.35
121.01
119.16
111.95
110.07
44.74
39.94 DMSO
39.80 DMSO
39.66 DMSO
39.52 DMSO
39.38 DMSO
39.24 DMSO
39.10 DMSO
20.34
f1 (ppm)

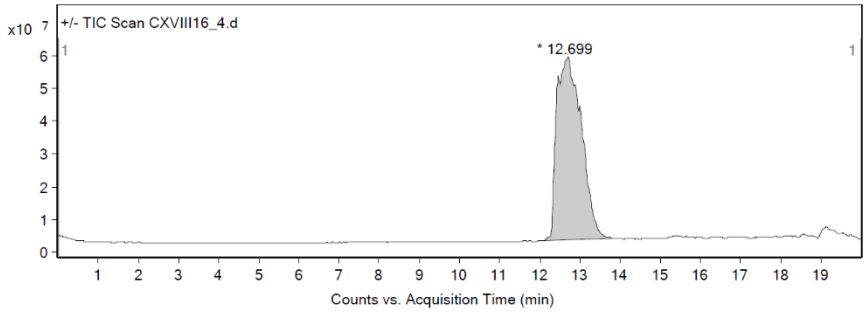

Integration Peak List

Peak	Start	RT	End	Height	Area	Area %
1	12.096	12.699	13.8	55710478.75	2381574826.24	100

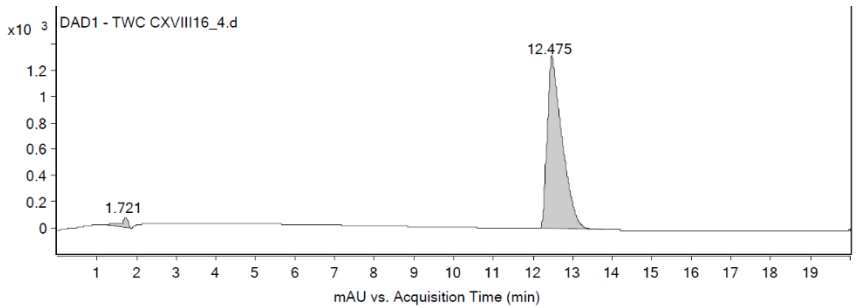

Integration Peak List

Peak	Start	RT	End	Height	Area	Area %
1	1.19	1.721	1.858	81.05	1119.76	3.27
2	12.181	12.475	13.774	1317.81	34232.96	100

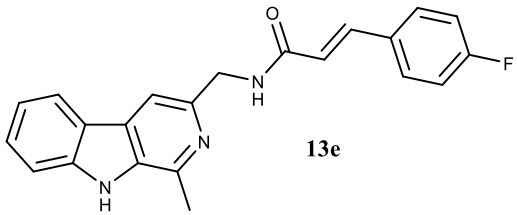
O
N
H
F
N
N
H

13e

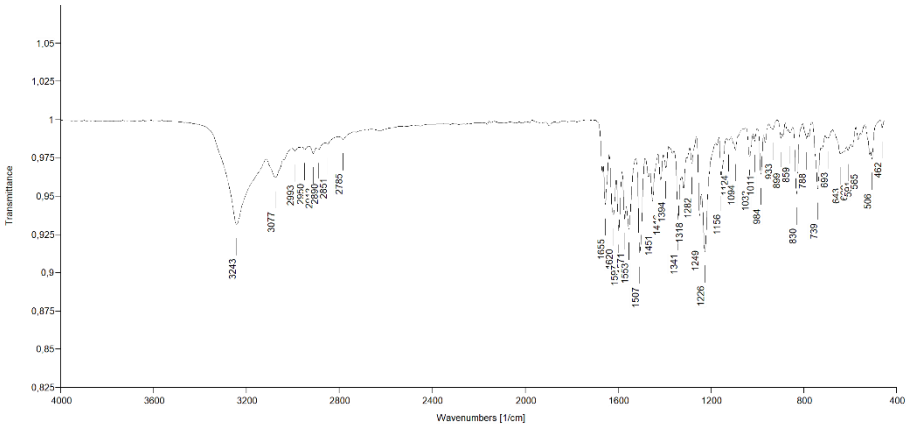
Transmittance
Wavenumbers [1/cm]
3243
3077
2953
2920
2850
2851
2786
1655
1620
1597
1571
1557
1507
1451
1394
1341
1318
1282
1249
1226
1156
1124
1094
1031
1011
984
933
889
859
830
788
739
693
643
597
565
506
462

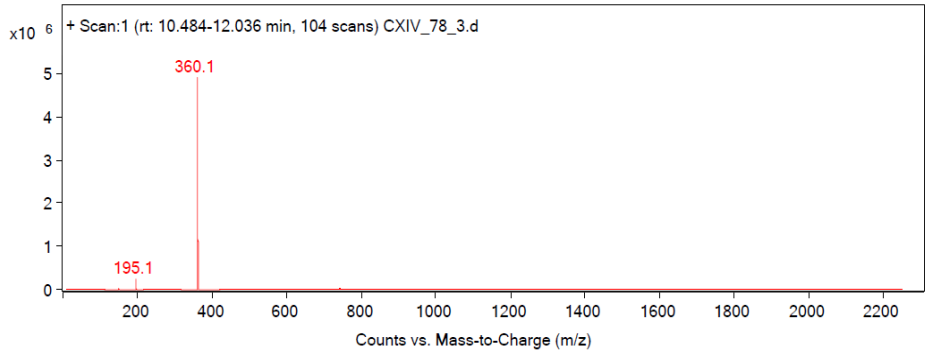
x10
+ Scan:1 (rt: 10.484-12.036 min, 104 scans) CXIV_78_3.d
360.1
195.1
Counts vs. Mass-to-Charge (m/z)

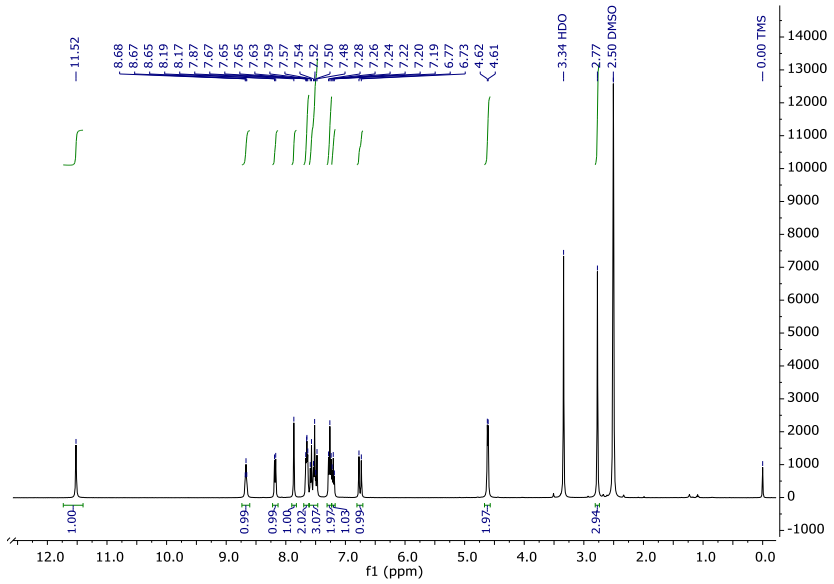
11.52
8.68
8.67
8.65
8.19
8.17
7.87
7.67
7.65
7.63
7.59
7.57
7.54
7.52
7.50
7.48
7.28
7.26
7.24
7.22
7.20
7.19
6.77
6.73
4.62
4.61
3.34 HDO
2.77
2.50 DMSO
0.00 TMS
f1 (ppm)

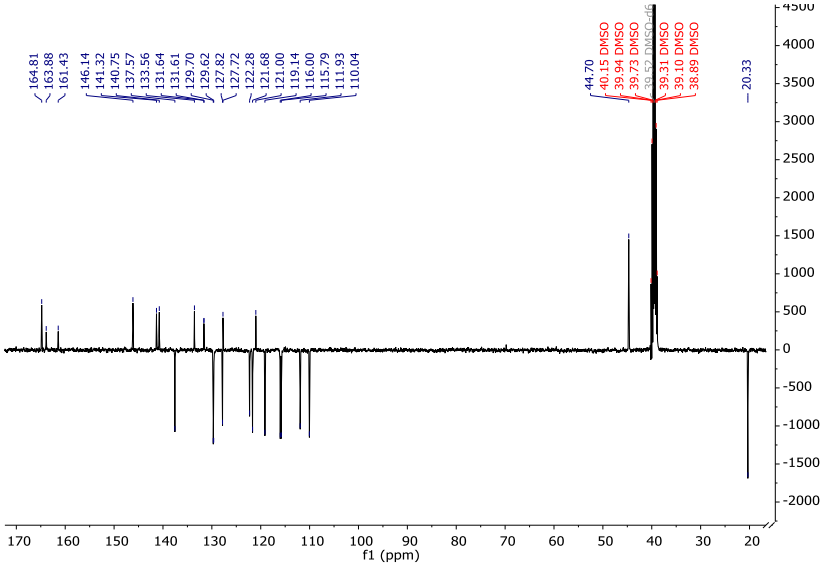
164.81
163.88
161.43
146.14
141.32
140.75
137.57
133.56
131.64
131.61
129.70
129.62
127.82
127.72
122.28
121.68
121.00
119.14
116.00
115.79
111.93
110.04
44.70
40.15 DMSO
39.94 DMSO
39.73 DMSO
39.31 DMSO
39.10 DMSO
38.89 DMSO
20.33
f1 (ppm)

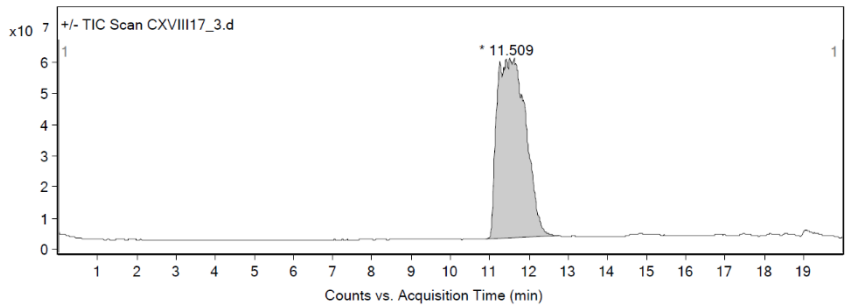

Integration Peak List

Peak	Start	RT	End	Height	Area	Area %
1	10.891	11.509	12.775	57728310.74	2943704055.09	100

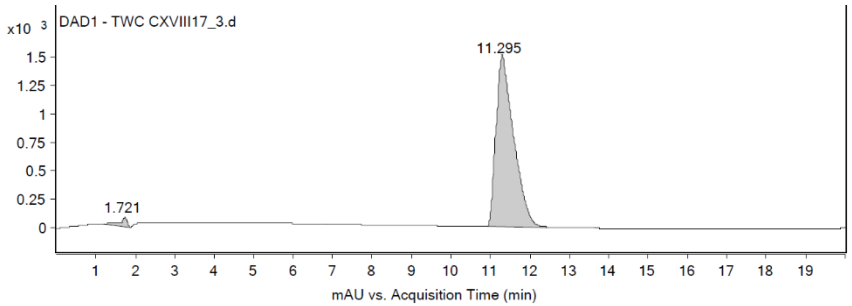

Integration Peak List

Peak	Start	RT	End	Height	Area	Area %
1	1.201	1.721	1.858	78.77	1095.21	2.35
2	10.914	11.295	12.461	1507.45	46652.12	100

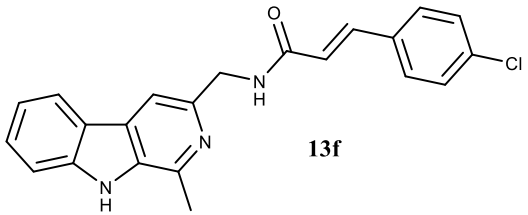
O
N
H
Cl
N
N
H

13f

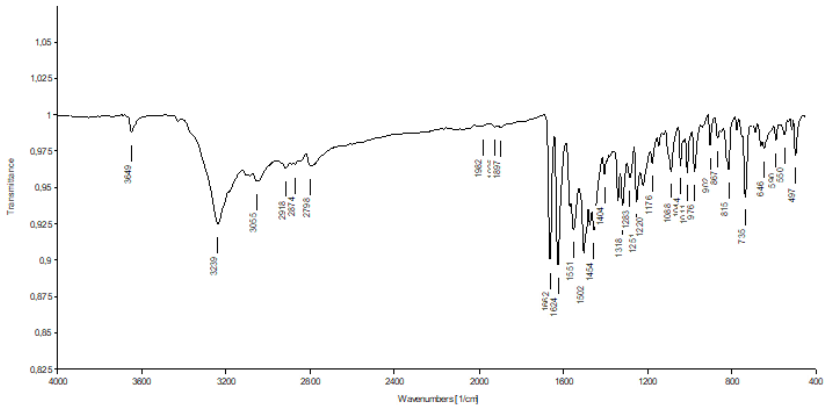
Transmittance
Wavenumbers[1/cm]

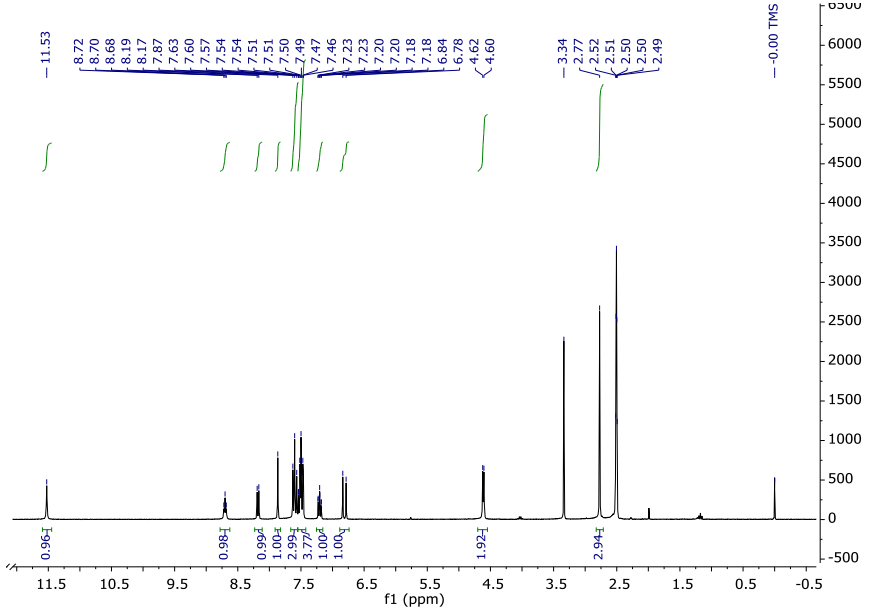
f1 (ppm)

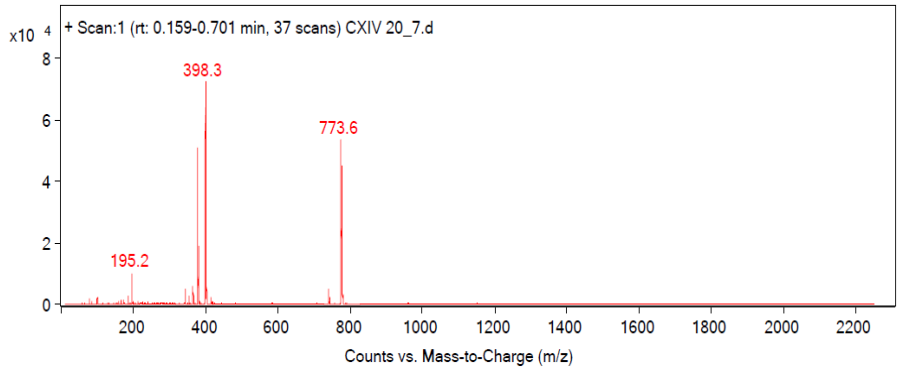
+ Scan:1 (rt: 0.159-0.701 min, 37 scans) CXIV 20_7.d
398.3
773.6
195.2
Counts vs. Mass-to-Charge (m/z)

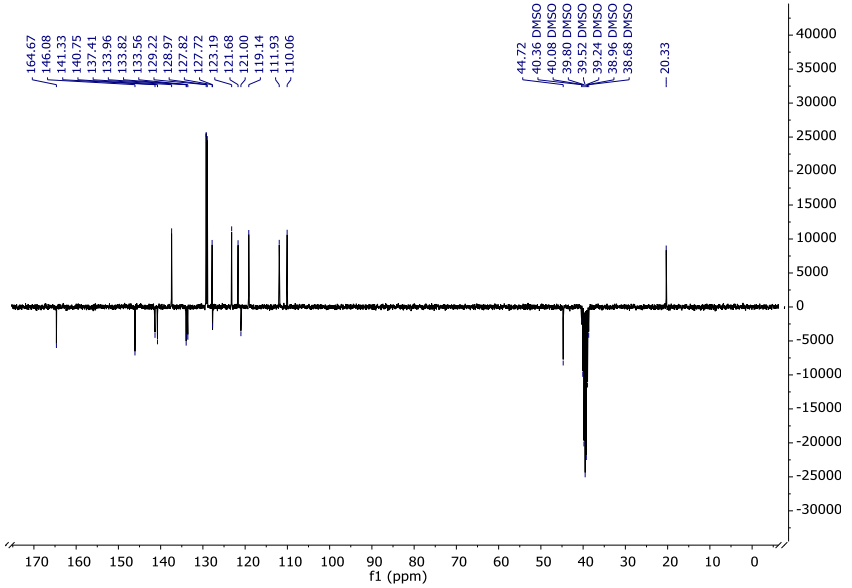
f1 (ppm)

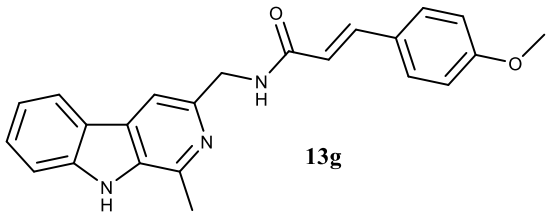

13g

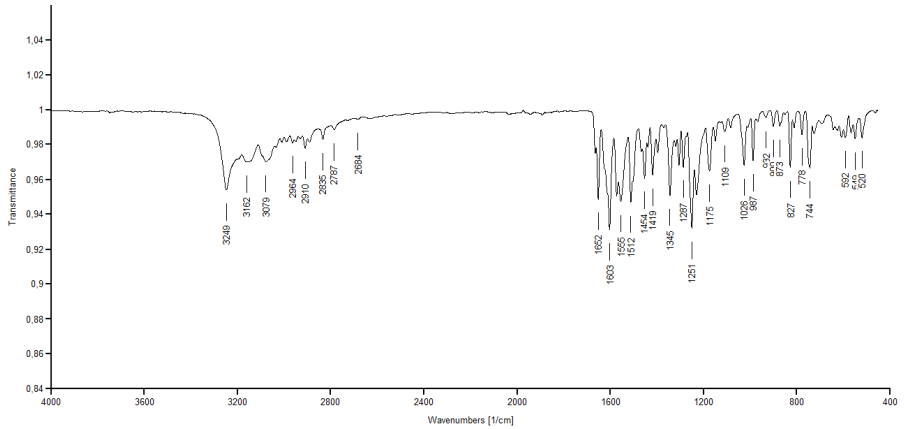
Transmittance
Wavenumbers [1/cm]
3249
3162
3079
2964
2910
2838
2787
2684
1652
1603
1565
1512
1459
1418
1345
1287
1251
1175
1109
1026
967
932
875
827
778
744
592
540
520

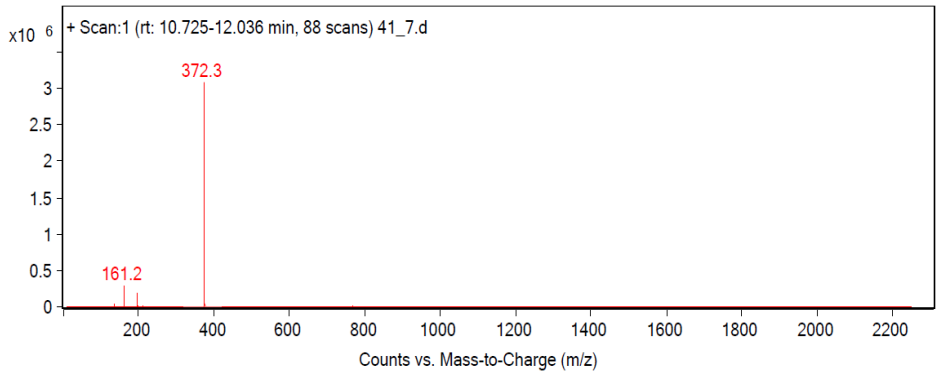
x10 6
+ Scan:1 (rt: 10.725-12.036 min, 88 scans) 41_7.d
372.3
161.2
Counts vs. Mass-to-Charge (m/z)

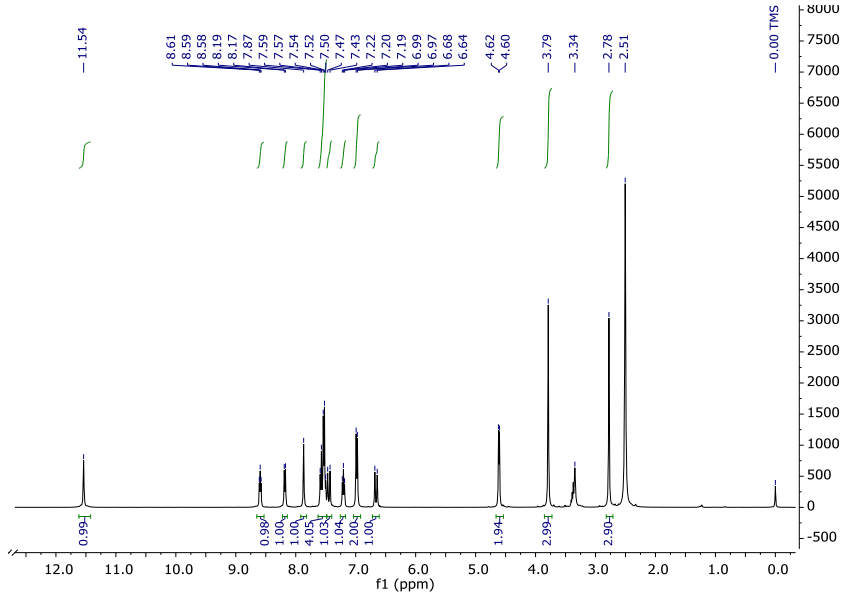
11.54
8.61
8.59
8.58
8.19
8.17
7.87
7.59
7.57
7.54
7.52
7.50
7.47
7.43
7.22
7.20
7.19
6.99
6.97
6.68
6.64
4.62
4.60
3.79
3.34
2.78
2.51
0.00 TMS
0.99
0.98
1.00
1.00
1.00
4.05
1.03
1.04
2.00
1.00
1.94
2.99
2.90
f1 (ppm)

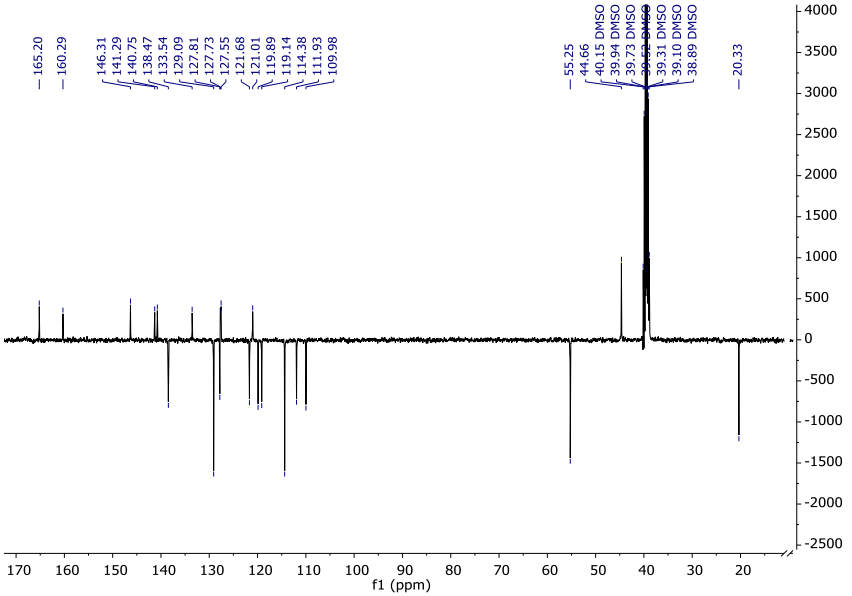
165.20
160.29
146.31
141.29
140.75
138.47
133.54
129.09
127.81
127.73
127.55
121.68
121.01
119.89
119.14
114.38
111.93
109.98
55.25
44.66
40.15 DMSO
39.94 DMSO
39.73 DMSO
39.31 DMSO
39.10 DMSO
38.89 DMSO
20.33
f1 (ppm)

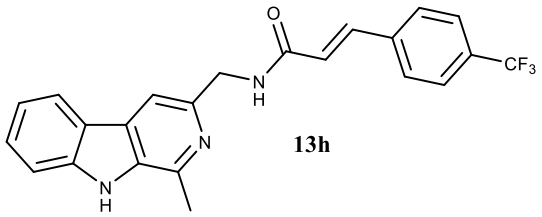
O
N
H
CF3
N
N
H

13h

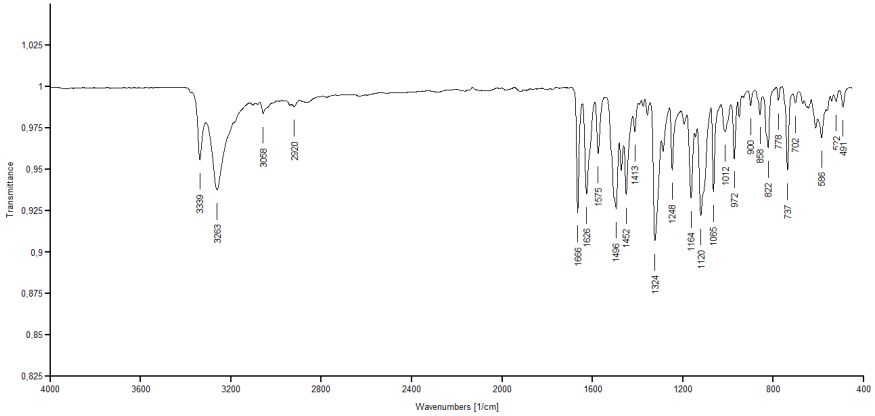
Transmittance
Wavenumbers [1/cm]
3339
3263
3058
2920
1656
1626
1575
1496
1452
1413
1324
1248
1164
1120
1065
1012
972
900
868
822
778
737
702
586
572
491

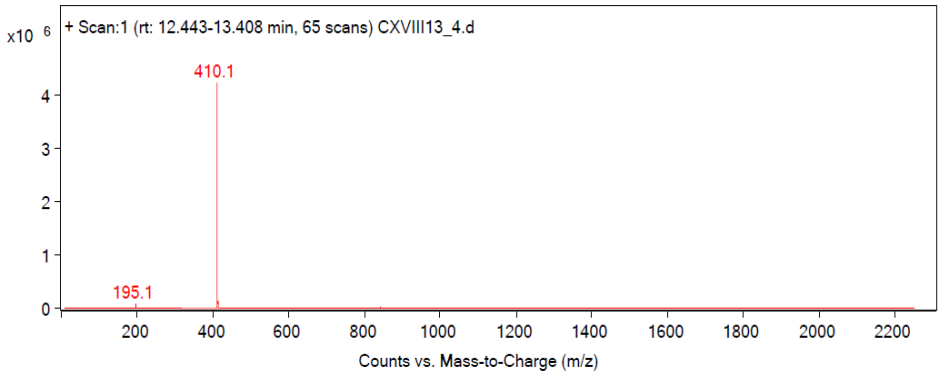
x10 6
+ Scan:1 (rt: 12.443-13.408 min, 65 scans) CXVIII13_4.d
410.1
195.1
Counts vs. Mass-to-Charge (m/z)

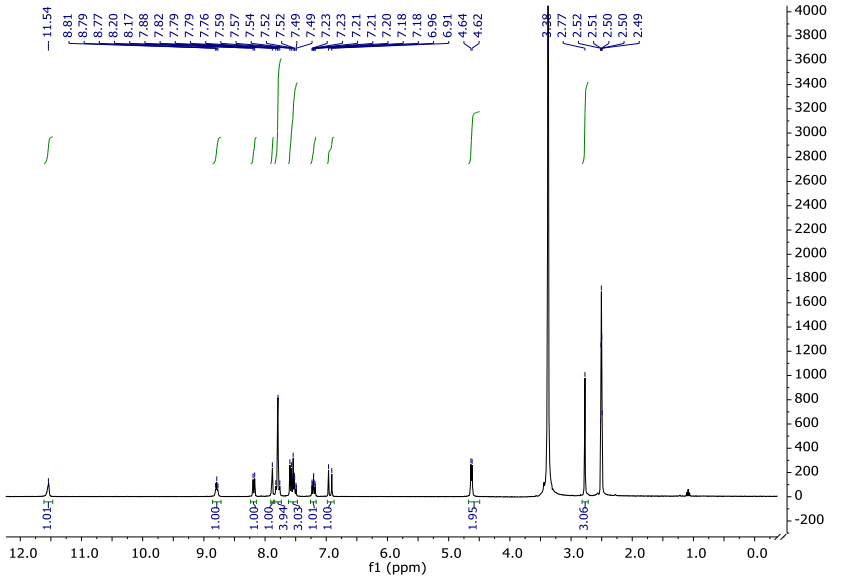
11.54
8.81
8.79
8.77
8.20
8.17
7.88
7.82
7.79
7.79
7.76
7.59
7.57
7.54
7.52
7.52
7.49
7.49
7.23
7.23
7.21
7.21
7.20
7.18
7.18
6.96
6.91
4.64
4.62
3.38
2.77
2.52
2.51
2.50
2.50
2.49
1.01
1.00
1.00
1.00
3.94
3.03
1.01
1.00
1.95
3.06
f1 (ppm)

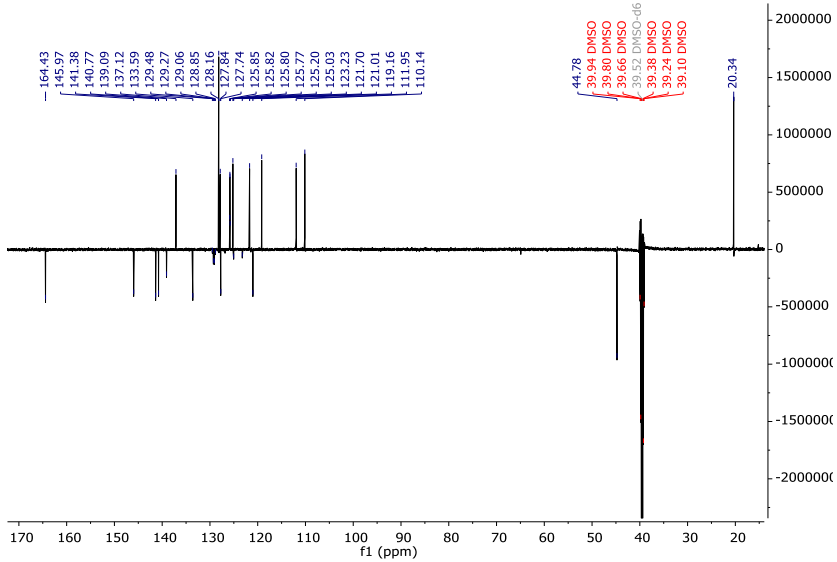
164.43
145.97
141.38
140.77
139.09
137.12
133.59
129.48
129.27
129.06
128.85
128.16
127.84
127.74
125.85
125.82
125.80
125.77
125.20
125.03
123.23
121.70
121.01
119.16
111.95
110.14
44.78
39.94 DMSO
39.80 DMSO
39.66 DMSO
39.52 DMSO-d6
39.38 DMSO
39.24 DMSO
39.10 DMSO
20.34
f1 (ppm)

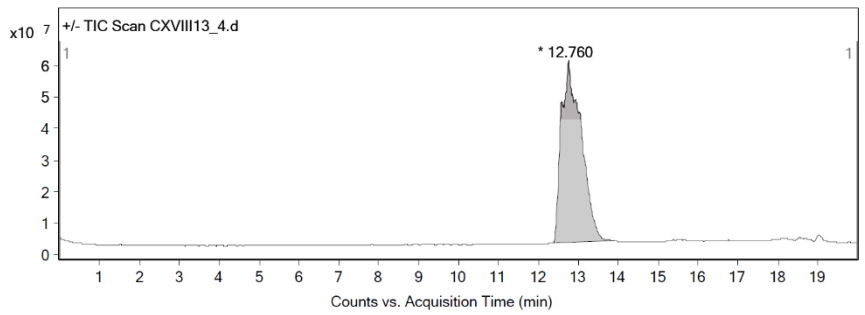

Integration Peak List

Peak	Start	RT	End	Height	Area	Area %
1	12.353	12.76	13.89	58039571.83	2018923492.95	100

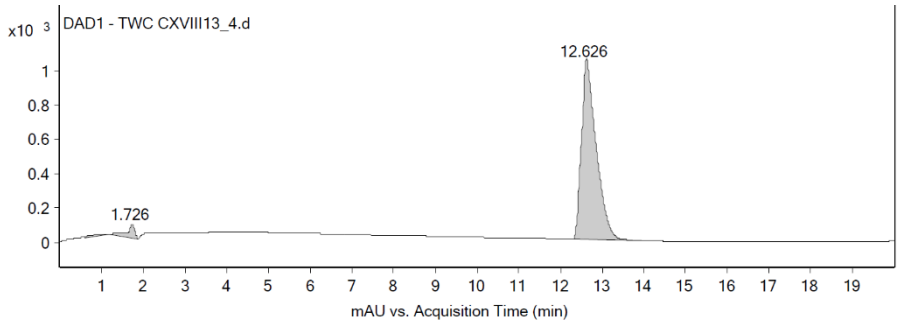

Integration Peak List

Peak	Start	RT	End	Height	Area	Area %
1	0.58	1.046	1.174	8.88	299.74	1.17
2	1.179	1.726	1.863	78.02	1096.15	4.28
3	12.306	12.626	13.964	1054.59	25629.37	100

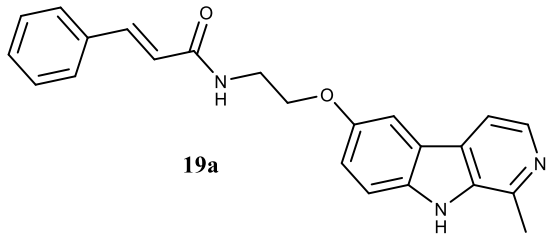

19a

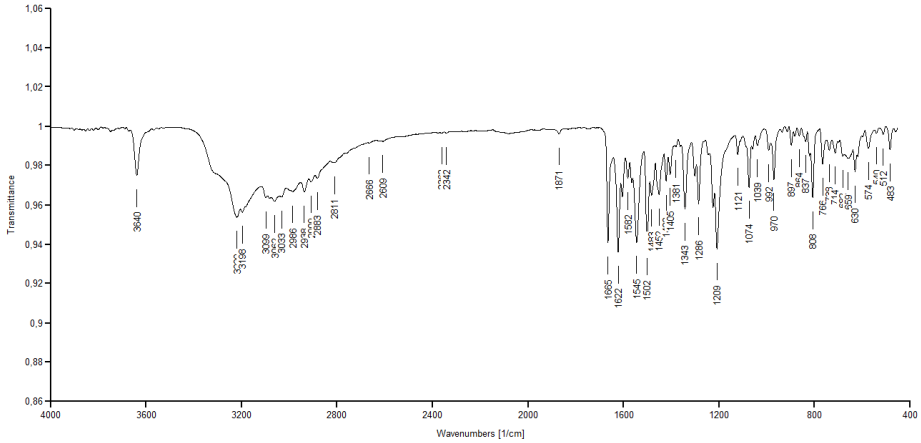
Transmittance
Wavenumbers [1/cm]
3640
3196
2966
2811
2696
2609
2342
1671
1622
1545
1502
1381
1343
1286
1209
1121
1074
1039
970
897
808
766
630
574
512
483

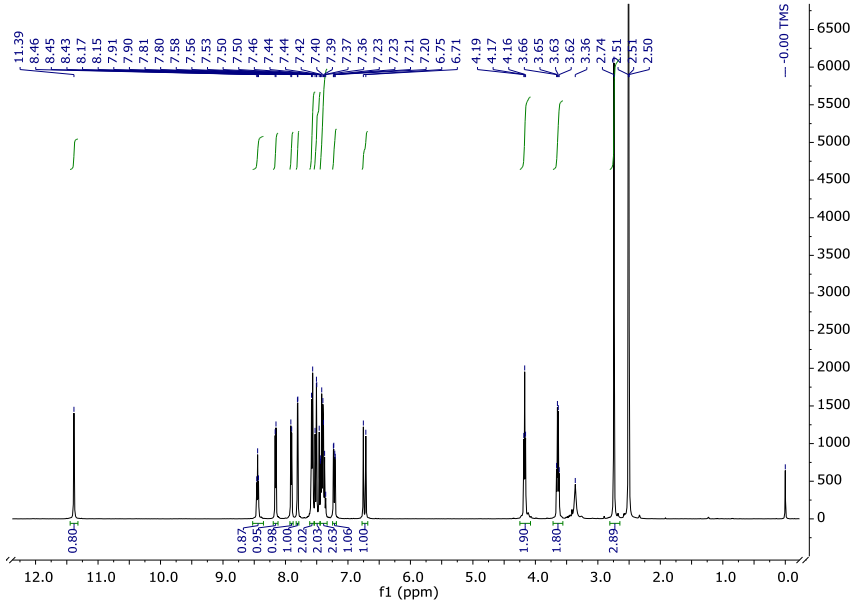
11.39
8.46
8.45
8.43
8.17
8.15
7.91
7.90
7.81
7.80
7.58
7.56
7.53
7.50
7.50
7.46
7.44
7.44
7.42
7.40
7.39
7.37
7.36
7.23
7.23
7.21
7.20
6.75
6.71
4.19
4.17
4.16
3.66
3.65
3.63
3.62
3.36
2.74
2.51
2.51
2.50
-0.00 TMS
0.80
0.87
0.95
0.98
1.00
2.02
2.03
2.63
1.06
1.00
1.90
1.80
2.89
f1 (ppm)

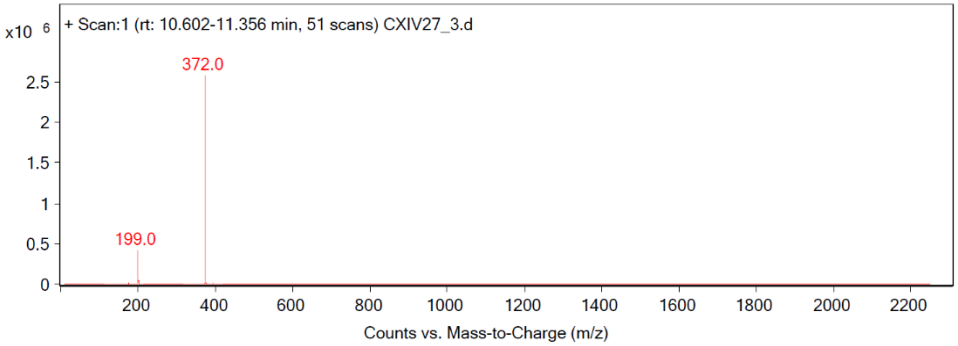
x10 6
+ Scan:1 (rt: 10.602-11.356 min, 51 scans) CXIV27_3.d
372.0
199.0
Counts vs. Mass-to-Charge (m/z)

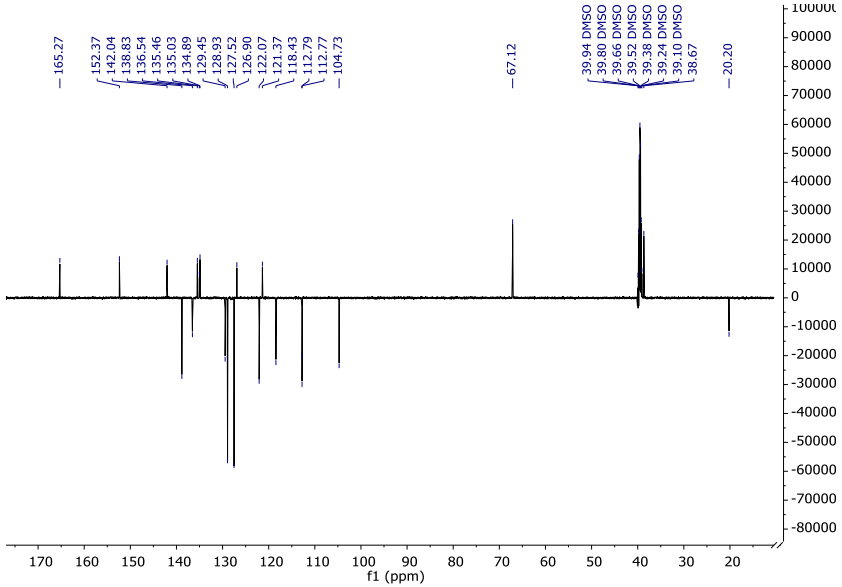
165.27
152.37
142.04
138.83
136.54
135.46
135.03
134.89
129.45
128.93
127.52
126.90
122.07
121.37
118.43
112.79
112.77
104.73
67.12
39.94 DMSO
39.80 DMSO
39.66 DMSO
39.52 DMSO
39.38 DMSO
39.24 DMSO
39.10 DMSO
38.67
20.20
f1 (ppm)

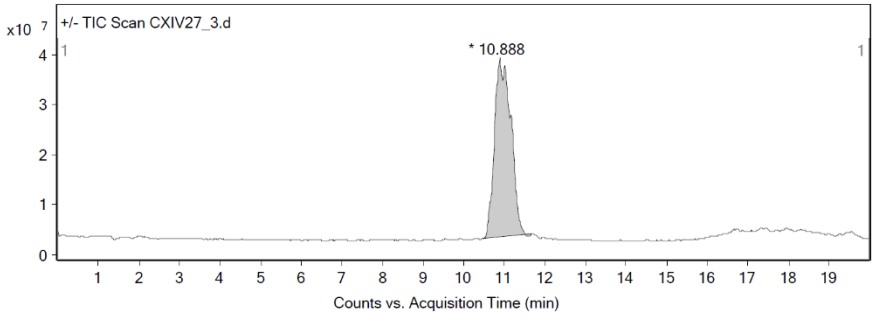

Integration Peak List

Peak	Start	RT	End	Height	Area	Area %
1	10.451	10.888	11.657	35954556.78	1004464336.75	100

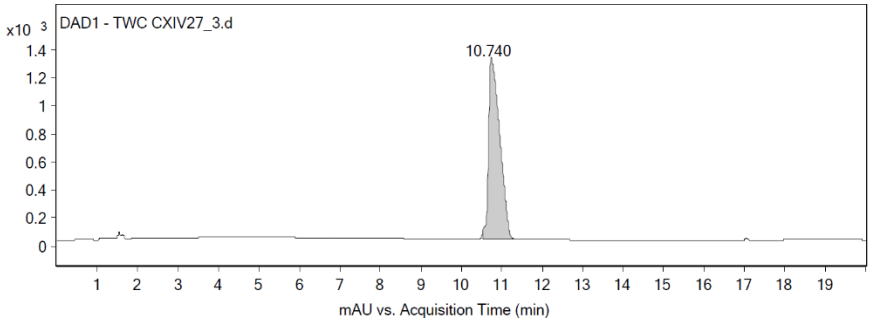

Integration Peak List

Peak	Start	RT	End	Height	Area	Area %
1	10.533	10.74	11.52	1297.17	25099.32	100

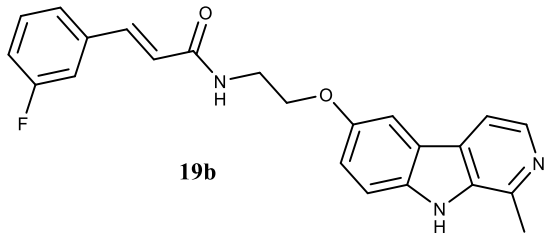
O
N
H
O
F
N
N
H

19b

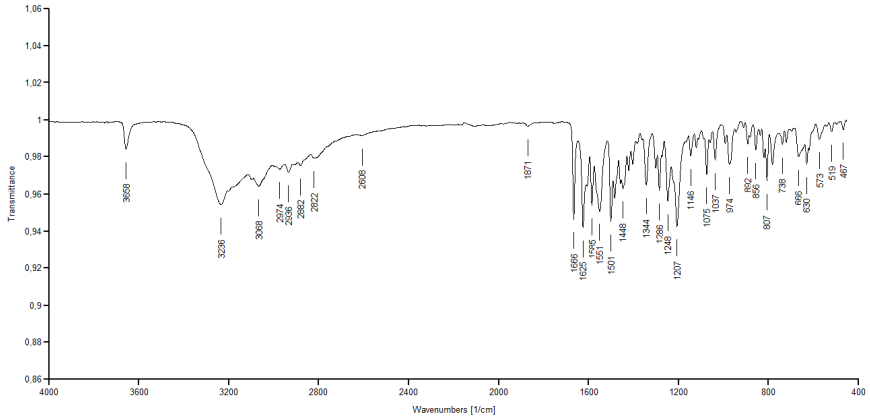
Transmittance
Wavenumbers [1/cm]
3658
3236
3068
2974
2928
2882
2822
2008
1871
1686
1625
1595
1551
1501
1448
1344
1286
1246
1207
1146
1075
1037
974
892
856
807
736
695
665
573
519
467

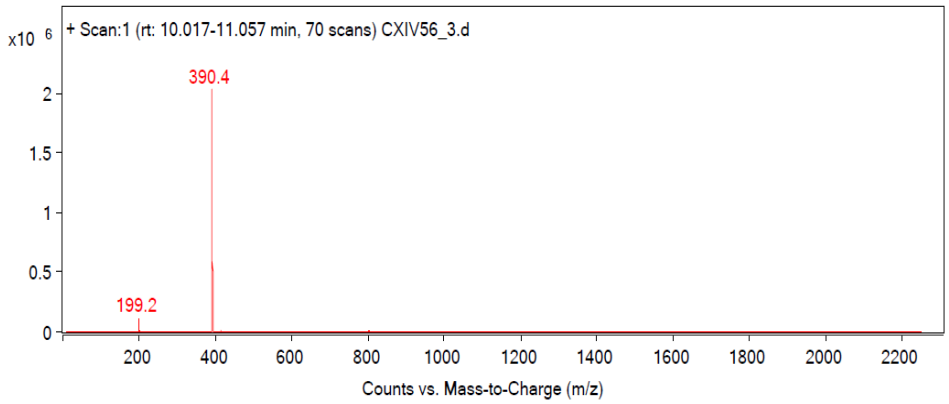
+ Scan:1 (rt: 10.017-11.057 min, 70 scans) CXIV56_3.d
x10 6
390.4
199.2
Counts vs. Mass-to-Charge (m/z)

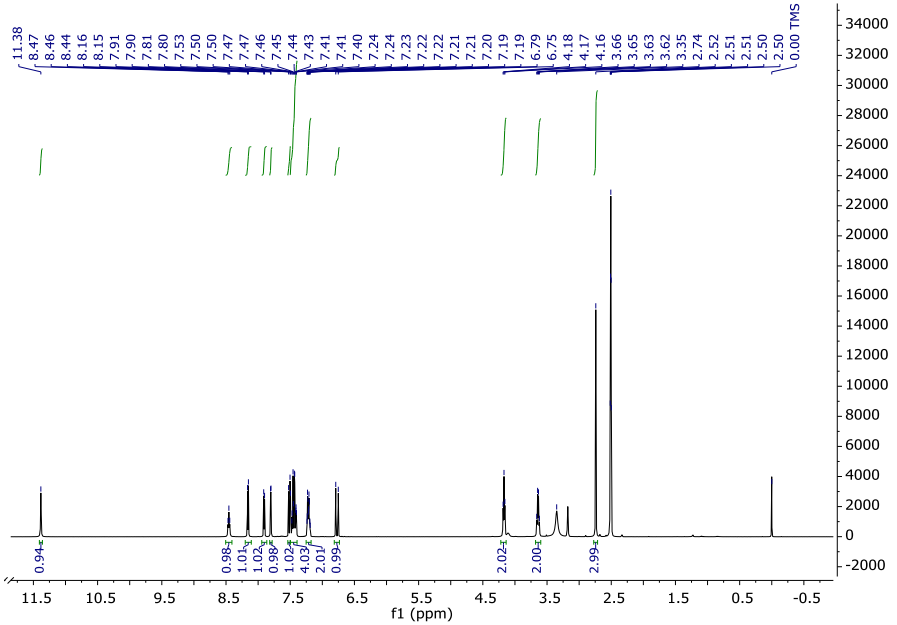
11.38
8.47
8.46
8.44
8.16
8.15
7.91
7.90
7.81
7.80
7.53
7.50
7.50
7.47
7.47
7.46
7.45
7.44
7.43
7.41
7.41
7.40
7.24
7.24
7.23
7.22
7.22
7.21
7.21
7.20
7.19
7.19
6.79
6.75
4.18
4.17
4.16
3.66
3.65
3.63
3.62
3.35
2.74
2.52
2.51
2.51
2.50
2.50
0.00 TMS
0.94
0.98
1.01
1.02
0.98
1.02
4.03
2.01
0.99
2.02
2.00
2.99
f1 (ppm)

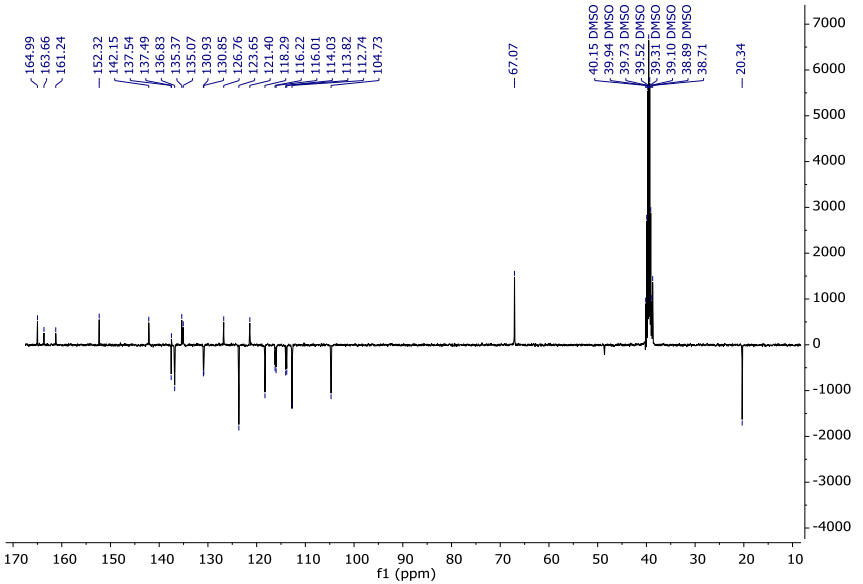
164.99
163.66
161.24
152.32
142.15
137.54
137.49
136.83
135.37
135.07
130.93
130.85
126.76
123.65
121.40
118.29
116.22
116.01
114.03
113.82
112.74
104.73
67.07
40.15 DMSO
39.94 DMSO
39.73 DMSO
39.52 DMSO
39.31 DMSO
39.10 DMSO
38.89 DMSO
38.71
20.34
f1 (ppm)

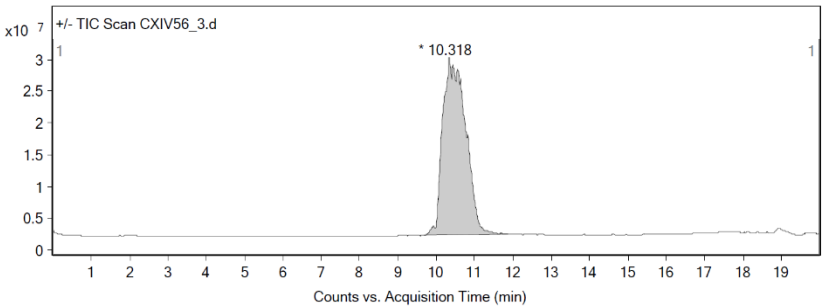

Integration Peak List

Peak	Start	RT	End	Height	Area	Area %
1	9.685	10.318	11.871	27940163.54	1164726317.11	100

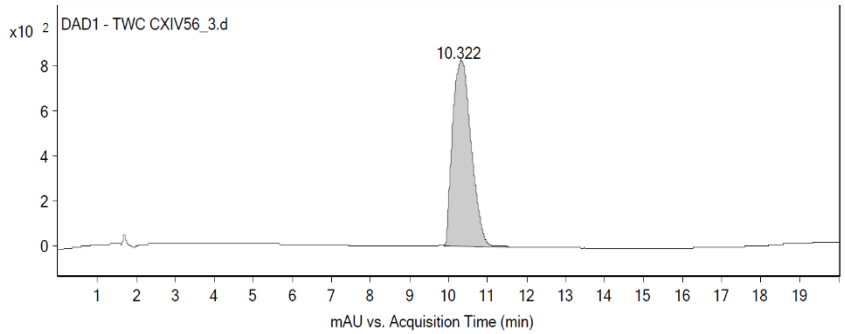

Integration Peak List

Peak	Start	RT	End	Height	Area	Area %
1	9.888	10.322	11.588	827.88	27550.35	100

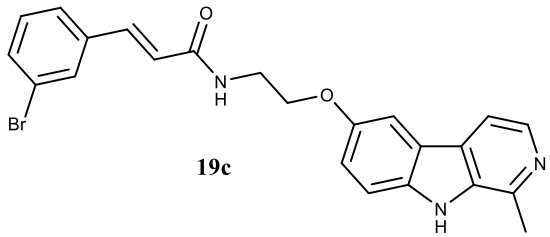
Br
O
N
H
O
N
H
N

19c

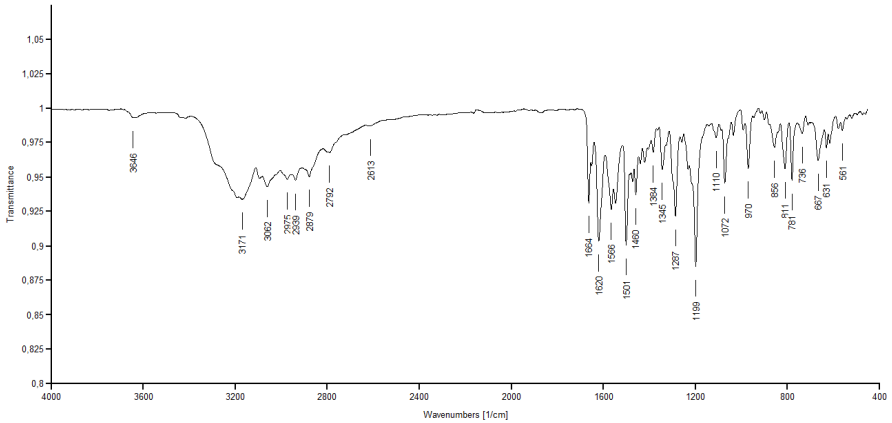
Transmittance
Wavenumbers [1/cm]
3646
3171
3062
2976
2939
2879
2792
2613
1664
1620
1566
1501
1460
1384
1345
1287
1199
1110
1072
970
856
811
781
736
667
631
561

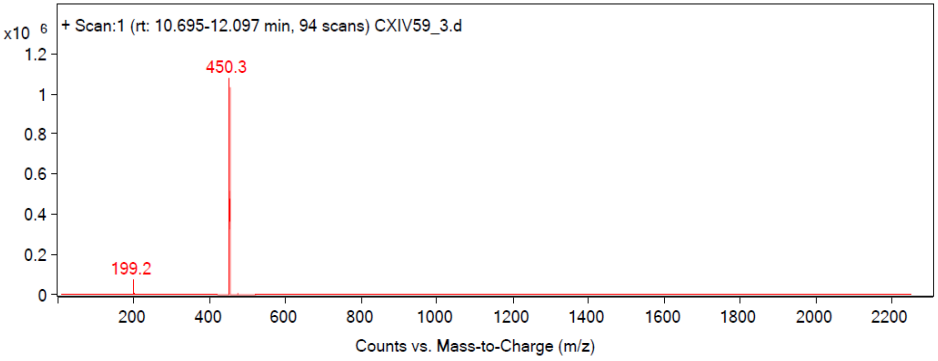
x10 6
+ Scan:1 (rt: 10.695-12.097 min, 94 scans) CXIV59_3.d
450.3
199.2
Counts vs. Mass-to-Charge (m/z)

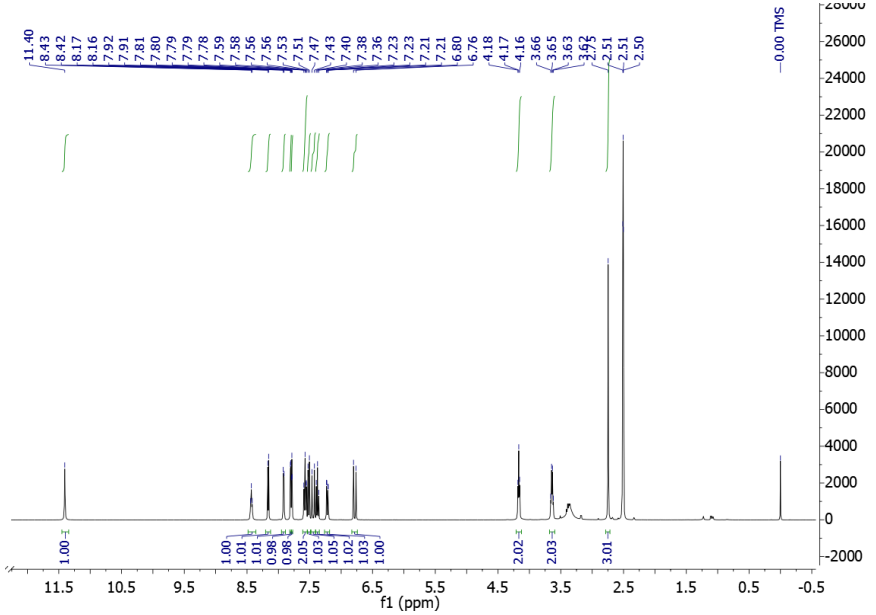
11.40
8.43
8.42
8.17
8.16
7.92
7.91
7.81
7.80
7.79
7.79
7.78
7.59
7.58
7.56
7.56
7.53
7.51
7.47
7.43
7.40
7.38
7.36
7.23
7.23
7.21
7.21
6.80
6.76
4.18
4.17
4.16
3.66
3.65
3.63
3.62
2.75
2.51
2.51
2.50
0.00 TMS
1.00
1.00
1.01
1.01
0.98
0.98
2.05
1.03
1.05
1.02
1.03
1.00
2.02
2.03
3.01
f1 (ppm)

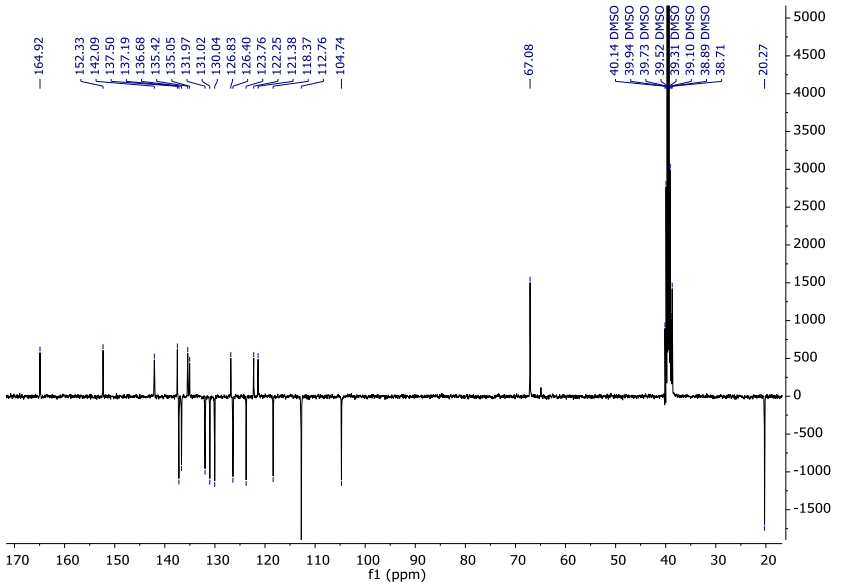
164.92
152.33
142.09
137.50
137.19
136.68
135.42
135.05
131.97
131.02
130.04
126.83
126.40
123.76
122.25
121.38
118.37
112.76
104.74
67.08
40.14 DMSO
39.94 DMSO
39.73 DMSO
39.52 DMSO
39.31 DMSO
39.10 DMSO
38.89 DMSO
38.71
20.27
f1 (ppm)

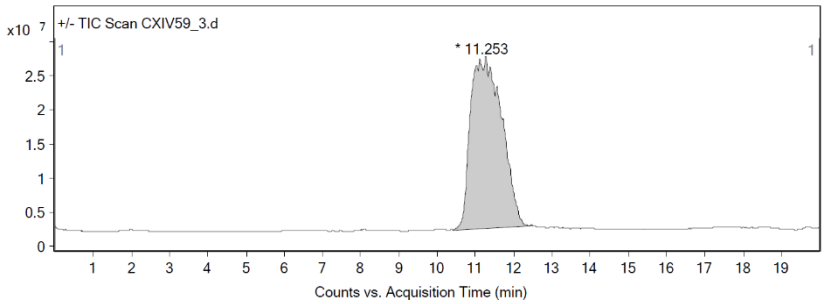

Integration Peak List

Peak	Start	RT	End	Height	Area	Area %
1	10.408	11.253	12.504	25258548.76	1434722266.58	100

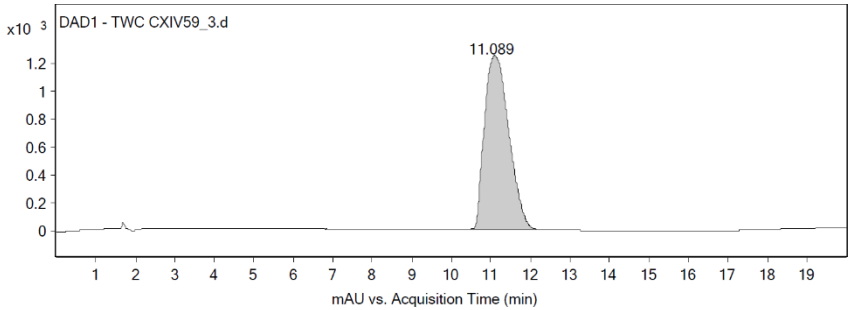

Integration Peak List

Peak	Start	RT	End	Height	Area	Area %
1	10.349	11.089	12.652	1248.75	54050.11	100

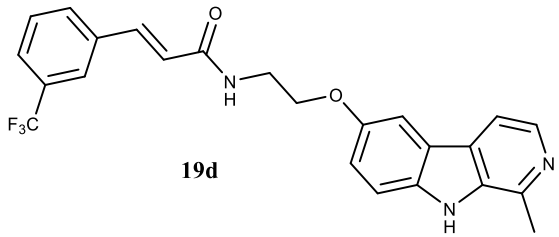
O
N
H
O
F3C
N
H

19d

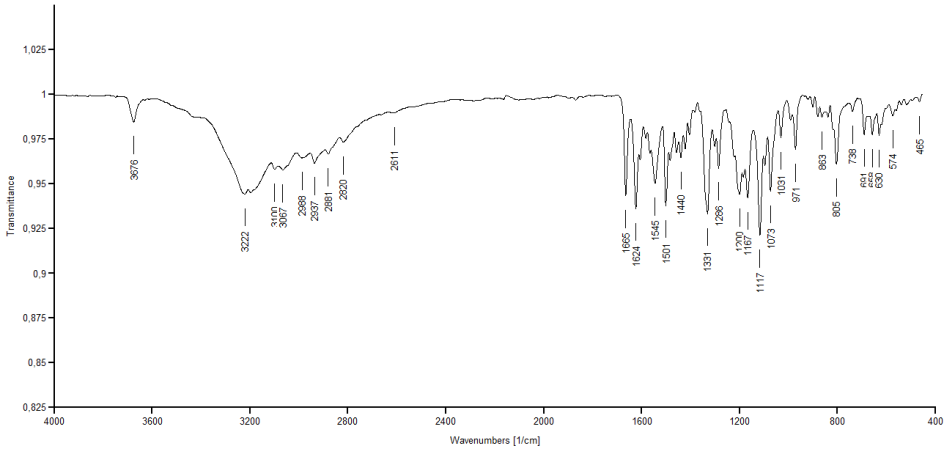
Transmittance
Wavenumbers [1/cm]
3676
3222
3100
3057
2986
2937
2861
2620
2511
1955
1624
1545
1501
1440
1331
1286
1220
1167
1117
1073
1031
971
905
863
738
694
650
574
465

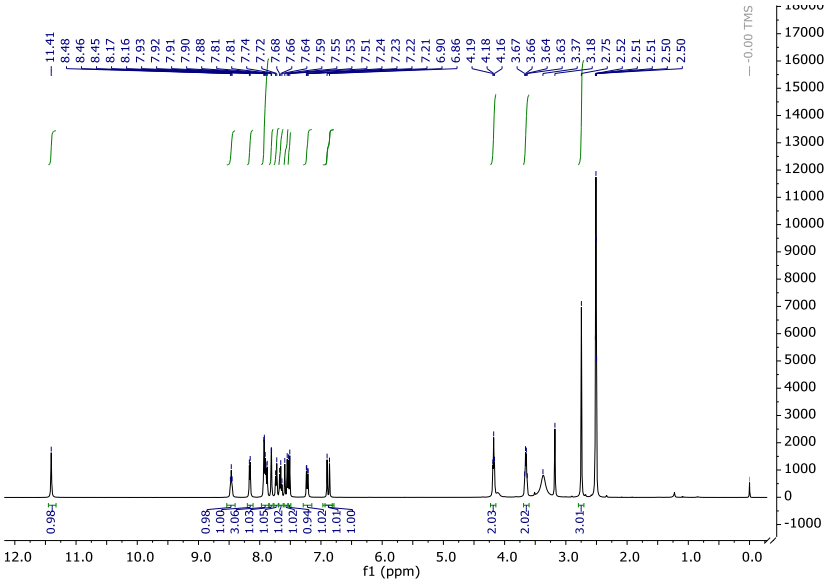
f1 (ppm)

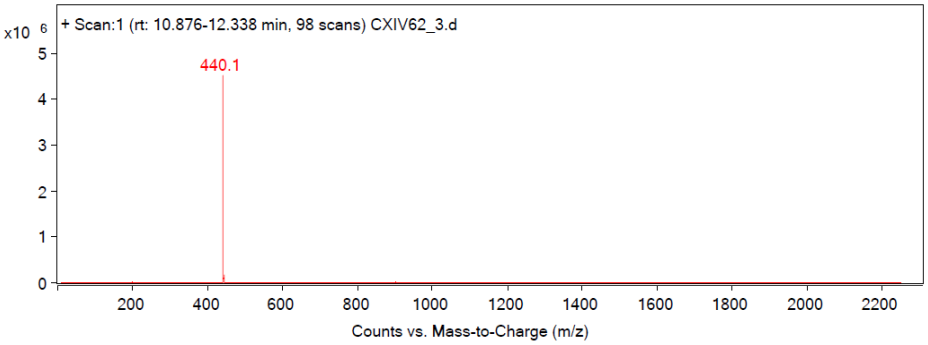
x10 6
+ Scan:1 (rt: 10.876-12.338 min, 98 scans) CXIV62_3.d
440.1
Counts vs. Mass-to-Charge (m/z)

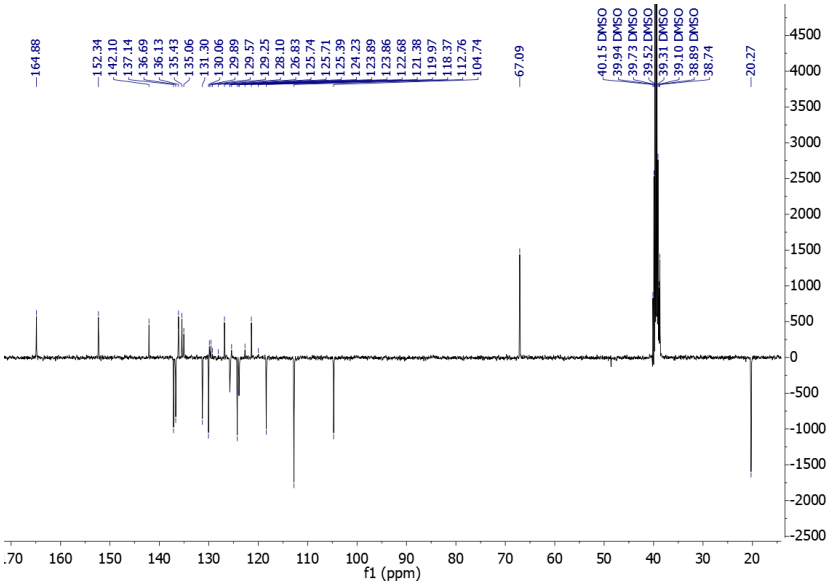
f1 (ppm)

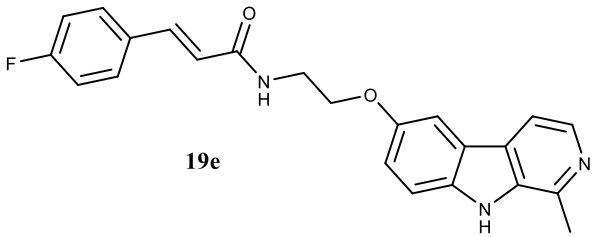
F
O
N
H
O
N
N
H

19e

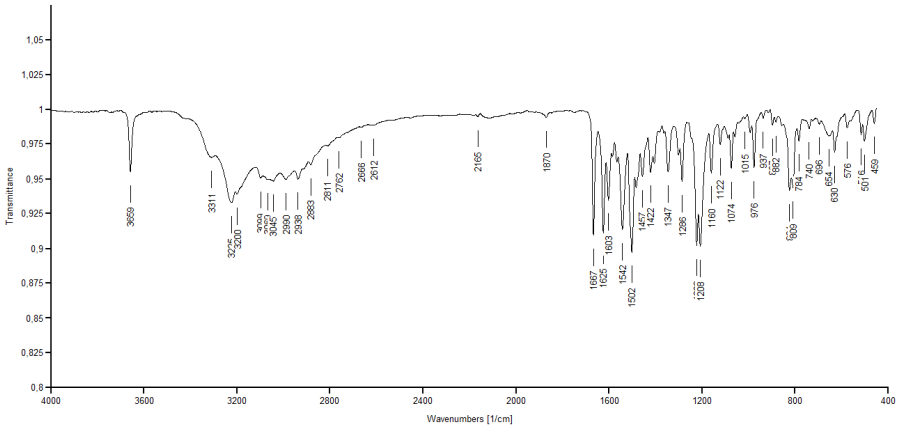
Transmittance
Wavenumbers [1/cm]

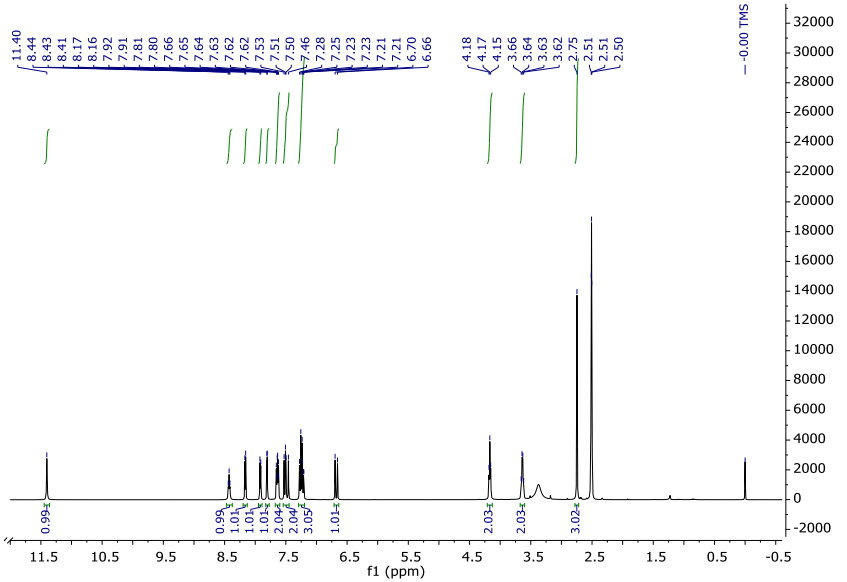
f1 (ppm)

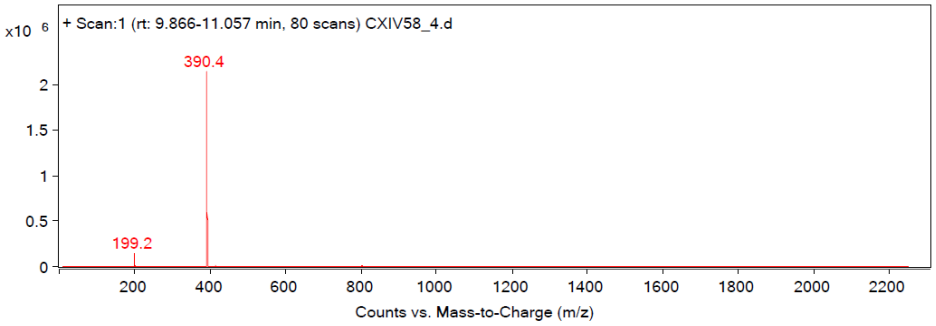
+ Scan:1 (rt: 9.866-11.057 min, 80 scans) CXIV58_4.d
390.4
199.2
Counts vs. Mass-to-Charge (m/z)

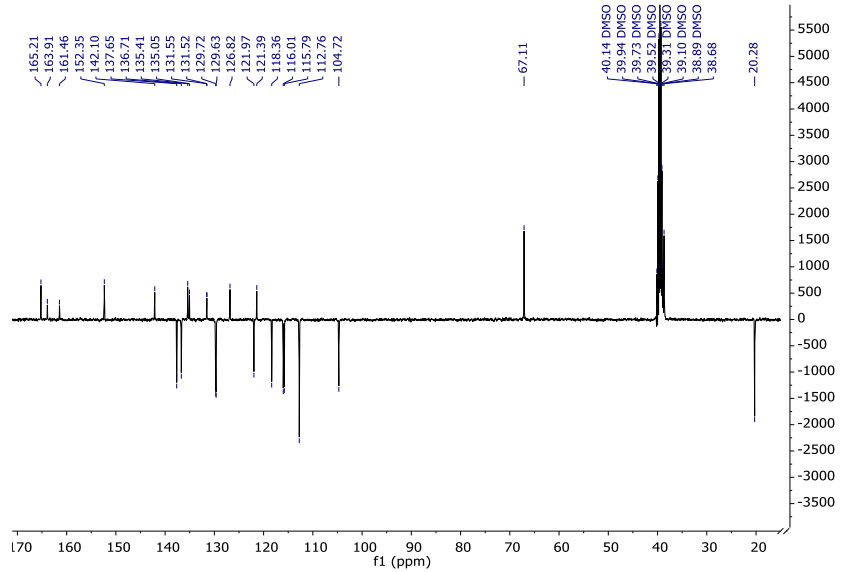
f1 (ppm)

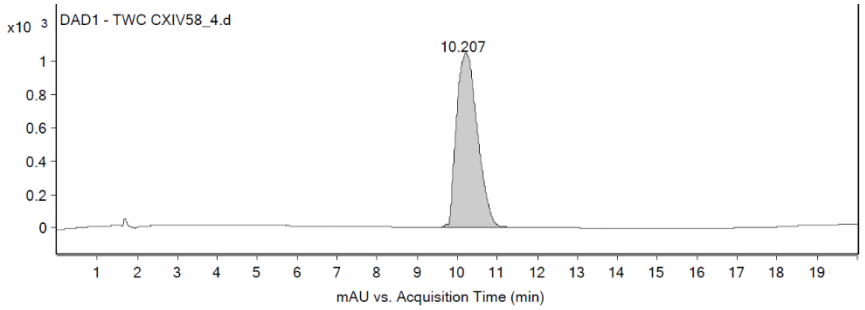

Integration Peak List

Peak	Start	RT	End	Height	Area	Area %
1	9.58	10.207	11.553	1042.29	38083.93	100

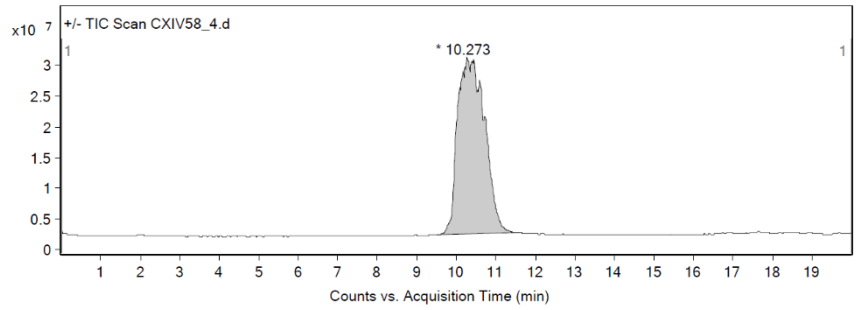

Integration Peak List

Peak	Start	RT	End	Height	Area	Area %
1	9.489	10.273	11.614	28927856.68	1386582983.74	100

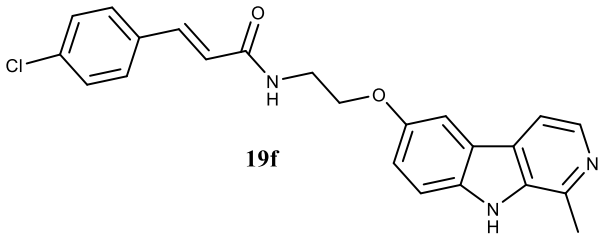
Cl
O
N
H
O
N
N
H

19f

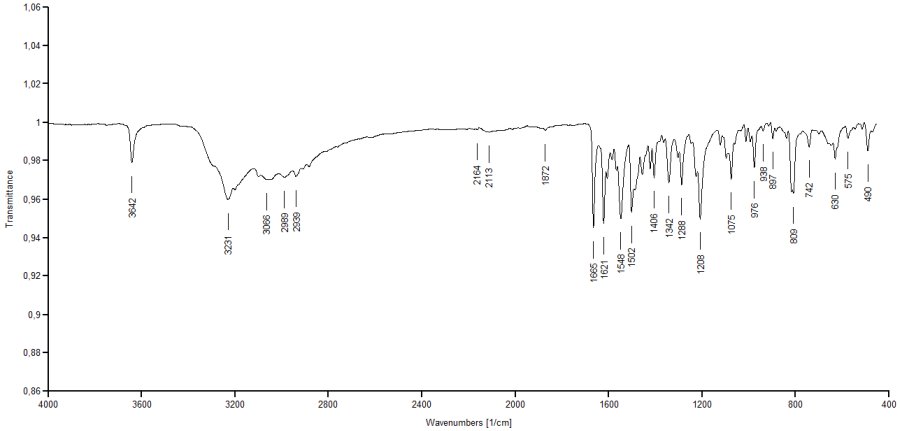
Transmittance
Wavenumbers [1/cm]
3642
3231
3066
2989
2939
2164
2113
1872
1695
1621
1548
1502
1406
1342
1288
1209
1075
976
938
897
809
742
630
575
490

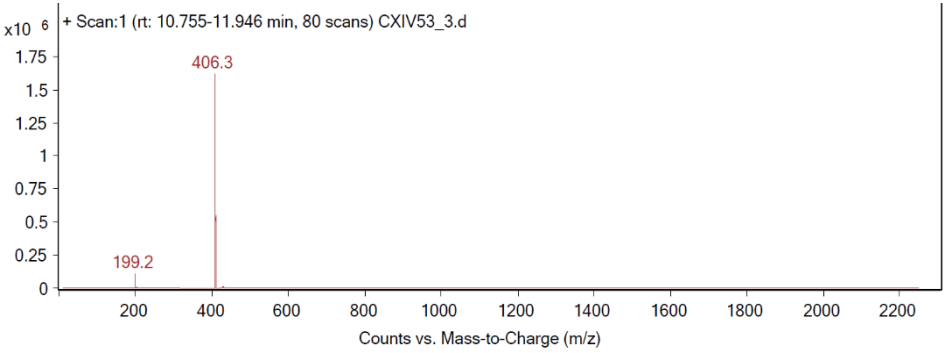
x10 6
+ Scan:1 (rt: 10.755-11.946 min, 80 scans) CXIV53_3.d
406.3
199.2
Counts vs. Mass-to-Charge (m/z)

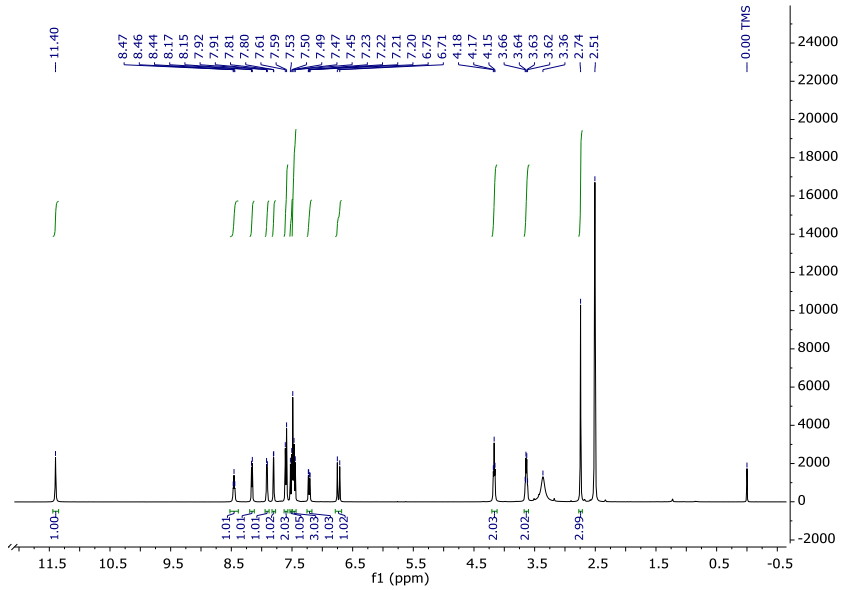
11.40
8.47
8.46
8.44
8.17
8.15
7.92
7.91
7.81
7.80
7.61
7.59
7.53
7.50
7.49
7.47
7.45
7.23
7.22
7.21
7.20
6.75
6.71
4.18
4.17
4.15
3.66
3.64
3.63
3.62
3.36
2.74
2.51
0.00 TMS
1.00
1.01
1.01
1.01
1.02
2.03
1.05
3.03
1.03
1.02
2.03
2.02
2.99
f1 (ppm)

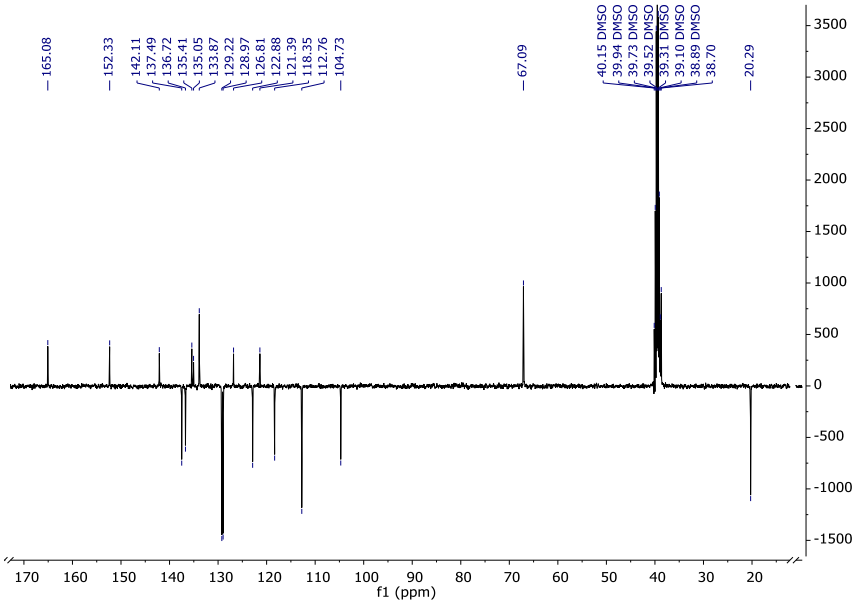
165.08
152.33
142.11
137.49
136.72
135.41
135.05
133.87
129.22
128.97
126.81
122.88
121.39
118.35
112.76
104.73
67.09
40.15 DMSO
39.94 DMSO
39.73 DMSO
39.52 DMSO
39.31 DMSO
39.10 DMSO
38.89 DMSO
38.70
20.29
f1 (ppm)

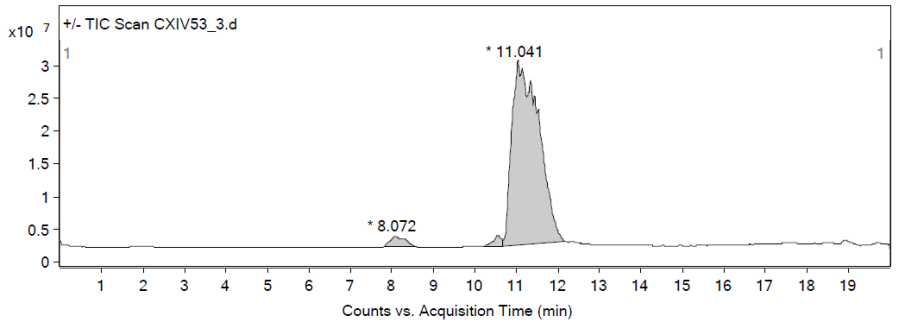

Integration Peak List

Peak	Start	RT	End	Height	Area	Area %
1	7.816	8.072	8.569	1541039.92	37249299.82	2.92
2	10.197	10.559	10.68	1745457.36	23653245.12	1.86
3	10.68	11.041	12.157	28328735.83	1273587700.89	100

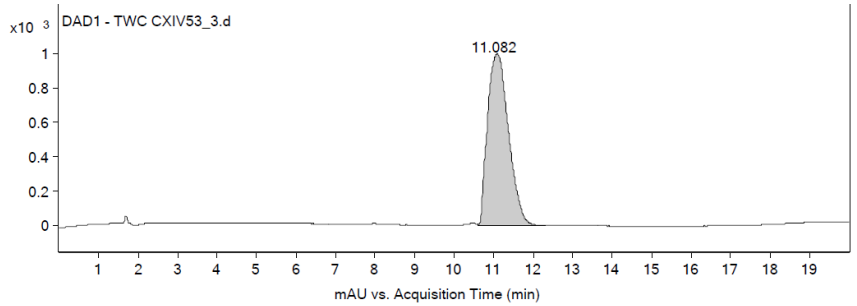

Integration Peak List

Peak	Start	RT	End	Height	Area	Area %
1	10.616	11.082	12.313	1000.83	36770.61	100

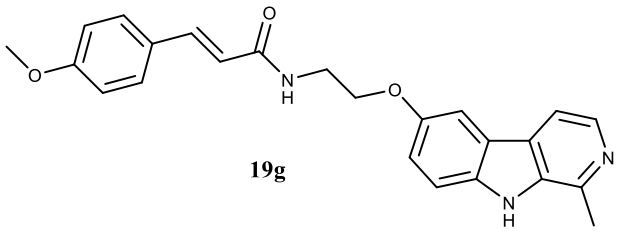

19g

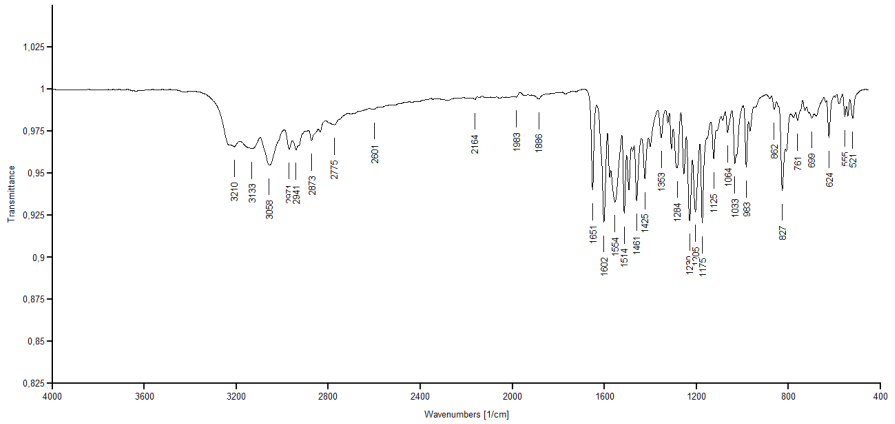
Transmittance
Wavenumbers [1/cm]
3210
3133
3058
2971
2941
2873
2775
2631
2164
1983
1886
1651
1632
1554
1514
1461
1425
1353
1284
1220
1205
1175
1125
1084
1033
983
927
862
761
699
624
555
521

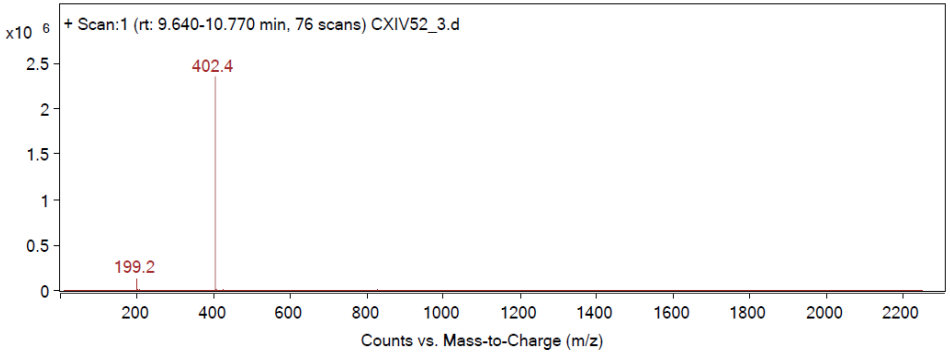
x10 6
+ Scan:1 (rt: 9.640-10.770 min, 76 scans) CXIV52_3.d
402.4
199.2
Counts vs. Mass-to-Charge (m/z)

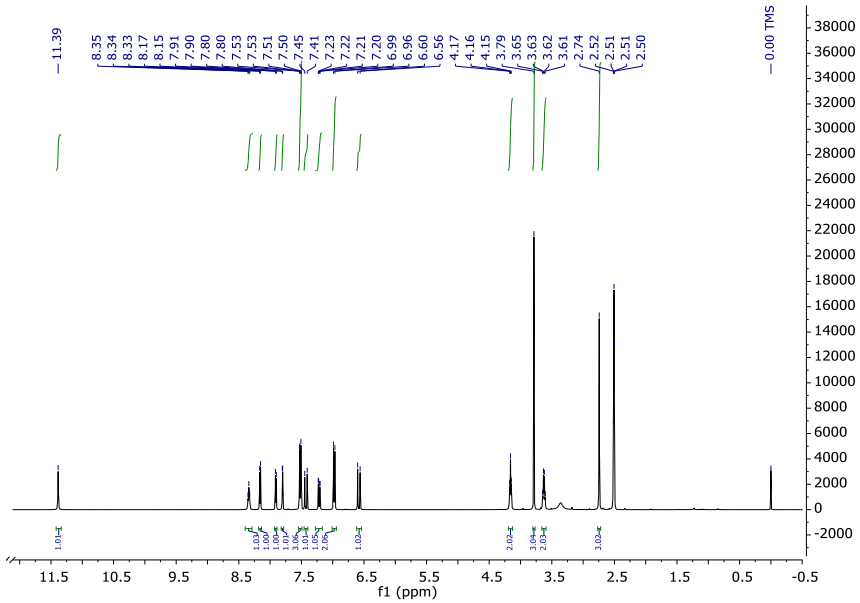
11.39
8.35
8.34
8.33
8.17
8.15
7.91
7.90
7.80
7.80
7.53
7.53
7.51
7.50
7.45
7.41
7.23
7.22
7.21
7.20
6.99
6.96
6.60
6.56
4.17
4.16
4.15
3.79
3.65
3.63
3.62
3.61
2.74
2.52
2.51
2.51
2.50
0.00 TMS
f1 (ppm)

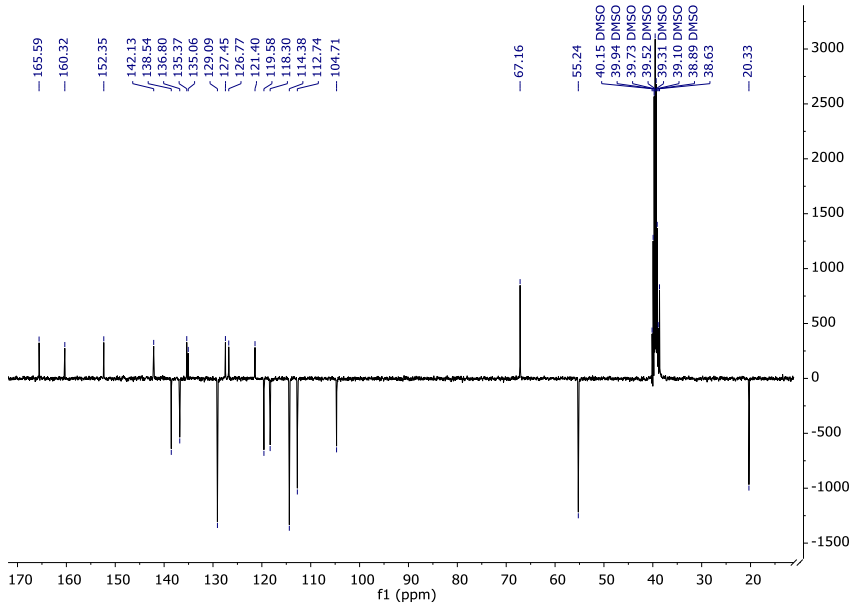
165.59
160.32
152.35
142.13
138.54
136.80
135.37
135.06
129.09
127.45
126.77
121.40
119.58
118.30
114.38
112.74
104.71
67.16
55.24
40.15 DMSO
39.94 DMSO
39.73 DMSO
39.52 DMSO
39.31 DMSO
39.10 DMSO
38.89 DMSO
38.63
20.33
f1 (ppm)

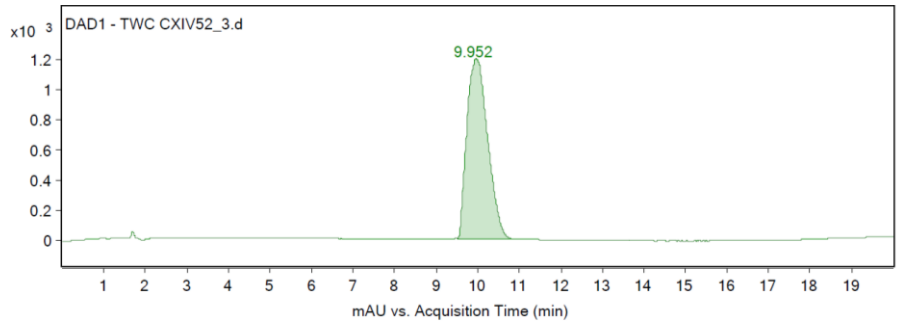

Integration Peak List

Peak	Start	RT	End	Height	Area	Area %
1	9.512	9.952	11.229	1200.44	42013.49	100

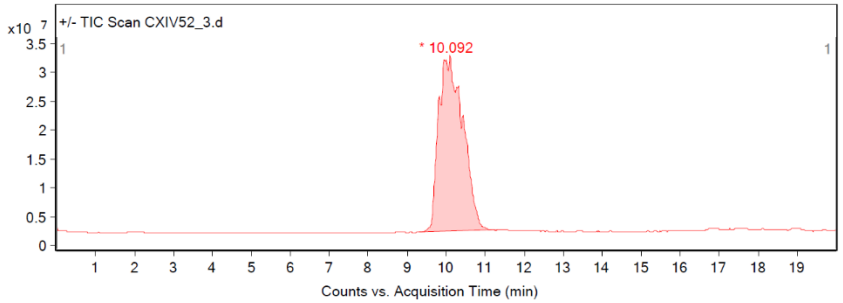

Integration Peak List

Peak	Start	RT	End	Height	Area	Area %
1	9.308	10.092	11.328	30600059.72	1325842457.19	100

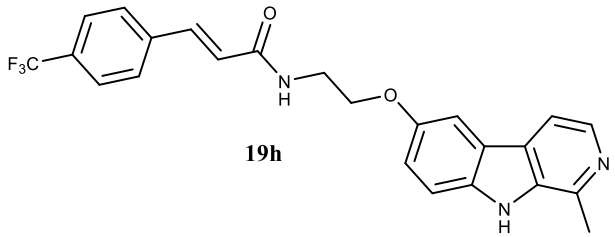
F3C
O
N
H
O
N
N
H

19h

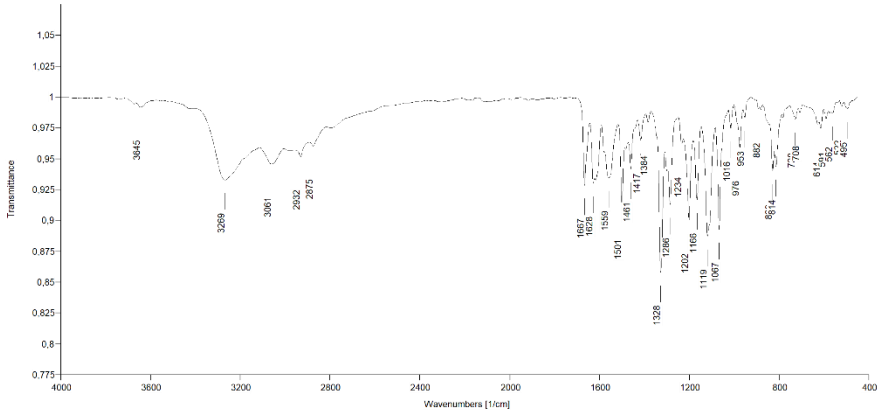
Transmittance
Wavenumbers [1/cm]
3645
3259
3061
2932
2875
1687
1628
1559
1501
1461
1417
1384
1328
1286
1234
1202
1166
1119
1067
1016
976
953
882
814
770
708
614
562
495

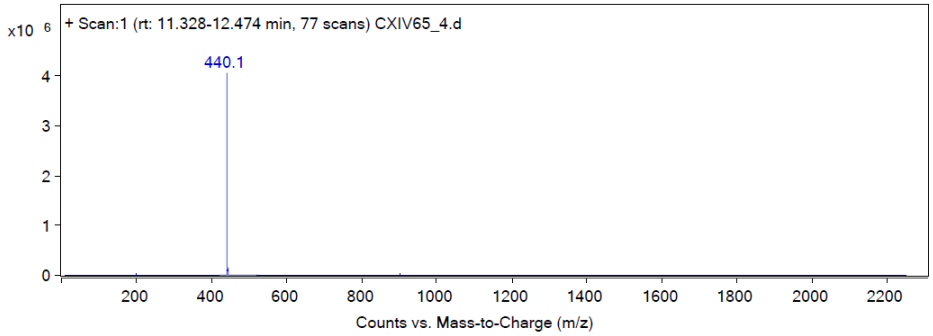
x10 6
+ Scan:1 (rt: 11.328-12.474 min, 77 scans) CXIV65_4.d
440.1
Counts vs. Mass-to-Charge (m/z)

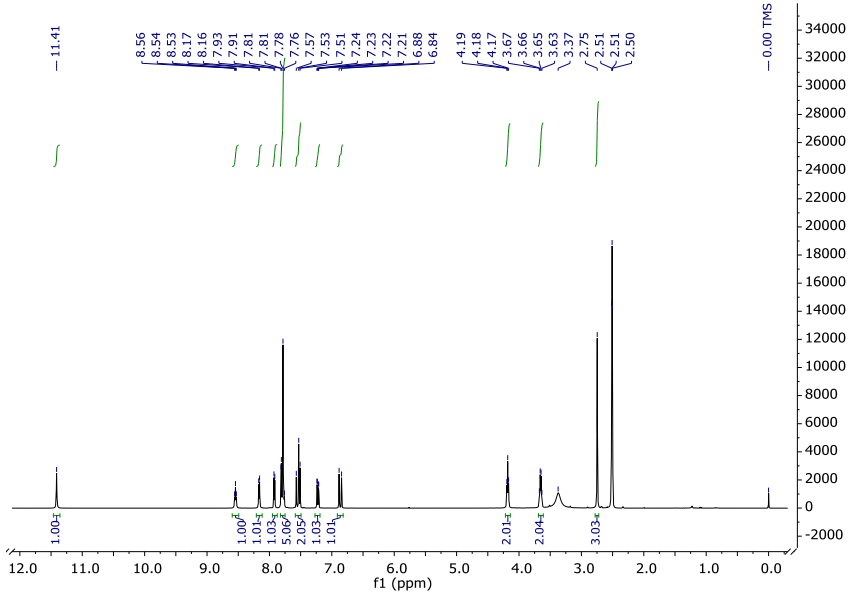
11.41
8.56
8.54
8.53
8.17
8.16
7.93
7.91
7.81
7.81
7.78
7.76
7.57
7.53
7.51
7.24
7.23
7.22
7.21
6.88
6.84
4.19
4.18
4.17
3.67
3.66
3.65
3.63
3.37
2.75
2.51
2.51
2.50
0.00 TMS
f1 (ppm)

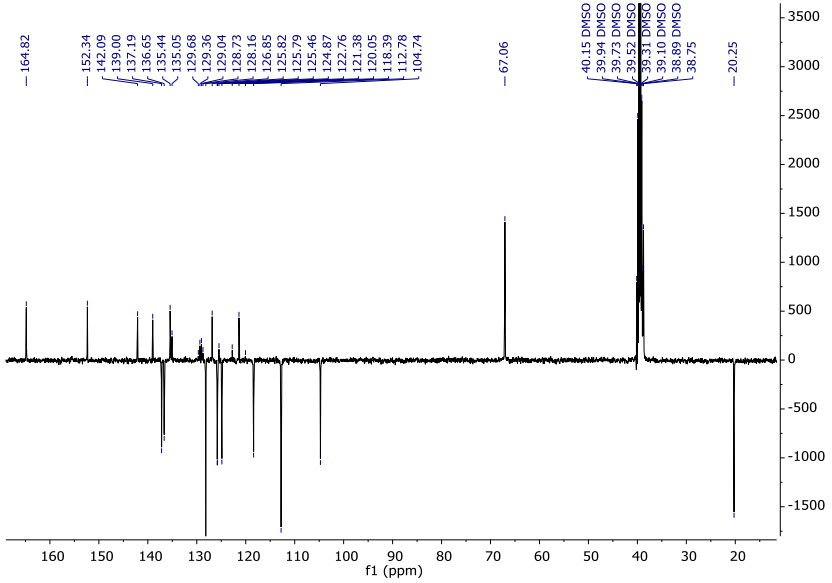
164.82
152.34
142.09
139.00
137.19
136.65
135.44
135.05
129.68
129.36
129.04
128.73
128.16
126.85
125.82
125.79
125.46
124.87
122.76
121.38
120.05
118.39
112.78
104.74
67.06
40.15 DMSO
39.94 DMSO
39.73 DMSO
39.52 DMSO
39.31 DMSO
39.10 DMSO
38.89 DMSO
38.75
20.25
f1 (ppm)

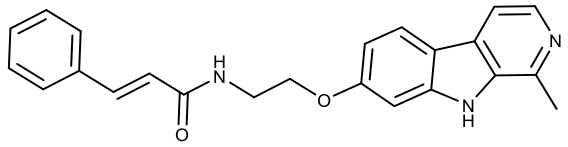

22a

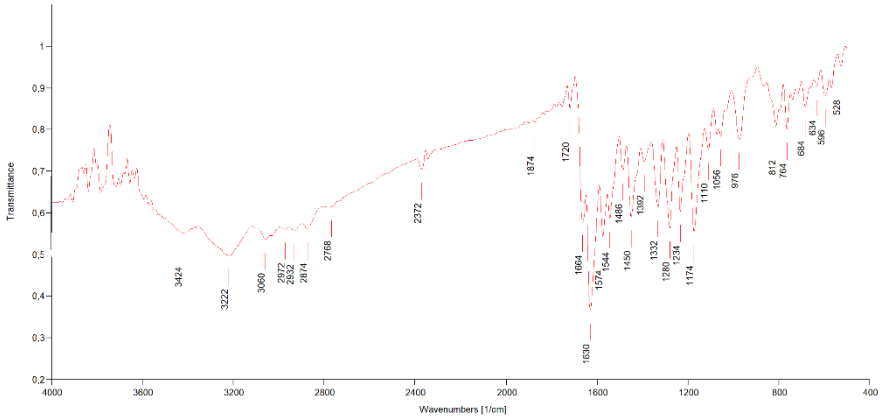
Transmittance
Wavenumbers [1/cm]
3424
3222
3060
2972
2932
2874
2768
2372
1874
1720
1664
1630
1574
1544
1486
1450
1392
1332
1280
1234
1174
1110
1056
976
812
764
684
634
596
528

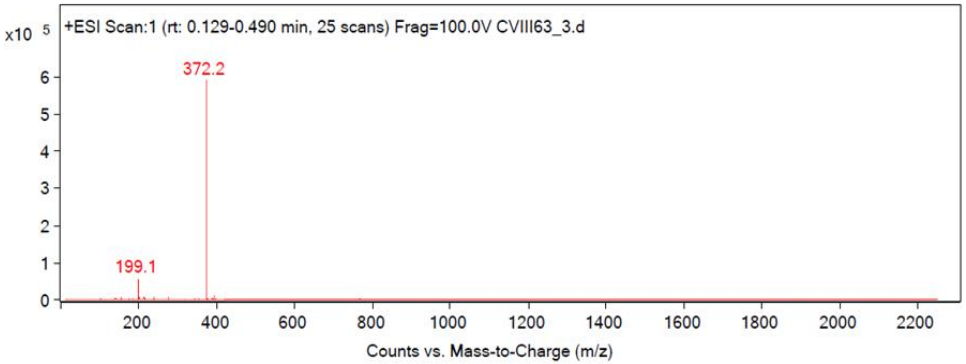
x10 5
+ESI Scan:1 (rt: 0.129-0.490 min, 25 scans) Frag=100.0V CVIII63_3.d
372.2
199.1
Counts vs. Mass-to-Charge (m/z)

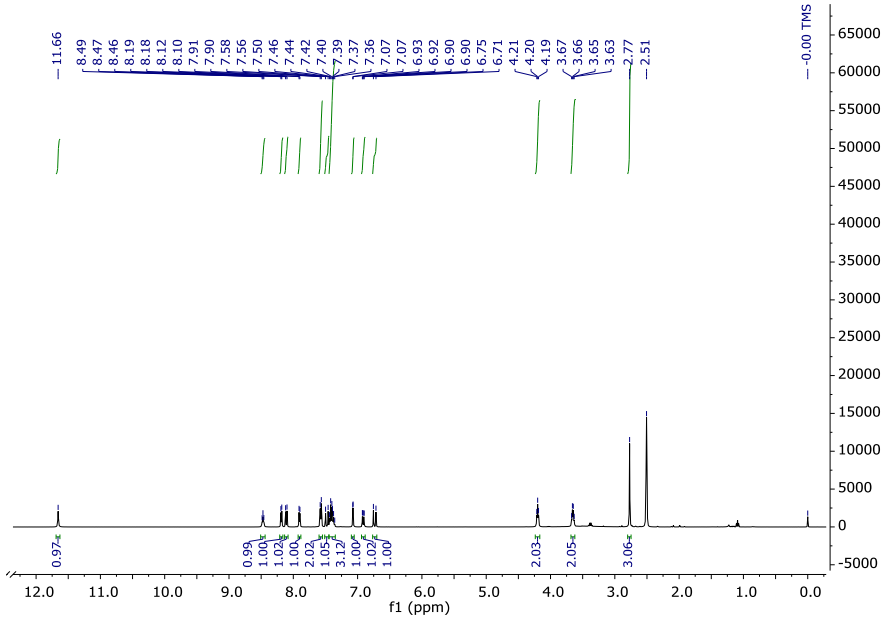
11.66
8.49
8.47
8.46
8.19
8.18
8.12
8.10
7.91
7.90
7.58
7.56
7.50
7.46
7.44
7.42
7.40
7.39
7.37
7.36
7.07
7.07
6.93
6.92
6.90
6.90
6.75
6.71
4.21
4.20
4.19
3.67
3.66
3.65
3.63
2.77
2.51
-0.00 TMS
0.97
0.99
1.00
1.02
1.00
2.02
1.05
3.12
1.00
1.02
1.00
2.03
2.05
3.06
f1 (ppm)

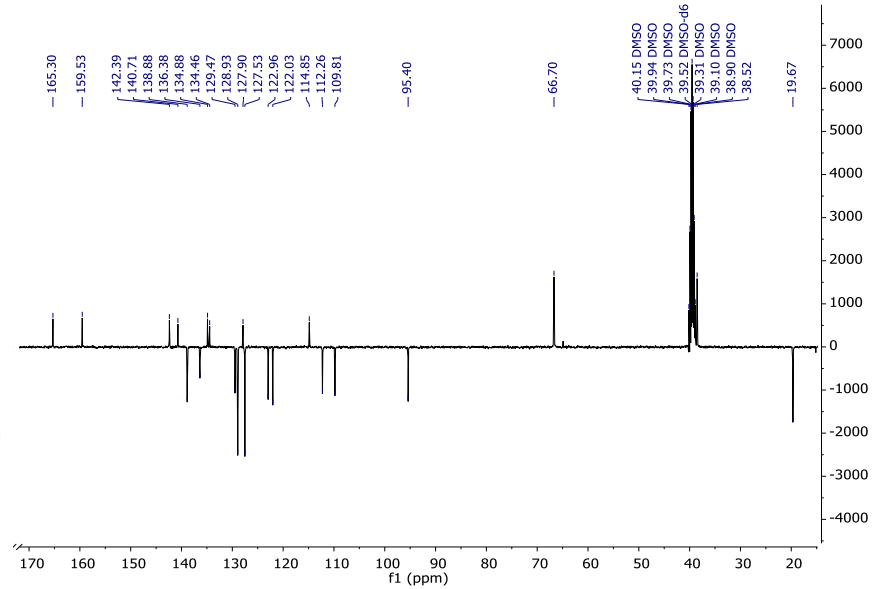
165.30
159.53
142.39
140.71
138.88
136.38
134.88
134.46
129.47
128.93
127.90
127.53
122.96
122.03
114.85
112.26
109.81
95.40
66.70
40.15 DMSO
39.94 DMSO
39.73 DMSO
39.52 DMSO-d6
39.31 DMSO
39.10 DMSO
38.90 DMSO
38.52
19.67
f1 (ppm)

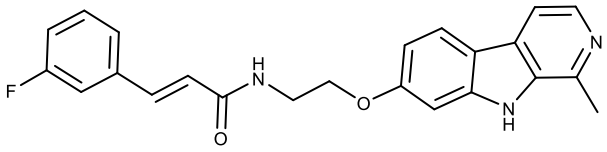
F
O
H
N
O
N
H
N

22b

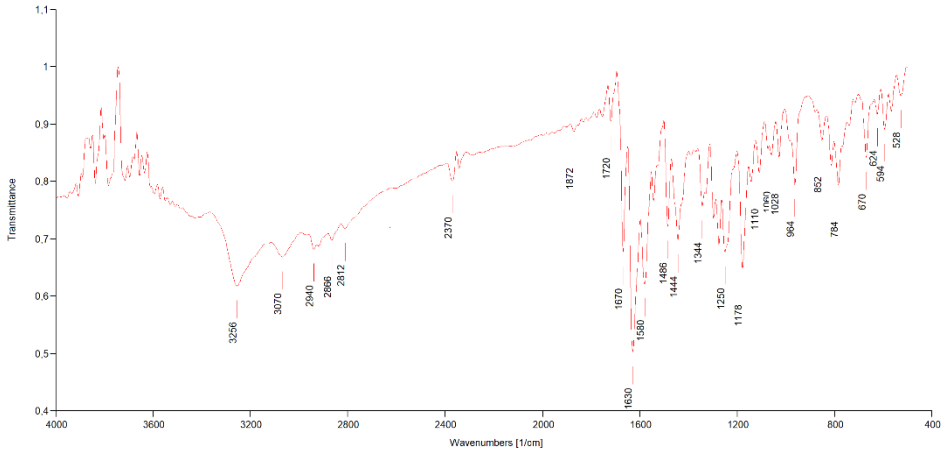
Transmittance
Wavenumbers [1/cm]
3256
3070
2940
2866
2812
2370
1872
1720
1670
1630
1580
1486
1444
1344
1250
1178
1110
1028
964
852
784
670
624
594
528

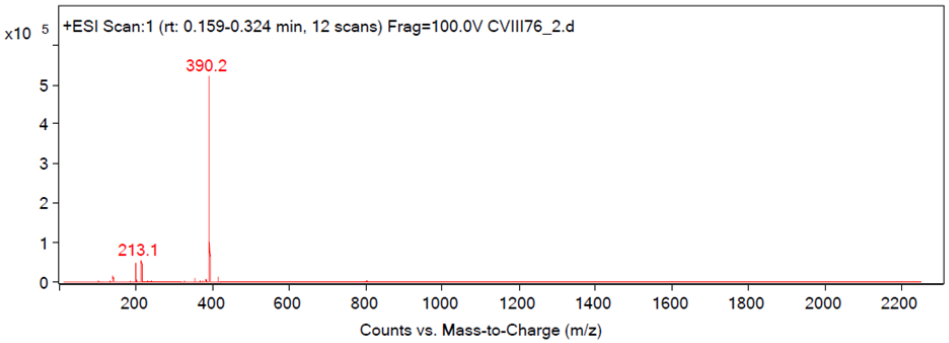
x10 5
+ESI Scan:1 (rt: 0.159-0.324 min, 12 scans) Frag=100.0V CVIII76_2.d
390.2
213.1
Counts vs. Mass-to-Charge (m/z)

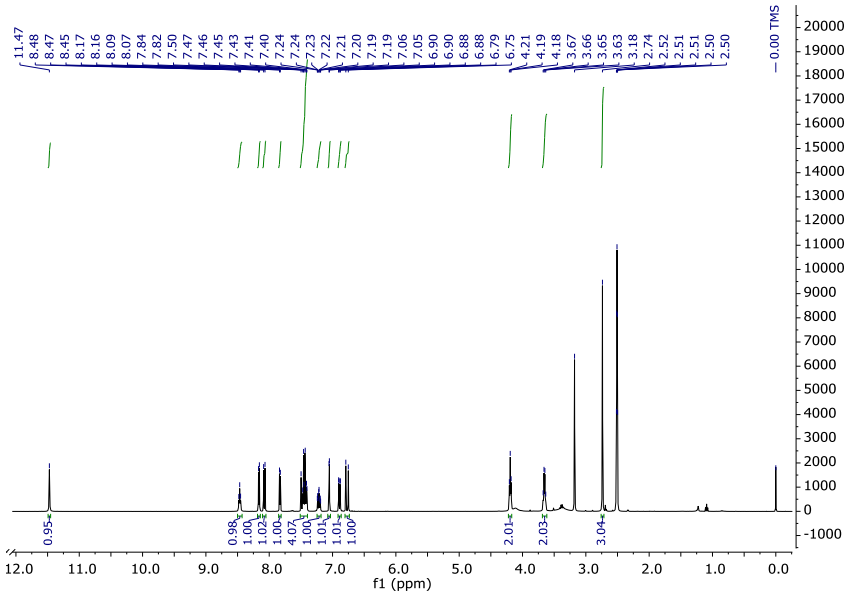
0.00 TMS
f1 (ppm)

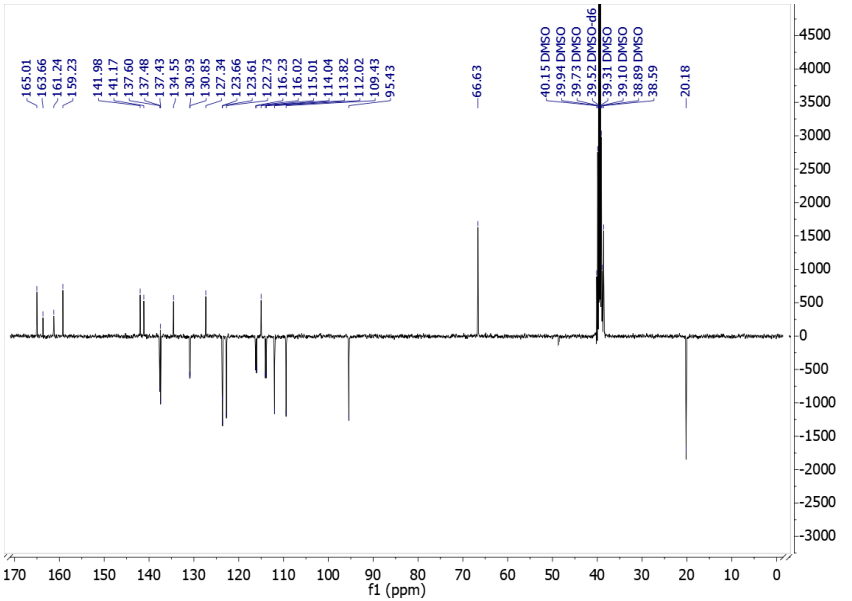
DMSO
DMSO-d6
f1 (ppm)

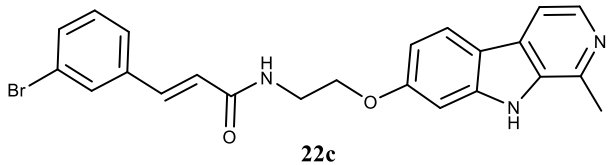
Br
H
N
O
O
N
H
N

22c

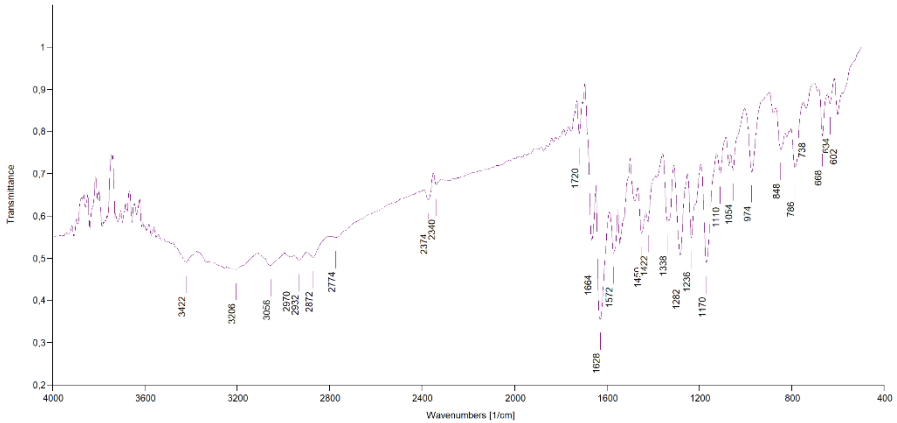
Transmittance
Wavenumbers [1/cm]
3422
3086
3058
2970
2932
2872
2774
2374
2340
1720
1664
1572
1628
1450
1422
1338
1282
1236
1170
1110
1054
974
848
786
738
668
602

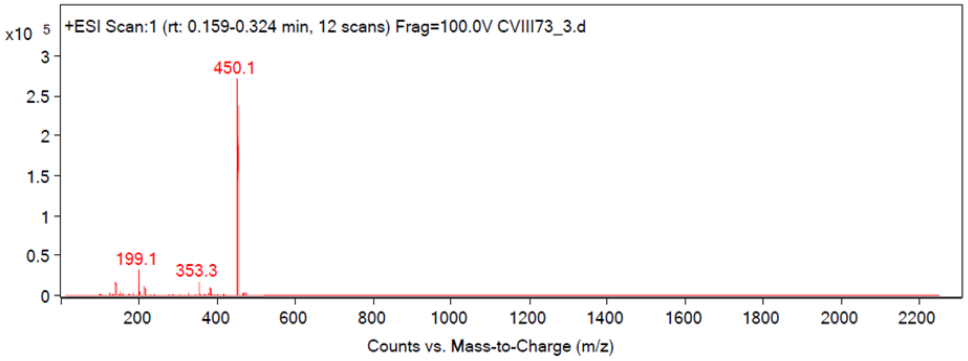
x10 5
+ESI Scan:1 (rt: 0.159-0.324 min, 12 scans) Frag=100.0V CVIII73_3.d
450.1
199.1
353.3
Counts vs. Mass-to-Charge (m/z)

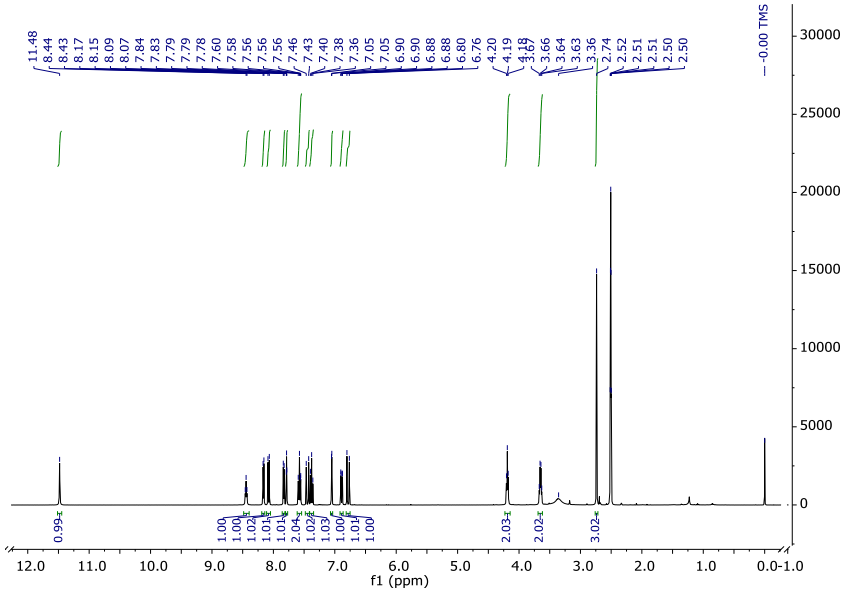
11.48
8.44
8.43
8.17
8.15
8.09
8.07
7.84
7.83
7.79
7.79
7.78
7.60
7.58
7.56
7.56
7.56
7.46
7.43
7.40
7.38
7.36
7.05
7.05
6.90
6.90
6.88
6.88
6.80
6.76
4.20
4.19
3.66
3.64
3.63
3.36
2.74
2.52
2.51
2.51
2.50
2.50
-0.00 TMS
0.99
1.00
1.00
1.02
1.01
1.01
2.04
1.02
1.00
1.01
1.00
2.03
2.02
3.02
f1 (ppm)

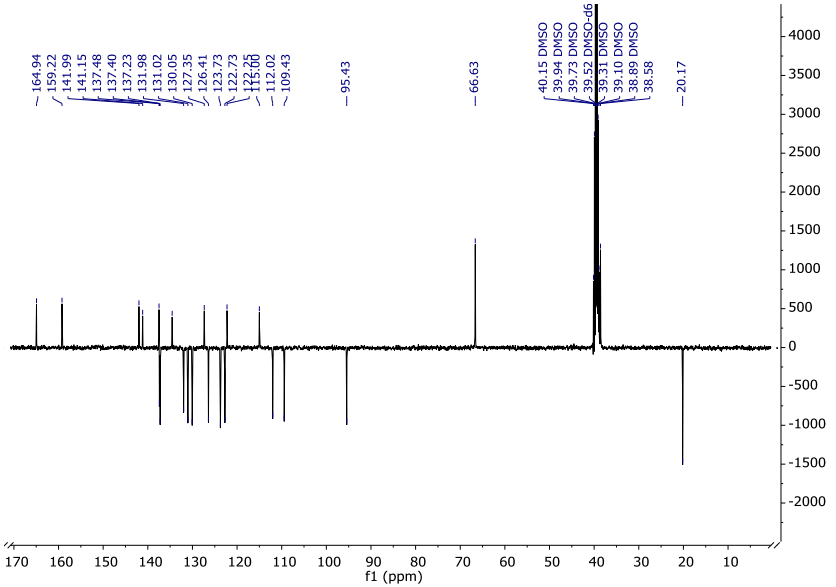
164.94
159.22
141.99
141.15
137.48
137.40
137.23
131.98
131.02
130.05
127.35
126.41
123.73
122.73
115.00
112.02
109.43
95.43
66.63
40.15 DMSO
39.94 DMSO
39.73 DMSO
39.52 DMSO-d6
39.31 DMSO
39.10 DMSO
38.89 DMSO
38.58
20.17
f1 (ppm)

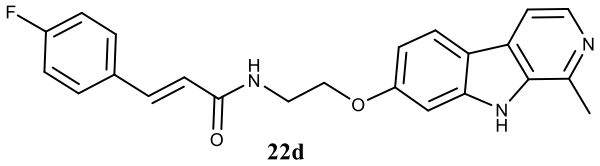
F
H
N
O
O
N
H
N

22d

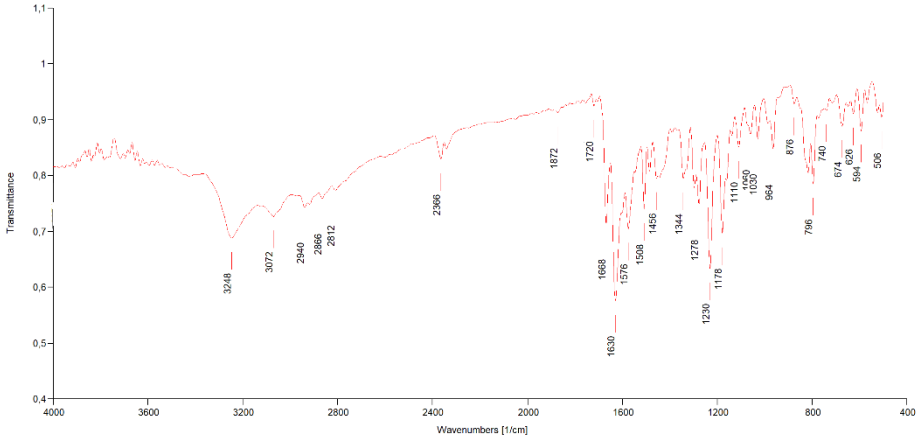
Transmittance
Wavenumbers [1/cm]
3248
3072
2940
2866
2812
2366
1872
1720
1668
1630
1576
1508
1456
1344
1278
1230
1178
1110
1050
1030
964
876
796
740
674
626
594
506

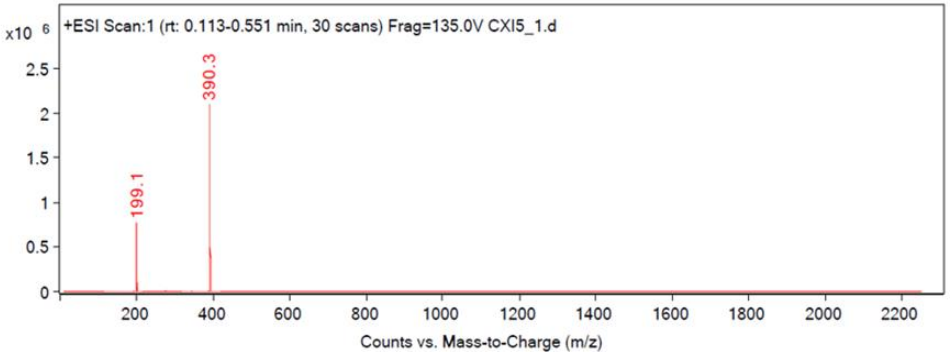
x10 6
+ESI Scan:1 (rt: 0.113-0.551 min, 30 scans) Frag=135.0V CXI5_1.d
390.3
199.1
Counts vs. Mass-to-Charge (m/z)

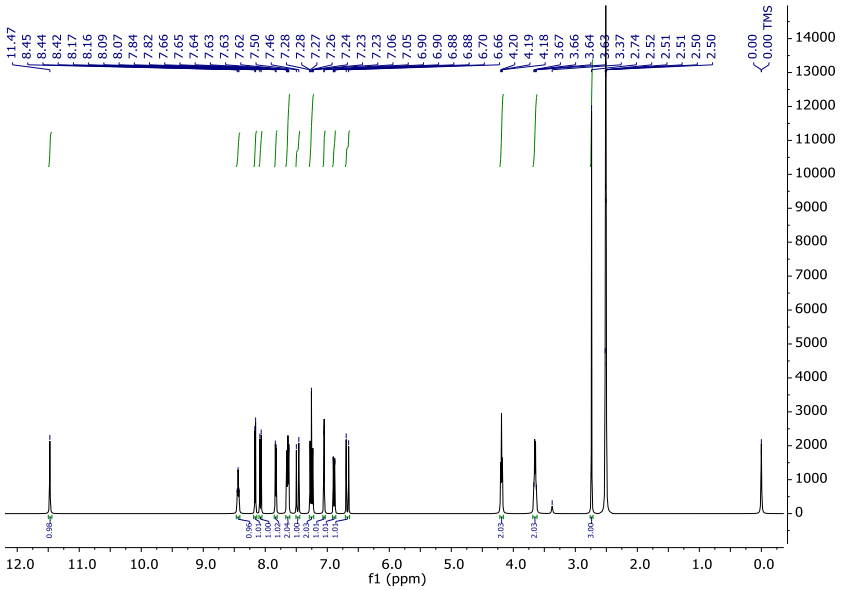
11.47
8.45
8.44
8.42
8.17
8.16
8.09
8.07
7.84
7.82
7.66
7.65
7.64
7.63
7.63
7.62
7.50
7.46
7.28
7.28
7.27
7.26
7.24
7.23
7.23
7.06
7.05
6.90
6.90
6.88
6.88
6.70
6.66
4.20
4.19
4.18
3.67
3.66
3.64
3.63
3.37
2.74
2.52
2.51
2.51
2.50
2.50
0.00
0.00 TMS
f1 (ppm)

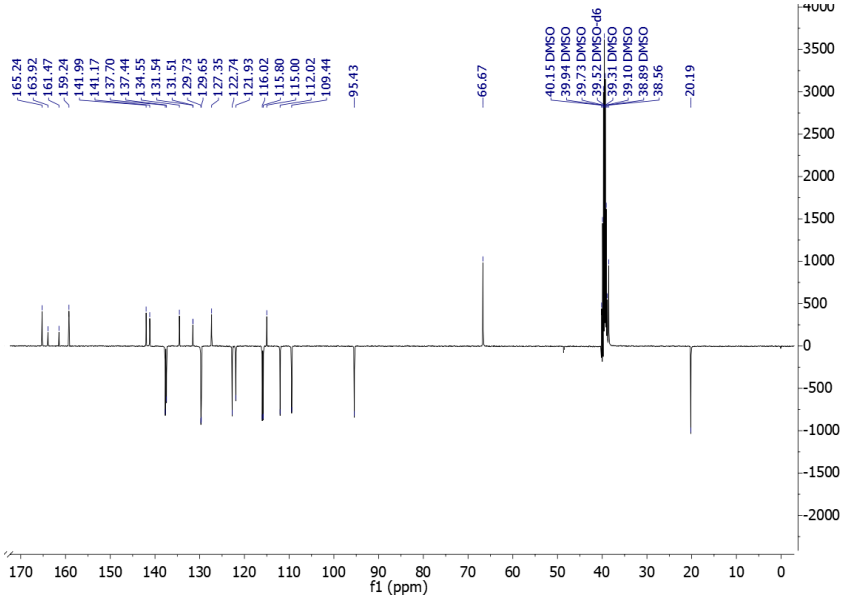
165.24
163.92
161.47
159.24
141.99
141.17
137.70
137.44
134.55
131.54
131.51
129.73
129.65
127.35
122.74
121.93
116.02
115.80
115.00
112.02
109.44
95.43
66.67
40.15 DMSO
39.94 DMSO
39.73 DMSO
39.52 DMSO-d6
39.31 DMSO
39.10 DMSO
38.89 DMSO
38.56
20.19
f1 (ppm)

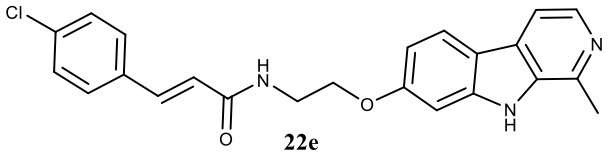
Cl
H
N
O
O
N
H
N

22e

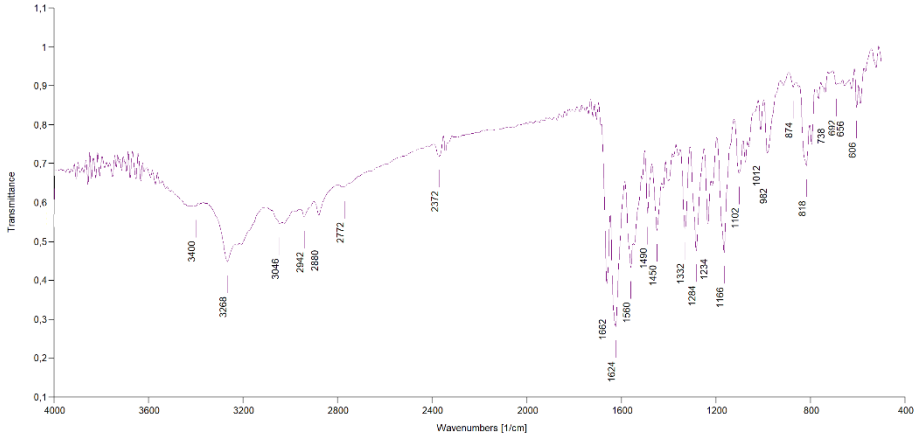
Transmittance
Wavenumbers [1/cm]
3400
3268
3046
2942
2880
2772
2372
1662
1624
1560
1490
1450
1332
1284
1234
1166
1102
1012
982
874
818
738
692
656
606

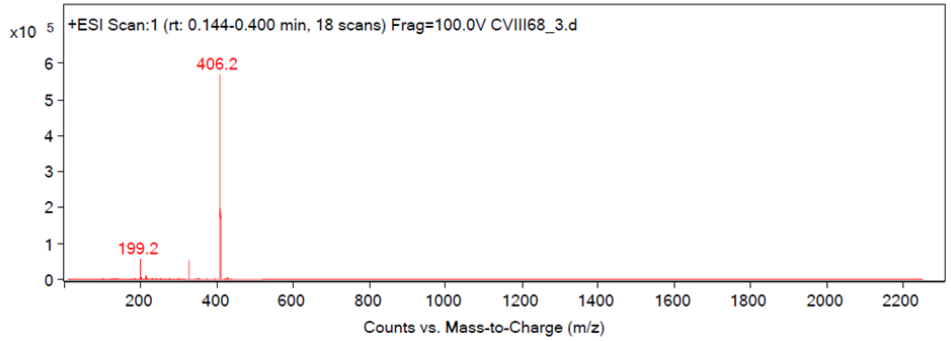
x10 5
+ESI Scan:1 (rt: 0.144-0.400 min, 18 scans) Frag=100.0V CVIII68_3.d
406.2
199.2
Counts vs. Mass-to-Charge (m/z)

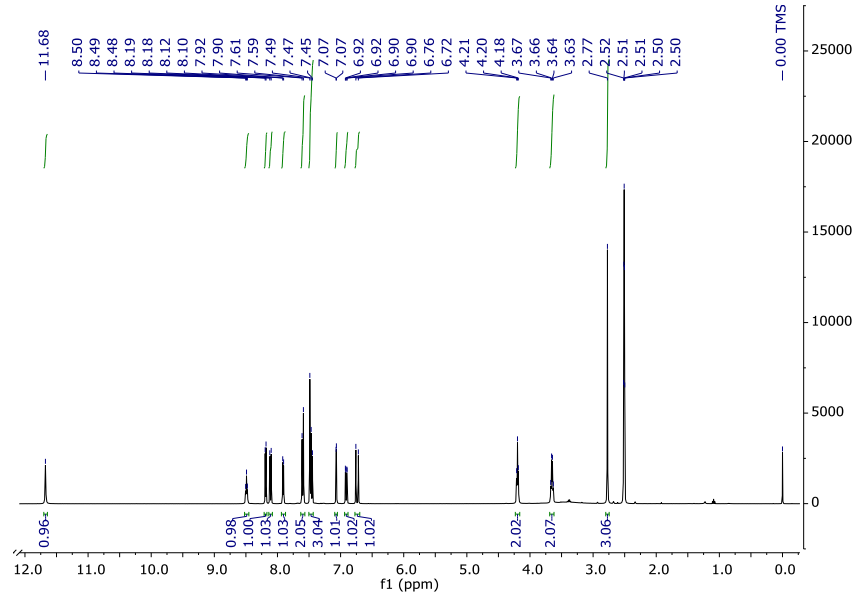
11.68
8.50
8.49
8.48
8.19
8.18
8.12
8.10
7.92
7.90
7.61
7.59
7.49
7.47
7.45
7.07
7.07
6.92
6.92
6.90
6.90
6.76
6.72
4.21
4.20
4.18
3.67
3.66
3.64
3.63
2.77
2.52
2.51
2.51
2.50
2.50
0.00 TMS
0.96
0.98
1.00
1.03
1.03
2.05
3.04
1.01
1.02
1.02
2.02
2.07
3.06
f1 (ppm)

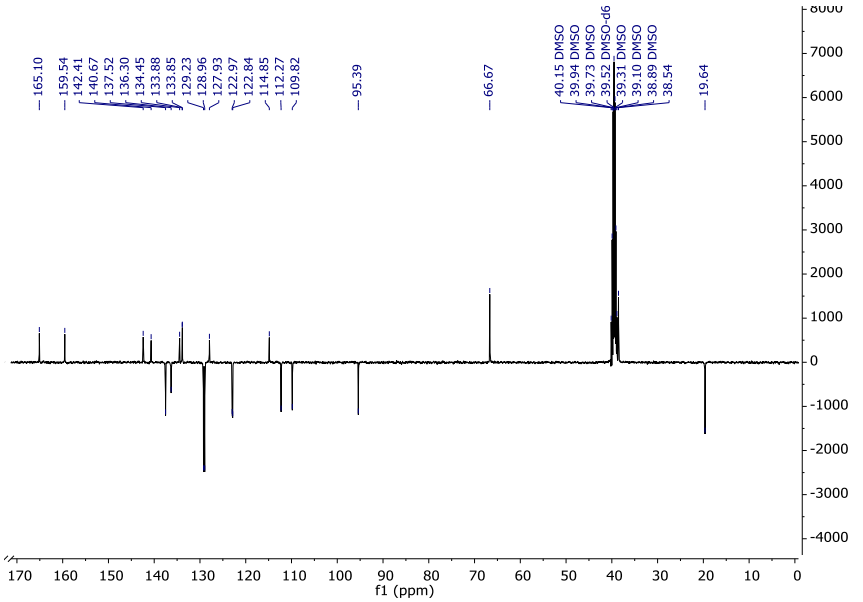
165.10
159.54
142.41
140.67
137.52
136.30
134.45
133.88
133.85
129.23
128.96
127.93
122.97
122.84
114.85
112.27
109.82
95.39
66.67
40.15 DMSO
39.94 DMSO
39.73 DMSO
39.52 DMSO-d6
39.31 DMSO
39.10 DMSO
38.89 DMSO
38.54
19.64
f1 (ppm)

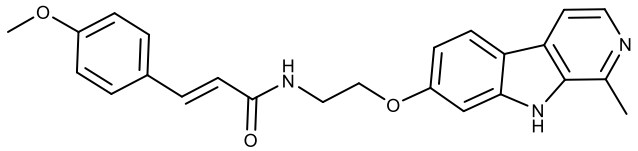

22f

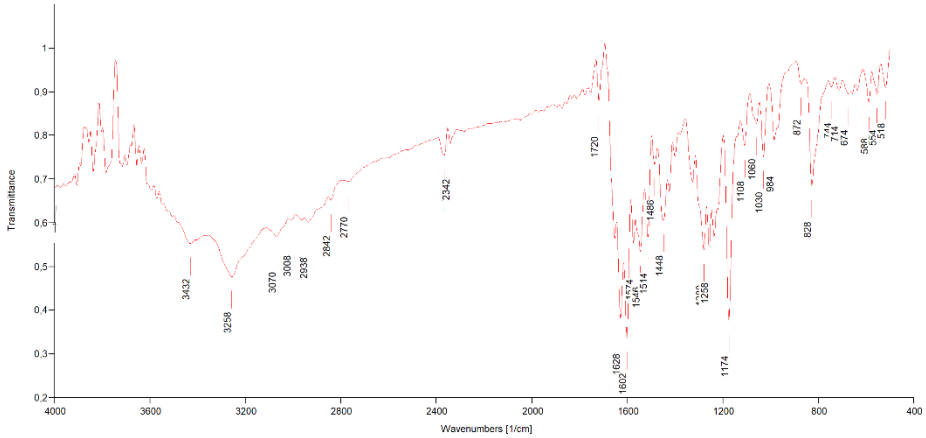
Transmittance
Wavenumbers [1/cm]
3432
3258
3070
3008
2938
2842
2770
2342
1720
1628
1602
1514
1486
1448
1258
1174
1108
1060
1030
984
872
828
774
714
674
588
554
518

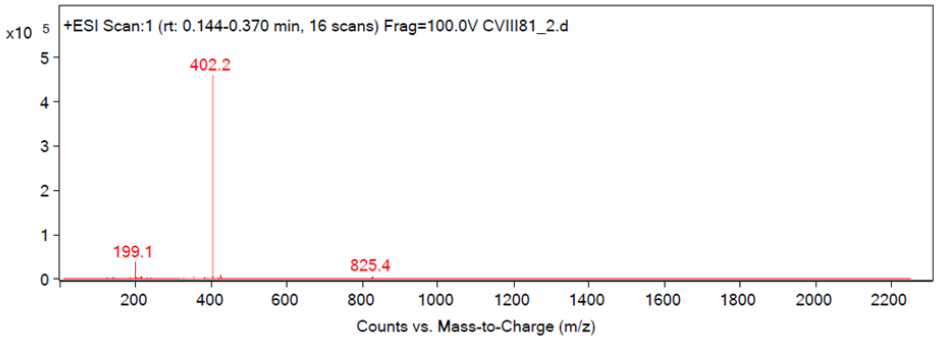
x10 5
+ESI Scan:1 (rt: 0.144-0.370 min, 16 scans) Frag=100.0V CVIII81_2.d
402.2
199.1
825.4
Counts vs. Mass-to-Charge (m/z)

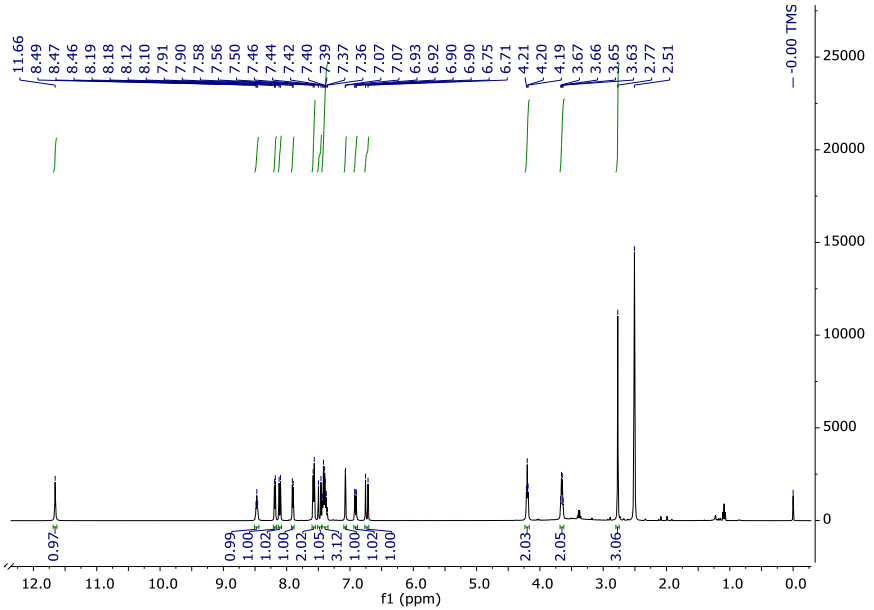
11.66
8.49
8.47
8.46
8.19
8.18
8.12
8.10
7.91
7.90
7.58
7.56
7.50
7.46
7.44
7.42
7.40
7.39
7.37
7.36
7.07
7.07
6.93
6.92
6.90
6.90
6.75
6.71
4.21
4.20
4.19
3.67
3.66
3.65
3.63
2.77
2.51
-0.00 TMS
0.97
0.99
1.00
1.02
1.00
2.02
1.05
3.12
1.00
1.02
1.00
2.03
2.05
3.06
f1 (ppm)

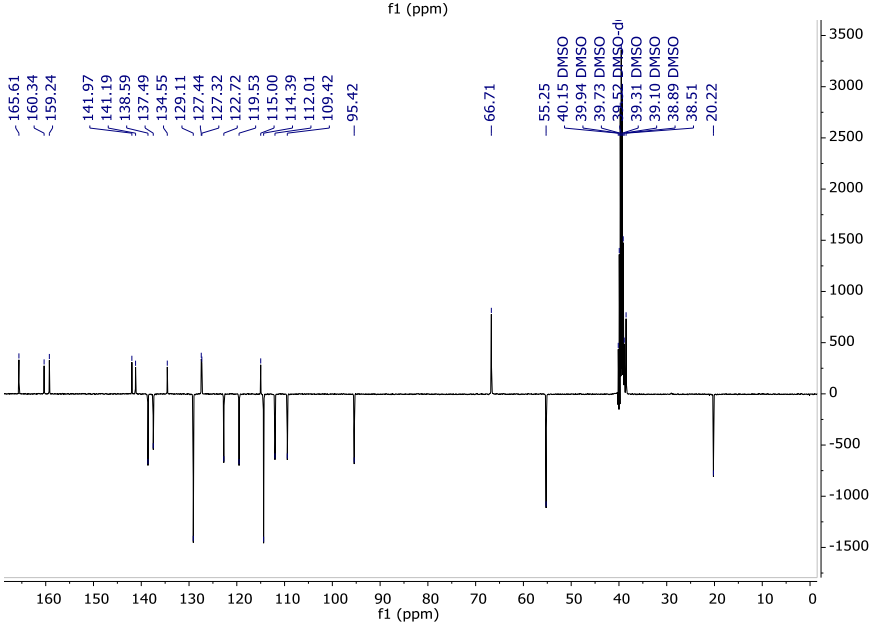
165.61
160.34
159.24
141.97
141.19
138.59
137.49
134.55
129.11
127.44
127.32
122.72
119.53
115.00
114.39
112.01
109.42
95.42
66.71
55.25
40.15 DMSO
39.94 DMSO
39.73 DMSO
39.52 DMSO-d
39.31 DMSO
39.10 DMSO
38.89 DMSO
38.51
20.22
f1 (ppm)

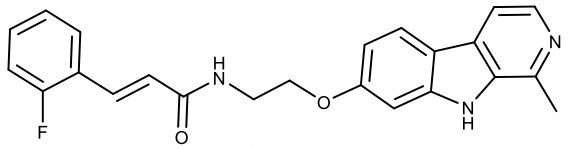

22g

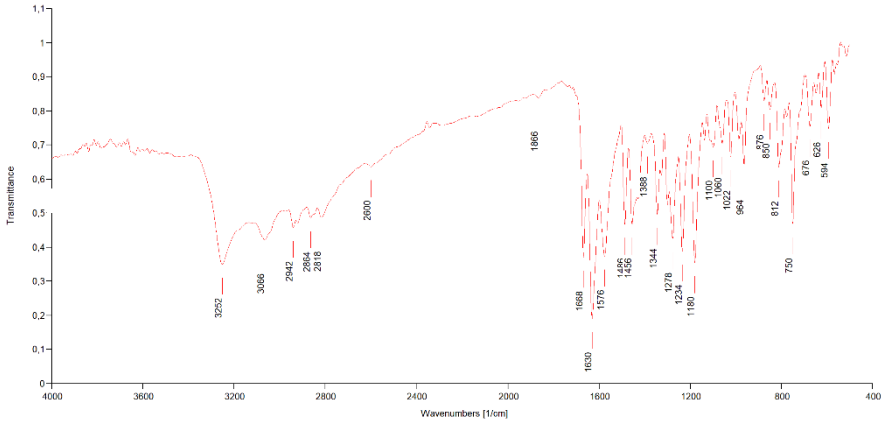
Transmittance
Wavenumbers [1/cm]
3252
3066
2942
2864
2818
2600
1866
1668
1630
1576
1496
1456
1388
1344
1278
1234
1180
1100
1060
1022
964
876
850
812
750
676
626
594

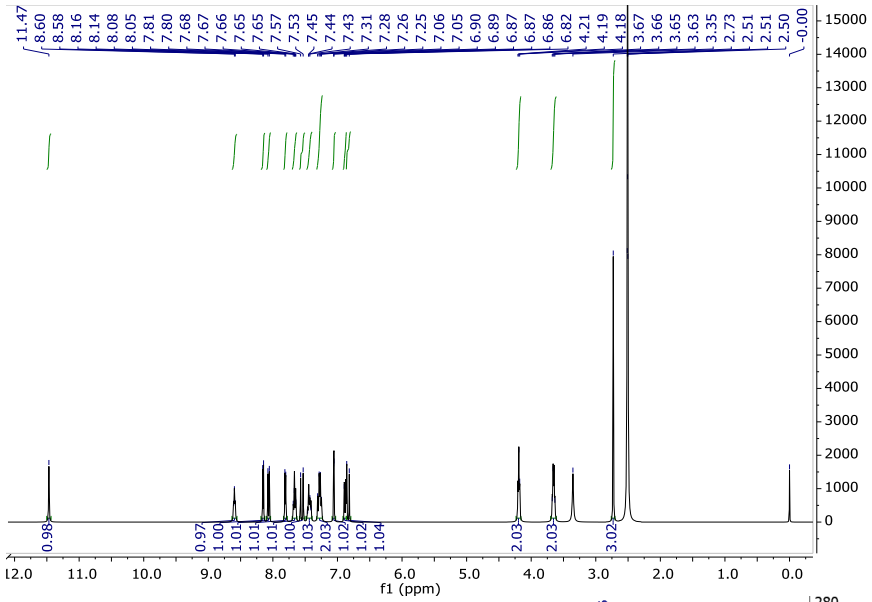
f1 (ppm)
0.98
0.97
1.00
1.01
1.01
1.01
1.00
1.03
2.03
1.02
1.02
1.04
2.03
2.03
3.02

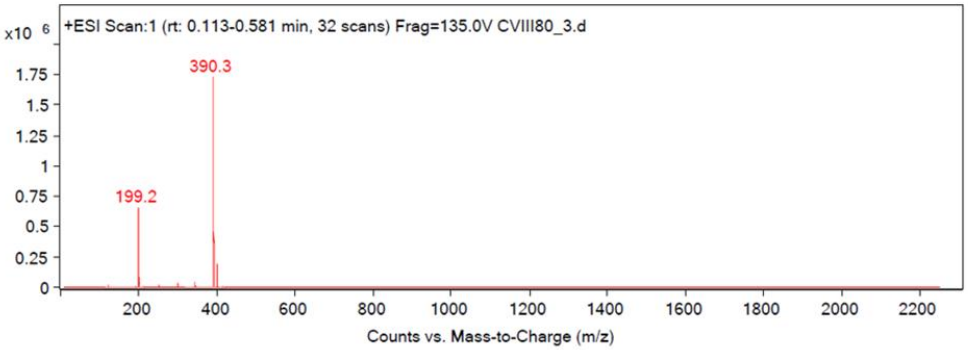
+ESI Scan:1 (rt: 0.113-0.581 min, 32 scans) Frag=135.0V CVIII80_3.d
x10 6
390.3
199.2
Counts vs. Mass-to-Charge (m/z)

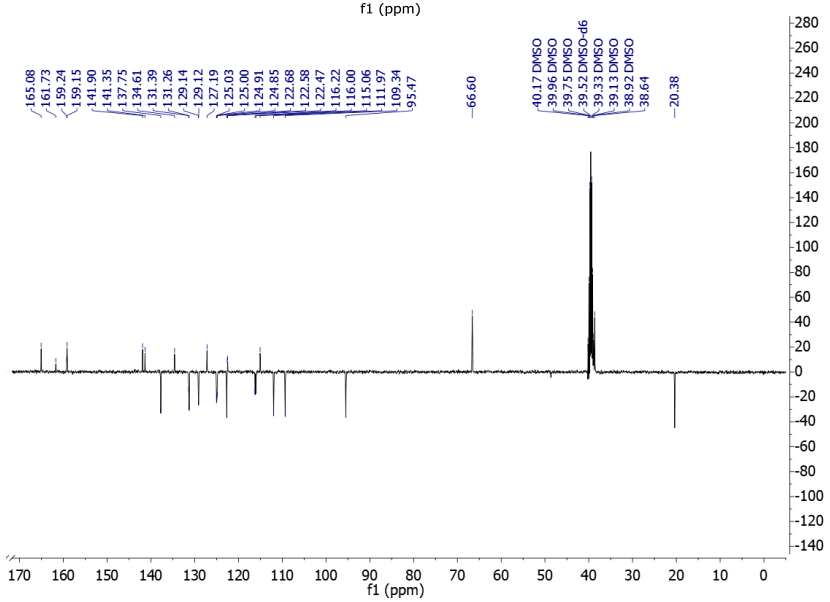
f1 (ppm)
165.08
161.73
159.24
159.15
141.90
141.35
137.75
134.61
131.39
131.26
129.14
129.12
127.19
125.03
125.00
124.91
124.85
122.68
122.58
122.47
116.22
116.00
115.06
111.97
109.34
95.47
66.60
40.17 DMSO
39.96 DMSO
39.75 DMSO
39.52 DMSO-d6
39.33 DMSO
39.13 DMSO
38.92 DMSO
38.64
20.38

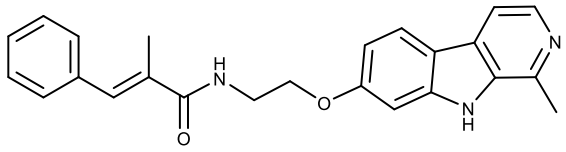

22h

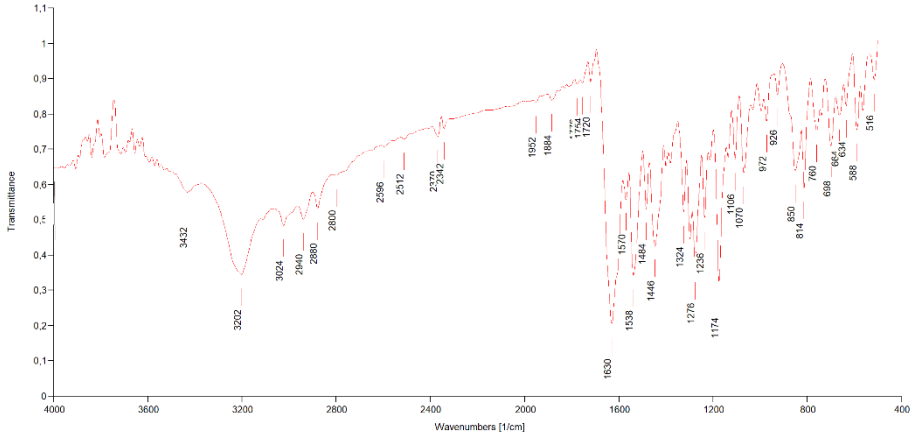
Transmittance
Wavenumbers [1/cm]
3432
3202
3024
2940
2880
2800
2598
2512
2370
2342
1952
1884
1754
1720
1630
1570
1538
1484
1446
1324
1276
1236
1174
1106
1070
972
926
850
814
760
698
664
634
588
516

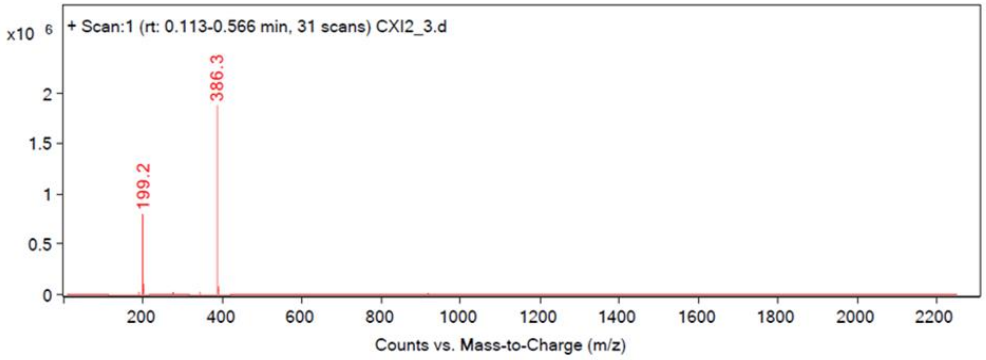
x10 6
+ Scan:1 (rt: 0.113-0.566 min, 31 scans) CXI2_3.d
386.3
199.2
Counts vs. Mass-to-Charge (m/z)

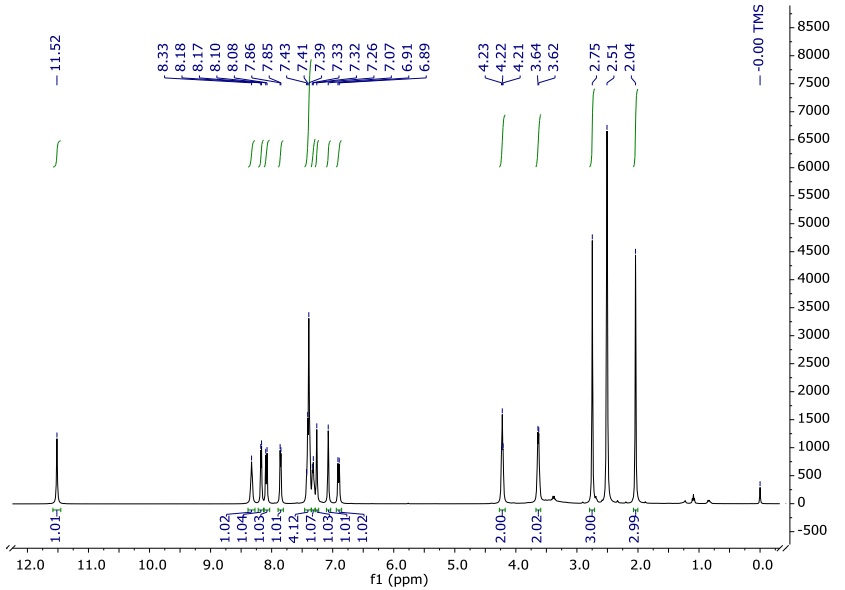
11.52
8.33
8.18
8.17
8.10
8.08
7.86
7.85
7.43
7.41
7.39
7.33
7.32
7.26
7.07
6.91
6.89
4.23
4.22
4.21
3.64
3.62
2.75
2.51
2.04
0.00 TMS
1.01
1.02
1.04
1.03
1.01
4.12
1.07
1.03
1.01
1.02
2.00
2.02
3.00
2.99
f1 (ppm)

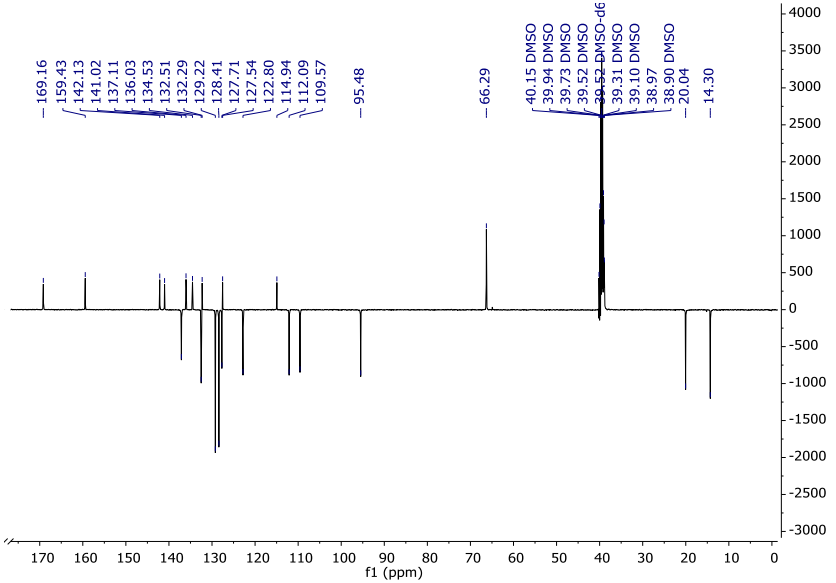
169.16
159.43
142.13
141.02
137.11
136.03
134.53
132.51
132.29
129.22
128.41
127.71
127.54
122.80
114.94
112.09
109.57
95.48
66.29
40.15 DMSO
39.94 DMSO
39.73 DMSO
39.52 DMSO
39.52 DMSO-d6
39.31 DMSO
39.10 DMSO
38.97
38.90 DMSO
20.04
14.30
f1 (ppm)

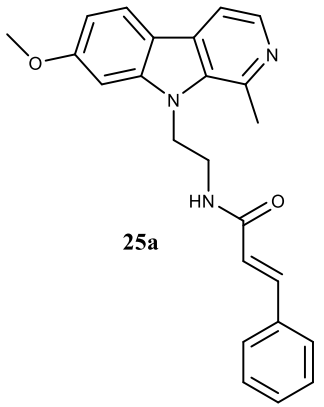
O
N
N
HN
O

25a

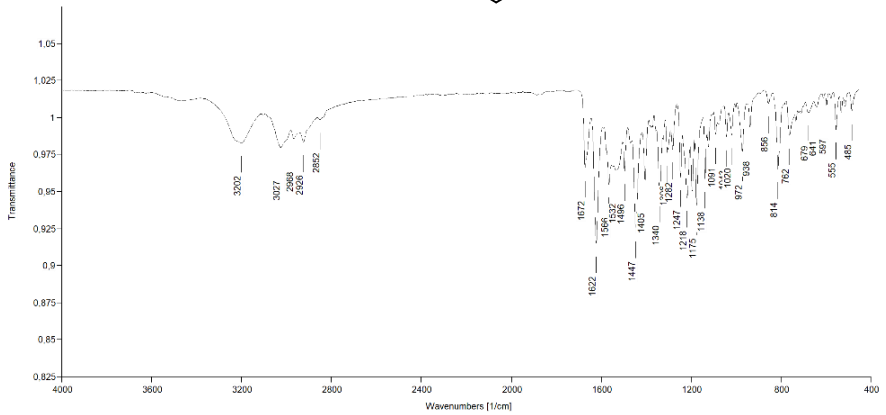
Transmittance
Wavenumbers [1/cm]
3202
3027
2908
2836
2852
1672
1622
1566
1497
1496
1447
1405
1340
1262
1247
1218
1175
1138
1091
1053
1020
972
938
856
814
762
679
641
597
555
485

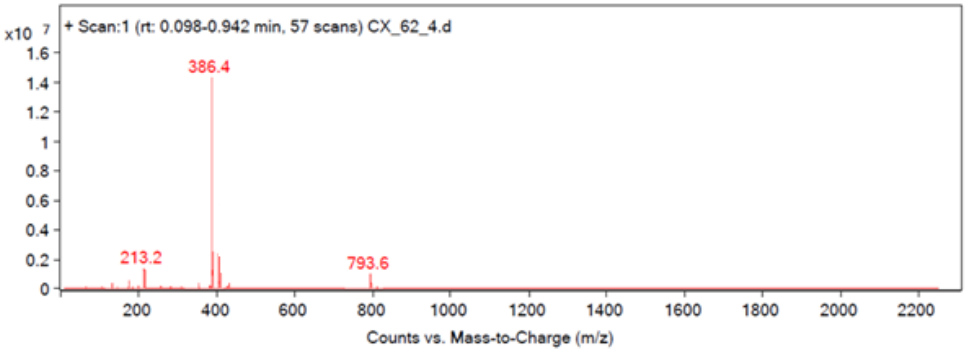
x10 7
+ Scan:1 (rt: 0.098-0.942 min, 57 scans) CX_62_4.d
386.4
213.2
793.6
Counts vs. Mass-to-Charge (m/z)

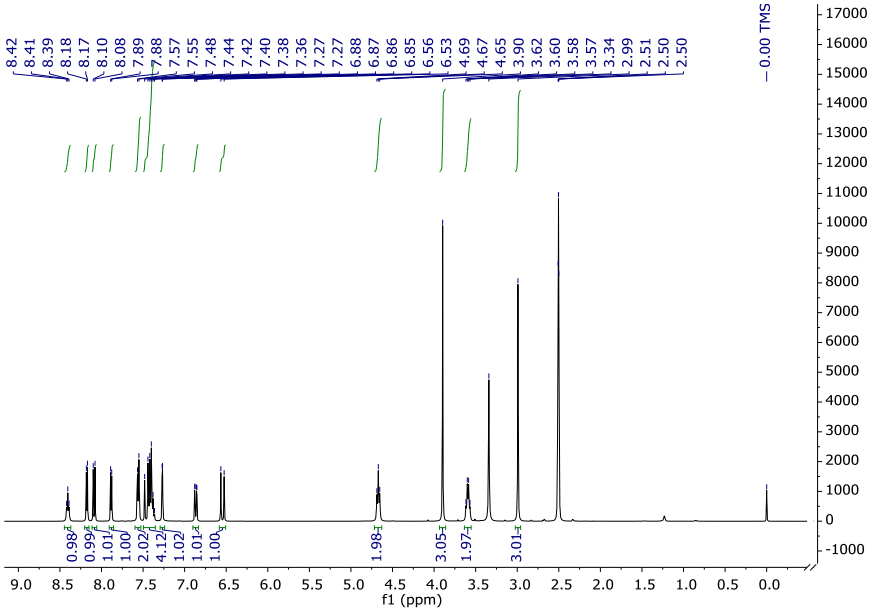
8.42
8.41
8.39
8.18
8.17
8.10
8.08
7.89
7.88
7.57
7.55
7.48
7.44
7.42
7.40
7.38
7.36
7.27
7.27
6.88
6.87
6.86
6.85
6.56
6.53
4.69
4.67
4.65
3.90
3.62
3.60
3.58
3.57
3.34
2.99
2.51
2.50
2.50
0.00 TMS
0.98
0.99
1.01
1.00
2.02
4.12
1.02
1.01
1.00
1.98
3.05
1.97
3.01
f1 (ppm)

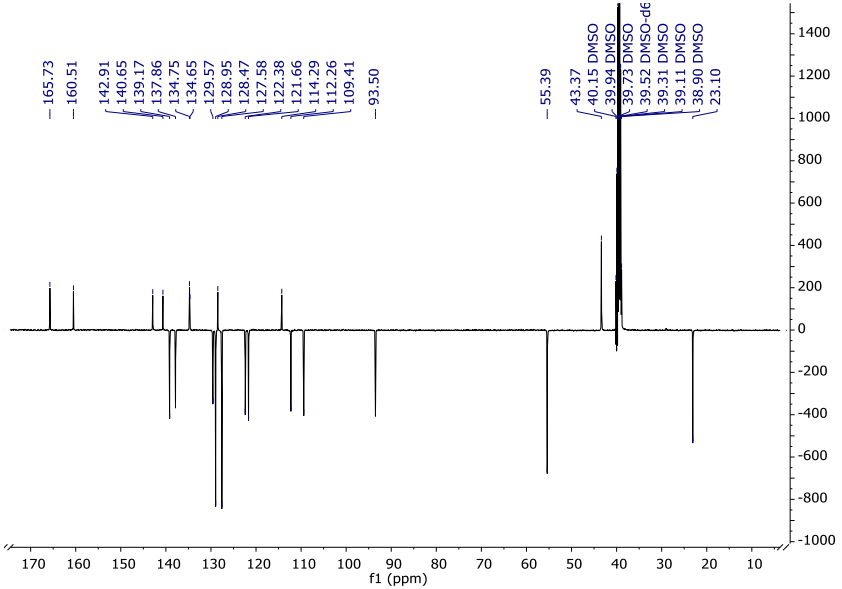
165.73
160.51
142.91
140.65
139.17
137.86
134.75
134.65
129.57
128.95
128.47
127.58
122.38
121.66
114.29
112.26
109.41
93.50
55.39
43.37
40.15 DMSO
39.94 DMSO
39.73 DMSO
39.52 DMSO-d6
39.31 DMSO
39.11 DMSO
38.90 DMSO
23.10
f1 (ppm)

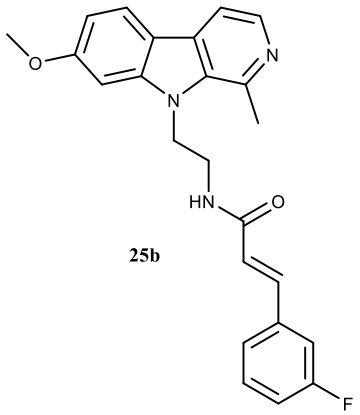
O
N
N
HN
O
F

25b

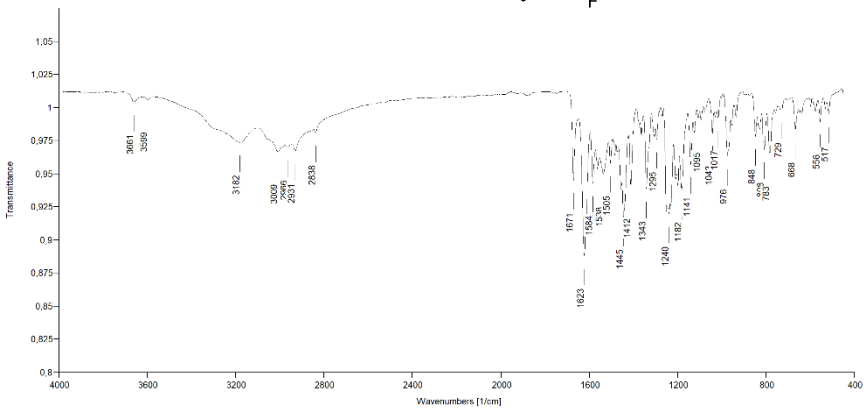
Transmittance
Wavenumbers [1/cm]
3661
3599
3182
3069
2969
2931
2838
1671
1623
1584
1535
1505
1445
1412
1343
1295
1240
1182
1141
1095
1017
976
848
829
783
729
668
556
517

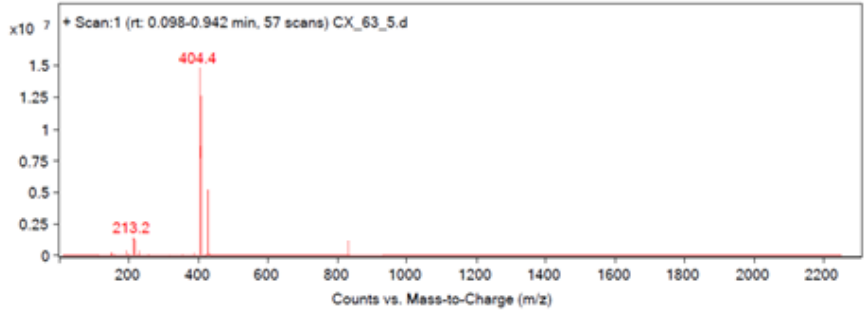
x10 7
+ Scan:1 (rt: 0.098-0.942 min, 57 scans) CX_63_5.d
404.4
213.2
Counts vs. Mass-to-Charge (m/z)

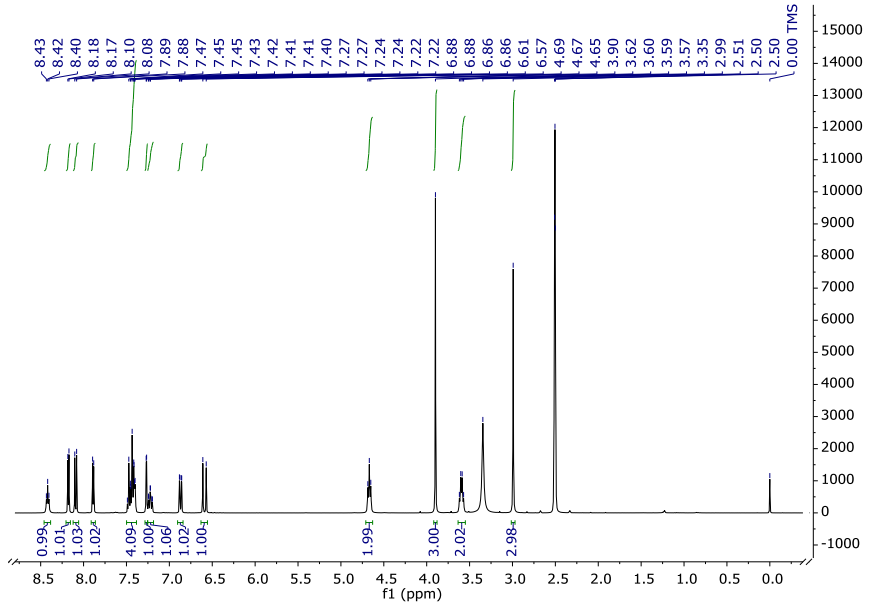
8.43
8.42
8.40
8.18
8.17
8.10
8.08
7.89
7.88
7.47
7.45
7.45
7.43
7.42
7.41
7.41
7.40
7.27
7.27
7.24
7.24
7.22
7.22
6.88
6.88
6.86
6.86
6.61
6.57
4.69
4.67
4.65
3.90
3.62
3.60
3.59
3.57
3.35
2.99
2.51
2.50
2.50
0.00 TMS
0.99
1.01
1.03
1.02
4.09
1.00
1.06
1.02
1.00
1.99
3.00
2.02
2.98
f1 (ppm)

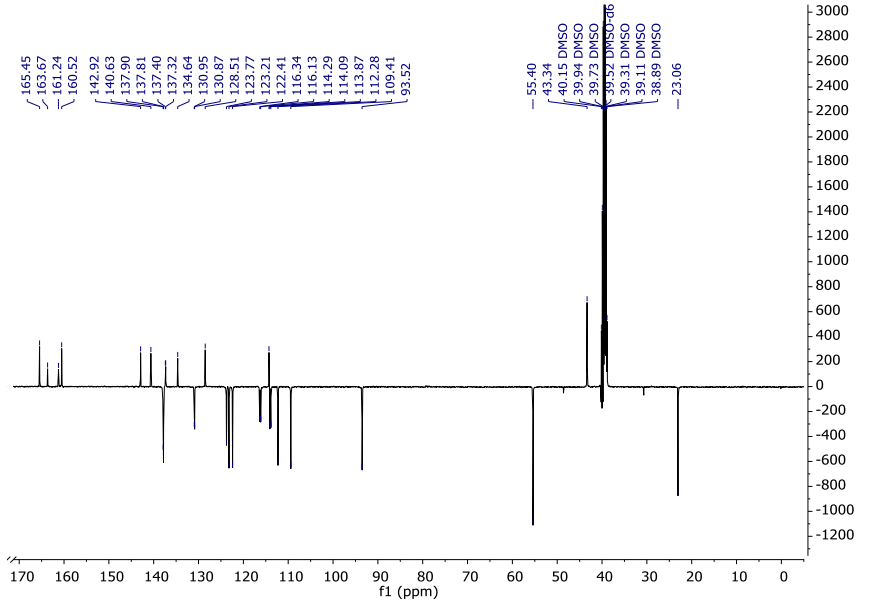
165.45
163.67
161.24
160.52
142.92
140.63
137.90
137.81
137.40
137.32
134.64
130.95
130.87
128.51
123.77
123.21
122.41
116.34
116.13
114.29
114.09
113.87
112.28
109.41
93.52
55.40
43.34
40.15 DMSO
39.94 DMSO
39.73 DMSO
39.52 DMSO-d6
39.31 DMSO
39.11 DMSO
38.89 DMSO
23.06
f1 (ppm)

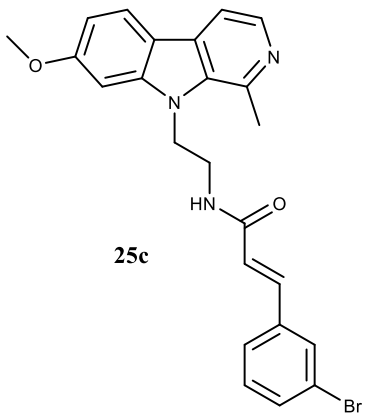
O
N
N
HN
O
Br

25c

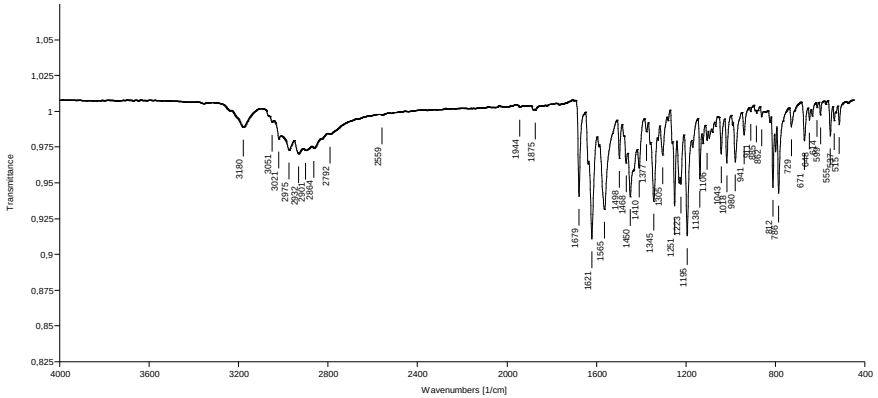
Transmittance
Wavenumbers [1/cm]

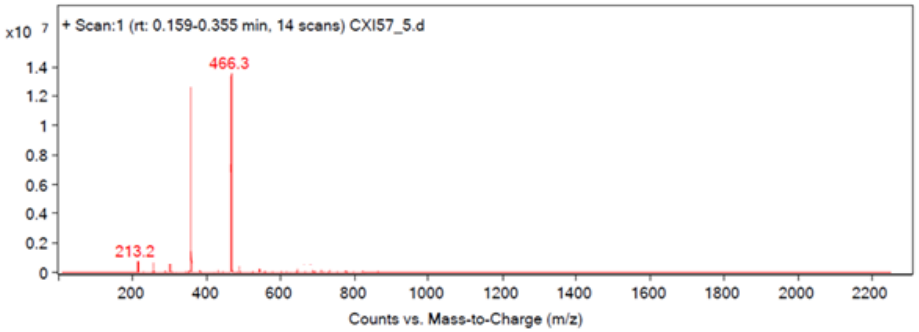
x10 7
+ Scan:1 (rt: 0.159-0.355 min, 14 scans) CXI57_5.d
466.3
213.2
Counts vs. Mass-to-Charge (m/z)

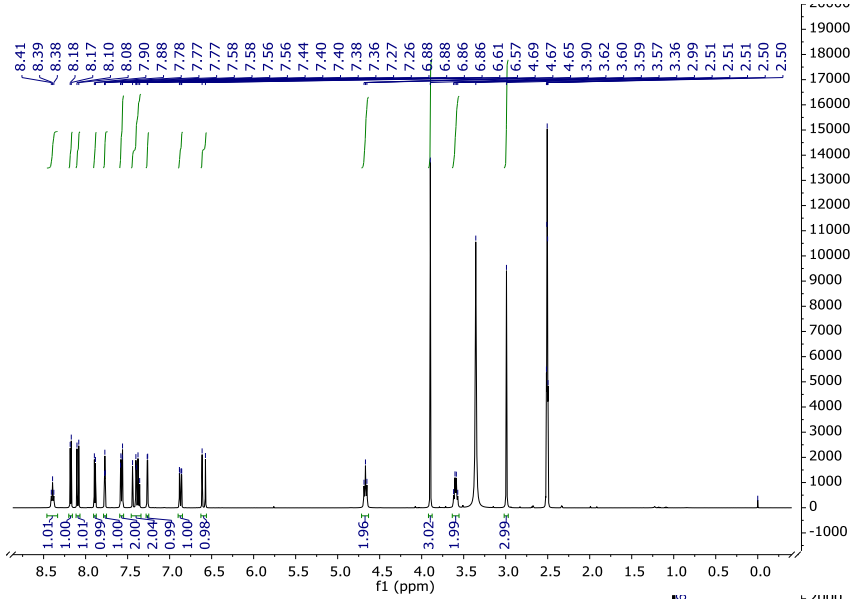
f1 (ppm)

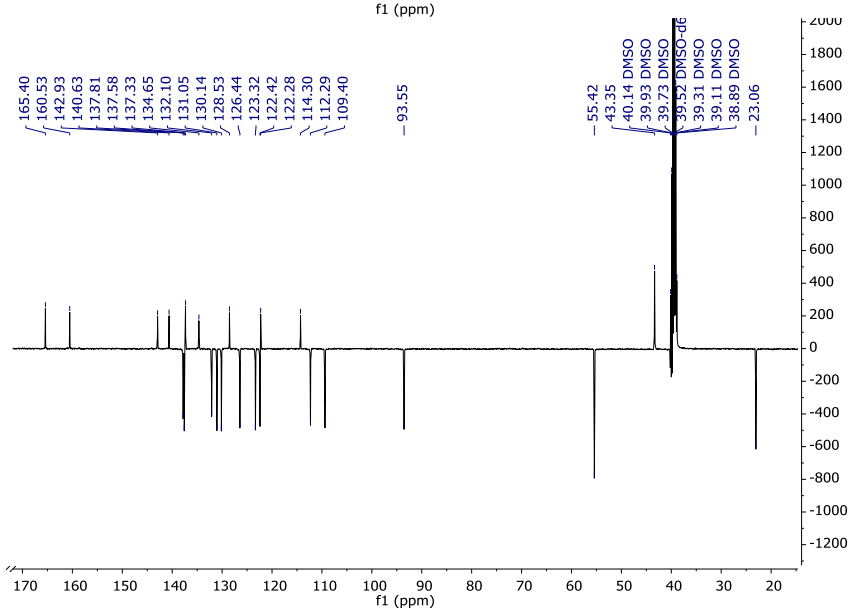
f1 (ppm)

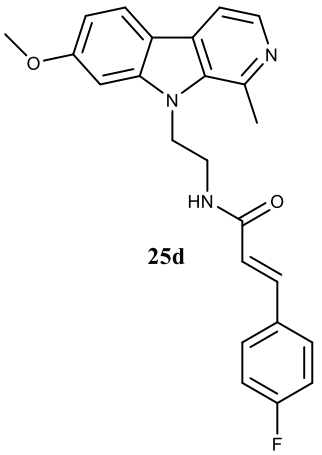
O
N
N
HN
O
F

25d

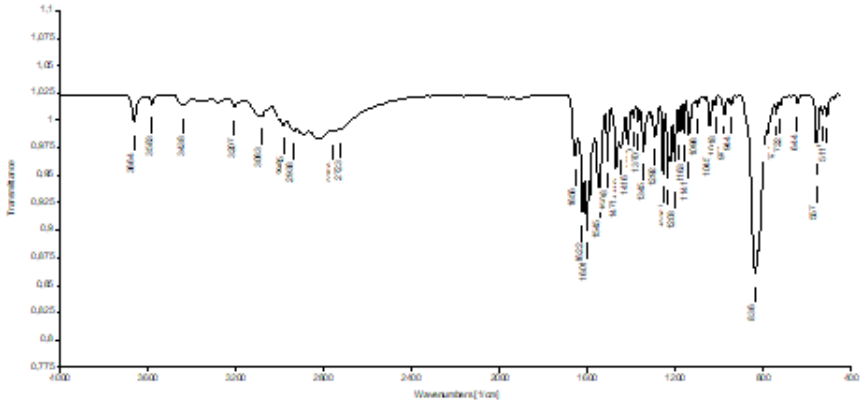
Transmittance
Wavenumbers[1/cm]

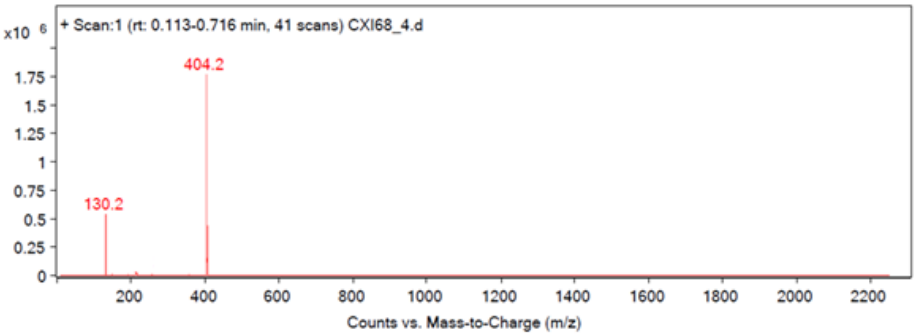
x10 6
+ Scan:1 (rt: 0.113-0.716 min, 41 scans) CXI68_4.d
404.2
130.2
Counts vs. Mass-to-Charge (m/z)

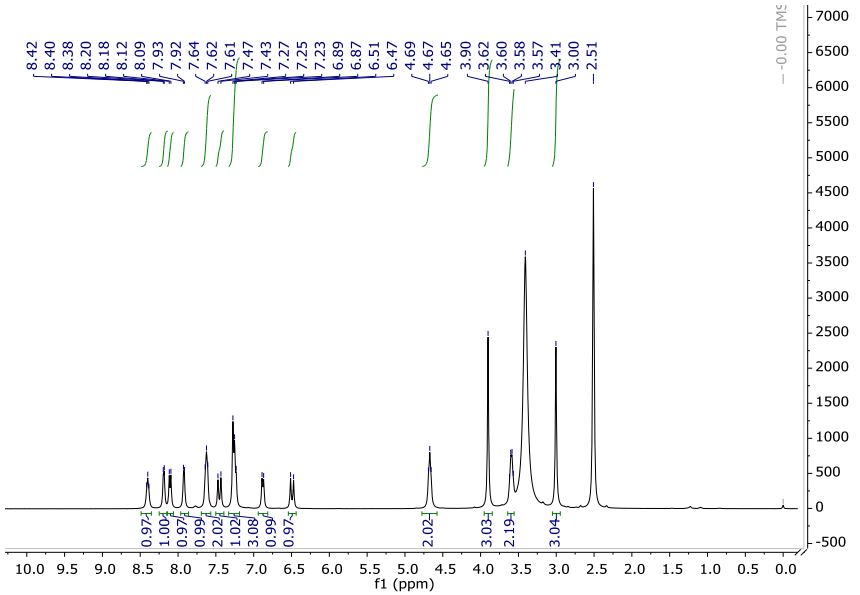
f1 (ppm)

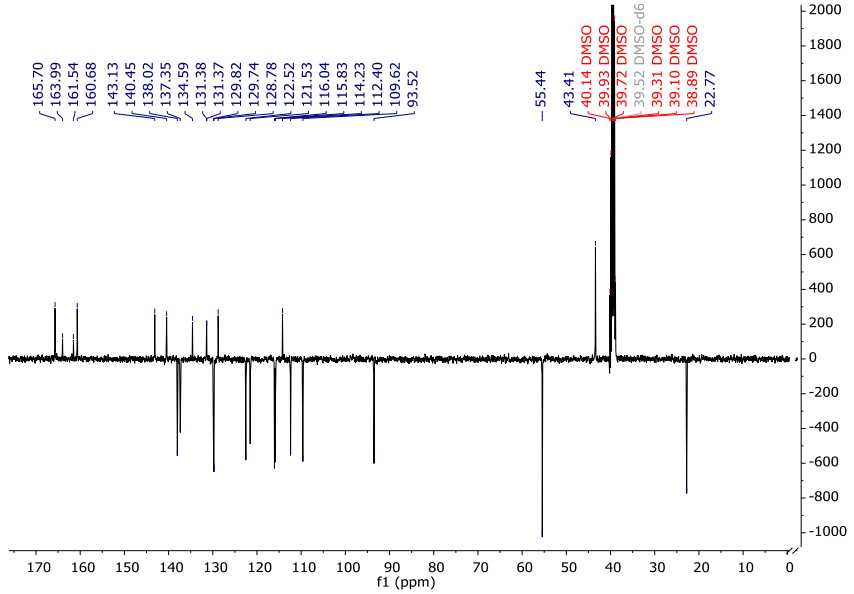
f1 (ppm)

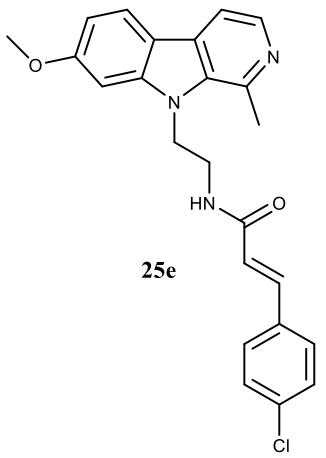
O
N
N
HN
O
Cl

25e

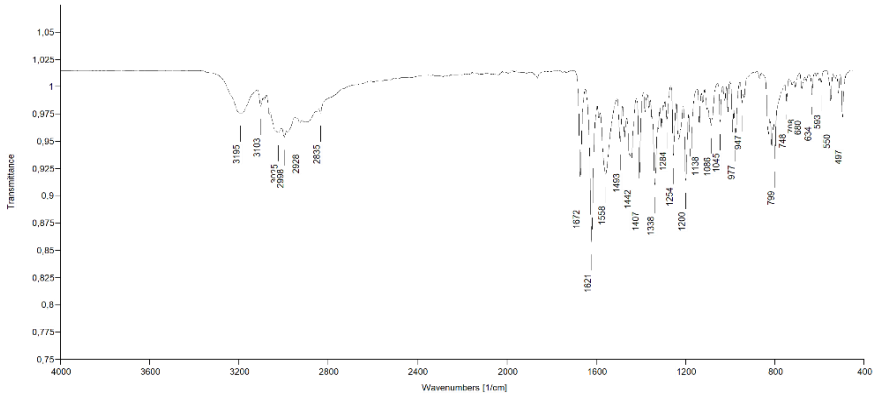
Transmittance
Wavenumbers [1/cm]
3195
3103
2915
2908
2928
2835
1872
1621
1558
1493
1442
1407
1338
1284
1254
1200
1138
1085
1045
977
947
799
748
660
634
550
497

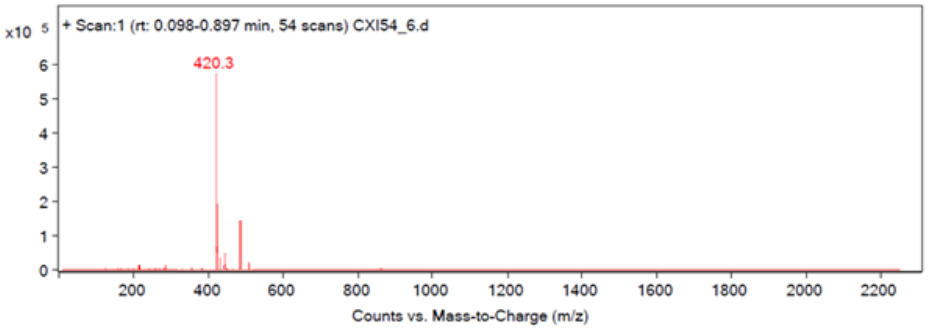
x10
+ Scan:1 (rt: 0.098-0.897 min, 54 scans) CXI54_6.d
420.3
Counts vs. Mass-to-Charge (m/z)

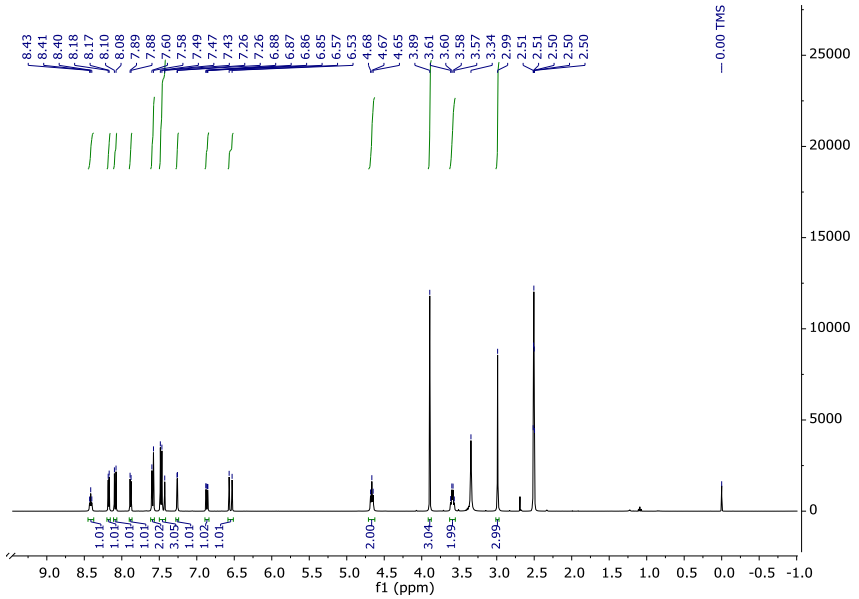
0.00 TMS
f1 (ppm)

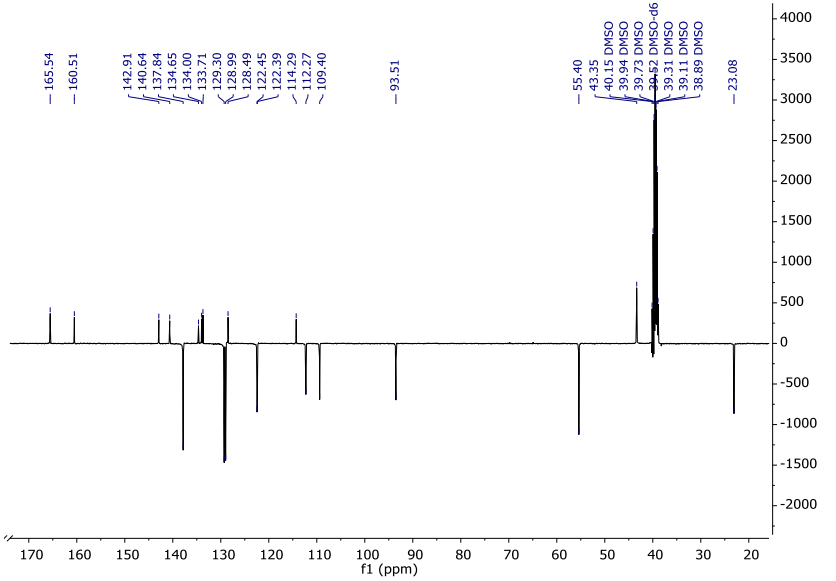
DMSO
DMSO-d6
f1 (ppm)

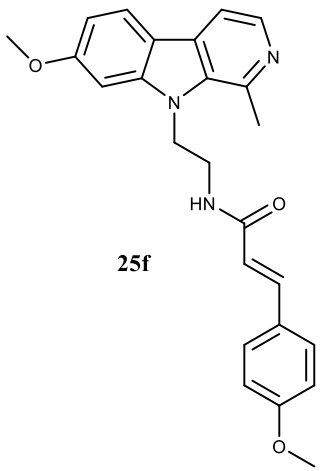
O
N
N
HN
O
O

25f

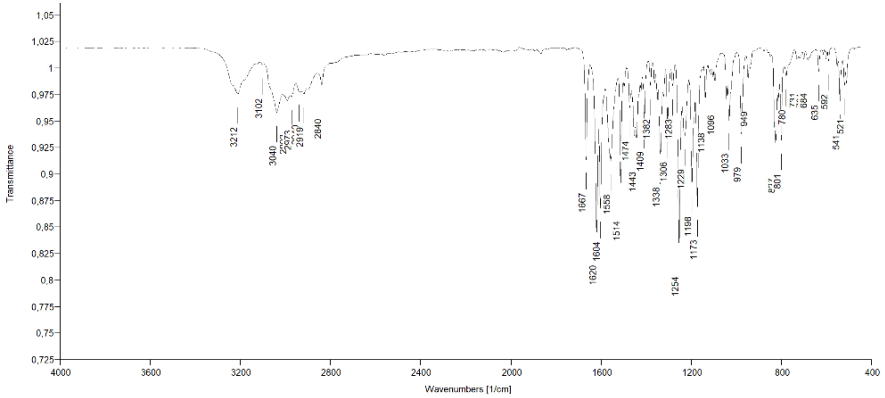
Transmittance
Wavenumbers [1/cm]
3212
3102
3040
2973
2919
2840
1667
1620
1604
1558
1514
1474
1443
1409
1382
1338
1306
1269
1229
1198
1173
1138
1096
1033
979
949
877
801
780
731
694
635
592
541
521
1254

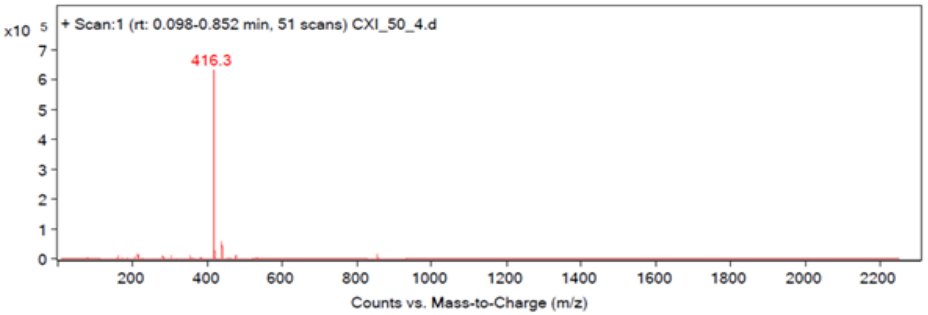
x10 5
+ Scan:1 (rt: 0.098-0.852 min, 51 scans) CXI_50_4.d
416.3
Counts vs. Mass-to-Charge (m/z)

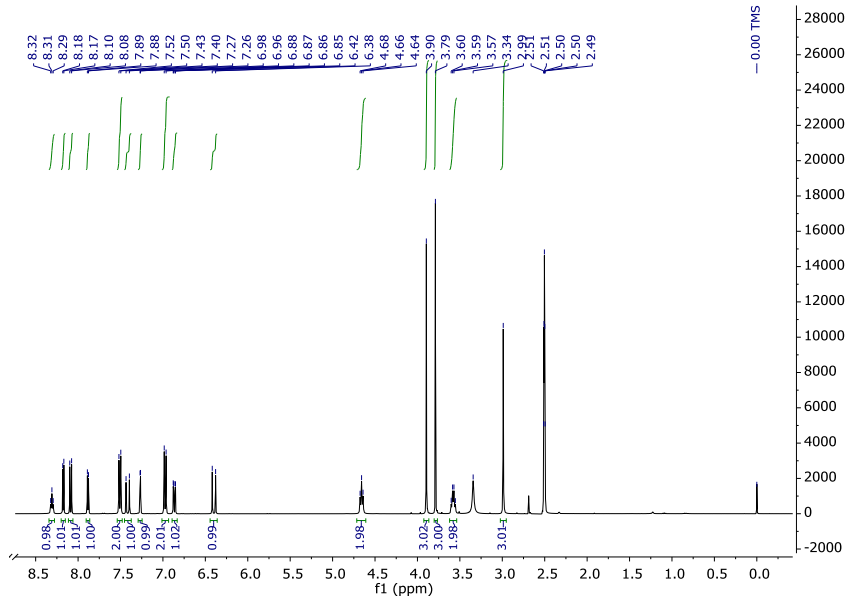
8.32
8.31
8.29
8.18
8.17
8.10
8.08
7.89
7.88
7.52
7.50
7.43
7.40
7.27
7.26
6.98
6.96
6.88
6.87
6.86
6.85
6.42
6.38
4.68
4.66
4.64
3.90
3.79
3.60
3.59
3.57
3.34
2.51
2.50
2.50
2.49
0.00 TMS
0.98
1.01
1.01
1.00
2.00
1.00
0.99
2.01
1.02
0.99
1.98
3.02
3.00
1.98
3.01
f1 (ppm)

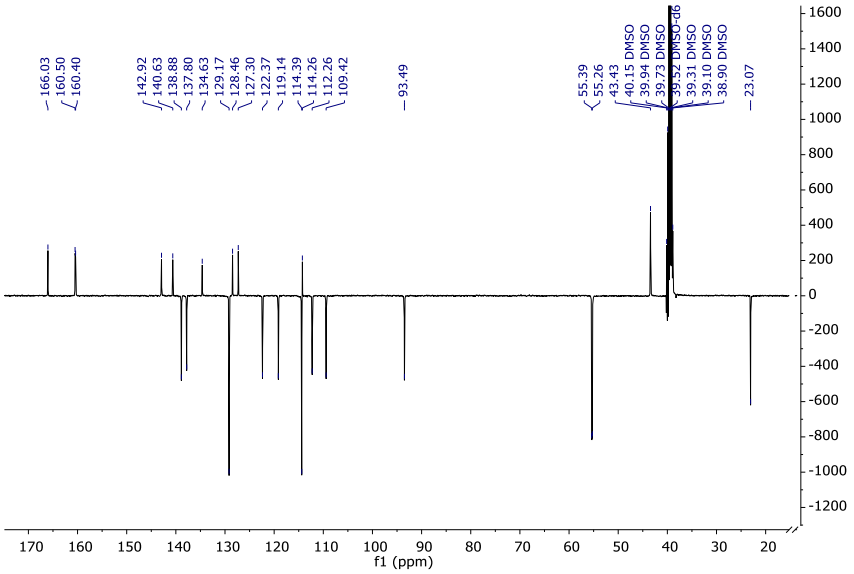
166.03
160.50
160.40
142.92
140.63
138.88
137.80
134.63
129.17
128.46
127.30
122.37
119.14
114.39
114.26
112.26
109.42
93.49
55.39
55.26
43.43
40.15 DMSO
39.94 DMSO
39.73 DMSO
39.52 DMSO-d6
39.31 DMSO
39.10 DMSO
38.90 DMSO
23.07
f1 (ppm)

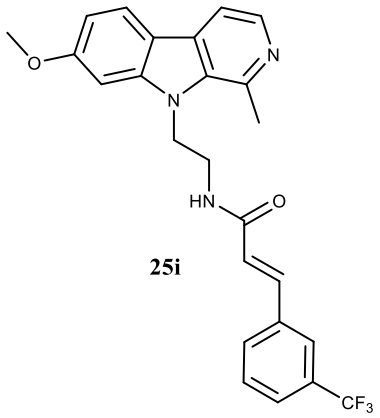
O
N
N
HN
O
CF3

25i

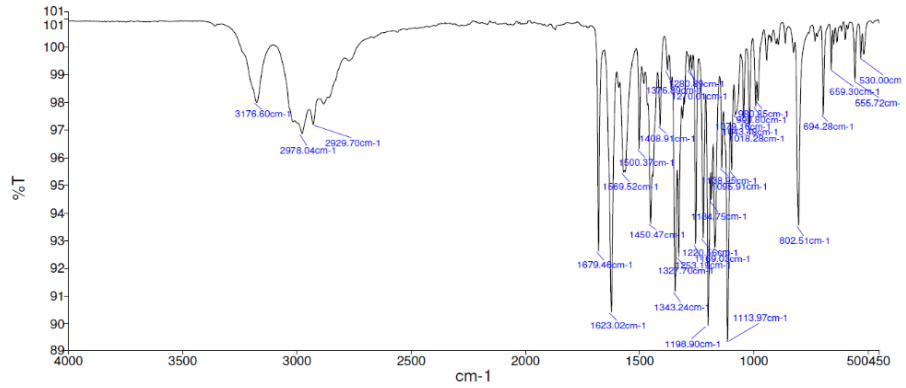
%T
cm-1
3176.60cm-1
2978.04cm-1
2929.70cm-1
1679.46cm-1
1623.02cm-1
1450.47cm-1
1343.24cm-1
1198.90cm-1
1113.97cm-1
802.51cm-1
694.28cm-1
659.30cm-1
555.72cm-1
530.00cm

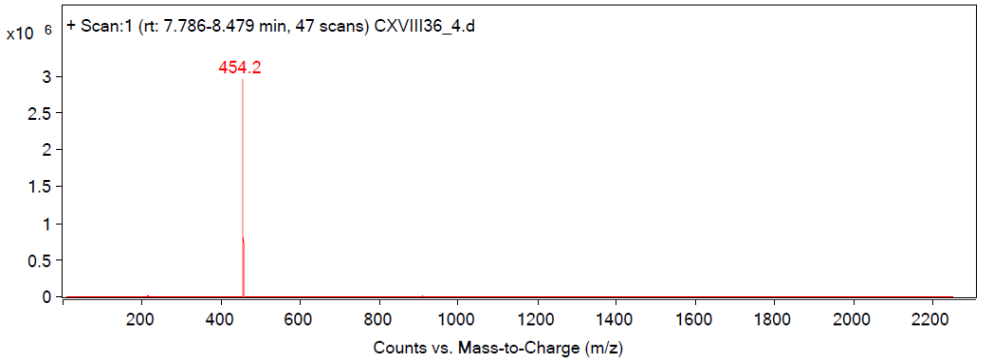
+ Scan:1 (rt: 7.786-8.479 min, 47 scans) CXVIII36_4.d
x10 6
454.2
Counts vs. Mass-to-Charge (m/z)

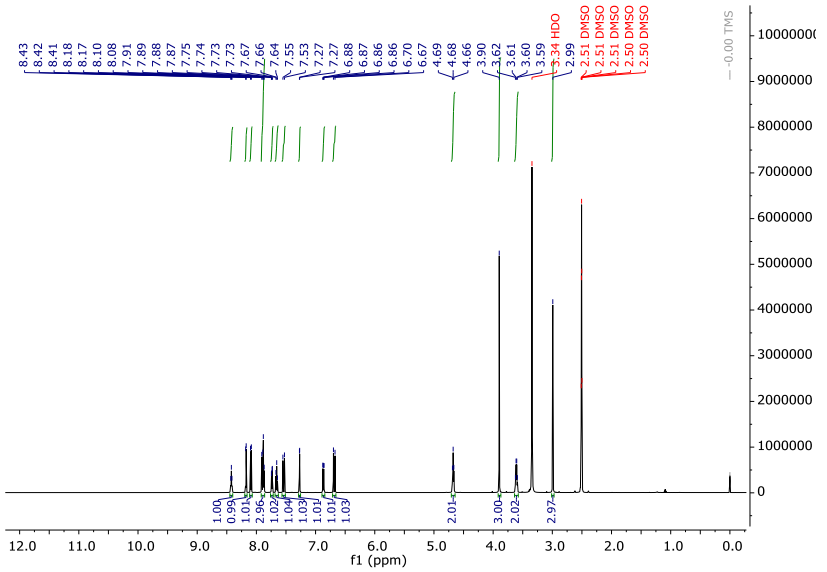
f1 (ppm)

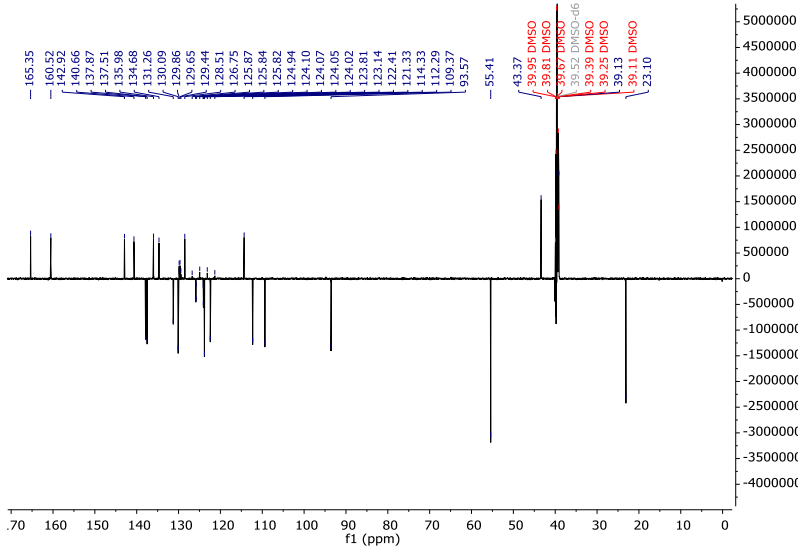
f1 (ppm)

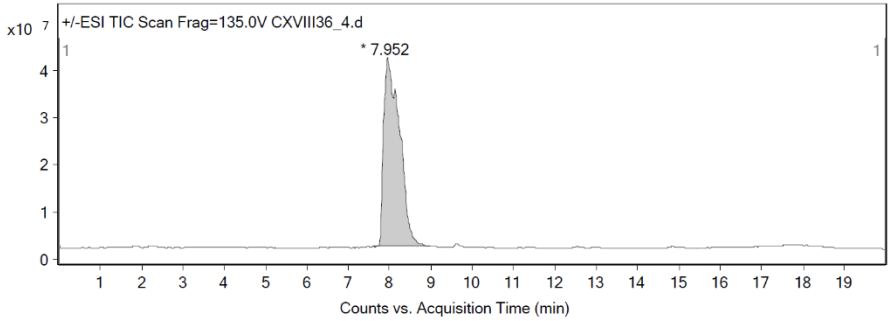

Integration Peak List

Peak	Start	RT	End	Height	Area	Area %
1	7.62	7.952	8.977	39933813.93	1078870199.24	100

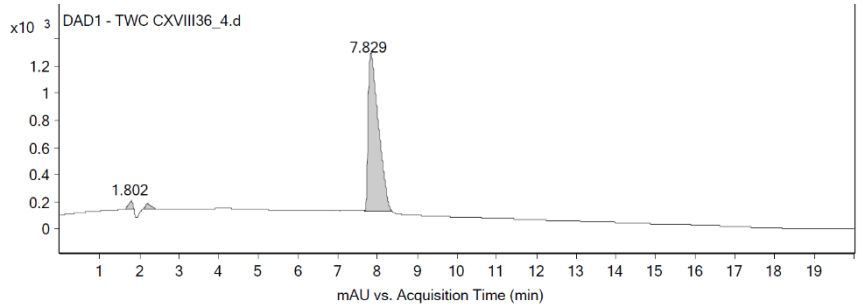

Integration Peak List

Peak	Start	RT	End	Height	Area	Area %
1	1.642	1.802	1.856	61.07	415.1	1.99
2	2.089	2.202	2.389	37.76	345.95	1.66
3	7.682	7.829	8.364	1155.8	20895.2	100

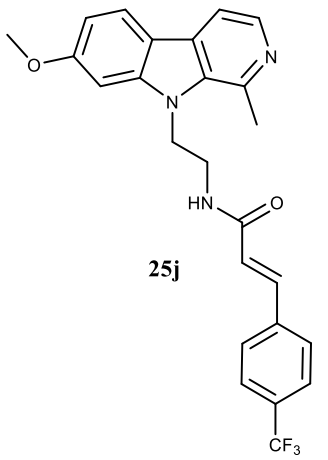
O
N
N
HN
O
CF3

25j

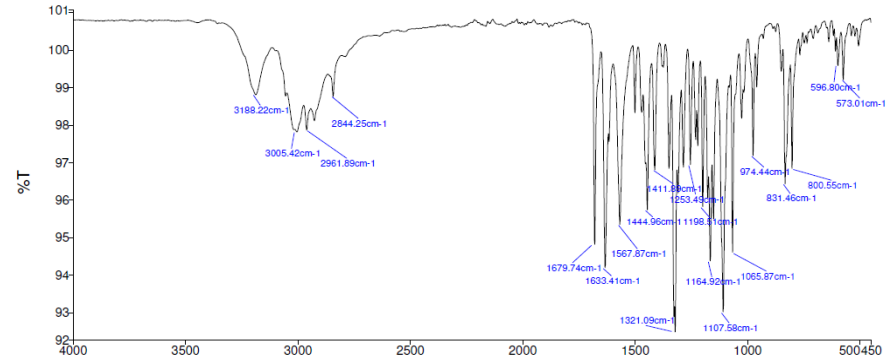
%T
3188.22cm-1
3005.42cm-1
2961.89cm-1
2844.25cm-1
1679.74cm-1
1633.41cm-1
1567.87cm-1
1444.96cm-1
1411.88cm-1
1321.09cm-1
1253.49cm-1
1198.31cm-1
1164.92cm-1
1107.58cm-1
1065.87cm-1
974.44cm-1
831.46cm-1
800.55cm-1
596.80cm-1
573.01cm-1

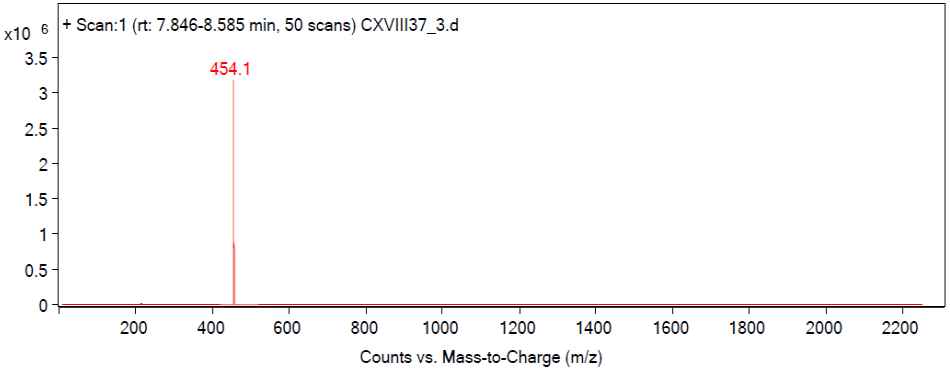
+ Scan:1 (rt: 7.846-8.585 min, 50 scans) CXVIII37_3.d
x10 6
454.1
Counts vs. Mass-to-Charge (m/z)

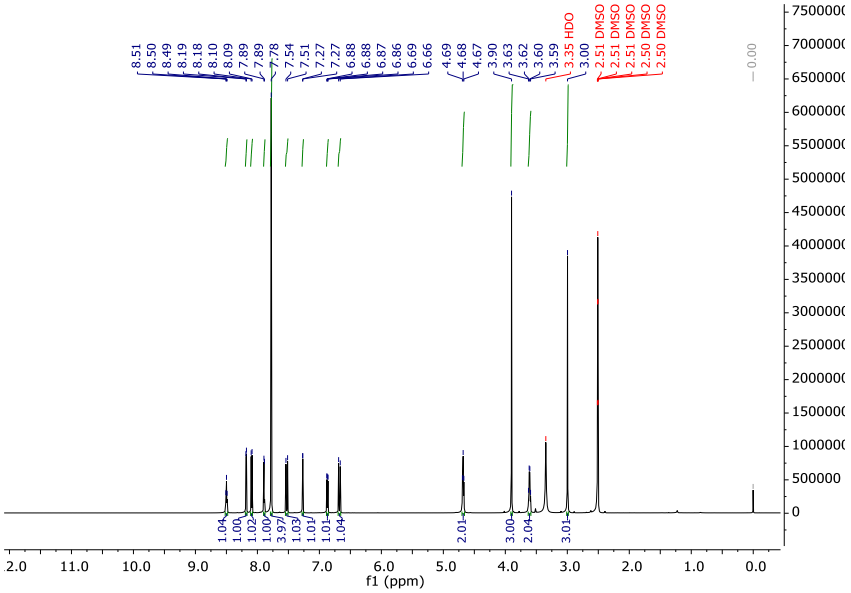
8.51
8.50
8.49
8.19
8.18
8.10
8.09
7.89
7.89
7.78
7.54
7.51
7.27
7.27
6.88
6.88
6.87
6.86
6.69
6.66
4.69
4.68
4.67
3.90
3.63
3.62
3.60
3.59
3.35 HDO
3.00
2.51 DMSO
2.51 DMSO
2.51 DMSO
2.50 DMSO
2.50 DMSO
f1 (ppm)

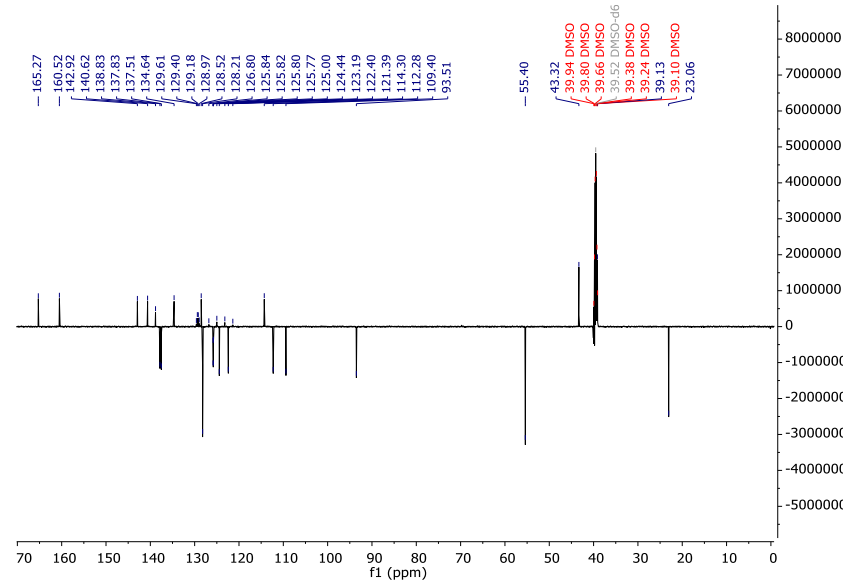
165.27
160.52
142.92
140.62
138.83
137.83
137.51
134.64
129.61
129.40
129.18
128.97
128.52
128.21
126.80
125.84
125.82
125.80
125.77
125.00
124.44
123.19
122.40
121.39
114.30
112.28
109.40
93.51
55.40
43.32
39.94 DMSO
39.80 DMSO
39.66 DMSO
39.52 DMSO-d6
39.38 DMSO
39.24 DMSO
39.13
39.10 DMSO
23.06
f1 (ppm)

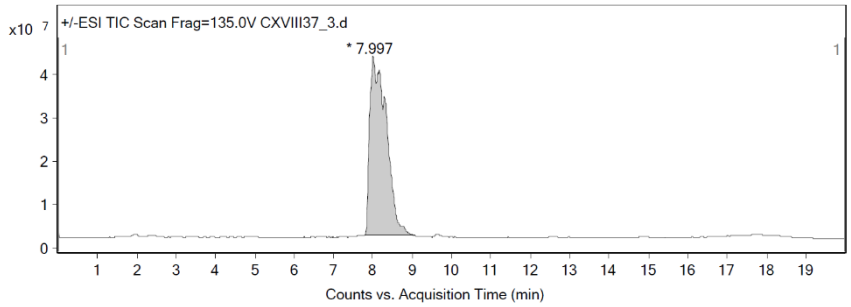

Integration Peak List

Peak	Start	RT	End	Height	Area	Area %
1	7.786	7.997	9.067	41241284.59	1225928227.28	100

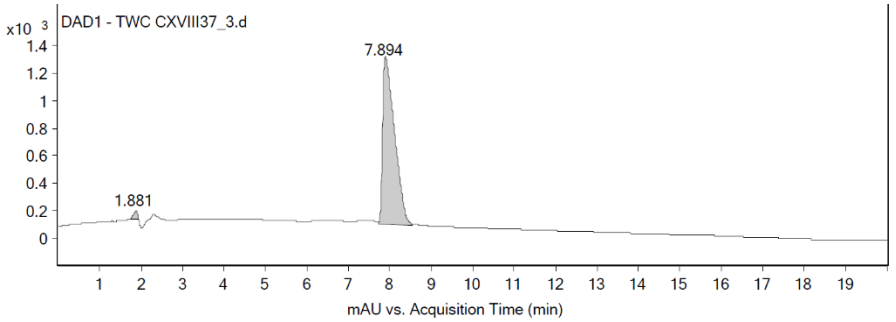

Integration Peak List

Peak	Start	RT	End	Height	Area	Area %
1	1.754	1.881	1.936	60.31	416.8	1.72
2	7.728	7.894	8.534	1216.78	24279.93	100

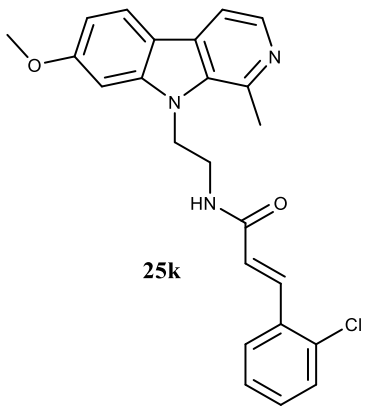

25k

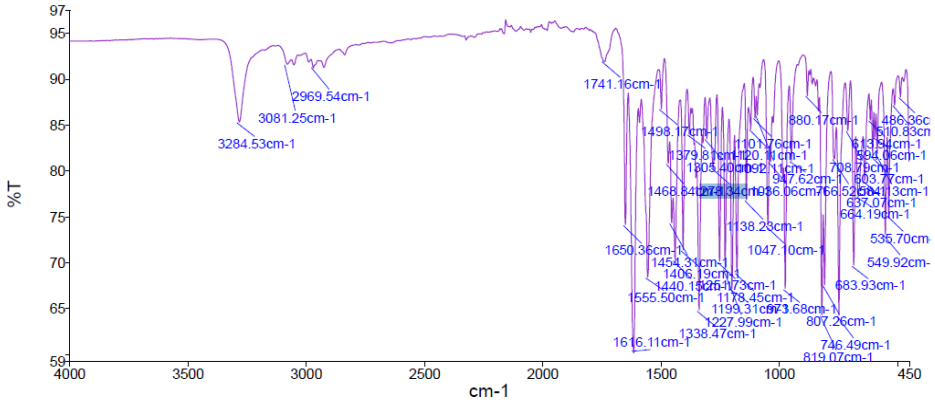

Line#:1 R.Time:----(Scan#:----)
MassPeaks:5
Spectrum Mode:Averaged 0.367-0.433(23-27) Base Peak:420(7452311)
BG Mode:Calc Segment 1 - Event 1

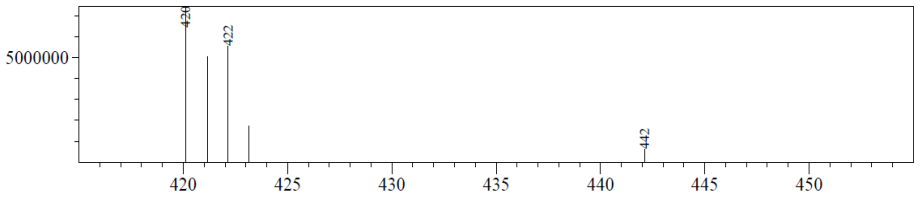

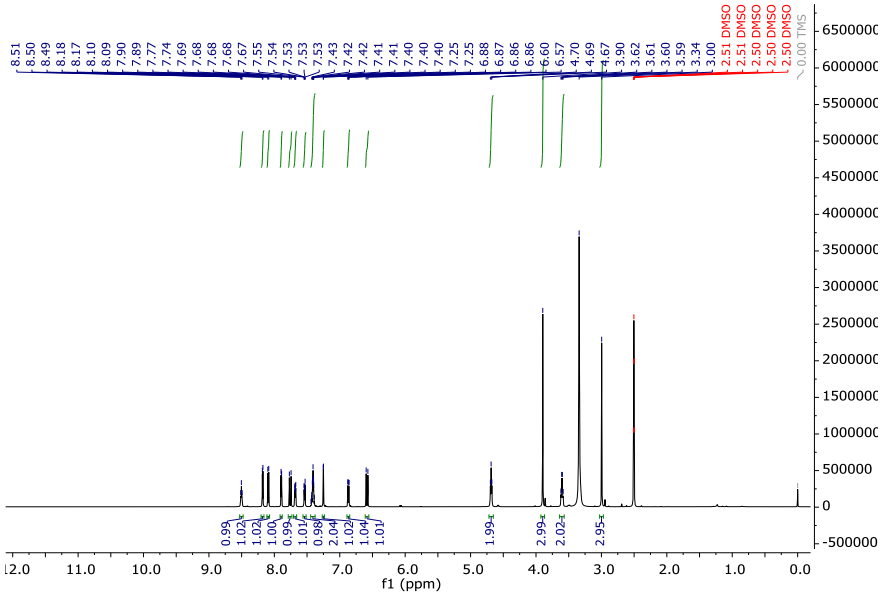

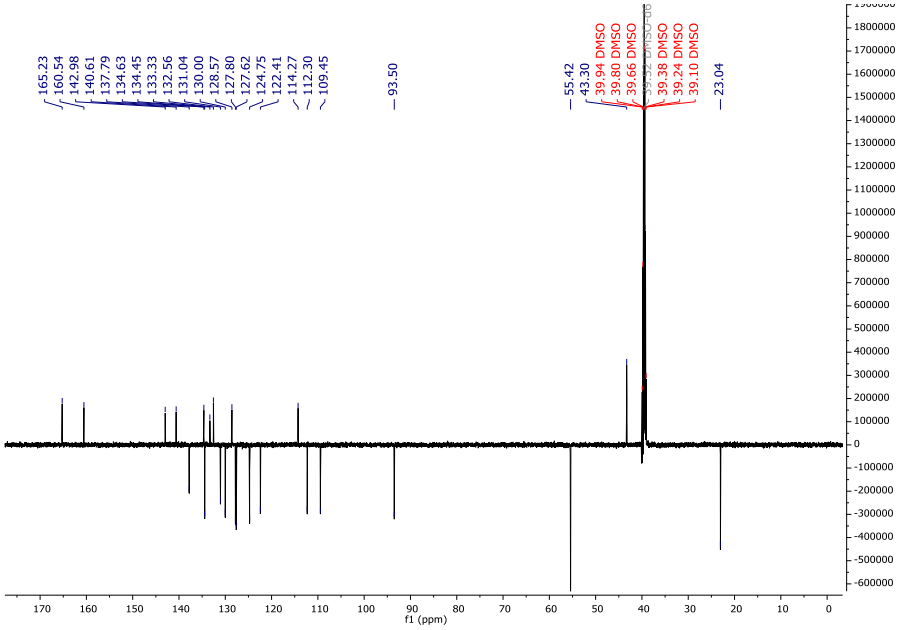

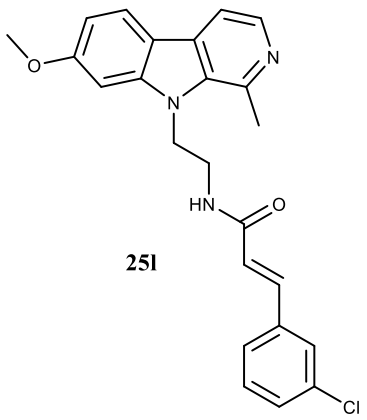

25l

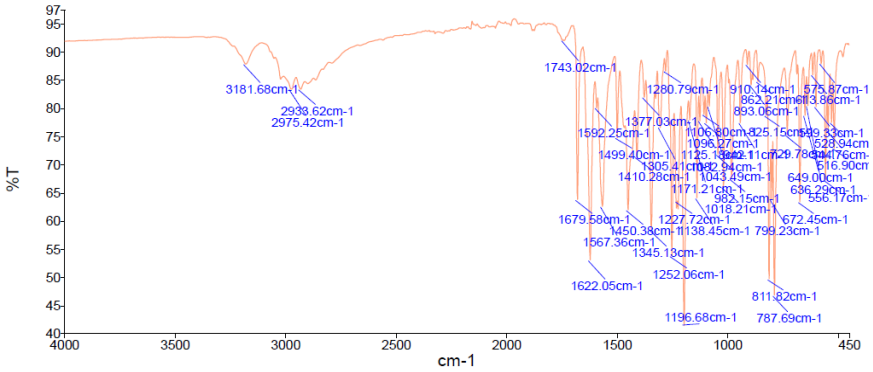

MassPeaks:4
Spectrum Mode:Averaged 0.333-0.400(21-25) Base Peak:420(9047188)
BG Mode:Calc Segment 1 - Event 1

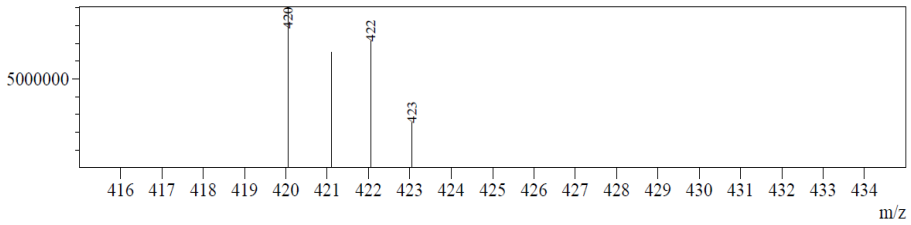

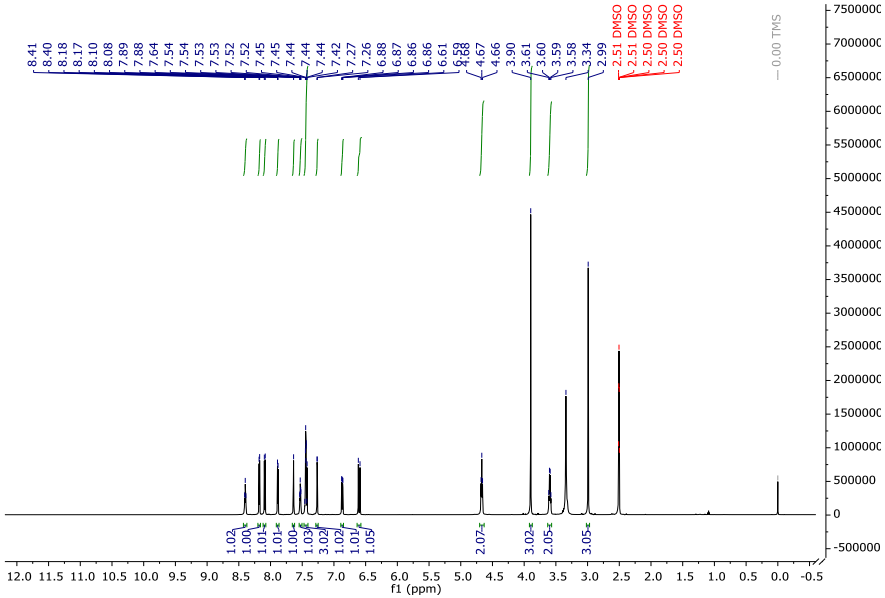

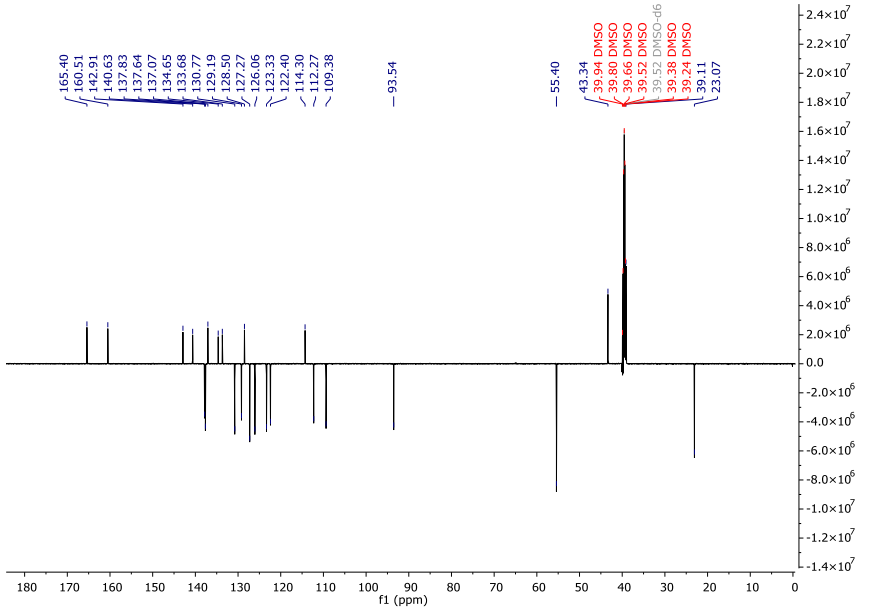

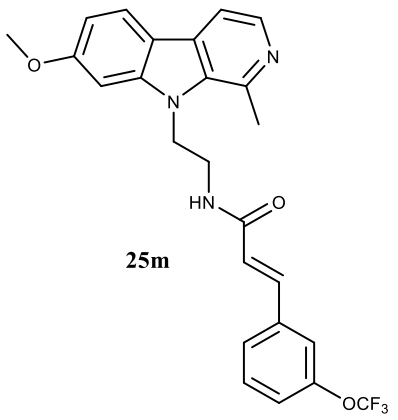

25m

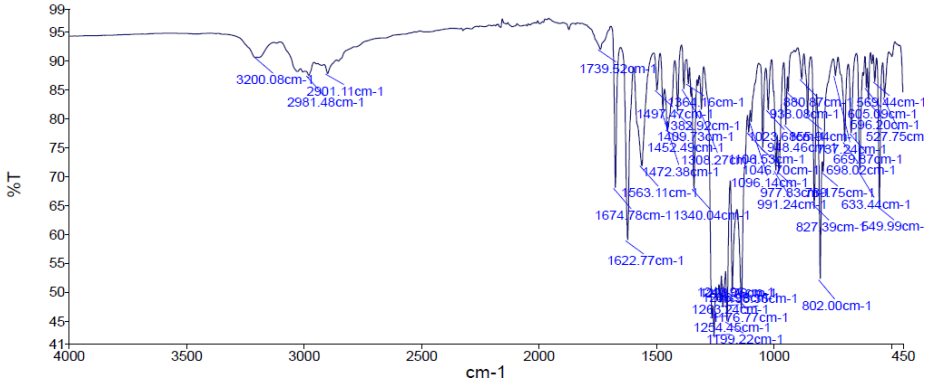

Line#:1 R.Time:----(Scan#:----)
MassPeaks:3
Spectrum Mode:Averaged 0.300-0.367(19-23) Base Peak:470(9488439)
BG Mode:Calc Segment 1 - Event 1

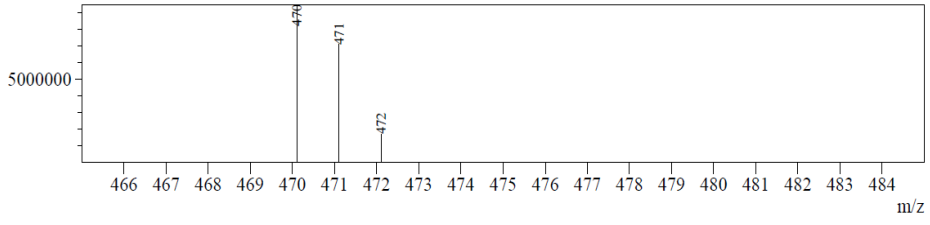

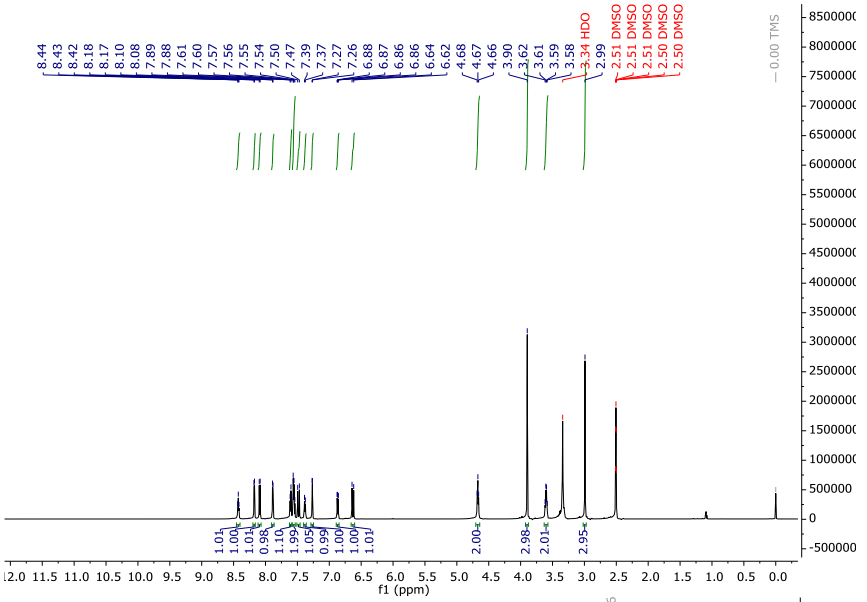

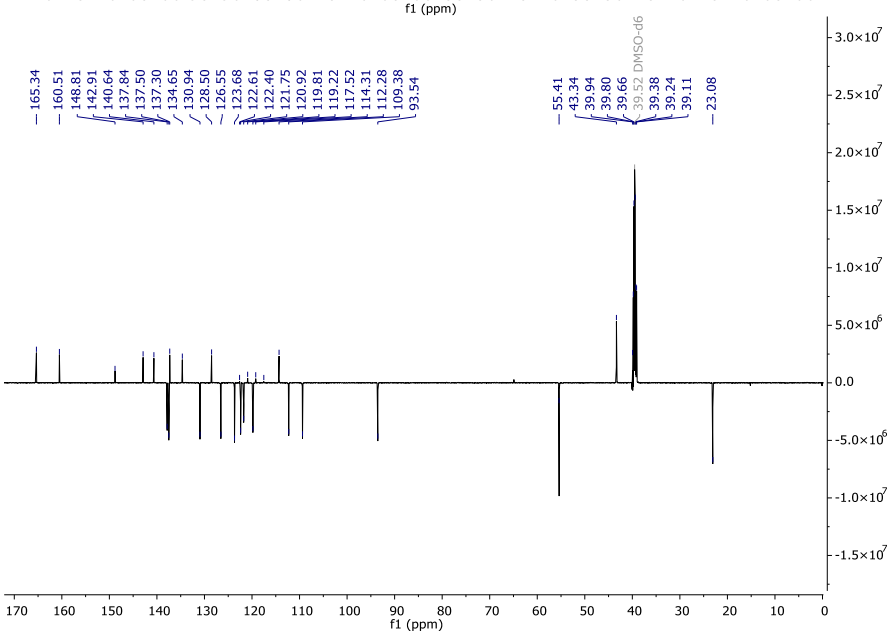

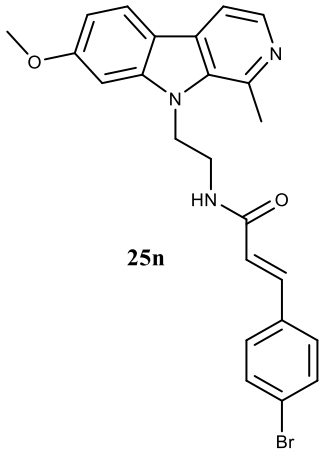

25n

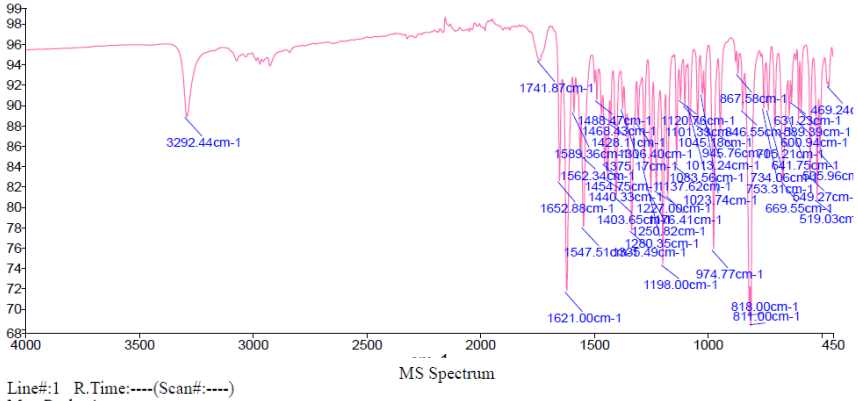

Line#:1 R.Time:----(Scan#:----)
MassPeaks:4
Spectrum Mode:Averaged 0.333-0.400(21-25) Base Peak:466(8537085)
BG Mode:Calc Segment 1 - Event 1

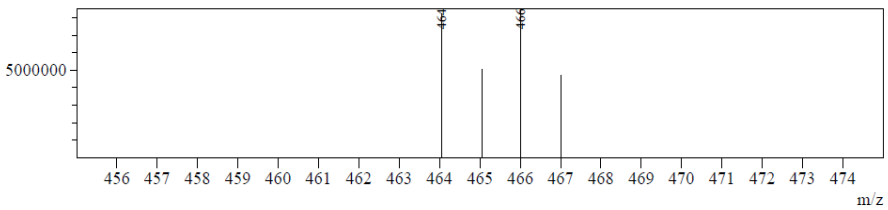

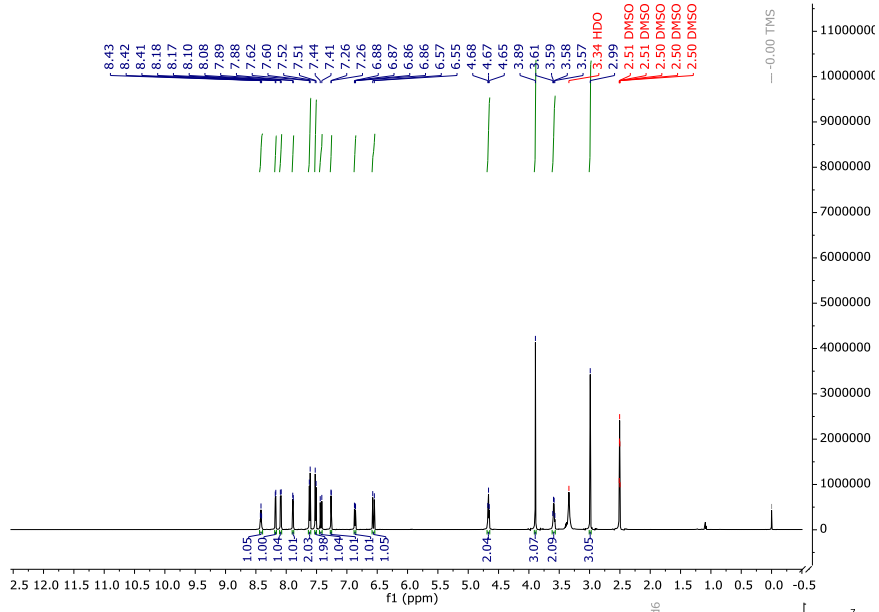

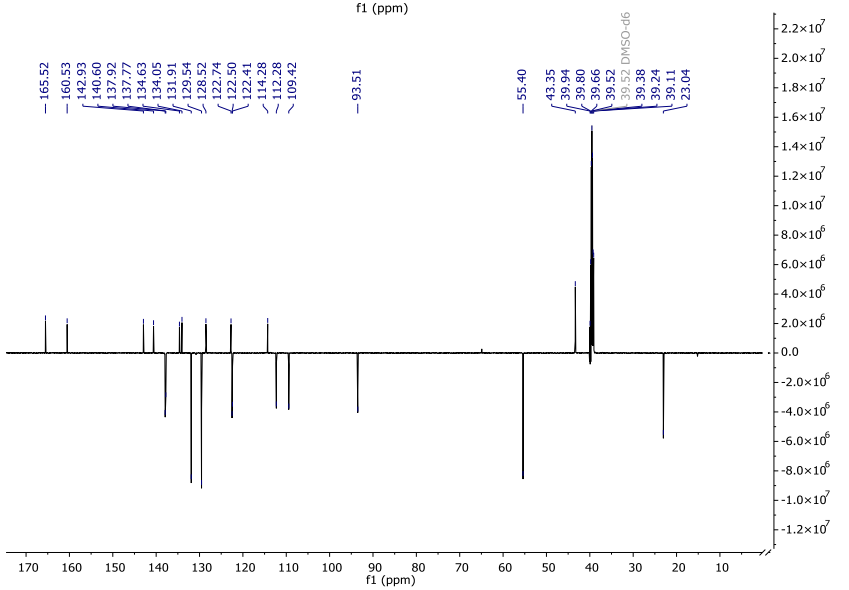

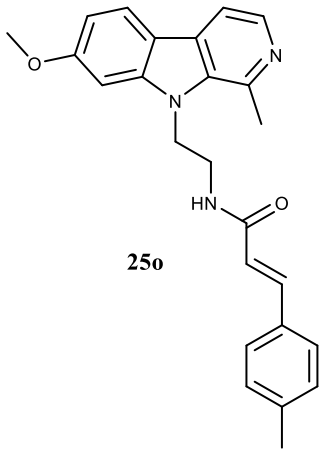

25o

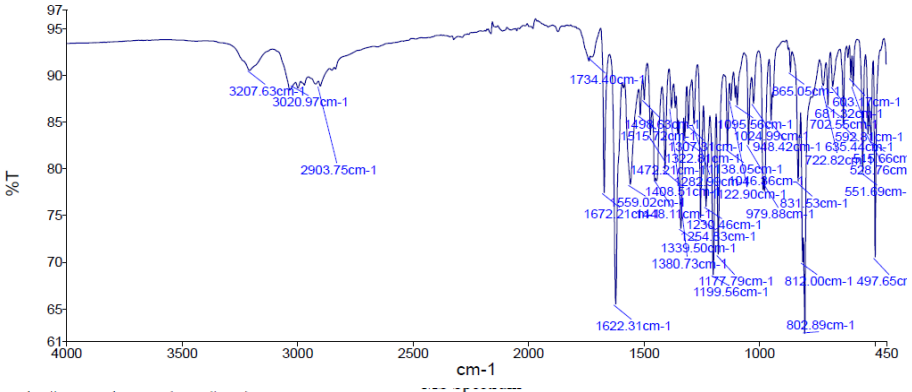

Line#:1 R.Time:----(Scan#:----)
MassPeaks:6
Spectrum Mode:Averaged 0,333-0,400(21-25) Base Peak:400(9422003)
BG Mode:Calc Segment 1 - Event 1

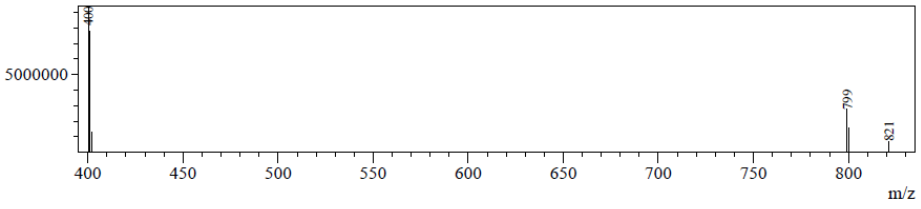

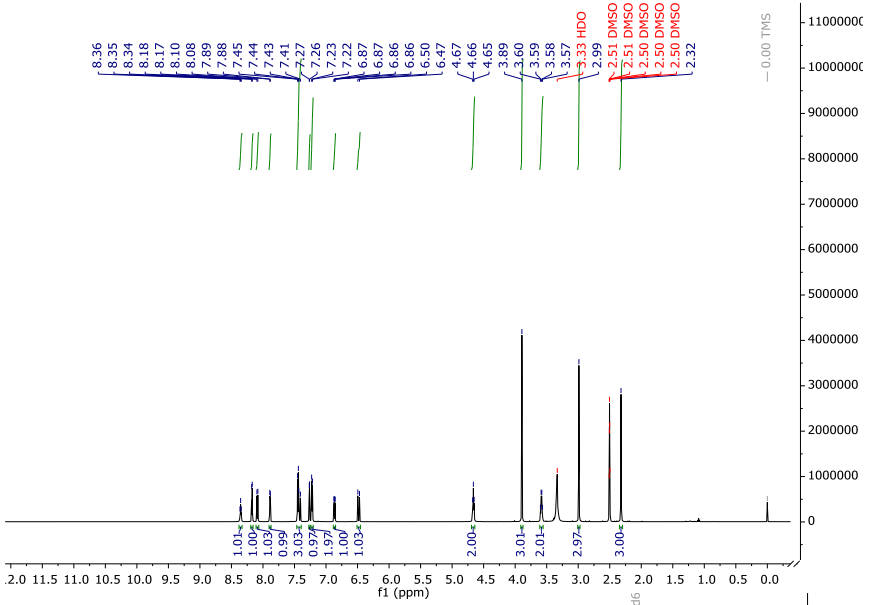

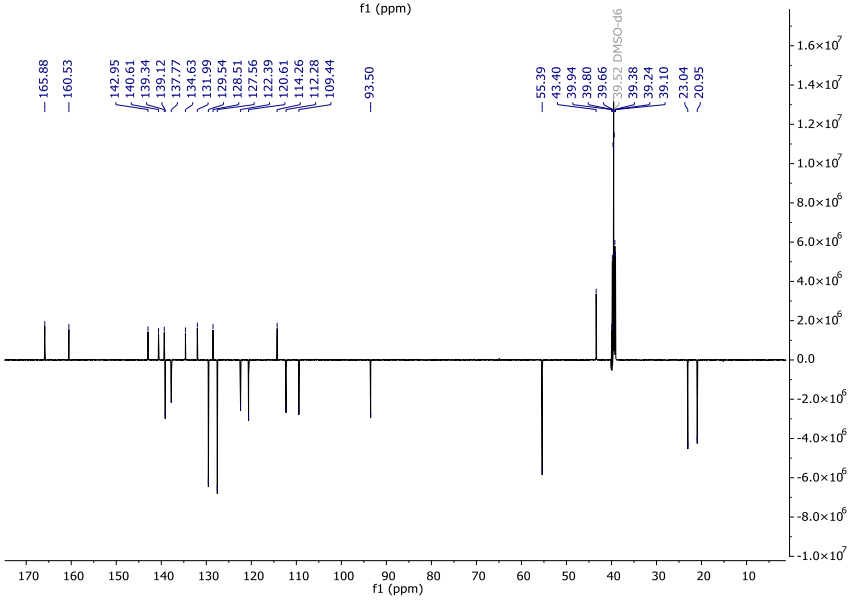

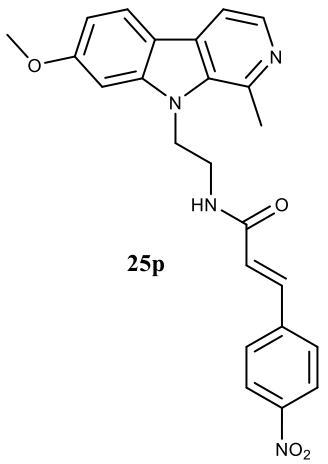

25p

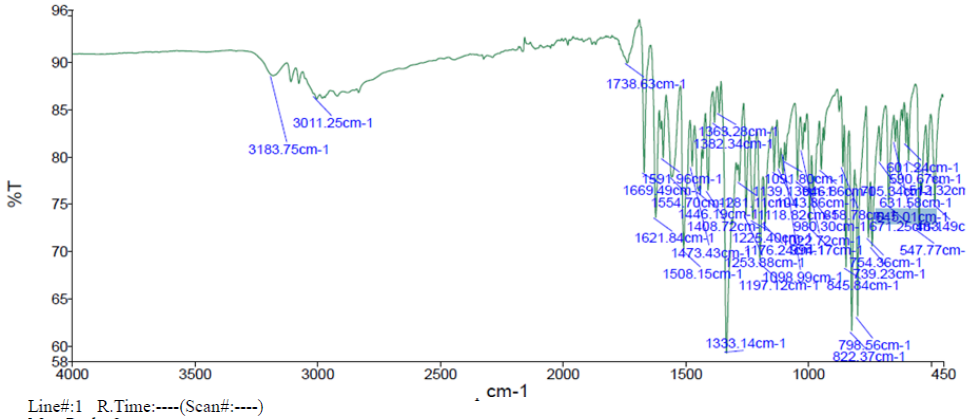

Line#:1 R.Time:----(Scan#:----)
MassPeaks:2
Spectrum Mode:Averaged 0.300-0.367(19-23) Base Peak:431(6290496)
BG Mode:Calc Segment 1 - Event 1

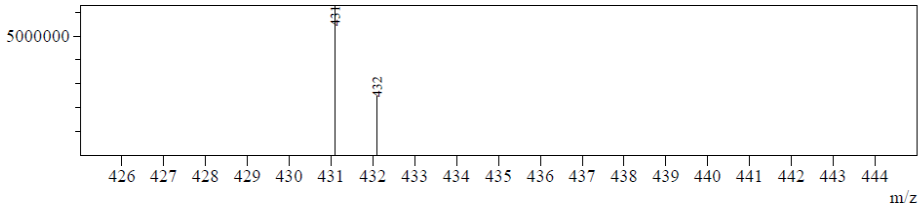

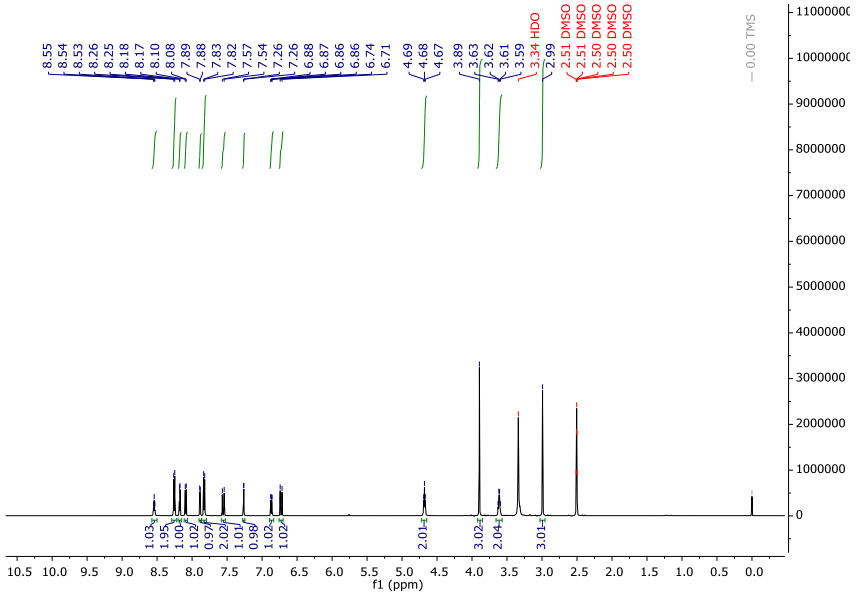

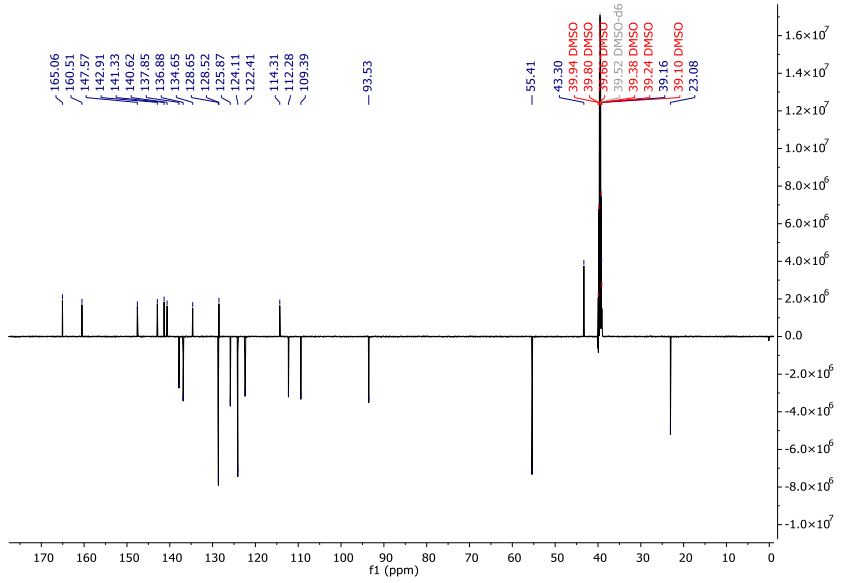

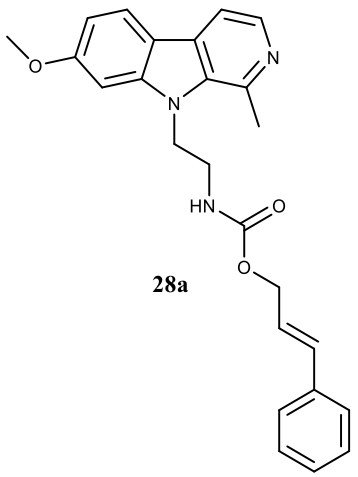

28a

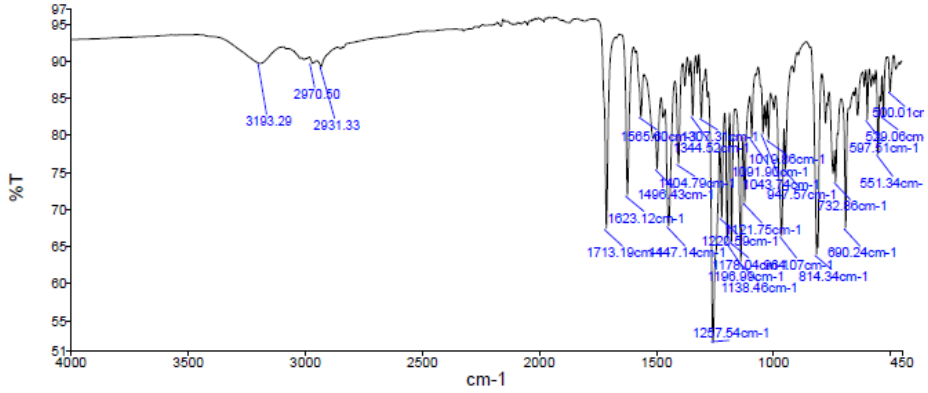
%T
cm-1
3193.29
2970.50
2931.33
1623.12cm-1
1713.19cm-1
1447.14cm-1
1257.54cm-1
1138.46cm-1
814.34cm-1
690.24cm-1
732.86cm-1
551.34cm-

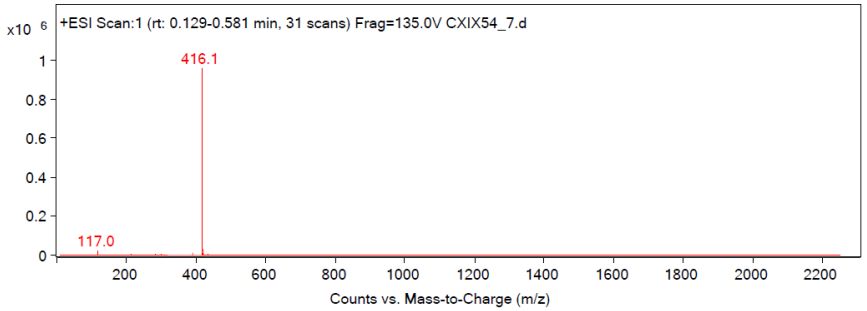
x10 6
+ESI Scan:1 (rt: 0.129-0.581 min, 31 scans) Frag=135.0V CXIX54_7.d
416.1
117.0
Counts vs. Mass-to-Charge (m/z)

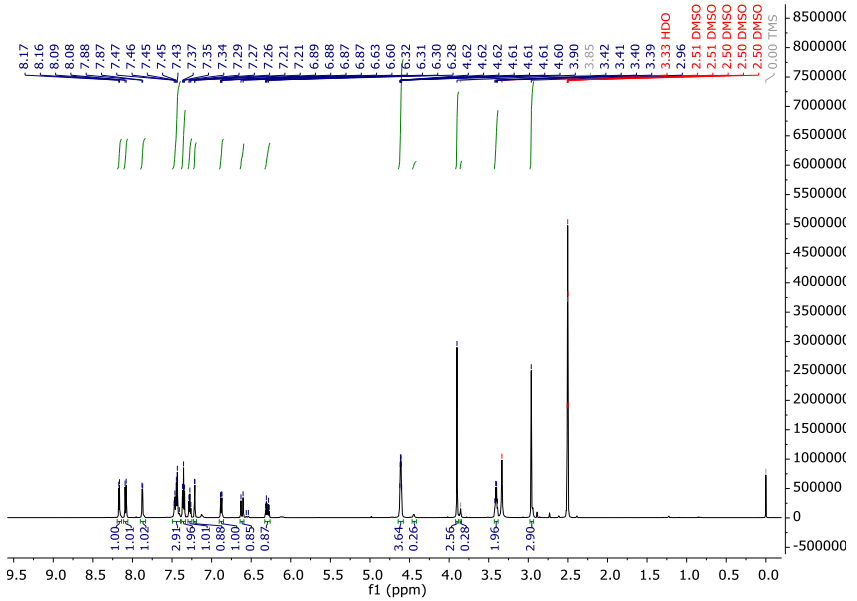
f1 (ppm)

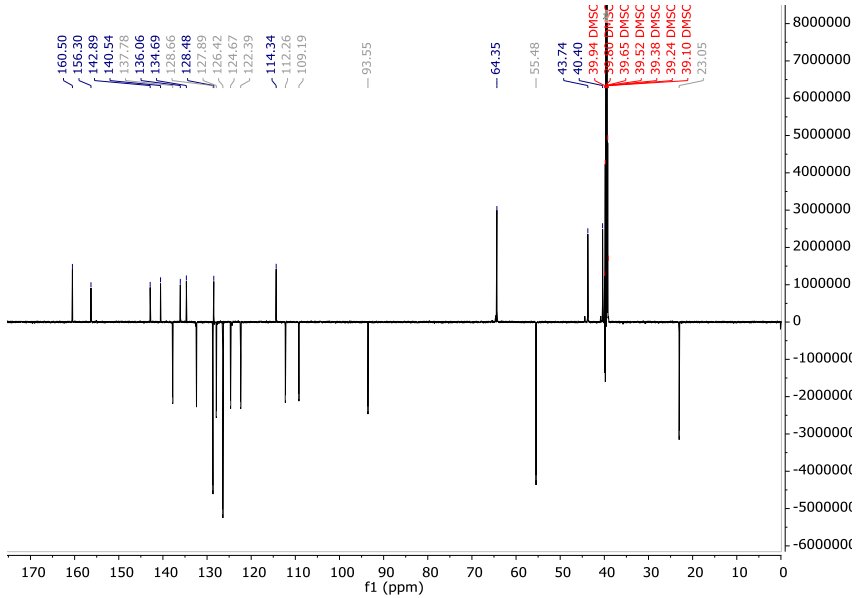
f1 (ppm)

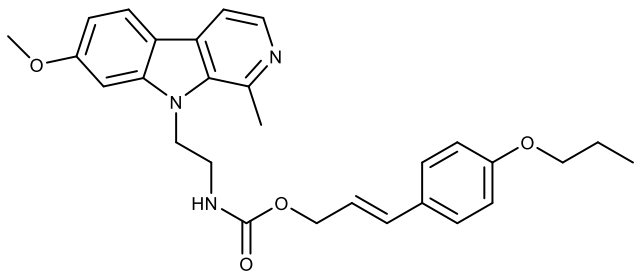

28b

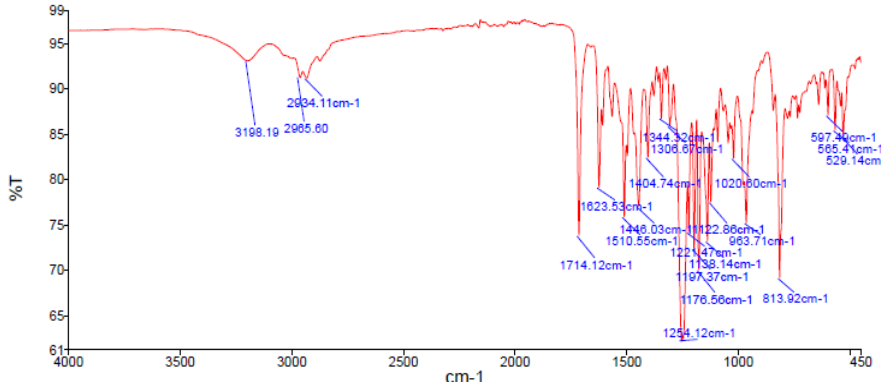
%T
cm-1
3198.19
2965.60
2934.11cm-1
1714.12cm-1
1623.53cm-1
1510.55cm-1
1404.74cm-1
1344.32cm-1
1306.67cm-1
1020.60cm-1
963.71cm-1
813.92cm-1
597.44cm-1
565.41cm-1
529.14cm

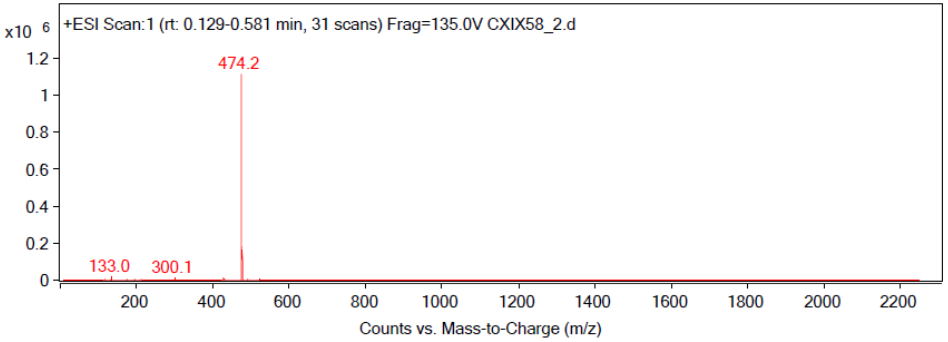
+ESI Scan:1 (rt: 0.129-0.581 min, 31 scans) Frag=135.0V CXIX58_2.d
474.2
133.0
300.1
Counts vs. Mass-to-Charge (m/z)

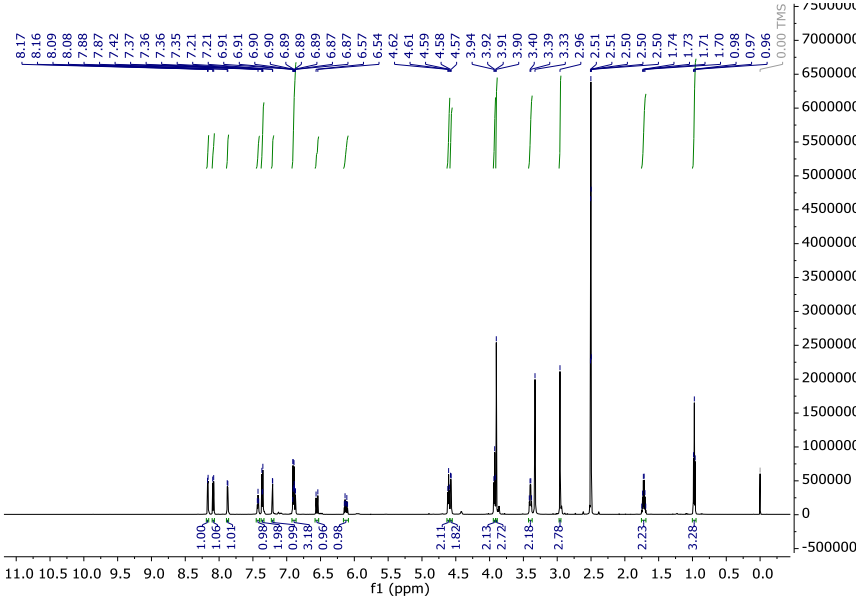
f1 (ppm)

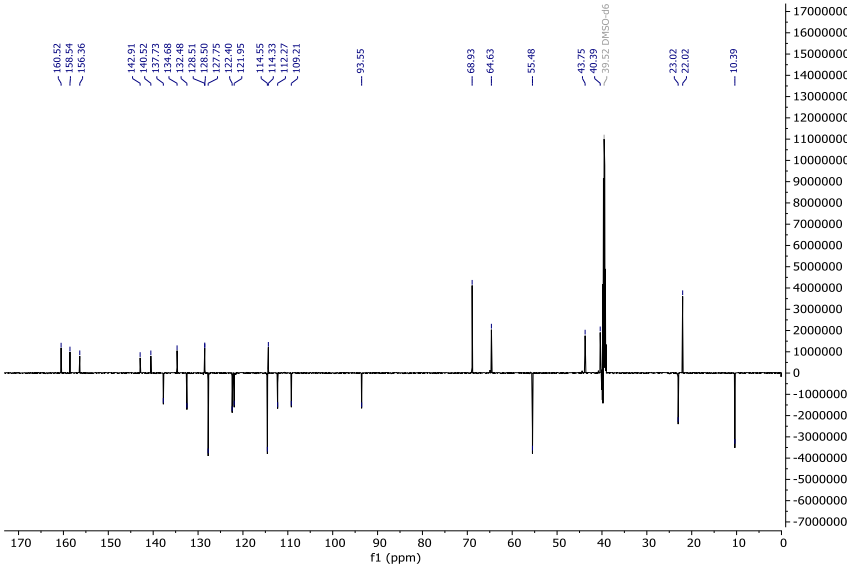
f1 (ppm)

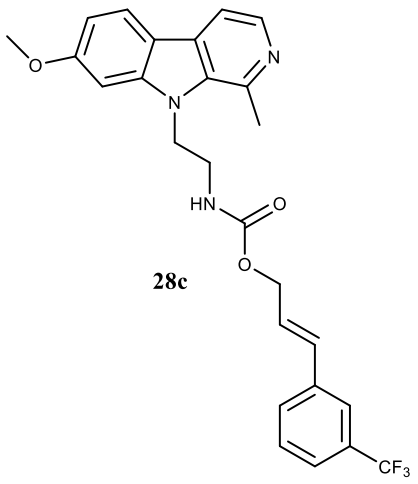
O
N
N
HN
O
O
CF3

28c

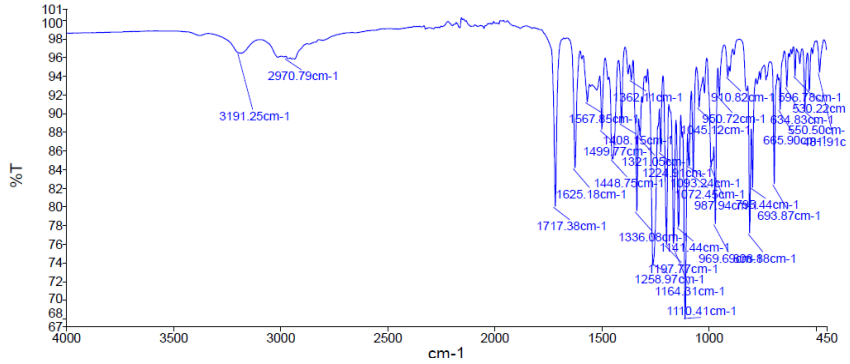
%T
cm-1
3191.25cm-1
2970.79cm-1
1717.38cm-1
1625.18cm-1
1448.75cm-1
1336.08cm-1
1258.97cm-1
1164.31cm-1
1110.41cm-1

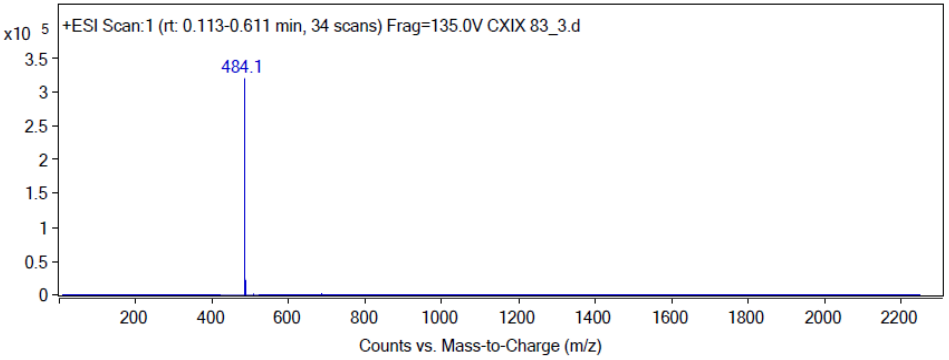
+ESI Scan:1 (rt: 0.113-0.611 min, 34 scans) Frag=135.0V CXIX 83_3.d
x10 5
484.1
Counts vs. Mass-to-Charge (m/z)

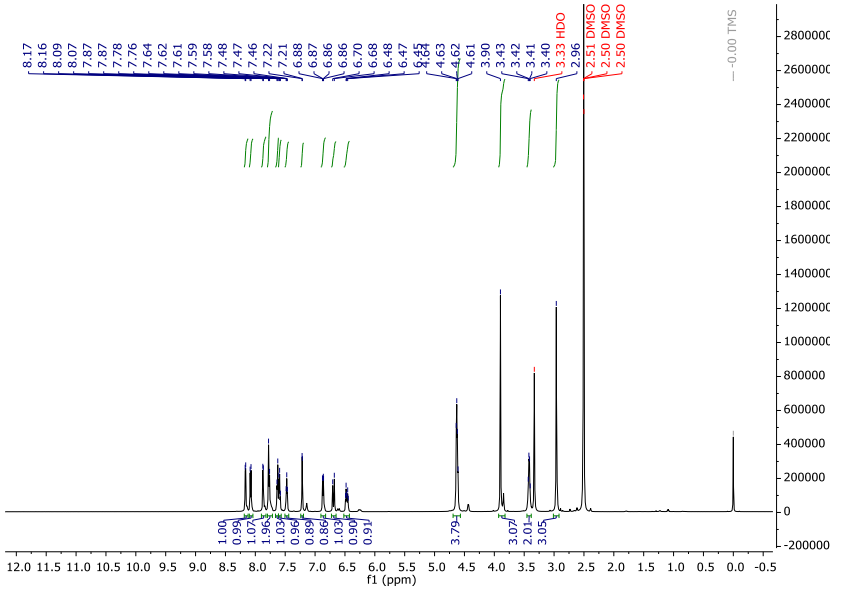
8.17
8.16
8.09
8.07
7.87
7.87
7.78
7.76
7.64
7.62
7.61
7.59
7.58
7.48
7.47
7.46
7.22
7.21
6.88
6.87
6.86
6.86
6.70
6.68
6.48
6.47
4.64
4.63
4.62
4.61
3.90
3.43
3.42
3.41
3.40
3.33 HDO
2.96
2.51 DMSO
2.50 DMSO
2.50 DMSO
0.00 TMS
f1 (ppm)

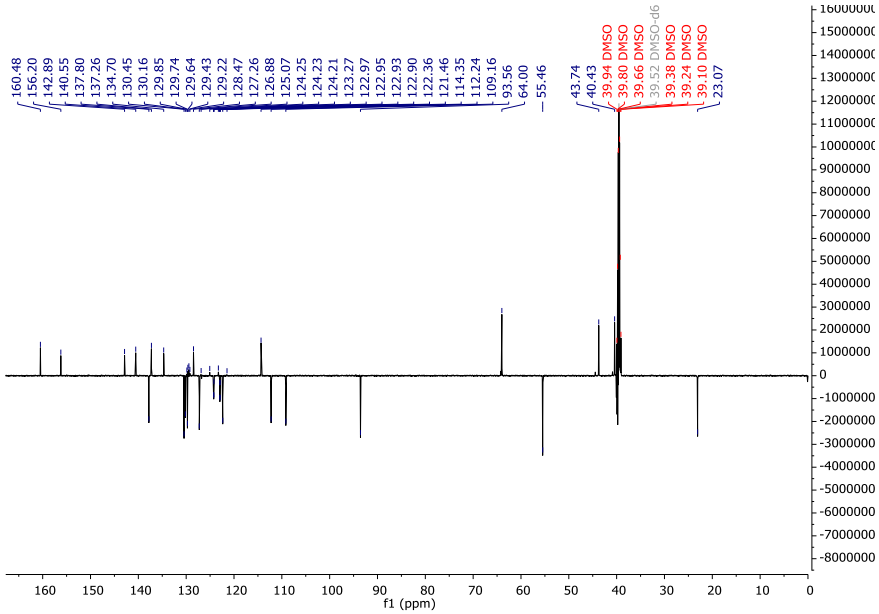
160.48
156.20
142.89
140.55
137.80
137.26
134.70
130.45
130.16
129.85
129.74
129.64
129.43
129.22
128.47
127.26
126.88
125.07
124.25
124.23
124.21
123.27
122.97
122.95
122.93
122.90
122.36
121.46
114.35
112.24
109.16
93.56
64.00
55.46
43.74
40.43
39.94 DMSO
39.80 DMSO
39.66 DMSO
39.52 DMSO-d6
39.38 DMSO
39.24 DMSO
39.10 DMSO
23.07
f1 (ppm)

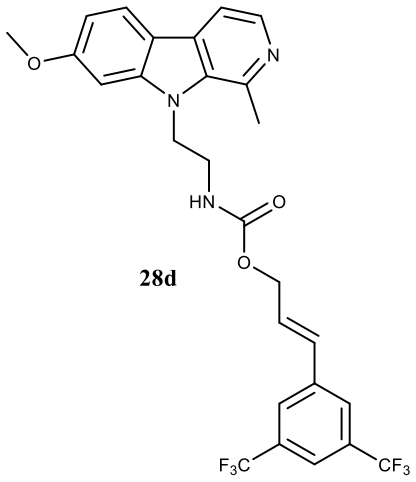
O
N
N
HN
O
O
F3C
CF3

28d

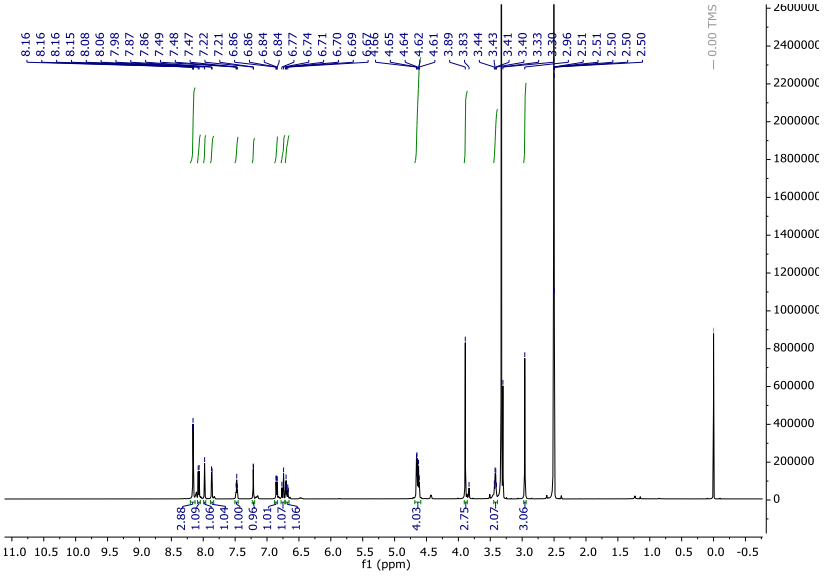
f1 (ppm)

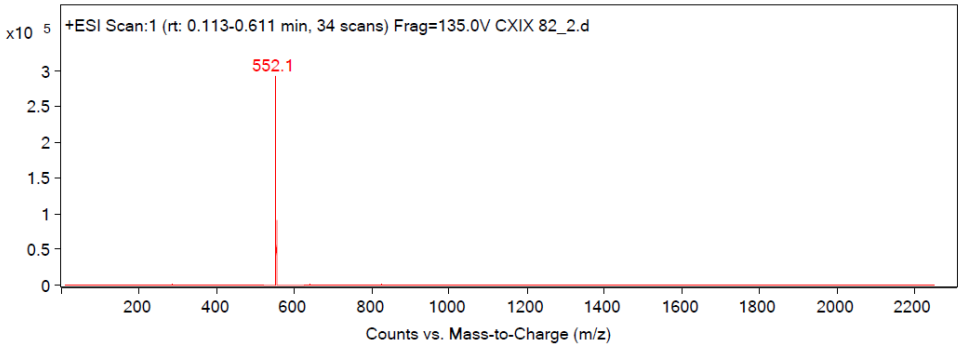
+ESI Scan:1 (rt: 0.113-0.611 min, 34 scans) Frag=135.0V CXIX 82_2.d
552.1
Counts vs. Mass-to-Charge (m/z)

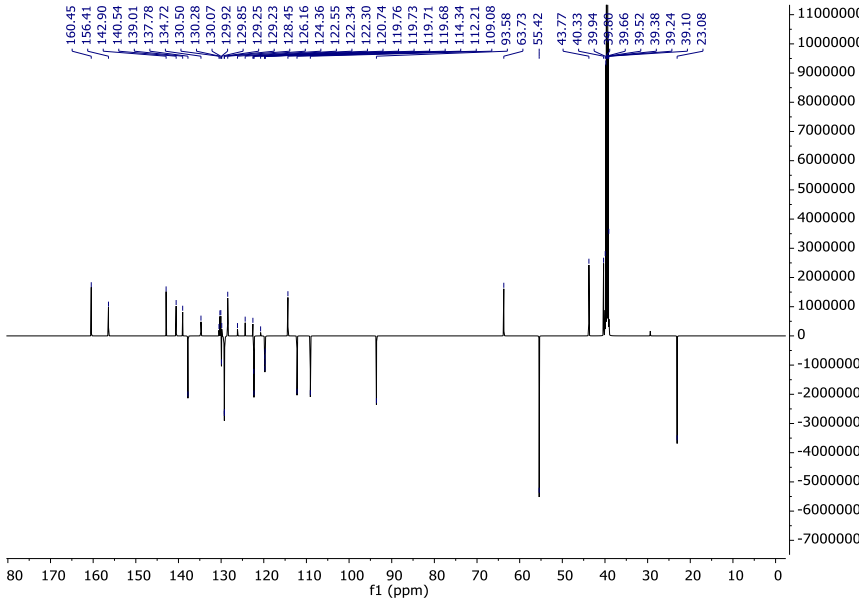
f1 (ppm)

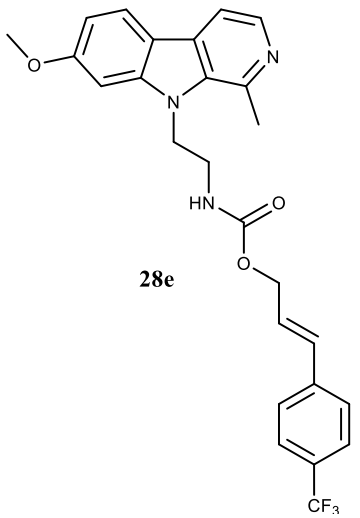

28e

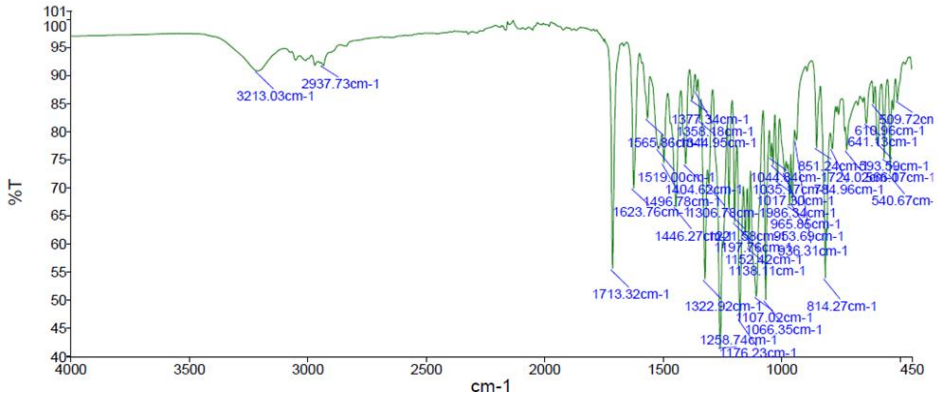

Line#:1 R.Time:----(Scan#:----)
MassPeaks:3
Spectrum Mode:Averaged 0,333-0,400(21-25) Base Peak:484(8195174)
BG Mode:Calc Segment 1 - Event 1

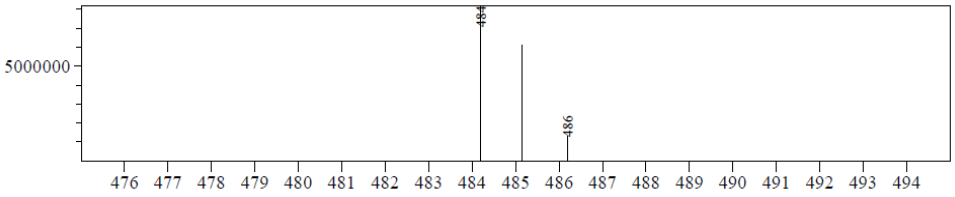

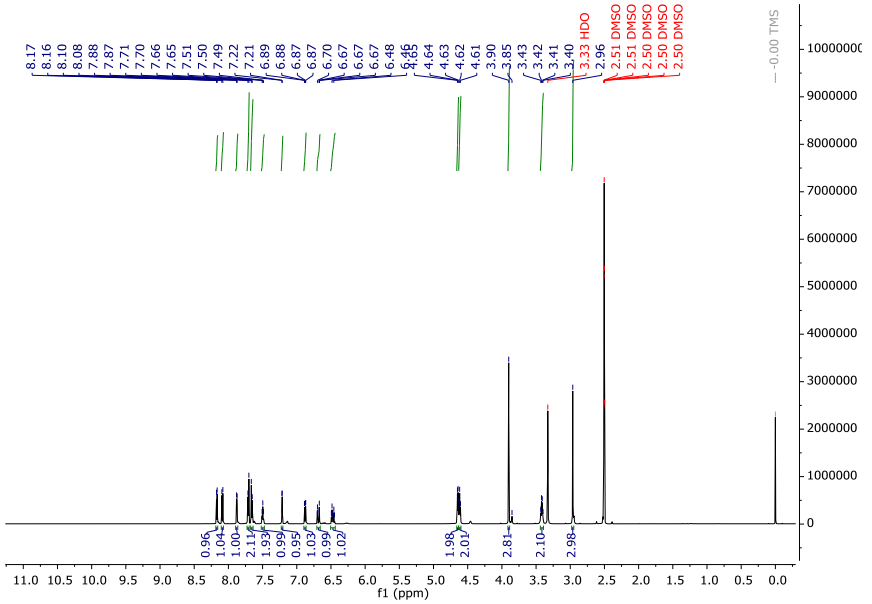

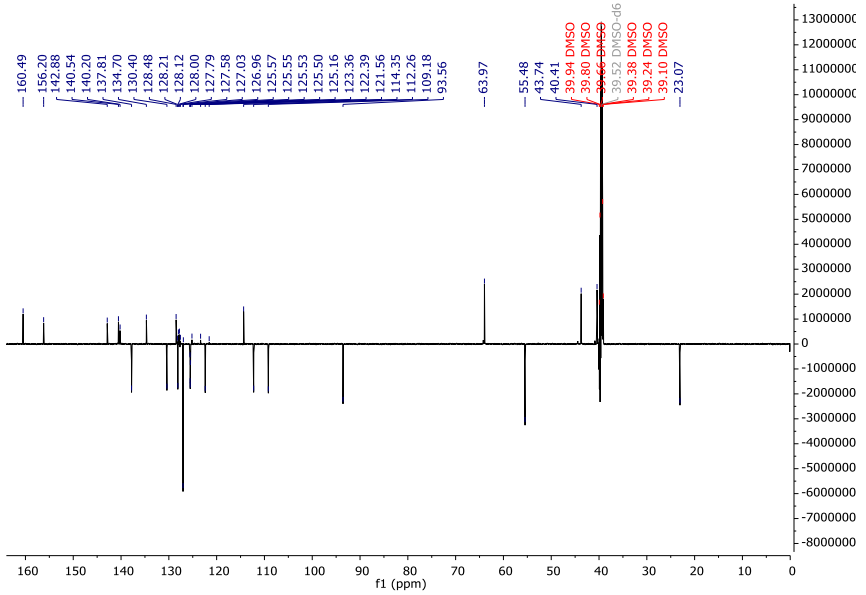

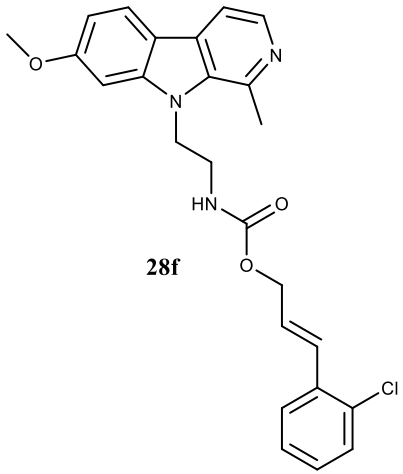

28f

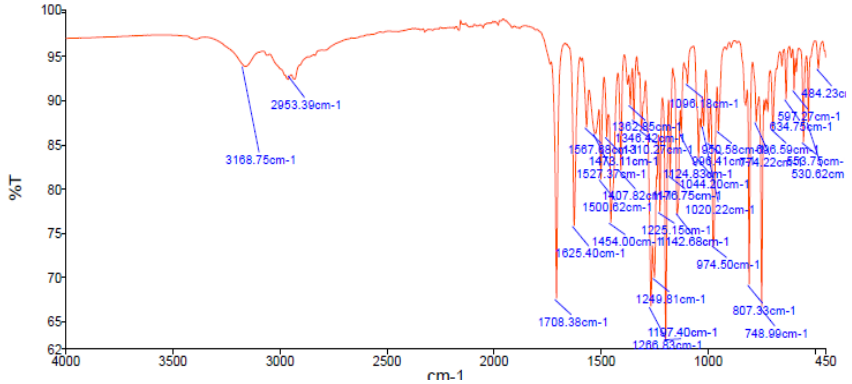

Spectrum Mode:Averaged 0,367-0,433(23-27) Base Peak:450(7556820)
BG Mode:Calc Segment 1 - Event 1

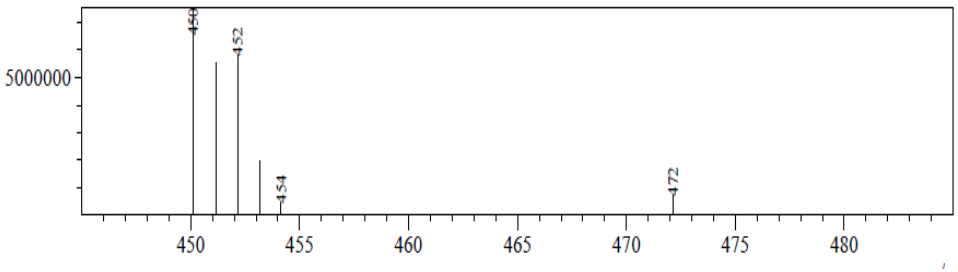

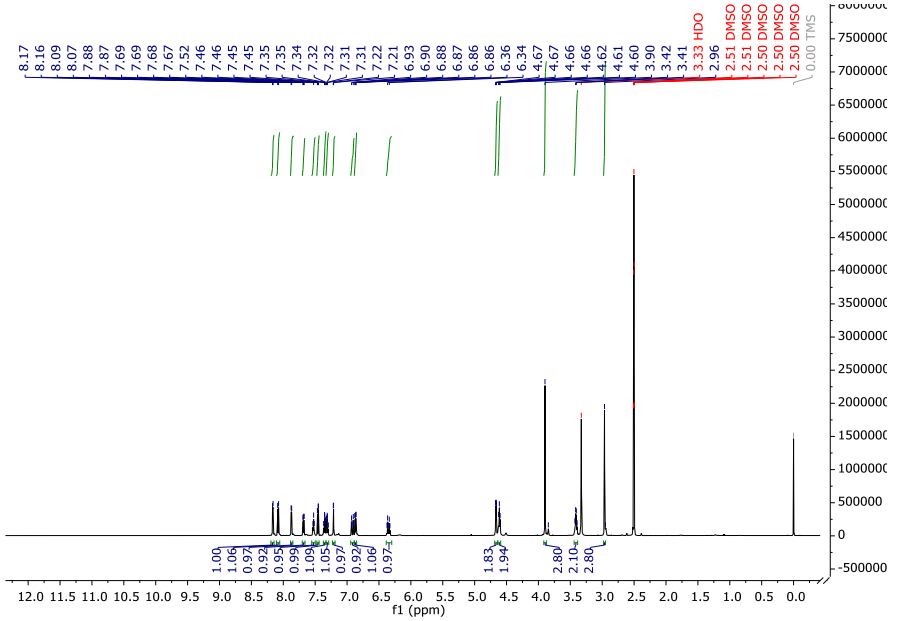

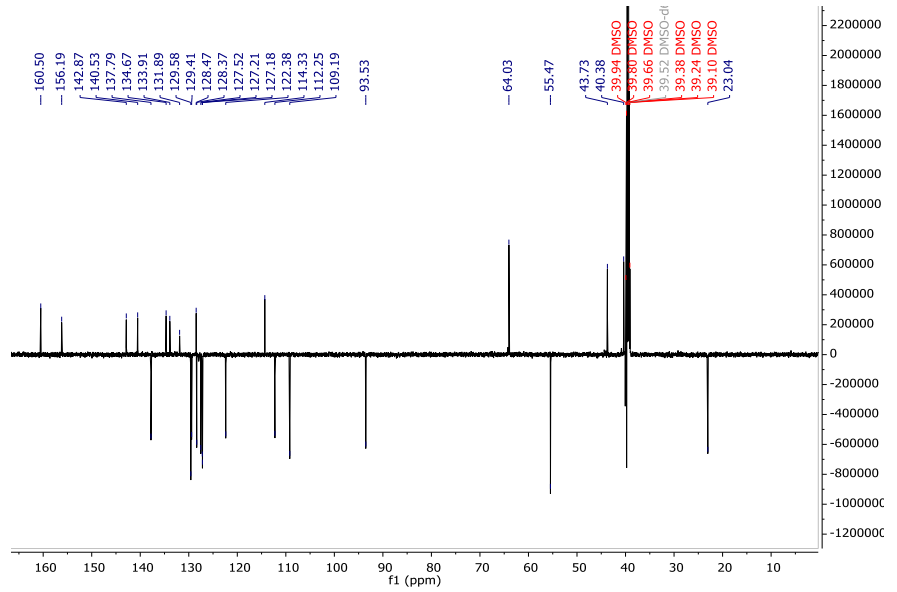

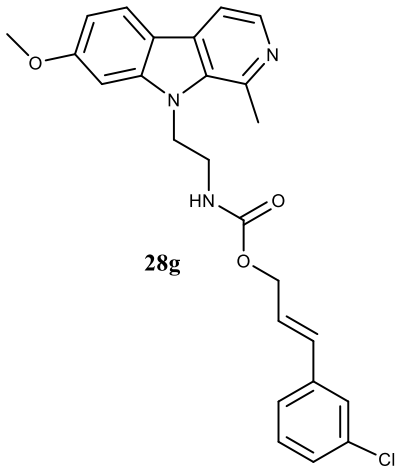

28g

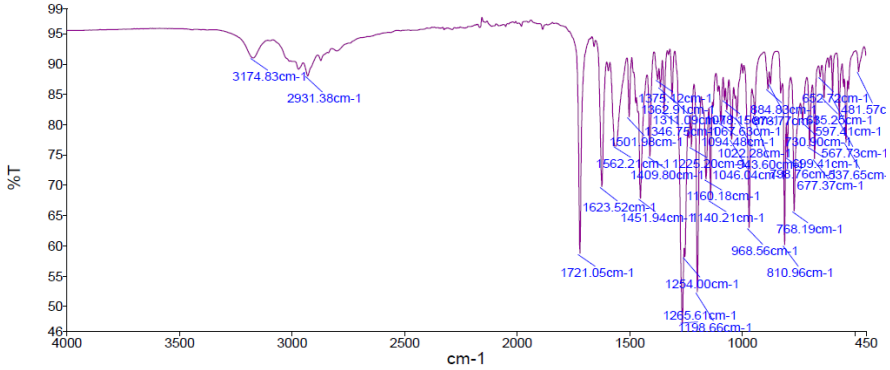

Spectrum Mode:Averaged 0,333-0,400(21-25) Base Peak:450(7321728)
BG Mode:Calc Segment 1 - Event 1

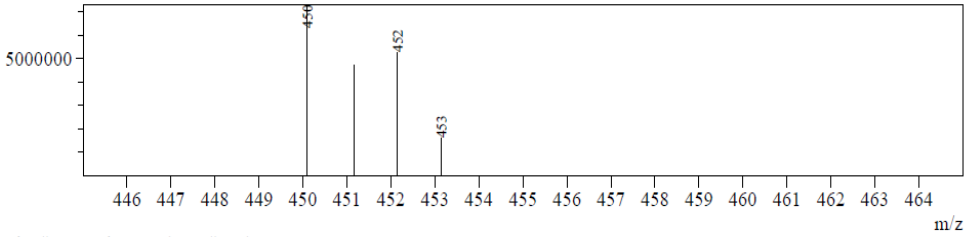

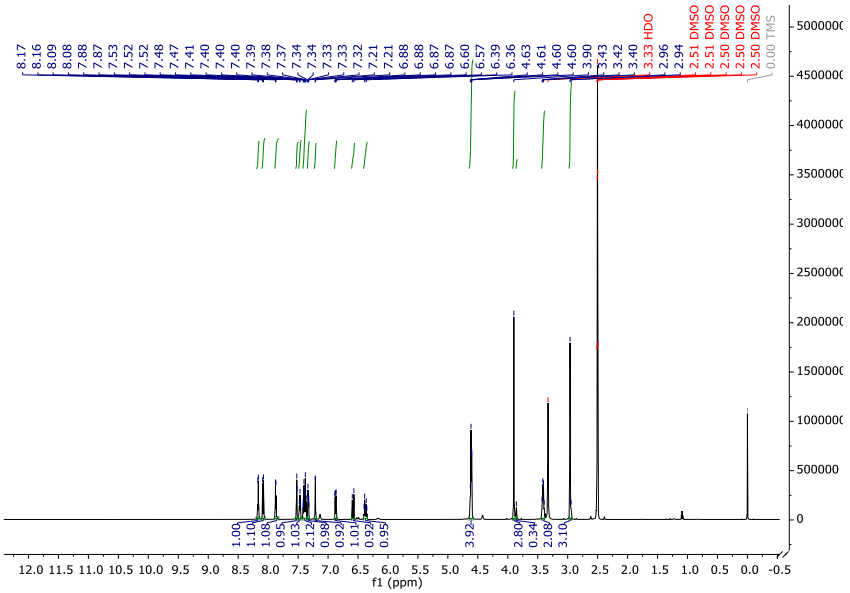

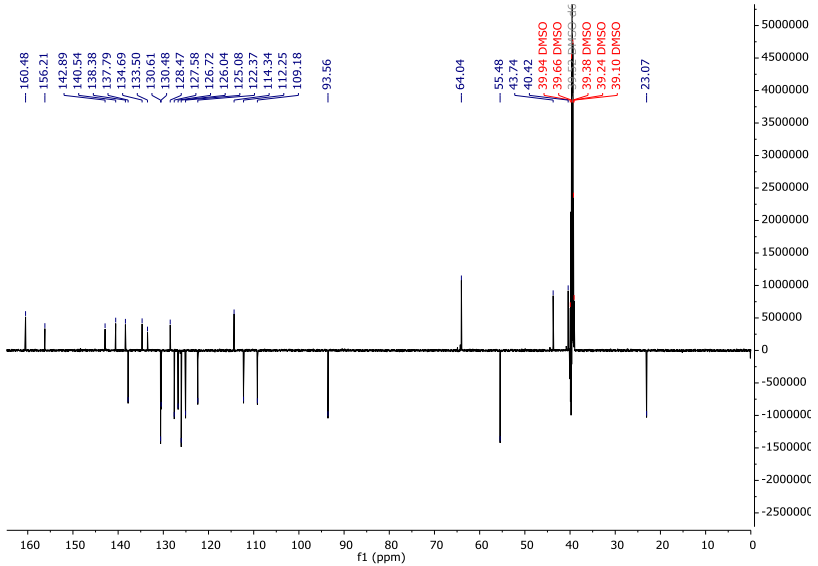

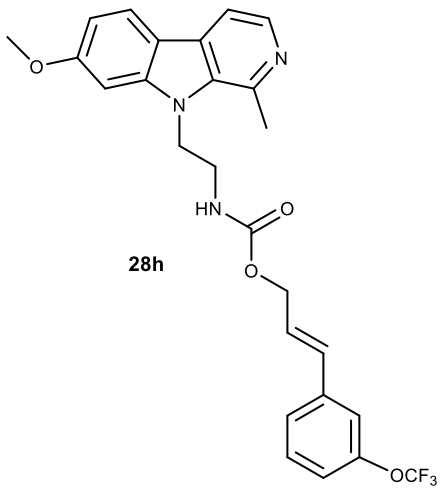

28h

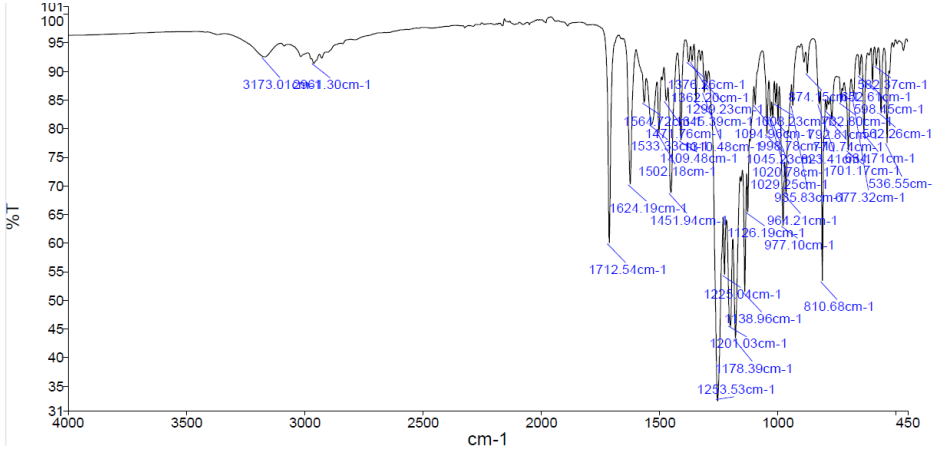

Spectrum Mode:Averaged 0,333-0,400(21-25) Base Peak:500(8480285)
BG Mode:Calc Segment 1 - Event 1

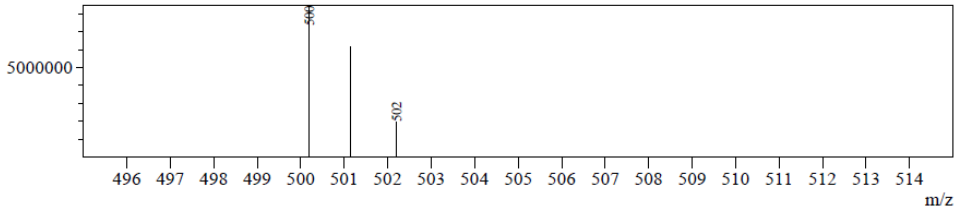

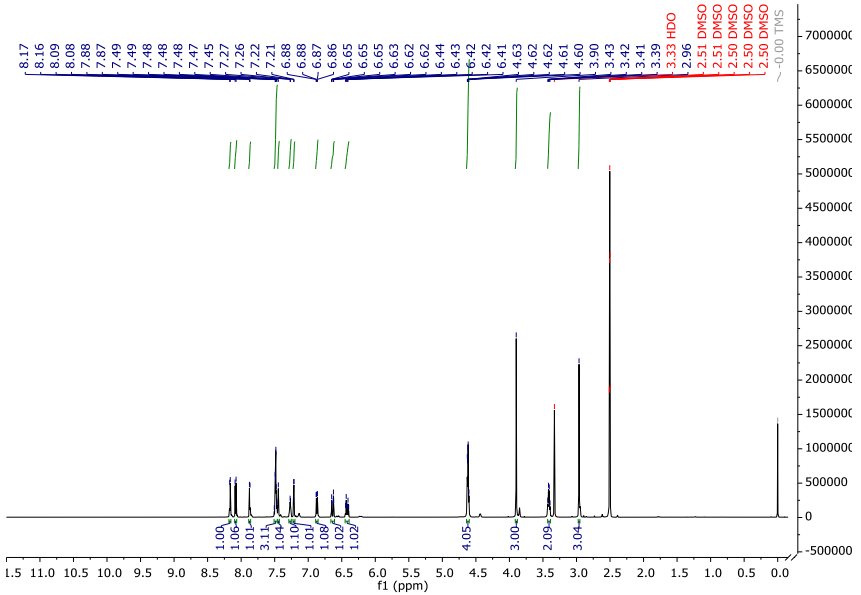

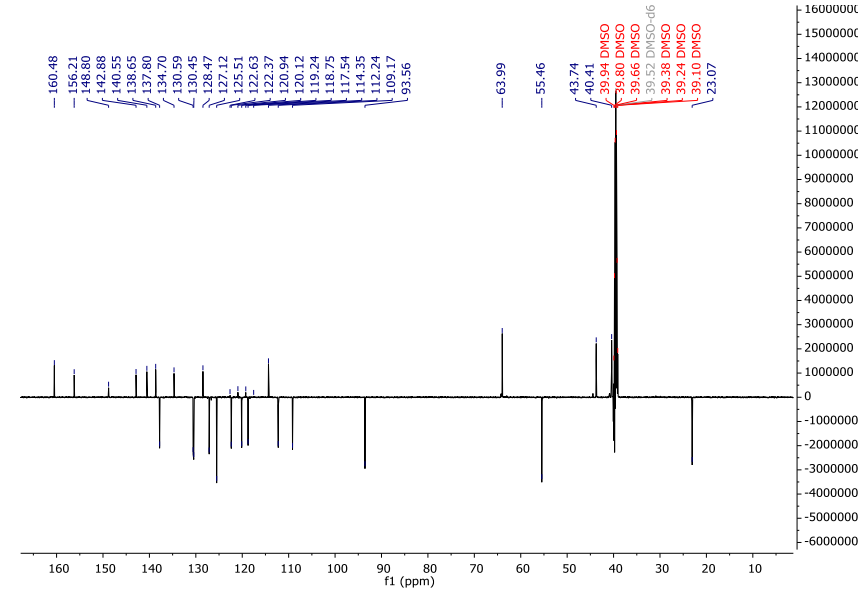

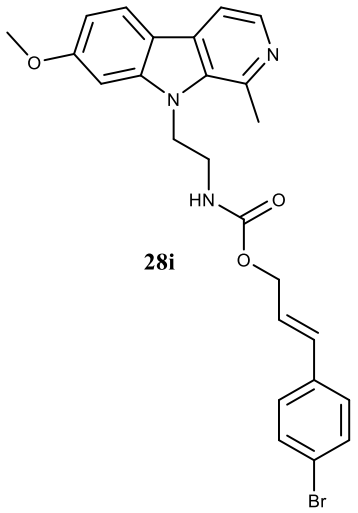

28i

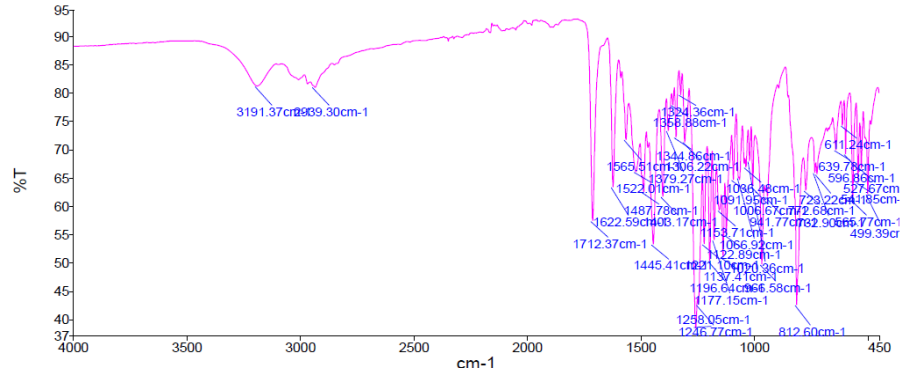

Spectrum Mode:Averaged 0,333-0,400(21-25) Base Peak:496(6133959)
BG Mode:Calc Segment 1 - Event 1

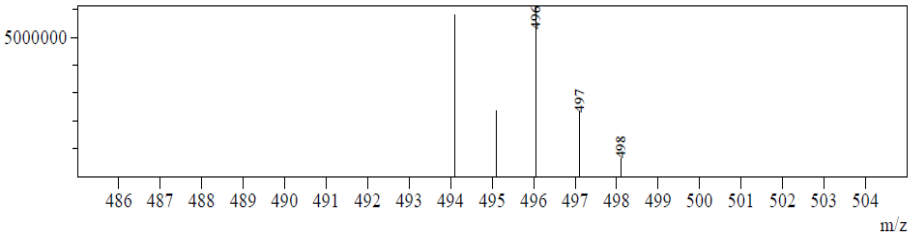

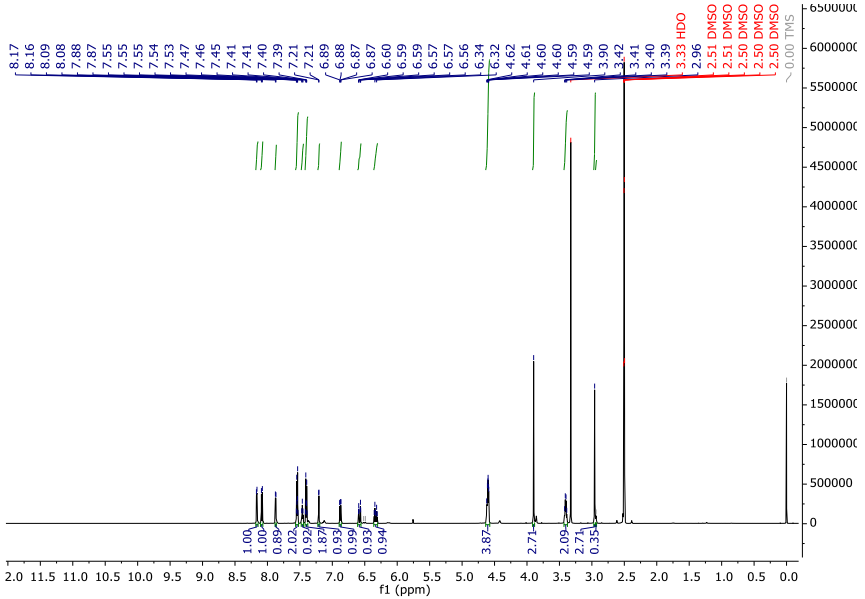

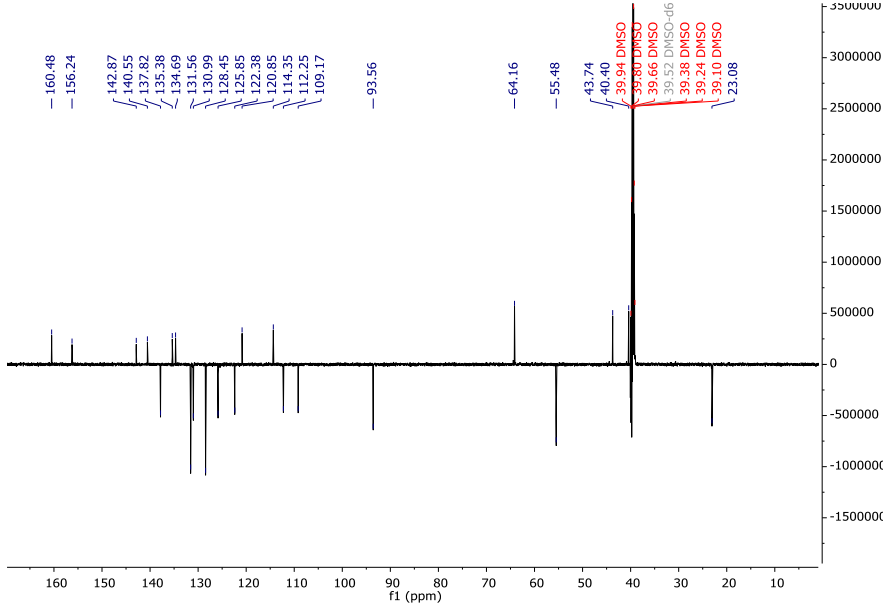

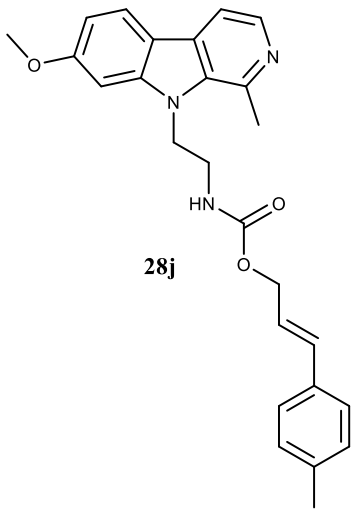

28j

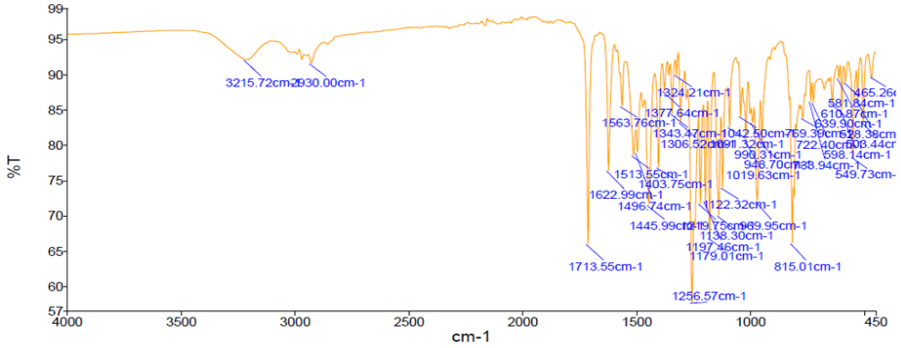

Spectrum Mode:Averaged 0.333-0.400(21-25) Base Peak:430(8075340)
BG Mode:Calc Segment 1 - Event 1

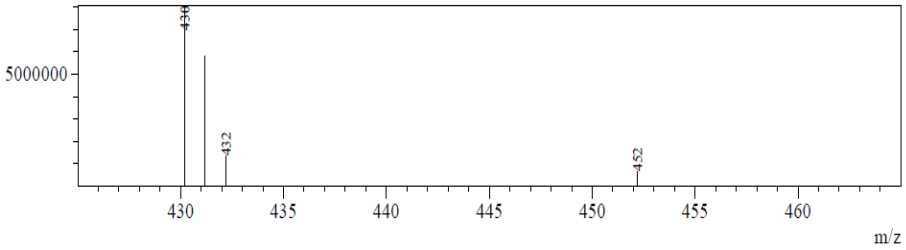

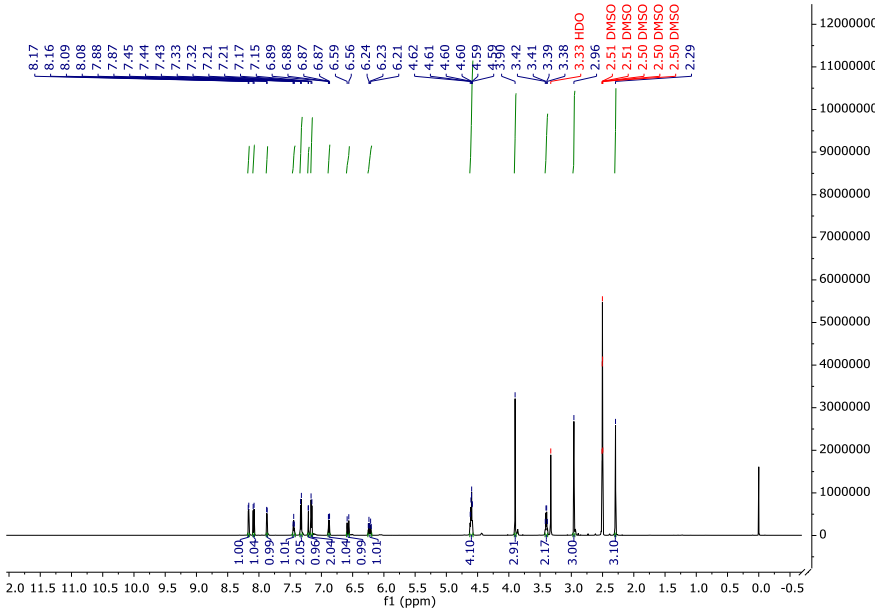

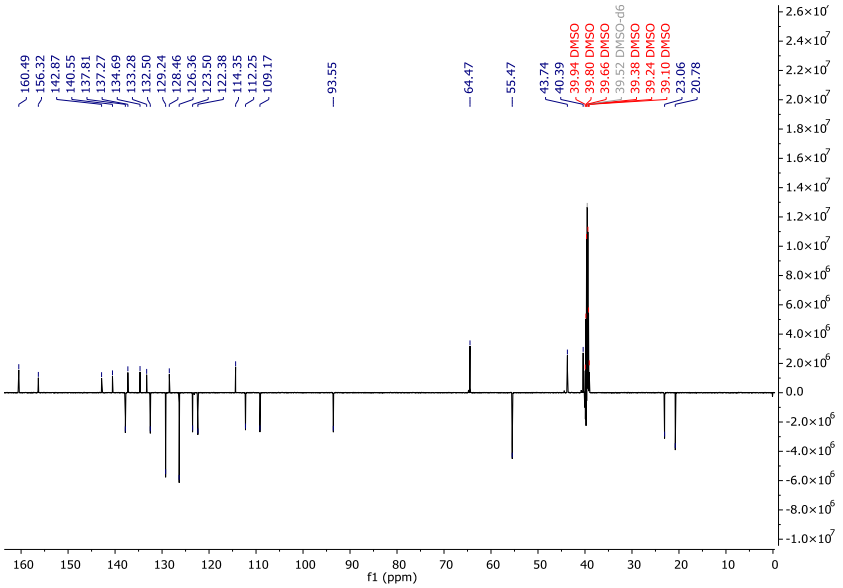

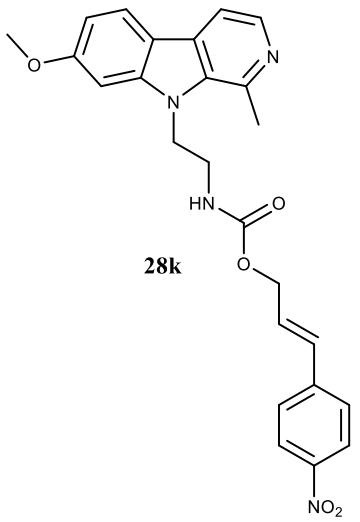

28k

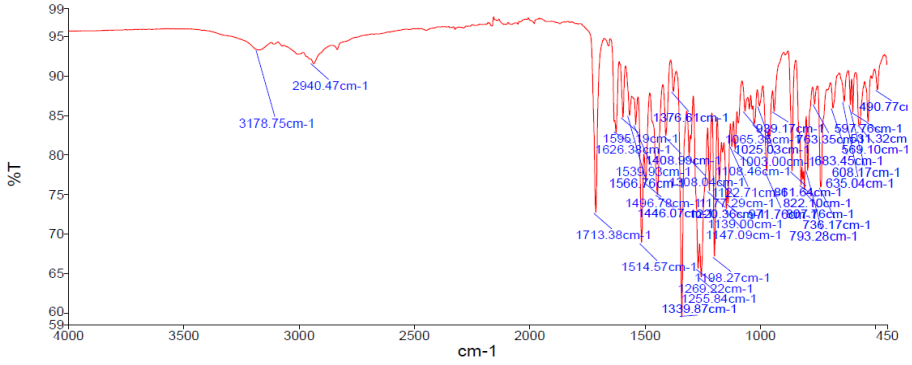

Spectrum Mode:Averaged 0,333-0,400(21-25) Base Peak:461(7767411)
BG Mode:Calc Segment 1 - Event 1

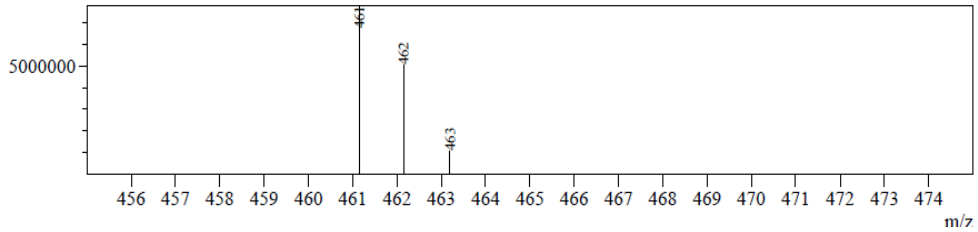

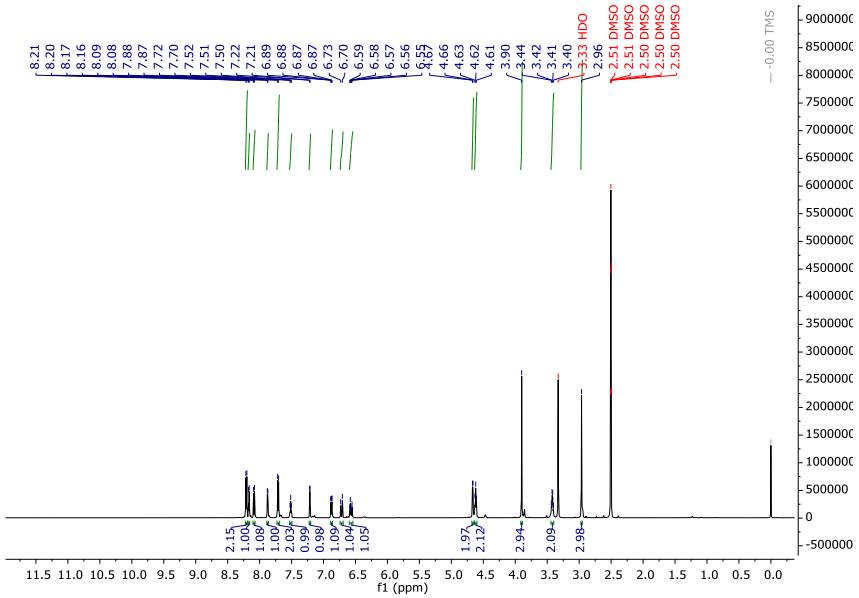

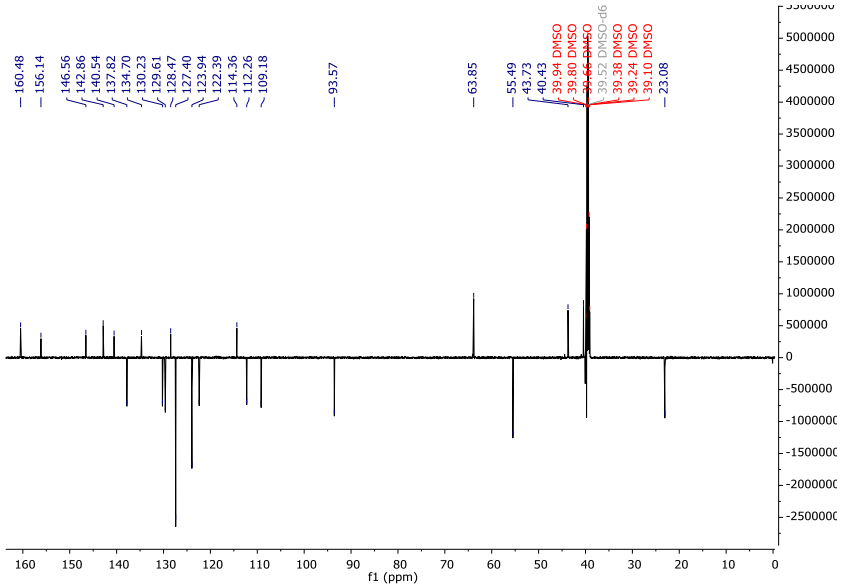

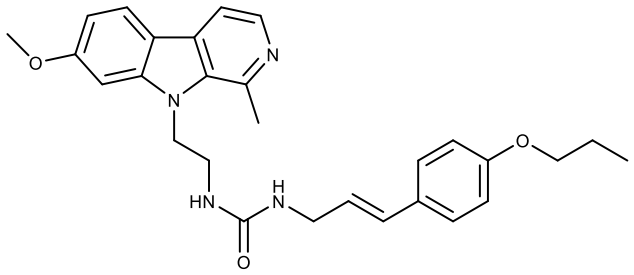

32b

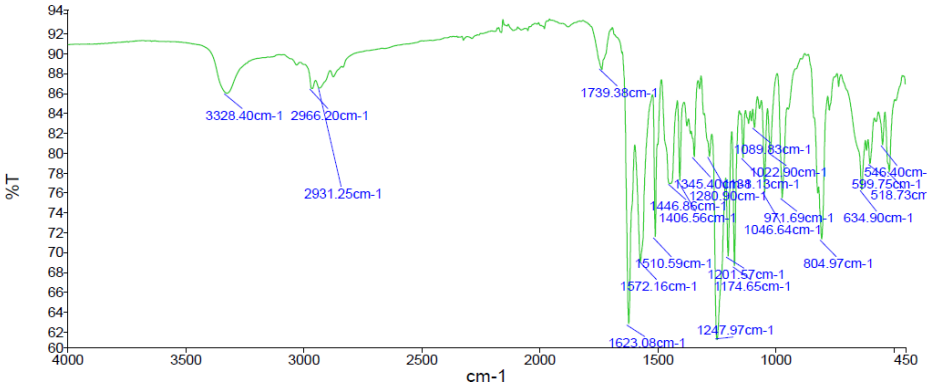
%T
cm-1
3328.40cm-1
2966.20cm-1
2931.25cm-1
1739.38cm-1
1623.08cm-1
1572.16cm-1
1510.59cm-1
1446.86cm-1
1406.56cm-1
1345.40cm-1
1280.90cm-1
1247.97cm-1
1201.57cm-1
1174.65cm-1
1089.83cm-1
1046.64cm-1
1022.90cm-1
971.69cm-1
804.97cm-1
634.90cm-1
599.75cm-1
546.40cm-1
518.73cm-1

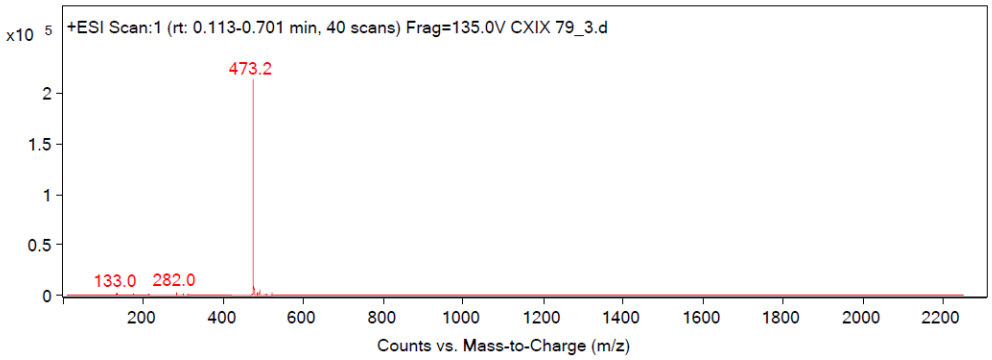
x10
+ESI Scan:1 (rt: 0.113-0.701 min, 40 scans) Frag=135.0V CXIX 79_3.d
473.2
133.0
282.0
Counts vs. Mass-to-Charge (m/z)

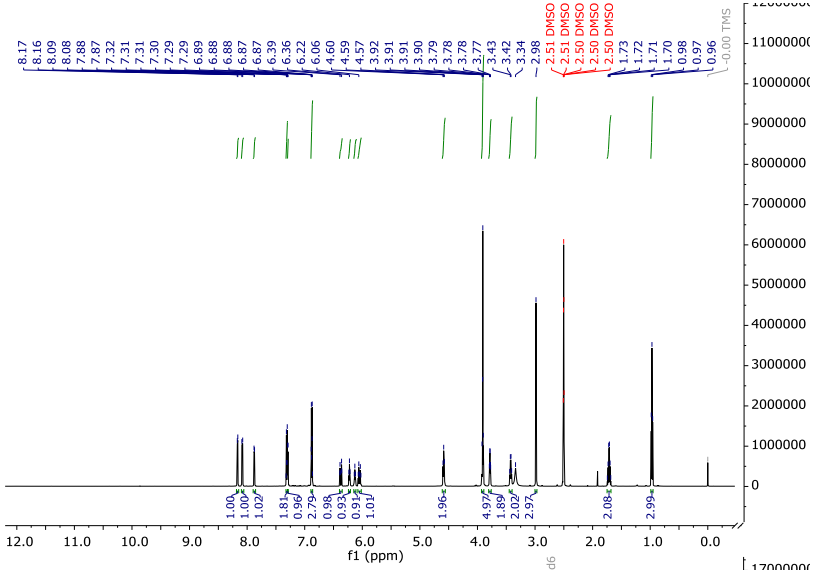
f1 (ppm)

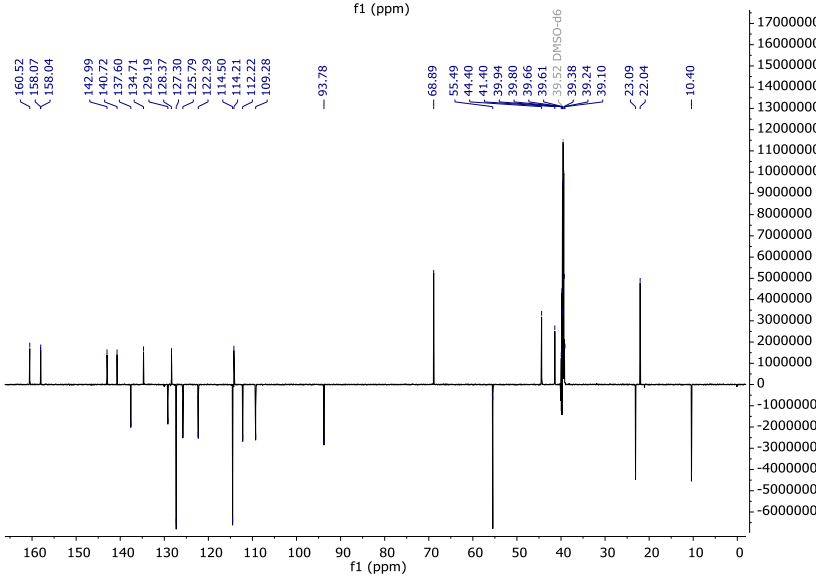
f1 (ppm)

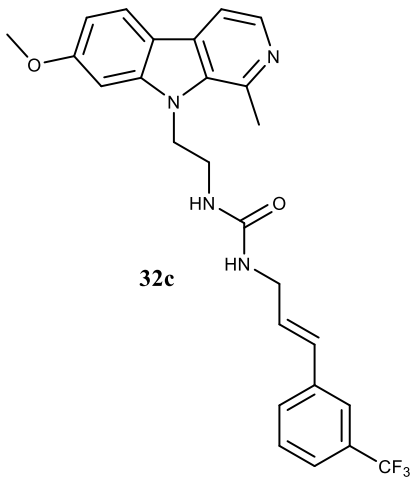
O
N
N
HN
O
HN
CF3

32c

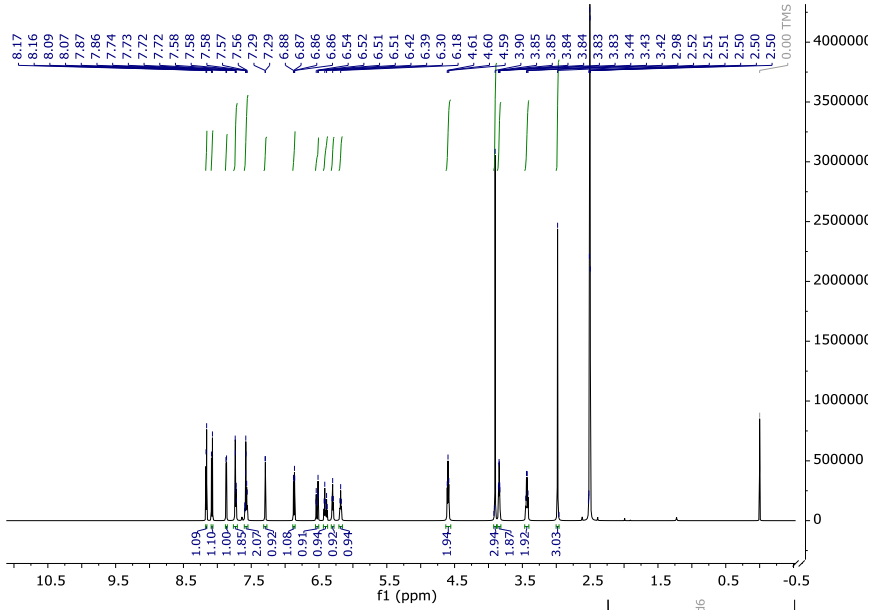
8.17
8.16
8.09
8.07
7.87
7.86
7.74
7.73
7.72
7.72
7.58
7.58
7.58
7.57
7.56
7.29
7.29
6.88
6.87
6.86
6.86
6.54
6.52
6.51
6.51
6.42
6.39
6.30
6.18
4.61
4.60
4.59
3.90
3.85
3.85
3.84
3.84
3.83
3.83
3.44
3.43
3.42
2.98
2.52
2.51
2.51
2.50
2.50
2.50
0.00 TMS
1.09
1.10
1.00
1.85
2.07
0.92
1.08
0.91
0.94
0.92
0.94
1.94
2.94
1.87
1.92
3.03
10.5
9.5
8.5
7.5
6.5
5.5
4.5
3.5
2.5
1.5
0.5
-0.5
f1 (ppm)
4000000
3500000
3000000
2500000
2000000
1500000
1000000
500000
0

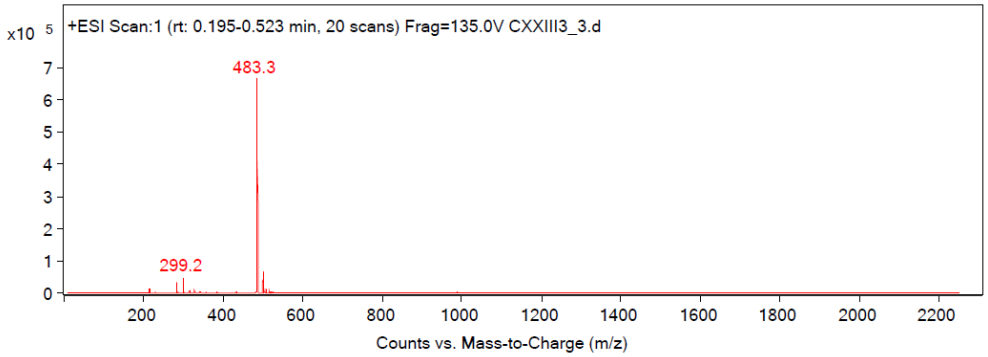
x10 5
+ESI Scan:1 (rt: 0.195-0.523 min, 20 scans) Frag=135.0V CXXIII3_3.d
483.3
299.2
7
6
5
4
3
2
1
0
200
400
600
800
1000
1200
1400
1600
1800
2000
2200
Counts vs. Mass-to-Charge (m/z)

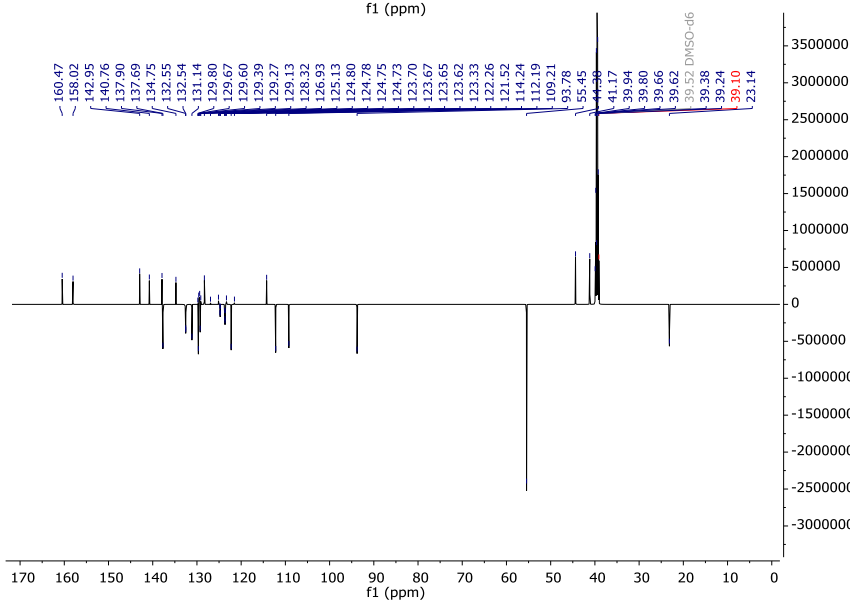
160.47
158.02
142.95
140.76
137.90
137.69
134.75
132.55
132.54
131.14
129.80
129.67
129.60
129.39
129.27
129.13
128.32
126.93
125.13
124.80
124.78
124.75
124.73
123.70
123.67
123.65
123.62
123.33
122.26
121.52
114.24
112.19
109.21
93.78
55.45
44.38
41.17
39.94
39.80
39.66
39.62
39.52 DMSO-d6
39.38
39.24
39.10
23.14
3500000
3000000
2500000
2000000
1500000
1000000
500000
0
-500000
-1000000
-1500000
-2000000
-2500000
-3000000
170
160
150
140
130
120
110
100
90
80
70
60
50
40
30
20
10
0
f1 (ppm)

PRILOG B

Prilog sadrži dva znanstvena rada objavljena u časopisima zastupljenim u bazi Current Contents koji obrađuju problematiku iznesenu u ovom doktorskom radu:

1. **Marinović M**, Perković I, Fontinha D, Prudêncio M, Held J, Pessanha de Carvalho L, Tandarić T, Vianello R, Zorc B, Rajić Z. Novel harmicines with improved potency against *Plasmodium*. Molecules 2020;25:4376.

2. **Marinović M**, Poje G, Perković I, Fontinha D, Prudêncio M, Held J, Pessanha de Carvalho L, Tandarić T, Vianello R, Rajić Z. Further investigation of harmicines as novel antiplasmodial agents: synthesis, structure-activity relationship and insight into the mechanism of action. Eur J Med Chem 2021;224:113687.

molecules

MDPI

Article

Novel Harmicines with Improved Potency against *Plasmodium*

Marina Marinović [1], Ivana Perković [1], Diana Fontinha [2], Miguel Prudêncio [2], Jana Held [3], Lais Pessanha de Carvalho [3], Tana Tandarić [4], Robert Vianello [4], Branka Zorc [1] and Zrinka Rajić [1,*]

1 Faculty of Pharmacy and Biochemistry, University of Zagreb, A. Kovačića 1, HR-10 000 Zagreb, Croatia; mmarinovic@pharma.hr (M.M.); iperkovic@pharma.hr (I.P.); bzorc@pharma.hr (B.Z.)
2 Instituto de Medicina Molecular, Faculdade de Medicina, Universidade de Lisboa, Av. Prof. Egas Moniz, 1649-028 Lisboa, Portugal; dfontinha@medicina.ulisboa.pt (D.F.); mprudencio@medicina.ulisboa.pt (M.P.)
3 Institute of Tropical Medicine, University of Tübingen, Wilhelmstraße 27, 72074 Tübingen, Germany; janaheld@hotmail.de (J.H.); lais_pessanha@hotmail.com (L.P.d.C.)
4 Computational Organic Chemistry and Biochemistry Group, Rudjer Bošković Institute, Bijenička cesta 54, HR-10 000 Zagreb, Croatia; tana.tandaric@irb.hr (T.T.); Robert.vianello@irb.hr (R.V.)
* Correspondence: zrajic@pharma.hr

Academic Editor: Silvie Rimpelová
Received: 6 September 2020; Accepted: 22 September 2020; Published: 23 September 2020

Abstract: Harmicines represent hybrid compounds composed of β-carboline alkaloid harmine and cinnamic acid derivatives (CADs). In this paper we report the synthesis of amide-type harmicines and the evaluation of their biological activity. *N*-harmicines **5a**–**f** and *O*-harmicines **6a**–**h** were prepared by a straightforward synthetic procedure, from harmine-based amines and CADs using standard coupling conditions, 1-[bis(dimethylamino)methylene]-1*H*-1,2,3-triazolo [4,5-*b*]pyridinium 3-oxid hexafluorophosphate (HATU) and *N*,*N*-diisopropylethylamine (DIEA). Amide-type harmicines exerted remarkable activity against the erythrocytic stage of *P. falciparum*, in low submicromolar concentrations, which was significantly more pronounced compared to their antiplasmodial activity against the hepatic stages of *P. berghei*. Furthermore, a cytotoxicity assay against the human liver hepatocellular carcinoma cell line (HepG2) revealed favorable selectivity indices of the most active harmicines. Molecular dynamics simulations demonstrated the binding of ligands within the ATP binding site of *Pf*Hsp90, while the calculated binding free energies confirmed higher activity of *N*-harmicines **5** over their *O*-substituted analogues **6**. Amino acids predominantly affecting the binding were identified, which provided guidelines for the further derivatization of the harmine framework towards more efficient agents.

Keywords: harmine; cinnamic acid; amide; antiplasmodial activity; *Pf*Hsp90; molecular dynamics simulations; *P. berghei*; P. falciparum

1. Introduction

Malaria is a life-threatening parasitic disease that kills over 400,000 people each year, mainly children under 5 years of age in sub-Saharan Africa [1]. Five species of *Plasmodium* cause malaria in humans, and the most severe form of the disease is caused by *P. falciparum*, which is also the most prevalent malaria parasite [2]. The complex life cycle of *Plasmodium* includes two hosts, *Anopheles* mosquitoes and mammals. In the latter, a clinically silent phase of hepatic infection obligatorily precedes a subsequent erythrocytic infection stage, responsible for the symptoms of malaria [3]. Since 2001, when the WHO recommended the use of artemisinin-based combination therapies (ACTs) for treating *P. falciparum* malaria, ACTs have become the mainstay of malaria therapy due to their high

efficacy, safety and lack of serious side effects [4]. Although malaria-caused deaths continuously drop and several countries report either none or under 100 new cases each year, the rise of drug-resistant parasites has slowed down that progress, especially in Asia. Failure rates of *P. falciparum* treatments to the first-line ACTs were found to be above 10% in the Southeast Asia Region, and were as high as 93% in Thailand [1]. Despite numerous efforts to develop an effective vaccine against malaria, it still remains out of reach [5–7]. Taken together, the rising number of drug-resistant parasite strains and the unavailability of an effective vaccine exemplify the need to look for novel antimalarial agents.

Hybrid drugs, compounds with at least two distinct pharmacophores, represent one of the possible strategies for finding novel biologically active molecules [8,9]. As previously shown by us and others, the preparation of hybrids based on known antimalarial agents and cinnamic acid (*trans*-3-phenyl-2-propenoic acid) or its derivatives (CAD) resulted in an increase in the former's in vitro antiplasmodial activity [10–15]. In our previous publication, we reported the synthesis and biological activity of triazole-type harmicines, hybrids based on the alkaloid harmine and CAD, linked via 1*H*-1,2,3-triazole (Figure 1) [15]. Harmine, a natural β-carboline alkaloid, was chosen as a CAD partner due to its known in vitro and in vivo antiplasmodial activity [16,17]. We showed that triazole-type harmicines exert a significant activity against both erythrocytic and hepatic stages of *Plasmodium* infection. In addition, molecular dynamics (MD) simulations confirmed the binding of the most active compound within the ATP binding site of *P. falciparum* heat shock protein 90 (*Pf*Hsp90) [15], which is essential for the parasite's development, and may play a major role in drug resistance [16–20].

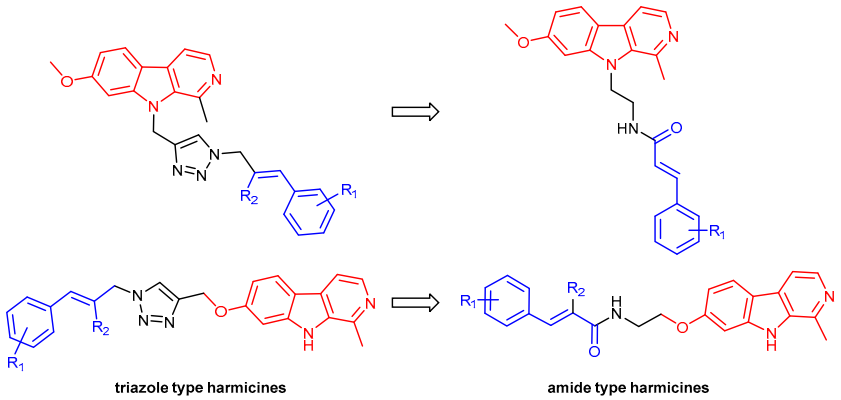

Figure 1. Triazole and amide-type harmicines (harmine is marked in red, while the cinnamic acid derivative (CAD) scaffold is marked in blue).

Since our earlier MD simulations did not identify the triazole ring as being crucial for binding to *Pf*Hsp90 [15], we decided to simplify the linker between two main fragments, harmine and CAD. To this end, triazole was replaced with its bioisostere, an amide bond, resulting in novel, amide-type harmicines. Here, we report the synthesis of amide-type harmicines, their activity against both erythrocytic and hepatic stages of *Plasmodium* infection, and their cytotoxicity. We also discuss how binding to *Pf*Hsp90 affects their activity.

2. Results and Discussion

2.1. Chemistry

As a continuation of our work on hybrids based on harmine and CADs, we decided to focus on amide-type harmicines **5** and **6**. Before synthesis, we evaluated the drug-like properties of the planned compounds, by calculating relevant physico-chemical parameters included in the Lipinski's rule of five and Gelovani's rules for small molecules, using Chemicalize.org software [21]. To our delight, all compounds were in complete agreement with both sets of rules (Table S1).

The chosen synthetic pathway towards novel harmicines involved three reaction steps, depicted in Scheme 1. In the first step, harmine and harmole were alkylated with 2-(Boc-amino)ethyl bromide to yield *N*- and *O*-alkylated compounds **1** and **2**, respectively. The alkylation of harmine proceeded smoothly with four equivalents of 2-(Boc-amino)ethyl bromide in the presence of four equivalents of Cs_2CO_3, at 75 °C for 24 h, whereas employing the same reaction conditions for the alkylation of harmole resulted in the formation of an *N*,*O*-bis alkylated product. A careful optimization of the reaction conditions allowed the selective *O*-alkylation of harmole. Only traces of the *N*,*O*-bis alkylated product were obtained when 2.6 equivalents of the alkylating agent and 1.35 equivalents of Cs_2CO_3 were employed at 110 °C for 4 h.

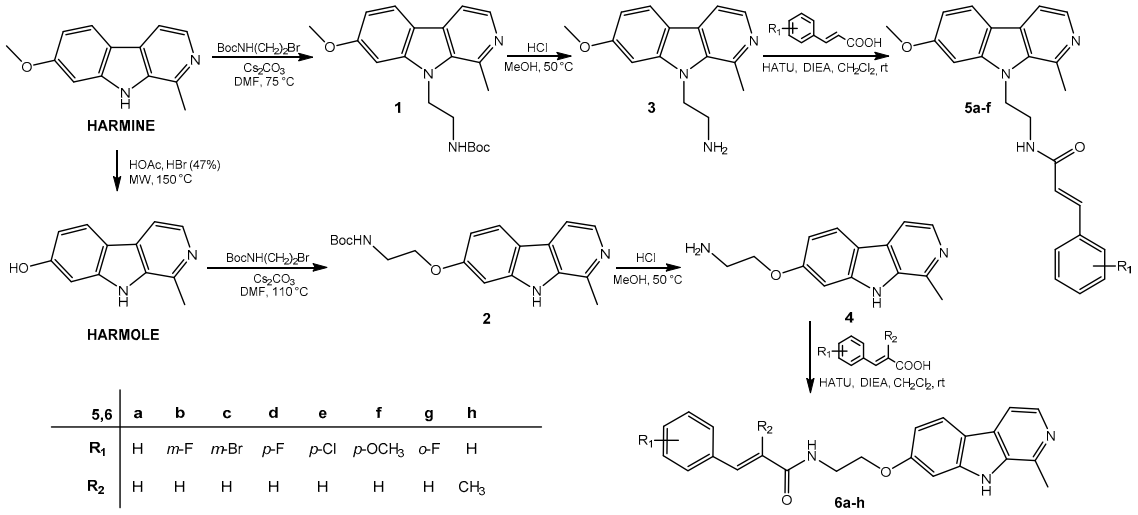

Scheme 1. Synthesis of harmicines **5** and **6**.

The Boc-protecting group was efficiently removed under acidic conditions, to attain primary amines **3** and **4**. In the final reaction step, the coupling between amines **3** or **4** and CADs was accomplished by using standard coupling conditions, 1-[bis(dimethylamino)methylene]-1*H*-1,2,3-triazolo [4,5-*b*]pyridinium 3-oxid hexafluorophosphate (HATU) and *N*,*N*-diisopropylethylamine (DIEA) in dichloromethane (DCM). The employed CADs were chosen according to the results of biological assays obtained earlier [15]. Coupling reactions were performed at room temperature, reaction times were short (1–2 h), and synthetic yields were moderate to high (47–77%). Purification of the crude products by column chromatography and/or crystallization was straightforward. Structures of the final products were confirmed by standard spectroscopic/spectrometric methods (^{1}H and ^{13}C NMR, IR, MS), while their purity was assessed by elemental analyses. The data obtained are provided in short in the Materials and Methods section, and in detail in the Supplementary Information.

2.2. Biological Evaluations

2.2.1. Antiplasmodial Activity

After the successful preparation and characterization of the title compounds, we sought to assess their in vitro activities against the erythrocytic and hepatic stages of *Plasmodium* infection and to investigate whether they differ from those activities of the triazole-type harmicines reported earlier [15].

In Vitro Activity against *P. falciparum* Erythrocytic Stage

The in vitro antiplasmodial activity of harmicines against *P. falciparum* erythrocytic stage was assessed employing both the chloroquine-sensitive (*Pf*3D7) and the chloroquine-resistant (*Pf*Dd2) strains, as previously described [22–24] (Table 1). Chloroquine and harmine were included as positive controls in these assays, and the activity of amide-type harmicines was compared with that of the

previously prepared triazole-type harmicines [15]. The conjugation of harmine to CADs yielded compounds with significantly higher antiplasmodial activity against *P. falciparum* blood stages than the parent compound, harmine. Remarkably, the activities were in the low submicromolar (*Pf*3D7) and submicromolar (*Pf*Dd2) concentrations, which is an activity one order of magnitude stronger than that exerted by the triazole-type harmicines. To our surprise, and in contrast with the data obtained for the triazole-type harmicines, analysis of the IC_{50} (concentration of the tested compound necessary for 50% growth inhibition) values for homologues *N*- and *O*-harmicines showed that the antiplasmodial activity of *N*-harmicines **5** is significantly higher than that of *O*-harmicines **6** against both strains, except in the case of compounds **5f** and **6f** (*Pf*3D7), as well as **5c** and **6c** (*Pf*Dd2).

Table 1. In vitro screening of antiplasmodial activity of amide-type harmicines **5** and **6** against erythrocytic stage of *P. falciparum* (*Pf*3D7 and *Pf*Dd2 strains), cytotoxicity of human liver hepatocellular carcinoma cell line (HepG2) and calculated selectivity indices. Data for harmine and chloroquine are taken from [15].

Compd.	IC_{50} [1] (μM)			SI [2]
	*Pf*3D7	*Pf*Dd2	HepG2	
5a	0.49 ± 0.25 [3]	1.11 ± 0.15 [3]	350.31 ± 13.02 [3]	715
5b	0.07 ± 0.03	0.78 ± 0.32	54.11 ± 13.36	773
5c	0.07 ± 0.03	0.41 ± 0.01	2.88 ± 0.42	41
5d	0.09 ± 0.06	0.33 ± 0.11	20.99 ± 0.88	233
5e	0.04 ± 0.02	0.17 ± 0.01	2.91 ± 1.75	73
5f	0.26 ± 0.001	0.49 ± 0.24	74.69 ± 7.61	287
6a	0.98 ± 0.12	4.7 ± 2.65	12.74 ± 0.66	13
6b	2.75 ± 1.6	5.01 ± 0.83	12.86 ± 3.31	5
6c	0.37 ± 0.22	0.48 ± 0.28	6.11 ± 2.07	16
6d	0.15 ± 0.06	0.69 ± 0.18	7.63 ± 2.47	51
6e	0.32 ± 0.03	0.4 ± 0.24	7.72 ± 3.04	24
6f	0.21 ± 0.14	1.09 ± 0.49	10.53 ± 0.43	50
6g	0.93 ± 0.28	3.92 ± 1.35	16.17 ± 1.86	17
6h	6.78 ± 0.72	19.53 ± 11.83	61.28 ± 2.75	9
CQ [4]	0.003 ± 0.002	0.20 ± 0.10	n.d.	n.d.
Harmine	8.25 ± 2.83	>27.7	> 250	30

[1] IC_{50}, the concentration of the tested compound necessary for 50% growth inhibition. [2] SI, selectivity index, ratio between IC_{50} (HepG2) and IC_{50} (*Pf*3D7). [3] Results represent mean ± SD, $n > 2$. [4] CQ, chloroquine.

We further compared the IC_{50} values within both series and found that the effects of the substituents in the cinnamic scaffold on the antiplasmodial activity were more pronounced for the *Pf*3D7 strain. As shown in Table 1, *N*-harmicines bearing halogens either in the *p*- or the *m*-positions (**5b–e**) exhibited significantly higher activities than unsubstituted and *p*-methoxy substituted compounds. In the *O*-harmicines **6** series, a substitution in the *p*-position was preferred, regardless of the type of substituent. Interestingly, the substitution of hydrogen with its isostere fluorine in the *p*-position yielded the most active compound among *O*-harmicines (**6d**), while the same substitution in the *m*-position resulted in decreased activity. The replacement of hydrogen with fluorine in the *o*-position had no significant influence on the antiplasmodial activity. Conversely, the substitution of the hydrogen with a methyl group in the α-position yielded compound **6h**, with at least one order of magnitude weaker antiplasmodial activity than other *O*-harmicines. The influence of lipophilicity was estimated by the comparison of IC_{50} and calculated log *P* values (Table S1). More lipophilic *N*-harmicines exerted more pronounced activity, while *O*-harmicines did not follow the same pattern. The most active compound against both strains was *N*-harmicine **5e** (IC_{50}(*Pf*3D7) = 0.04 μM, IC_{50}(*Pf*Dd2) = 0.17 μM).

In Vitro Activity against *P. berghei* Hepatic Stages

The in vitro activity of harmicines against the hepatic stages of *Plasmodium* infection was evaluated by employing rodent *P. berghei* parasites and a human hepatoma cell line (Huh7), as previously described [25,26]. Each compound was assessed at 1 and 10 μM (Figure 2), with harmine and DMSO serving as positive and negative controls, respectively. Concomitantly, the compounds' cytotoxicity to Huh7 cells was assessed by cell confluency measurement. The results obtained show that amide-type harmicines do not exert significant activity against the hepatic stages of *P. berghei* infection. The compounds' activity at 1 μM is similar to that of the parent compound harmine, but they are significantly more active than the latter at 10 μM. The marked cytotoxicity observed to Huh7 cells, even at 1 μM, precluded the determination of IC_{50} values for the compounds' hepatic stages antiplasmodial activity.

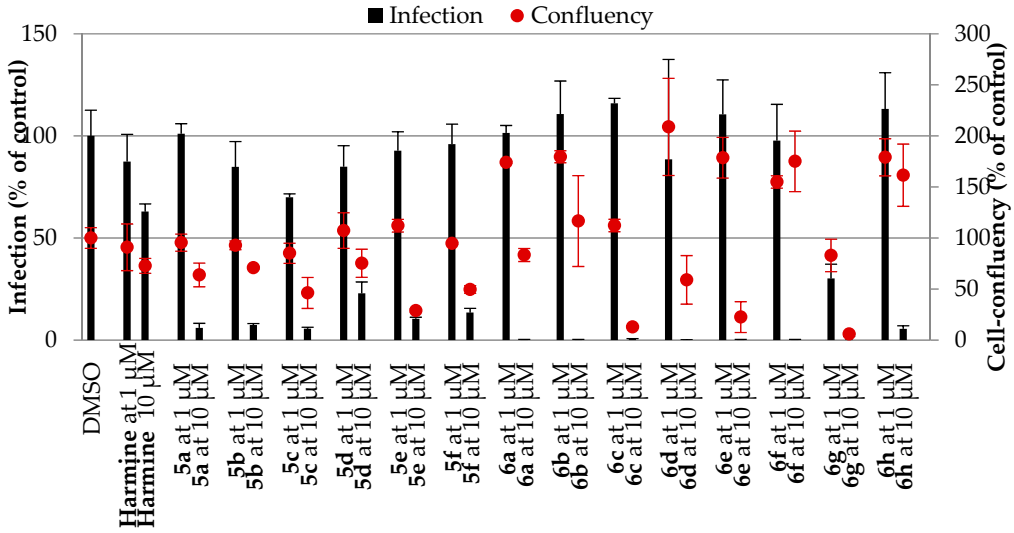

Figure 2. In vitro activity against *P. berghei* liver stages of harmicines **5a–f** and **6a–h** at 1 and 10 μM concentrations. Total parasite load (infection scale, bars) and cell viability (cell confluency scale, dots) are shown. Results were normalized to the negative control, DMSO, and are represented as mean ± SD, $n = 1$.

2.2.2. Cytotoxicity Assay

A cytotoxicity assay was performed using the neutral red assay, as described previously, against human liver hepatocellular carcinoma cell line (HepG2) [27] (Table 1). For the safety assessment, a selectivity index (SI) for each compound was calculated as the fractional ratio between the IC_{50} values for HepG2 and *P. falciparum Pf*3D7 strain (Table 2). In general, *N*-harmicines **5** are less cytotoxic than *O*-harmicines **6**, which is in agreement with the results obtained for triazole-type harmicines. Furthermore, all *N*-harmicines, but only two *O*-harmicines, **6d** and **6f**, have more favorable SIs than the parent compound harmine (SI = 30). A close inspection of the IC_{50} values within the series of *N*-harmicines revealed that substitution of hydrogen in the cinnamic moiety by F, Cl or Br led to a significant increase in cytotoxicity (H < F < Cl ≈ Br). *O*-harmicines showed similar levels of cytotoxicity, independently of the cinnamic substituent. Compound **6h**, with a methyl group in the α-position in the CAD region, was the only exception, as it was significantly less toxic than the other *O*-harmicines. Compound **5b**, with a *m*-fluorine substituent in the cinnamic scaffold, exerted the highest selectivity (SI = 773), followed by **5a**, an amide with unsubstituted cinnamic acid (SI = 715). Two other compounds, namely **5f** and **5d**, also showed pronounced selectivity (SIs 287 and 233, respectively), whereas **6h** and **6b** displayed low selectivity (SIs 9 and 5, respectively).

Table 2. Calculated total binding free energies (ΔG_{BIND}) from molecular dynamics trajectories using MM-GBSA approach, and their decomposition on a per-residue basis for selected derivatives. [1] Data for harmines are taken from [15].

Residue	5a	5d	5e	6a	6d	6e	Harmine
Asn37	−1.82	−1.33	−2.01	−2.09	−1.69	−1.81	0.00
Asp79	1.47	1.36	1.58	1.11	1.30	0.74	0.00
Arg98	−0.05	−0.93	−1.39	−2.00	−2.45	−2.24	0.00
Phe124	−1.44	−1.68	−0.64	−0.58	−0.35	−0.37	0.00
Met84	−2.50	−2.63	−2.70	−2.05	−2.25	−2.02	0.00
Gly83	−0.79	−1.28	−1.63	−1.00	−1.69	−1.56	0.00
Ile82	−0.88	−1.50	−1.51	−1.28	−1.49	−1.43	0.00
Thr171	−1.60	−1.92	−1.51	−0.74	−0.51	−0.53	0.00
Ala41	−1.39	−1.37	−1.44	−1.32	−1.40	−1.27	0.00
Ile173	−1.05	−1.13	−1.18	−0.46	−0.42	−0.32	−0.01
Asn92	−0.96	−0.94	−1.06	−1.64	−1.43	−1.41	0.00
Ala38	−0.90	−0.91	−0.89	−0.56	−0.53	−0.50	0.00
Leu93	−0.63	−0.60	−0.80	−0.46	−0.52	−0.59	0.00
Leu34	−0.68	−0.82	−0.75	−0.16	−0.14	−0.12	0.00
Val136	−0.67	−0.72	−0.64	−0.11	−0.14	−0.12	−0.02
Gly81	−0.33	−0.49	−0.54	−0.37	−0.42	−0.35	0.00
Thr95	0.03	0.03	0.03	0.03	0.04	0.04	0.00
Asp142	0.04	0.03	0.04	0.03	0.03	0.03	0.00
Glu48	0.03	0.05	0.04	0.05	0.06	0.06	0.00
Total ΔG_{BIND}	−33.9	−38.1	−40.9	−34.6	−35.7	−37.5	−7.5

[1] Residues are selected to list those identified as belonging to the ATP binding pocket (Asn37, Asp79, Arg98, Phe124) and all of those with contributions higher than −0.50 and lower than 0.03 kcal mol^{-1} to the most potent **5e**. All values are in kcal mol^{-1}.

2.3. Molecular Dynamics Simulations

Computational analysis was performed to gain an insight into the binding of a representative set of ligands, involving both *N*-substituted (**5a**, **5d** and **5e**) and *O*-substituted derivatives (**6a**, **6d** and **6e**), and to interpret their observed affinities towards *Pf*Hsp90. To this end, MD simulations were employed to obtain the binding poses and the accompanying binding free energies, as well as to identify residues governing the binding. These results were compared with those previously obtained for the parent harmine [15].

We calculated the selected compounds' binding free energies (ΔG_{BIND}), as well as their decomposition into contributions from individual residues (Table 2). The specific residues considered for the analysis include those responsible for the binding of **5e** within the ATP binding pocket (Asn37, Asp79, Arg98, Phe124) [28,29], and all those with contributions higher than −0.50 and lower than 0.03 kcal mol^{-1}, leading to the identification of the residues that are the most and the least responsible for the binding of **5e** to *Pf*Hsp90.

Our data reveal that all evaluated compounds are associated with negative ΔG_{BIND}, in agreement with their high antiplasmodial activity. In addition, a very good agreement between calculated data and experimentally measured activities is observed. Firstly, with the highest binding free energy of ΔG_{BIND} = −40.9 kcal mol^{-1}, computations clearly predict **5e** to have the highest activity, which was confirmed experimentally. It is worth noting that this value exceeds that of an analogous triazole-based *N*-substituted derivative studied earlier [15], where the computed value was −39.0 kcal mol^{-1}, being strongly in line with a general tendency of a higher activity for the amide-based derivatives examined here. Moreover, the calculated difference of −1.9 kcal mol^{-1} nicely agrees with a trend in the matching IC_{50}(*Pf*3D7) activities of 0.04 μM for **5e** and 0.44 μM for its triazole-based analogue [15], which predicts a difference of $\Delta\Delta G_{BIND}$ = −1.6 kcal mol^{-1}. Secondly, computed values evidently distinguish between *O*-substituted and *N*-substituted derivatives, with the latter group involving better binders amid the

two families. Lastly, among each set, the calculated ΔG_{BIND} values indicate identical binding trends regarding the substituents introduced, which assume *p*-Cl (**5e**) > *p*-F (**5d**) > *p*-H (**5a**), in the same way as the matching *O*-substituted derivatives **6e** > **6d** > **6a**. With this in mind, we can safely conclude that the excellent agreement between computations and experiments lends strong credence to the computational methodology employed.

The calculated ΔG_{BIND} value for **5e** is the most exergonic, suggesting it is optimally positioned within *Pf*Hsp90. Its decomposition into contributions from specific residues reveals that **5e** is clearly positioned within the ATP binding site, as its binding is dominated by residues that define this cavity (Figure 3). This holds in particular for Asn37 and Arg98, where the contributions obtained are −2.01 and −1.39 kcal mol^{-1}, respectively, closely followed by Phe124, where it is −0.64 kcal mol^{-1}. The corresponding MD trajectories show that the tricyclic aromatic ring and the attached –OMe group on **5e** are responsible for these favorable contributions. Specifically, side chains of both Asn37 and Phe124 are located above the aromatic framework of **5e**, forming positive N–H···π and π···π stacking interactions, respectively, while Arg98 uses its cationic guanidine moiety to donate hydrogen bonding to the ligand's methoxy oxygen. The overall effect of these three residues is somewhat reduced by the unfavorable effect of Asp79, which is overcome by the contribution of several other residues that promote the binding (Table 2), and which are positioned close to the ATP binding site. The reason behind the negative contribution of Asp79 lies in the repulsion between its carboxylic moiety and the –CH_2–CH_2– linker in **5e** connecting the amide substituent with the harmine *N*-position. This might suggest that the parent harmine, containing all of the positively contributing structural elements—both the tricyclic ring and the –OMe group—while being deprived of the mentioned linker, let alone having the acidic N–H instead that could engage in favorable interactions with Asp79, would represent a much better binder than **5e**. However, quite the opposite occurs, as harmine reveals very poor binding properties, displaying a significantly lower ΔG_{BIND} (−7.5 kcal mol^{-1}) (Table 2), consistent with the significantly higher IC_{50} value of 8.25 μM (Table 1). Moreover, although the relationship between IC_{50} and ΔG_{BIND} values is not so straightforward, the IC_{50} value measured for harmine roughly translates to a binding energy of −6.9 kcal mol^{-1}, which again confirms the validity of our computational setup and nicely ties into our computational and experimental results. Additionally, the data shown in Table 2 clearly indicate that, aside from a very low ΔG_{BIND} value, harmine binds even outside the ATP binding pocket (Figure 3), as none of the residues either defining it or close to it are contributing to the binding. All of these observations underline the importance of the *N*-site of harmine for the inactivation of *Pf*Hsp90, and justify the synthetic strategy employed here, as carefully tailored *N*-substituents can overcome unfavorable interactions with the anionic Asp79 through their positive interactions with the rest of the protein. This valuable insight might provide precious information for further harmine derivatization. Lastly, besides the ATP binding site residues mentioned above, the binding of **5e** is particularly promoted by Met84, which uses its –SMe side chain to form the stabilizing C–H···π interactions with the aromatic unit in **5e** (Figure 3), thus allowing for the highest individual contribution among all amino acid residues.

Interestingly, although *N*-derivatives **5** with different *para*-groups exhibit different antiplasmodial activities (Table 1), we did not observe any significant interactions between moieties placed at this position and the protein (Figure 3). Instead, this site points outside the *Pf*Hsp90. Thus, it is presently unclear what the immediate effect of this position for the ligand affinity is, and how to eventually advance the binding properties with such further substitutions. Still, the extent of this effect is modest and is likely channeled through electron-donating or electron-accepting features of the introduced substituent that modulate the electron density throughout each derivative, which, in turn, affect its interactions with the protein. This conclusion is justified by the data in Table 1, considering that all six *N*-derivatives stretch over only one order of magnitude in the affinities measured, from 0.49 μM in **5a** to 0.04 μM in **5e**, thus confirming only a minor effect of the introduced *para*-substituent. Therefore, it is unlikely that a potential insertion of additional *para*-moieties in **5** will considerably improve the

compounds' activity. Instead, redesigning the employed –CH_2–CH_2– linker emerges as a promising strategy that will be exploited in our future work.

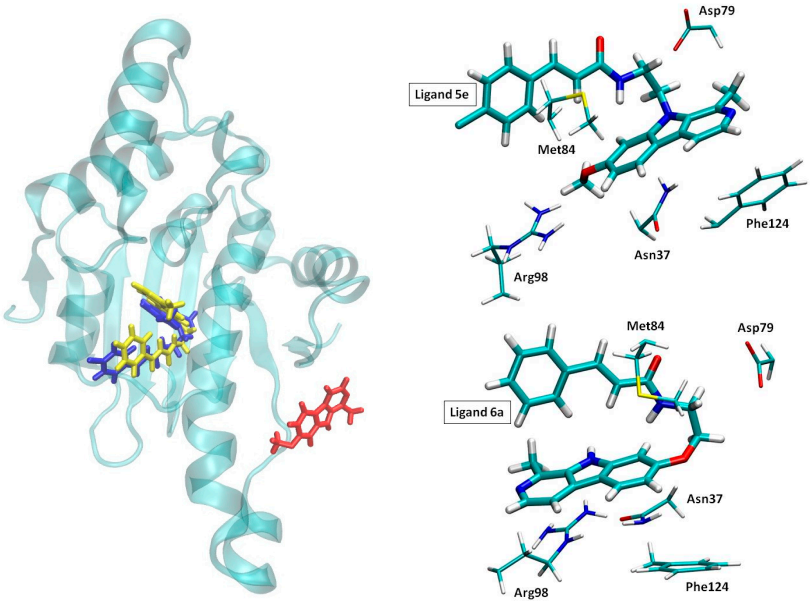

Figure 3. Binding positions of ligands **5e** (in blue) and **6a** (in yellow) within the ATP binding site in *Pf*Hsp90 and harmine (in red) outside of it (left). The interaction of **5e** (top right) and **6a** (bottom right) with the relevant binding site residues.

Replacing *p*-Cl (**5e**) with *p*-F (**5d**) decreases the IC_{50} value by a factor of two and is supported by the 2.8 kcal mol^{-1} lower binding energy of ΔG_{BIND}(**5d**) = −38.1 kcal mol^{-1}. In **5d**, reduced contributions from the ATP binding site residues are observed, which suggests a slight change in the binding pose, except for Phe124, which benefits from the modified ligand's positions by gaining a full kcal mol^{-1} relative to **5e**, as a result of the more optimized π···π stacking interactions in that case. Lastly, complete removal either of the *para*-halogens, as in **5a**, yields a further reduction in both IC_{50} and ΔG_{BIND} values and results in a slightly changed binding pose. The latter appears enough to position the –OMe group away from Arg98, leading to a significant reduction in its binding contribution, while lowering the impact of other residues as well. Given the lowest affinity of **5a** among all *N*-derivatives, these results suggest the predominant role of the introduced *para*-substituent through tuning the position of ligands within the binding site, thus allowing for the optimization of ligand contacts with the protein residues.

Derivatives **6** have a functionalized harmine –OMe group, while maintaining the unsubstituted secondary amine on the central aromatic ring. In line with the above, this is immediately evident in diminishing the negative contribution of Asp79 from 1.58 kcal mol^{-1} in **5e** to 1.11, 1.30 and even 0.74 kcal mol^{-1} in **6a**, **6d** and **6e**, respectively. Yet, these highly positive values do not indicate any favorable hydrogen bonding among Asp79 carboxylate and the ligands amino group, which was also not observed in our simulations. On the other hand, derivatives **6** are also positioned within the ATP binding site in *Pf*Hsp90, but in a way which does not allow for an efficient interaction with Asp79 (Figure 3). This change in the binding pose is evident in the increase in the contribution of Arg98, which moves from forming hydrogen bonding with the ligand's methoxy oxygen, as in **5**, into forming cation···π interactions with aromatic fragments in the *O*-substituted derivatives **6** that turned out as even more favorable (Table 2). The latter also allows Asn92 to optimize its N–H···π interactions with systems **6**, evident in its increased contributions. Other than those, in general, most of the ATP binding site residues and those in their vicinity have reduced contributions relative to the analogous systems **5**, ultimately leading to the lower activities observed for the matching *O*-substituted derivatives **6**. A likely reason for that is the observed tendency of these systems to assume geometries that enable the intramolecular C–H···π stacking interactions among aromatic fragments within the

ligands **6** themselves (Figure 3), which diminish a number of potential contacts with the protein. Additionally, data in Table 2 shows a significant drop in the individual contributions of Thr171, Ile173, Leu34 and Val136, which are considerably lower in **6** than in **5**. These residues form a hydrophobic pocket around the unsubstituted –OMe group and vicinal fragments in **5**, thus promoting the binding, which is not possible upon substituting this part in systems **6**, thus explaining the lower affinities of the latter. Overall, this indicates that the *O*-site in the harmine derivatives provides fewer promising opportunities for the synthesis of successful *Pf*Hsp90 binders, in agreement with our experimental data.

3. Materials and Methods

3.1. Chemistry

3.1.1. General Information

Melting points were determined on a Stuart Melting Point Apparatus (Barloworld Scientific, England, UK) in open capillaries and were uncorrected. FTIR-ATR spectra were recorded using a Fourier-Transform Infrared Attenuated Total Reflection UATR Two Spectrometer (PerkinElmer, Waltham, MA, USA) in the range from 450 to 4000 cm^{-1}. ^{1}H and ^{13}C NMR spectra were recorded on a Bruker Avance III HD operating at 300 or 400 MHz for the ^{1}H and 75, 101 or 151 MHz for the ^{13}C nuclei (Bruker, Billerica, MA, USA). Samples were measured in DMSO-d_6 solutions at 20 °C in 5 mm NMR tubes. Chemical shifts (δ) are reported in parts per million (ppm) using tetramethylsilane (TMS) as a reference in the ^{1}H and DMSO residual peak as a reference in the ^{13}C spectra (39.51 ppm). Coupling constants (J) are reported in hertz (Hz). Mass spectra were recorded on HPLC-MS/MS (HPLC, Agilent Technologies 1200 Series; MS, Agilent Technologies 6410 Triple Quad, San Jose, CA, USA). Mass determination was performed using electrospray ionization (ESI) in a positive mode. Elemental analyses were performed on a CHNS LECO analyzer (LECO Corporation, St. Joseph, MI, USA). Analyses indicated by the symbols of the elements were within ±0.4% of their theoretical values. Microwave-assisted reactions were performed in a microwave reactor CEM Discover (CEM, Matthews, NC, USA) in a glass reaction vessel. All compounds were routinely checked by TLC with silica gel 60F-254 glass plates (Merck KGaA, Darmstadt, Germany) using DCM/methanol 8:1 and 85:15 as the solvent system. Spots were visualized by short-wave UV light (λ = 254 nm) and iodine vapor. Column chromatography was performed on silica gel 0.063–0.200 mm (Sigma-Aldrich, St. Louis, MO, USA) with the same eluents used for TLC. All chemicals and solvents were of analytical grade and purchased from commercial sources. CADs were purchased as predominantly *trans* stereoisomers (≥99%). Harmine, acetic acid, hydrochloric acid, cinnamic acid, α-methylcinnamic acid, 2-fluorocinnamic acid, 3-fluorocinnamic acid, 4-fluorocinnamic acid, 4-methoxycinnamic acid and 4-chlorocinnamic acid were purchased from Sigma-Aldrich (St. Louis, MO, USA). Cesium carbonate, 2-(Boc-amino)ethyl bromide, HATU and 3-bromocinnamic acid were purchased from TCI Chemicals (Tokyo, Japan). Hydrobromic acid (47%) was purchased from Merck (Darmstadt, Germany), DIEA from Alfa Aesar (Kandel, Germany), DCM from Fischer Scientific (Waltham, MA, USA), diethyl ether from ITW Reagents (Darmstadt, Germany), anhydrous sodium sulphate from Gram-Mol (Zagreb, Croatia) and *N*,*N*-dimethylformamide (DMF) from Kemika (Zagreb, Croatia). Harmole was prepared according to the modified literature procedure for harmine using HBr/glacial acetic acid mixture, under MW irradiation [30].

3.1.2. Synthesis of tert-butyl (2-(7-methoxy-1-methyl-9H-pyrido[3,4-b]indol-9-yl)ethyl)carbamate (**1**)

To a stirred solution of harmine (0.200 g, 0.94 mmol) in anhydrous DMF (3 mL) at 75 °C under an argon atmosphere, Cs_2CO_3 (1.228 g, 3.77 mmol, 4 equivalents) was added. The resulting suspension was stirred at 75 °C for 20 min, followed by the addition of 2-(Boc-amino)ethyl bromide (0.844 g, 3.77 mmol, 4 equivalents). The reaction mixture was stirred at 75 °C for 24 h, cooled down, poured into H_2O (40 mL) and extracted with ethyl acetate (3 × 40 mL). The collected organic layers were washed

with H_2O, dried over anhydrous sodium sulfate, filtered, and evaporated under the reduced pressure. After purification by column chromatography (DCM:MeOH = 8:1) and trituration with diethyl ether, 0.195 g (58%) of **1** was obtained; mp 197.5–199 °C; IR (ATR, ν/cm^{-1}) 3183, 3065, 3013, 2993, 2969, 2937, 1701, 1623, 1567, 1502, 1447, 1409, 1366, 1343, 1330, 1313, 1278, 1247, 1195, 1166, 1146, 1124, 1092, 1048, 1018, 970, 944, 876, 841, 803, 768, 727, 684, 639, 598, 559, 534; ^{1}H NMR (DMSO-d_6) δ 8.15 (d, 1H, J = 5.1 Hz), 8.07 (d, 1H, J = 8.5 Hz), 7.85 (d, 1H, J = 5.0 Hz), 7.22 (s, 1H), 7.02 (t, 1H, J = 5.2 Hz), 6.87 (dd, 1H, J = 8.4, 1.6 Hz), 4.55 (t, 2H, J = 6.6 Hz), 3.92 (s, 3H), 3.33–3.31 (m, 2H), 2.95 (s, 3H), 1.29 (s, 8H), 1.01 (s, 1H); ^{13}C NMR (DMSO-d_6) δ 160.45, 155.62, 142.84, 140.46, 137.63, 134.70, 128.39, 122.20, 114.35, 112.10, 108.95, 93.80, 77.77, 55.47, 43.98, 39.97, 28.01, 22.99; ESI-MS: *m/z* 356.2 (M + 1)$^+$.

3.1.3. Synthesis of tert-butyl (2-((1-methyl-9H-pyrido[3,4-b]indol-7-yl)oxy)ethyl)carbamate (**2**)

To a stirred solution of harmole (0.257 g, 1.30 mmol) in anhydrous DMF (3 mL), under an argon atmosphere, Cs_2CO_3 (0.570 g, 1.75 mmol, 1.35 equivalents) was added. The resulting suspension was stirred at room temperature for 20 min, followed by the addition of 2-(Boc-amino)ethyl bromide (0.755 g, 3.37 mmol, 2.6 equivalents). The reaction mixture was stirred at 110 °C for 4 h, cooled down, poured into H_2O (30 mL) and extracted with ethyl acetate (3 × 40 mL). The collected organic layers were washed with H_2O, dried over anhydrous sodium sulfate, filtered, and evaporated under the reduced pressure. After purification by column chromatography (DCM:MeOH = 8:1) and trituration with diethyl ether, 0.278 g (63%) of **2** was obtained; mp 189.5–190.5 °C; IR (ATR, ν/cm^{-1}) 3380, 3134, 3052, 2978, 2944, 2872, 2764, 2726, 2582, 2406, 1692, 1634, 1568, 1530, 1480, 1448, 1394, 1368, 1334, 1296, 1260, 1174, 1114, 1052, 1010, 964, 872, 846, 820, 788, 720, 686, 634, 604, 522; ^{1}H NMR (DMSO-d_6) δ 11.42 (s, 1H), 8.15 (d, 1H, J = 5.3 Hz), 8.05 (d, 1H, J = 8.6 Hz), 7.81 (d, 1H, J = 5.3 Hz), 7.06 (t, 1H, J = 5.4 Hz), 7.00 (d, 1H, J = 2.1 Hz), 6.85 (dd, 1H, J = 8.7, 2.2 Hz), 4.08 (t, 2H, J = 5.8 Hz), 3.41–3.35 (m, 2H), 2.73 (s, 3H), 1.40 (s, 9H); ^{13}C NMR (DMSO-d_6) δ 159.21, 155.72, 141.91, 141.20, 137.58, 134.54, 127.25, 122.65, 114.95, 111.95, 109.32, 95.38, 77.79, 66.65, 28.22, 20.25; ESI-MS: *m/z* 342.3 (M + 1)$^+$.

3.1.4. General Procedure for the Synthesis of Amines **3** and **4**

A solution of the corresponding compound **1** or **2** (0.70 mmol) and 1.76 mL 4 M HCl (7 mmol) in MeOH (4 mL) was stirred at 50 °C for 16 h (compound **1**) or 2 h (compound **2**). Upon completion, solvent was removed under the reduced pressure. The residue was dissolved in H_2O (20 mL), basified to pH 12 with 5% NaOH, and extracted with ethyl acetate (5 × 40 mL). The collected organic layers were dried over anhydrous sodium sulfate, filtered, and evaporated under reduced pressure. The crude product was triturated with diethyl ether.

2-(7-Methoxy-1-methyl-9*H*-pyrido[3,4-*b*]indol-9-yl)ethan-1-amine (**3**)

Yield: 0.179 g, (76%); mp 133.5–135.5 °C; IR (ATR, ν/cm^{-1}); 3354, 3327, 3274, 3054, 3039, 2966, 2932, 2837, 1751, 1621, 1563, 1496, 1443, 1404, 1343, 1302, 1283, 1236, 1219, 1151, 1136, 1117, 1089, 1040, 1021, 973, 941, 922, 887, 848, 815, 768, 723, 643, 599, 551, 528; ^{1}H NMR (DMSO-d_6) δ 8.16 (d, 1H, J = 5.2 Hz), 8.07 (d, 1H, J = 8.6 Hz), 7.86 (d, 1H, J = 5.2 Hz), 7.24 (d, 1H, J = 2.1 Hz), 6.87 (dd, 1H, J = 8.6, 2.2 Hz), 4.54 (t, 2H, J = 7.3 Hz), 3.91 (s, 3H), 2.97 (s, 3H), 2.93 (t, 2H, 2′, J = 7.3 Hz); ^{13}C NMR (DMSO-d_6) δ 160.51, 142.95, 140.67, 137.64, 134.79, 128.22, 122.33, 114.17, 112.23, 109.14, 93.79, 55.63, 47.15, 42.11, 23.33; ESI-MS: *m/z* 256.3 (M + 1)$^+$.

2-((1-Methyl-9*H*-pyrido[3,4-*b*]indol-7-yl)oxy)ethan-1-amine (**4**)

Yield: 0.169 g, (66%); mp 172.5–173 °C; IR (ATR, ν/cm^{-1}) 3954, 3908, 3838, 3786, 3716, 3656, 3530, 3394, 3332, 3250, 3156, 3068, 2930, 2864,2774, 2372, 1892, 1756, 1720, 1628, 1568, 1486, 1444, 1326, 1284, 1238, 1180, 1104, 1028, 996, 908, 860, 812, 636, 590; ^{1}H NMR (DMSO-d_6) δ 11.38 (s, 1H), 8.15 (d, 1H, J = 5.3 Hz), 8.04 (d, 1H, J = 8.6 Hz), 7.79 (d, 1H, J = 5.3 Hz), 7.01 (d, 1H, J = 2.2 Hz), 6.85 (dd, 1H, J = 8.6, 2.2 Hz), 4.03 (t, 2H, J = 5.7 Hz), 2.95 (t, 2H, J = 5.7 Hz), 2.73 (s, 3H), 1.57 (s, 2H); ^{13}C NMR (DMSO-d_6) δ 159.47,

141.90, 141.23, 137.73, 134.53, 127.19, 122.57, 114.82, 111.89, 109.37, 95.27, 70.46, 41.02, 20.32; ESI-MS: *m/z* 242.2 $(M + 1)^+$.

3.1.5. General Procedure for the Synthesis of Harmicines **5a–f**

A solution of CAD (0.18 mmol), DIEA (0.061 mL, 0.35 mmol) and HATU (0.067 g, 0.18 mmol) in DCM (3 mL) was stirred at room temperature for 15 min, followed by the addition of amine **3** (0.045 g, 0.18 mmol). The resulting solution was stirred at room temperature for 2 h. Purification was performed by either Method A or Method B.

Method A: The reaction mixture was extracted with brine (2 × 20 mL) and water (1 × 20 mL). The organic layer was dried over anhydrous sodium sulfate, filtered and evaporated under the reduced pressure. The crude product was purified by column chromatography (DCM:MeOH = 8:1) and triturated with diethyl ether.

Method B: The resulting precipitate was filtered off. The mother liquor was extracted with brine (2 × 20 mL) and water (1 × 20 mL). The organic layer was dried over anhydrous sodium sulfate, filtered, evaporated under the reduced pressure and residue combined with the filtered precipitate. The crude product was purified by column chromatography (DCM:MeOH = 8:1) and triturated with diethyl ether.

N-(2-(7-methoxy-1-methyl-9*H*-pyrido[3,4-*b*]indol-9-yl)ethyl)cinnamamide (**5a**)

CAD: 0.026 g of *trans*-cinnamic acid; purification: Method A; yield: 0.034 g, (51%); mp 201.5–203 °C; IR (ATR, ν/cm^{-1}) 3202, 3027, 2968, 2926, 2852, 1672, 1622, 1566, 1532, 1496, 1447, 1405, 1340, 1306, 1282, 1247, 1218, 1196, 1175, 1138, 1091, 1043, 1020, 972, 938, 856, 814, 762, 679, 641, 597, 555, 485; ^{1}H NMR (DMSO-d_6) δ 8.41 (t, 1H, J = 5.9 Hz), 8.18 (d, 1H, J = 5.2 Hz), 8.09 (d, 1H, J = 8.6 Hz), 7.88 (d, 1H, J = 5.2 Hz), 7.57–7.55 (m, 2H), 7.48–7.36 (m, 4H), 7.27 (d, 1H, J = 1.9 Hz), 6.87 (dd, 1H, J = 8.6, 2.0 Hz), 6.54 (d, 1H, J = 15.8 Hz), 4.67 (t, 2H, J = 6.8 Hz), 3.90 (s, 3H), 3.59 (q, 2H, J = 6.5 Hz), 2.99 (s, 3H); ^{13}C NMR (DMSO-d_6) δ 165.72, 160.49, 142.90, 140.64, 139.16, 137.85, 134.74, 134.64, 129.56, 128.94, 128.46, 127.57, 122.37, 121.65, 114.27, 112.25, 109.40, 93.49, 55.38, 43.36, 39.10, 23.09; ESI-MS: *m/z* 386.4 $(M + 1)^+$; Anal. Calcd. for $C_{24}H_{23}N_3O_2$: C, 74.78; H, 6.01; N, 10.90, found: C, 74.88; H, 6.21; N, 10.75.

(*E*)-3-(3-fluorophenyl)-*N*-(2-(7-methoxy-1-methyl-9*H*-pyrido[3,4-*b*]indol-9-yl)ethyl)acrylamide (**5b**)

CAD: 0.029 g of 3-fluorocinnamic acid; purification: Method A; yield: 0.033 g, (47%); mp 226.5–228 °C; IR (ATR, ν/cm^{-1}); 3661, 3599, 3182, 3009, 2931, 2838, 1671, 1623, 1584, 1538, 1505, 1445, 1412, 1343, 1295, 1240, 1182, 1141, 1095, 1043, 1017, 976, 848, 808, 783, 729, 668, 556, 517; ^{1}H NMR (DMSO-d_6) δ 8.42 (t, 1H, J = 5.9 Hz), 8.18 (d, 1H, J = 5.2 Hz), 8.09 (d, 1H, J = 8.6 Hz), 7.89 (d, 1H, J = 5.2 Hz), 7.49–7.39 (m, 4H), 7.27 (d, 1H, J = 2.0 Hz), 7.25–7.18 (m, 1H), 6.87 (dd, 1H, J = 8.6, 2.1 Hz), 6.59 (d, 1H, J = 15.8 Hz), 4.67 (t, 2H, J = 6.9 Hz), 3.90 (s, 3H), 3.59 (q, 2H, J = 6.5 Hz), 2.99 (s, 3H); ^{13}C NMR (DMSO-d_6) δ 165.44, 162.45 (d, J = 243.8 Hz), 160.51, 142.91, 140.62, 137.89, 137.80, 137.35 (d, J = 7.9 Hz), 134.63, 130.90 (d, J = 8.4 Hz), 128.50, 123.76, 123.20, 122.40, 116.23 (d, J = 21.3 Hz), 114.28, 113.97 (d, J = 21.8 Hz), 112.27, 109.40, 93.51, 55.39, 43.33, 39.10, 23.05; ESI-MS: *m/z* 404.4 $(M + 1)^+$; Anal. Calcd. for $C_{24}H_{22}FN_3O_2$: C, 71.45; H, 5.50; N, 10.42, found: C, 71.26; H, 5.79; N, 10.59.

(*E*)-3-(3-bromophenyl)-*N*-(2-(7-methoxy-1-methyl-9*H*-pyrido[3,4-*b*]indol-9-yl)ethyl)acrylamide (**5c**)

CAD: 0.040 g of 3-bromocinnamic acid; purification: Method B; yield: 0.057 g, (70%); mp 225–226 °C; IR (ATR, ν/cm^{-1}); 3180, 3051, 3021, 2975, 2932, 2901, 2864, 2792, 2559, 1944, 1875, 1679, 1621, 1565, 1498, 1468, 1450, 1410, 1377, 1345, 1305, 1251, 1223, 1195, 1138, 1106, 1043, 1018, 980, 941, 911, 885, 862, 812, 786, 729, 671, 648, 614, 599, 555, 537, 515; ^{1}H NMR (DMSO-d_6) δ 8.39 (t, 1H, J = 6.0 Hz), 8.18 (d, 1H, J = 5.2 Hz), 8.09 (d, 1H, J = 8.6 Hz), 7.89 (d, 1H, J = 5.2 Hz), 7.77 (t, 1H, J = 1.7 Hz), 7.57 (dd, 2H, J = 8.1, 1.4 Hz), 7.44–7.35 (m, 2H), 7.26 (d, 1H, J = 2.1 Hz), 6.87 (dd, 1H, J = 8.6, 2.2 Hz), 6.59 (d, 1H, J = 15.8 Hz), 4.67 (t, 2H, J = 6.9 Hz), 3.90 (s, 3H), 3.60 (q, 2H, J = 6.5 Hz), 2.99 (s, 3H); ^{13}C NMR (DMSO-d_6) 165.39, 160.52, 142.92, 140.62, 137.80, 137.57, 137.33, 134.64, 132.09, 131.04, 130.13, 128.52, 126.43, 123.32, 122.41,

122.27, 114.29, 112.29, 109.39, 93.54, 55.41, 43.34, 39.10, 23.05; ESI-MS: *m/z*, 464.3 $(M + 1)^+$, 466.3 $(M + 1)^+$; Anal. Calcd. for $C_{24}H_{22}BrN_3O_2$: C, 62.08; H, 4.78; N, 9.05, found: C, 62.31; H, 4.89; N, 9.27.

(*E*)-3-(4-fluorophenyl)-*N*-(2-(7-methoxy-1-methyl-9*H*-pyrido[3,4-*b*]indol-9-yl)ethyl)acrylamide (**5d**)

CAD: 0.029 g of 4-fluorocinnamic acid; purification: Method B; yield: 0.042 g, (57%); mp 202.5–204 °C; IR (ATR, ν/cm^{-1}); 3664, 3583, 3438, 3207, 3083, 2985, 2938, 2756, 2723, 1656, 1622, 1601, 1545, 1508, 1471, 1449, 1416, 1390, 1370, 1345, 1292, 1256, 1223, 1203, 1181, 1163, 1141, 1098, 1045, 1018, 976, 944, 836, 741, 722, 644, 557, 530, 511; ^{1}H NMR (DMSO-d_6) δ 8.40 (s, 1H), 8.19 (d, 1H, J = 4.3 Hz), 8.11 (d, 1H, J = 8.4 Hz), 7.92 (d, 1H, J = 4.2 Hz), 7.62 (t, 2H, J = 6.6 Hz), 7.45 (d, 1H, J = 15.7 Hz), 7.28–7.23 (m, 3H), 6.88 (d, 1H, J = 8.0 Hz), 6.49 (d, 1H, J = 15.7 Hz), 4.67 (t, 2H, J = 6.7 Hz), 3.90 (s, 3H), 3.59 (q, 2H, J = 6.8 Hz), 3.00 (s, 3H); ^{13}C NMR (DMSO-d_6) δ 165.69, 162.76 (d, J = 247.0 Hz), 160.67, 143.12, 140.44, 138.01, 137.34, 134.59, 131.38 (d, J = 2.5 Hz), 129.77 (d, J = 8.3 Hz), 128.78, 122.52, 121.53, 115.93 (d, J = 21.7 Hz), 114.22, 112.40, 109.62, 93.52, 55.44, 43.40, 39.09, 22.76; ESI-MS: *m/z* 404.2 $(M + 1)^+$; Anal. Calcd. for $C_{24}H_{22}FN_3O_2$: C, 71.45; H, 5.50; N, 10.42, found: C, 71.58; H, 5.37; N, 10.48.

(*E*)-3-(4-chlorophenyl)-*N*-(2-(7-methoxy-1-methyl-9*H*-pyrido[3,4-*b*]indol-9-yl)ethyl)acrylamide (**5e**)

CAD: 0.032 g of 4-chlorocinnamic acid; purification: Method B; yield: 0.039 g, (53%); mp 245 °C (decomp.); IR (ATR, ν/cm^{-1}) 3195, 3103, 3025, 2998, 2928, 2835, 1672, 1621, 1558, 1493, 1442, 1407, 1338, 1284, 1254, 1200, 1138, 1086, 1045, 977, 947, 799, 748, 708, 680, 634, 593, 550, 497; ^{1}H NMR (DMSO-d_6) δ 8.41 (t, 1H, J = 5.9 Hz), 8.17 (d, 1H, J = 5.2 Hz), 8.09 (d, 1H, J = 8.6 Hz), 7.88 (d, 1H, J = 5.2 Hz), 7.59 (d, 2H, J = 8.5 Hz), 7.49–7.42 (m, 3H), 7.26 (d, 1H, J = 2.0 Hz), 6.87 (dd, 1H, J = 8.6, 2.1 Hz), 6.55 (d, 1H, J = 15.8 Hz), 4.67 (t, 2H, J = 6.8 Hz), 3.89 (s, 3H), 3.59 (q, 2H, J = 6.5 Hz), 2.99 (s, 3H); ^{13}C NMR (DMSO-d_6) δ 165.53, 160.50, 142.90, 140.63, 137.83, 134.64, 133.99, 133.70, 129.29, 128.98, 128.48, 122.44, 122.38, 114.28, 112.26, 109.39, 93.50, 55.39, 43.34, 39.10, 23.07; ESI-MS: *m/z* 420.3 $(M + 1)^+$; Anal. Calcd. for $C_{24}H_{22}ClN_3O_2$: C, 68.65; H, 5.28; N, 10.01, found: C, 68.90; H, 5.11; N, 10.23.

(*E*)-*N*-(2-(7-methoxy-1-methyl-9*H*-pyrido[3,4-*b*]indol-9-yl)ethyl)-3-(4-methoxyphenyl)acrylamide (**5f**)

CAD: 0.031 g of 4-methoxycinnamic acid; purification: Method A; yield: 0.046 g, (61%); mp 216–217.5 °C; IR (ATR, ν/cm^{-1}); 3212, 3102, 3040, 2993, 2973, 2940, 2919, 2840, 1667, 1620, 1604, 1558, 1514, 1474, 1443, 1409, 1382, 1338, 1306, 1283, 1254, 1229, 1198, 1173, 1138, 1096, 1033, 979, 949, 827, 801, 780, 731, 701, 684, 635, 592, 541, 521; ^{1}H NMR (DMSO-d_6) δ 8.31 (t, 1H, J = 5.9 Hz), 8.17 (d, 1H, J = 5.2 Hz), 8.09 (d, 1H, J = 8.6 Hz), 7.88 (d, 1H, J = 5.2 Hz), 7.51 (d, 2H, J = 8.8 Hz), 7.41 (d, 1H, J = 15.8 Hz), 7.27 (d, 1H, J = 2.1 Hz), 6.97 (d, 2H, J = 8.8 Hz), 6.87 (dd, 1H, J = 8.6, 2.2 Hz), 6.40 (d, 1H, J = 15.8 Hz), 4.66 (t, 2H, J = 6.9 Hz), 3.90 (s, 3H), 3.79 (s, 3H), 3.58 (q, 2H, J = 6.6 Hz), 2.99 (s, 3H); ^{13}C NMR (DMSO-d_6) δ 166.04, 160.51, 160.41, 142.92, 140.63, 138.88, 137.81, 134.64, 129.17, 128.47, 127.30, 122.38, 119.15, 114.39, 114.26, 112.26, 109.43, 93.49, 55.38, 55.26, 43.42, 39.09, 23.06; ESI-MS: *m/z* 416.3 $(M + 1)^+$; Anal. Calcd. for $C_{25}H_{25}N_3O_3$: C, 72.27; H, 6.07; N, 10.11, found: C, 72.43; H, 6.32; N, 10.35.

3.1.6. General Procedure for the Synthesis of Harmicines **6a–h**

A solution of CAD (0.20 mmol), DIEA (0.070 mL, 0.40 mmol) and HATU (0.077 g, 0.20 mmol) in DCM (4 mL) was stirred at room temperature for 15 min, followed by the addition of amine **4** (0.049 g, 0.20 mmol). The resulting solution was stirred at room temperature for 1 h. The formed precipitate was filtered off. After purification by column chromatography (DCM:MeOH = 85:15) and trituration with diethyl ether, compounds **6a**–**h** were obtained.

N-(2-((1-methyl-9*H*-pyrido[3,4-*b*]indol-7-yl)oxy)ethyl)cinnamamide (**6a**)

CAD: 0.030 g of *trans*-cinnamic acid; yield: 0.045 g, (60%); mp 151.5 °C (decomp.); IR (ATR, ν/cm^{-1}) 3994, 3908, 3838, 3784, 3718, 3656, 3424, 3222, 3060, 2972, 2932, 2874, 2768, 2372, 1898, 1720, 1630, 1574, 1544, 1486, 1450, 1392, 1332, 1280, 1234, 1174, 1110, 1056, 976, 812, 764, 684, 596; ^{1}H NMR (DMSO-d_6)

δ 11.66 (s, 1H), 8.47 (t, 1H, J = 5.3 Hz,), 8.19 (d, 1H, J = 5.4 Hz), 8.11 (d, 1H, J = 8.7 Hz), 7.90 (d, 1H, J = 5.4 Hz), 7.57 (d, 2H, J = 7.0 Hz), 7.48 (d, 1H, J = 15.8 Hz), 7.44–7.35 (m, 3H), 7.07 (d, 1H, J = 1.8 Hz), 6.91 (dd, 1H, J = 8.7, 2.0 Hz), 6.73 (d, 1H, J = 15.8 Hz), 4.20 (t, 2H, J = 5.4 Hz), 3.65 (q, 2H, 5.3 Hz), 2.77 (s, 3H); ^{13}C NMR (DMSO-d_6) δ 165.29, 159.52, 142.38, 140.70, 138.87, 136.37, 134.87, 134.45, 129.46, 128.92, 127.89, 127.52, 122.95, 122.02, 114.84, 112.25, 109.80, 95.39, 66.68, 38.51, 19.66; ESI-MS: *m/z* 372.2 $(M + 1)^+$; Anal. Calcd. for $C_{23}H_{21}N_3O_2$: C, 74.37; H, 5.70; N, 11.31, found: C, 74.67; H, 5.75; N, 11.22.

(*E*)-3-(3-fluorophenyl)-*N*-(2-((1-methyl-9*H*-pyrido[3,4-*b*]indol-7-yl)oxy)ethyl)acrylamide (**6b**)

CAD: 0.034 g of 3-fluorocinnamic acid; yield: 0.053 g, (67%); mp 210–212.5 °C; (ATR, ν/cm^{-1}); 3954, 3908, 3838, 3784, 3718, 3656, 3256, 3070, 2940, 2866, 2812, 2370, 1872, 1778, 1720, 1670, 1630, 1580, 1486, 1444, 1344, 1250, 1178, 1110, 1060, 1028, 964, 852, 784, 670, 624, 594, 528; ^{1}H NMR (DMSO-d_6) δ 11.47 (s, 1H), 8.47 (t, 1H, J = 5.5 Hz), 8.16 (d, 1H, J = 5.3 Hz), 8.08 (d, 1H, J = 8.7 Hz), 7.83 (d, 1H, J = 5.3 Hz), 7.50–7.40 (m, 4H), 7.21 (ddd, 1H, J = 9.9, 3.9, 2.0 Hz), 7.05 (d, 1H, J = 2.1 Hz), 6.89 (dd, 1H, J = 8.7, 2.2 Hz), 6.77 (d, 1H, J = 15.8 Hz), 4.19 (t, 2H, J = 5.4 Hz), 3.65 (q, 2H, J = 5.4 Hz), 2.74 (s, 3H); ^{13}C NMR (DMSO-d_6) δ 165.00, 162.44 (d, J = 243.8 Hz), 159.22, 141.97, 141.16, 137.59, 137.47, 137.42, 134.54, 130.88 (d, J = 8.4 Hz), 127.33, 123.65, 123.60, 122.72, 116.12 (d, J = 21.3 Hz), 115.00, 113.92 (d, J = 21.8 Hz), 112.01, 109.42, 95.42, 66.62, 38.58, 20.17; ESI-MS: *m/z* 390.2 $(M + 1)^+$; Anal. Calcd. for $C_{23}H_{20}FN_3O_2$: C, 70.94; H, 5.18; N, 10.79, found: C, 70.83; H, 5.27; N, 10.99.

(*E*)-3-(3-bromophenyl)-*N*-(2-((1-methyl-9*H*-pyrido[3,4-*b*]indol-7-yl)oxy)ethyl)acrylamide (**6c**)

CAD: 0.046 g of 3-bromocinnamic acid; yield: 0.043 g, (47%); mp 135–137.5 °C; IR (ATR, ν/cm^{-1}) 3908, 3840, 3784, 3718, 3656, 3424, 3206, 3056, 2970, 2932, 2872, 2774, 2374, 1874, 1720, 1666, 1630, 1572, 1450, 1338, 1282, 1234, 1168, 1110, 1054, 972, 846, 786, 668, 602; ^{1}H NMR (DMSO-d_6) δ 11.48 (s, 1H), 8.44 (t, 1H, J = 5.5 Hz), 8.16 (d, 1H, J = 5.3 Hz), 8.08 (d, 1H, J = 8.7 Hz), 7.83 (d, 1H, J = 5.3 Hz), 7.79 (t, 1H, J = 1.5 Hz), 7.60–7.55 (m, 2H), 7.45 (d, 1H, J = 15.8 Hz), 7.38 (t, 1H, J = 7.9 Hz), 7.05 (d, 1H, J = 2.1 Hz), 6.89 (dd, 1H, J = 8.7, 2.2 Hz), 6.78 (d, 1H, J = 15.8 Hz), 4.19 (t, 2H, J = 5.4 Hz), 3.65 (q, 2H, J = 5.4 Hz), 2.74 (s, 3H); ^{13}C NMR (DMSO-d_6) δ 164.93, 159.21, 141.97, 141.14, 137.47, 137.39, 137.22, 134.53, 131.97, 131.01, 130.04, 127.34, 126.40, 123.72, 122.72, 122.24, 114.99, 112.01, 109.42, 95.42, 66.62, 38.57, 20.16; ESI-MS: *m/z* 450.1 $(M + 1)^+$, 452.1 $(M + 1)^+$; Anal. Calcd. for $C_{23}H_{20}BrN_3O_{22}$: C, 61.34; H, 4.48; N, 9.33, C, 61.29; H, 4.67; N, 9.68.

(*E*)-3-(4-fluorophenyl)-*N*-(2-((1-methyl-9*H*-pyrido[3,4-*b*]indol-7-yl)oxy)ethyl)acrylamide (**6d**)

CAD: 0.034 g of 4-fluorocinnamic acid; yield: 0.057 g, (73%); mp 199.5–200 °C; IR (ATR, ν/cm^{-1}) 3952, 3908, 3840, 3786, 3718, 3634, 3572, 3430, 3248, 3072, 2940, 2866, 2812, 2600, 2366, 2050, 1872, 1720, 1668, 1630, 1576, 1508, 1456, 1344, 1278, 1230, 1178, 1110, 1030, 694, 796, 674, 626, 594, 506; ^{1}H NMR (DMSO-d_6) δ 11.47 (s, 1H), 8.44 (t, 1H, J = 5.5 Hz), 8.16 (d, 1H, J = 5.3 Hz), 8.08 (d, 1H, J = 8.7 Hz), 7.83 (d, 1H, J = 5.3 Hz), 7.66–7.60 (m, 2H), 7.48 (d, 1H, J = 15.8 Hz), 7.29–7.22 (m, 2H), 7.05 (d, 1H, J = 2.1 Hz), 6.89 (dd, 1H, J = 8.7, 2.2 Hz), 6.68 (d, 1H, J = 15.8 Hz), 4.19 (t, 2H, J = 5.5 Hz), 3.65 (q, 2H, J = 5.4 Hz), 2.74 (s, 3H); ^{13}C NMR (DMSO-d_6) δ 165.23, 162.69 (d, J = 247.1 Hz), 159.23, 141.98, 141.16, 137.69, 137.43, 134.54, 131.51 (d, J = 2.7 Hz), 129.68 (d, J = 8.4 Hz), 127.34, 122.73, 121.92, 115.90 (d, J = 21.7 Hz), 114.99, 112.01, 109.43, 95.42, 66.66, 38.55, 20.18; ESI-MS: *m/z* 390.2 $(M + 1)^+$; Anal. Calcd. for $C_{23}H_{20}FN_3O_2$: C, 70.94; H, 5.18; N, 10.79, found: C, 70.81; H, 5.39; N, 10.63.

(*E*)-3-(4-chlorophenyl)-*N*-(2-((1-methyl-9*H*-pyrido[3,4-*b*]indol-7-yl)oxy)ethyl)acrylamide (**6e**)

CAD: 0.037 g of 4-chlorocinnamic acid; yield: 0.052 g, (64%); mp 230.5–234 °C; IR (ATR, ν/cm^{-1}) 3908, 3838, 3784, 3716, 3656, 3268, 3044, 2942, 2880, 2774, 2372, 1720, 1662, 1626, 1560, 1488, 1450, 1330, 1284, 1234, 1168, 1102, 982, 874, 820, 740, 654, 588; ^{1}H NMR (DMSO-d_6) δ 11.68 (s, 1H), 8.49 (t, 1H, J = 5.5 Hz), 8.19 (d, 1H, J = 5.5 Hz), 8.11 (d, 1H, J = 8.7 Hz), 7.91 (d, 1H, J = 5.4 Hz), 7.60 (d, 2H, J = 8.5 Hz), 7.49–7.45 (m, 3H), 7.07 (d, 1H, J = 2.1 Hz), 6.91 (dd, 1H, J = 8.7, 2.2 Hz), 6.74 (d, 1H, J = 15.8 Hz), 4.20 (t, 2H, J = 5.4 Hz), 3.65 (q, 2H, J = 5.4 Hz), 2.77 (s, 3H); ^{13}C NMR (DMSO-d_6) δ 165.09, 159.53, 142.40, 140.66,

137.51, 136.29, 134.44, 133.87, 133.84, 129.22, 128.95, 127.92, 122.96, 122.83, 114.84, 112.26, 109.81, 95.38, 66.66, 38.53, 19.63; ESI-MS: *m/z* 390.2 $(M + 1)^+$; Anal. Calcd. for $C_{23}H_{20}ClN_3O_2$: C, 68.06; H, 4.97; N, 10.35, found: C, 68.18; H, 4.84; N, 10.44.

(*E*)-3-(4-methoxyphenyl)-*N*-(2-((1-methyl-9*H*-pyrido[3,4-*b*]indol-7-yl)oxy)ethyl)acrylamide (**6f**)

CAD: 0.036 g of 4-methoxycinnamic acid; yield: 0.051 g, (63%); mp 191–194.5 °C; (ATR, ν/cm^{-1}); 3976, 3908, 3838, 3784, 3718, 3656, 3432, 3258, 3070, 2938, 2770, 2368, 2050, 1874, 1720, 1602, 1546, 1514, 1448, 1280, 1174, 1108, 1030, 984, 872, 828, 744, 714, 674, 588, 554, 518; ^{1}H NMR (DMSO-d_6) δ 11.46 (s, 1H), 8.35 (t, 1H, J = 5.5 Hz), 8.16 (d, 1H, J = 5.3 Hz), 8.07 (d, 1H, J = 8.7 Hz), 7.83 (d, 1H, J = 5.3 Hz), 7.52 (d, 2H, J = 8.8 Hz), 7.43 (d, 1H, J = 15.8 Hz), 7.05 (d, 1H, J = 2.1 Hz), 6.98 (d, 2H, J = 8.8 Hz), 6.89 (dd, 1H, J = 8.7, 2.2 Hz), 6.58 (d, 1H, J = 15.8 Hz), 4.18 (t, 2H, J = 5.5 Hz), 3.79 (s, 3H), 3.64 (q, 2H, J = 5.4 Hz), 2.73 (s, 3H); ^{13}C NMR (DMSO-d_6) δ 165.60, 160.33, 159.23, 141.96, 141.18, 138.58, 137.48, 134.54, 129.10, 127.43, 127.31, 122.71, 119.52, 114.99, 114.38, 112.00, 109.41, 95.41, 66.70, 55.24, 38.50, 20.21; ESI-MS: *m/z* 402.2 $(M + 1)^+$; Anal. Calcd. for $C_{24}H_{23}N_3O_3$: C, 71.80; H, 5.77; N, 10.47, found: C, C, 71.89; H, 5.54; N, 10.36.

(*E*)-3-(2-fluorophenyl)-*N*-(2-((1-methyl-9*H*-pyrido[3,4-*b*]indol-7-yl)oxy)ethyl)acrylamide (**6g**)

CAD: 0.034 g of 2-fluorocinnamic acid; yield: 0.061 g, (77%); mp 241.5 °C (decomp.); IR (ATR, ν/cm^{-1}) 3838, 3784, 3716, 3636, 3570, 3252, 3066, 2942, 2864, 2818, 2600, 1866, 1668, 1630, 1576, 1486, 1456, 1344, 1278, 1234, 1180, 1100, 1060, 1022, 964, 850, 812, 750, 676, 626, 594; ^{1}H NMR (DMSO-d_6) δ 11.47 (s, 1H), 8.60 (t, 1H, J = 5.4 Hz), 8.15 (d, 1H, J = 5.3 Hz), 8.07 (d, 1H, J = 8.6 Hz), 7.81 (d, 1H, J = 5.3 Hz), 7.70–7.63 (m, 1H, 7.55 (d, 1H, J = 16.0 Hz), 7.48–7.39 (m, 1H), 7.28 (dd, 2H, J = 15.7, 8.3 Hz), 7.06 (d, 1H, J = 2.0 Hz), 6.88 (dd, 1H, J = 8.7, 2.1 Hz), 6.84 (d, 1H, J = 16.0 Hz), 4.19 (t, 2H, J = 5.4 Hz), 3.65 (q, 2H, J = 5.4 Hz), 2.73 (s, 3H); ^{13}C NMR (DMSO-d_6) δ 165.05, 160.45 (d, J = 250.4 Hz), 159.12, 141.87, 141.31, 137.72, 134.57, 131.35, 131.23, 129.08, 127.15, 124.97, 124.85 (d, J = 5.9 Hz), 122.65, 122.49 (d, J = 11.5 Hz), 116.08 (d, J = 21.8 Hz), 115.03, 111.93, 109.30, 95.44, 66.57, 38.61, 20.35; ESI-MS: m/z 390.3 $(M + 1)^+$; Anal. Calcd. for $C_{23}H_{20}FN_3O_2$: C, 70.94; H, 5.18; N, 10.79, found: C, 70.99; H, 4.97; N, 11.01.

(*E*)-2-methyl-*N*-(2-((1-methyl-9*H*-pyrido[3,4-*b*]indol-7-yl)oxy)ethyl)-3-phenylacrylamide (**6h**)

CAD: 0.033 g of α-methylcinnamic acid; yield: 0.047 g, (61%); mp 221.5–222.5 °C; (ATR, ν/cm^{-1}) 3996, 3954, 3908, 3838, 3786, 3716, 3656, 3432, 3202, 3024, 2940, 2880, 2800, 2596, 2512, 2370, 1952, 1884, 1776, 1720, 1630, 1538, 1484, 1446, 1276, 1236, 1174, 1106, 1070, 972, 926, 850, 814, 760, 698, 664, 588, 516; ^{1}H NMR (DMSO-d_6) δ 11.52 (s, 1H), 8.33 (t, 1H, J = 5.3 Hz), 8.17 (d, 1H, J = 5.2 Hz), 8.09 (d, 1H, J = 8.6 Hz), 7.85 (d, 1H, J = 5.1 Hz), 7.43–7.36 (m, 4H), 7.34–7.30 (m, 1H), 7.26 (s, 1H), 7.07 (s, 1H), 6.90 (d, 1H, J = 8.4 Hz), 4.22 (t, 2H, J = 5.2 Hz), 3.63 (q, J = 5.4 Hz, 2H), 2.75 (s, 3H), 2.04 (s, 3H); ^{13}C NMR (DMSO-d_6) δ 169.15, 159.42, 142.12, 141.01, 137.10, 136.02, 134.52, 132.50, 132.28, 129.21, 128.40, 127.70, 127.53, 122.79, 114.93, 112.08, 109.56, 95.47, 66.28, 38.96, 20.03, 14.29; ESI-MS: *m/z* 386.3 $(M + 1)^+$; Anal. Calcd. for $C_{24}H_{23}N_3O_2$: C, 74.78; H, 6.01; N, 10.90, found: C, 74.99; H, 6.32; N, 10.73.

3.2. In Vitro Drug Sensitivity Assay against Erythrocytic Stages of P. falciparum

The antiplasmodial activity of harmicines **5** and **6** was evaluated against two laboratory *P. falciparum* strains (3D7 – CQ-sensitive, and Dd2 – CQ-resistant), as previously described, using the histidine-rich protein 2 (HRP2) assay [23,24]. Briefly, 96-well plates were pre-coated with the tested compounds in a three-fold dilution before ring stage parasites were added in complete culture medium at a hematocrit of 1.5% and a parasitemia of 0.05%. After three days of incubation at 37 °C, 5% CO_2 and 5% oxygen, plates were frozen until analyzed by HRP2-ELISA. All compounds were evaluated in duplicate in at least two independent experiments. The IC_{50} was determined by nonlinear regression analysis of log concentration–response curves using the drc package v0.9.0 of R v2.6.1 [22].

3.3. In Vitro Activity against P. berghei Hepatic Stages

The in vitro activity of harmicines **5** and **6** against the liver stages of *P. berghei* infection was assessed as previously described [25,26]. Briefly, Huh7 cells were routinely cultured in 1640 Roswell Park Memorial Institute (RPMI) medium supplemented with 10% (*v/v*) fetal bovine serum, 1% (*v/v*) glutamine, 1% (*v/v*) penicillin/streptomycin, 1% non-essential amino acids, and 10 mM 2-(4-(2-hydroxyethyl)piperazin-1-yl)ethanesulfonic acid (HEPES). For drug screening experiments, Huh7 cells were seeded at 1×10^4 cell/well of a 96-well plate and incubated overnight at 37 °C with 5% CO_2. Stock solutions of test compounds (10 mM) were prepared in DMSO and were serially diluted in infection medium, i.e., culture medium supplemented with gentamicin (50 µg/mL) and amphotericin B (0.8 µg/mL), in order to obtain the test concentrations. On the day of the infection, the culture medium was replaced by serial dilutions of test compounds and incubated for 1 h at 37 °C with 5% CO_2. Next, 1×10^4 firefly luciferase-expressing *P. berghei* sporozoites, freshly isolated from the salivary glands of female infected *Anopheles stephensi* mosquitoes, were added to the cultures, plates were centrifuged at 1800× *g* for 5 min at room temperature and incubated at 37 °C with 5% CO_2. To assess the effect of each compound concentration on cell viability, cultures were incubated with Alamar Blue (Invitrogen, Waltham, MA, USA) at 46 h post infection (hpi), according to the manufacturer's recommendations. The parasite load was then assessed by a bioluminescence assay (Biotium, Fremont, CA, USA), using a multi-plate reader, Infinite M200 (Tecan, Männedorf, Switzerland). Nonlinear regression analysis was employed to fit the normalized results of the dose–response curves, and IC_{50} values were determined using GraphPad Prism 6.0 (GraphPad software, La Jolla, CA, USA).

3.4. In Vitro Cytotoxicity Assay

Cytotoxicity against a human cell line (HepG2) was evaluated using the neutral red assay [27]. In brief, human cells were seeded to a 96 well plate in complete culture medium, before on the following day a serial dilution of the respective compound was added. After one day of incubation, cytotoxicity was evaluated by the addition of Neutral Red, subsequent lysis of cells and the measurement of absorbance in a plate reader. The IC_{50} was determined as for the in vitro drug assay against *P. falciparum.* To assess the safety of a compound, SI was calculated as the fractional ratio between the IC_{50} values for HepG2 and the *P. falciparum* 3D7 strain.

3.5. Molecular Dynamics Simulations

The starting point of our molecular dynamics simulations was a *Pf*Hsp90 N-terminal domain structure obtained by X-ray crystallography from the Protein Data Bank (accession code 3K60). Ligands (ADP and SO_4^{2-}) were removed from the model and selected compounds were placed in the ATP binding pocket, including harmine as a reference. Original crystal waters were removed from the structure so that water molecules from the bulk solvent could diffuse into the protein during equilibration and production MD runs. In order to parameterize the investigated ligands, geometry optimization and RESP charge calculations were performed using the Gaussian 16 program [31] at the HF/6–31G(d) level to be consistent with the employed GAFF force field, while the *Pf*Hsp90 protein was modeled using the AMBER ff14SB force field. Such protein complexes were solvated in a truncated octahedral box of TIP3P water molecules spanning a 10-Å-thick buffer, neutralized by Na^+ ions and submitted to geometry optimization in the AMBER 16 program [32] by employing periodic boundary conditions in all directions. Optimized systems were gradually heated from 0 to 300 K and equilibrated during 30 ps using NVT conditions, followed by productive and unconstrained MD simulations of 300 ns by employing a time step of 2 fs at a constant pressure (1 atm) and temperature (300 K), with the latter held constant using a Langevin thermostat with a collision frequency of 1 ps^{-1}. Bonds involving hydrogen atoms were constrained using the SHAKE algorithm [33] while the long-range electrostatic interactions were calculated employing the Particle Mesh Ewald method [34]. The nonbonded interactions were truncated at 10.0 Å.

The binding free energies, ΔG_{BIND}, of each ligand within the *Pf*Hsp90 ATP binding site were calculated using the established MM-GBSA protocol [35,36] available in AmberTools16 [32], and in line with our earlier reports [15,37,38]. MM-GBSA is a widely used method for binding free energy calculations from snapshots of MD trajectory with an estimated standard error of 1–3 kcal mol^{-1} [36]. For that purpose, 1000 snapshots collected from the last 30 ns of the corresponding MD trajectories were utilized. The calculated MM-GBSA binding free energies were decomposed into specific residue contributions on a per-residue basis according to the established procedure [39,40]. This protocol calculates contributions to ΔG_{BIND} arising from each amino acid residue and identifies the nature of the energy change in terms of interaction and solvation energies or entropic contributions.

4. Conclusions

In this paper, we have presented a synthesis of the amide-type harmicines, which is simpler and more efficient than the synthesis of the triazole-type harmicines. This, in turn, offers significant advantages in terms of the cost and availability of those compounds. We also investigated their biological activities against erythrocytic and hepatic stages of *Plasmodium*, as well as against the HepG2 cell line and performed computational analysis in order to gain more insight into their binding to *Pf*Hsp90. Amide-type harmicines exerted stronger antiplasmodial activities against the erythrocytic stage of infection than their triazole counterparts. At the same time, their activities against hepatic stages of *P. berghei* were not significant. Furthermore, *N*-harmicines displayed favorable selectivity indices. Molecular dynamics simulations indicated that their binding to *Pf*Hsp90 might be crucial for the inhibition of *Plasmodium* development. These results pave the way for the future enrichment of the harmicines library, towards the establishment of a relevant QSAR model and the identification of a lead compound for further development.

Supplementary Materials: Table S1: Properties of novel compounds calculated with Chemicalize.org program. The Lipinski's and Gelovani's parameters; Table S2: IR, ^{1}H and ^{13}C NMR spectroscopic data for compounds **1** and **3**; Table S3: IR, ^{1}H and ^{13}C NMR spectroscopic data for compounds **2** and **4**; Table S4: Analytical and MS data for harmicines **5a–f**; Table S5: IR, ^{1}H and ^{13}C NMR spectroscopic data for harmicines **5a–f**; Table S6: Analytical and MS data for harmicines **6a–h**; Table S7: IR, ^{1}H and ^{13}C NMR spectroscopic data for harmicines **6a–h**; spectra of all compounds are available online.

Author Contributions: Conceptualization, Z.R.; methodology, M.M., I.P., D.F., M.P., J.H., L.P.d.C., T.T., R.V.; writing—original draft, R.V., B.Z., Z.R. All authors have read and agreed to the published version of the manuscript.

Funding: The authors acknowledge the financial support of the Croatian Science Foundation (research project UIP-2017-05-5160), the University of Zagreb (support for 2019), and Fundação para a Ciência e Tecnologia, Portugal (FCT) (grant 02/SAICT/2017/29550). The work of doctoral student M. Marinović was fully supported by the Young researcher's career development project—training of doctoral students of the Croatian Science Foundation, founded by the European Union through the European Social Fund.

Acknowledgments: T.T. and R.V. would like to thank the Zagreb University Computing Centre (SRCE) for granting us the computational resources on the ISABELLA cluster.

Conflicts of Interest: The authors declare no conflict of interest. The funders had no role in the design of the study; in the collection, analyses, or interpretation of data; in the writing of the manuscript, or in the decision to publish the results.

Abbreviations

ADP	adenosine diphosphate
ATR	attenuated total reflectance
Boc	*tert*-butyloxycarbonyl
CAD	cinnamic acid derivative
DCM	dichloromethane
DIEA	*N*,*N*-diisopropylethylamine
DMF	*N*,*N*-dimethylformamide
ESI	electrospray ionization
GAFF	generalized Amber force field

HATU	1-[bis(dimethylamino)methylene]-1*H*-1,2,3-triazolo[4,5-*b*]pyridinium-3-oxidhexafluorophosphate
HEPES	2-(4-(2-hydroxyethyl)piperazin-1-yl)ethanesulfonic acid
HRP2	histidine-rich protein 2
HepG2	human liver hepatocellular carcinoma cell line
IC_{50}	the concentration of the tested compound necessary for 50% growth inhibition
MD	chloroquine-sensitive strain of *P. falciparum*
MM-GBSA	molecular mechanics/generalized born surface area
MW	microwave
*Pf*Dd2	chloroquine-resistant strain of *P. falciparum*
*Pf*Hsp90	*P. falciparum* heat shock protein 90
QSAR	quantitative structure–activity relationship
RESP	restrained electrostatic potential
SI	selectivity index
TIP3P	transferable intermolecular potential with 3 points
TMS	tetramethylsilane
UATR	universal attenuated total reflectance

References

1. WHO. World Malaria Report 2019. World Health Organisation, 2019. Available online: https://apps.who.int/iris/bitstream/handle/10665/330011/9789241565721-eng.pdf?sequence=1&isAllowed=y (accessed on 15 July 2020).
2. Mishra, M.; Mishra, V.K.; Kashaw, V.; Iyer, A.K.; Kashaw, S.K. Comprehensive review on various strategies for antimalarial drug discovery. *Eur. J. Med. Chem.* **2017**, *125*, 1300–1320. [CrossRef] [PubMed]
3. Fernández-Álvaro, E.; Hong, W.D.; Nixon, G.L.; O'Neill, P.M.; Calderón, F. Antimalarial Chemotherapy: Natural Product Inspired Development of Preclinical and Clinical Candidates with Diverse Mechanisms of Action. *J. Med. Chem.* **2016**, *59*, 5587–5603. [CrossRef] [PubMed]
4. Grimberg, B.T.; Mehlotra, R.K. Expanding the antimalarial drug arsenal-now, but how? *Pharmaceuticals* **2011**, *4*, 681–712. [CrossRef] [PubMed]
5. Available online: https://www.ema.europa.eu/en/news/first-malaria-vaccine-receives-positive-scientific-opinion-ema (accessed on 15 July 2020).
6. Wilby, K.J.; Lau, T.T.; Gilchrist, S.E.; Ensom, M.H. Mosquirix (RTS,S): A Novel Vaccine for the Prevention of Plasmodium falciparum Malaria. *Ann. Pharmacother.* **2012**, *46*, 384–393. [CrossRef]
7. Malaria Vaccine Pilot Launched in Malawi. Available online: https://www.who.int/news-room/detail/23-04-2019-malaria-vaccine-pilot-launched-in-malawi (accessed on 14 July 2020).
8. Mishra, S.; Singh, P. Hybrid molecules: The privileged scaffolds for various pharmaceuticals. *Eur. J. Med. Chem.* **2016**, *124*, 500–536. [CrossRef]
9. Meunier, B. Hybrid molecules with a dual mode of action: Dream or reality? *Acc. Chem. Res.* **2008**, *41*, 69–77. [CrossRef]
10. Pérez, B.C.; Teixeira, C.; Albuquerque, I.S.; Gut, J.; Rosenthal, P.J.; Gomes, J.R.B.; Prudeîncio, M.; Gomes, P. N-Cinnamoylated chloroquine analogues as dual-stage antimalarial leads. *J. Med. Chem.* **2013**, *56*, 556–567. [CrossRef]
11. Pérez, B.; Teixeira, C.; Albuquerque, I.S.; Gut, J.; Rosenthal, P.J.; Prudêncio, M.; Gomes, P. Primacins, N-cinnamoyl-primaquine conjugates, with improved liver-stage antimalarial activity. *Medchemcomm* **2012**, *3*, 1170–1172. [CrossRef]
12. Pérez, B.; Teixeira, C.; Gut, J.; Rosenthal, P.J.; Gomes, J.R.B.; Gomes, P. Cinnamic Acid/Chloroquinoline Conjugates as Potent Agents against Chloroquine-Resistant Plasmodium falciparum. *ChemMedChem* **2012**, *7*, 1537–1540. [CrossRef]
13. Pérez, B.; Teixeira, C.; Gomes, A.S.; Albuquerque, I.S.; Gut, J.; Rosenthal, P.J.; Prudêncio, M.; Gomes, P. In Vitro efficiency of 9-(N-cinnamoylbutyl)aminoacridines against blood- and liver-stage malaria parasites. *Bioorg. Med. Chem. Lett.* **2013**, *23*, 610–613. [CrossRef]
14. Pérez, B.C.; Teixeira, C.; Figueiras, M.; Gut, J.; Rosenthal, P.J.; Gomes, J.R.B.; Gomes, P. Novel cinnamic acid/4-aminoquinoline conjugates bearing non-proteinogenic amino acids: Towards the development of potential dual action antimalarials. *Eur. J. Med. Chem.* **2012**, *54*, 887–899. [CrossRef] [PubMed]

15. Perković, I.; Raić-Malić, S.; Fontinha, D.; Prudêncio, M.; Pessanha de Carvalho, L.; Held, J.; Tandarić, T.; Vianello, R.; Zorc, B.; Rajić, Z. Harmicines—Harmine and cinnamic acid hybrids as novel antiplasmodial hits. *Eur. J. Med. Chem.* **2020**, *187*. [CrossRef] [PubMed]
16. Shahinas, D.; MacMullin, G.; Benedict, C.; Crandall, I.; Pillaid, D.R. Harmine is a potent antimalarial targeting Hsp90 and synergizes with chloroquine and artemisinin. *Antimicrob. Agents Chemother.* **2012**, *56*, 4207–4213. [CrossRef] [PubMed]
17. Shahinas, D.; Liang, M.; Datti, A.; Pillai, D.R. A repurposing strategy identifies novel synergistic inhibitors of plasmodium falciparum heat shock protein 90. *J. Med. Chem.* **2010**, *53*, 3552–3557. [CrossRef]
18. Bayih, A.G.; Folefoc, A.; Mohon, A.N.; Eagon, S.; Anderson, M.; Pillai, D.R. In vitro and in vivo anti-malarial activity of novel harmine-analog heat shock protein 90 inhibitors: A possible partner for artemisinin. *Malar. J.* **2016**, *15*, 1–11. [CrossRef]
19. Shahinas, D.; Folefoc, A.; Pillai, D.R. Targeting plasmodium falciparum Hsp90: Towards reversing antimalarial resistance. *Pathogens* **2013**, *2*, 33–54. [CrossRef]
20. Wang, T.; Mäser, P.; Picard, D. Inhibition of Plasmodium falciparum Hsp90 Contributes to the Antimalarial Activities of Aminoalcohol-carbazoles. *J. Med. Chem.* **2016**, *59*, 6344–6352. [CrossRef]
21. Chemicalize. Available online: https://chemicalize.com/ (accessed on 20 July 2020).
22. R Core Team. *A Language and Environment for Statistical Computing*; R Foundation for Statistical Computing: Vienna, Austria, 2020; Available online: https://www.r-project.org/ (accessed on 20 July 2020).
23. Noedl, H.; Bronnert, J.; Yingyuen, K.; Attlmayr, B.; Kollaritsch, H.; Fukuda, M. Simple histidine-rich protein 2 double-site sandwich enzyme-linked immunosorbent assay for use in malaria drug sensitivity testing. *Antimicrob. Agents Chemother.* **2005**, *49*, 3575–3577. [CrossRef]
24. Held, J.; Gebru, T.; Kalesse, M.; Jansen, R.; Gerth, K.; Müller, R.; Mordmüller, B. Antimalarial activity of the myxobacterial macrolide chlorotonil A. *Antimicrob. Agents Chemother.* **2014**, *58*, 6378–6384. [CrossRef]
25. Ploemen, I.H.J.; Prudêncio, M.; Douradinha, B.G.; Ramesar, J.; Fonager, J.; van Gemert, G.-J.; Luty, A.J.F.; Hermsen, C.C.; Sauerwein, R.W.; Baptista, F.G.; et al. Visualisation and Quantitative Analysis of the Rodent Malaria Liver Stage by Real Time Imaging. *PLoS ONE* **2009**, *4*, e7881. [CrossRef]
26. Machado, M.; Sanches-Vaz, M.; Cruz, J.P.; Mendes, A.M.; Prudêncio, M. Inhibition of Plasmodium hepatic infection by antiretroviral compounds. *Front. Cell. Infect. Microbiol.* **2017**, *7*. [CrossRef] [PubMed]
27. Borenfreund, E.; Puerner, J.A. A simple quantitative procedure using monolayer cultures for cytotoxicity assays (HTD/NR-90). *J. Tissue Cult. Methods* **1985**, *9*, 7–9. [CrossRef]
28. Roe, S.M.; Prodromou, C.; O'Brien, R.; Ladbury, J.E.; Piper, P.W.; Pearl, L.H. Structural basis for inhibition of the Hsp90 molecular chaperone by the antitumor antibiotics radicicol and geldanamycin. *J. Med. Chem.* **1999**, *42*, 260–266. [CrossRef] [PubMed]
29. Corbett, K.D.; Berger, J.M. Structure of the ATP-binding domain of Plasmodium falciparum Hsp90. *Proteins Struct. Funct. Bioinform.* **2010**, *78*, 2738–2744. [CrossRef]
30. Frédérick, R.; Bruyére, C.; Vancraeynest, C.; Reniers, J.; Meinguet, C.; Pochet, L.; Backlund, A.; Masereel, B.; Kiss, R.; Wouters, J. Novel trisubstituted harmine derivatives with original in vitro anticancer activity. *J. Med. Chem.* **2012**, *55*, 6489–6501. [CrossRef]
31. Frisch, M.J.; Trucks, G.W.; Schlegel, H.B.; Scuseria, G.E.; Robb, M.A.; Cheeseman, J.R.; Scalmani, G.; Barone, V.; Petersson, G.A.; Nakatsuji, H.; et al. *Gaussian 16*; Revision C.01; Gaussian, Inc.: Wallingford, CT, USA, 2016.
32. Case, D.A.; Betz, R.M.; Cerutti, D.S.; Darden, T.A.; Duke, R.E.; Giese, T.J.; Gohlke, H.; Goetz, A.W.; Homeyer, N.; Izadi, S.; et al. *Amber 2016*; University of California, San Francisco: San Francisco, CA, USA, 2016.
33. Ryckaert, J.P.; Ciccotti, G.; Berendsen, H.J.C. Numerical integration of the cartesian equations of motion of a system with constraints: Molecular dynamics of n-alkanes. *J. Comput. Phys.* **1977**, *23*, 327–341. [CrossRef]
34. Darden, T.; York, D.; Pedersen, L. Particle mesh Ewald: An N·log(N) method for Ewald sums in large systems. *J. Chem. Phys.* **1993**, *98*, 10089–10092. [CrossRef]
35. Hou, T.; Wang, J.; Li, Y.; Wang, W. Assessing the performance of the MM/PBSA and MM/GBSA methods. 1. The accuracy of binding free energy calculations based on molecular dynamics simulations. *J. Chem. Inf. Model.* **2011**, *51*, 69–82. [CrossRef]
36. Genheden, S.; Ryde, U. The MM/PBSA and MM/GBSA methods to estimate ligand-binding affinities. *Expert Opin. Drug Discov.* **2015**, *10*, 449–461. [CrossRef]

37. Tandarić, T.; Vianello, R. Computational Insight into the Mechanism of the Irreversible Inhibition of Monoamine Oxidase Enzymes by the Antiparkinsonian Propargylamine Inhibitors Rasagiline and Selegiline. *ACS Chem. Neurosci.* **2019**, *10*, 3532–3542. [CrossRef]
38. Matić, J.; Šupljika, F.; Tandarić, T.; Dukši, M.; Piotrowski, P.; Vianello, R.; Brozovic, A.; Piantanida, I.; Schmuck, C.; Stojković, M.R. DNA/RNA recognition controlled by the glycine linker and the guanidine moiety of phenanthridine peptides. *Int. J. Biol. Macromol.* **2019**, *134*, 422–434. [CrossRef] [PubMed]
39. Rastelli, G.; Del Rio, A.; Degliesposti, G.; Sgobba, M. Fast and accurate predictions of binding free energies using MM-PBSA and MM-GBSA. *J. Comput. Chem.* **2010**, *31*, 797–810. [CrossRef] [PubMed]
40. Gohlke, H.; Kiel, C.; Case, D.A. Insights into protein-protein binding by binding free energy calculation and free energy decomposition for the Ras-Raf and Ras-RalGDS complexes. *J. Mol. Biol.* **2003**, *330*, 891–913. [CrossRef]

Sample Availability: Not available.

European Journal of Medicinal Chemistry 224 (2021) 113687

Contents lists available at ScienceDirect

European Journal of Medicinal Chemistry

journal homepage: http://www.elsevier.com/locate/ejmech

Further investigation of harmicines as novel antiplasmodial agents: Synthesis, structure-activity relationship and insight into the mechanism of action

Marina Marinović [a, 1], Goran Poje [a, 1], Ivana Perković [a], Diana Fontinha [b], Miguel Prudêncio [b], Jana Held [c], Lais Pessanha de Carvalho [c], Tana Tandarić [d], Robert Vianello [d], Zrinka Rajić [a, *]

[a] University of Zagreb Faculty of Pharmacy and Biochemistry, A. Kovačića 1, 10000, Zagreb, Croatia
[b] Instituto de Medicina Molecular João Lobo Antunes, Faculdade de Medicina, Universidade de Lisboa, Av. Prof. Egas Moniz, 1649-028, Lisboa, Portugal
[c] University of Tübingen, Institute of Tropical Medicine, Wilhelmstraße 27, 72074, Tübingen, Germany
[d] Rudjer Bošković Institute, Division of Organic Chemistry and Biochemistry, Bijenička Cesta 54, 10 000, Zagreb, Croatia

ARTICLE INFO

Article history:
Received 26 April 2021
Received in revised form
2 July 2021
Accepted 3 July 2021
Available online 5 July 2021

Keywords:
Harmine
β-Carboline
Cinnamic acid
Hybrid compounds
Antiplasmodial activity
*Pf*Hsp90
P. berghei
P. falciparum

ABSTRACT

The rise of the resistance of the malaria parasite to the currently approved therapy urges the discovery and development of new efficient agents. Previously we have demonstrated that harmicines, hybrid compounds composed from β-carboline alkaloid harmine and cinnamic acid derivatives, linked *via* either triazole or amide bond, exert significant antiplasmodial activity. In this paper, we report synthesis, antiplasmodial activity and cytotoxicity of expanded series of novel triazole- and amide-type harmicines. Structure-activity relationship analysis revealed that amide-type harmicines **27**, prepared at N-9 of the β-carboline core, exhibit superior potency against both erythrocytic stage of *P. falciparum* and hepatic stages of *P. berghei*. Notably, harmicine **27a**, *m*-(trifluoromethyl)cinnamic acid derivative, exhibited the most favourable selectivity index (SI = 1105). Molecular dynamics simulations revealed the ATP binding site of *P. falciparum* heat shock protein 90 as a druggable binding location, confirmed the usefulness of the harmine's N-9 substitution and identified favourable N–H … π interactions involving Lys45 and the aromatic phenyl unit in the attached cinnamic acid fragment as crucial for the enhanced biological activity. Thus, those compounds were identified as promising and valuable leads for further derivatization in the search of novel, more efficient antiplasmodial agents.

1. Introduction

Malaria is the deadliest human protozoan infectious disease widely spread in the tropical and subtropical areas of the world. Five identified species of the parasite responsible for causing human malaria are *Plasmodium falciparum*, *P. vivax*, *P. ovale*, *P. malariae* and *P. knowlesi*. Of these, *P. falciparum* and *P. vivax* are responsible for more than 95% of malaria cases in the world [1–3]. Despite years of continuous efforts, it is still a major cause of morbidity and mortality (229 million cases and 409 000 deaths in 2019), especially among young children and pregnant women [3]. As existing antimalarial drugs are becoming less effective due to the emergence of resistant strains of *P. falciparum*, there is an urgent need for novel and effective agents to combat malaria [2].

One of the widely employed approaches to find novel antimalarial chemotherapeutic agents is the design of hybrid molecules [4–8]. Hybrids represent chemical entities in which at least two pharmacological agents, acting on the same disease, are covalently linked in a single molecule. Ideally, the novel molecule should have greater activity than the sum of its parts and reduce the risk of drug resistance, drug-drug interactions and adverse effects. In the antimalarial field, hybrids comprised of agents belonging to the most of the known antimalarial drug classes have shown enhanced activity *in vitro* and *in vivo* [5]. Among those compounds, conjugates with cinnamic acid and its derivatives (CADs) have been extensively explored by us and others [9–13] and recently reviewed by Gomes and co-workers [14].

* Corresponding author.
E-mail address: zrajic@pharma.hr (Z. Rajić).
[1] Both authors contributed equally to this work.

https://doi.org/10.1016/j.ejmech.2021.113687
0223-5234/

In our previous work, we presented harmicines, hybrid compounds derived from harmine, a β-carboline alkaloid with antiplasmodial properties, and CADs [10,15]. The reported harmicines differ in 1) the type of the linker between two moieties, which is either a triazole ring or an amide bond, 2) the position of the substitution on the harmine's β-carboline core, which is either O-7 or N-9, and 3) type of CAD. Harmicines exerted remarkable antiplasmodial activity against erythrocytic and hepatic stages of the *Plasmodium* infection, while molecular dynamics (MD) simulations confirmed binding of the most active compounds within the ATP binding site of *P. falciparum* heat shock protein 90 (*Pf*Hsp90), crucial for the intraerythrocytic development of *Plasmodium* [16,17].

To further extend our knowledge of the harmicines structure-activity relationship, we decided to derivatize the harmine scaffold at C-1, C-3, O-6 and N-9 of the β-carboline core and combine it with different CADs (Fig. 1). Both triazole-type (TT) and amide-type (AT) harmicines were prepared. As a continuation of our research, we investigated their antiplasmodial activity against both erythrocytic and hepatic stages of the *Plasmodium* parasite, as well as cytotoxicity against human liver hepatocellular carcinoma cell line (HepG2). We also report computational analysis of their binding to *Pf*Hsp90 using MD simulations.

2. Results and discussion

2.1. Chemistry

The synthetic part of this work could be divided into two parts: 1) synthesis of TT harmicines and 2) synthesis of AT harmicines, with a general synthetic scheme shown in Fig. 2, while the detailed reactions and conditions are given in Schemes 1–4.

TT harmicines (**5a-e**, **14a-e**, **15a-e**, **20a-e**) were prepared by Cu(I) catalysed azide-alkyne cycloaddition (CuAAC). Different reagents and reaction conditions were used depending on the position of the β-carboline ring functionalization. Harmine-based azides **3** or **10** and CAD-based alkynes **4a-e** served as building blocks for the synthesis of TT harmicines at C-1 (**5a-e**) or C-3 (**15a-e**), respectively. CuAAC was performed with $CuSO_4 \times 5H_2O$ in the presence of sodium ascorbate, as a source of Cu(I) ions, in *t*-BuOH/H_2O 1:1 mixture. On the contrary, the starting compounds for the synthesis of TT harmicines at O-6 (**20a-e**) and N-9 (**14a-e**) were harmine-based alkynes **12** or **19** and cinnamyl azides **13a-e**. In this case, the reaction was carried out in MeOH, with Cu(II) acetate (MeOH acts as a reducing agent to generate Cu(I)).

To obtain the required starting compounds for CuAAC, synthetic routes to alkynes and azides were developed. Harmine-based azides **3** and **10** were generated in several steps: 1) synthesis of substituted β-carbolines **1** and **8** at positions 1 and 3 [18,19], 2) synthesis of the corresponding alcohols **2** and **9** [20], and 3) conversion of alcohols to azides **3** and **10** *via* 2-azido-1,3-dimethylimidazolinium hexafluorophosphate (ADMP) and 1,8-diazabicyclo(5.4.0)undec-7-ene (DBU) [21]. Alcohol **9** was also alkylated at N-9 with propargyl bromide in the presence of Cs_2CO_3, to obtain alkyne **12**. Next, we have prepared β-carboline **17**, substituted with a methoxy group at C-6, a starting compound for harmicines **20a-e** and **23a-h**. Subsequent demethylation yielded phenol **18**, which was further propargylated to yield alkyne **19**. CADs were efficiently transformed to CAD-based alkynes **4a-e** and cinnamyl azides **13a-e**. Alkynes **4a-e** were successfully prepared by the reaction of CAD with propargyl bromide, in the presence of K_2CO_3, while the synthesis of cinnamyl azides **13a-e** involved several steps: esterification of CADs, reduction to the corresponding alcohols, and conversion to azides *via* ADMP/DBU, as described previously [10].

On the other hand, synthesis of AT harmicines (**7a-h**, **16a-h**, **23a-h**, **27a**,**b**) was straightforward and involved two steps: 1) synthesis of harmine-based primary amines **6**, **11**, **22** and **26** and 2) coupling reactions with different CADs. The above listed primary amines were obtained by either the reduction of azides **3** and **10** by catalytic hydrogenation or the O-6 alkylation of phenol **18**/N-9 alkylation of harmine with 2-(Boc-amino)ethyl bromide, followed by the removal of the Boc-protecting group under acidic conditions [15]. Coupling reactions were efficiently performed by activating CADs with 1-[bis(dimethylamino)methylene]-1*H*-1,2,3-triazolo

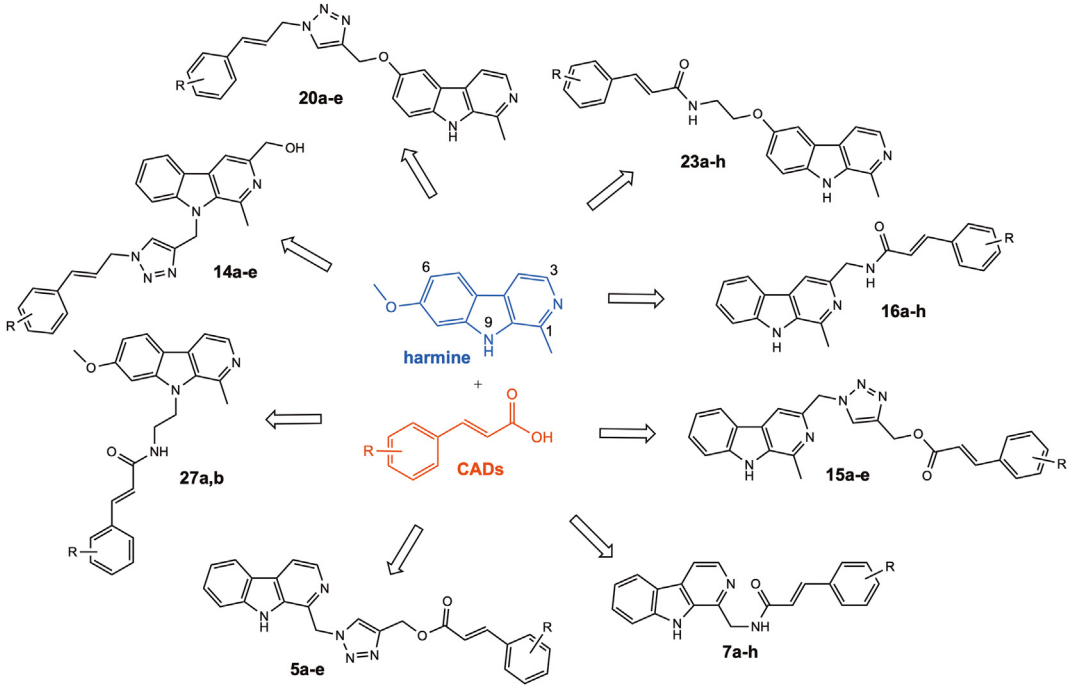

Fig. 1. Novel harmicines.

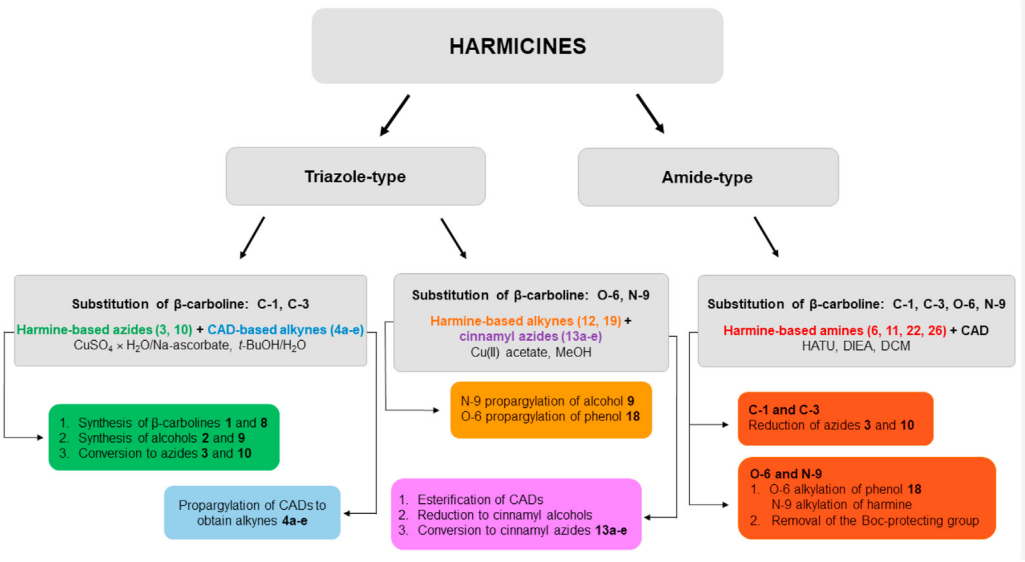

Fig. 2. Synthesis of triazole-type (TT) and amide-type (AT) harmicines.

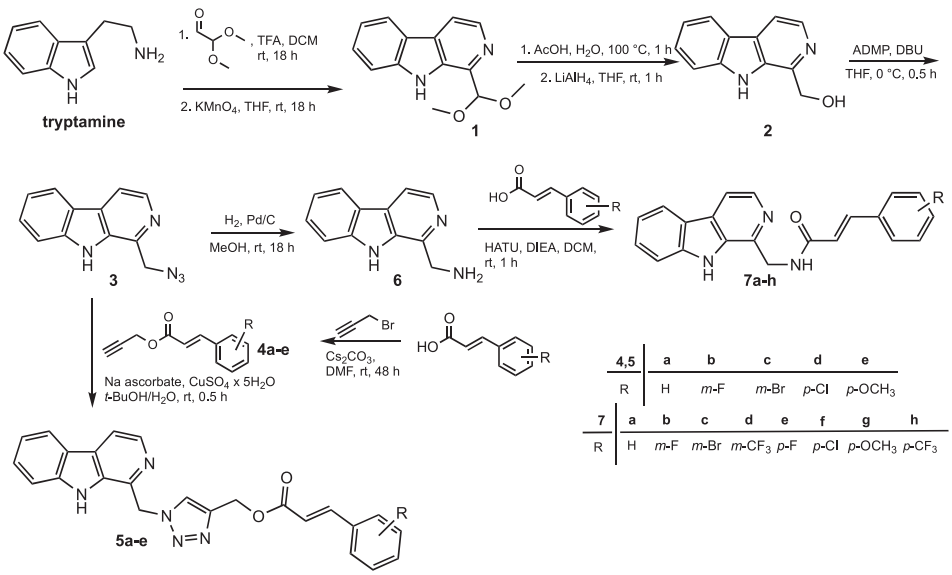

Scheme 1. Synthesis of TT harmicines **5a**-**e** and AT harmicines **7a**-**h**.

[4,5-*b*]pyridinium-3-oxide hexafluorophosphate (HATU), in the presence of *N,N*-diisopropylethylamine (DIEA), followed by the addition of an appropriate harmine-based amine. The reactions proceeded smoothly, in dichloromethane at room temperature for 1 h.

Altogether, we have obtained 45 new compounds in high purity, as determined by HPLC-ESI/MS analysis (>95%) or CHN analysis (values for C, H, and N within 0.4% of the calculated values for the proposed formula). Spectroscopic and spectrometric methods (^{1}H and ^{13}C NMR, IR, MS) were used to confirm the proposed structures. The data obtained are provided in short in the Materials and Methods section, and in detail in the Supplementary Material. The evaluation of the drug-like properties, *i.e.* relevant physicochemical parameters included in the Lipinski's rule and Gelovani's rules, using Chemicalize.org software [22] disclosed that both TT and AT harmicines are in complete agreement with both sets of rules, respectively (Table S15).

2.2. Biological evaluations

2.2.1. In vitro antiplasmodial activity and SAR analysis

The ability of novel harmicines to inhibit the erythrocytic stage of *P. falciparum* infection (chloroquine-sensitive (*Pf*3D7) and chloroquine-resistant (*Pf*Dd2) strains), as well as infection of the human hepatoma cell line (Huh7) by *P. berghei* parasites, was evaluated as described previously [23–27]. The diversity of the harmicines allowed us to explore the significance of certain structural features for the activity: 1) position of the substitution at the β-carboline ring, 2) linker between β-carboline and CAD, and 3) position and the type of substituent on the phenyl ring in CAD.

The results of the *in vitro* screening of blood schizonticidal activity indicated significant differences in antiplasmodial activities between harmicines prepared at the different positions of the β-carboline ring (Table 1). In general, the activity decreased according to the pattern: N-9 > O-6 > C-3 > C-1, except for TT harmicines **14**

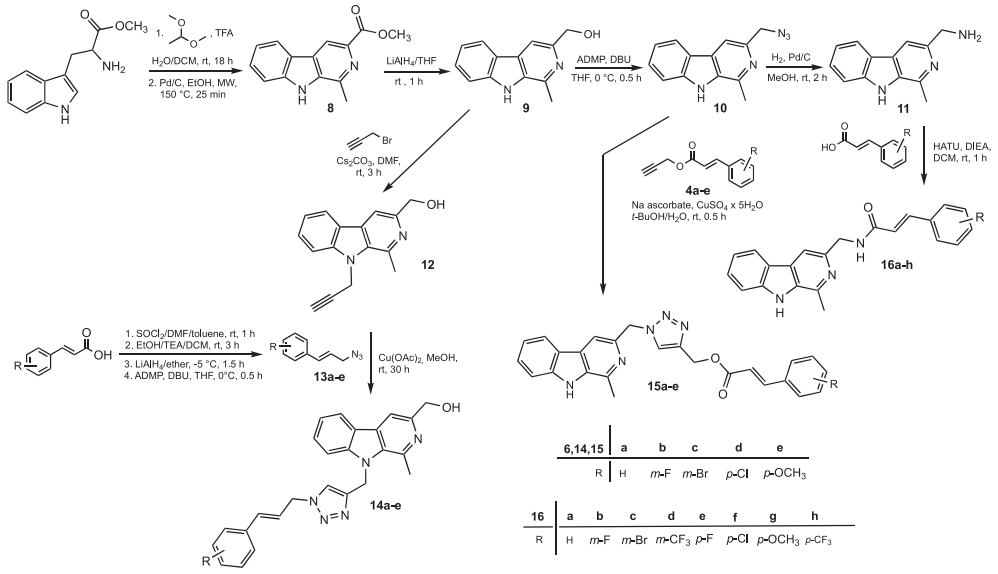

Scheme 2. Synthesis of TT harmicines **14a**-**e**, **15a**-**e** and AT harmicines **16a**-**h**.

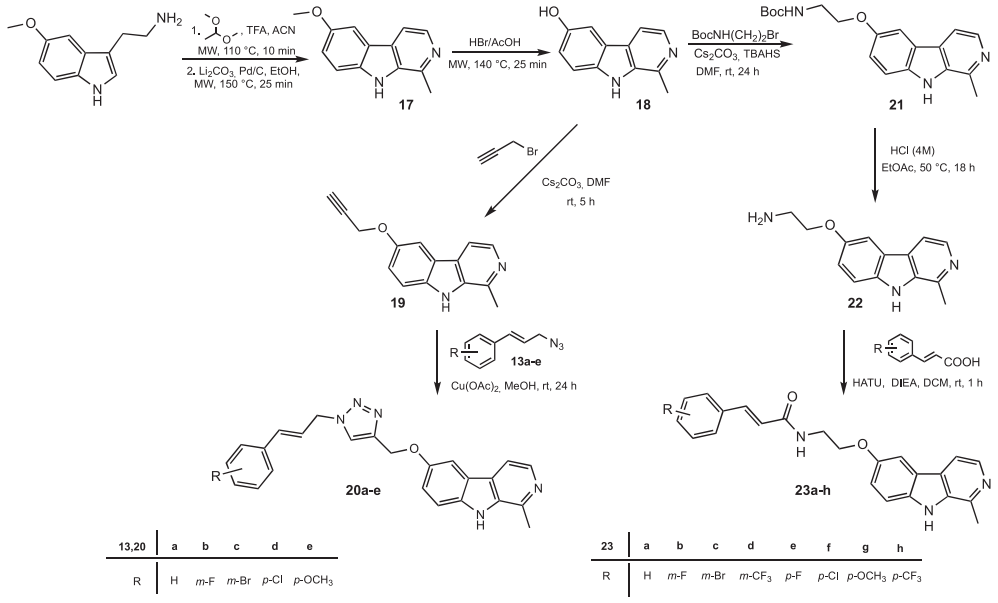

Scheme 3. Synthesis of TT harmicines **20a**-**e** and AT harmicines **23a**-**h**.

(substitution at N-9), which were among the least active compounds.

The most active compounds, AT harmicines **27a**,**b**, hybrids comprised of harmine-based amine at N-9 (compound **26**) and *m*- or *p*-(trifluoromethyl)cinnamic acid, displayed at least two orders of magnitude stronger activities than the parent compound, harmine, in nanomolar (*Pf*3D7) and submicromolar concentrations (*Pf*Dd2). These results are in agreement with IC_{50} values obtained previously for the series of AT harmicines, in which the derivative with *p*-chloro substituent (trifluoromethyl isostere) in the cinnamic scaffold exerted the highest activity [15]. Interestingly, harmicines **14**, also hybrids at N-9, with triazole linker and an additional hydroxymethyl substituent at C-3, exerted lower activity than harmine, with the exception of compound **14c**, *m*-bromocinnamic acid derivative. It is noteworthy that the analogues TT harmicines reported by Perković et al., without C-3 hydroxymethyl substituent, exhibited activities in submicromolar concentrations, suggesting that such substitution results in the loss of activity [10].

Harmicines **20** and **23**, both bearing substituents at O-6, showed similar activities in submicromolar and micromolar concentrations, regardless of the type of the linker. Comparison of the antiplasmodial activities within the series of TT harmicines **20** showed that the substituent R^1 on cinnamic moiety had a minor effect on the activity. Compound **20c**, a *m*-bromocinnamic acid derivative, exerted on average 2.2-fold higher activity than the other compounds. Among the AT harmicines, compounds **23d** and **23h**, *m*- and *p*-(trifluoromethyl)cinnamic acid derivatives, exhibited the highest antiplasmodial activities, which were still 2 to 3-fold lower than the activities of analogous compounds **27a** and **27b**.

On the other hand, considering the antiplasmodial activities of the AT and TT harmicines **16** and **15**, hybrids at C-3, two conclusions could be drawn. First, the IC_{50} values were in the micromolar range.

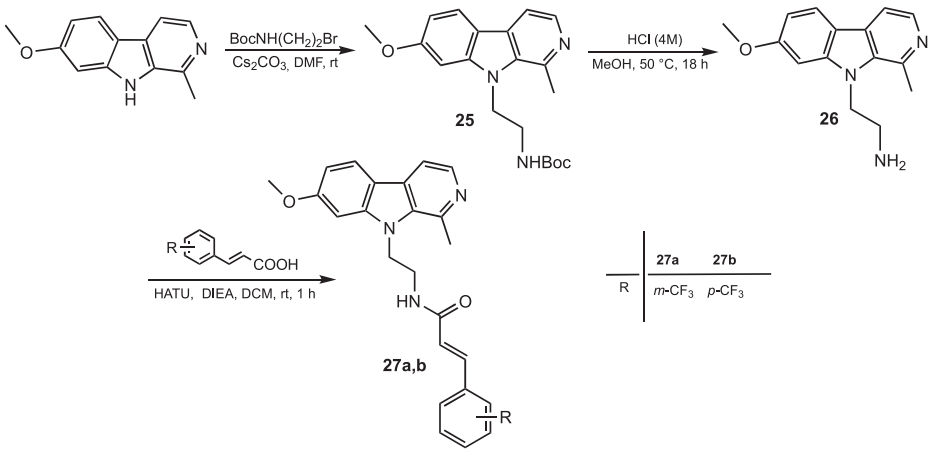

Scheme 4. Synthesis of harmicines **27**.

Table 1
In vitro antiplasmodial activity of harmicines **5**, **7**, **14**–**16**, **20**, **23** and **27** against the erythrocytic stage of *P. falciparum* (*Pf*3D7 and *Pf*Dd2 strains).

TT harmicines	β-carboline substitution	IC_{50}[a] (μM)		AT harmicines	IC_{50} (μM)	
		*Pf*3D7	*Pf*Dd2		*Pf*3D7	*Pf*Dd2
5a	C-1	>27.78[b]	>20.25	**7a**	>27.99	>55.56
5b		>17.32	>20.07	**7b**	>27.78	>27.78
5c		>13.24	>19.07	**7c**	>27.78	>27.78
				7d	>27.78	>27.78
				7e	>13.89	>13.89
5d		>55.56	>55.56	**7f**	>27.78	>27.78
5e		>55.56	39.20 ± 0.25	**7g**	>27.78	>27.78
				7h	>55.56	>55.56
15a	C-3	>20.04	>27.78	**16a**	5.78 ± 1.05	10.18 ± 1.68
15b		>27.78	>27.78	**16b**	5.74 ± 0.33	12.71 ± 1.76
15c		16.41 ± 3.35	11.14 ± 2.76	**16c**	3.23 ± 0.32	1.48 ± 035
				16d	2.01 ± 0.09	7.40 ± 0.74
				16e	4.13 ± 0.61	13.30 ± 7.41
15d		21.44 ± 2.27	>27.78	**16f**	2.92 ± 0.03	8.38 ± 3.16
15e		>27.78	>27.78	**16g**	6.50 ± 0.29	10.72 ± 3.18
				16h	2.30 ± 0.41	5.97 ± 1.33
20a	O-6	0.61 ± 0.09	2.12 ± 0.40	**23a**	1.55 ± 0.45	2.47 ± 0.25
20b		0.55 ± 0.08	2.28 ± 0.33	**23b**	1.11 ± 0.14	1.30 ± 0.09
20c		0.26 ± 0.17	0.73 ± 0.40	**23c**	0.19 ± 0.02	0.63 ± 0.22
				23d	0.12 ± 0.02	0.32 ± 0.08
				23e	0.95 ± 0.06	1.67 ± 0.06
20d		0.57 ± 0.06	0.95 ± 0.16	**23f**	0.36 ± 0.02	0.92 ± 0.06
20e		0.60 ± 0.03	1.81 ± 0.04	**23g**	1.17 ± 0.03	2.86 ± 0.52
				23h	0.12 ± 0.02	0.35 ± 0.06
14a	N-9	>27.78	>19.78			
14c		6.28 ± 1.04	18.41 ± 2.42			
14d		>19.92	>23.60			
14e		18.19	>16.93			
				27a	0.06 ± 0.02	0.33 ± 0.06
				27b	0.04 ± 0.003	0.17 ± 0.01
CQ[d]		0.003 ± 0.002	0.20 ± 0.10	HAR[e]	8.25 ± 2.83	>27.7

[c] Results represent mean ± SD, $n \geq 2$.
[a] IC_{50}, the concentration of the tested compound necessary for 50% growth inhibition.
[b] The exact IC_{50} could not be obtained, as activity could only be detected at the highest tested concentration.
[d] CQ, chloroquine;[e] HAR, harmine.

This result, together with those obtained for harmicines **14**, indicate that the position 3 of the β-carboline ring is not optimal for substitution. Secondly, there is a marked difference in the antiplasmodial activities of harmicines **15** and **16**. AT harmicines **16** were significantly more potent than their triazole-linker counterparts, compounds **15**. Comparison of the activities of the homologous compounds from the series **16** and **15** revealed at least a 3.5-fold (**16a** *vs* **15a**) increase in the activity. The most pronounced effect was observed for harmicines **16g** and **15d** (a 7.3-fold increase in the activity). Remarkably, the comparison of IC_{50} values of AT and TT harmicines, hybrids at N-9 of the β-carboline, reported earlier, revealed the same tendency [10,15].

Harmicines **5** and **7**, prepared at C-1of the β-carboline core, were inactive against the erythrocytic stage of *P. falciparum*, at the highest concentration tested, regardless of the type of the linker and CAD used for conjugation.

As a continuation of our research, screening of *in vitro* activities of harmicines **5**, **7**, **14**, **15**, **16**, **20**, **23** and **27** against the hepatic stages

of *Plasmodium* parasite was performed. Both AT and TT harmicines were initially tested at two concentrations, 1 and 10 μM. The results obtained have shown that the potency of harmicines against the hepatic stages followed a similar pattern as against the erythrocytic stage of *Plasmodium* infection (Fig. 3). The most pronounced activity was observed for harmicines **27** and **14**, prepared at N-9 of the β-carboline ring, followed by **20** and **23** (O-6), **15** and **16** (C-3) and finally harmicines **5** and **7** (C-1), which were mostly inactive. In general, AT harmicines exhibited better activity, *i.e.* **27** > **14**, **23** > **20**, **16** > **15**. In view of those results, compound **27a**, *m*-(trifluoromethyl)cinnamic acid derivative, was selected as the most promising for IC_{50} determination (Fig. S1). The obtained IC_{50} value was 4.3-fold lower than IC_{50} of the reference drug primaquine (1.94 ± 0.68 μM *vs* 8.4 ± 3.4 μM) [28].

2.2.2. *In vitro cytotoxicity screening and selectivity*

Cytotoxicity of the harmicines active against the erythrocytic stage of *P. falciparum* was evaluated against HepG2, as described previously [29] (Table 2). In addition, the selectivity index (SI) for each harmicine was calculated as the fractional ratio between the IC_{50}s for HepG2 and *P. falciparum Pf*3D7 strain (Table 2).

To our delight, the most active compounds against *Pf*3D7, **27a**,**b**, exhibited favourable SIs. Remarkably, the most selective compound of all prepared harmicines was **27a** (SI = 1105). A comparison of the IC_{50} values obtained for harmicines prepared at O-6 revealed that, in general, TT harmicines **20** were more cytotoxic to HepG2 cells than AT harmicines **23** ($IC_{50} \leq 10$ μM, with the exception of the compound **20e**). It is worth mentioning that harmicines **23e**-**g** were not cytotoxic at all at the highest concentration tested.

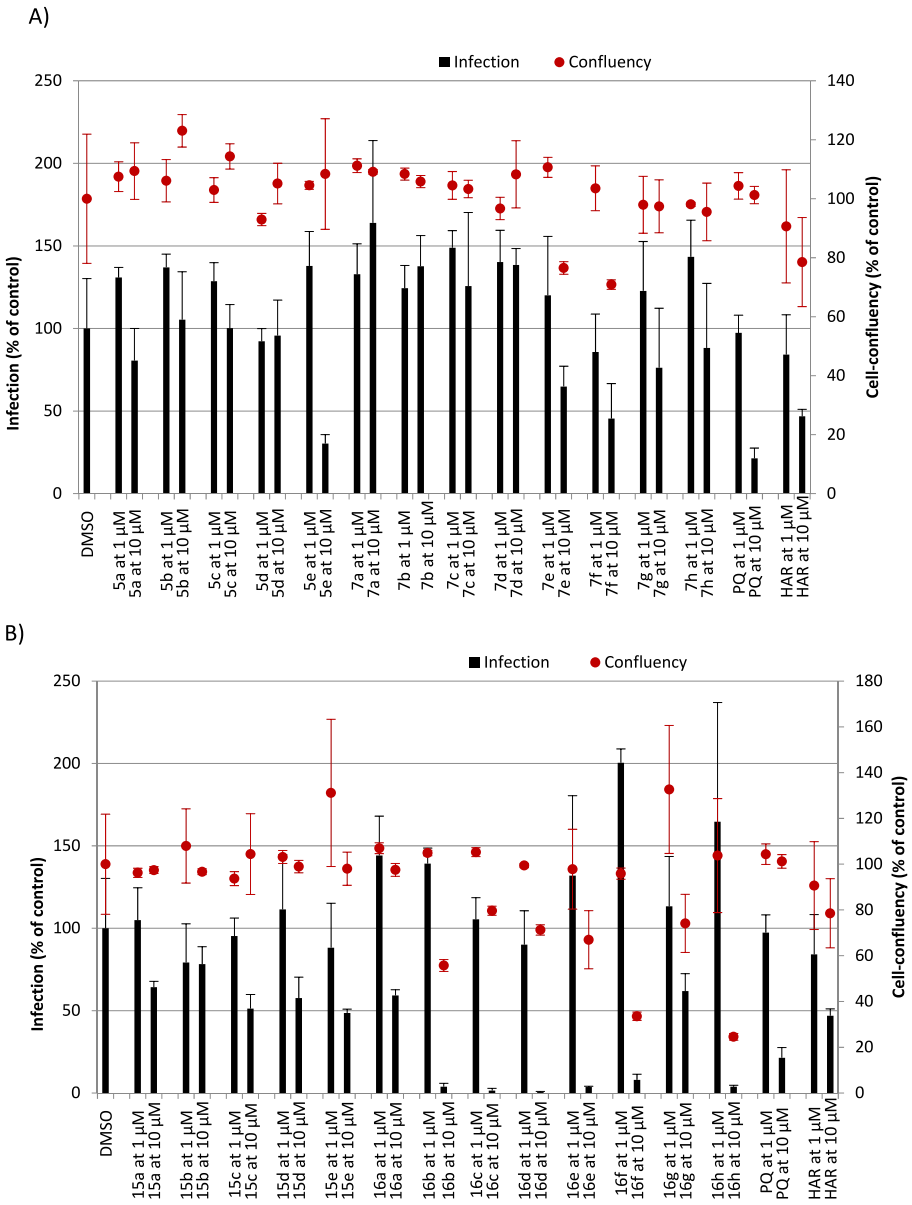

Fig. 3. *In vitro* activity of harmicines against *P. berghei* liver stages: a) **5a**-**e** and **7a**-**h**, b) **15a**-**e** and **16a**-**h**, c) **20a**-**e** and **23a**-**h** and d) **14a**,**c**-**d** and **27a**,**b** at 1 and 10 μM concentrations. Total parasite load (infection scale, bars) and cell viability (cell confluency scale, dots) are shown. Results were normalized to the negative control, DMSO, and are represented as mean ± SD, n = 1 (PQ, primaquine; HAR, harmine).

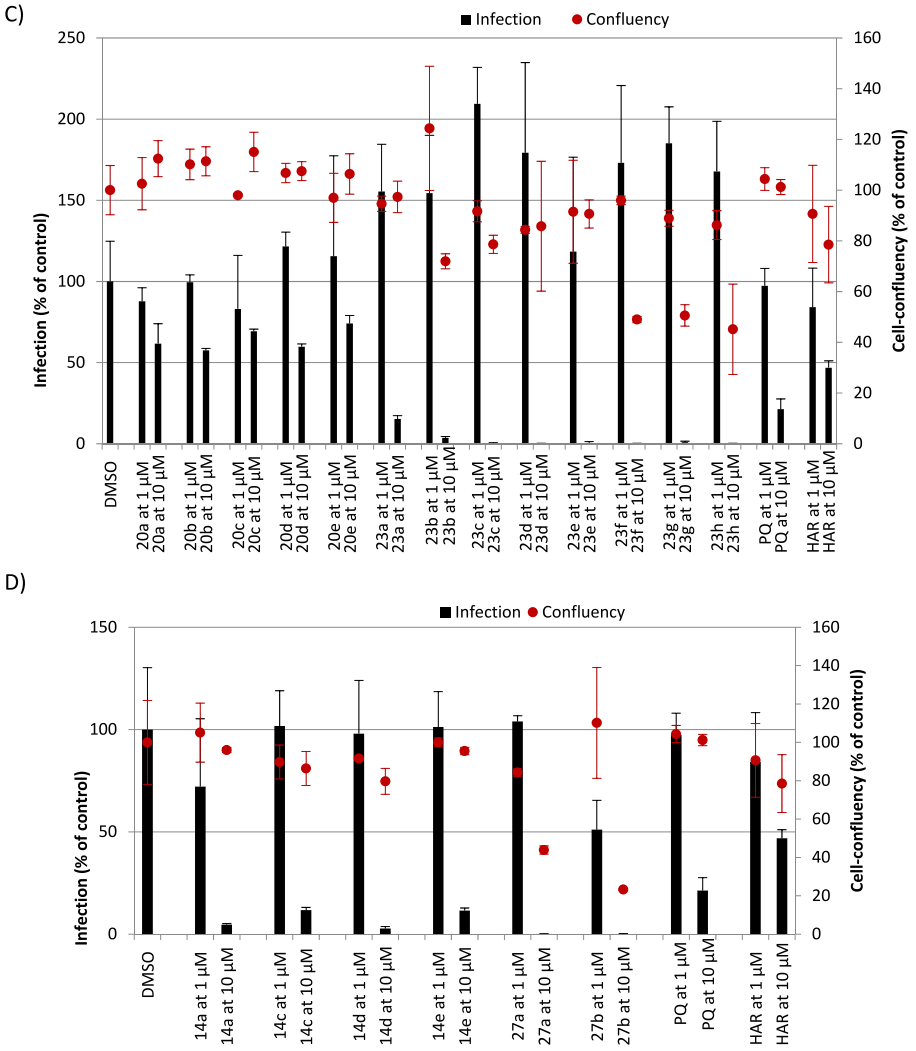

Fig. 3. (*continued*).

Cytotoxicity of other tested harmicines did not differ much from their antiplasmodial activities against erythrocytic stages (in most cases their SI was below 7). Therefore, those compounds can't be considered for future development as antimalarial agents. However, those results open the window for their repurposing as anticancer agents, which will be explored in our future investigations.

2.3. Molecular dynamics simulations

Given a very large number of compounds evaluated in this work, we utilized MD simulations on a representative set of systems, selected to feature the most potent derivative **27b**, together with **7b**, **16a** and **23h**, which should provide enough structural and electronic information to discriminate among various substitution patterns and their biological activities, while offering guidelines how to focus subsequent synthetic efforts towards even more effective analogues based on the employed organic framework.

The calculated binding free energies (ΔG_{BIND}) for the studied systems are given in Table 3, together with their decomposition into contributions from individual residues. The residues considered for the analysis include those identified as responsible for the

Table 2
In vitro cytotoxicity screening of harmicines against HepG2 and calculated selectivity indices.

Compd.	IC_{50}[a] (μM)	SI[b]	Compd.	IC_{50}[a] (μM)	SI[b]
14c	>125[c]	19.90	**20d**	3.95 ± 0.83	6.93
15c	110.19 ± 56.92	6.71	**20e**	88.01 ± 50.81	146.68
15d	70.50 ± 25.64	3.29	**23a**	12.02 ± 4.95	7.75
16a	7.05 ± 0.11	1.29	**23b**	37.57 ± 3.10	33.85
16b	15.83 ± 3.23	2.76	**23c**	7.57 ± 2.56	39.84
16c	9.64 ± 4.71	2.98	**23d**	6.14 ± 0.11	51.17
16d	9.37 ± 4.90	4.66	**23e**	>250	263.16
16e	12.46 ± 5.26	2.99	**23f**	>250	694.44
16f	11.33 ± 0.65	3.88	**23g**	>250	213.68
16g	10.38 ± 4.15	1.60	**23h**	3.59 ± 1.26	29.92
16h	33.26 ± 1.66	14.46	**27a**	66.32 ± 3.79	1105.33
20a	10.13 ± 3.50	16.61	**27b**	5.84 ± 1.67	146
20b	10.51 ± 5.39	19.11	HAR[d]	>250	30
20c	6.13 ± 2.71	23.58			

[a] IC_{50}, the concentration of the tested compound necessary for 50% growth inhibition.
[b] SI, selectivity index, the ratio between IC_{50} (HepG2) and IC_{50} (*Pf*3D7).
[c] The exact IC_{50} could not be obtained, as activity could only be detected at the highest tested concentration.
[d] HAR, harmine.

Table 3
Total binding free energies (ΔG_{BIND}) and their decomposition on a per-residue basis following the MM-GBSA analysis of the obtained molecular dynamics trajectories.[a].

System	7b	16a	23h	27b	HAR[b]
Total ΔG_{BIND}	−21.3	−25.8	−22.9	−30.0	−7.5
Lys44	−0.13	−1.41	−0.51	−1.89	0.00
Arg98	−1.63	0.04	−1.71	−1.67	0.00
Asn37	−2.25	−2.17	−1.80	−1.40	0.00
Met84	−0.89	−1.63	−2.06	−1.26	0.00
Ala41	−0.58	−1.51	−1.59	−1.02	0.00
Tyr47	0.01	−0.02	0.01	−0.68	0.00
Phe124	−0.78	−0.73	−0.74	−0.68	0.00
Ile82	−0.10	−0.98	−1.30	−0.64	0.00
Asp40	0.14	−0.79	−0.48	−0.63	0.00
Leu93	−0.61	−0.61	−0.58	−0.47	0.00
Ile173	−0.21	−0.66	−0.56	−0.43	−0.01
Thr171	−0.37	−1.03	−0.75	−0.37	0.00
Leu34	−0.13	−0.48	−0.19	−0.31	0.00
Ala38	−0.15	−0.82	−0.69	−0.23	0.00
Lys102	0.01	0.01	0.01	0.03	−0.34
Asp52	0.01	0.01	0.01	0.04	0.00
Thr95	0.02	0.03	0.03	0.04	0.00
Arg167	0.03	0.04	0.02	0.05	0.00
Glu48	0.03	0.06	0.08	0.13	0.00
Asp43	0.05	0.04	0.04	0.20	0.00
Asp79	0.23	1.51	1.62	0.31	0.00

[a] Residues are selected to list those belonging to the ATP binding pocket (Asn37, Asp79, Arg98, Phe124, in bold) and all of those with contributions higher than −0.20 and lower than 0.03 kcal mol^{-1} for the most potent **27b**. All values are in kcal mol^{-1}.
[b] HAR, harmine.

binding of ATP within the ATP binding pocket of *Pf*Hsp90 (Asn37, Asp79, Arg98, Phe124) [30,31] and all those with contributions higher than −0.20 and lower than 0.03 kcal mol^{-1} for the most potent **27b**.

It turns out that all compounds are associated with negative ΔG_{BIND} values, implying that their binding is exergonic and favourable. All four systems are clearly positioned within the ATP binding site of *Pf*Hsp90 (Fig. 4), as they form significant interactions with residues that define that site, which underlines the importance of this structural element as a druggable target. Still, their orientations and specific ligand-protein interactions are largely different, thus resulting in diverse affinities.

The binding of **27b** is the most exergonic, ΔG_{BIND}(**27b**) = −30.0 kcal mol^{-1}, thus confirming its highest biological activity measured here. Its harmine fragment enters deeper within the binding site, where it uses its aromatic framework to interact with Asn37 (N−H … π interactions) and Met84 (C−H … π interactions), evidenced in their significant individual contributions

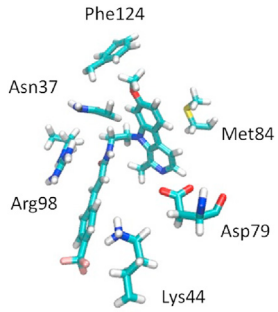

Fig. 5. Specific interactions governing the binding of the most potent **27b** within the ATP binding site of the *Pf*Hsp90 protein.

of −1.40 and −1.26 kcal mol^{-1}, respectively (Fig. 5), or its attached −OMe group to form C−H … π interactions with Phe124 (−0.68 kcal mol^{-1}). The mentioned three residues already contribute around 11% of the total binding energy, which is significant. In addition, the introduced N-9 amide functionality further promotes the binding, first by allowing Arg98 to stack above the amide linker (−1.67 kcal mol^{-1}), and second, even more significantly, to facilitate positive N−H … π contacts between the cationic Lys44 residue and the terminal *p*-CF_3-phenyl unit, being persistent during simulations (Fig. S2). The latter promotes Lys44 as the most dominant *Pf*Hsp90 residue in binding **27b**, related with the individual contribution of −1.89 kcal mol^{-1}. Taken together, indicated five residues already account for 23% of the total binding energy, suggesting that **27b** is rather well positioned within the binding site. All of this clearly confirms the suitability of the N-9 substitution as a useful strategy in designing effective compounds and justifies placing an aromatic unit at an appropriate distance from the harmine N-9 site to benefit the binding, where the amide linker seems to be optimal and well-tuned for the purpose. In addition, knowing that the *p*-CF_3 group exerts an electron-withdrawing effect on the attached phenyl ring, which likely diminishes the mentioned N−H … π interactions with Lys44, it would be useful to consider replacing *p*-CF_3 with different electron-donating groups, which will be tackled in the subsequent synthetic work. Having said that, among others, *p*-OMe does not appear suitable as such a derivative possesses reduced activity [15], albeit lower toxicity, so other substituents would have to be evaluated.

The effect of the anionic Asp79 is also interesting and worth discussing. This is a significant residue, since it is also identified as part of the ATP binding motif, yet its interactions with **27b** are strongly

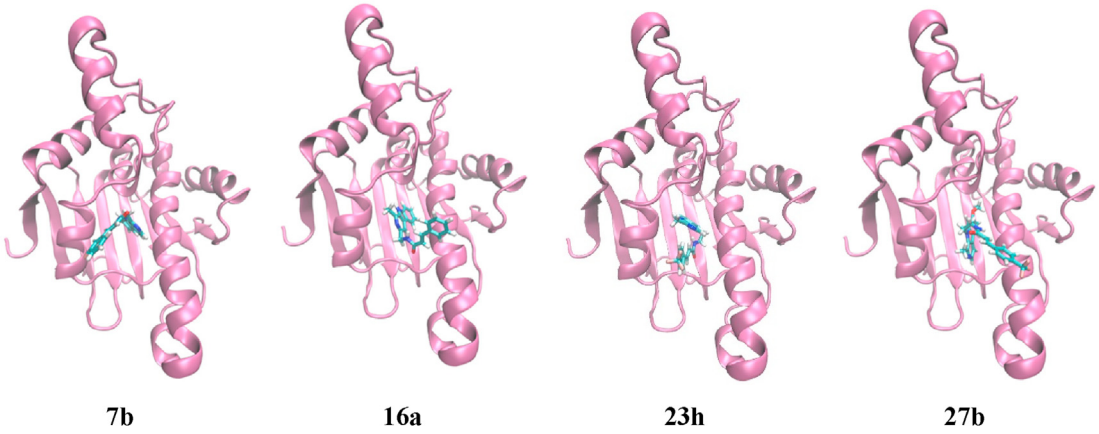

Fig. 4. Position of the investigated ligands within the ATP binding site of the *Pf*Hsp90 protein.

disfavouring the binding, as Asp79 is associated with a positive contribution of +0.31 kcal mol^{-1}, being the highest endergonic among all residues. The underlying reason is that Asp79 is located in the vicinity of the harmine's pyridine unit without any notable favourable contacts that could counterbalance a negative steric and electronic interference from the anionic carboxylate. This suggests that despite its mostly optimal design, **27b** could further benefit from modifying its pyridine unit with something that could revert this fragment into a favourable pairing with Asp79. Yet, this is not achieved in **16a**, as the binding affinity of this C-3 derivative is reduced by 4.2 kcal mol^{-1} to ΔG_{BIND}(**16a**) = −25.8 kcal mol^{-1}, suggesting that the introduced amide-linked cinnamic acid moiety is likely too large for this purpose. There, the unfavourable interaction with Asp79 is even enhanced (Fig. S3), as its individual contribution rises from +0.31 in **27b** to +1.51 kcal mol^{-1}. Such structural modification even changes the binding orientation so that, for example, the entire positive contribution from Arg98, observed in **27b**, is lost here, which leads to a reduced affinity, being in line with experiments. An even less favourable outcome is seen in **7b**, where an analogous structural modification occurs on the other part of the pyridine ring, the C-1 atom, where the resulting binding affinity is further reduced to ΔG_{BIND}(**7b**) = −21.3 kcal mol^{-1}, being the lowest among considered systems, thus confirming its low activity observed experimentally. Even though **7b** seems to be able to compensate the unfavourable contribution from Asp79 down to +0.23 kcal mol^{-1}, its position within the ATP binding site disfavours favourable contributions from several significant residues, including Lys44, which is diminished to only −0.13 kcal mol^{-1}, despite, for example, improving the contribution of Asn37 up to −2.25 kcal mol^{-1} due to positive N−H … π interactions.

In general, all considered systems, selected to correspond to different substitution patterns, show much more exergonic binding affinities than the parent harmine, which justifies the utilized synthetic strategy. The calculated value of ΔG_{BIND}(harmine) = −7.5 kcal mol^{-1}, demonstrates its poor binding features, being consistent with its elevated IC_{50} value of 8.25 μM (Table 1). In addition, although the relationship between IC_{50} and ΔG_{BIND} values is not so straightforward in absolute terms, their relative ratio is connected through the Cheng-Prusoff equation [32]. In this context, harmine's IC_{50} value roughly translates to the binding energy of −6.9 kcal mol^{-1}, thus placing our calculations in close agreement with experiments, and confirming the validity of the employed computational setup. Harmine seems like a good reference, since it was identified as a selective inhibitor of *Pf*Hsp90, which is essential for the erythrocytic development of *Plasmodium* [16,33] and our calculations show it predominantly binds outside the ATP binding site (Table 3). Hence, the approach to structurally modify harmine is likely to lead to more efficient compounds, although, in some cases evaluated here, the introduced amide/triazole-linked cinnamic acid unit, despite being placed at right positions on the harmine's scaffold, appears as too bulky or electronically less optimized to maximize the effect. Nevertheless, computations confirm the substitution at the N-9 position as the most promising route in this respect, which likely opens the door towards further improvements in the desired biological activities.

3. Conclusions

In conclusion, we have successfully prepared and characterized 45 novel harmicines of the triazole- and amide-type in the positions 1, 3, 6 and 9 of the β-carboline ring. Further, we evaluated their antiplasmodial activities against erythrocytic and hepatic stages of the *Plasmodium* infection and cytotoxicity against HepG2. The results clearly showed remarkable blood shizontocidal activity in nanomolar concentrations, as well as selectivity of amide-type harmicines **27**, in comparison to other compounds. Harmicines **27** were also the most active against hepatic stages of *P. berghei* (4.3-fold more active than the reference drug primaquine). Molecular dynamics simulations revealed that all investigated compounds bind within the ATP binding site and confirmed **27b** as the most potent derivative. In addition, Lys44 was identified as crucial for the enhanced activity, evident in favourable N−H … π contacts with the phenyl ring within the attached cinnamic acid unit, particularly when the latter is introduced at the harmine's N-9 position, being in line with the experiments. Lastly, computations underlined the unfavourable contribution from the ATP binding site residue Asp79, seen in the steric and electronic interference with the bound ligands, which defines a promising route to advance the developed synthetic methodology towards even more efficient compounds based on the employed organic framework. Taken together with previously obtained results, this study revealed amide-type harmicines at N-9 of the β-carboline ring as the best performers against *Plasmodium*. Our ongoing work focuses on establishing a reliable quantitative structure-activity relationship model, with the final goal of identifying lead compounds for further development.

4. Materials and Methods

4.1. Chemistry

4.1.1. General information

Melting points were determined on a Stuart Melting Point Apparatus (Barloworld Scientific, UK) in open capillaries and were uncorrected. FTIR-ATR spectra were recorded using a Fourier-Transform Infrared Attenuated Total Reflection UATR Two spectrometer (PerkinElmer, Waltham, MA, USA) in the range from 450 to 4000 cm^{-1}. ^{1}H and ^{13}C NMR spectra were recorded on a Bruker Avance III HD operating at 300, 400 or 600 MHz for the ^{1}H and 75, 101 or 151 MHz for the ^{13}C nuclei (Bruker, Billerica, MA, USA). Samples were measured in DMSO-d_6 solutions at 20 °C in 5 mm NMR tubes. Chemical shifts (δ) are reported in parts per million (ppm) using tetramethylsilane (TMS) as a reference in the ^{1}H and DMSO residual peak as a reference in the ^{13}C spectra (39.52 ppm). Coupling constants (J) are reported in hertz (Hz). Mass spectra were recorded on Agilent 1200 Series HPLC coupled with Agilent 6410 Triple Quad (Agilent Technologies, St. Clara, CA, USA). The mobile phase consisted of Milli Q water as component A and MeOH (HPLC grade, J. T. Baker) as component B, and as the stationary phase, Zorbax XDC C18 column (4.6 × 75 mm, 3.5 μm) was used. Gradient elution was used at a flow rate of 0.5 mL/min, and 5 μL of analyte solution was injected per analysis. The starting conditions and gradient steepness were adjusted according to the analyte polarity. Diode array detector was utilized, while the data were presented as a total wavelength chromatogram (TWC). Mass spectrometry conditions were as follows: electrospray ionization (ESI) in positive and negative mode was used. Capillary voltage and current were set to 4.0 kV and 20 nA, respectively. Nebulizer pressure was set to 15 psi, while the drying gas (nitrogen) temperature and flow were 300 °C and 11 L/min. For the MS data analysis, Agilent MassHunter software (Agilent Technologies, St. Clara, CA, USA) was used. Elemental analyses were performed on a CHNS LECO analyser (LECO Corporation, St. Joseph, MI, USA). Analyses indicated by the symbols of the elements were within ±0.4% of their theoretical values. Microwave-assisted reactions were performed in a microwave reactor CEM Discover (CEM, USA) in a glass reaction vessel. All compounds were routinely checked by TLC with silica gel 60F-254 glass plates (Merck, Germany) using DCM/MeOH 8:1, 85:15, 95:5, 97:3, cyclohexane/EtOAc/MeOH 1:1:0.5 and cyclohexane/EtOAc 2:1, 9:1 as the solvent systems. Spots were visualized by UV light (λ = 254 nm; 365 nm) and iodine vapour. Column chromatography was performed on silica gel 0.063−0.200 mm (Sigma-Aldrich, USA)

with the same eluents used for TLC, with an additional Al_2O_3 layer to remove Cu-salts (compounds **5a**-**e**, **14a**,**c**-**d**, **15a**-**e**, **20a**-**e**). All chemicals and solvents were of analytical grade and purchased from commercial sources. CADs were purchased as predominantly *trans* stereoisomers (≥99%).

Harmine, acetic acid, hydrochloric acid, cinnamic acid, *m*-fluorocinnamic acid, *p*-fluorocinnamic acid, *p*-methoxycinnamic acid, *p*-chlorocinnamic acid, *m*-(trifluoromethyl)cinnamic acid, *p*-(trifluoromethyl)cinnamic acid, *t*-BuOH, acetaldehyde dimethyl acetal, 2,2-dimethoxyacetaldehyde, DBU, lithium aluminium hydride, toluene, lithium carbonate, 10% palladium on activated charcoal were purchased from Sigma-Aldrich (USA). Caesium carbonate, 2-(*tert*-butoxycarbonylamino)ethyl bromide, tryptamine, 5-methoxytryptamine, L-tryptophan methyl ester hydrochloride, tetrabutylammonium hydrogensulfate, ADMP, HATU, *m*-bromocinnamic acid, propargyl bromide and DMF were purchased from TCI Chemicals (Japan). Hydrobromic acid (47%), dry tetrahydrofuran and aluminium oxide were purchased from Merck (Germany), DIEA, copper(II) acetate and TEA from Alfa Aesar (USA), 1 M hydrochloric acid in EtOAc, trifluoroacetic acid, DCM and dry diethyl ether from Thermo Fischer Scientific (USA), diethyl ether from ITW Reagents (Germany), cyclohexane, EtOAc, MeOH, absolute EtOH and petroleum ether from Honeywell (USA), acetonitrile from CARLO ERBA Reagents (France), DMF, sodium hydroxide, sodium bicarbonate and potassium carbonate from Kemika (Croatia), anhydrous sodium sulphate, potassium permanganate, ammonium chloride and sodium chloride from Gram-Mol (Croatia), thionyl chloride from Fluka (Switzerland), sodium ascorbate from Acros Organics (Belgium), copper(II) sulphate pentahydrate from Zorka Šabac (Serbia).

β-carbolines **1**, **8**, **17** and alcohol **9** were prepared according to the literature procedures [18–20,34]. Alcohol **2** is a known compound, but prepared by alternative methods [35,36]. Phenol **18** was prepared according to the modified literature procedure from β-carboline **17** using HBr/glacial acetic acid mixture, under the MW irradiation [37]. Among alkynes **4**, only **4c** is a new compound. Nevertheless, the established synthetic method for their preparation differs from the one described in the literature [38]. Although amine **6** is commercially available, we have included its synthesis and characterization, since those data are not available. Cinnamyl azides **13a**-**e**, as well as compounds **25** and **26** were prepared according to our published methods [10,15].

*4.1.2. Synthesis of (9H-pyrido [3,4]-b]indol-1-yl)methanol (**2**)*

A solution of β-carboline **1** (0.700 g, 2.889 mmol), AcOH (3.63 mL) and H_2O (5.45 mL) was refluxed for 1 h at 100 °C. After cooling to rt, pH was adjusted to 9 with 5% NaOH and the reaction mixture extracted with EtOAc (3 × 50 mL). The collected organic layers were filtered through phase separator and solvent evaporated under the reduced pressure. Obtained yellow crude (0.453 g, 2.309 mmol) was suspended in dry THF (6 mL). Afterwards $LiAlH_4$ (0.175 g, 4.618 mmol) was added in small portions, and the reaction mixture was stirred under argon atmosphere for 1 h at rt. The reaction was quenched with H_2O (20 mL), pH adjusted to 8 with 1% HCl, and the resulting solution extracted with EtOAc (4 × 50 mL). The collected organic layers were filtered through phase separator and solvent evaporated under the reduced pressure. The crude product was triturated with diethyl ether, to obtain alcohol **2**. Yield: 0.417 g (91%).

*4.1.3. General procedure for the synthesis of azides **3** and **10***

To a solution of **2** or **9** (1.447 mmol) in dry THF (5 mL), ADMP (1.032 g, 3.618 mmol) and DBU (0.584 mL, 3.907 mmol) were added at 0 °C. The reaction was stirred at 0 °C for 0.5 h, diluted with saturated NH_4Cl solution (40 mL) and extracted with DCM (2 × 30 mL). Organic layers were collected and extracted with brine (2 × 30 mL) and H_2O (1 × 20 mL), filtered through phase separator and solvent evaporated under the reduced pressure. The crude product (brownish oil) was purified by column chromatography (cyclohexane/EtOAc/MeOH 1:1:0.5).

*4.1.3.1. 1-(azidomethyl)-9H-pyrido[3,4-b]indole (**3**).* Alcohol **2**: 0.287 g. Yield: 0.236 g (73%); oil; IR (ATR, ν/cm^{-1}) 3663, 3451, 3288, 3059, 2937, 2855, 2105, 1730, 1631, 1566, 1493, 1428, 1371, 1321, 1248, 1118, 1052, 971, 938, 873, 824, 751, 718, 620, 579, 432; ^{1}H NMR (DMSO-d_6) δ 11.78 (s, 1H), 8.36 (d, 1H, J = 5.2 Hz), 8.29-8.23 (m, 1H), 8.13 (d, 1H, J = 5.2 Hz), 7.64 (dt, 1H, J = 8.3, 0.9 Hz), 7.60-7.57 (m, 1H), 7.29-7.26 (m, 1H), 4.89 (s, 2H); ^{13}C NMR (DMSO-d_6) δ 140.58, 139.19, 137.75, 133.86, 128.50, 128.44, 121.87, 120.74, 119.57, 114.77, 112.02, 51.59.

*4.1.3.2. 3-(azidomethyl)-1-methyl-9H-pyrido[3,4-b]indole (**10**).* Alcohol **9**: 0.307 g. Yield: 0.261 g (76%); oil; IR (ATR, ν/cm^{-1}) 3671, 3451, 3239, 3051, 2937, 2863, 2447, 2325, 2104, 1689, 1631, 1566, 1509, 1452, 1403, 1354, 1264, 1085, 1036, 971, 848, 759, 718, 644, 579, 431; ^{1}H NMR (DMSO-d_6) δ 11.66 (s, 1H), 8.20 (d, 1H, J = 7.9 Hz), 8.00 (s, 1H), 7.62-7.60 (m, 1H), 7.57-7.53 (m, 1H), 7.26-7.23 (m, 1H), 4.57 (s, 2H), 2.78 (s, 3H); ^{13}C NMR (DMSO-d_6) δ 143.23, 142.12, 140.74, 133.94, 128.02, 127.56, 121.74, 121.01, 119.39, 112.07, 111.72, 55.30, 20.41.

*4.1.4. General procedure for the synthesis of alkynes **4a**-**e***

An appropriate CAD (3.375 mmol) and K_2CO_3 (0.653 g, 4.725 mmol) were suspended in dry DMF (5 mL). Under the argon atmosphere, propargyl bromide (0.601 mL, 5.4 mmol, 80% solution in toluene) was added dropwise, and the reaction was stirred at rt for 48 h. Upon completion, the reaction mixture was diluted with H_2O (50 mL) and extracted with EtOAc (3 × 40 mL). The collected organic layers were washed with H_2O (2 × 100 mL), dried over anhydrous sodium sulphate and solvent evaporated under the reduced pressure. The crude product (oil) was purified by column chromatography (cyclohexane/EtOAc/MeOH 1:1:0.5).

*4.1.4.1. Prop-2-yn-1-yl cinnamate (**4a**).* CAD: 0.500 g of *trans*-cinnamic acid; yield: 0.584 g (93%).

*4.1.4.2. Prop-2-yn-1-yl (E)-3-(3-fluorophenyl)acrylate (**4b**).* CAD: 0.561 g of *m*-fluorocinnamic acid; yield: 0.648 g (94%).

*4.1.4.3. Prop-2-yn-1-yl (E)-3-(3-bromophenyl)acrylate (**4c**).* CAD: 0.766 g of *m*-bromocinnamic acid; yield: 0.779 g (87%); mp 79.0–81.0 °C; IR (ATR, ν/cm^{-1}) 3416, 3279, 3060, 3042, 2940, 2132, 1716, 1637, 1561, 1479, 1419, 1360, 1295, 1201, 1169, 1073, 991, 965, 851, 780, 754, 696, 665, 632, 554; ^{1}H NMR (DMSO-d_6) δ 8.02 (t, 1H, J = 1.8 Hz), 7.78 (dt, 1H, J = 7.7, 1.4 Hz), 7.69 (d, 1H, J = 16.1 Hz), 7.64-7.62 (m, 1H), 7.39 (t, 1H, J = 7.9 Hz), 6.79 (d, 1H, J = 16.1 Hz), 4.84 (d, 2H, J = 2.4 Hz), 3.59 (t, 1H, J = 2.5 Hz); ^{13}C NMR (DMSO-d_6) δ 165.21, 143.81, 136.38, 133.17, 130.99, 130.97, 127.45, 122.32, 118.90, 77.80, 51.93; ESI-MS: decomposition.

*4.1.4.4. Prop-2-yn-1-yl (E)-3-(4-chlorophenyl)acrylate (**4d**).* CAD: 0.616 g of *p*-chlorocinnamic acid; yield: 0.7 g, (94%).

*4.1.4.5. Prop-2-yn-1-yl (E)-3-(4-methoxyphenyl)acrylate (**4e**).* CAD: 0.601 g of *p*-methoxycinnamic acid; yield: 0.540 g, (74%).

*4.1.5. General procedure for the synthesis of harmicines **5a**-**e***

Azide **3** (0.04 g, 0.179 mmol) and a corresponding alkyne **4a-e** (0.197 mmol) were suspended in 5 mL of a 1:1 H_2O/*t*-BuOH mixture. Sodium ascorbate (0.2 mmol, 200 μL of freshly prepared 1 M

solution in H_2O) was added, followed by $CuSO_4 \times 5H_2O$ (0.02 mmol, 20 μL of 1 M solution in H_2O). The mixture was stirred at rt for 0.5 h, diluted with 5 mL of ice-cold H_2O and filtered. A yellow precipitate was washed with H_2O (3 × 2 mL), dried under vacuum, purified by column chromatography (mobile phase DCM/MeOH 95:5). The crude product was triturated with diethyl ether/petroleum ether mixture/recrystallized from EtOH.

*4.1.5.1. (1-((9H-pyrido[3,4-b]indol-1-yl)methyl)-1H-1,2,3-triazol-4-yl)methyl cinnamate (**5a**).* Alkyne **4a**: 0.037 g; purification: trituration with diethyl ether/petroleum ether mixture; yield: 0.036 g (49%); mp 181.5–183.5 °C; IR (ATR, ν/cm^{-1}) 3220, 3168, 3093, 3059, 3029, 2994, 2961, 2898, 2877, 2798, 2776, 1713, 1637, 1567, 1505, 1452, 1432, 1402, 1370, 1346, 1325, 1307, 1281, 1243, 1203, 1167, 1066, 1038, 1003, 972, 859, 820, 804, 764, 739, 707, 682, 641, 605, 593, 573, 547, 525, 483; ^{1}H NMR (DMSO-d_6) δ 11.98 (s, 1H), 8.32 (s, 1H), 8.30 (d, 1H, J = 5.2 Hz), 8.27 (d, 1H, J = 7.9 Hz), 8.13 (d, 1H, J = 5.2 Hz), 7.73-7.66 (m, 4H), 7.62-7.58 (m, 1H), 7.44-7.38 (m, 3H), 7.31-7.26 (m, 1H), 6.66 (d, 1H, J = 16.0 Hz), 6.11 (s, 2H), 5.28 (s, 2H); ^{13}C NMR (DMSO-d_6) δ 165.93, 145.03, 141.79, 140.70, 137.98, 137.88, 133.92, 133.84, 130.57, 128.91, 128.74, 128.57, 128.42, 125.73, 121.92, 120.74, 119.66, 117.65, 114.87, 112.07, 57.29, 51.21; ESI-MS: *m/z* 410.1 (M+1)$^+$; Anal. Calcd. for $C_{24}H_{19}N_5O_2$: C, 70.40; H, 4.68; N, 17.10; found: C, 70.27; H, 4.47; N, 17.35.

*4.1.5.2. (1-((9H-pyrido[3,4-b]indol-1-yl)methyl)-1H-1,2,3-triazol-4-yl)methyl (E)-3-(3-fluorophenyl)acrylate (**5b**).* Alkyne **4b**: 0.040 g; purification: trituration with diethyl ether/petroleum ether mixture; yield: 0.043 g (56%); mp 185.5–187.5 °C; IR (ATR, ν/cm^{-1}) 3311, 3230, 3198, 3147, 3105, 3063, 3019, 2998, 2973, 1715, 1639, 1585, 1569, 1502, 1485, 1472, 1449, 1429, 1403, 1390, 1349, 1323, 1272, 1234, 1190, 1168, 1147, 1122, 1075, 1060, 1035, 983, 954, 939, 874, 858, 837, 819, 780, 728, 671, 643, 605, 582, 562, 534, 521; ^{1}H NMR (DMSO-d_6) δ 11.98 (s, 1H), 8.32 (s, 1H), 8.30 (d, 1H, J = 5.2 Hz), 8.27 (d, 1H, J = 7.9 Hz), 8.13 (d, 1H, J = 5.2 Hz), 7.69-7.63 (m, 3H), 7.61-7.59 (m, 1H), 7.56 (dt, 1H, J = 7.8, 1.2 Hz), 7.47-7.43 (m, 1H), 7.30-7.24 (m, 2H), 6.75 (d, 1H, J = 16.1 Hz), 6.11 (s, 2H), 5.28 (s, 2H); ^{13}C NMR (DMSO-d_6) δ 165.75, 162.40 (d, J = 243.8 Hz), 143.66, 141.71, 140.71, 137.99, 137.89, 136.49 (d, J = 8.1 Hz), 133.85, 130.87 (d, J = 8.4 Hz), 128.75, 128.59, 125.78, 124.94 (d, J = 2.5 Hz), 121.94, 120.75, 119.68, 119.30, 117.26 (d, J = 21.4 Hz), 114.89, 114.58 (d, J = 22.1 Hz), 112.08, 57.40, 51.22; ESI-MS: *m/z* 428.1 (M+1)$^+$; Anal. Calcd. for $C_{24}H_{18}FN_5O_2$: C, 67.44; H, 4.24; N, 16.38; found: C, 67.40; H, 4.49; N, 16.21.

*4.1.5.3. (1-((9H-pyrido[3,4-b]indol-1-yl)methyl)-1H-1,2,3-triazol-4-yl)methyl (E)-3-(3-bromophenyl)acrylate (**5c**).* Alkyne **4c**: 0.052 g; purification: recrystallisation from EtOH; yield: 0.032 g (37%); mp 184.0–186.0 °C; IR (ATR, ν/cm^{-1}) 3311, 3223, 3194, 3147, 3102, 3060, 2997, 2971, 1715, 1640, 1607, 1564, 1501, 1472, 1457, 1428, 1404, 1389, 1347, 1308, 1276, 1234, 1189, 1168, 1122, 1090, 1060, 1036, 984, 860, 830, 812, 777, 735, 670, 643, 605, 578, 542; ^{1}H NMR (DMSO-d_6) δ 11.97 (s, 1H), 8.32 (s, 1H), 8.30 (d, 1H, J = 5.2 Hz), 8.26 (d, 1H, J = 7.8 Hz), 8.13 (d, 1H, J = 5.2 Hz), 7.98 (t, 1H, J = 1.8 Hz), 7.73 (dt, 1H, J = 7.8, 1.3 Hz), 7.69-7.57 (m, 4H), 7.36 (t, 1H, J = 7.9 Hz), 7.31-7.27 (m, 1H), 6.75 (d, 1H, J = 16.0 Hz), 6.11 (s, 2H), 5.28 (s, 2H); ^{13}C NMR (DMSO-d_6) δ 165.68, 143.33, 141.71, 140.69, 137.97, 137.87, 136.45, 133.83, 133.03, 130.93, 128.74, 128.57, 127.32, 125.74, 122.28, 121.92, 120.73, 119.66, 119.37, 114.87, 112.07, 57.40, 51.21; ESI-MS: *m/z* 488.0 (M+1)$^+$, 489.9 (M+1)$^+$; Anal. Calcd. for $C_{24}H_{18}BrN_5O_2$: C, 59.03; H, 3.72; N, 14.34; found: C, 59.19; H, 3.94; N, 14.52.

*4.1.5.4. (1-((9H-pyrido[3,4-b]indol-1-yl)methyl)-1H-1,2,3-triazol-4-yl)methyl (E)-3-(4-chlorophenyl)acrylate (**5d**).* Alkyne **4d**: 0.043 g; purification: trituration with diethyl ether/petroleum ether mixture; yield: 0.02 g (25%); mp 201.0–203.5 °C; IR (ATR, ν/cm^{-1}) 3227, 3192, 3096, 3061, 2993, 2965, 2926, 2894, 2872, 1713, 1642, 1594, 1568, 1503, 1490, 1468, 1453, 1431, 1404, 1370, 1346, 1308, 1271, 1242, 1201, 1171, 1148, 1087, 1068, 1038, 1012, 972, 868, 818, 775, 737, 695, 683, 669, 637, 593, 560, 547, 529, 491, 455; ^{1}H NMR (DMSO-d_6) δ 11.97 (s, 1H), 8.31 (s, 1H), 8.30 (d, 1H, J = 5.3 Hz), 8.27 (d, 1H, J = 7.9 Hz), 8.13 (d, 1H, J = 5.2 Hz), 7.77-7.74 (m, 2H), 7.70-7.64 (m, 2H), 7.62-7.58 (m, 1H), 7.50-7.45 (m, 2H), 7.31-7.26 (m, 1H), 6.69 (d, 1H, J = 16.1 Hz), 6.11 (s, 2H), 5.28 (s, 2H); ^{13}C NMR (DMSO-d_6) δ 165.79, 143.60, 141.74, 140.69, 137.97, 137.87, 135.08, 133.83, 132.91, 130.15, 128.94, 128.74, 128.57, 125.73, 121.92, 120.73, 119.66, 118.49, 114.87, 112.07, 57.35, 51.21; ESI-MS: *m/z* 444.0 (M+1)$^+$; Anal. Calcd. for $C_{24}H_{18}ClN_5O_2$: C, 64.94; H, 4.09; N, 15.78; found: C, 64.75; H, 4.27; N, 15.93.

*4.1.5.5. (1-((9H-pyrido[3,4-b]indol-1-yl)methyl)-1H-1,2,3-triazol-4-yl)methyl (E)-3-(4-methoxyphenyl)acrylate (**5e**).* Alkyne **4e**: 0.043 g; purification: trituration with diethyl ether/petroleum ether mixture; yield: 0.032 g (41%); mp 155.0–157.5 °C; IR (ATR, ν/cm^{-1}) 3223, 3170, 3131, 3094, 3082, 2996, 2965, 2934, 2900, 2837, 1712, 1636, 1607, 1573, 1513, 1455, 1429, 1402, 1375, 1322, 1308, 1287, 1258, 1240, 1202, 1163, 1065, 1037, 1002, 971, 867, 852, 824, 774, 734, 592, 547, 527, 513; ^{1}H NMR (DMSO-d_6) δ 11.98 (s, 1H), 8.32-8.29 (m, 2H), 8.27 (d, 1H, J = 7.9 Hz), 8.12 (d, 1H, J = 5.2 Hz), 7.69-7.59 (m, 5H), 7.28 (t, 1H, J = 7.5 Hz), 6.96 (d, 2H, J = 8.4 Hz), 6.50 (d, 1H, J = 16.0 Hz), 6.11 (s, 2H), 5.25 (s, 2H), 3.79 (s, 3H); ^{13}C NMR (DMSO-d_6) δ 166.22, 161.24, 144.85, 141.92, 140.71, 138.01, 137.88, 133.85, 130.26, 128.74, 128.58, 126.56, 125.70, 121.94, 120.75, 119.67, 114.88, 114.38, 112.09, 57.11, 55.34, 51.21; ESI-MS: *m/z* 440.1 (M+1)$^+$; Anal. Calcd. for $C_{25}H_{21}N_5O_3$: C, 68.33; H, 4.82; N, 15.94; found: C, 68.27; H, 4.99; N, 15.68.

*4.1.6. General procedure for the synthesis of amines **6** and **11***

A suspension of **3** or **10** (0.856 mmol) and 10% Pd/C (0.041 g) in MeOH (5 mL) was stirred at rt under hydrogen atmosphere for 18 h (compound **6**) or 2 h (compound **11**). Upon completion, the reaction mixture was filtered through celite, and the solvent was removed under the reduced pressure. The crude product was triturated with diethyl ether/petroleum ether mixture.

*4.1.6.1. (9H-pyrido[3,4-b]indol-1-yl)methanamine (**6**).* Azide **3**: 0.191 g; yield: 0.120 g (71%); IR (ATR, ν/cm^{-1}) 3347, 3282, 3120, 3051, 2955, 2856, 2776, 1625, 1600, 1562, 1501, 1477, 1460, 1430, 1355, 1327, 1316, 1240, 1212, 1163, 1127, 1108, 1071, 960, 896, 848, 829, 772, 747, 671, 595, 564, 516; ^{1}H NMR (DMSO-d_6) δ 8.26 (d, 1H, J = 5.2 Hz), 8.21 (dt, 1H, J = 7.8, 1.0 Hz), 7.97 (d, 1H, J = 5.2 Hz), 7.63-7.62 (m, 1H), 7.55-7.52 (m, 1H), 7.24-7.22 (m, 1H), 4.19 (s, 2H); ^{13}C NMR (DMSO-d_6) δ 146.51, 140.35, 137.18, 133.23, 127.82, 127.42, 121.60, 120.88, 119.15, 113.19, 112.01, 44.59; ESI-MS: *m/z* 196.0 (M − 1)$^-$.

*4.1.6.2. (1-methyl-9H-pyrido[3,4-b]indol-3-yl)methanamine (**11**).* Azide **10**: 0.203 g; yield: 0.110 g (61%); IR (ATR, ν/cm^{-1}) 3338, 3239, 3130, 3057, 2978, 2940, 2914, 2882, 2850, 2783, 2737, 2690, 2637, 1626, 1606, 1566, 1503, 1453, 1401, 1374, 1344, 1317, 1284, 1250, 1176, 1147, 1103, 1083, 1009, 970, 945, 891, 838, 813, 775, 734, 643, 588, 545; ^{1}H NMR (DMSO-d_6) δ 11.42 (s, 1H), 8.14 (d, 1H, J = 7.6 Hz), 7.91 (s, 1H), 7.57-7.47 (m, 2H), 7.20 (t, 1H, J = 6.9 Hz), 3.89 (s, 2H), 2.73 (s, 3H); ^{13}C NMR (DMSO-d_6) δ 151.13, 140.89, 140.74, 133.29, 127.76, 127.62, 121.53, 121.19, 118.98, 111.89, 109.01, 47.59, 20.38; ESI-MS: *m/z* 210.0 (M − 1)$^-$.

*4.1.7. General procedure for the synthesis of harmicines **7a-h***

A solution of a corresponding CAD (0.212 mmol), DIEA (0.073 mL, 0.424 mmol) and HATU (0.081 g, 0.212 mmol) in DCM

(4 mL) was stirred at rt for 20 min, followed by the addition of amine **6** (0.038 g, 0.193 mmol). The reaction mixture was stirred at rt for 1 h. The formed precipitate was filtered off. After purification by column chromatography (DCM/MeOH 8:1) and trituration with diethyl ether, compounds **7a-h** were obtained.

*4.1.7.1. N-((9H-pyrido[3,4-b]indol-1-yl)methyl)cinnamamide (**7a**).* CAD: 0.031 g of *trans*-cinnamic acid; yield: 0.033 g (52%); mp 225.0–227.0 °C; IR (ATR, ν/cm^{-1}) 3375, 3328, 3226, 3195, 3101, 3060, 2901, 1661, 1623, 1576, 1514, 1435, 1404, 1325, 1243, 1205, 994, 914, 811, 767, 731, 718, 706, 620, 565, 490, 478; ^{1}H NMR (DMSO-d_6) δ 11.64 (s, 1H), 8.79 (t, 1H, J = 5.4 Hz), 8.33 (d, 1H, J = 5.2 Hz), 8.25 (d, 1H, J = 7.9 Hz), 8.08 (d, 1H, J = 5.3 Hz), 7.67-7.64 (m, 1H), 7.61-7.50 (m, 4H), 7.46-7.35 (m, 3H), 7.29-7.24 (m, 1H), 6.88 (d, 1H, J = 15.8 Hz), 4.92 (d, 2H, J = 5.3 Hz); ^{13}C NMR (DMSO-d_6) δ 165.43, 141.41, 140.45, 139.04, 137.34, 134.92, 133.52, 129.49, 128.94, 128.17, 127.82, 127.58, 122.10, 121.76, 120.87, 119.45, 113.96, 112.08, 41.65; ESI-MS: m/z 328.1 (M+1)$^+$; HPLC purity > 99.5%.

*4.1.7.2. (E)-N-((9H-pyrido[3,4-b]indol-1-yl)methyl)-3-(3-fluorophenyl)acrylamide (**7b**).* CAD: 0.035 g of *m*-fluorocinnamic acid; yield: 0.034 g (51%); mp 224.5–225.5 °C; IR (ATR, ν/cm^{-1}) 3350, 3217, 3149, 3080, 2995, 2905, 2814, 1672, 1627, 1586, 1516, 1448, 1409, 1325, 1273, 1239, 1225, 1146, 1011, 968, 878, 851, 807, 784, 728, 611, 564, 521; ^{1}H NMR (DMSO-d_6) δ 11.63 (s, 1H), 8.78 (t, 1H, J = 5.4 Hz), 8.32 (d, 1H, J = 5.2 Hz), 8.24 (d, 1H, J = 7.8 Hz), 8.07 (d, 1H, J = 5.2 Hz), 7.64 (d, 1H, J = 8.2 Hz), 7.57 (t, 1H, J = 7.6 Hz), 7.52 (d, 1H, J = 15.8 Hz), 7.49-7.43 (m, 3H), 7.26 (t, 1H, J = 7.4 Hz), 7.23-7.20 (m, 1H), 6.94 (d, 1H, J = 15.8 Hz), 4.92 (d, 2H, J = 5.3 Hz); ^{13}C NMR (DMSO-d_6) δ 165.08, 162.46 (d, J = 244.0 Hz), 141.26, 140.45, 137.71 (d, J = 2.4 Hz), 137.58 (d, J = 7.8 Hz), 137.37, 133.48, 130.90 (d, J = 8.4 Hz), 128.16, 127.80, 123.75 (d, J = 2.5 Hz), 123.70, 121.76, 120.87, 119.44, 116.14 (d, J = 21.2 Hz), 113.96 (d, J = 21.8 Hz), 112.07, 41.65; ESI-MS: m/z 346.1 (M+1)$^+$; HPLC purity 98.2%.

*4.1.7.3. (E)-N-((9H-pyrido[3,4-b]indol-1-yl)methyl)-3-(3-bromophenyl)acrylamide (**7c**).* CAD: 0.048 g of *m*-bromocinnamic acid; yield: 0.056 g (72%); mp 236.5–239.0 °C; IR (ATR, ν/cm^{-1}) 3191, 3016, 1671, 1626, 1564, 1497, 1471, 1437, 1392, 1328, 1222, 1128, 1078, 971, 929, 820, 778, 722, 667, 584; ^{1}H NMR (DMSO-d_6) δ 11.62 (s, 1H), 8.74 (t, 1H, J = 5.4 Hz), 8.31 (d, 1H, J = 5.2 Hz), 8.23 (d, 1H, J = 7.8 Hz), 8.06 (d, 1H, J = 5.2 Hz), 7.80 (t, 1H, J = 1.9 Hz), 7.63 (d, 1H, J = 8.2 Hz), 7.59 (d, 1H, J = 7.8 Hz), 7.57-7.54 (m, 2H), 7.47 (d, 1H, J = 15.8 Hz), 7.37 (t, 1H, J = 7.9 Hz), 7.25 (t, 1H, J = 7.4 Hz), 6.94 (d, 1H, J = 15.8 Hz), 4.91 (d, 2H, J = 5.3 Hz); ^{13}C NMR (DMSO-d_6) δ 165.01, 141.20, 140.46, 137.53, 137.34, 137.30, 133.46, 131.98, 131.02, 130.06, 128.17, 127.82, 126.49, 123.82, 122.26, 121.76, 120.85, 119.44, 113.96, 112.06, 41.62; ESI-MS: m/z 405.9 (M+1)$^+$, 407.9 (M+1)$^+$; HPLC purity 99.4%.

*4.1.7.4. (E)-N-((9H-pyrido[3,4-b]indol-1-yl)methyl)-3-(3-(trifluoromethyl)phenyl)acrylamide (**7d**).* CAD: 0.046 g of *m*-(trifluoromethyl)cinnamic acid; yield: 0.040 g (52%); mp 225.5–226.5 °C; IR (ATR, ν/cm^{-1}) 3197, 3014, 1669, 1628, 1560, 1498, 1438, 1329, 1226, 1177, 1167, 1109, 1077, 972, 885, 804, 742, 721, 691, 581; ^{1}H NMR (DMSO-d_6) δ 11.65 (s, 1H), 8.78 (t, 1H, J = 5.3 Hz), 8.33 (d, 1H, J = 5.2 Hz), 8.24 (dt, 1H, J = 7.9, 1.0 Hz), 8.07 (d, 1H, J = 5.2 Hz), 7.96 (t, 1H, J = 2.0 Hz), 7.90 (d, 1H, J = 7.8 Hz), 7.73 (d, 1H, J = 7.8 Hz), 7.67-7.63 (m, 2H), 7.60 (d, 1H, J = 15.8 Hz), 7.58-7.55 (m, 1H), 7.28-7.25 (m, 1H), 7.06 (d, 1H, J = 15.9 Hz), 4.93 (d, 2H, J = 5.3 Hz); ^{13}C NMR (DMSO-d_6) δ 164.96, 141.19, 140.47, 137.35, 137.26, 136.19, 133.47, 131.37, 130.05, 129.74 (q, J = 31.7 Hz), 128.15, 127.80, 125.72 (q, J = 2.7 Hz), 124.33, 124.06 (q, J = 273.3 Hz), 123.92 (q, J = 3.6 Hz), 121.75, 120.87, 119.44, 113.96, 112.07, 41.67; ESI-MS: m/z 396.1 (M+1)$^+$; HPLC purity 97.3%.

*4.1.7.5. (E)-N-((9H-pyrido[3,4-b]indol-1-yl)methyl)-3-(4-fluorophenyl)acrylamide (**7e**).* CAD: 0.035 g of *p*-fluorocinnamic acid; yield: 0.045 g (67%); mp 231.5–233.0 °C; IR (ATR, ν/cm^{-1}) 3380, 3244, 3147, 3075, 2989, 2900, 1655, 1616, 1599, 1556, 1505, 1430, 1426, 1413, 1354, 1325, 1239, 1220, 1161, 1128, 1098, 1010, 977, 828, 755, 734, 628, 508; ^{1}H NMR (DMSO-d_6) δ 11.62 (s, 1H), 8.75 (t, 1H, J = 5.4 Hz), 8.32 (d, 1H, J = 5.2 Hz), 8.24 (d, 1H, J = 7.8 Hz), 8.06 (d, 1H, J = 5.2 Hz), 7.66-7.63 (m, 3H), 7.56 (t, 1H, J = 7.6 Hz), 7.51 (d, 1H, J = 15.8 Hz), 7.27-7.24 (m, 3H), 6.83 (d, 1H, J = 15.8 Hz), 4.91 (d, 2H, J = 5.3 Hz); ^{13}C NMR (DMSO-d_6) δ 165.31, 162.69 (d, J = 247.0 Hz), 141.39, 140.42, 137.80, 137.35, 133.49, 131.56 (d, J = 3.0 Hz), 129.71 (d, J = 8.4 Hz), 128.12, 127.77, 122.00 (d, J = 1.7 Hz), 121.73, 120.86, 119.41, 115.89 (d, J = 21.8 Hz), 113.92, 112.05, 41.64; ESI-MS: m/z 346.1 (M+1)$^+$; Anal. Calcd. for $C_{21}H_{16}FN_3O$: C, 73.03; H, 4.67; N, 12.17; found: C, 73.15; H, 4.81; N, 12.29.

*4.1.7.6. (E)-N-((9H-pyrido[3,4-b]indol-1-yl)methyl)-3-(4-chlorophenyl)acrylamide (**7f**).* CAD: 0.039 g of *p*-chlorocinnamic acid; yield: 0.036 g (52%); mp 241.0–243.5 °C (decomp.); IR (ATR, ν/cm^{-1}) 3384, 3275, 3053, 1671, 1627, 1532, 1505, 1494, 1457, 1435, 1405, 1323, 1237, 1219, 1094, 1028, 1013, 972, 819, 732, 609, 589, 573, 495; ^{1}H NMR (DMSO-d_6) δ 11.62 (s, 1H), 8.79 (t, 1H, J = 5.4 Hz), 8.32 (d, 1H, J = 5.2 Hz), 8.24 (d, 1H, J = 7.8 Hz), 8.06 (d, 1H, J = 5.2 Hz), 7.65-7.61 (m, 3H), 7.58-7.55 (m, 1H), 7.52-7.48 (m, 3H), 7.26 (t, 1H, J = 7.4 Hz), 6.89 (d, 1H, J = 15.8 Hz), 4.91 (d, 2H, J = 5.4 Hz); ^{13}C NMR (DMSO-d_6) δ 165.20, 141.35, 140.45, 137.67, 137.38, 133.92, 133.51, 129.29, 128.99, 128.16, 127.80, 122.93, 121.77, 120.88, 119.45, 113.96, 112.08, 41.66; ESI-MS: m/z 362.1 (M+1)$^+$; Anal. Calcd. for $C_{21}H_{16}ClN_3O$: C, 69.71; H, 4.46; N, 11.61; found: C, 69.95; H, 4.31; N, 11.99.

*4.1.7.7. (E)-N-((9H-pyrido[3,4-b]indol-1-yl)methyl)-3-(4-methoxyphenyl)acrylamide (**7g**).* CAD: 0.038 g of *p*-methoxycinnamic acid; yield: 0.034 g (49%); mp 230.5–232.0 °C; IR (ATR, ν/cm^{-1}) 3350, 3173, 3097, 3006, 1662, 1624, 1603, 1511, 1432, 1366, 1325, 1254, 1240, 1174, 1029, 981, 914, 818, 791, 733, 596, 528, 506; ^{1}H NMR (DMSO-d_6) δ 11.58 (s, 1H), 8.66 (t, 1H, J = 5.5 Hz), 8.29 (d, 1H, J = 5.3 Hz), 8.22 (d, 1H, J = 7.8 Hz), 8.04 (d, 1H, J = 4.7 Hz), 7.62 (d, 1H, J = 8.2 Hz), 7.56-7.51 (m, 3H), 7.44 (d, 1H, J = 15.7 Hz), 7.24 (t, 1H, J = 7.5 Hz), 6.96 (d, 2H, J = 8.2 Hz), 6.69 (d, 1H, J = 15.7 Hz), 4.88 (d, 2H, J = 5.5 Hz), 3.77 (s, 3H); ^{13}C NMR (DMSO-d_6) δ 165.82, 160.39, 141.57, 140.46, 138.83, 137.34, 133.54, 129.20, 128.20, 127.85, 127.49, 121.78, 120.90, 119.57, 119.48, 114.42, 113.98, 112.10, 55.28, 41.67; ESI-MS: m/z 358.1 (M+1)$^+$; HPLC purity 99.0%.

*4.1.7.8. (E)-N-((9H-pyrido[3,4-b]indol-1-yl)methyl)-3-(4-(trifluoromethyl)phenyl)acrylamide (**7h**).* CAD: 0.046 g of *p*-(trifluoromethyl)cinnamic acid; yield: 0.050 g (65%); mp 262.5–265.0 °C; IR (ATR, ν/cm^{-1}) 3341, 3236, 1664, 1622, 1504, 1436, 1416, 1323, 1239, 1217, 1155, 1116, 1068, 1013, 988, 826, 755, 740, 572, 532, 494; ^{1}H NMR (DMSO-d_6) δ 11.65 (s, 1H), 8.87 (t, 1H, J = 5.4 Hz), 8.33 (d, 1H, J = 5.3 Hz), 8.25 (d, 1H, J = 7.9 Hz), 8.08 (d, 1H, J = 5.3 Hz), 7.83-7.76 (m, 4H), 7.66-7.54 (m, 3H), 7.29-7.24 (m, 1H), 7.03 (d, 1H, J = 15.8 Hz), 4.94 (d, 2H, J = 5.3 Hz); ^{13}C NMR (DMSO-d_6) δ 164.89, 141.23, 140.46, 139.04, 137.38, 137.32, 133.49, 129.21 (q, J = 32.3 Hz), 128.20, 128.16, 127.81, 125.81 (q, J = 3.0 Hz), 124.95, 124.12 (q, J = 272.7 Hz), 121.76, 120.87, 119.44, 113.96, 112.07, 41.66; ESI-MS: m/z 396.1 (M+1)$^+$; HPLC purity 99.4%.

*4.1.8. Synthesis of (1-methyl-9-(prop-2-yn-1-yl)-9H-pyrido[3,4-b]indol-3-yl)methanol (**12**)*

Alcohol **9** (0.200 g, 0.942 mmol) was dissolved in dry DMF (5 mL). Under argon atmosphere caesium carbonate (0.430 g, 1.319 mmol) was added, followed by dropwise addition of

propargyl bromide (0.126 mL, 1.130 mmol, 80% solution in toluene). The reaction mixture was stirred at rt for 5 h. Upon completion, the reaction mixture was diluted with H_2O (50 mL) and extracted with EtOAc (3 × 40 mL). The collected organic layers were washed with H_2O (2 × 100 mL), dried over anhydrous sodium sulphate and the solvent evaporated under the reduced pressure. After purification by column chromatography (DCM/MeOH 95:5) and trituration with diethyl ether, alkyne **12** was obtained as a white solid.

Yield: 0.170 g (72%); mp 225.0–230.0 °C (decomp.); IR (ATR, ν/cm^{-1}) 3154, 2929, 2823, 2109, 1621, 1561, 1475, 1453, 1360, 1333, 1283, 1206, 1139, 1063, 1040, 965, 933, 877, 744, 724, 641, 578; ^{1}H NMR (DMSO-d_6) δ 8.25 (d, 1H, J = 7.8 Hz), 8.03 (s, 1H), 7.78 (d, 1H, J = 8.3 Hz), 7.63-7.58 (m, 1H), 7.29 (t, 1H, J = 7.4 Hz), 5.45 (d, 2H, J = 2.4 Hz), 5.35 (t, 1H, J = 5.8 Hz), 4.68 (d, 2H, J = 5.8 Hz), 3.35 (t, 1H, J = 2.4 Hz), 3.04 (s, 3H); ^{13}C NMR (DMSO-d_6) δ 150.83, 141.27, 140.52, 133.22, 129.53, 128.23, 121.52, 121.05, 120.04, 110.37, 109.11, 75.50, 64.34, 34.19, 22.45; ESI-MS: m/z 251.1 (M+1)$^+$.

*4.1.9. General procedure for the synthesis of harmicines **14a-e***

To a solution of alkyne **12** (0.040 g, 0.160 mmol) and the corresponding cinnamyl azide **13a-e** (0.176 mmol) in MeOH (5 mL), a catalytic amount of $Cu(OAc)_2$ was added. The reaction mixture was stirred at rt for 24 h. Upon completion of the reaction, the solvent was removed under the reduced pressure. The residue was purified by column chromatography with DCM/MeOH, cyclohexane/EtOAc/MeOH or EtOAc/MeOH as a mobile phase. The crude product was triturated with diethyl ether/petroleum ether to obtain harmicines **14a-e**. Compound **14b** was obtained, but decomposed quickly at −20 °C.

*4.1.9.1. (9-((1-cinnamyl-1H-1,2,3-triazol-4-yl)methyl)-1-methyl-9H-pyrido[3,4-b]indol-3-yl)methanol (**14a**).* **13a**: 0.028 g; mobile phase: cyclohexane/EtOAc/MeOH 3:1:0.5; yield: 0.032 g (49%); mp 197.0–200.0 °C; IR (ATR, ν/cm^{-1}) 3113, 3060, 2966, 2917, 2859, 1657, 1619, 1560, 1512, 1445, 1402, 1362, 1337, 1290, 1252, 1220, 1190, 1156, 1136, 1122, 1062, 1043, 962, 934, 860, 842, 813, 780, 748, 691, 638, 620, 577, 530, 511, 477, 463; ^{1}H NMR (DMSO-d_6) δ 8.23 (d, 1H, J = 7.7 Hz), 8.02 (s, 1H), 7.98 (s, 1H), 7.82 (d, 1H, J = 8.3 Hz), 7.59-7.55 (m, 1H), 7.40-7.24 (m, 6H), 6.51 (d, 1H, J = 15.9 Hz), 6.47-6.35 (m, 1H), 5.90 (s, 2H), 5.33 (t, 1H, J = 5.7 Hz), 5.07 (d, 2H, J = 6.0 Hz), 4.67 (d, 2H, J = 5.7 Hz), 3.05 (s, 3H); ^{13}C NMR (DMSO-d_6) δ 150.27, 144.17, 141.35, 140.55, 135.63, 133.45, 133.41, 129.10, 128.66, 128.10, 128.06, 126.51, 123.66, 122.72, 121.41, 120.99, 119.71, 110.61, 109.07, 64.35, 51.27, 39.73, 23.15; ESI-MS: m/z 410.3 (M+1)$^+$; Anal. Calcd. for $C_{25}H_{23}N_5O$: C, 73.33; H, 5.66; N, 17.10; found: C, 73.19; H, 5.39; N, 17.34.

*4.1.9.2. (E)-(9-((1-(3-(3-bromophenyl)allyl)-1H-1,2,3-triazol-4-yl)methyl)-1-methyl-9H-pyrido[3,4-b]indol-3-yl)methanol (**14c**).* **13c**: 0.042 g; mobile phase: DCM/MeOH 95:5; yield: 0.031 g, (39%); mp 164.5–167.5 °C; IR (ATR, ν/cm^{-1}) 3117, 3060, 2959, 2922, 2861, 1619, 1592, 1560, 1471, 1460, 1445, 1380, 1358, 1336, 1290, 1252, 1222, 1199, 1154, 1120, 1095, 1062, 1044, 995, 965, 934, 875, 861, 829, 786, 747, 719, 685, 668, 636, 621, 577, 534, 492, 463; ^{1}H NMR (DMSO-d_6) δ 8.23 (d, 1H, J = 7.7 Hz), 8.02 (s, 1H), 7.97 (s, 1H), 7.82 (d, 1H, J = 8.3 Hz), 7.70 (t, 1H, J = 2.2 Hz), 7.57 (t, 1H, J = 8.0 Hz), 7.47-7.42 (m, 2H), 7.30-7.24 (m, 2H), 6.67-6.60 (m, 2H), 5.93 (s, 2H), 5.32 (t, 1H, J = 5.7 Hz), 5.07 (d, 2H, J = 5.1 Hz), 4.67 (d, 2H, J = 5.6 Hz), 3.08 (s, 3H); ^{13}C NMR (DMSO-d_6) δ 150.26, 144.16, 141.34, 140.54, 138.20, 133.45, 131.73, 130.74, 130.69, 129.09, 129.00, 128.04, 125.64, 125.56, 122.78, 122.12, 121.40, 120.99, 119.71, 110.60, 109.06, 64.34, 51.11, 39.72, 23.13; ESI-MS: m/z 488.1 (M+1)$^+$, 490.1 (M+1)$^+$; Anal. Calcd. for $C_{25}H_{22}BrN_5O$: C, 61.48; H, 4.54; N, 14.34; found: C, 61.78; H, 4.59; N, 14.62.

*4.1.9.3. (E)-(9-((1-(3-(4-chlorophenyl)allyl)-1H-1,2,3-triazol-4-yl)methyl)-1-methyl-9H-pyrido[3,4-b]indol-3-yl)methanol (**14d**).* **13d**: 0.034 g; mobile phase: EtOAc/MeOH 10:0.5; yield: 0.029 g, (41%); mp 183.0–186.5 °C; IR (ATR, ν/cm^{-1}) 3111, 3064, 2971, 2918, 2858, 2822, 1727, 1658, 1619, 1592, 1559, 1489, 1471, 1447, 1405, 1361, 1336, 1292, 1254, 1221, 1192, 1158, 1121, 1085, 1041, 1014, 964, 938, 861, 837, 819, 799, 779, 748, 719, 685, 637, 577, 537, 502, 462; ^{1}H NMR (DMSO-d_6) δ 8.23 (d, 1H, J = 7.8 Hz), 8.02 (s, 1H), 7.97 (s, 1H), 7.82 (d, 1H, J = 8.3 Hz), 7.57 (t, 1H, J = 7.5 Hz), 7.43-7.35 (m, 4H), 7.27 (t, 1H, J = 7.4 Hz), 6.52-6.41 (m, 2H), 5.90 (s, 2H), 5.32 (t, 1H, J = 5.7 Hz), 5.07 (d, 2H, J = 5.1 Hz), 4.67 (d, 2H, J = 5.7 Hz), 3.05 (s, 3H); ^{13}C NMR (DMSO-d_6) δ 150.27, 144.18, 141.35, 140.55, 134.61, 133.44, 132.47, 132.05, 129.10, 128.64, 128.24, 128.06, 124.71, 122.76, 121.41, 120.99, 119.72, 110.60, 109.06, 64.35, 51.17, 39.73, 23.15; ESI-MS: m/z 444.2 (M+1)$^+$; Anal. Calcd. for $C_{25}H_{22}ClN_5O$: C, 67.64; H, 5.00; N, 15.78; found: C, 67.34; H, 5.16; N, 15.63.

*4.1.9.4. (E)-(9-((1-(3-(4-methoxyphenyl)allyl)-1H-1,2,3-triazol-4-yl)methyl)-1-methyl-9H-pyrido[3,4-b]indol-3-yl)methanol (**14e**).* **13e**: 0.033 g; mobile phase: DCM/MeOH 95:5; yield: 0.030 g, (43%); mp 202.0–205.0 °C; IR (ATR, ν/cm^{-1}) 3180, 3119, 3067, 3024, 3002, 2945, 2923, 2869, 1622, 1563, 1488, 1462, 1441, 1379, 1364, 1333, 1298, 1254, 1222, 1203, 1160, 1135, 1122, 1067, 1037, 1003, 965, 915, 857, 771, 745, 696, 636, 582, 533, 509, 471, 454; ^{1}H NMR (DMSO-d_6) δ 8.23 (d, 1H, J = 7.8 Hz), 8.02 (s, 1H), 7.96 (s, 1H), 7.82 (d, 1H, J = 8.3 Hz), 7.57 (t, 1H, J = 7.5 Hz), 7.34-7.30 (m, 2H), 7.26 (t, 1H, J = 7.5 Hz), 6.89-6.85 (m, 2H), 6.47 (d, 1H, J = 15.8 Hz), 6.25 (dt, 1H, J = 15.8, 6.5 Hz), 5.90 (s, 2H), 5.33 (t, 1H, J = 5.7 Hz), 5.03 (d, 2H, J = 7.2 Hz), 4.67 (d, 2H, J = 5.7 Hz), 3.74 (s, 3H), 3.05 (s, 3H); ^{13}C NMR (DMSO-d_6) δ 159.20, 150.26, 144.14, 141.35, 140.56, 133.45, 133.19, 129.09, 128.24, 128.05, 127.86, 122.61, 121.40, 121.05, 120.98, 119.71, 114.06, 110.60, 109.07, 64.35, 55.11, 51.41, 39.73, 23.15; ESI-MS: m/z 440.3 (M+1)$^+$; Anal. Calcd. for $C_{26}H_{25}N_5O_2$: C, 71.05; H, 5.73; N, 15.93; found: C, 71.27; H, 5.79; N, 15.72.

*4.1.10. General procedure for the synthesis of harmicines **15a-e***

To a suspension of azide **10** (0.04 g, 0.169 mmol) and a corresponding alkyne **4a-e** (0.186 mmol) in 5 mL of a 1:1H_2O/*t*-BuOH mixture, sodium ascorbate (0.2 mmol, 200 μL of freshly prepared 1 M solution in H_2O) and $CuSO_4 \times 5H_2O$ (0.02 mmol, 20 μL of 1 M solution in H_2O) were added. The mixture was stirred at rt for 0.5 h, diluted with 5 mL of ice-cold H_2O and filtered. A yellow precipitate was washed with H_2O (3 × 2 mL) and dried under vacuum. After purification by column chromatography (mobile phase DCM/MeOH 95:5) and trituration with diethyl ether/petroleum ether mixture, compounds **15a-e** were obtained as white solids.

*4.1.10.1. (1-((1-methyl-9H-pyrido[3,4-b]indol-3-yl)methyl)-1H-1,2,3-triazol-4-yl)methyl cinnamate (**15a**).* Alkyne **4a**: 0.035 g; yield: 0.026 g (36%); mp 194.5–195.5 °C; IR (ATR, ν/cm^{-1}) 3220, 3194, 3175, 3145, 3101, 3060, 3030, 2989, 2945, 1712, 1694, 1644, 1626, 1605, 1565, 1503, 1451, 1392, 1376, 1356, 1329, 1312, 1271, 1254, 1223, 1202, 1170, 1116, 1059, 1037, 1002, 972, 934, 898, 859, 843, 827, 804, 765, 752, 738, 708, 681, 642, 611, 587, 524, 480; ^{1}H NMR (DMSO-d_6) δ 11.67 (s, 1H), 8.26 (s, 1H), 8.17 (d, 1H, J = 7.9 Hz), 7.99 (s, 1H), 7.72-7.70 (m, 2H), 7.67 (d, 1H, J = 16.0 Hz), 7.60 (dt, 1H, J = 8.2, 1.0 Hz), 7.55-7.53 (m, 1H), 7.44-7.39 (m, 3H), 7.24-7.21 (m, 1H), 6.65 (d, 1H, J = 16.1 Hz), 5.77 (s, 2H), 5.27 (s, 2H), 2.75 (s, 3H); ^{13}C NMR (DMSO-d_6) δ 165.94, 145.02, 142.54, 142.16, 141.92, 140.78, 134.00, 133.93, 130.58, 128.91, 128.42, 128.10, 127.60, 125.13, 121.72, 120.91, 119.46, 117.66, 112.10, 112.05, 57.34, 55.25, 20.40; ESI-MS: m/z 424.0 (M+1)$^+$; Anal. Calcd. for $C_{25}H_{21}N_5O_2$: C, 70.91; H, 5.00; N, 16.54; found: C, 70.83; H, 5.17; N, 16.69.

*4.1.10.2. (1-((1-methyl-9H-pyrido[3,4-b]indol-3-yl)methyl)-1H-1,2,3-triazol-4-yl)methyl (E)-3-(3-fluorophenyl)acrylate (**15b**).* Alkyne **4b**: 0.038 g, yield: 0.045 g (60%); mp 197.0–198.5 °C; IR (ATR, ν/cm^{-1}) 3223, 3198, 3166, 3104, 3067, 3043, 3012, 2970, 2895, 1707, 1627, 1608, 1583, 1568, 1506, 1483, 1449, 1387, 1355, 1320, 1271, 1252, 1213, 1151, 1115, 1084, 1057, 1036, 1008, 980, 942, 911, 898, 864, 832, 788, 766, 738, 693, 675, 649, 609, 586, 555, 537, 520, 480; ^{1}H NMR (DMSO-d_6) δ 11.67 (s, 1H), 8.26 (s, 1H), 8.18 (d, 1H, J = 7.9 Hz), 8.00 (s, 1H), 7.67 (d, 1H, J = 16.1 Hz), 7.65-7.62 (m, 1H), 7.61-7.59 (m, 1H), 7.56-7.53 (m, 2H), 7.46-7.43 (m, 1H), 7.27-7.22 (m, 2H), 6.74 (d, 1H, J = 16.0 Hz), 5.77 (s, 2H), 5.28 (s, 2H), 2.75 (s, 3H); ^{13}C NMR (DMSO-d_6) δ 165.73, 162.39 (d, J = 243.8 Hz), 143.61, 142.52, 142.16, 141.83, 140.77, 136.47 (d, J = 8.1 Hz), 134.00, 130.84 (d, J = 8.4 Hz), 128.09, 127.60, 125.14, 124.91 (d, J = 2.5 Hz), 121.71, 120.90, 119.44, 119.29, 117.23 (d, J = 21.3 Hz), 114.56 (d, J = 22.1 Hz), 112.09, 112.06, 57.43, 55.25, 20.40; ESI-MS: m/z 442.1 (M+1)$^+$; HPLC purity 97.6%.

*4.1.10.3. (1-((1-methyl-9H-pyrido[3,4-b]indol-3-yl)methyl)-1H-1,2,3-triazol-4-yl)methyl (E)-3-(3-bromophenyl)acrylate (**15c**).* Alkyne **4c**: 0.049 g; yield: 0.045 g (53%); mp 204.5–205.5 °C; IR (ATR, ν/cm^{-1}) 3347, 3281, 3170, 3080, 3054, 3023, 2970, 2950, 1708, 1684, 1638, 1592, 1569, 1498, 1474, 1455, 1423, 1383, 1354, 1341, 1313, 1290, 1272, 1247, 1231, 1188, 1146, 1110, 1073, 1053, 1032, 1009, 980, 928, 899, 872, 829, 791, 766, 731, 697, 666, 649, 623, 586, 563, 549, 527; ^{1}H NMR (DMSO-d_6) δ 11.67 (s, 1H), 8.26 (s, 1H), 8.17 (d, 1H, J = 7.9 Hz), 7.99 (s, 1H), 7.97 (t, 1H, J = 1.8 Hz), 7.75-7.71 (m, 1H), 7.64 (d, 1H, J = 16.0 Hz), 7.62-7.58 (m, 2H), 7.56-7.52 (m, 1H), 7.36 (t, 1H, J = 7.9 Hz), 7.25-7.21 (m, 1H), 6.74 (d, 1H, J = 16.1 Hz), 5.77 (s, 2H), 5.28 (s, 2H), 2.75 (s, 3H); ^{13}C NMR (DMSO-d_6) δ 165.67, 143.31, 142.52, 142.14, 141.84, 140.77, 136.44, 133.99, 133.01, 130.91, 128.08, 127.59, 127.29, 125.11, 122.27, 121.70, 120.90, 119.43, 119.38, 112.08, 112.03, 57.44, 55.24, 20.39; ESI-MS: m/z 501.9 (M+1)$^+$, 503.9 (M+1)$^+$; HPLC purity 97.4%.

*4.1.10.4. (1-((1-methyl-9H-pyrido[3,4-b]indol-3-yl)methyl)-1H-1,2,3-triazol-4-yl)methyl (E)-3-(4-chlorophenyl)acrylate (**15d**).* Alkyne **4d**: 0.041 g; yield: 0.044 g (57%); mp 209.0–211.0 °C; IR (ATR, ν/cm^{-1}) 3250, 3157, 3103, 3086, 3067, 3052, 1703, 1633, 1592, 1566, 1493, 1475, 1456, 1428, 1408, 1388, 1356, 1305, 1278, 1251, 1222, 1204, 1182, 1160, 1117, 1089, 1058, 1036, 1004, 964, 899, 865, 840, 823, 805, 753, 739, 719, 702, 646, 605, 586, 550, 524, 501, 456; ^{1}H NMR (DMSO-d_6) δ 11.67 (s, 1H), 8.26 (s, 1H), 8.18 (d, 1H, J = 7.9 Hz), 8.00 (s, 1H), 7.76-7.73 (m, 2H), 7.66 (d, 1H, J = 16.0 Hz), 7.60 (dt, 1H, J = 8.3, 1.0 Hz), 7.56-7.53 (m, 1H), 7.48-7.45 (m, 2H), 7.24-7.22 (m, 1H), 6.68 (d, 1H, J = 16.1 Hz), 5.77 (s, 2H), 5.28 (s, 2H), 2.75 (s, 3H); ^{13}C NMR (DMSO-d_6) δ 165.80, 143.60, 142.53, 142.17, 141.88, 140.78, 135.09, 134.01, 132.92, 130.15, 128.94, 128.11, 127.61, 125.13, 121.72, 120.91, 119.46, 118.51, 112.10, 112.07, 57.40, 55.26, 20.41; ESI-MS: m/z 458.0 (M+1)$^+$; HPLC purity 98.3%.

*4.1.10.5. (1-((1-methyl-9H-pyrido[3,4-b]indol-3-yl)methyl)-1H-1,2,3-triazol-4-yl)methyl (E)-3-(4-methoxyphenyl)acrylate (**15e**).* Alkyne **4e**: 0.040 g; yield: 0.048 g (62%); mp 240.5–243.0 °C; IR (ATR, ν/cm^{-1}) 3236, 3201, 3165, 3103, 3068, 3036, 3007, 2965, 2940, 2911, 2839, 1699, 1626, 1601, 1574, 1514, 1456, 1426, 1389, 1357, 1307, 1290, 1252, 1223, 1207, 1179, 1155, 1115, 1056, 1023, 1009, 992, 971, 937, 898, 868, 830, 810, 776, 751, 735, 710, 693, 663, 652, 637, 608, 586, 555, 521; ^{1}H NMR (DMSO-d_6) δ 11.67 (s, 1H), 8.25 (s, 1H), 8.18 (d, 1H, J = 7.9 Hz), 7.99 (s, 1H), 7.68-7.64 (m, 2H), 7.64-7.59 (m, 2H), 7.55-7.53 (m, 1H), 7.24-7.22 (m, 1H), 6.97-6.94 (m, 2H), 6.49 (d, 1H, J = 16.0 Hz), 5.77 (s, 2H), 5.25 (s, 2H), 3.79 (s, 3H), 2.75 (s, 3H); ^{13}C NMR (DMSO-d_6) δ 166.19, 161.20, 144.80, 142.53, 142.14, 142.03, 140.76, 133.99, 130.22, 128.08, 127.59, 126.54, 125.05, 121.70, 120.90, 119.44, 114.88, 114.35, 112.08, 112.04, 57.14, 55.32, 55.23, 20.39; ESI-MS: m/z 454.1 (M+1)$^+$; HPLC purity 98.6%.

*4.1.11. General procedure for the synthesis of harmicines **16a-h***

A solution of a corresponding CAD (0.162 mmol), DIEA (0.056 mL, 0.324 mmol) and HATU (0.062 g, 0.162 mmol) in DCM (4 mL) was stirred at rt for 20 min, followed by the addition of amine **11** (0.031 g, 0.147 mmol). The resulting solution was stirred at rt for 1 h. Purification was performed by either Method A or Method B.

Method A: The resulting precipitate was filtered off, purified by column chromatography (DCM/MeOH 8:1) and triturated with diethyl ether/petroleum ether mixture.

Method B: After completion of the reaction, the solvent was evaporated and EtOAc (10 mL) was added. The formed precipitate was filtered off, purified by column chromatography (DCM/MeOH 8:1) and triturated with diethyl ether/petroleum ether mixture.

*4.1.11.1. N-((1-methyl-9H-pyrido[3,4-b]indol-3-yl)methyl)cinnamamide (**16a**).* CAD: 0.024 g of *trans*-cinnamic acid; purification: Method A; yield: 0.032 g (64%); mp 207.0–208.0; IR (ATR, ν/cm^{-1}) 3352, 3284, 3089, 3048, 2896, 2851, 1659, 1621, 1568, 1510, 1451, 1388, 1354, 1319, 1284, 1246, 1206, 1176, 1075, 1015, 973, 899, 871, 741, 714, 643, 612, 587, 557, 487; ^{1}H NMR (DMSO-d_6) δ 11.54 (s, 1H), 8.69 (t, 1H, J = 5.7 Hz), 8.19 (d, 1H, J = 7.8 Hz), 7.88 (s, 1H), 7.60-7.58 (m, 3H), 7.53-7.49 (m, 2H), 7.44-7.41 (m, 2H), 7.39-7.37 (m, 1H), 7.21 (t, 1H, J = 7.4 Hz), 6.81 (d, 1H, J = 15.8 Hz), 4.62 (d, 2H, J = 5.8 Hz), 2.78 (s, 3H); ^{13}C NMR (DMSO-d_6) δ 164.89, 146.07, 141.27, 140.79, 138.77, 134.98, 133.55, 129.41, 128.92, 127.86, 127.79, 127.52, 122.38, 121.70, 120.99, 119.17, 111.93, 110.08, 44.64, 20.26; ESI-MS: m/z 342.4 (M+1)$^+$; HPLC purity 97.1%.

*4.1.11.2. (E)-3-(3-fluorophenyl)-N-((1-methyl-9H-pyrido[3,4-b]indol-3-yl)methyl)acrylamide (**16b**).* CAD: 0.027 g of *m*-fluorocinnamic acid; purification: Method A; yield: 0.022 g (41%); mp 118.0–119.0 °C; IR (ATR, ν/cm^{-1}) 3242, 3080, 2972, 2907, 2783, 1658, 1620, 1571, 1501, 1451, 1420, 1341, 1247, 1144, 1032, 983, 899, 859, 779, 740, 632, 561, 517; ^{1}H NMR (DMSO-d_6) δ 11.52 (s, 1H), 8.69 (t, 1H, J = 5.5 Hz), 8.18 (d, 1H, J = 7.4 Hz), 7.87 (s, 1H), 7.59-7.42 (m, 6H), 7.24-7.19 (m, 2H), 6.85 (d, 1H, J = 15.7 Hz), 4.61 (d, 2H, J = 4.3 Hz), 2.77 (s, 3H); ^{13}C NMR (DMSO-d_6) δ 164.59, 162.46 (d, J = 243.9 Hz), 146.03, 141.35, 140.75, 137.63 (d, J = 7.9 Hz), 137.47, 133.57, 130.89 (d, J = 8.3 Hz), 127.83, 127.73, 123.97, 123.67, 121.68, 121.00, 119.15, 116.07 (d, J = 21.4 Hz), 113.92 (d, J = 21.8 Hz), 111.94, 110.07, 44.73, 20.34; ESI-MS: m/z 360.3 (M+1)$^+$; Anal. Calcd. for $C_{22}H_{18}FN_3O$: C, 73.52; H, 5.05; N, 11.69; found: C, 73.35; H, 5.27; N, 11.83.

*4.1.11.3. (E)-3-(3-bromophenyl)-N-((1-methyl-9H-pyrido[3,4-b]indol-3-yl)methyl)acrylamide (**16c**).* CAD: 0.037 g of *m*-bromocinnamic acid; purification: Method A; yield: 0.018 g (28%); mp 121.5–123.5 °C; IR (ATR, ν/cm^{-1}) 3243, 3082, 1743, 1725, 1655, 1617, 1562, 1501, 1452, 1419, 1470, 1396, 1340, 1248, 1234, 1150, 1069, 1029, 984, 899, 863, 779, 741, 697, 666, 638, 609, 561; ^{1}H NMR (DMSO-d_6) δ 11.54 (s, 1H), 8.68 (t, 1H, J = 5.8 Hz), 8.18 (d, 1H, J = 7.9 Hz), 7.87 (s, 1H), 7.80 (t, 1H, J = 1.8 Hz), 7.61-7.56 (m, 3H), 7.52 (t, 1H, J = 7.4 Hz), 7.47 (d, 1H, J = 15.8 Hz), 7.39 (t, 1H, J = 7.9 Hz), 7.21 (t, 1H, J = 7.4 Hz), 6.87 (d, 1H, J = 15.8 Hz), 4.62 (d, 2H, J = 5.8 Hz), 2.78 (s, 3H); ^{13}C NMR (DMSO-d_6) δ 164.53, 146.00, 141.36, 140.76, 137.60, 137.12, 133.58, 131.93, 131.03, 130.03, 127.83, 127.73, 126.42, 124.09, 122.26, 121.68, 121.00, 119.15, 111.94, 110.06, 44.73, 20.34; ESI-MS: m/z 420.0 (M+1)$^+$, 422.0 (M+1)$^+$; HPLC purity 98.3%.

*4.1.11.4. (E)-N-((1-methyl-9H-pyrido[3,4-b]indol-3-yl)methyl)-3-(3-(trifluoromethyl)phenyl)acrylamide (**16d**).* CAD: 0.035 g of *m*-(trifluoromethyl)cinnamic acid; purification: Method B; yield: 0.023 g

(39%); mp 235.5–237.0 °C (decomp.); IR (ATR, ν/cm^{-1}) 3339, 3251, 3084, 2992, 2950, 2893, 2855, 2786, 1664, 1622, 1570, 1517, 1470, 1451, 1396, 1331, 1284, 1249, 1229, 1165, 1122, 1095, 1072, 1020, 969, 937, 899, 864, 803, 777, 738, 695, 657, 596, 559, 524, 507; ^{1}H NMR (DMSO-d_6) δ 11.53 (s, 1H), 8.70 (t, 1H, J = 5.8 Hz), 8.18 (d, 1H, J = 7.9 Hz), 7.95 (t, 1H, J = 2.0 Hz), 7.90 (d, 1H, J = 7.8 Hz), 7.88 (s, 1H), 7.74 (d, 1H, J = 7.8 Hz), 7.67 (t, 1H, J = 7.8 Hz), 7.61-7.58 (m, 2H), 7.54-7.51 (m, 1H), 7.22-7.20 (m, 1H), 6.96 (d, 1H, J = 15.9 Hz), 4.63 (d, 2H, J = 5.8 Hz), 2.78 (s, 3H); ^{13}C NMR (DMSO-d_6) δ 164.49, 145.97, 141.37, 140.77, 137.06, 136.23, 133.58, 131.31, 130.07, 129.73 (q, J = 31.7 Hz), 127.85, 127.75, 125.69 (q, J = 3.5 Hz), 124.06 (q, J = 272.8 Hz), 124.56, 123.88 (q, J = 3.5 Hz), 121.69, 121.01, 119.16, 111.95, 110.07, 44.74, 20.34; ESI-MS: m/z 410.1 (M+1)$^+$; HPLC purity 98.4%.

*4.1.11.5. E)-3-(4-fluorophenyl)-N-((1-methyl-9H-pyrido[3,4-b]indol-3-yl)methyl)acrylamide (**16e**).* CAD: 0.027 g of *p*-fluorocinnamic acid; purification: Method A; yield: 0.018 g (34%); mp 217.5–219.5 °C (decomp.); IR (ATR, ν/cm^{-1}) 3243, 3077, 2993, 2950, 2913, 2890, 2851, 2785, 1655, 1620, 1597, 1571, 1553, 1507, 1451, 1416, 1394, 1341, 1318, 1282, 1249, 1226, 1156, 1124, 1094, 1033, 1011, 984, 933, 899, 859, 830, 788, 739, 693, 643, 608, 591, 565, 506, 462; ^{1}H NMR (DMSO-d_6) δ 11.52 (s, 1H), 8.67 (t, 1H, J = 5.1 Hz), 8.18 (d, 1H, J = 7.8 Hz), 7.87 (s, 1H), 7.67-7.63 (m, 2H), 7.59-7.48 (m, 3H), 7.26 (t, 2H, J = 8.7 Hz), 7.20 (t, 1H, J = 7.4 Hz), 6.75 (d, 1H, J = 15.8 Hz), 4.61 (d, 2H, J = 5.5 Hz), 2.77 (s, 3H); ^{13}C NMR (DMSO-d_6) δ 164.81, 162.66 (d, J = 246.9 Hz), 146.14, 141.32, 140.75, 137.57, 133.56, 131.62 (d, J = 3.2 Hz), 129.66 (d, J = 8.4 Hz), 127.82, 127.72, 122.28, 121.68, 121.00, 119.14, 115.90 (d, J = 21.7 Hz), 111.93, 110.04, 44.70, 20.33; ESI-MS: m/z 360.1 (M+1)$^+$; HPLC purity 98.8%.

*4.1.11.6. (E)-3-(4-chlorophenyl)-N-((1-methyl-9H-pyrido[3,4-b]indol-3-yl)methyl)acrylamide (**16f**).* CAD: 0.030 g of *p*-chlorocinnamic acid; purification: Method A; yield: 0.012 g (21%); mp 255.0–257.5 °C (decomp.); IR (ATR, ν/cm^{-1}) 3649, 3239, 3055, 2918, 2874, 2798, 1982, 1925, 1897, 1662, 1624, 1551, 1502, 1454, 1404, 1318, 1283, 1251, 1220, 1176, 1088, 1044, 1011, 976, 902, 867, 815, 735, 646, 590, 550, 497; ^{1}H NMR (DMSO-d_6) δ 11.53 (s, 1H), 8.70 (t, 1H, J = 5.8 Hz), 8.18 (d, 1H, J = 7.9 Hz), 7.87 (s, 1H), 7.63-7.56 (m, 3H), 7.54-7.46 (m, 4H), 7.23-7.18 (m, 1H), 6.81 (d, 1H, J = 15.8 Hz), 4.61 (d, 2H, J = 5.7 Hz), 2.77 (s, 3H); ^{13}C NMR (DMSO-d_6) δ 164.67, 146.08, 141.33, 140.75, 137.41, 133.96, 133.82, 133.56, 129.22, 128.97, 127.82, 127.72, 123.19, 121.68, 121.00, 119.14, 111.93, 110.06, 44.72, 20.33; ESI-MS: m/z 374.0 (M − 1)$^-$; Anal. Calcd. for $C_{22}H_{18}ClN_3O$: C, 70.30; H, 4.83; N, 11.18; found: C, 70.39; H, 4.65; N, 11.37.

*4.1.11.7. (E)-3-(4-methoxyphenyl)-N-((1-methyl-9H-pyrido[3,4-b]indol-3-yl)methyl)acrylamide (**16g**).* CAD: 0.029 g of *p*-methoxycinnamic acid; purification: Method A; yield: 0.028 g (51%); mp 263.0–264.0 °C (decomp.); IR (ATR, ν/cm^{-1}) 3249, 3162, 3079, 2964, 2910, 2835, 2787, 2684, 1652, 1603, 1555, 1512, 1454, 1419, 1345, 1287, 1251, 1175, 1109, 1026, 987, 932, 900, 873, 827, 778, 744, 592, 549, 520; ^{1}H NMR (DMSO-d_6) δ 11.54 (s, 1H), 8.59 (t, 1H, J = 5.6 Hz), 8.18 (d, 1H, J = 7.9 Hz), 7.87 (s, 1H), 7.59-7.50 (m, 4H), 7.45 (d, 1H, J = 15.8 Hz), 7.20 (t, 1H, J = 7.5 Hz), 6.98 (d, 2H, J = 8.2 Hz), 6.66 (d, 1H, J = 15.8 Hz), 4.61 (d, 2H, J = 5.9 Hz), 3.79 (s, 3H), 2.78 (s, 3H); ^{13}C NMR (DMSO-d_6) δ 165.20, 160.29, 146.31, 141.29, 140.75, 138.47, 133.54, 129.09, 127.81, 127.73, 127.55, 121.68, 121.01, 119.89, 119.14, 114.38, 111.93, 109.98, 55.25, 44.66, 20.33; ESI-MS: m/z 372.3 (M+1)$^+$; Anal. Calcd. for $C_{23}H_{21}N_3O_2$: C, 74.37; H, 5.70; N, 11.31; found: C, 74.19; H, 5.93; N, 11.54.

*4.1.11.8. (E)-N-((1-methyl-9H-pyrido[3,4-b]indol-3-yl)methyl)-3-(4-(trifluoromethyl)phenyl)acrylamide (**16h**).* CAD: 0.035 g of *p*-(trifluoromethyl)cinnamic acid; purification: Method A; yield: 0.026 g (43%); mp 264.5–266.5 °C; IR (ATR, ν/cm^{-1}) 3339, 3263, 3058, 2920, 1666, 1626, 1575, 1496, 1452, 1413, 1324, 1248, 1164, 1120, 1065, 1012, 972, 900, 858, 822, 778, 737, 702, 586, 522, 491; ^{1}H NMR (DMSO-d_6) δ 11.54 (s, 1H), 8.79 (t, 1H, J = 5.8 Hz), 8.18 (d, 1H, J = 7.9 Hz), 7.88 (s, 1H), 7.82-7.76 (m, 4H), 7.59-7.49 (m, 3H), 7.23-7.18 (m, 1H), 6.94 (d, 1H, J = 15.8 Hz), 4.63 (d, 2H, J = 5.7 Hz), 2.77 (s, 3H); ^{13}C NMR (DMSO-d_6) δ 164.43, 145.97, 141.38, 140.77, 139.09, 137.12, 133.59, 129.17 (q, J = 31.8 Hz), 128.16, 127.84, 127.74, 125.81 (q, J = 3.9 Hz), 125.20, 124.13 (q, J = 272.0 Hz), 121.70, 121.01, 119.16, 111.95, 110.14, 44.78, 20.34; ESI-MS: m/z 410.1 (M+1)$^+$; HPLC purity 97.3%.

*4.1.12. Synthesis of 1-methyl-6-(prop-2-yn-1-yloxy)-9H-pyrido[3,4-b]indole (**19**)*

To a solution of compound **18** (0.200 g, 1.009 mmol) in dry DMF (5 mL), under argon atmosphere caesium carbonate (0.460 g, 1.413 mmol) was added, followed by the dropwise addition of propargyl bromide (0.135 mL, 1.211 mmol, 80% solution in toluene). The reaction mixture was stirred at rt for 6 h. Upon completion, reaction mixture was diluted with H_2O (50 mL) and extracted with EtOAc (3 × 40 mL). The collected organic layers were washed with H_2O (2 × 100 mL), dried over anhydrous sodium sulphate and the solvent was evaporated under the reduced pressure. After purification by column chromatography (DCM/MeOH = 97:3 → 95:5) and trituration with diethyl ether, **19** was obtained as a white solid. Yield: 0.122 g (51%); mp 175.5–177.5 °C; IR (ATR, ν/cm^{-1}) 3292, 3122, 3054, 2950, 2860, 2766, 2716, 2366, 2330, 2128, 2058, 1866, 1764, 1736, 1606, 1570, 1506, 1476, 1448, 1412, 1380, 1334, 1292, 1260, 1200, 1120, 1068, 1030, 986, 944, 914, 886, 818, 758, 646, 524; ^{1}H NMR (DMSO-d_6) δ 11.42 (s, 1H), 8.17 (d, 1H, J = 5.4 Hz), 7.88 (d, 1H, J = 5.3 Hz), 7.81 (d, 1H, J = 2.5 Hz), 7.53 (d, 1H, J = 8.9 Hz), 7.23 (dd, 1H, J = 8.8, 2.5 Hz), 4.88 (d, 2H, J = 2.4 Hz), 3.56 (t, 1H, J = 2.4 Hz), 2.75 (s, 3H); ^{13}C NMR (DMSO-d_6) δ 151.09, 142.26, 137.03, 135.67, 135.12, 126.63, 121.27, 118.34, 112.72, 112.62, 105.62, 78.04, 56.26, 20.40; ESI-MS: m/z 237.1 (M+1)$^+$.

*4.1.13. General procedure for the synthesis of harmicines **20a-e***

To a solution of alkyne **19** (0.050 g, 0.212 mmol) and the corresponding cinnamyl azide **13a-e** (0.254 mmol) in MeOH (5 mL), catalytic amount of $Cu(OAc)_2$ was added. The reaction mixture was stirred at rt for 24 h. Upon completion of the reaction, the solvent was removed under the reduced pressure. The residue was purified by column chromatography with DCM/MeOH or cyclohexane/EtOAc/MeOH as a mobile phase. The crude product was triturated with diethyl ether/petroleum ether mixture to obtain harmicines **20a-e**.

*4.1.13.1. 6-((1-Cinnamyl-1H-1,2,3-triazol-4-yl)methoxy)-1-methyl-9H-pyrido[3,4-b]indole (**20a**).* **13a**:0.040 g; mobile phase: DCM/MeOH 8:1; yield: 0.059 g (70%); mp 205.0–206.5 °C; IR (ATR, ν/cm^{-1}) 3136, 3120, 3030, 2945, 2856, 2760, 2693, 2676, 1632, 1604, 1579, 1565, 1504, 1481, 1460, 1412, 1389, 1361, 1335, 1289, 1237, 1202, 1123, 1054, 1034, 1002, 967, 888, 858, 817, 780, 755, 725, 705, 694, 625, 584, 520, 502; ^{1}H NMR (DMSO-d_6) δ 11.39 (s, 1H), 8.30 (s, 1H), 8.16 (d, 1H, J = 5.3 Hz), 7.91-7.89 (m, 2H), 7.51 (d, 1H, J = 8.8 Hz), 7.45-7.22 (m, 6H), 6.65-6.49 (m, 2H), 5.26 (s, 2H), 5.21 (d, 2H, J = 6.3 Hz), 2.74 (s, 3H); ^{13}C NMR (DMSO-d_6) δ 151.94, 143.26, 142.22, 136.98, 135.70, 135.42, 135.10, 133.62, 128.68, 128.14, 126.70, 126.56, 124.43, 123.72, 121.36, 118.35, 112.76, 112.69, 105.12, 61.89, 51.34, 20.42; ESI-MS: m/z 396.3 (M+1)$^+$; Anal. Calcd. for $C_{24}H_{21}N_5O$: C, 72.89; H, 5.35; N, 17.71; found: C, 72.74; H, 5.52; N, 17.56.

*4.1.13.2. (E)-6-((1-(3-(3-fluorophenyl)allyl)-1H-1,2,3-triazol-4-yl)methoxy)-1-methyl-9H-pyrido[3,4-b]indole (**20b**).* **13b**: 0.045 g; mobile phase: cyclohexane/EtOAc/MeOH 1:1:0.5 and DCM/MeOH 9:1; yield: 0.039 g (44%); mp 145.0–147.0 °C; IR (ATR, ν/cm^{-1}) 3357,

3293, 3166, 3071, 3052, 2975, 2937, 2900, 2866, 1601, 1583, 1568, 1493, 1473, 1459, 1404, 1379, 1365, 1330, 1286, 1262, 1207, 1149, 1120, 1067, 1054, 1039, 976, 938, 884, 847, 812, 792, 776, 752, 736, 715, 675, 641, 620, 593, 561, 528, 493, 456; ^{1}H NMR (DMSO-d_6) δ 11.41 (s, 1H), 8.31 (s, 1H), 8.17 (d, 1H, J = 5.4 Hz), 7.91-7.89 (m, 2H), 7.52 (d, 1H, J = 8.8 Hz), 7.39-7.32 (m, 2H), 7.27-7.23 (m, 2H), 7.13-7.08 (m, 1H), 6.64-6.62 (m, 2H), 5.26 (s, 2H), 5.23-5.21 (m, 2H), 2.75 (s, 3H); ^{13}C NMR (DMSO-d_6) δ 162.49 (d, J = 243.3 Hz), 151.97, 143.26, 142.16, 138.36 (d, J = 7.9 Hz), 136.80, 135.48, 135.07, 132.34, 130.58 (d, J = 8.5 Hz), 126.78, 125.50, 124.47, 130.00 (d, J = 1.7 Hz), 121.34, 118.42, 114.81 (d, J = 21.3 Hz), 112.80 (d, J = 17.4 Hz), 112.77, 112.67, 105.11, 61.89, 51.16, 20.32; ESI-MS: m/z 414.2 $(M+1)^+$; Anal. Calcd. for $C_{24}H_{20}FN_5O$: C, 69.72; H, 4.88; N, 16.94; found: C, 69.47; H, 4.61; N, 17.15.

*4.1.13.3. (E)-6-((1-(3-(3-bromophenyl)allyl)-1H-1,2,3-triazol-4-yl) methoxy)-1-methyl-9H-pyrido[3,4-b]indole (**20c**).* **13c**: 0.060 g; mobile phase: cyclohexane/EtOAc/MeOH 3:1:0.75; yield: 0.051 g (50%); mp 181.5–183.0 °C; IR (ATR, ν/cm^{-1}) 3252, 3198, 3151, 3089, 3064, 3039, 3015, 2965, 2945, 2916, 2892, 1601, 1584, 1566, 1495, 1475, 1422, 1400, 1373, 1350, 1337, 1289, 1256, 1233, 1217, 1199, 1129, 1095, 1066, 1052, 1033, 1008, 977, 944, 882, 857, 807, 782, 738, 707, 674, 620, 589, 563, 542, 479; ^{1}H NMR (DMSO-d_6) δ 11.40 (s, 1H), 8.31 (s, 1H), 8.16 (d, 1H, J = 5.4 Hz), 7.92-7.89 (m, 2H), 7.71 (t, 1H, J = 2.0 Hz), 7.51 (d, 1H, J = 8.8 Hz), 7.48-7.43 (m, 2H), 7.30 (t, 1H, J = 7.8 Hz), 7.24 (dd, 1H, J = 8.8, 2.5 Hz), 6.68-6.58 (m, 2H), 5.26 (s, 2H), 5.21 (d, 2H, J = 4.6 Hz), 2.74 (s, 3H); ^{13}C NMR (DMSO-d_6) δ 151.98, 143.28, 142.20, 138.30, 136.89, 135.46, 135.09, 132.03, 130.77, 129.05, 126.75, 125.67, 124.47, 122.17, 121.36, 118.40, 112.78, 112.71, 105.10, 61.91, 51.20, 20.37; ESI-MS: m/z 474.2 $(M+1)^+$, 476.2 $(M+1)^+$. Anal. Calcd. for $C_{24}H_{20}BrN_5O$: C, 60.77; H, 4.25; N, 14.76; C, 60.92; H, 4.43; N, 14.56.

*4.1.13.4. (E)-6-((1-(3-(4-chlorophenyl)allyl)-1H-1,2,3-triazol-4-yl) methoxy)-1-methyl-9H-pyrido[3,4-b]indole (**20d**).* **13d**: 0.049 g; mobile phase: cyclohexane/EtOAc/MeOH 1:1:0.5; yield: 0.046 g (51%); mp 195.0–196.5 °C; IR (ATR, ν/cm^{-1}) 3208, 3136, 3089, 3069, 2969, 2923, 2893, 2870, 2802, 1602, 1582, 1567, 1494, 1480, 1459, 1405, 1385, 1340, 1289, 1257, 1237, 1207, 1163, 1127, 1094, 1054, 1033, 1015, 987, 971, 950, 884, 857, 843, 818, 742, 702, 687, 662, 623, 583, 563, 533, 487; ^{1}H NMR (DMSO-d_6) δ 11.39 (s, 1H), 8.30 (s, 1H), 8.16 (d, 1H, J = 5.4 Hz), 7.91-7.89 (m, 2H), 7.51 (d, 1H, J = 8.8 Hz), 7.47-7.44 (m, 2H), 7.39-7.36 (m, 2H), 7.23 (dd, 1H, J = 8.9, 2.5 Hz), 6.62-6.51 (m, 2H), 5.26 (s, 2H), 5.21 (d, 2H, J = 5.1 Hz), 2.74 (s, 3H); ^{13}C NMR (DMSO-d_6) δ 151.93, 143.27, 142.22, 136.98, 135.44, 135.10, 134.68, 132.51, 132.23, 128.65, 128.28, 126.71, 124.77, 124.48, 121.36, 118.38, 112.76, 112.69, 105.15, 61.89, 51.23, 20.41; ESI-MS: m/z 430.4 $(M+1)^+$; Anal. Calcd. for $C_{24}H_{20}ClN_5O$: C, 67.05; H, 4.69; N, 16.29; found: C, 67.22; H, 4.78; N, 16.31.

*4.1.13.5. (E)-6-((1-(3-(4-methoxyphenyl)allyl)-1H-1,2,3-triazol-4-yl) methoxy)-1-methyl-9H-pyrido[3,4-b]indole (**20e**).* **13e**: 0.048 g; mobile phase: cyclohexane/EtOAc/MeOH 1:1:0.5; yield: 0.069 g (77%); mp 200.0–203.0 °C; IR (ATR, ν/cm^{-1}) 3208, 3138, 3069, 2953, 2929, 2894, 2873, 2836, 2802, 1743, 1607, 1582, 1567, 1513, 1498, 1480, 1460, 1441, 1405, 1386, 1337, 1289, 1257, 1238, 1207, 1175, 1127, 1109, 1054, 1032, 1015, 987, 968, 884, 856, 819, 760, 741, 703, 666, 624, 582, 563, 529, 498, 477; ^{1}H NMR (DMSO- d_6) δ 11.39 (s, 1H), 8.28 (s, 1H), 8.16 (d, 1H, J = 5.4 Hz), 7.92-7.89 (m, 2H), 7.51 (d, 1H, J = 8.8 Hz), 7.37 (d, 2H, J = 8.2 Hz), 7.23 (d, 1H, J = 8.9 Hz), 6.88 (d, 2H, J = 8.2 Hz), 6.58 (d, 1H, J = 15.8 Hz), 6.39-6.32 (m, 1H), 5.25 (s, 2H), 5.16 (d, 2H, J = 6.5 Hz), 3.75 (s, 3H), 2.74 (s, 3H); ^{13}C NMR (DMSO-d_6) δ 159.22, 151.94, 143.23, 142.21, 136.98, 135.42, 135.09, 133.36, 128.30, 127.89, 126.70, 124.31, 121.36, 121.11, 118.34, 114.06, 112.75, 112.68, 105.12, 61.89, 55.11, 51.46, 20.41; ESI-MS: m/z 426.3 $(M+1)^+$; Anal. Calcd. for $C_{25}H_{23}N_5O_2$: C, 70.57; H, 5.45; N, 16.46; found: C, 70.72; H, 5.63; N, 16.65.

*4.1.14. Tert-butyl (2-((1-methyl-9H-pyrido[3,4-b]indol-6-yl)oxy) ethyl)carbamate (**21**)*

To a stirred solution of **18** (0.647 g, 3.264 mmol) in dry DMF (6 mL), under argon atmosphere, caesium carbonate (2.978 g, 9.139 mmol) and tetrabutylammonium hydrogensulphate (0.887 g, 2.611 mmol) was added. The resulting suspension was stirred at rt for 20 min, followed by the addition of 2-(*tert*-butoxycarbonylamino)ethyl bromide (2.926 g, 13.056 mmol). The reaction mixture was stirred at rt for 24 h, poured into H_2O (50 mL) and extracted with EtOAc (3 × 50 mL). The collected organic layers were washed with H_2O, filtered through phase separator and evaporated under the reduced pressure. After purification by column chromatography (DCM/MeOH 8:1) and trituration with diethyl ether/petroleum ether mixture, compound **21** was obtained. Yield: 0.624 g (56%); ^{1}H NMR (DMSO-d_6) δ 11.42 (s, 1H), 8.16 (d, 1H, J = 5.3 Hz), 7.92 (d, 1H, J = 5.3 Hz), 7.77 (d, 1H, J = 1.7 Hz), 7.51 (d, 1H, J = 8.8 Hz), 7.18 (dd, 1H, J = 8.8, 2.3 Hz), 7.06 (t, 1H, J = 5.0 Hz), 4.05 (t, 2H, J = 5.8 Hz), 3.39-3.34 (m, 2H), 2.75 (s, 3H), 1.40 (s, 9H); ^{13}C NMR (DMSO-d_6) δ 155.73, 152.39, 142.04, 136.57, 135.41, 135.03, 126.88, 121.35, 118.42, 112.78, 112.75, 104.68, 77.76, 67.19, 39.61, 28.24, 20.23; ESI-MS: m/z 342.4 $(M+1)^+$.

*4.1.15. 2-((1-Methyl-9H-pyrido[3,4-b]indol-6-yl)oxy)ethan-1-amine (**22**)*

A solution of the **21** (0.642 g, 1.880 mmol) and 4.7 mL 4 M HCl (18.80 mmol) in EtOAc (6 mL) was stirred at 50 °C for 18 h. Upon completion, solvent was removed under the reduced pressure. The residue was dissolved in H_2O (20 mL), basified to pH 11 with 5% NaOH. The resulting precipitate was filtered off. After trituration with diethyl ether, 0.313 g, (69%) of **22** was obtained; mp 170.5–172.0 °C; IR (ATR, ν/cm^{-1}) 3645, 3359, 3241, 3065, 2925, 2869, 1605, 1581, 1566, 1500, 1478, 1458, 1401, 1288, 1234, 1211, 1126, 1071, 1059, 992, 905, 884, 847, 825, 816, 741, 703, 632; ^{1}H NMR (DMSO-d_6) δ 11.36 (s, 1H), 8.15 (d, 1H, J = 5.3 Hz), 7.90 (d, 1H, J = 5.3 Hz), 7.74 (d, 1H, J = 2.3 Hz), 7.50 (d, 1H, J = 8.8 Hz), 7.19 (dd, 1H, J = 8.8, 2.5 Hz), 4.02 (t, 2H, J = 5.8 Hz), 2.94 (t, 2H, J = 5.7 Hz), 2.74 (s, 3H); ^{13}C NMR (DMSO-d_6) δ 152.47, 141.87, 136.70, 135.19, 134.93, 126.54, 121.29, 117.98, 112.34, 112.18, 104.86, 71.06, 40.87, 19.97; ESI-MS: m/z 242.2 $(M+1)^+$.

*4.1.16. General procedure for the synthesis of harmicines **23a-h***

A solution of a corresponding CAD (0.249 mmol), DIEA (0.086 mL, 0.498 mmol) and HATU (0.095 g, 0.249 mmol) in DCM (4 mL) was stirred at rt for 20 min, followed by the addition of amine **22** (0.050 g, 0.208 mmol). The resulting solution was stirred at rt for 1 h. The formed precipitate was filtered off. After purification by column chromatography (DCM/MeOH 8:1) and trituration with diethyl ether/petroleum ether mixture compounds **23a-h** were obtained.

*4.1.16.1. N-(2-((1-methyl-9H-pyrido[3,4-b]indol-6-yl)oxy)ethyl)cinnamamide (**23a**).* CAD: 0.037 g of *trans*-cinnamic acid; yield: 0.045 g (58%); mp 128.0–129.5 °C; IR (ATR, ν/cm^{-1}) 3640, 3220, 3062, 2986, 2938, 2811, 2609, 1871, 1665, 1622, 1545, 1502, 1458, 1422, 1343, 1286, 1209, 1121, 1074, 970, 897, 808, 766, 714, 659, 630, 574, 512, 483; ^{1}H NMR (DMSO-d_6) δ 11.39 (s, 1H), 8.45 (t, 1H, J = 5.6 Hz), 8.16 (d, 1H, J = 5.3 Hz), 7.91 (d, 1H, J = 5.3 Hz), 7.81 (d, 1H, J = 2.5 Hz), 7.57 (d, 2H, J = 7.3 Hz), 7.53-7.46 (m, 2H), 7.44-7.36 (m, 3H), 7.22 (dd, 1H, J = 8.9, 2.6 Hz), 6.73 (d, 1H, J = 15.9 Hz), 4.17 (t, 2H, J = 5.6 Hz), 3.64 (q, 2H, J = 5.6 Hz), 2.74 (s, 3H); ^{13}C NMR (DMSO-d_6) δ 165.27, 152.37, 142.04, 138.83, 136.54, 135.46, 135.03, 134.89, 129.45, 128.93, 127.52, 126.90, 122.07, 121.37, 118.43, 112.79, 112.77,

104.73, 67.12, 38.67, 20.20; ESI-MS: *m/z* 372.0 $(M+1)^+$; HPLC purity > 99.5%.

*4.1.16.2. (E)-3-(3-fluorophenyl)-N-(2-((1-methyl-9H-pyrido[3,4-b]indol-6-yl)oxy)ethyl)acrylamide (**23b**).* CAD: 0.041 g of *m*-fluorocinnamic acid; yield: 0.062 g (76%); mp 225.0–226.0 °C; IR (ATR, ν/cm^{-1}) 3658, 3236, 3068, 2974, 2936, 2882, 2822, 2608, 1871, 1666, 1625, 1585, 1551, 1501, 1448, 1344, 1286, 1248, 1207, 1146, 1075, 1037, 974, 902, 856, 807, 738, 666, 630, 573, 519, 467; ^{1}H NMR (DMSO-d_6) δ 11.38 (s, 1H), 8.46 (t, 1H, J = 5.5 Hz), 8.16 (d, 1H J = 5.4 Hz), 7.91 (d, 1H, J = 5.3 Hz), 7.80 (d, 1H, J = 2.4 Hz), 7.51 (d, 1H, J = 8.9 Hz), 7.50-7.40 (m, 4H), 7.24-7.19 (m, 2H), 6.77 (d, 1H, J = 15.8 Hz), 4.17 (t, 2H, J = 5.5 Hz), 3.64 (q, 2H, J = 5.5 Hz), 2.74 (s, 3H); ^{13}C NMR (DMSO-d_6) δ 164.99, 162.45 (d, J = 243.8 Hz), 152.32, 142.15, 137.54, 137.49, 136.83, 135.37, 135.07, 130.89 (d, J = 8.4 Hz), 126.76, 123.65, 121.40, 118.29, 116.11 (d, J = 21.2 Hz), 113.93 (d, J = 21.8 Hz), 112.74, 112.72, 104.73, 67.07, 38.71, 20.34; ESI-MS: *m/z* 390.4 $(M+1)^+$; HPLC purity > 99.5%.

*4.1.16.3. (E)-3-(3-bromophenyl)-N-(2-((1-methyl-9H-pyrido[3,4-b]indol-6-yl)oxy)ethyl)acrylamide (**23c**).* CAD: 0.057 g of *m*-bromocinnamic acid; yield: 0.062 g (77%); mp 230.5–232.5 °C; IR (ATR, ν/cm^{-1}) 3646, 3171, 3062, 2975, 2939, 2879, 2792, 2613, 1664, 1620, 1566, 1501, 1460, 1384, 1345, 1287, 1199, 1110, 1072, 970, 856, 811, 781, 736, 667, 631, 561; ^{1}H NMR (DMSO-d_6) δ 11.40 (s, 1H), 8.43 (t, 1H, J = 5.5 Hz), 8.16 (d, 1H, J = 5.4 Hz), 7.92 (d, 1H, J = 5.4 Hz), 7.81 (d, 1H, J = 2.3 Hz), 7.79 (t, 1H, J = 1.8 Hz), 7.59-7.56 (m, 2H), 7.52 (d, 1H, J = 8.8 Hz), 7.45 (d, 1H, J = 15.8 Hz), 7.38 (t, 1H, J = 7.9 Hz), 7.22 (dd, 1H, J = 8.8, 2.4 Hz), 6.78 (d, 1H, J = 15.8 Hz), 4.17 (t, 2H, J = 5.5 Hz), 3.64 (q, 2H, J = 5.4 Hz), 2.75 (s, 3H); ^{13}C NMR (DMSO-d_6) δ 164.92, 152.33, 142.09, 137.50, 137.19, 136.68, 135.42, 135.05, 131.97, 131.02, 130.04, 126.83, 126.40, 123.76, 122.25, 121.38, 118.37, 112.76, 104.74, 67.08, 38.71, 20.27; ESI-MS: *m/z* 450.3 $(M+1)^+$, 452.3 $(M+1)^+$; HPLC purity > 99.5%.

*4.1.16.4. (E)-N-(2-((1-methyl-9H-pyrido[3,4-b]indol-6-yl)oxy)ethyl)-3-(3-(trifluoromethyl)phenyl)acrylamide (**23d**).* CAD: 0.054 g of *p*-(trifluoromethyl)cinnamic acid; yield: 0.058 g (64%); mp 216.5–218.0 °C; IR (ATR, ν/cm^{-1}) 3676, 3222, 3100, 3067, 2988, 2937, 2881, 2820, 2611, 1665, 1624, 1545, 1501, 1440, 1331, 1286, 1200, 1167, 1117, 1073, 1031, 971, 863, 805, 738, 691, 658, 630, 574, 465; ^{1}H NMR (DMSO-d_6) δ 11.41 (s, 1H), 8.46 (t, 1H, J = 5.6 Hz), 8.16 (d, 1H, J = 5.4 Hz), 7.93-7.88 (m, 3H), 7.81 (d, 1H, J = 2.6 Hz), 7.73 (d, 1H, J = 7.8 Hz), 7.66 (t, 1H, J = 7.8 Hz), 7.57 (d, 1H, J = 15.8 Hz), 7.52 (d, 1H, J = 8.8 Hz), 7.22 (dd, 1H, J = 8.8, 2.5 Hz), 6.88 (d, 1H, J = 15.9 Hz), 4.18 (t, 2H, J = 5.5 Hz), 3.65 (q, 2H, J = 5.6 Hz), 2.75 (s, 3H); ^{13}C NMR (DMSO-d_6) δ 164.88, 152.34, 142.10, 137.14, 136.69, 136.13, 135.43, 135.06, 131.30, 130.06, 129.73 (q, J = 32.3 Hz), 126.83, 125.73 (q, J = 3.0 Hz), 124.23, 124.04 (q, J = 273.7 Hz), 123.88 (q, J = 3.0 Hz), 121.38, 118.37, 112.76, 104.74, 67.09, 38.74, 20.27; ESI-MS: *m/z* 440.1 $(M+1)^+$; Anal. Calcd. for $C_{24}H_{20}F_3N_3O_2$: C, 65.60; H, 4.59; N, 9.56; found C, 65.80; H, 4.37; N, 9.71.

*4.1.16.5. (E)-3-(4-fluorophenyl)-N-(2-((1-methyl-9H-pyrido[3,4-b]indol-6-yl)oxy)ethyl)acrylamide (**23e**).* CAD: 0.041 g of *p*-fluorocinnamic acid; yield: 0.065 g (80%); mp 226.5–227.5 °C; IR (ATR, ν/cm^{-1}) 3659, 3311, 3225, 3099, 3045, 2990, 2938, 2165, 1870, 1667, 1625, 1542, 1502, 1422, 1347, 1286, 1208, 1160, 1122, 1074, 976, 897, 824, 740, 630, 576, 501, 459; ^{1}H NMR (DMSO-d_6) δ 11.40 (s, 1H), 8.43 (t, 1H, J = 5.4 Hz), 8.16 (d, 1H, J = 5.4 Hz), 7.92 (d, 1H, J = 5.3 Hz), 7.81 (d, 1H, J = 2.2 Hz), 7.66-7.62 (m, 2H), 7.53-7.46 (m, 2H), 7.28-7.21 (m, 3H), 6.68 (d, 1H, J = 15.8 Hz), 4.17 (t, 2H, J = 5.5 Hz), 3.64 (q, 2H, J = 5.4 Hz), 2.75 (s, 3H); ^{13}C NMR (DMSO-d_6) δ 165.21, 162.68 (d, J = 247.0 Hz), 152.35, 142.10, 137.65, 136.71, 135.41, 135.05, 131.53 (d, J = 2.6 Hz), 129.68 (d, J = 8.4 Hz), 126.82, 121.97, 121.39, 118.36, 115.90 (d, J = 21.7 Hz), 112.76, 104.72, 67.11, 38.68, 20.28; ESI-MS: *m/z* 390.4 $(M+1)^+$; HPLC purity > 99.5%.

*4.1.16.6. (E)-3-(4-chlorophenyl)-N-(2-((1-methyl-9H-pyrido[3,4-b]indol-6-yl)oxy)ethyl)acrylamide (**23f**).* CAD: 0.045 g of *p*-chlorocinnamic acid; yield: 0.071 g (84%); mp 228.5–229.5 °C; IR (ATR, ν/cm^{-1}) 3642, 3231, 3066, 2989, 2939, 2164, 2113, 1872, 1665, 1621, 1548, 1502, 1406, 1342, 1288, 1208, 1075, 976, 938, 897, 809, 742, 630, 575, 490; ^{1}H NMR (DMSO-d_6) δ 11.40 (s, 1H), 8.46 (t, 1H, J = 5.3 Hz), 8.16 (d, 1H, J = 5.3 Hz), 7.91 (d, 1H, J = 5.3 Hz), 7.80 (d, 1H, J = 2.0 Hz), 7.60 (d, 2H, J = 8.4 Hz), 7.51 (d, 1H, J = 8.9 Hz), 7.49-7.45 (m, 3H), 7.22 (dd, 1H, J = 8.8, 2.3 Hz), 6.73 (d, 1H, J = 15.8 Hz), 4.17 (t, 2H, J = 5.4 Hz), 3.64 (q, 2H, J = 5.3 Hz), 2.74 (s, 3H); ^{13}C NMR (DMSO-d_6) δ 165.08, 152.33, 142.11, 137.49, 136.72, 135.41, 135.05, 133.87, 129.22, 128.97, 126.81, 122.88, 121.39, 118.35, 112.76, 104.73, 67.09, 38.70, 20.29; ESI-MS: *m/z* 406.3 $(M+1)^+$; Anal. Calcd. for $C_{23}H_{20}ClN_3O_2$: C, 68.06; H, 4.97; N, 10.35; found C, 68.16; H, 4.78; N, 10.25.

*4.1.16.7. (E)-3-(4-methoxyphenyl)-N-(2-((1-methyl-9H-pyrido[3,4-b]indol-6-yl)oxy)ethyl)acrylamide (**23g**).* CAD: 0.044 g of *p*-methoxycinnamic acid; yield: 0.063g (75%); mp 241.5–242.5 °C; IR (ATR, ν/cm^{-1}) 3210, 3133, 3058, 2971, 2941, 2873, 2775, 2601, 2164, 1983, 1886, 1651, 1602, 1554, 1514, 1461, 1425, 1353, 1284, 1230, 1205, 1175, 1125, 1064, 1033, 983, 862, 827, 761, 699, 624, 555, 521; ^{1}H NMR (DMSO-d_6) δ 11.39 (s, 1H), 8.34 (t, 1H, J = 5.5 Hz), 8.16 (d, 1H, J = 5.4 Hz), 7.91 (d, 1H, J = 5.3 Hz), 7.80 (d, 1H, J = 2.4 Hz), 7.53-7.50 (m, 3H), 7.43 (d, 1H, J = 15.8 Hz), 7.22 (dd, 1H, J = 8.8, 2.5 Hz), 6.98 (d, 2H, J = 8.8 Hz), 6.58 (d, 1H, J = 15.8 Hz), 4.16 (t, 2H, J = 5.6 Hz), 3.79 (s, 3H), 3.63 (q, 2H, J = 5.5 Hz), 2.74 (s, 3H); ^{13}C NMR (DMSO-d_6) δ 165.59, 160.32, 152.35, 142.13, 138.54, 136.80, 135.37, 135.06, 129.09, 127.45, 126.77, 121.40, 119.58, 118.30, 114.38, 112.74, 104.71, 67.16, 55.24, 38.63, 20.33; ESI-MS: *m/z* 402.4 $(M+1)^+$; HPLC purity > 99.5%.

*4.1.16.8. (E)-N-(2-((1-methyl-9H-pyrido[3,4-b]indol-6-yl)oxy)ethyl)-3-(4-(trifluoromethyl)phenyl)acrylamide (**23h**).* CAD: 0.054 g of *p*-(trifluoromethyl)cinnamic acid; yield: 0.057 g (62%); mp 231.5–233.5 °C; IR (ATR, ν/cm^{-1}) 3645, 3269, 3061, 2932, 2875, 1667, 1628, 1559, 1501, 1461, 1417, 1384, 1328, 1286, 1234, 1202, 1166, 1119, 1067, 1016, 976, 953, 882, 829, 814, 728, 708, 614, 591, 562, 522, 495; ^{1}H NMR (DMSO-d_6) δ 11.41 (s, 1H), 8.54 (t, 1H, J = 5.5 Hz), 8.16 (d, 1H, J = 5.3 Hz), 7.92 (d, 1H, J = 5.3 Hz), 7.81-7.76 (m, 5H), 7.57-7.51 (m, 2H), 7.22 (dd, 1H, J = 8.9, 2.5 Hz), 6.86 (d, 1H, J = 15.8 Hz), 4.18 (t, 2H, J = 5.5 Hz), 3.65 (q, 2H, J = 5.4 Hz), 2.75 (s, 3H); ^{13}C NMR (DMSO-d_6) δ 164.82, 152.34, 142.09, 139.00, 137.19, 136.65, 135.44, 135.05, 129.20 (q, J = 32.3 Hz), 128.16, 126.85, 125.80 (q, J = 3.0 Hz), 124.87, 124.11 (q, J = 272.7 Hz), 121.38, 118.39, 112.78, 104.74, 67.06, 38.75, 20.25; MS: *m/z* 440.1 $(M+1)^+$; Anal. Calcd. for $C_{24}H_{20}F_3N_3O_2$: C, 65.60; H, 4.59; N, 9.56; found: C, 65.72; H, 4.37; N, 9.21.

*4.1.17. General procedure for the synthesis of harmicines **27a,b***

Harmicines **27a**,**b** were prepared according to the published procedure [26,27]. In short, a solution of a corresponding CAD (0.182 mmol), DIEA (0.063 mL, 0.364 mmol) and HATU (0.069 g, 0.182 mmol) in DCM (4 mL) was stirred at rt for 20 min, followed by the addition of amine **26** (0.042 g, 0.165 mmol). The resulting solution was stirred at rt for 1 h. The formed precipitate was filtered off. After purification by column chromatography (DCM/MeOH 8:1) and trituration with diethyl ether/petroleum ether mixture compounds **27a**,**b** were obtained.

*4.1.17.1. (E)-N-(2-(7-methoxy-1-methyl-9H-pyrido[3,4-b]indol-9-yl)ethyl)-3-(3-(trifluoromethyl)phenyl)acrylamide (**27a**).* CAD: 0.039 g

of *m*-(trifluoromethyl)cinnamic acid; yield: 0.033 g (44%); mp 220.5–222.5 °C; IR (ATR, ν/cm^{-1}) 3177, 2978, 2930, 1679, 1623, 1570, 1500, 1450, 1409, 1377, 1343, 1328, 1281, 1270, 1253, 1221, 1199, 1185, 1169, 1139, 1114, 1096, 1079, 1043, 1018, 991, 981, 803, 694, 659, 556, 530; ^{1}H NMR (DMSO-d_6) δ 8.42 (t, 1H, J = 6.0 Hz), 8.18 (d, 1H, J = 5.2 Hz), 8.09 (d, 1H, J = 8.5 Hz), 7.91-7.87 (m, 3H), 7.74 (dd, 1H, J = 7.7, 1.6 Hz), 7.66 (t, 1H, J = 7.8 Hz), 7.54 (d, 1H, J = 15.8 Hz), 7.27 (d, 1H, J = 2.2 Hz), 6.87 (dd, 1H, J = 8.6, 2.2 Hz), 6.68 (d, 1H, J = 15.8 Hz), 4.68 (t, 2H, J = 7.0 Hz), 3.90 (s, 3H), 3.61 (q, 2H, J = 6.6 Hz), 2.99 (s, 3H); ^{13}C NMR (DMSO-d_6) δ 165.35, 160.52, 142.92, 140.66, 137.87, 137.51, 135.98, 134.68, 131.26, 130.09, 129.76 (q, J = 31.7 Hz), 128.51, 125.86 (q, J = 3.6 Hz), 124.06 (q, J = 3.6 Hz), 124.04 (q, J = 272.5 Hz), 123.81, 122.41, 114.33, 112.29, 109.37, 93.57, 55.41, 43.37, 39.13, 23.10; ESI-MS: *m/z* 454.2 (M+1)$^+$; HPLC purity 98.2%.

*4.1.17.2. (E)-N-(2-(7-methoxy-1-methyl-9H-pyrido[3,4-b]indol-9-yl) ethyl)-3-(4-(trifluoromethyl)phenyl)acrylamide (**27b**).* CAD: 0.039 g of *p*-(trifluoromethyl)cinnamic acid; yield: 0.034 g (45%); mp 252.0–254.5 °C; IR (ATR, ν/cm^{-1}) 3188, 3005, 2962, 2844, 1680, 1633, 1569, 1445, 1412, 1321, 1253, 1199, 1165, 1108, 1066, 974, 831, 801, 597, 573; ^{1}H NMR (DMSO-d_6) δ 8.50 (t, 1H, J = 6.0 Hz), 8.18 (d, 1H, J = 5.1 Hz), 8.09 (d, 1H, J = 8.6 Hz), 7.89 (d, 1H, J = 5.2 Hz), 7.78 (s, 4H), 7.53 (d, 1H, J = 15.8 Hz), 7.27 (d, 1H, J = 2.2 Hz), 6.87 (dd, 1H, J = 8.6, 2.2 Hz), 6.68 (d, 1H, J = 15.8 Hz), 4.68 (t, 2H, J = 6.9 Hz), 3.90 (s, 3H), 3.61 (q, 2H, J = 6.7 Hz), 3.00 (s, 3H); ^{13}C NMR (DMSO-d_6) δ 165.27, 160.52, 142.92, 140.62, 138.83, 137.83, 137.51, 134.64, 129.29 (q, J = 31.8 Hz), 128.52, 128.21, 125.81 (q, J = 3.5 Hz), 124.44, 124.09 (q, J = 272.0 Hz), 122.40, 114.30, 112.28, 109.40, 93.51, 55.40, 43.32, 39.13, 23.06; ESI-MS: *m/z* 454.1 (M+1)$^+$; HPLC purity 99.1%.

4.2. In vitro drug sensitivity assay against P. falciparum erythrocytic stages

Antiplasmodial activity of harmicines **5**, **7**, **14**–**16**, **20** and **23** was evaluated against two laboratory *P. falciparum* strains (3D7, CQ-sensitive strain, and Dd2, CQ-resistant strain), as previously described, using the histidine-rich protein 2 (HRP2) assay [23,24]. Briefly, 96-well plates were pre-coated with the tested compounds in a three-fold dilution before ring-stage parasites were added in complete culture medium at a haematocrit of 1.5% and a parasitaemia of 0.05%. After three days of incubation at 37 °C, 5% CO_2 and 5% oxygen, plates were frozen until analysed by HRP2-ELISA. All compounds were evaluated in duplicate in at least two independent experiments. The IC_{50} was determined by nonlinear regression analysis of log concentration-response curves using the drc-package v0.9.0 of R v2.6.1 [25].

4.3. In vitro activity against P. berghei hepatic stages

In vitro activity of harmicines **5**, **7**, **14**–**16**, **20** and **23** against the liver stage of *P. berghei* infection was assessed as previously described [26,27]. Briefly, Huh7 cells were routinely cultured in 1640 Roswell Park Memorial Institute (RPMI) medium supplemented with 10% (*v*/*v*) fetal bovine serum, 1% (*v*/*v*) glutamine, 1% (*v*/*v*) penicillin/streptomycin, 1% non-essential amino acids, and 10 mM 2-[4-(2-hydroxyethyl)piperazin-1-yl]ethane-1-sulphonic acid (HEPES). For drug screening experiments, Huh7 cells were seeded at 1 × 10^4 cell/well of a 96-well plate and incubated overnight at 37 °C with 5% CO_2. 10 mM stock solutions of test compounds were prepared in DMSO and were serially diluted in infection medium, *i.e.* culture medium supplemented with gentamicin (50 μg/ml) and amphotericin B (0.8 μg/ml), to obtain the test concentrations. On the day of the infection, the culture medium was replaced by the serial dilutions of test compounds and incubated for 1 h at 37 °C with 5% CO_2. Next, 1 × 10^4 firefly luciferase-expressing *P. berghei* sporozoites, freshly isolated from the salivary glands of female infected *Anopheles stephensi* mosquitoes, were added to the cultures, plates were centrifuged at 1800×*g* for 5 min at room temperature and incubated at 37 °C with 5% CO_2. To assess the effect of each compound concentration on cell viability, cultures were incubated with Alamar Blue (Invitrogen, UK) at 46 h post infection (hpi), according to the manufacturer's recommendations. Parasite load was then assessed by a bioluminescence assay (Biotium, Fremont, CA, USA), using a multi-plate reader Infinite M200 (Tecan, Switzerland). Nonlinear regression analysis was employed to fit the normalized results of the dose-response curves, and IC_{50} values were determined using GraphPad Prism 6.0 (GraphPad software, La Jolla, CA, USA).

4.4. In vitro cytotoxicity assay

Cytotoxicity against a human cell line (HepG2) was evaluated using the neutral red assay [29]. In brief, human cells were seeded to a 96 well plate in a complete culture medium, before on the following day a serial dilution of the respective compound was added. After one day incubation, cytotoxicity was evaluated by the addition of Neutral Red, subsequent lysis of cells and measurement of absorbance in a plate reader. The IC_{50} was determined as for the *in vitro* drug assay against *P. falciparum*. To assess the safety of a compound, SI was calculated as the fractional ratio between the IC_{50}s for HepG2 and *P. falciparum* 3D7 strain.

4.5. Molecular dynamics simulations

MD simulations were performed on a *Pf*Hsp90 *N*-terminal domain X-ray structure collected from the Protein Data Bank (accession code 3K60). Ligands (ADP and SO_4^{2-}) were removed from the model and selected compounds were placed in the ATP binding pocket, including harmine as a reference. Original crystal waters were removed so that the water molecules from the bulk solvent could diffuse into the protein during equilibration and production MD runs. The investigated ligands were parameterized by performing the geometry optimization and RESP charge calculations in the Gaussian 16 program [39] at the HF/6–31G(d) level to be consistent with the employed GAFF force field, while the *Pf*Hsp90 protein was modelled with the AMBER ff14SB force field. Such protein complexes were solvated in a truncated octahedral box of TIP3P water molecules (10 Å-thick buffer), neutralized by Na^+ ions and submitted to geometry optimization in the AMBER 16 program [39] by employing periodic boundary conditions in all directions. Optimized systems were gradually heated from 0 to 300 K and equilibrated during 30 ps using NVT conditions, followed by productive and unconstrained MD simulations of 300 ns by employing a time step of 2 fs at a constant pressure (1 atm) and temperature (300 K), with the latter held constant using a Langevin thermostat with a collision frequency of 1 ps^{-1}. Bonds involving hydrogen atoms were constrained using the SHAKE algorithm [40] while the long-range electrostatic interactions were calculated employing the Particle Mesh Ewald method [41] The nonbonded interactions were truncated at 10.0 Å.

The binding free energies, ΔG_{BIND}, of each ligand within the *Pf*Hsp90 ATP binding site were calculated using the established MM-GBSA protocol [42,43] available in AmberTools16 [39], and in line with our earlier reports [10,15,44,45]. For that purpose, 1000 snapshots collected from the last 30 ns of the corresponding MD trajectories were utilized. The calculated MM-GBSA binding free energies were decomposed into specific residue contributions on a per-residue basis according to the established procedure [46,47]. This protocol calculates contributions to ΔG_{BIND} arising from each amino

acid residue and identifies the nature of the energy change in terms of interaction and solvation energies or entropic contributions.

Declaration of competing interest

The authors declare that they have no known competing financial interests or personal relationships that could have appeared to influence the work reported in this paper.

Acknowledgement

The authors acknowledge the financial support by the Croatian Science Foundation (research project UIP-2017-05-5160), University of Zagreb (support for 2019), and Fundação para a Ciência e Tecnologia, Portugal (FCT) (grant 02/SAICT/2017/29550). The work of doctoral student M. Marinović has been fully supported by the Young researcher's career development project - training of doctoral students of the Croatian Science Foundation founded by the European Union from the European Social Fund. T.T. and R.V. would like to thank the Zagreb University Computing Centre (SRCE) for granting computational resources on the ISABELLA cluster.

Abbreviations

ADMP	2-azido-1,3-dimethylimidazolinium hexafluorophosphate
AT	amide-type
ATR	attenuated total reflection
Boc	*tert*-butyloxycarbonyl
CAD	cinnamic acid derivative;
CQ	chloroquine;
DBU	1,8-diazabicyclo(5.4.0)undec-7-ene
DCM	dichloromethane
DIEA	*N,N*-diisopropylethylamine;
DMF	*N,N*-dimethylformamide;
ESI	electrospray ionization
EtOAc	ethyl acetate
EtOH	ethanol
ΔG_{BIND}	binding free energies
HAR	harmine
HATU	1-[bis(dimethylamino)methylene]-1*H*-1,2,3-triazolo [4,5-*b*]pyridinium-3-oxidhexafluorophosphate
HEPES	2-[4-(2-hydroxyethyl)piperazin-1-yl]ethane-1-sulphonic acid; hpi, hours post infection
HRP2	histidine-rich protein 2
HepG2	human liver hepatocellular carcinoma cell line;
IC_{50}	the concentration of the tested compound necessary for 50% growth inhibition
MD	molecular dynamics
MeOH	methanol
*Pf*3D7	chloroquine-sensitive strain of *P. falciparum*
*Pf*Dd2	chloroquine-resistant strain of *P. falciparum*
*Pf*Hsp90	*P. falciparum* heat shock protein 90
PQ	primaquine
SI	selectivity index
t-BuOH	*t*-buthanol
TEA	triethylamine
TMS	tetramethylsilane
TT	triazole-type
TWC	total wavelength chromatogram

Appendix A. Supplementary data

Supplementary data to this article can be found online at https://doi.org/10.1016/j.ejmech.2021.113687.

References

[1] M. Mishra, V.K. Mishra, V. Kashaw, A.K. Iyer, S.K. Kashaw, Comprehensive review on various strategies for antimalarial drug discovery, Eur. J. Med. Chem. 125 (2017) 1300–1320, https://doi.org/10.1016/j.ejmech.2016.11.025.
[2] P. Jourdan, J.P. Schneider, J. Dassonville-Klimpt, A. Sonnet, Recent Advances in Antimalarial Drugs: Structures, Mechanisms of Action and Clinical Trials, in: A. Méndez-Vilas (Ed.), Antimicrob. Res. Nov. Bioknowledge Educ. Programs, Formatex Research Center, Badajoz, 2017, pp. 599–609.
[3] WHO, World Malaria Report 2019, 2019. Colombia.
[4] A. Müller-Schiffmann, H. Sticht, C. Korth, Hybrid compounds: from simple combinations to nanomachines, BioDrugs 26 (2012) 21–31, https://doi.org/10.2165/11597630-000000000-00000.
[5] R. Oliveira, D. Miranda, J. Magalhães, R. Capela, M.J. Perry, P.M.O. Neill, R. Moreira, F. Lopes, From hybrid compounds to targeted drug delivery in antimalarial therapy, Bioorg. Med. Chem. 23 (2015) 5120–5130, https://doi.org/10.1016/j.bmc.2015.04.017.
[6] S. Shaveta, P. Mishra, Singh, Hybrid molecules: the privileged scaffolds for various pharmaceuticals, Eur. J. Med. Chem. 124 (2016) 500–536, https://doi.org/10.1016/j.ejmech.2016.08.039.
[7] J.J. Walsh, A. Bell, Hybrid drugs for malaria, Curr. Pharmaceut. Des. 15 (2009) 2970–2985.
[8] M. Fonte, N. Tassi, P. Gomes, C. Teixeira, Acridine-based antimalarials-from the very first synthetic antimalarial to recent developments, Molecules 26 (2021) 600, https://doi.org/10.3390/molecules26030600.
[9] B. Pérez, C. Teixeira, J. Gut, P.J. Rosenthal, J.R.B. Gomes, P. Gomes, Cinnamic acid/chloroquinoline conjugates as potent agents against chloroquine-resistant plasmodium falciparum, ChemMedChem 7 (2012) 1537–1540, https://doi.org/10.1002/cmdc.201200257.
[10] I. Perković, S. Raić-Malić, D. Fontinha, M. Prudêncio, L. Pessanha de Carvalho, J. Held, T. Tandarić, R. Vianello, B. Zorc, Z. Rajić, Harmicines - harmine and cinnamic acid hybrids as novel antiplasmodial hits, Eur. J. Med. Chem. 187 (2020), 111927, https://doi.org/10.1016/j.ejmech.2019.111927.
[11] B.C. Pérez, C. Teixeira, M. Figueiras, J. Gut, P.J. Rosenthal, J.R.B. Gomes, P. Gomes, Novel cinnamic acid/4-aminoquinoline conjugates bearing non-proteinogenic amino acids: towards the development of potential dual action antimalarials, Eur. J. Med. Chem. 54 (2012) 887–899, https://doi.org/10.1016/j.ejmech.2012.05.022.
[12] B.C. Pérez, C. Teixeira, I.S. Albuquerque, J. Gut, P.J. Rosenthal, J.R.B. Gomes, M. Prudeîncio, P. Gomes, N-Cinnamoylated chloroquine analogues as dual-stage antimalarial leads, J. Med. Chem. 56 (2013) 556–567, https://doi.org/10.1021/jm301654b.
[13] B. Pérez, C. Teixeira, I.S. Albuquerque, J. Gut, P.J. Rosenthal, M. Prudêncio, P. Gomes, PRIMACINS, N-cinnamoyl-primaquine conjugates, with improved liver-stage antimalarial activity, Medchemcomm 3 (2012) 1170–1172, https://doi.org/10.1039/c2md20113e.
[14] A. Teresa Silva, C.M. Bento, A.C. Pena, L.M. Figueiredo, C. Prudêncio, L. Aguiar, T. Silva, R. Ferraz, M. Salomé Gomes, C. Teixeira, P. Gomes, F. Borges, J. Garrido, T. Barros Silva, Cinnamic acid conjugates in the rescuing and repurposing of classical antimalarial drugs, Molecules 25 (2020) 66, https://doi.org/10.3390/molecules25010066.
[15] M. Marinović, I. Perković, D. Fontinha, M. Prudêncio, J. Held, L.P. de Carvalho, T. Tandarić, R. Vianello, B. Zorc, Z. Rajić, Novel harmicines with improved potency against Plasmodium, Molecules 25 (2020) 4376, https://doi.org/10.3390/molecules25194376.
[16] D. Shahinas, G. MacMullin, C. Benedict, I. Crandall, D.R. Pillaid, Harmine is a potent antimalarial targeting Hsp90 and synergizes with chloroquine and artemisinin, Antimicrob. Agents Chemother. 56 (2012) 4207–4213, https://doi.org/10.1128/AAC.00328-12.
[17] T. Wang, P. Mäser, D. Picard, Inhibition of plasmodium falciparum Hsp90 contributes to the antimalarial activities of aminoalcohol-carbazoles, J. Med. Chem. 59 (2016) 6344–6352, https://doi.org/10.1021/acs.jmedchem.6b00591.
[18] S. Eagon, M.O. Anderson, Microwave-assisted synthesis of tetrahydro-β-carbolines and β-carbolines, Eur. J. Org Chem. 2014 (2014) 1653–1665, https://doi.org/10.1002/ejoc.201301580.
[19] N. Devi, D. Singh, Honey, S. Mor, S. Chaudhary, R.K. Rawal, V. Kumar, A.K. Chowdhury, V. Singh, In(OTf)3 catalysed an expeditious synthesis of β-carboline-imidazo[1,2-: A] pyridine and imidazo[1,2- a] pyrazine conjugates, RSC Adv. 6 (2016) 43881–43891, https://doi.org/10.1039/c6ra04841b.
[20] D. Singh, C.K. Hazra, C.C. Malakar, S.K. Pandey, B.S. Kaith, V. Singh, Indium-mediated domino allylation-lactonisation approach: diastereoselective synthesis of β-carboline C-3 tethered α-methylene γ-butyrolactones, Chemistry 3 (2018) 4859–4864, https://doi.org/10.1002/slct.201800006.
[21] M. Kitamura, T. Koga, M. Yano, T. Okauchi, Direct synthesis of organic azides from alcohols using 2-azido-1,3- dimethylimidazolinium hexafluorophosphate, Synlett 23 (2012) 1335–1338, https://doi.org/10.1055/s-0031-1290958.
[22] Chemicalize ChemAxon. https://chemicalize.com/, 2018. (Accessed 20 July 2020).
[23] J. Held, T. Gebru, M. Kalesse, R. Jansen, K. Gerth, R. Müller, B. Mordmüller, Antimalarial activity of the myxobacterial macrolide chlorotonil A, Antimicrob. Agents Chemother. 58 (2014) 6378–6384, https://doi.org/10.1128/AAC.03326-14.
[24] H. Noedl, J. Bronnert, K. Yingyuen, B. Attlmayr, H. Kollaritsch, M. Fukuda,

Simple histidine-rich protein 2 double-site sandwich enzyme-linked immunosorbent assay for use in malaria drug sensitivity testing, Antimicrob. Agents Chemother. 49 (2005) 3575–3577, https://doi.org/10.1128/AAC.49.8.3575-3577.2005.
[25] R Core Team, A Language and Environment for Statistical Computing, R Foundation for Statistical Computing, Vienna, Austria, 2018. https://www.r-project.org/. (Accessed 20 July 2020).
[26] M. Machado, M. Sanches-Vaz, J.P. Cruz, A.M. Mendes, M. Prudêncio, Inhibition of Plasmodium hepatic infection by antiretroviral compounds, Front. Cell. Infect. Microbiol. 7 (2017) 329, https://doi.org/10.3389/fcimb.2017.00329.
[27] I.H.J. Ploemen, M. Prudêncio, B.G. Douradinha, J. Ramesar, J. Fonager, G.-J. van Gemert, A.J.F. Luty, C.C. Hermsen, R.W. Sauerwein, F.G. Baptista, M.M. Mota, A.P. Waters, I. Que, C.W.G.M. Lowik, S.M. Khan, C.J. Janse, B.M.D. Franke-Fayard, Visualisation and quantitative analysis of the rodent malaria liver stage by real time imaging, PloS One 4 (2009), e7881, https://doi.org/10.1371/journal.pone.0007881.
[28] M. Beus, D. Fontinha, J. Held, Z. Rajić, L. Uzelac, M. Kralj, M. Prudêncio, B. Zorc, Primaquine and chloroquine fumardiamides as promising antiplasmodial agents, Molecules 24 (2019) 2812, https://doi.org/10.3390/molecules24152812.
[29] E. Borenfreund, J.A. Puerner, A simple quantitative procedure using monolayer cultures for cytotoxicity assays (HTD/NR-90), J. Tissue Cult. Methods 9 (1985) 7–9, https://doi.org/10.1007/BF01666038.
[30] K.D. Corbett, J.M. Berger, Structure of the ATP-binding domain of plasmodium falciparum Hsp90, Proteins Struct. Funct. Bioinforma. 78 (2010) 2738–2744, https://doi.org/10.1002/prot.22799.
[31] S.M. Roe, C. Prodromou, R. O'Brien, J.E. Ladbury, P.W. Piper, L.H. Pearl, Structural basis for inhibition of the Hsp90 molecular chaperone by the antitumor antibiotics radicicol and geldanamycin, J. Med. Chem. 42 (1999) 260–266, https://doi.org/10.1021/jm980403y.
[32] H.C. Cheng, The power issue: determination of KB or Ki from IC50 - a closer look at the Cheng-Prusoff equation, the Schild plot and related power equations, J. Pharmacol. Toxicol. Methods 46 (2001) 61–71, https://doi.org/10.1016/S1056-8719(02)00166-1.
[33] D. Shahinas, M. Liang, A. Datti, D.R. Pillai, A repurposing strategy identifies novel synergistic inhibitors of plasmodium falciparum heat shock protein 90, J. Med. Chem. 53 (2010) 3552–3557, https://doi.org/10.1021/jm901796s.
[34] M. Cain, R.W. Weber, F. Guzman, J.M. Cook, S.A. Barker, K.C. Rice, J.N. Crawley, S.M. Paul, P. Skolnick, β-Carbolines: synthesis and neurochemical and pharmacological actions on brain benzodiazepine receptors, J. Med. Chem. 25 (1982) 1081–1091, https://doi.org/10.1021/jm00351a015.
[35] T. Szabó, V. Hazai, B. Volk, G. Simig, M. Milen, First total synthesis of the β-carboline alkaloids trigonostemine A, trigonostemine B and a new synthesis of pityriacitrin and hyrtiosulawesine, Tetrahedron Lett. 60 (2019) 1471–1475, https://doi.org/10.1016/j.tetlet.2019.04.044.
[36] G. Lin, Y. Wang, Q. Zhou, W. Tang, J. Wang, T. Lu, A facile synthesis of 1-substituted βcarboline derivatives via minisci-reaction, Synth. Commun. 41 (2011) 3541–3550, https://doi.org/10.1080/00397911.2010.519092.
[37] Y. Schott, M. Decker, H. Rommelspacher, J. Lehmann, 6-Hydroxy- and 6-methoxy-β-carbolines as acetyl- and butyrylcholinesterase inhibitors, Bioorg, Med. Chem. Lett. 16 (2006) 5840–5843, https://doi.org/10.1016/j.bmcl.2006.08.067.
[38] W. Seppelt, H.-J. Neubauer, H. Adolphi, P. Hofmeister, Propargyl Cinnamates, Process for Their Production and Their Application in Pest Control, EP0235722B1, 1989. https://patents.google.com/patent/EP0235722B1/en. (Accessed 15 March 2021).
[39] D.A. Case, R.M. Betz, D.S. Cerutti, T.E. Cheatham, T.A. Darden, R.E. Duke, T.J. Giese, H. Gohlke, A.W. Goetz, N. Homeyer, S. Izadi, P. Janowski, J. Kaus, A. Kovalenko, T.S. Lee, S. LeGrand, P. Li, C. Lin, T. Luchko, R. Luo, B. Madej, D. Mermelstein, K.M. Merz, G. Monard, H. Nguyen, H.T. Nguyen, I. Omelyan, A. Onufriev, D.R. Roe, A. Roitberg, C. Sagui, C.L. Simmerling, W.M. Botello-Smith, J. Swails, R.C. Walker, J. Wang, R.M. Wolf, X. Wu, L. Xiao, P.A. Kollman, Amber 16 (2016).
[40] J.P. Ryckaert, G. Ciccotti, H.J.C. Berendsen, Numerical integration of the cartesian equations of motion of a system with constraints: molecular dynamics of n-alkanes, J. Comput. Phys. 23 (1977) 327–341, https://doi.org/10.1016/0021-9991(77)90098-5.
[41] T. Darden, D. York, L. Pedersen, Particle mesh Ewald: an N·log(N) method for Ewald sums in large systems, J. Chem. Phys. 98 (1993) 10089–10092, https://doi.org/10.1063/1.464397.
[42] T. Hou, J. Wang, Y. Li, W. Wang, Assessing the performance of the MM/PBSA and MM/GBSA methods. 1. The accuracy of binding free energy calculations based on molecular dynamics simulations, J. Chem. Inf. Model. 51 (2011) 69–82, https://doi.org/10.1021/ci100275a.
[43] S. Genheden, U. Ryde, The MM/PBSA and MM/GBSA methods to estimate ligand-binding affinities, Expet Opin. Drug Discov. 10 (2015) 449–461, https://doi.org/10.1517/17460441.2015.1032936.
[44] T. Tandarić, R. Vianello, Computational insight into the mechanism of the irreversible inhibition of monoamine oxidase enzymes by the anti-parkinsonian propargylamine inhibitors rasagiline and selegiline, ACS Chem. Neurosci. 10 (2019) 3532–3542, https://doi.org/10.1021/acschemneuro.9b00147.
[45] L. Hok, J. Mavri, R. Vianello, The effect of deuteration on the H2 receptor histamine binding profile: a computational insight into modified hydrogen bonding interactions, Molecules 25 (2020) 1–17, https://doi.org/10.3390/molecules25246017.
[46] G. Rastelli, A. Del Rio, G. Degliesposti, M. Sgobba, Fast and accurate predictions of binding free energies using MM-PBSA and MM-GBSA, J. Comput. Chem. 31 (2010) 797–810, https://doi.org/10.1002/jcc.21372.
[47] H. Gohlke, C. Kiel, D.A. Case, Insights into protein-protein binding by binding free energy calculation and free energy decomposition for the Ras-Raf and Ras-RalGDS complexes, J. Mol. Biol. 330 (2003) 891–913, https://doi.org/10.1016/S0022-2836(03)00610-7.

TEMELJNA DOKUMENTACIJSKA KARTICA/
BASIC DOCUMENTATION CARD

Temeljna dokumentacijska kartica

Sveučilište u Zagrebu
Farmaceutsko-biokemijski fakultet
Zavod za farmaceutsku kemiju
A. Kovačića 1, 10000 Zagreb, Hrvatska

Doktorski rad

HARMICINI AMIDNOGA TIPA KAO POTENCIJALNI ANTIMALARICI

Marina Marinović

SAŽETAK

U prvom dijelu istraživanja ovog doktorskog rada sintetizirano je četrdeset harmicina amidnoga tipa (**7a-h**, **13a-h**, **19a-h**, **22a-h**, **25a-f**, **i-p**), hibridnih spojeva harmina/srodnih β-karbolinskih alkaloida i cimetne kiseline/odabranih derivata cimetne kiseline (DCK-a) međusobno povezanih amidnom vezom. U tu svrhu pripravljeni su amini **6**, **12**, **18**, **21** i **24**, čime je primarna amino skupina uvedena u pet položaja β-karbolina: 1, 3, 6, 7 i 9. U idućem koraku sintetizirani su harmicini amidnoga tipa reakcijama povezivanja dobivenih amina s cimetnom kiselinom/DCK-ima korištenjem standardnih reakcijskih uvjeta (HATU/DIEA). Harmicini su karakterizirani spektroskopskim (^{1}H, ^{13}C NMR, IR) i spektrometrijskim (MS) tehnikama te im je određeno talište. Svim spojevima ispitano je antiplazmodijsko djelovanje *in vitro* na eritrocitnu fazu životnog ciklusa dva soja *Plasmodium falciparum* (*Pf*3D7 i *Pf*Dd2), hepatocitnu fazu životnog ciklusa *P. berghei* i citotoksičnost na humanu staničnu liniju hepatocelularnog karcinoma (HepG2).

U drugom dijelu istraživanja provedena je analiza kvantitativnog odnosa strukture i djelovanja (engl. *quantitative structure-activity relationship*, QSAR). Antiplazmodijsko djelovanje harmicina na eritrocitnu fazu *Pf*3D7 povezano je s pripadajućim izračunatim molekulskim deskriptorima te je primjenom metode višestruke linearne regresije dobiven prediktivni model ovisnosti log IC_{50} o dvije varijable: izoelektričnoj točki (p*I*) i Abrahamovom deskriptoru E (Abr E). Model je validiran unutarnjom 10-strukom unakrsnom validacijom.

U trećem dijelu istraživanja, za provedbu vanjske validacije modela predložene su strukture 356 novih harmicina te su im, prema dobivenom modelu, izračunate predviđene IC_{50} vrijednosti. Potom je odabrano, sintetizirano i karakterizirano ukupno 19 harmicina: šest harmicina amidnoga tipa (**25k-p**), 11 harmicina karbamatnog tipa (**28a-k**) i dva harmicina ureidnog tipa (**32b**,**c**) u položaju N-9 β-karbolina, te je ispitano njihovo antiplazmodijsko djelovanje *in vitro* na eritrocitnu fazu životnog ciklusa plazmodija (*Pf*3D7 i *Pf*Dd2). Na temelju dobivenih rezultata izračunate su razlike između eksperimentalnih i predviđenih vrijednosti i srednja apsolutna pogreška predviđanja. Najjače djelovanje, gotovo dva reda veličine jače od harmina, pokazali su harmicini amidnoga tipa u položaju N-9 β-karbolina (**25b-e**,**i**,**j**).

Rezultati ovog doktorskog rada predstavljaju temelj za daljnji razvoj novih harmicina amidnoga tipa s pojačanim antiplazmodijskim djelovanjem.

Rad je pohranjen u Središnjoj knjižnici Farmaceutsko-biokemijskog fakulteta Sveučilišta u Zagrebu.

Rad sadrži: 253 stranice, 41 sliku, 50 tablica, 10 shema i 181 literaturni navod. Izvornik je na hrvatskom jeziku.

Ključne riječi: β-karbolin, harmicini, DCK, sinteza, antiplazmodijsko djelovanje, QSAR

Mentor: **Dr. sc. Zrinka Rajić**, *redovita profesorica, Farmaceutsko-biokemijski fakultet Sveučilišta u Zagrebu*

Ocjenjivači: **Dr. sc. Ivana Perković**, *izvanredna profesorica, Farmaceutsko-biokemijski fakultet Sveučilišta u Zagrebu*

Dr. sc. Jasmina Lovrić, *redovita profesorica, Farmaceutsko-biokemijski fakultet Sveučilišta u Zagrebu*

Dr. sc. Bono Lučić, *viši znanstveni suradnik, Institut Ruđer Bošković*

Rad prihvaćen: Prosinac 2022.

Basic documentation card

University of Zagreb
Faculty of Pharmacy and Biochemistry
Department of Medicinal Chemistry
A. Kovačića 1, 10000 Zagreb, Croatia

Doctoral dissertation

AMIDE-TYPE HARMICINES AS POTENTIAL ANTIMALARIAL AGENTS

Marina Marinović

SUMMARY

The first part of this thesis includes the synthesis of forty amide-type harmicines (**7a-h**, **13a-h**, **19a-h**, **22a-h**, **25a-f**, **i-p)**, hybrid compounds in which harmine/β-carboline alkaloids and cinnamic acid or cinnamic acid derivatives (CADs) are linked *via* an amide bond. First, the primary amino group was introduced in five positions of the β-carboline ring: 1, 3, 6, 7 and 9, which resulted in the synthesis of amines **6**, **12**, **18**, **21** and **24**. Subsequently, the coupling reaction of amines and cinnamic acid/CADs were preformed using standard conditions (HATU/DIEA). The synthesized compounds were characterized by spectroscopic (^{1}H, ^{13}C NMR, IR) and spectrometric (MS) techniques, as well as determination of their melting points. Finally, we evaluated biological activities of the prepared harmicines, *i.e. in vitro* antiplasmodial activity against the erythrocytic stage of the *Plasmodium falciparum* life cycle (*Pf*3D7 and *Pf*Dd2) and hepatic stage of the *P. berghei* life cycle, as well as cytotoxicity against human hepatocellular carcinoma cell line (HepG2).

In the second part of this thesis quantitative structure-activity relationship (QSAR) analysis was performed using a multiple linear regression technique. A set of molecular descriptors underwent the forward stepwise regression procedure and the predictive model was built by selecting two molecular descriptors: isoelectric point (p*I*) and Abraham descriptor E (Abr E). The constructed model was internally validated using 10-fold cross-validation.

For the purpose of external validation of the constructed model, in the third part of this thesis 356 novel harmicines were designed and their predicted logIC_{50} values calculated, followed by the synthesis and characterization of six amide-type harmicines (**25k-p**), eleven carbamate type-harmicines (**28a-k**) and two ureido-type harmicines (**32b**,**c**) in the position N-9 of the β-carboline. Next, we evaluated *in vitro* antiplasmodial activity of novel harmicines against the erythrocytic stage of the *P. falciparum* life cycle (*Pf*3D7 and *Pf*Dd2). Based on the obtained results, the absolute differences between the experimental and predicted values as well as mean absolute error were calculated. The most active compounds, amide-type harmicines in the position N-9 of the β-carboline (**25b-e**,**i**,**j**), displayed at least two orders of magnitude stronger activities than the parent compound, harmine. The results of this doctoral thesis represent the basis for the further development of novel amide-type harmicines with enhanced antiplasmodial activity.

The dissertation is deposited in the Central Library of the Faculty of Pharmacy and Biochemistry University of Zagreb.

Dissertation includes: 253 pages, 41 figures, 50 tables, 10 schemes and 181 references. Original is in Croatian language.

Keywords: β-carboline, harmicines, CAD, synthesis, antiplasmodial activity, QSAR

Mentor: **Zrinka Rajić, Ph.D.**, *Full Professor, Faculty of Pharmacy and Biochemistry, University of Zagreb*

Reviewers: **Ivana Perković, Ph.D.**, *Associate Professor, Faculty of Pharmacy and Biochemistry, University of Zagreb*

Jasmina Lovrić, Ph.D., *Full Professor, Faculty of Pharmacy and Biochemistry, University of Zagreb*

Bono Lučić, Ph.D., *Senior Research Associate, Ruđer Bošković Institute*

The thesis was accepted: December 2022